

509p.
NASA Conference Publication 2327
Part 2

Recent Experiences in Multidisciplinary Analysis and Optimization

*Proceedings of a symposium held at
NASA Langley Research Center
Hampton, Virginia
April 24-26, 1984*

NASA

*NASA Conference Publication 2327
Part 2*

Recent Experiences in Multidisciplinary Analysis and Optimization

*Compiled by
Jaroslaw Sobieski
Langley Research Center*

Proceedings of a symposium held at
NASA Langley Research Center
Hampton, Virginia
April 24-26, 1984

NASA

National Aeronautics
and Space Administration

**Scientific and Technical
Information Branch**

1984

PREFACE

This conference publication contains the papers presented at the NASA Symposium on Recent Experiences in Multidisciplinary Analysis and Optimization, held at NASA Langley Research Center, Hampton, Virginia, April 24-26, 1984. The purposes of the symposium were to exchange information about the status of the application of optimization and associated analyses in industry or research laboratories to real life problems, and to examine the directions of future developments.

Within the broad statement of the symposium's purposes, information exchange has encompassed the following:

Examples of successful applications

"Attempt and failure" examples, particularly to describe the reasons for failure and lessons learned

Identification of potential applications and benefits, even though no attempt to apply optimization may have been made as yet

Synergistic effects of optimized interaction and trade-offs occurring among two or more engineering disciplines (e.g., structural engineering and aerodynamics) and/or subsystems in a system (e.g., propulsion and airframe in aircraft)

Traditional organization of a design process as a vehicle for or an impediment to the progress in the design methodology

Computer technology in the context of the foregoing

This information exchange has covered aerospace and other industries as well as universities and government agencies.

The goal of the meeting was to reach a better understanding of the extent to which optimization and the associated analyses are being used, development directions, the future potential, and actions that ought to be taken to realize the potential sooner. That goal was attained and the symposium showed through both the diversity and quality of papers and the active participation of the attendees that the activities in the subject area are vigorous beyond the initial expectations. There was a consensus that multidisciplinary analysis and optimization have an important potential as aids to human intellect in the design process, and that cooperation of industry, academia, and government, under NASA leadership, is needed to realize that potential.

PRECEDING PAGE BLANK NOT FILMED

CONTENTS

| | |
|-------------------|-----|
| PREFACE | iii |
|-------------------|-----|

Part 1*

SESSION 1: INTRODUCTION AND GENERAL CONSIDERATIONS Co-Chairmen: L. A. McCullers and J. Sobieski

| | |
|---|-----|
| STRUCTURAL SYNTHESIS - PRECURSOR AND CATALYST | 1 |
| L. A. Schmit | |
| OPTIMIZATION IN THE SYSTEMS ENGINEERING PROCESS | 19 |
| Loren A. Lemmerman | |
| PRACTICAL CONSIDERATIONS IN AEROELASTIC DESIGN | 35 |
| Bruce A. Rommel and Alan J. Dodd | |
| FLUTTER OPTIMIZATION IN FIGHTER AIRCRAFT DESIGN | 47 |
| William E. Triplett | |
| APPLICATION OF THE GENERALIZED REDUCED GRADIENT METHOD TO CONCEPTUAL AIRCRAFT DESIGN | 65 |
| Gary A. Gabriele | |
| EXPERIENCES PERFORMING CONCEPTUAL DESIGN OPTIMIZATION OF TRANSPORT AIRCRAFT | 87 |
| P. Douglas Arbuckle and Steven M. Sliwa | |
| THE ROLE OF OPTIMIZATION IN STRUCTURAL MODEL REFINEMENT | 103 |
| L. L. Lehman | |
| PIAS, A PROGRAM FOR AN ITERATIVE AEROELASTIC SOLUTION | 111 |
| Marjorie E. Manro | |

SESSION 2: OPTIMIZATION IN VARIOUS INDUSTRIES Chairman: W. J. Stroud

| | |
|---|-----|
| OPTIMIZATION PROCESS IN HELICOPTER DESIGN | 127 |
| A. H. Logan and D. Banerjee | |
| ROLE OF OPTIMIZATION IN INTERDISCIPLINARY ANALYSES OF NAVAL STRUCTURES | 139 |
| S. K. Dhir and M. M. Hurwitz | |
| APPLICATION OF OPTIMIZATION TECHNIQUES TO VEHICLE DESIGN - A REVIEW | 147 |
| B. Prasad and C. L. Magee | |
| STRUCTURAL OPTIMIZATION IN AUTOMOTIVE DESIGN | 173 |
| J. A. Bennett and M. E. Botkin | |

*Part 1 is presented under separate cover.

| | |
|--|-----|
| TRADEOFF METHODS IN MULTIOBJECTIVE INSENSITIVE DESIGN OF AIRPLANE CONTROL SYSTEMS | 189 |
| Albert A. Schy and Daniel P. Giesy | |

SESSION 3A: APPLICATIONS 1
Chairman: J. H. Starnes, Jr.

| | |
|--|-----|
| STAEBL -- STRUCTURAL TAILORING OF ENGINE BLADES (PHASE II) | 205 |
| M. S. Hirschbein and K. W. Brown | |
| OPTIMIZATION OF CASCADE BLADE MISTUNING UNDER FLUTTER AND FORCED RESPONSE CONSTRAINTS | 219 |
| Durbha V. Murthy and Raphael T. Haftka | |
| SIZING-STIFFENED COMPOSITE PANELS LOADED IN THE POSTBUCKLING RANGE | 235 |
| S. B. Biggers and J. N. Dickson | |
| OPTIMAL REDESIGN STUDY OF THE HARM WING | 251 |
| S. C. McIntosh, Jr., and M. E. Weynand | |
| COMPOSITE MATERIAL DESIGN, ANALYSIS, AND PROCESSING OF SPACE MOTOR NOZZLE COMPONENTS | 265 |
| Edward L. Stanton | |

SESSION 3B: APPLICATIONS 2
Chairman: I. Abel

| | |
|---|-----|
| A NONLINEAR PROGRAMMING METHOD FOR SYSTEM DESIGN WITH RESULTS THAT HAVE BEEN IMPLEMENTED | 267 |
| Frank Hauser | |
| APPLICATION OF OPTIMIZATION TECHNIQUES TO THE DESIGN OF A FLUTTER SUPPRESSION CONTROL LAW FOR THE DAST ARW-2 | 279 |
| William A. Adams, Jr., and Sherwood H. Tiffany | |
| APPLICATION OF CONMIN TO WING DESIGN OPTIMIZATION WITH VORTEX FLOW EFFECT | 297 |
| C. Edward Lan | |
| CALCULATED EFFECTS OF VARYING REYNOLDS NUMBER AND DYNAMIC PRESSURE ON FLEXIBLE WINGS AT TRANSONIC SPEEDS | 309 |
| Richard L. Campbell | |
| INFLUENCE OF ANALYSIS AND DESIGN MODELS ON MINIMUM WEIGHT DESIGN | 329 |
| M. Salama, R. K. Ramanathan, L. A. Schmit, and I. S. Sarma | |

SESSSION 4: METHODS AND TOOLS 1
Co-Chairmen: R. T. Haftka and H. Miura

| | |
|--|-----|
| MULTIDISCIPLINARY SYSTEMS OPTIMIZATION BY LINEAR DECOMPOSITION | 343 |
| J. Sobieski | |

| | |
|--|-----|
| STRUCTURAL SENSITIVITY ANALYSIS: METHODS, APPLICATIONS, AND NEEDS | 367 |
| Howard M. Adelman, Raphael T. Haftka, Charles J. Camarda, and Joanne L. Walsh | |
| SENSITIVITY ANALYSIS IN COMPUTATIONAL AERODYNAMICS | 385 |
| Dean R. Bristow | |
| AIRCRAFT CONFIGURATION OPTIMIZATION INCLUDING OPTIMIZED FLIGHT PROFILES | 395 |
| L. A. McCullers | |
| THE ADS GENERAL-PURPOSE OPTIMIZATION PROGRAM | 413 |
| G. N. Vanderplaats | |
| SHAPE DESIGN SENSITIVITY ANALYSIS OF BUILT-UP STRUCTURES | 423 |
| Kyung K. Choi | |
| MULTIDISCIPLINARY OPTIMIZATION APPLIED TO A TRANSPORT AIRCRAFT | 439 |
| Gary L. Giles and G. A. Wrenn | |
| SOME EXPERIENCES IN AIRCRAFT AEROELASTIC DESIGN USING PRELIMINARY AEROELASTIC DESIGN OF STRUCTURES (PADS) | 455 |
| Nick A. Radovcich | |
| DESIGN ENHANCEMENT TOOLS IN MSC/NASTRAN | 505 |
| D. V. Wallerstein | |
| PROGRESS REPORT ON THE "AUTOMATED STRENGTH-AEROELASTIC DESIGN OF AEROSPACE STRUCTURES" PROGRAM | 527 |
| E. H. Johnson and V. B. Venkayya | |

Part 2

SESSION 5A: ROTORCRAFT APPLICATIONS Co-Chairmen: C. E. Hammond and R. J. Huston

| | |
|---|-----|
| OVERVIEW: APPLICATIONS OF NUMERICAL OPTIMIZATION METHODS TO HELICOPTER DESIGN PROBLEMS | 539 |
| H. Miura | |
| APPLICATION OF MODERN STRUCTURAL OPTIMIZATION TO VIBRATION REDUCTION IN ROTORCRAFT | 553 |
| P. P. Friedmann | |
| HELICOPTER ROTOR BLADE AERODYNAMIC OPTIMIZATION BY MATHEMATICAL PROGRAMING | 567 |
| Joanne L. Walsh, Gene J. Bingham, and Michael F. Riley | |
| REGRESSION ANALYSIS AS A DESIGN OPTIMIZATION TOOL | 579 |
| Richmond Perley | |

| | |
|--|-----|
| A ROTOR OPTIMIZATION USING REGRESSION ANALYSIS | 595 |
| N. Giansante | |
| OPTIMIZATION OF HELICOPTER ROTOR BLADE DESIGN FOR MINIMUM VIBRATION | 609 |
| M. W. Davis | |
| APPLICATION OF NUMERICAL OPTIMIZATION TO ROTOR AERODYNAMIC DESIGN | 627 |
| W. A. Pleasants III and T. J. Wiggins | |
| AEROELASTIC/AERODYNAMIC OPTIMIZATION OF HIGH SPEED HELICOPTER/ COMPOUND ROTOR | 643 |
| L. R. Sutton and R. L. Bennett | |
| THE STRUCTURAL OPTIMIZATION OF A SPREADER BAR FOR TWIN LIFT HELICOPTER OPERATIONS | 663 |
| Alan Dobyns | |
| MULTIOBJECTIVE OPTIMIZATION TECHNIQUES FOR STRUCTURAL DESIGN | 675 |
| S. S. Rao | |

SESSION 5B: SPACE APPLICATIONS

Chairman: A. W. Wilhite

| | |
|--|-----|
| IDEAS, A MULTIDISCIPLINARY COMPUTER-AIDED CONCEPTUAL DESIGN SYSTEM FOR SPACECRAFT | 683 |
| Melvin J. Ferebee, Jr. | |
| AVID II, A MULTIDISCIPLINARY COMPUTER AIDED CONCEPTUAL DESIGN SYSTEM FOR LAUNCH VEHICLES AND ORBITAL TRANSFER VEHICLES [†] | |
| A. W. Wilhite | |
| MICROCOMPUTER DESIGN AND ANALYSIS OF THE CABLE CATENARY LARGE SPACE ANTENNA SYSTEM | 705 |
| W. Akle | |
| DESIGN OPTIMIZATION OF THE 34-METER DSN-NCP ANTENNAS | 719 |
| Roy Levy | |
| POST AND A RANDOM-WALK SEARCH MODE | 735 |
| James A Martin | |
| COMPONENT TESTING FOR DYNAMIC MODEL VERIFICATION | 759 |
| T. K. Hasselman and Jon D. Chrostowski | |
| DUAL STRUCTURAL-CONTROL OPTIMIZATION OF LARGE SPACE STRUCTURES | 775 |
| Achille Messac and James Turner | |
| STRUCTURAL OPTIMIZATION WITH CONSTRAINTS ON TRANSIENTS RESPONSE | 803 |
| Robert Riess | |

[†]Paper not available for publication.

| | |
|---|-----|
| OPTIMIZATION APPLICATIONS IN AIRCRAFT ENGINE DESIGN AND TEST | 815 |
| T. K. Pratt | |
| ON OPTIMAL DESIGN FOR THE BLADE-ROOT/HUB INTERFACE IN JET ENGINES | 833 |
| Noboru Kikuchi and John E. Taylor | |

SESSION 6: METHODS AND TOOLS 2
Co-Chairmen: H. M. Adelman and G. L. Giles

| | |
|---|------|
| PROBLEMS IN LARGE-SCALE STRUCTURAL OPTIMIZATION | 847 |
| Jasbir S. Arora and Ashok D. Belegundu | |
| STRUCTURAL OPTIMIZATION OF LARGE OCEAN-GOING STRUCTURES | 873 |
| Owen F. Hughes | |
| FUNDAMENTAL DIFFERENCES BETWEEN OPTIMIZATION CODE TEST PROBLEMS AND ENGINEERING APPLICATIONS | 891 |
| E. D. Eason | |
| A CONCEPTUAL BASIS FOR THE DESIGN OF DAMAGE-TOLERANT STRUCTURAL SYSTEMS | 907 |
| Farrokh Mistree, Jon A. Shupe, and Owen F. Hughes | |
| COMMENTS ON GUST RESPONSE CONSTRAINED OPTIMIZATION | 943 |
| Prabhat Hajela | |
| APPLYING OPTIMIZATION SOFTWARE LIBRARIES TO ENGINEERING PROBLEMS | 957 |
| M. J. Healy | |
| OPTDES.BYU: AN INTERACTIVE OPTIMIZATION PACKAGE WITH 2D/3D GRAPHICS | 979 |
| R. J. Balling, A. R. Parkinson, and J. C. Free | |
| ON THE UTILIZATION OF ENGINEERING KNOWLEDGE IN DESIGN OPTIMIZATION | 991 |
| Panos Papalambros | |
| COMPUTER AIDED ANALYSIS AND OPTIMIZATION OF MECHANICAL SYSTEM DYNAMICS | 1007 |
| E. J. Haug | |
| SHAPE OPTIMIZATION INCLUDING FINITE ELEMENT GRID ADAPTATION | 1027 |
| Noboru Kikuchi and J. E. Taylor | |
| MULTIDISCIPLINARY APPROACH TO THE DESIGN OF HIGH PRESSURE OXYGEN SYSTEMS | 1037 |
| R. L. Johnston | |

N87-11751

OVERVIEW: APPLICATIONS OF NUMERICAL OPTIMIZATION METHODS
TO HELICOPTER DESIGN PROBLEMS

H. Miura
NASA Ames Research Center
Moffett Field, California

INTRODUCTION

The term "optimization" covers wide spectrum of technology, but this presentation is limited to the applications of numerical optimization methods (in other words, mathematical programming or multi-variable search methods) as applied to helicopter design problems. The potential benefits of this technology were recognized as early as ten years ago, but as can be clearly seen in the table shown below, serious effort to exploit its capabilities started only very recently. It is interesting to note that the helicopter industry started incorporating this technology much faster than the fixed wing industry. The current active interest of the helicopter industry may be accurately reflected in the organization of a special session at the 1983 AHS Forum (ref. 1). This situation can probably be attributed to the existence of many difficult and urgent problems associated with helicopter design. Also, the relatively small and flexible organizational structure of helicopter manufacturers might be a contributing factor. A great deal of research and development effort is still required to ship numerical optimization methods out of R&D departments into production design divisions. However, design optimization methods will be considered increasingly important to win basic research contracts, and even to win major military aircraft design contracts in the near future.

One commonly expressed criticism of using numerical optimization in helicopter design problems is the adequacy of analysis techniques. For example, it is important to design a rotor system that applies minimum vibratory forces and moments to the airframe, but prediction of dynamic airloads for a given rotor system for any specified flight condition is still an active research subject. Under such circumstances, we often have to face R&D resource allocation problems. In my opinion, it is important to have a system that can carry out design optimization based on the best available analysis or test data. Such a system will provide a framework to accommodate new technology developments by replacing outdated modules with new modules. Recent developments in computer engineering provide opportunities to build such an adaptive program system that will be allowed to grow with new technology developments. The benefits of multi-disciplinary analysis and design will be captured readily if the framework to integrate necessary modules is available. Also it should be recognized that the contributions of any analysis tools or sophisticated tests are enhanced if there are mechanisms to promptly reflect results in aircraft design. Human engineers have been the only link between analysis and design capabilities in the past, but design engineers in the helicopter industry may be able to use numerical design optimization as a convenient practical tool in the near future.

| Year | Conceptual Preliminary Design | Structural Design | Aerodynamic Acoustic Design | Rotor System Design | Flight Trajectory Design | Control System Design |
|------|-------------------------------|-------------------|-----------------------------|---------------------|--------------------------|-----------------------|
| 1970 | 2 | | | | | |
| 71 | | | | 18 | | |
| 72 | | | | 19 | | |
| 73 | | | | | | |
| 74 | | 6 | | | 28 | |
| 75 | | | | | | |
| 76 | 3 | 7, 8 | | | 29 | |
| 77 | | | | | | |
| 78 | 4 | | | | | |
| 79 | | 9 | | | | |
| 1980 | | 10 | 15, 16 | | | |
| 81 | 5 | 11, 12, 13 | | | | |
| 82 | | 14 | | 20, 21, 22 | 30 | |
| 83 | | | | 23, 24, 25 | | 31 |
| 84 | | | 17 | 26, 27 | | |

CONCEPTUAL AND PRELIMINARY DESIGN OPTIMIZATION

Design optimization is more effective if introduced into the early design stages, where many important decisions are yet to be made. Selection of the basic configuration of an aircraft to accomplish a given set of missions in an optimal fashion has been identified as a critically important decision in the recent JVX exercise. The wide spectrum of modern aircraft with a variety of characteristics makes the conceptual design decision extremely complicated and delicate. On the other hand, there is usually not sufficient time or funding to have many preliminary design study contracts.

There are a number of papers dealing with the applications of numerical optimization to the general area of conceptual to preliminary design of rotorcraft; the first paper by Stepniewski (ref. 2) appeared as early as 1970. A Polish group (ref. 3) applied the same technology and even the same optimization program (Automatic Engineering and Science Optimization Program (AESOP)) to preliminary design of compound helicopters. Later Stepniewski and Sloan attempted the formulation of the optimal design of transport helicopters (ref. 4). Their purpose was to come up with a sensible formulation of the lowest possible total operating cost per revenue-seat and nautical mile. This is probably the first published attempt to integrate helicopter performance analysis and cost models aimed specifically at helicopter design optimization.

Ramos and Taylor wrote a comprehensive report (ref. 5) on the optimal preliminary design of helicopters. The program, named HELISOTON, developed at the University of Southampton, appears to have relatively comprehensive coverage of the performance of helicopters with resizing algorithms. The only reason that formal multi-variable design optimization was not carried out seems to be excessive computer run times. Formulation and program structure may already be prepared to couple with a numerical optimization code.

No published literature was found regarding the use of numerical optimization methods for the preliminary design of helicopters in the U.S., although every helicopter manufacturer has some form of helicopter sizing program. One of the two subjects addressed by Bell Helicopter Textron within the scope of the ongoing contract with NASA Ames will identify the preliminary design process used at Bell and formulate design optimization problems. Preliminary program modules will be written to examine the feasibility of adopted approaches. This study will be completed by December 1984. There is an in-house development effort being carried out at NASA Ames to build a preliminary design optimization system as part of integrated design and analysis system.

- o Design optimization should be applied in conceptual and preliminary design where many design decisions are not frozen yet.
- o Design optimization is necessary to compare the "best apples" with the "best oranges".
- o Stepniewski's work in 1970 was not well recognized by the U.S. industry, but stimulated European engineers.
- o Contract: Bell-NASA Ames (Sep.83-Dec.84) will address preliminary design optimization as one of two subjects.

STRUCTURAL DESIGN OPTIMIZATION

Reflecting current interests and needs for controlling vibration of helicopters, all the papers reviewed here addressed structural modification to control steady state vibration levels excited by periodic forces or moments. Typically these studies aim at cockpit vibration reduction caused by main rotor vibratory excitation forces and moments. Done et al. applied the Vincent circle method (refs. 7, 11, and 12), presenting the feasibility of this method to design optimization. Hanson and Calapodas compared, in references 9 and 10, the Vincent circle method with the strain energy method proposed by Sciarra (ref. 6). Their conclusions were that the strain energy method was better for stiffness modification, although it did not provide any data for mass tuning and absorber design/positioning. Finite matrix perturbation techniques were also applied (refs. 13 and 14) to this class of problems with reasonable success. Applications of formal optimization methods were not found in literature. Disjoint feasible design space reported by Johnson (ref. 8) and recently by Mills-Currah and Schmit (ref. 32) for undamped structures has not yet been noticed by the helicopter industry. A finite element modelling exercise program sponsored by NASA Langley Research Center will address the airframe design problem, aiming at vibration prediction and control, and may generate a broad technical data-base and provide adequate guidance for the future development of practical tools. However, helicopter vibration problems are extremely complex aeroelastic phenomena that should involve main rotor dynamics, rotor/airframe coupling, and aerodynamic interference, and therefore must be considered as multi-disciplinary problems.

Structural weight reduction is probably more important for helicopters than for fixed wing aircraft; hence there must be a number of applications carried out in industry, but no formal documentation was found. The critical problem until now has been lack of appropriate software. The implementation of sensitivity analysis in MSC-NASTRAN and the development of CASADAS by Northrop under an AFWAL contract will provide desperately needed tools for structural weight reduction with static and dynamic constraints.

There is a strong trend toward the extensive use of modern composite materials for the primary and secondary load-carrying structures of helicopters. Automated design technology such as that represented by the PASCO program (ref. 33) will be useful but has not penetrated the helicopter industry yet, probably because of the lack of experience and confidence at this time in using such a tool in the practical design environment. Enormously challenging design optimization problems also exist in the design of solid three-dimensional composite structures; for example, rotor hub components and power train mechanical parts. These areas remain virtually untouched.

- o Airframe design optimization studies focused mostly on control of vibration excited by main rotor vibratory forces and moments.
Vincent circle method, strain energy method, matrix perturbation
- o General structural optimization codes are emerging.
MSC-NASTRAN sensitivity analysis capability
CASADAS
- o Composite structural design will need numerical design optimization.
- o A Langley program to develop national capability to analyze vibration as part of helicopter structural design may include structural optimization in 86-88.

AERODYNAMIC AND ACOUSTIC DESIGN OPTIMIZATION

Reduction of helicopter noise level is, just like vibration control, an extremely important and urgent problem that the helicopter industry is facing today. We have just started understanding the primary generation mechanisms of helicopter noise. The real challenges are to design low noise helicopters without degrading the aerodynamic performance of the aircraft, or even to aim at its simultaneous improvement. Analyses of aerodynamic responses and noise characteristics of the main rotor blades, especially in the important transonic regime, are still research subjects. Although some computer codes have become available recently, these codes require a great deal of numerical data processing effort. Therefore, simple coupling with numerical optimization codes will not be productive at this time, even on the fastest computers available. It is believed that the innovative use of approximation concepts will be instrumental in obtaining design tools that can be used in the practical environment.

In the past, attempts were made to transfer technology developed for fixed wing airfoil optimization to rotary wing design problems (refs. 15 and 16). The results are encouraging in general, but a great deal of advanced research (theoretical, computational and experimental) will be required for the development of a mature technology base and design tools.

Significant research efforts are expended at NASA Ames to integrate currently available best-analysis techniques with a numerical optimization code. Some preliminary results associated with this effort were presented at the AHS Forum by Tauber (ref. 17).

- o Computational fluid dynamics technology coupled with numerical optimization will become a practical design tool. Research will be needed to integrate analysis capabilities into numerical optimization to reduce the overall computation effort.
- o Optimization of airfoil of rotor blades has been studied using CFD and math programming methods. One of the advantages recognized over the traditional method is the capability to take multiple conditions simultaneously.
- o Numerical optimization will become useful to design low noise rotor blades.
 Providing theoretically optimum design based on the best analysis available
 Reduction of test time and cost

MAIN ROTOR DESIGN OPTIMIZATION

The application of numerical optimization to rotor blade design problems was presented by Bielawa (ref. 18) in 1971. He solved blade weight minimization problems under a constraint on the first aeroelastic mode damped frequency. The study was preliminary in nature and the optimization technique used might be classified as one of the optimality criteria approaches. However, his formulation of the rotor design problem was in the general standard form that could be used with any of today's general mathematical programming codes. Stepniewski's paper (ref. 2) was referenced in an extensive review by Huber (ref. 19). Despite excellent pioneering work by Bielawa, there were no significant publications in the next ten years in this area. But in 1982, Bennett (ref. 20) presented an epoch making paper at the AHS Forum in Anaheim. He gave several rotor design problems formulated in standard mathematical programming forms, and solved them by coupling analysis codes with a general purpose optimization code, OPT. This paper appears to have had a significant effect on the helicopter technical community regarding applicability of numerical optimization methods. At the same AHS Forum, Taylor (ref. 21) presented an interesting paper aimed at blade design modification for vibratory root force reduction, although his redesign algorithm was not an automated numerical search method.

In 1982-1983, two reports were written by McIntosh under two separate contracts with the U.S. Army (AVRADCOM). Reference 22 describes a bearingless rotor flexbeam shape designed to minimize various combinations of bending and centrifugal stresses for a given oscillatory excitation force distribution. Reference 23 presented an ambitious effort to couple a linear rotor airframe coupled vibration analysis code, QVR, with the general optimization code CONMIN to reduce a measure of the fuselage vibration by modifying the rotor system design parameters. Both of the studies reported by McIntosh were preliminary and warranted further investigation, although some of the results looked encouraging.

There are at least three government supported research activities in this area. This reflects the current interests and importance of rotor design problems. Two of them are reported in this session (refs. 26 and 27) and the other is described in references 24 and 25. Although it is not explicitly stated, ongoing rotor system study projects such as ITR or FRR programs will use design optimization methods at various levels of the design effort.

- o Interests in the U.S. revived in 1982, more than ten years after the first paper was published. Bennett's work on rotor structural design optimization was a significant step.
- o Current interest in design of low vibration rotor systems. There are a number of areas in which analysis capabilities must be developed or improved to obtain modules that are usable in the design process with sufficient confidence.
 - Unsteady air load prediction capability
 - Dynamic stall models
 - Adequacy of rotor design procedures
- o Three government supported research activities:
 - NASA Langley - Univ. of Washington/Univ. of Southern Illinois
 - U.S. Army ATL - Bell Helicopter Textron
 - NASA Ames - Univ. of California, Los Angeles

FLIGHT PATH OPTIMIZATION

This problem is obviously not a helicopter design problem. It addresses the determination of an optimal flight condition path to accomplish a specified mission with a given helicopter, payload and weather conditions. The objective can be minimum fuel, minimum cost, minimum time, obstacle clearance or statistical survivability. Traditionally, this type of problem was solved using optimal control theory, which seeks solutions in the form of time dependent control inputs (refs. 28 to 30). However, assuming that missions can be broken into a relatively small number of segments and that flight conditions are kept constant in each segment, this problem may be cast into a standard form to be solved by nonlinear programming methods.

Recent trends in microcomputer technology indicate rapid growth in the capabilities of on-board, portable or even hand-held computers. The U.S. Army has a project to use an HP-41 hand-held calculator for flight planning and on-board flight management to reduce operational cost, improve operational safety and reduce pilot workload. If sufficient computer capabilities are available, optimization of the parameters displayed to pilots will be possible. A futuristic version of this picture is to work with an autopilot system to reduce the pilot workload in the relatively trivial mission segments. A preliminary study of this problem, especially from the viewpoint of the application of numerical optimization methods, will be carried out by Bell Helicopter under a contract with NASA Ames. An ongoing in-house study to generate or store necessary aircraft performance data with minimum CPU power and memory requirement is planned to be integrated into the program that will be developed by Bell under the contract.

- o Optimization of flight trajectory plan has been exercised for fixed wing airplanes, but not a great deal has been done for helicopters.
- o Techniques used in the past were dynamic programming and optimal control theory, not static numerical optimization methods.
- o Computerization will be necessary to reduce the pilot workload, especially for military helicopters.
 - Army program to use HP-41 for flight management of UH-1H
- o Feasibility of applying numerical optimization methods will be studied by Bell Helicopter under the contract with NASA Ames.
 - Development of sensible analytical models and their sensitivity to results
 - Requirements for the on-board computers
 - Evaluation of practical pay-offs

CONTROL SYSTEM DESIGN OPTIMIZATION

Multi-variable function minimization methods have been used in the design of linear control systems for some time. For example, minimization of a quadratic merit function of state variables has been commonly used to obtain closed loop gain schedule for linearized models. If properly coupled with rotor dynamics, control system design optimization may take aircraft performance and handling quality constraints into account. In fact, in reference 3 aircraft handling quality constraints were considered in the scope of preliminary design. The addition of control system design variables should be straightforward, even though such tasks will not be simple.

Vibration reduction by applying higher harmonic blade pitch variation has been studied extensively using optimal estimation and control theory. However, Jacob and Lehmann (ref. 31) presented an interesting concept to transform the dynamic blade pitch control scheduling problem into non-time-dependent discrete variables. The idea was to expand the pitch angle distribution of the blade with the weighted sum of Tschebysheff polynomials (spanwise) and Fourier series (azimuthwise). Coefficients of the product terms in this summation were design variables to be modified by an optimization program to reduce the vibratory hub load amplitudes. The mathematical model used in this study was probably over-simplified, but it showed the feasibility of using this concept as an alternative approach to optimal control techniques. Note that coefficients may be computed at a certain number of discrete trim conditions and a numerical interpolation scheme can then be implemented. Compared to the approaches using optimal estimation and control techniques, this 'static' control scheduling cannot respond to unexpected loads such as gust induced airload disturbances.

- o Control system design optimization coupled with aircraft performance and handling quality analysis models will be useful.
- o Higher harmonic blade pitch variation scheduling for vibratory load reduction can be formulated in a 'static' numerical optimization problem. However, it will be necessary to obtain pitch variation scheduling for each flight condition. Also this static scheduling approach cannot respond to external disturbances.

IMPORTANCE OF APPROXIMATION CONCEPTS

Helicopter response analyses are difficult and many of them can be very expensive. For example, straightforward coupling of a numerical optimization code with a transonic aerodynamic analysis code for optimal design of blade tip geometry is not currently feasible for this reason. Rotor performance analysis, acoustic noise estimation or rotor system aeroelastic stability analysis could be quite expensive if repeated many times. Structural optimization technology developed in the early 1970s (ref. 34) provides valuable clues to overcoming the economic barrier mentioned above. The key idea is to make full use of approximations to reduce the amount of data processing. Except for the evaluation of the final design, accurate response analyses are not necessarily required; instead, we need only enough information to guide the design to a nearly optimal and practical design point. One of the most important concepts is to build explicit approximate expressions for all functions that are likely to affect the design modification process.

For structural design, the Taylor series expansions of displacements and stresses with respect to reciprocals of sizing variables have been found to be effective. Complete analysis is carried out only when it becomes necessary to update the Taylor series expansion coefficients. Vanderplaats, in reference 35, introduced a procedure to gradually build second order approximations of all the functions while the design is being improved. The advantage of this scheme is that all the analysis results in the past can contribute to improve the quality of the approximation models. In other words, the accuracy of the model keeps improving as the design approaches an optimum. An innovative application of this concept was presented in reference 36, in which the system responses were evaluated by tests, not computer runs. This idea should be helpful in planning tests in helicopter research and development.

An alternative idea is to distribute trial analysis points within the limited design subspace and evaluate all the functions at those discrete points. Then, approximate interpolation functions are constructed by means of regression analyses if a sufficient amount of data is available, or by means of certain estimation techniques if the amount of data points is not enough. In certain cases, additional data acquisition by complete analyses or tests may be performed. This scheme will be useful to obtain a global picture within the design space of interest, but should be used with caution due to the nature of approximate functions. If the number of design variables increases, applications of this approach will be increasingly difficult. Also, all the analysis effort on the designs that grossly violate constraints may be wasted without contributing to the design process.

There are various intermediate approaches to compromise between the two strategies mentioned above. In any case, the generation of appropriate explicit approximate functions is the critically important technique necessary to make use of the results of sophisticated advanced analysis tools in the design process.

- o Helicopter analyses are very complicated. Aerodynamics and acoustic analysis require especially large amount of computation. Introduction of approximation will be essential.
- o Approximation concepts developed for structural optimization will be applicable to helicopter problems. In addition, various variations of approximation techniques are not available. Innovative use of available techniques will be helpful.

SUMMARY

There are a number of helicopter design problems that are well suited to applications of numerical design optimization techniques. Adequate implementation of this technology will provide high pay-offs. There are a number of numerical optimization programs available, and there are many excellent response/performance analysis programs developed or being developed. But integration of these programs in a form that is usable in the design phase should be recognized as important. It is also necessary to attract the attention of engineers engaged in the development of analysis capabilities and to make them aware that analysis capabilities are much more powerful if integrated into design oriented codes. Frequently, the shortcomings of analysis capabilities are revealed by coupling them with an optimization code.

Most of the published work has addressed problems in preliminary system design, rotor system/blade design or airframe design. Very few published results were found in acoustics, aerodynamics and control system design. Currently major efforts are focused on vibration reduction, and aerodynamics/acoustics applications appear to be growing fast. The development of a computer program system to integrate the multiple disciplines required in helicopter design with numerical optimization technique is needed. The size of the helicopter industry is small compared to that of the fixed wing airplane industry; therefore it is necessary to look for help and to work together with other industries for the development of commonly usable engineering developments.

Activities in Britain, Germany and Poland are identified, but no published results from France, Italy, the USSR or Japan were found.

- o Helicopter design can make use of numerical optimization methods. High payoff will be expected if a system that integrates multi-disciplinary analysis capabilities with numerical optimization is to be created.
- o Development of advanced analysis programs that provide useful design oriented data should be recognized as an important mechanism for integration with numerical optimization.
- o Approximation concepts will be the critical item in this integration effort.
- o The U.S. helicopter industry became aware of the potential of this technology in the last 2-3 years. Activities in Britain, Germany and Poland are observed. The U.S. helicopter industry can take advantage of the developments made by other industries within the U.S.

REFERENCES

1. Optimal Design. Proc. of the AHS 39th Annual Forum, St. Louis, MO, May 1983.
2. Stepniewski, W. Z., and Kalmbach, C. F., Jr., Multi-Variable Search and Its Application to Aircraft Design Optimization. *Aeronautical Journal*, Royal Aeronautical Society, Vol. 74, No. 713, May 1970, pp. 419-432.
3. Szumanski, K., Optimization of the Rotor-Wing System from Helicopter Performance Point of View. CAS Paper No. 76-37, The Tenth Congress of the International Council of the Aeronautical Sciences, Ottawa, Canada, Oct. 1976.
4. Stepniewski, W. Z., Some Thoughts on Design Optimization of Transport Helicopters. *Vertica*, Vol. 6, 1982, pp. 1-17.
5. Ramos, O. R., and Taylor, P., "Helicopter Design Synthesis. 7th European Rotorcraft and Powered Lift Aircraft Forum, Garmish-Partenkirchen, West Germany, Sept. 1981.
6. Sciarra, J. J., Use of the Finite Element Damped Forced Response Strain Energy Distribution for Vibration Reduction. Boeing Vertol Company Report No. D21-10819-1 for U.S. Army Research Office, Durham, N.C., July 1974.
7. Done, G. T. S., and Hughes, A. D., Reducing Vibration by Structural Modification. *Vertica*, Vol. 1, 1976, pp. 31-38.
8. Johnson, E. J., Disjoint Design Spaces in the Optimization of Harmonically Excited Structures. *AIAA Journal*, Vol. 14, No. 2, Feb. 1976, pp. 259-261.
9. Hanson, H. W., and Calapodas, N. J., Evaluation of Practical Aspects of Vibration Reduction Using Structural Optimization Techniques. AHS 35th Annual Forum, Washington, D.C., May 1979.
10. Hanson, H. W., Investigation of Vibration Reduction Through Structural Optimization. USAVRADCOM-TR-80-D-13, 1980.
11. Done, G. T. S., and Rangacharyulu, M. A. V., Use of Optimization in Helicopter Vibration Control by Structural Modification. *Journal of Sound and Vibration*, Vol. 74, Feb. 1981.
12. Done, G. T. S., Use of Optimization in Helicopter Vibration Control by Structural Modification. AHS Northeast Region National Specialists' Meeting on Helicopter Vibration. Hartford, CT, Nov. 1981.
13. King, S. P., Assessment of the Dynamic Response of Structures When Modified by the Addition of Mass, Stiffness or Dynamic Absorbers. AHS Northeast Region National Specialists' Meeting on Helicopter Vibration, Hartford, CT, Nov. 1981.
14. Kitis, L., Pilkey, W. D., and Wang, B. P., Optimal Passive Frequency Response Control of Helicopters by Added Structures. AIAA paper no. N83-27976, backup document for a Synoptic in *Journal of Aircraft*, Sept. 1983.
15. Hicks, R. M., and McCroskey, W. J., An Experimental Evaluation of a Helicopter Rotor Section Designed by Numerical Optimization. NASA TM-78622, Mar. 1980.

16. Tauber, M. E., and Hicks, R. M., Computerized Three-Dimensional Aerodynamic Design of a Lifting Rotor Blade. AHS 36th Annual Forum, Washington, D.C., May 1980.
17. Tauber, M. E., Computerized Aerodynamic Design of a Transonically 'Quiet' Blade. AHS 40th Annual Forum, Crystal City, VA, May 1984.
18. Bielawa, R. L., Techniques for Stability Analysis and Design Optimization with Dynamic Constraints on Nonconservative Linear Systems. 17th AIAA/ASME Structures, Structural Dynamics and Materials Conference, Anaheim, CA, May 1971.
19. Huber, H., Parametric Trends and Optimization: Preliminary Selection of Configuration: Prototype Design and Manufacturing. AGARD Helicopter Aerodynamics and Dynamics, AGARD-LS-63, March 1973.
20. Bennett, R. L., Applications of Optimization Methods to Rotor Design Problems. AHS 38th Annual Forum, Anaheim, CA, May 1982. Also in Vertica, Vol. 7, No. 3, 1983.
21. Taylor, R. B., Helicopter Vibration Reduction by Rotor Blade Modal Shaping. AHS 38th Annual Forum, Anaheim, CA, May 1982.
22. McIntosh, S. C., A Feasibility Study of Bearingless Rotor Flexbeam Optimization. Nielsen Engineering and Research Report TR-243, Aug. 1982.
23. McIntosh, S. C., A Study of Optimization as a Means to Reduce Rotorcraft Vibrations. Nielsen Engineering and Research Report TR-293, Feb. 1983.
24. Ko, T., Design of Helicopter Rotor Blades for Optimum Dynamic Characteristics. D.Sc. Thesis, Washington Univ., St. Louis, MO, 1984.
25. Peters, D. A., Ko, T., Korn, A. E., and Rossow, M. P., Design of Helicopter Rotor Blades for Desired Placement of Natural Frequencies. Proceedings of the 39th Annual Forum of the American Helicopter Society, 1983, pp. 674-689.
26. Friedmann, P. P., Application of Modern Structural Optimization to Vibration Reduction in Rotorcraft. Recent Experiences in Multidisciplinary Analysis and Optimization, NASA CP-2327, Part 2, 1984, pp. 553-566.
27. Sutton, L. R., and Bennett, R. L., Aeroelastic/Aerodynamic Optimization of High Speed Helicopter/Compound Rotor. Recent Experiences in Multidisciplinary Analysis and Optimization, NASA CP-2327, Part 2, 1984, pp. 643-662.
28. Schmitz, F. H., A Simple, Near-Optimal Takeoff Control Policy for a Heavily Loaded Helicopter From a Restricted Area. AIAA Mechanics and Control of Flight Conference, Anaheim, CA, Aug. 1974.
29. Johnson, W., Helicopter Optimal Descent and Landing After Power Loss. NASA TM X-73244, May 1977.
30. Slater, G. L., and Erzberger, H., Optimal Short-Range Trajectories for Helicopters. NASA TM-84303, Dec. 1982.
31. Jacob, H. G., and Lehmann, G., Optimization of Blade Pitch Angle for Higher Harmonic Rotor Control. Vertica, Vol. 7, No. 3, 1983, pp. 271-286.

32. Mills-Curran, J., and Schmit, L. A., Structural Optimization with Dynamic Behavior Constraints. AIAA/ASME/ASCE/AHS 24th SDM Conference, Lake Tahoe, NV, May 1983.
33. Anderson, M. S., and Stroud, W. J., General Panel Sizing Computer Code and Its Application to Composite Structural Panels. AIAA Journal, Vol. 17, Aug. 1979, pp. 892-897.
34. Schmit, L. A., and Miura, H., Approximation Concepts for Efficient Structural Synthesis. NASA CR-2552, Mar. 1976.
35. Vanderplaats, G. N., Approximate Concepts for Numerical Airfoil Optimization. NASA TP-1370, Mar. 1979.
36. Garberoglio, J. E., Song, J. O., and Boudreaux, W. L., Optimization of Compressor Vane and Bleed Setting. ASME paper no. 82-GT-81, Proc. 27th International Gas Turbine Conference and Exhibit, London, April 1982.

N87-11752

**APPLICATION OF MODERN STRUCTURAL OPTIMIZATION
TO VIBRATION REDUCTION IN ROTORCRAFT**

P.P. Friedmann
University of California
Los Angeles, California

PRECEDING PAGE BLANK NOT FILMED

SCHEMATIC REPRESENTATION OF FOUR BLADED HELICOPTER ROTOR USED IN VIBRATION REDUCTION STUDY

The helicopter rotor model used in the study consists of a four bladed hingeless rotor attached to a fuselage as shown below. The helicopter is assumed to be in trimmed forward flight. Each blade is assumed to have flap, lag, and torsional degrees of freedom. The fuselage degrees of freedom are not included in the analysis. Thus the aeroelastic stability and response analysis upon which this study is based is an isolated blade analysis. The helicopter rotor vibration reduction problem expressed as a general class of structural synthesis problems can be stated in the following form:

$$\left. \begin{aligned} g_q(\bar{D}) &\geq 0 \quad ; \quad q = 1, \dots, Q \\ D_i^{(L)} &\leq D_i \leq D_i^{(U)} \quad ; \quad i = 1, \dots, n_{dv} \\ \text{and } J(\bar{D}) &\rightarrow \min \end{aligned} \right\} (1)$$

where $g_q(\bar{D})$ is the q^{th} constraint function in terms of the vector of design variables \bar{D} , D_i is the i^{th} design variable, superscripts L and U denote lower and upper bounds, respectively, and $J(\bar{D})$ is the objective function in terms of the design variables. For additional details see Refs. 1 and 2. Preassigned parameters are the blade pre-cone, the blade chord $2b$ and the blade cross sectional aerodynamic center offset from the elastic axis, x_A .

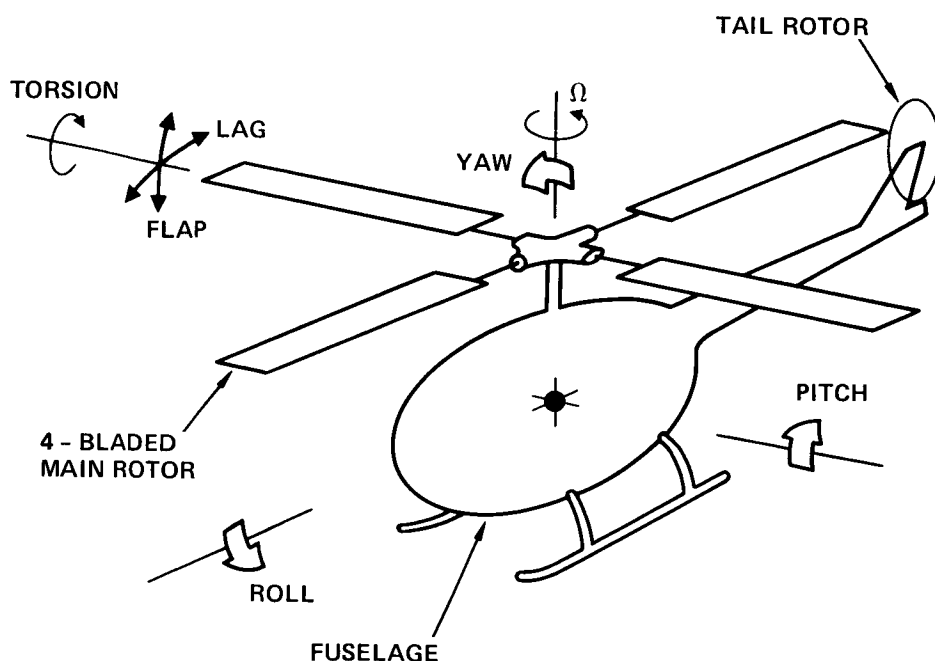


Figure 1

TYPICAL BLADE CROSS SECTION AND DESIGN VARIABLES

A typical cross section of the rotor blade is shown in the figure below. The free vibration mode shapes and frequencies are obtained from a finite element analysis using seven spanwise stations. The design variables are the breadth b , the height h_s and the thicknesses t_b and t_h of the thin rectangular box section^s, representing the structural member at each spanwise station. Elastic properties of the blade and bending torsion as well as the structural mass properties are expressed in terms of these design variables. The nonstructural mass of the blade is assumed to consist of two parts. The first portion is the nonstructural skin and honeycomb core surrounding the structural cell which provides the appropriate aerodynamic shape. The second contribution to the nonstructural mass is represented by m_{ns} in the figure below, which is a counter weight used as a tuning device for controlling blade frequency placement and mode shape pattern. The nonstructural masses m_{ns} at three outboards stations of the blade are also used as design variables, while the offsets x_m from the elastic axis are given parameters. The presence of the nonstructural mass introduces an offset between the cross sectional center of mass and the elastic axis. The average value of this offset is given by

$$X_{IAV} = \frac{x_m \int_{l_{os}}^l m_{ns} dx}{\int_0^l m dx + \int_{l_{os}}^l m_{ns} dx}$$

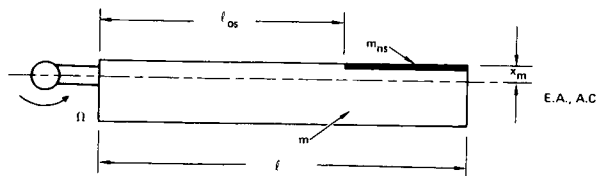
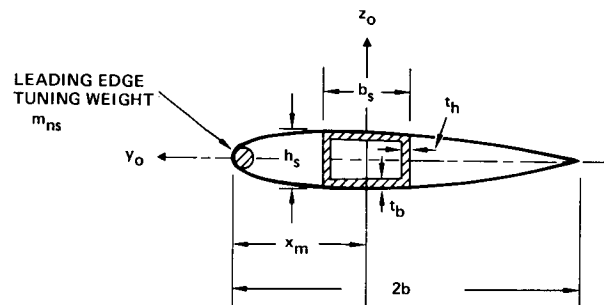


Figure 2

BEHAVIOR CONSTRAINTS AND OBJECTIVE FUNCTION

The two types of behavior constraints in this optimization study are frequency constraints and constraints on the aeroelastic stability margins in hover. The frequency constraints consist of the mathematical requirement that the fundamental rotating frequencies of the blade in flap, lag and torsion should be within certain specified upper and lower bounds. The higher frequencies are constrained so as to avoid four-per-revolution resonances. The aeroelastic constraints are the aeroelastic stability margins in hover which are assumed to be an adequate measure of stability for soft-in-plane hingeless blades. The objective function to be minimized is a mathematical expression representing the maximum peak-to-peak value of the oscillatory vertical hub shears or the oscillatory hub rolling moments due to flap-wise bending. Thus the objective functions are: $J(\bar{D}) = P_{z1\max}$ for hub shears and $J(\bar{D}) = m_{x1\max}$ for hub rolling moments. The blade root shears in the rotating system are obtained by integrating the distributed blade loads over the blade. The blade root moments are obtained by calculating the integrated bending moments due to the distributed loads, which consist of aerodynamic, inertia and damping loads. The total forces and moments acting at the rotor hub are obtained by resolving the rotating forces and moments in the nonrotating frame, as shown in the figure below, and summing over all four blades. In this process only the fourth harmonic remains the first order dominant contribution.

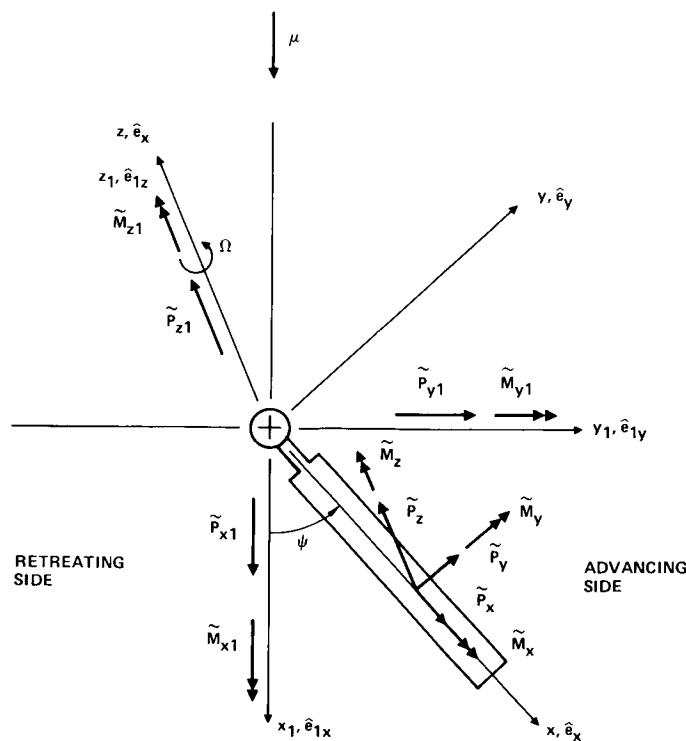


Figure 3

BASIC ORGANIZATION AND SOLUTION OF THE OPTIMIZATION PROBLEM

This study uses the SUMT optimizer based on the extended interior penalty function and a modified Newton's method implemented in a computer program called NEWSUMT. The optimization design process organization for the present study, using approximation concepts, is illustrated in the figure below. This process consists of the following steps.

- (1) An initial trial design \vec{D}_0 is chosen by selecting the values of b_s , h_s , t_h , t_b and m_{ns} at the various spanwise stations.
- (2) The uncoupled rotating modes and frequencies of the blade are obtained using a finite element model. Explicit first order and second order Taylor series approximations to the frequency constraints are calculated in closed form.
- (3) The aeroelastic stability in hover, the response in forward flight, and the vertical hub shears and moment (which constitute the objective function to be minimized) are calculated using the analysis given in Refs 3 and 4. The gradient information for the explicit approximation of the objective function is also calculated by finite differences.
- (4) The mathematical programming problem represented by Eq (1) is replaced by an approximate problem where the constraints $g_q(\vec{D})$ and the objective function $J(\vec{D})$ are expressed by explicit Taylor series approximations. The approximate problem is solved by the NEWSUMT optimizer to obtain an improved design.
- (5) The entire optimization process is repeated with the improved design as a starting point until the sequence of vectors \vec{D} converges to a solution \vec{D}^* where all inequality constraints are satisfied and $J(\vec{D}^*)$ is at least a local minimum.

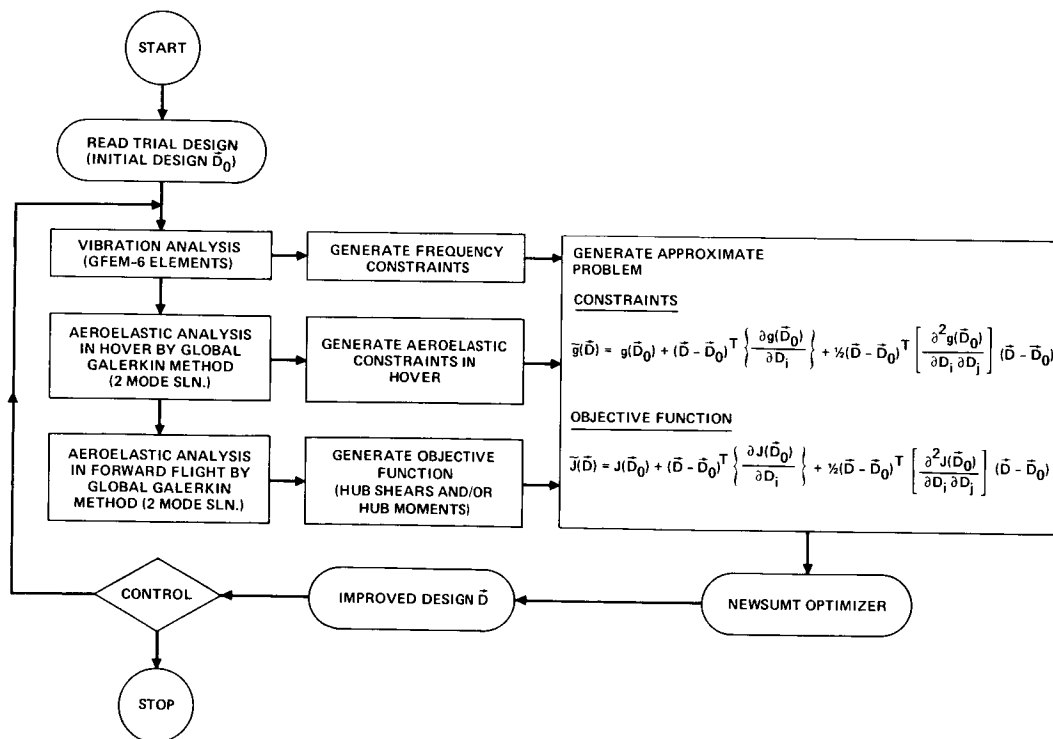


Figure 4

RESULTS FOR SOFT-IN-PLANE CONFIGURATION NO. 1

Configuration No. 1 is an initial design consisting of a uniform hingeless blade with properties resembling those of the MBB 105 rotor blade, which is one of the best hingeless rotors in production. Thus an improvement on this design is indicative of the benefits due to using modern structural optimization for vibration reduction in forward flight. The detailed properties of this blade can be found in Refs. 1 and 2. The properties given here are useful for a better physical understanding of the blade configuration:

$$\bar{\omega}_{F1} = 1.094; \quad \bar{\omega}_{L1} = 0.710; \quad \bar{\omega}_{T1} = 4.896; \quad \gamma = 5.5; \quad \sigma = 0.07; \quad a = 2\pi$$

$$n_b = 4; \quad \bar{b} = 0.0275; \quad \Omega = 425 \text{ RPM}; \quad m_{ns} = 0; \quad C_W = 0.005$$

The objective function used is the value of the four-per-revolution hub shears at $\mu=0.30$ in trimmed level flight. Two stages of optimization were performed for this configuration. The cross sectional dimensions corresponding to the improved designs D_1 and D_2 obtained after the first and second stage of the optimization are graphically illustrated in the figure below. The design variables used were the breadths b_s and the thicknesses t_h at seven spanwise stations of the blade. To reduce somewhat the number of design variables, the ratios $h_s/b_s = A_R$ and $t_b/t_h = A_{Rt}$ were treated as preassigned parameters. This approach is commonly denoted as design variable linking (Refs. 5 and 6) in structural optimization. The first stage of optimization results in a 15.9% reduction in the peak-to-peak vertical hub shears and the second stage of optimization yields an additional reduction of 1.03%. The maximum value of the hub shears remains almost unchanged.

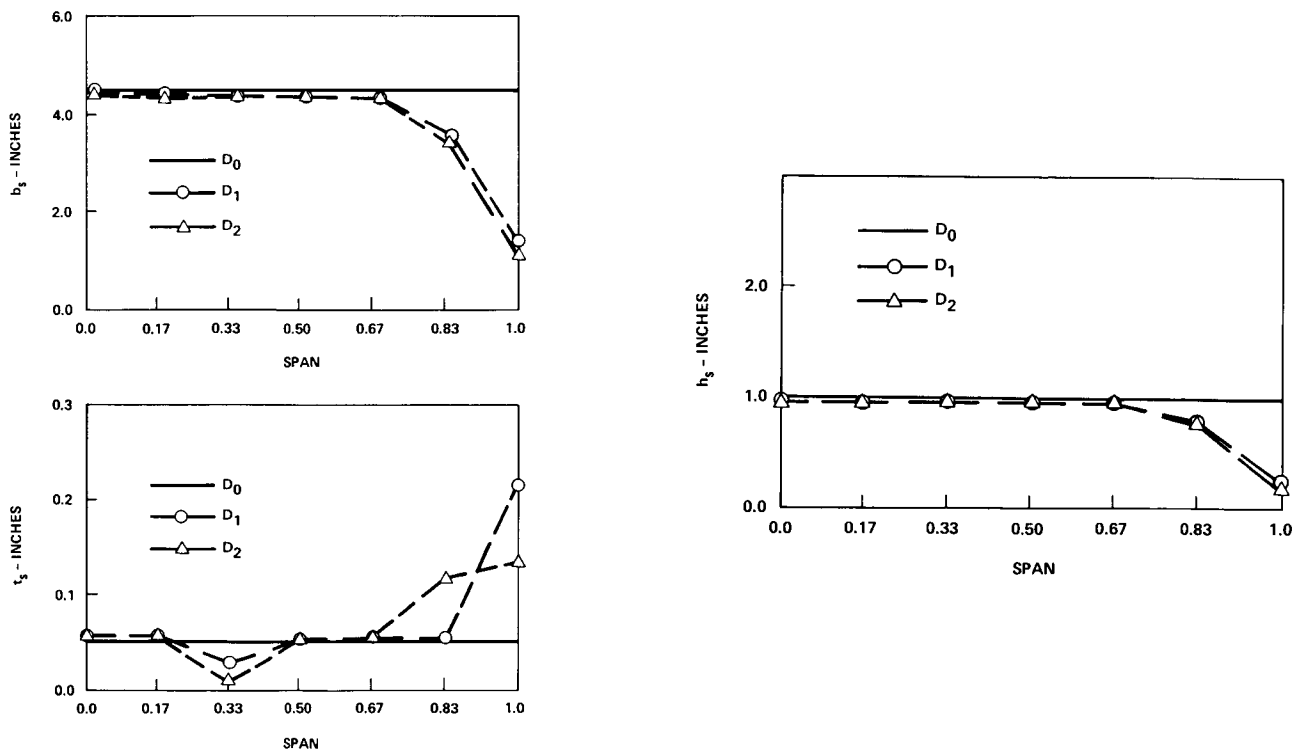


Figure 5

RESULTS FOR SOFT-IN-PLANE CONFIGURATION NO. 2

The results obtained for the previous configuration indicate that most changes in cross sectional dimensions, dictated by the optimization procedure, occur in the blade tip region. Since such changes can be easily introduced by considering non-structural tuning masses, the effects of these masses were examined by using a slightly different initial design, denoted configuration No. 2. This initial design is characterized by the following fundamental frequencies: $\bar{\omega}_{F1} = 1.125$; $\bar{\omega}_{L1} = 0.732$ and $\bar{\omega}_{T1} = 3.176$. The nonstructural tuning mass is distributed only at the three outboard segments of the blade, thus in this case there are a total of 17 design variables. Results for three different cases after one stage of optimization are presented in the first table below. Improved design D_1 is for configuration 2 without the nonstructural mass. The second case, where the nonstructural masses are located at the leading edge, is denoted by D_2 . The third case where the nonstructural masses are located on the elastic axis, which coincides with the line of aerodynamic centers, is denoted by D_3 . The results obtained indicate that the best choice for the location of the nonstructural mass is along the elastic axis, because it produces substantial reductions in oscillatory vertical hub shears without increasing hub rolling moments and without reducing the aeroelastic stability margins. The second table given below shows the rotating frequencies in flap, lag and torsion for designs D_1 , D_2 and D_3 compared to the initial design D_0 .

| VALUES | | 14 D.V. $m_{ns} = 0$ $\frac{(D_0 - D_1)\%}{D_0}$ | 17 D.V. $m_{ns, L.E.}$ $\frac{(D_0 - D_2)\%}{D_0}$ | 17 D.V. $m_{ns, E.A.}$ $\frac{(D_0 - D_3)\%}{D_0}$ |
|------------------------------------|-----|--|--|--|
| $\frac{P_{z1} \ell}{\Omega^2 I_b}$ | PTP | 40.69% | 20.17% | 29.04% |
| | M | 24.32% | 22.73% | 16.09% |
| $\frac{M_{x1} \ell}{\Omega^2 I_b}$ | PTP | 18.33% | -5.83% | 13.33% |
| | M | 39.07% | 14.89% | 54.84% |

| FREQ. | D_0 | 14 D.V. D_1 $m_{ns} = 0$ | 17 D.V. D_2 $m_{ns, L.E.}$ | 17 D.V. D_3 $m_{ns, EA}$ | UPPER BOUND $\bar{\omega} (U)$ | LOWER BOUND $\bar{\omega} (L)$ |
|---------------------|-------|----------------------------------|------------------------------------|----------------------------------|--------------------------------------|--------------------------------------|
| $\bar{\omega}_{F1}$ | 1.125 | 1.171 | 1.129 | 1.145 | 1.15 | 1.05 |
| $\bar{\omega}_{F2}$ | 3.408 | 3.336 | 3.387 | 3.338 | — | — |
| $\bar{\omega}_{L1}$ | 0.732 | 0.886 | 0.748 | 0.801 | 0.90 | 0.55 |
| $\bar{\omega}_{L2}$ | 4.483 | 4.588 | 4.518 | 4.523 | — | — |
| $\bar{\omega}_{T1}$ | 3.176 | 3.642 | 3.101 | 3.499 | 6.0 | 2.5 |
| $\bar{\omega}_{T2}$ | 9.099 | 9.087 | 8.247 | 9.167 | — | — |

Figure 6

RESULTS FROM A SECOND STAGE OF OPTIMIZATION FOR DESIGN D_3

As indicated on the previous page, nonstructural masses distributed along the elastic axis of the outboard one third segment of the blade appeared to be most effective for the configuration being considered. Thus a second stage of optimization was carried out with improved design D_3 as the initial design. These results are presented below, and to clarify the discussion improved design D_3 at the end of the first optimization stage is denoted improved design D_I while the final design obtained after the second stage of optimization is denoted as improved design D_{II} . The cross sectional dimensions of the improved designs D_I and D_{II} are compared with those of the initial design D_0 , which was assumed to be a uniform blade. The spanwise variations of b_s and h_s of the improved design D_{II} are similar to those of improved design D_I . However, the spanwise variations of the thicknesses t_b and t_h of the design D_{II} are quite different from those of design D_I . Design D_{II} exhibits reduced cross sectional thickness in the outboard 2/3 span, accompanied by nonstructural mass addition, m_{ns} , equal to 2.3% of blade mass distributed along the elastic axis of the outboard 1/3 portion of the blade.

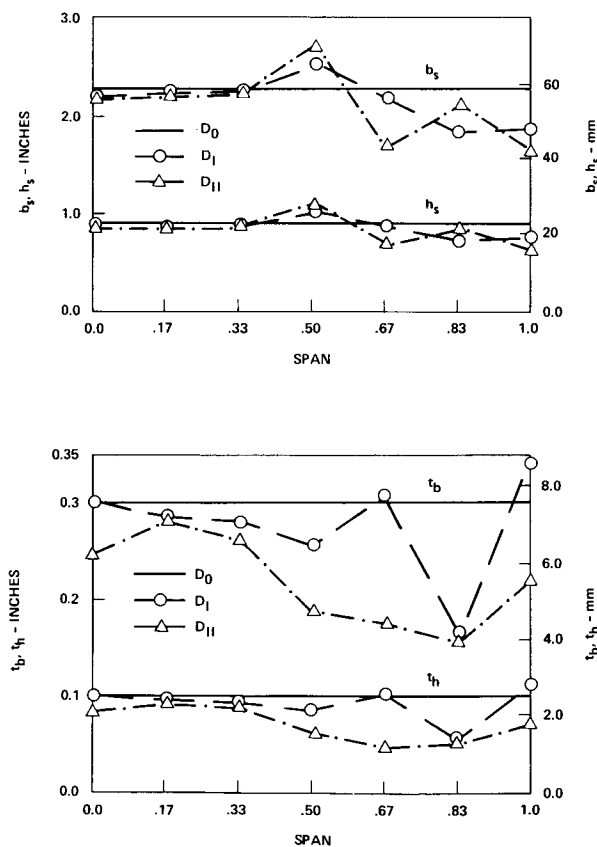


Figure 7

ADDITIONAL RESULTS FROM A SECOND STAGE OF OPTIMIZATION FOR DESIGN D₃

The objective function used in the optimization was the value of the linear peak-to-peak vertical hub shears at $\mu = 0.30$. In the tables presented below the reductions in vertical hub shears and rolling moments at $\mu = 0.30$ after two stages of optimization are presented. The terms linear and nonlinear in the tables refer to the inclusion of geometrically nonlinear effects due to moderate blade deflections in the aeroelastic response calculation from which the hub shears and rolling moment are obtained. In the nonlinear case the geometrical nonlinearities are included while in the linear case they are not. For design D_{II}, the linear peak-to-peak vertical hub shear was reduced by 37.9% and the nonlinear hub shear was reduced by 35.9%. The corresponding reductions in the hub rolling moments were 24.17% and 25.2%, respectively. An interesting byproduct of the optimization is a reduction of total blade mass which is shown at the bottom of the last table. In design D_I only 0.2% of the blade mass is added as nonstructural mass, whereas for design D_{II} 2.3% of the blade mass is added as nonstructural mass in the same locations. Design D_I produced a 8.7% reduction in total blade mass while design D_{II} resulted in a 19.7% reduction in total blade mass. An examination of the two designs reveals that the reduction in blade mass at the outboard segments of the blade is considerably higher than the reduction experienced by the inboard segments. This indicates that one should be careful about violating constraints associated with energy storage in the rotor, which can be important for autorotation.

| | | VALUES | INITIAL DESIGN D _O | IMPROVED DESIGN D _{II} | REDUCTION (D _O -D _{II})/ D _O % |
|--|----------------|----------------------|----------------------------------|------------------------------------|--|
| VERTICAL HUB SHEARS NONDIMENSIONALIZED W.R.T. (Ω ² I _b /ℓ) | LINEAR | PEAK- TO- PEAK | 0.0575 | 0.0357 | 37.91% |
| | | MAXIMUM | 0.2323 | 0.1787 | 23.07% |
| | NON- LINEAR | PEAK- TO- PEAK | 0.0602 | 0.0386 | 35.88% |
| | | MAXIMUM | 0.2363 | 0.1819 | 23.02% |

| | | | | | |
|--|----------------|----------------------|--------|--------------------|--------|
| HUB ROLLING MOMENTS NONDIMENSIONALIZED W.R.T. (Ω ² I _b) | LINEAR | PEAK- TO- PEAK | 0.0120 | 0.0091 | 24.17% |
| | | MAXIMUM | 0.1940 | 0.1331 | 31.39% |
| | NON- LINEAR | PEAK- TO- PEAK | 0.0119 | 0.0089 | 25.21% |
| | | MAXIMUM | 0.0946 | 0.1338 | 31.24% |
| BLADE MASS REDUCTION | | 1st STAGE 8.7% | | 2nd STAGE 19.7% | |

Figure 8

VERTICAL HUB SHEARS AND ROLLING MOMENTS FOR DESIGN D_{II} AS A FUNCTION OF μ

As mentioned before, the objective function used in the optimization procedure is the linear expression of the hub shears at $\mu = 0.30$. Therefore it is important to examine the variation of the vertical hub shears and hub rolling moments over the whole range of advance ratios $0 < \mu < 0.30$ considered. The figures below depict both the variations of the peak-to-peak and the maximum values of the four-per-rev vertical hub shears and hub rolling moments for the range of advance ratios $0 < \mu < 0.30$. Furthermore, for the sake of completeness both the linear and the non-linear versions of these quantities are plotted. These results demonstrate that for the soft-in-plane configurations studied in this paper the choice of linear vertical hub shears at one particular moderately high advance ratio ($\mu = 0.30$) as the objective function is sufficient to guarantee a similar amount of reduction in the oscillatory vertical hub shears at the intermediate advance ratios. This statement is also supported by the behavior of the hub rolling moments, also shown below, which shows that improved design D_{II} exhibits a consistent reduction in hub rolling moments compared to design D_0 over the whole range of advance ratios considered. Additional results (Ref. 2) not presented here indicate similar reductions in root torsional moments. However in-plane hub shears experience only a relatively minor reduction.

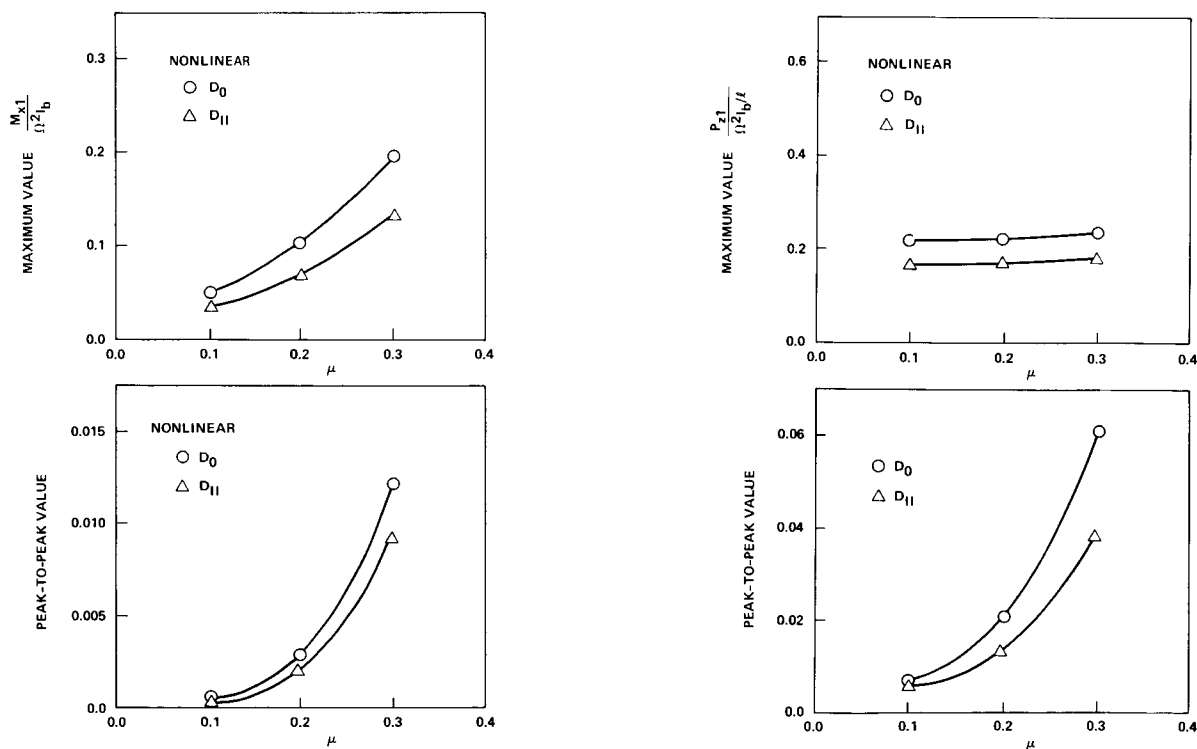


Figure 9

CONCLUSIONS AND ONGOING EXTENSION OF THIS RESEARCH

The results described in the previous pages have indicated that by applying modern structural optimization to the design of soft-in-plane hingeless rotors, vibratory hub shears in forward flight can be reduced by 15-40%. This reduction is achieved by relatively small modifications of the original design, which yield optimal frequency placement in flap, lag and torsion. It is also interesting to note that as a byproduct of optimization, the optimized blade configuration is between 9-20% lighter than the initial uniform blade. This result is obtained without using blade weight as the objective function in the optimization process. It is remarkable that these results are consistent with the needs expressed by Blackwell (Ref. 7) in a recent paper which advocates the need for designing blades in such a manner as to reduce vibrations in helicopters. In his excellent paper Blackwell provides practical physical insight by considering the sensitivity of blade vibrations to useful blade design parameters such as tip sweep, camber, blade mass and stiffness distribution, chordwise blade center of gravity offset from the aerodynamic center, chordwise center of gravity offset from the elastic axis, blade twist, and use of composite materials for tailoring of the vibrational characteristics. Our current research is aimed at incorporating some of these effects in a structural optimization process based on the blade model shown below. The important effects incorporated are the swept tip and improved unsteady aerodynamic modeling of the excitation. These two ingredients were selected because the swept tip is a powerful means for both modifying the vibratory response as well as optimizing the aerodynamic and acoustic performance of the rotor. Similarly, vibratory loads are strongly dependent on improved capability for modeling the unsteady aerodynamic environment.

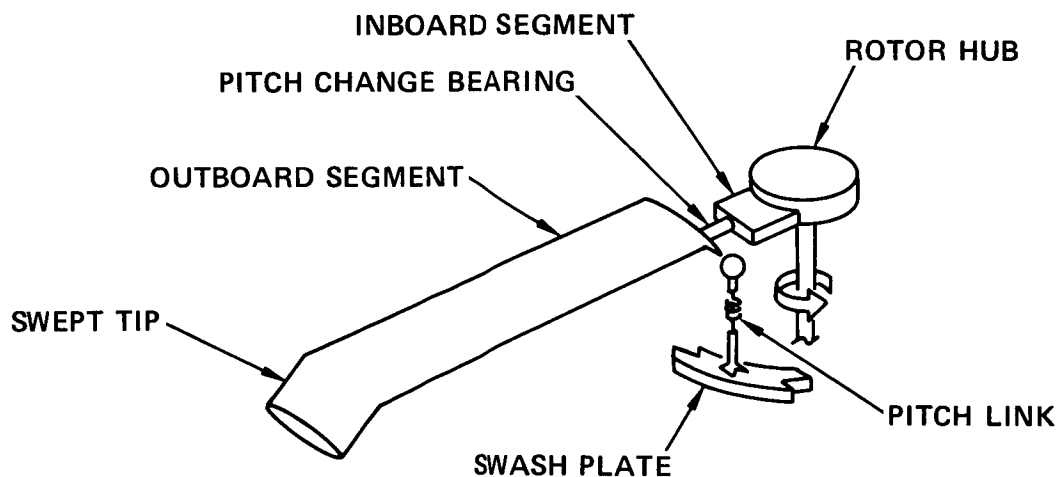


Figure 10

OTHER ASPECTS, LOCAL FUSELAGE VIBRATION REDUCTION BY STRUCTURAL MODIFICATION

The optimum blade design problem discussed previously attempts to reduce helicopter vibrations by reducing the source of the vibratory excitation, namely the vibratory loads applied at the hub, as indicated in the figure below. During the design cycle of the helicopter the need for local vibration reduction at specific locations in the fuselage or tail boom frequently arises. Various methods for local vibration reduction have been developed, such as vibration isolation devices vibration absorbers and the use of local structural modification, which has been introduced by Done in Ref. 8. When using the method of local structural modification the fuselage is represented by a number of easily identifiable substructures as shown below. A known excitation at the hub is assumed, and the sensitivity of the response at the pilot seat location (for example) is examined as a result of introducing a local structural modification consisting of either a change in mass at a point or a change in stiffness between two points (as represented by a spring), where these two quantities are assumed to be continuously varied. Using the frequency response matrix of a damped linear system, the sensitivity of the response at the pilot seat location to modifications in each substructure is tabulated and the best candidate for modification is selected by a visual inspection of the results. Since Done's work a number of researchers have applied various variants of this approach to vibration reduction in the helicopter fuselage (Refs. 9-12). However it should be noted that the method has not been coupled with an optimization approach based on the mathematical programming approach. It appears that this problem is quite suitable for treatment by multilevel decomposition along the lines indicated in Ref. 13, and in addition to constraints on vibration levels, other constraints can also be enforced on the substructure level.

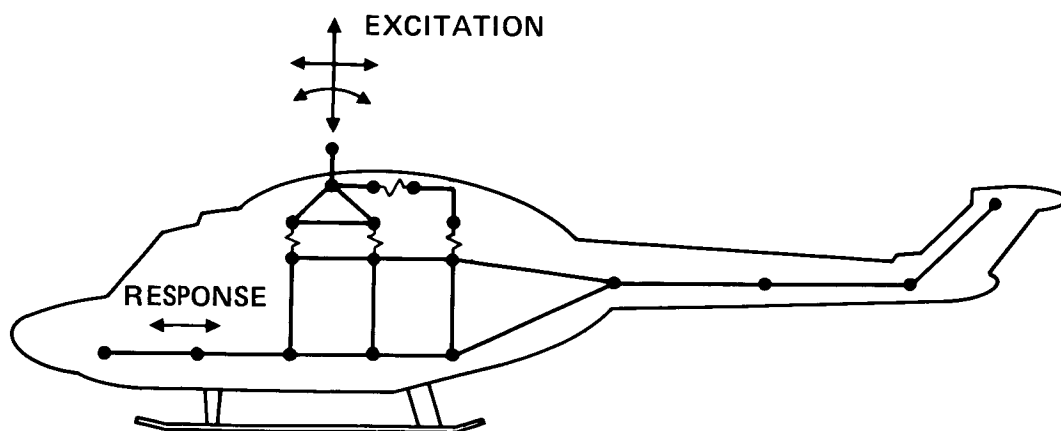


Figure 11

SYMBOLS

| | |
|---|--|
| A_R | = h_s/b_s |
| A_{Rt} | = t_b/t_h |
| \bar{b} | = semi-chord nondimensionalized with respect to R |
| C_W | = weight coefficient = $W/\pi\Omega^2 R^4$ |
| I_b | = blade flapping inertia |
| ℓ | = length of elastic part of blade |
| ℓ_{os} | = length defining outboard station where outboard blade segment starts |
| m_{ns} | = nonstructural mass per unit length of the blade used as a tuning weight |
| M_{x1} | = hub rolling moment |
| n_b | = number of blades |
| P_{z1} | = vertical hub shears |
| $\tilde{P}_x, \tilde{P}_y, \tilde{P}_z$ | = distributed loading vectors per unit length of blade |
| R | = radius of the blade |
| W | = weight of the helicopter |
| γ | = Lock number |
| σ | = blade solidity ratio |
| μ | = advance ratio |
| Ω | = speed of rotation (RPM) |
| $\bar{\omega}_{F1}, \bar{\omega}_{L1}, \bar{\omega}_{T1}$ | = rotating uncoupled fundamental frequency of the blade in flap, lag and torsion, respectively, nondimensionalized w.r.t. Ω |
| $\bar{\omega}_{Fi}, \bar{\omega}_{Li}, \bar{\omega}_{Ti}$ | = rotating uncoupled i^{th} fundamental frequency of the blade in flap, lag and torsion respectively, nondimensionalized w.r.t. Ω |

REFERENCES

1. Friedmann, P.P. and Shanthakumaran, P., "Aeroelastic Tailoring of Rotor Blades for Vibration Reduction in Forward Flight", AIAA Paper 83-0916-CP, Proceedings of AIAA/ASME/ASCE/AHS 24th Structures, Structural Dynamics and Materials Conference, Lake Tahoe, NV, May 2-4, 1983, pp. 344-359.
2. Friedmann, P.P. and Shathakumaran, P., "Optimum Design of Rotor Blades for Vibration Reduction in Forward Flight", Proceedings of the 39th Annual Forum of the American Helicopter Society, St. Louis, MO, May 9-11, 1983, pp. 656-673.
3. Shamie, J. and Friedmann, P., "Effects of Moderate Deflections on the Aeroelastic Stability of a Rotor Blade in Forward Flight", Paper No. 24, Proceedings of the Third European Rotorcraft and Powered Lift Aircraft Forum, Aix-en-Provence, France, 1977.
4. Friedmann, P.P. and Kottapalli, S.B.R., "Coupled Flap-Lag-Torsional Dynamics of Hingeless Rotor Blades in Forward Flight", Journal of the American Helicopter Society, Vol. 27, No. 4, pp. 28-36, October 1982.
5. Schmit, L.A. and Miura, H., "Approximation Concepts for Efficient Structural Synthesis", NASA CR-2552, March 1976.
6. Schmit, L.A., "Structural Optimization, Some Key Ideas and Insights", International Symposium on Optimum Structural Design, University of Arizona, Tucson, October 1981.
7. Blackwell, R.H., "Blade Design for Reduced Helicopter Vibration", Journal of the American Helicopter Society, Vol. 28, No. 3, July 1983, pp. 33-41.
8. Done, G.T.S., "Reducing Vibration by Structural Modification", Vertica, Vol. 1, No. 1, 1976, pp. 31-38.
9. Hanson, H.W. and Calapodas, N.J., "Evaluation of the Practical Aspects of Vibration Reduction Using Structural Optimization Techniques", Journal of the American Helicopter Society, Vol. 25, No. 3, July 1980, pp. 37-45.
10. Bartlett, F.D., "Flight Vibration Optimization Via Conformal Mapping", Journal of the American Helicopter Society, Vol. 28, No. 1, January 1983, pp. 49-55.
11. King, S.P., "The Modal Approach to Structural Modification", Journal of the American Helicopter Society, Vol. 28, No. 2, April 1983, pp. 30-36.
12. Wang, B.P., Kitis, L., Pilkey, W.D. and Palazollo, A.B., "Helicopter Vibration Reduction by Local Structural Modification", Journal of the American Helicopter Society, Vol. 27, No. 3, July 1982, pp. 43-47.
13. Sobieszczanki-Sobieski, J., James, B. and Dovit, A., "Structural Optimization by Multilevel Decomposition", AIAA Paper 83-0832, Proceedings of 24th AIAA/ASME/ASCE/AHS Structures, Structural Dynamics and Materials Conference, May 2-4, 1983, pp. 124-143.

ACKNOWLEDGEMENT

A part of this research was funded by NASA Langley Research Center under NSG 1578. This research is currently funded by NASA Ames Research Center under NAG 2-226.

HELICOPTER ROTOR BLADE AERODYNAMIC OPTIMIZATION
BY MATHEMATICAL PROGRAMING

Joanne L. Walsh
NASA Langley Research Center
Hampton, Virginia

Gene J. Bingham
NASA Langley Research Center
Structures Laboratory
U.S. Army Research Technology Laboratories (AVSCOM)
Hampton, Virginia

and

Michael F. Riley
Kentron International, Inc.
Hampton, Virginia

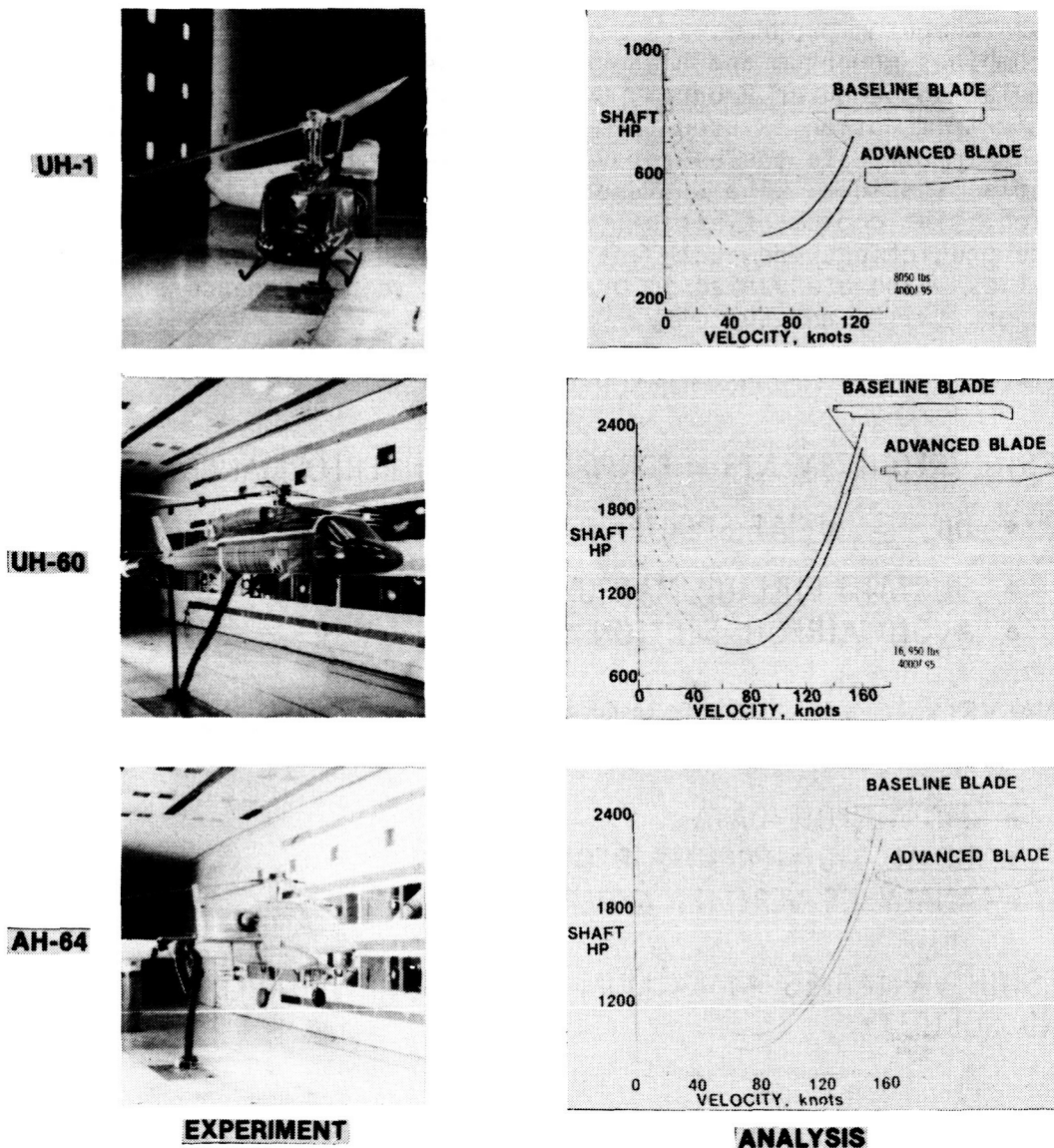
INTRODUCTION

One of the goals in helicopter design is to improve hover and forward flight performance. A way of achieving this goal is through the use of advanced (nonrectangular) rotor blades. Work in this area at the Army Structures Laboratory (AVSCOM) located at the Langley Research Center is reported in reference 1. The design goal is to reduce hover horsepower without degrading forward flight performance. Designs are generated by determining the influences of rotor blade design variables (twist, percent taper, taper ratio, and solidity) on rotor performance and by adjusting these design variables to obtain desired performance. In reference 1, an analytical procedure is described for evaluating the influences of the design variables on rotor performance. That procedure, referred to herein as the conventional approach, combines momentum and blade element theories (ref. 2) for the hover analysis and the Rotorcraft Flight Simulation Computer Program, C-81, (ref. 3) for the forward flight analysis. Advanced blades designed using the conventional approach have been evaluated in tests in the Langley 4 x 7 meter wind tunnel; for example, performance predictions have been verified for the UH-1 baseline and advanced rotor blades (ref. 4).

Although the conventional approach has produced blade designs exhibiting improved performance, it is a tedious and time-consuming procedure. A researcher typically spends several weeks manipulating the rotor blade design variables before reaching a final blade configuration. Using this approach, the researcher must have significant experience and data at hand. Any lack of experience and data tends to increase the design time.

To avoid the tedious and time-consuming aspects of the conventional approach, mathematical programming techniques are being applied. Mathematical programming has been used previously (refs. 5-8) to optimize helicopter rotor blades for various constraints, usually for improved aeroelastic behavior. The present work addresses the rotor aerodynamic design and consists of coupling the hover and forward flight analysis programs with a general-purpose mathematical programming procedure CONMIN (ref. 9). This mathematical programming design approach systematically searches for a blade design which minimizes hover horsepower while assuring satisfactory forward flight performance. This effort has been ongoing for about a year and has reached a stage where satisfactory designs are provided by the procedure. The purpose of this paper is to describe how the mathematical programming approach was used to design an advanced rotor blade for a representative army helicopter, and to compare the resulting design and effort with the design and effort for the conventional approach.

Researchers at the Langley Research Center are using experimental and analytical techniques to improve rotor blade performance in both hover and forward flight. In general, the blades on existing helicopters have a rectangular planform. Researchers have found that they can improve helicopter performance, i.e., lower the required horsepower, by tapering the rotor blades. Figure 1 shows horsepower required versus velocity plots for three different advanced (tapered) blades. In each case, the advanced blade requires less horsepower than the baseline (rectangular) blade. The performance predictions for both the baseline and advanced blades for the three helicopters (UH-1, UH-60, and AH-64) shown in the three plots were obtained using the analyses of references 2 and 3. Both the baseline and advanced blades have been evaluated experimentally at Langley, the UH-1, UH-60, and AH-64 for hover and the UH-1 and AH-64 for forward flight. In all cases, the analytical performance predictions agree well with the experimental results.



ROTOR BLADE AERODYNAMIC DESIGN

The key aspects of the aerodynamic rotor blade design problem are illustrated in figure 2. The design objective (goal) is to reduce the hover horsepower while not degrading forward-flight performance. This reduction in horsepower is to be achieved for a helicopter with a specified design gross weight operating at a specified altitude and temperature. In this study, forward-flight performance is defined in terms of three requirements (constraints). First, the horsepower required, hp_r , for forward flight at a specified maximum (or design) horizontal velocity, V_H , must be less than the available horsepower, hp_a . Second, the helicopter must be able to sustain a pullup maneuver, i.e., the aircraft must operate trimmed at a gross weight equal to a specified load factor multiplied by the design gross weight at a second specified horizontal velocity, V_{xf} , less than V_H . Third, the airfoil sections distributed along the rotor blade must operate at section drag coefficients (or pitching moment coefficients) less than a specified value (to avoid excessive helicopter vibration and control loads).

Two analysis computer programs are used to predict performance. The hover analysis combines momentum and blade element theories (ref. 2). The Rotorcraft Flight Simulation Computer Program, C-81, is used for forward flight. Only the quasi-static trim option is used from C-81. The analyses use experimentally derived 2-D airfoil data tables (provided by the designer) and segment the blade into 20 radial stations. The designer can assign one of five airfoil shapes at each station. The choice of airfoil remains fixed throughout the analyses. Performance predictions from both analyses have been verified experimentally. The quantities which are varied in order to improve performance are taper ratio, percent taper, twist, and solidity.

GOAL - REDUCE HOVER HORSEPOWER

DESIGN REQUIREMENTS - FORWARD FLIGHT PERFORMANCE

- $hp_r \leq hp_a$ AT SPECIFIED V_H AND GROSS WEIGHT
- SUSTAIN PULL-UP MANEUVER
- AVOID AIRFOIL SECTION STALL

ANALYSIS TOOLS - HOVER (MOMENTUM AND BLADE ELEMENT THEORIES) FORWARD FLIGHT (C-81)

- 2-D AIRFOIL DATA
- UP TO 5 DIFFERENT AIRFOIL SHAPES
- ANALYSES VERIFIED EXPERIMENTALLY

DESIGN VARIABLES - MAXIMUM TWIST, PERCENT TAPER, TAPER RATIO, AND SOLIDITY

Figure 2

ROTOR BLADE DESIGN VARIABLES

The design variables (percent taper, taper ratio, solidity, and twist) are illustrated in figure 3. The percent taper (also known as point of taper initiation), r/R , defines the relative radial location r at which taper begins. The blade is rectangular up to this point and then is tapered to the tip. A blade with zero percent taper is rectangular. The taper ratio is c_r/c_t , where c_r is the chord at the point of taper initiation and c_t is the tip chord. A blade with a taper ratio of 1.0 is rectangular. The blade solidity, σ , is the ratio of the sum of the blade areas to the rotor disk area, πR^2 , where R is the blade radius. In the present work, the design variable which defines solidity is the chord c_r . The dashed-line blade in figure 3 represents a blade with increased solidity over the solid-line blade. Twist, indicated in the lower portion of the figure, is varied linearly from the root to the tip. The twist design variable is the maximum twist indicated by τ_{\max} .

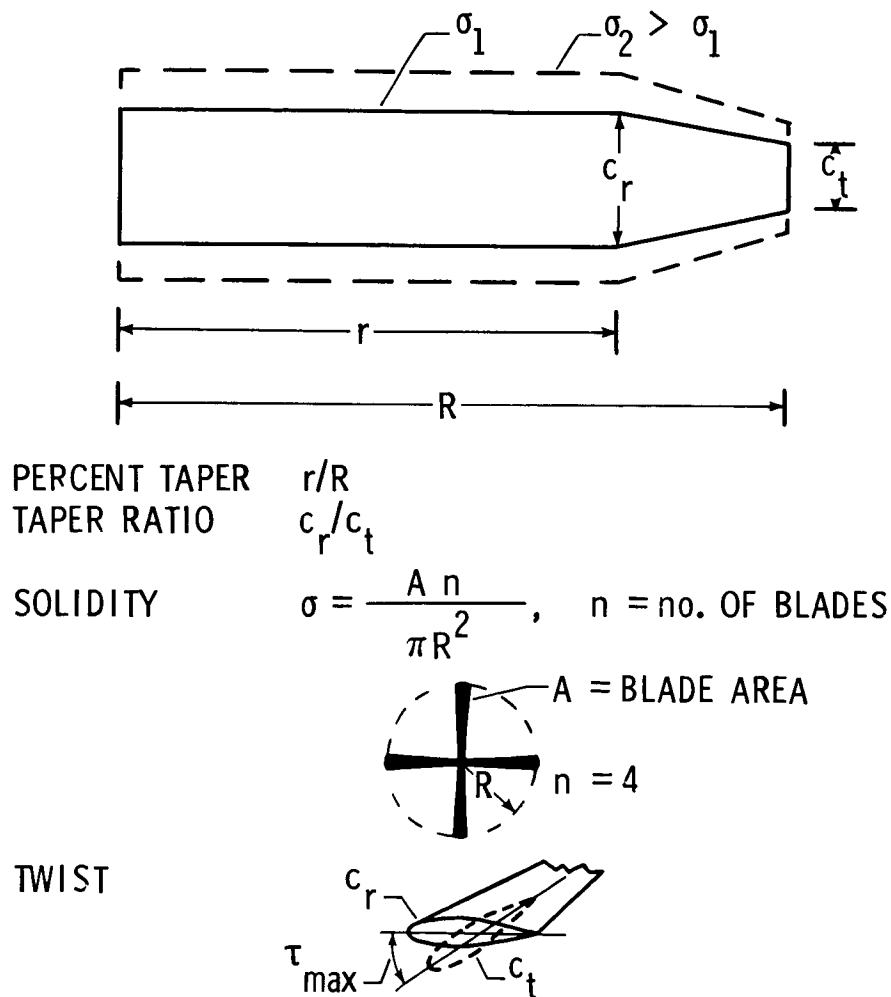


Figure 3

CONVENTIONAL APPROACH

The conventional rotor blade design approach is a two-step method as indicated in figure 4. Only a cursory description will be given here. A more detailed explanation can be found in reference 1. The rotor blade is designed first for hover using the analysis based on reference 2. The designer changes the values of taper ratio and percent taper to reduce hover horsepower. Then he changes the value of twist and repeats the above process. He continues to manipulate these three design variables until he arrives at the rotor blade configuration with the lowest hover horsepower. Next, he compromises this best hover design to meet forward flight requirements. He does this by varying the fourth design variable, solidity, as well as the original design variables. Solidity is primarily influenced by design requirements on the pullup maneuver and airfoil stall. The solidity must be adequate for the pullup maneuver. Greater solidity is generally required to meet the forward-flight design constraints but it compromises the best hover design by increasing the horsepower.

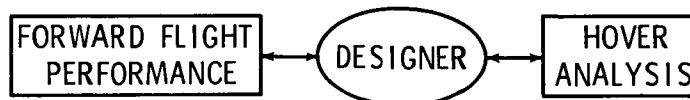
Using the conventional approach, the designer is actively involved in manipulating the design variables and deciding on design changes. He must rely on his previous experience and intuition. He is the communications link between the hover and forward flight analyses. This approach involves parametric studies and extensive cross-plots and is very time consuming. A typical design requires 4-6 weeks.

- METHOD

- DESIGN FOR HOVER ONLY. REDUCE HOVER HORSEPOWER BY CONSIDERING INFLUENCES OF
 - TAPER RATIO AND PERCENT TAPER
 - TWIST
- COMPROMISE "BEST HOVER" DESIGN TO MEET FORWARD FLIGHT REQUIREMENTS
 - $hp_r \leq hp_a$ AT V_H AND DESIGN GW
 - SUSTAIN PULLUP MANEUVER
 - AVOID AIRFOIL STALL

- DESIGNER ACTIVELY INVOLVED

- DATA BASE
- PREVIOUS EXPERIENCE



- TIME-CONSUMING

- PARAMETRIC STUDIES, CROSS PLOTS
- REQUIRES 4-6 WEEKS TOTAL DESIGNER TIME

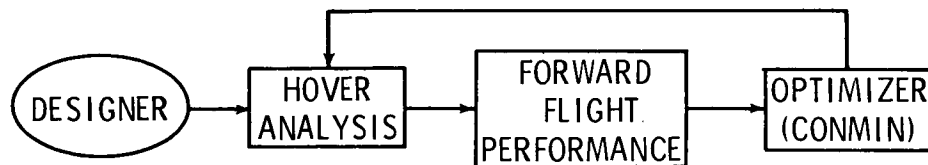
Figure 4

MATHEMATICAL PROGRAMING APPROACH

The mathematical programing approach is illustrated in figure 5. This approach uses the same rotor performance analyses discussed previously but, in addition, couples an optimizer to the analyses. When the designer uses mathematical programing methods, he must define the problem in terms of an objective function (the quantity to be minimized), a set of design variables (the quantities which are changed in order to minimize the objective function), and a set of constraints (requirements which must be satisfied). Once the designer has defined the problem in these terms, which is no easy task, he is not as actively involved in manipulating the design variables. Instead, the optimizer takes over the role of manipulating the design variables to arrive at the best blade design. With the mathematical programing approach, changes in the design variables simultaneously affect both the hover analysis and the forward flight performance analysis.

The optimizer used in this study is CONMIN (ref. 9) which is a well-established, general-purpose optimization program. CONMIN requires the use of gradients which in this application are determined by finite differences calculated internally by CONMIN.

- METHOD
 - COUPLE OPTIMIZER (CONMIN) TO ANALYSIS TOOLS
 - DEFINE
 - OBJECTIVE FUNCTION
 - DESIGN VARIABLES
 - CONSTRAINTS
- DESIGNER NOT AS ACTIVELY INVOLVED



- SIMULTANEOUSLY CONSIDERS INFLUENCES OF TWIST, PERCENT TAPER, TAPER RATIO, AND SOLIDITY ON BOTH HOVER AND FORWARD FLIGHT PERFORMANCE

Figure 5

FORMULATION OF OPTIMIZATION PROBLEM BY MATHEMATICAL PROGRAMING

The mathematical programing formulation of the rotor blade design problem is shown in figure 6. The objective function is the required hover horsepower. The design variables are twist, percent taper, taper ratio, and solidity. The chord c_r controls solidity. The forward flight requirements translate into 14 constraints and are obtained from the C-81 program. By CONMIN sign convention a constraint, g_i , is satisfied if it is negative or zero and violated if it is positive.

The first constraint (eq. (1)) is that horsepower required for forward flight at the design gross weight and the specified horizontal velocity V_H not exceed the horsepower available. The second constraint on pullup maneuver is more difficult to translate into a mathematical programing context. The constraint on pullup maneuver is implemented by determining from C-81 whether or not the helicopter can trim at a gross weight equal to a load factor multiplied by the design gross weight at a specified velocity V_{xf} . Since experience indicates that the failure of the helicopter to trim is an indication that the solidity is too small, the trim constraint, g_i , is formulated as shown in equation (2). The constraint is set equal to -0.5 (satisfied) if trim occurs and equal to $10 - 0.5c_r$ (not satisfied) if trim does not occur. The final design requirement on airfoil stall translates easily into mathematical programing language as shown in equation (3). This constraint is to impose restraints on the airfoil section drag coefficient, C_D . This requirement translates into 12 constraints since the C_D 's are evaluated every 30 degrees around the azimuth. An alternative (not yet implemented) would be to express the constraint in terms of the pitching moment coefficient, C_m , which is more consistent with aeroelastic design requirements.

- OBJECTIVE FUNCTION: HOVER HORSEPOWER
- DESIGN VARIABLES: TWIST, PERCENT TAPER, TAPER RATIO, SOLIDITY
- CONSTRAINTS: ($g_i \leq 0$ SATISFIED, $g_i > 0$ VIOLATED)

- HORSEPOWER REQUIRED

$$g_1 = hp_r / hp_a - 1 \quad (1)$$

- PULL-UP MANEUVER

$$g_2 = \begin{cases} -0.5, & \text{IF TRIMMED} \\ 10 - 0.5c_r, & \text{IF NOT TRIMMED} \end{cases} \quad (2)$$

- AIRFOIL SECTION STALL

$$g_k = C_D / C_{D_{\max}} - 1, \quad 12 \text{ AZIMUTHAL LOCATIONS} \quad (3)$$

Figure 6

COMPARISON OF RESULTS FOR ADVANCED ROTOR BLADE

Rotor blade designs obtained using both the conventional and mathematical programming approaches are shown for a representative army helicopter (fig. 7). The goal is to find the blade design which has the lowest hover horsepower for a four-bladed helicopter with a design gross weight of 15,000 pounds and a horizontal velocity of 160 knots. The selected pullup maneuver requires a load factor of 1.33 (or 20,000 pounds) at a velocity of 100 knots. Both approaches started from a rectangular blade which has a twist of -9.0 degrees and a solidity of 0.09285. Both designs are substantial improvements over the rectangular blade. The overall designs are very similar with slight variations in the details. There is a significant difference in the total design time. Results obtained using the mathematical programming approach took 2 days. Those obtained using the conventional approach took 5 weeks.

DESIGN GROSS WEIGHT = 15,000 lb
 HORIZONTAL VELOCITY = 160 knots
 LOAD FACTOR = 1.33 (20000 lb) AT $V_{LF} = 100$ knots

| | <u>BASELINE (RECTANGULAR)</u> | <u>CONVENTIONAL*</u> | <u>MATHEMATICAL PROGRAMING*</u> |
|-------------------------|-----------------------------------|----------------------|-------------------------------------|
| HOVER HORSEPOWER | 1672 hp | 1558 hp | 1555 hp |
| TWIST | -9° | -12° | -10.6° |
| PERCENT TAPER | 0 | .80 | .85 |
| TAPER RATIO | 1.0 | 3.0 | 3.1 |
| SOLIDITY (σ_T) | .093 | .098 | .092 |
| (c_r) | (1.75 ft) | (2.23 ft) | (2.0 ft) |
| DESIGN TIME | | 5 WEEKS | 2 DAYS |

*BOTH APPROACHES STARTED FROM BASELINE (RECTANGULAR) DESIGN

Figure 7

OBSERVATIONS ON DEVELOPMENT OF THE MATHEMATICAL PROGRAMING SYSTEM

In development of the mathematical programing system, communication played a major role. The participants had to bridge their knowledge gap between the rotorcraft aerodynamics and optimization disciplines. For example, the rotor blade designer had to explain helicopter aerodynamic terminology, while the optimization specialist had to explain mathematical programing terminology. Once they had exchanged jargon, they could begin the problem definition. The rotor blade designer had to explain the overall design problem - what he wanted to do, what analysis methods he used, and what trade-offs he considered. Some design requirements were easy to translate into mathematical programing terms. Others, such as the pullup maneuver, were very difficult to translate. Early discussions revealed most of the information, but some of the intuitive reasoning used in the conventional approach was slow to surface. In fact some of the intuitive reasoning is still surfacing. Practical design limits which are almost implicit in the conventional approach need to be made explicit in the mathematical programing approach. For example, the solidity was originally controlled by a chord multiplication factor which was allowed to vary within wide limits. However, in one extreme case this resulted in a blade design which was excessively wide and impractical to use on a helicopter. The rotor blade designer would intuitively disregard such a design, but the optimization process as formulated did not. A subsequent reformulation of the solidity design variable with appropriate limits eliminated this design. (See fig. 8.)

- BASIC COMMUNICATION
 - JARGON EXCHANGE
 - PROBLEM DEFINITION
- FINDING OUT HOW CONVENTIONAL DESIGNER APPROACHES THE PROBLEM
 - ANALYSIS METHODS
 - TRADE-OFFS
- A LOT OF TALKING REQUIRED
 - EARLY DISCUSSIONS REVEALED MOST OF THE INFORMATION
 - INTUITIVE REASONING MORE DIFFICULT TO SURFACE

Figure 8

PLANS

We plan to continue developing and improving the mathematical programming approach (fig. 9). Plans are to replace the drag coefficient in the airfoil section stall constraint (eq. 3, fig. 6) by the pitching moment coefficient to be consistent with aeroelastic design requirements. Plans include improving the trim constraint (eq. 2, fig. 6), a continuous trim constraint being evaluated speeds up convergence. Plans also include applying the mathematical programming approach to different helicopter configurations. We are also looking at ways to speed up clock turnaround time. This includes speeding up computation time by design variable scaling. We are presently limited to overnight turnaround because of the memory requirements for the C-81 program, which, even though it is overlaid, requires almost the entire memory of a CYBER 173 computer. We are looking at extracting only those subroutines needed for the quasi-static trim analysis. We also plan to use airfoils as design variables. Eventually, we plan to add static (loads) and dynamic (vibrations) structural constraints.

- CHANGE C_D TO C_M IN AIRFOIL SECTION STALL CONSTRAINTS
- IMPROVE TRIM (pullup maneuver) CONSTRAINT
- APPLY TO DIFFERENT HELICOPTER CONFIGURATIONS
- SPEED UP COMPUTER TIME
- AIRFOILS AS DESIGN VARIABLES
- INCLUDE STATIC AND DYNAMIC STRUCTURAL CONSTRAINTS

Figure 9

CONCLUDING REMARKS

Formal mathematical programming has been applied to the aerodynamic rotor blade design process. The approach is to couple hover and forward flight analysis programs with the general-purpose optimization program CONMIN to determine the blade taper ratio, percent taper, twist distribution, and solidity which minimize the horsepower required at hover while meeting constraints on forward flight performance. Designs obtained using this approach for the blade of a representative army helicopter compare well with those obtained using a conventional approach involving personnel-intensive parametric studies. Results from the present method can be obtained in 2 days as compared to 5 weeks required by the conventional procedure. Also the systematic manipulation of the design variables by the optimization procedure minimizes the need for the researcher to have a vast body of past experience and data in determining the influence of a design change on the performance. Plans are to continue evaluation of the method for additional rotor blade configurations and refine the procedure.

REFERENCES

1. Bingham, Gene J.: The Aerodynamic Influences of Rotor Blade Taper, Twist, Airfoils, and Solidity on Hover and Forward Flight Performance. 37th Annual Forum of the American Helicopter Society, New Orleans, Louisiana, May 1981.
2. Gessow, Alfred; and Myers, Garry C., Jr.: Aerodynamics of the Helicopters. Frederick Unger Publishing Company, New York, 1952.
3. Van Gaasbeck, J. R.: Rotorcraft Flight Simulation, Computer Program C-81. USARTL-TR-77-54B, 1979.
4. Berry, John D.: Quarter Scale Testing of an Advanced Rotor System for the UH-1 Helicopter. 37th Annual Forum of the American Helicopter Society, New Orleans, Louisiana, May 1981.
5. Kitis, L.; Pilkey, W. D.; and Wang, B. P.: Optimal Frequency Response Modification by Added Passive Structures. J. of Aircraft, Vol. 20, No. 11, November 1983.
6. Peters, D. A.; Ko, T.; and Rossow, M. P.: Design of Helicopter Rotor Blades for Desired Placement of Natural Frequencies. 39th Annual Forum of the American Helicopter Society, St. Louis, MO, May 1983.
7. Friedmann, P. P.; and Shanthakumaran, P.: Aeroelastic Tailoring of Rotor Blades for Vibration Reduction in Forward Flight. AIAA/ASME/ASCE/AHS 24th Structures, Structural Dynamics and Materials Conference, May 2-4, 1983, Lake Tahoe, Nevada.
8. Bennett, R. L.: Application of Optimization Methods to Rotor Design Problems. Vertica, Vol. 7, No. 3, pp 201-208, 1983.
9. Vanderplaats, G. N.: CONMIN - A Fortran Program for Constrained Function Minimization - User's Manual. NASA TM X-62282, August 1973.

REGRESSION ANALYSIS
AS A DESIGN OPTIMIZATION TOOL

Richmond Perley
Kaman Aerospace Corporation
Bloomfield, Connecticut

SUMMARY

This presentation is organized in four parts. First is a discussion of the generalized design problem and how it differs from a detailed, final design problem. The optimization process and a role for regression analysis are addressed. This is followed by the performance index, or objective function, and basic search strategy used.

The discussion of program implementation includes a description of some of the auxiliary outputs available. Finally, some conclusions are given about the value of regression analysis as a design optimization tool.

1. GENERALIZED DESIGN PROBLEM

- A. OPTIMIZATION LOOP**
- B. OPTIMIZATION LOOP CONSIDERATIONS**
- C. REGRESSION ANALYSIS CONSIDERATIONS**
- D. COMPUTATIONAL REQUIREMENTS - A FIGURE OF MERIT**

2. PERFORMANCE INDEX (OBJECTIVE FUNCTION)

- A. PERFORMANCE INDEX EQUATIONS**
- B. BASIC SEARCH STRATEGY**

3. PROGRAM IMPLEMENTATION

- A. SENSITIVITIES**
- B. TRADEOFF STUDY**
- C. CONTOUR PLOTS**

4. VALUE OF REGRESSION ANALYSIS

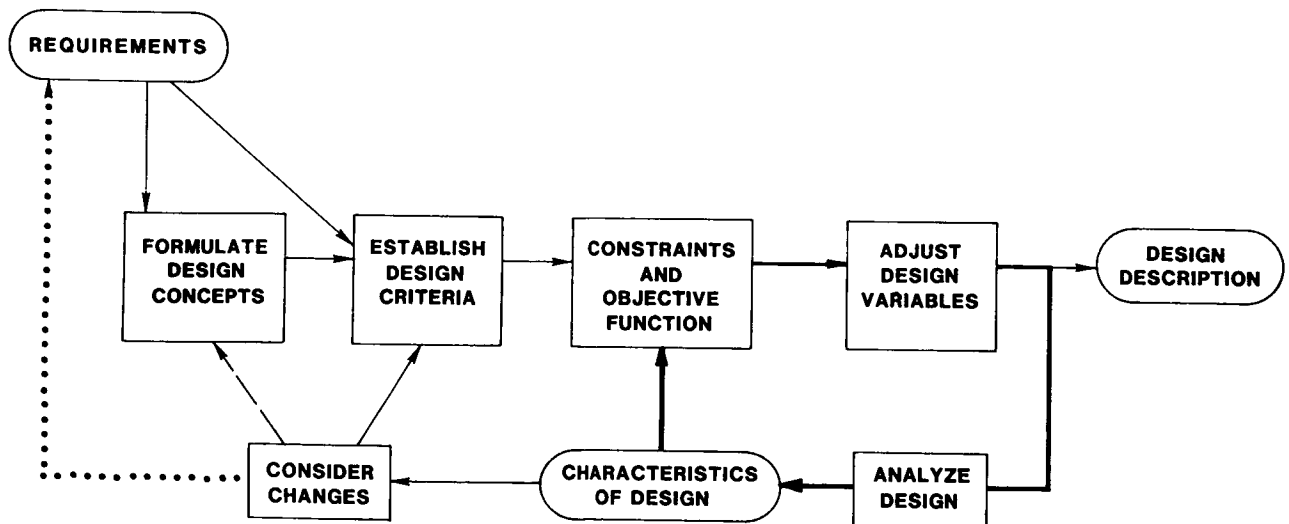
GENERALIZED DESIGN PROBLEM

The optimization concepts will be described in relation to an overall design process as opposed to a detailed, part-design process where the requirements are firmly stated, the optimization criteria are well established, and a design is known to be feasible.

The overall design process starts with the stated requirements. Some of the design criteria are derived directly from the requirements, but others are affected by the design concept. It is these design criteria that define the performance index, or objective function, that is to be minimized within some constraints. In general, there will be multiple objectives, some mutually exclusive, with no clear statement of their relative importance.

The optimization loop on the right adjusts the design variables and analyzes the resulting design, in an iterative fashion, until the objective function is minimized within the constraints. This provides a solution, but it is only the beginning. Is a better overall result achieved if one of the constraints is relaxed; if objective 1 is given less importance with respect to objective 2? We probably will want to change the design concepts in ways that affect the design criteria. We may even want to vary the requirements to determine the cost drivers.

In effect, the problem definition evolves as information is derived from the results. It becomes a learning process as we determine what the physics of the system can deliver in relation to the desirable system characteristics. As with any learning process, an interactive capability is a real attribute for investigating the many alternatives that will be suggested as learning progresses.

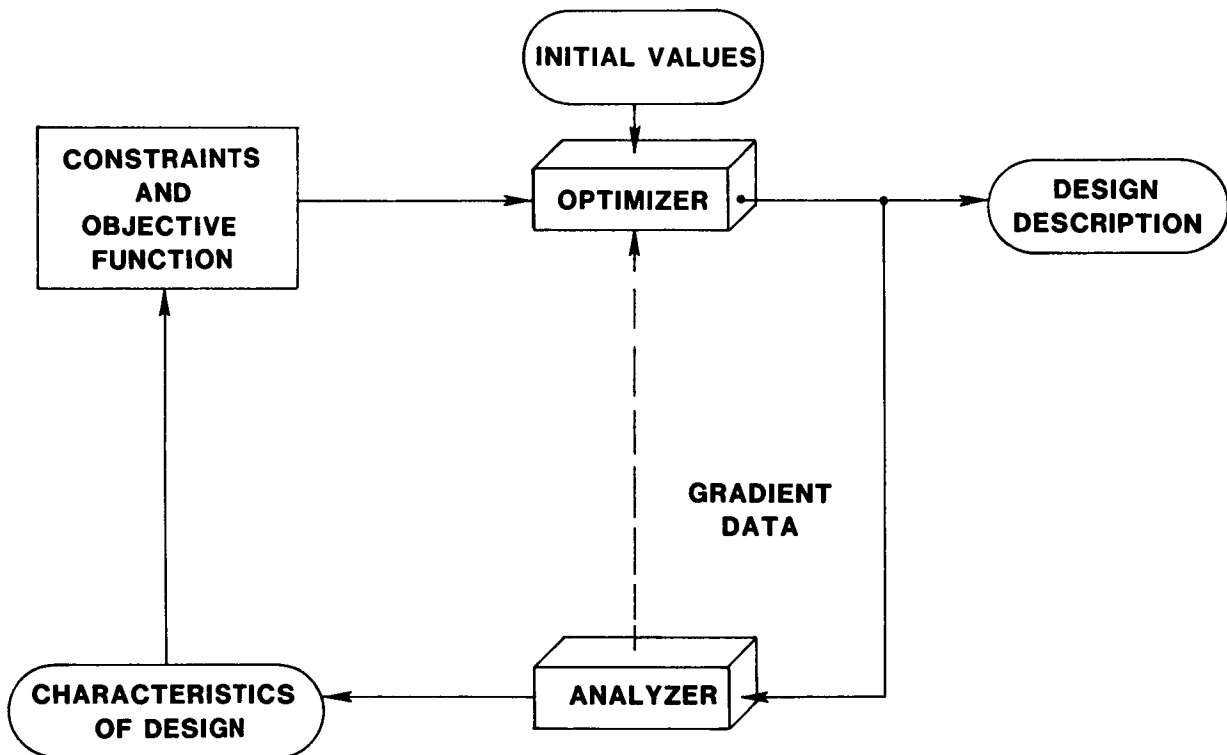


OPTIMIZATION LOOP

The optimization loop involves two functions. The optimizer contains the strategies for adjusting the design variables until the objective function is minimized. The analyzer determines the characteristics of the design from the values of the design variables.

The analyzer used is always a compromise between accuracy, or representativeness, and ease of use and computational requirements. The physical processes to be analyzed are often extremely complex and do not have direct solutions. Large matrix inversions, finite difference methods, and the iterative solutions of aeroelastic problems are a few examples. One approach to this compromise is to partition the analyzer into recurring and non-recurring portions, i.e., a portion that is a function of the design variables and a portion that is not.

Since most design optimization problems are non-linear, several iterations of the optimization loop are required to reach a solution for one set of initial values. Depending on the degree of non-linearity, there may be several minima and the solution found often depends on the starting point. Therefore, the process must be started from a number of points distributed throughout the design space in order to find the "global" minimum. This is further reason for minimizing computational requirements.



OPTIMIZATION LOOP CONSIDERATIONS

The efficacy of the optimizer is a function of the types and quality of information available from the analyzer. With first gradients, it can estimate directions in which to move. With second gradients, it can estimate how far to move along each axis of the design space. If gradient information is obtained from the analyzer through first and second differences, the convergence-limit "noise" of iterative solutions and the resolution-limit "noise" of matrix inversions can produce large errors in the first gradients and make the second gradients almost unusable. The analytical solutions to many of the physical processes of interest in design optimization do not provide direct calculation of gradients.

- o **FIRST GRADIENT**

- o **SECOND GRADIENT (HESSIAN)**

- o **FIRST AND SECOND DIFFERENCES**

- **CONVERGENCE "NOISE"**

- **RESOLUTION "NOISE"**

REGRESSION ANALYSIS CONSIDERATIONS

A useful approach to reducing the computational requirements of the analyzer and increasing the ease of use is the incorporation of polynomial approximating equations to represent the physical processes. The polynomial coefficients are readily found by regression analysis. Generally, second or third order equations provide a satisfactory representation over the design space of interest. These equations can be evaluated rapidly at each iteration of the optimization loop and the gradients are directly available from the coefficients. Furthermore, because of the redundancy used in the regression analysis, the approximating equations smooth the convergence limit "noise." This is particularly important in those portions of the design space where the analytic solutions converge slowly. A further advantage is that experimental as well as analytic data can be incorporated in the analysis using this technique.

The amount of data required "up front" for the regression analysis is considered by some as a disadvantage. However, the total computational requirements for the analytical procedures to produce this data are generally less than those for using the same analytical procedures directly in the optimization loop. A comparison of the two approaches follows.

- o SECOND OR THIRD ORDER POLYNOMIALS**
- o REPRESENTATIVE OVER DESIGN SPACE**
- o RAPIDLY EVALUATED AT EACH ITERATION**
- o CONTINUOUS FIRST AND SECOND GRADIENTS**
- o SMOOTHS CONVERGENCE LIMIT "NOISE"**
- o ANALYTIC AND EXPERIMENTAL DATA**
- o COMPUTATION REQUIREMENTS**

COMPUTATIONAL REQUIREMENTS - A FIGURE OF MERIT

The computational requirement for each data point required by the regression analysis is the same as the requirement for each call to the analytical procedure when it is used directly by the optimizer. Therefore, a figure of merit that reflects the computational advantage of the regression equations is the ratio of the number of calls to the analyzer by the optimizer to the number of data points required by the regression analysis.

Our experience shows that the number of data points required for the regression analysis lies somewhere between the number of terms in a full cubic and three times the number of terms in a full quadratic equation. These are shown as the upper and lower bounds as the number of design variables, N, becomes large.

The number of optimizer calls to the analyzer depends on a number of factors on which there is no universal agreement; however, upper and lower values for each are suggested. The number of starts/problem depends on the number of minima and is certainly conservative since the design space has 2^N "corners." The number of problems refers to the number of times the problem statement is changed, as discussed previously. The value of K depends on the newness of the design problem and the interests of the designer, but is certainly greater than unity.

It can be seen that the ratio is always greater than 1, a regression advantage, unless direct use is at its lower value; regression is at its upper bound; and the number of design variables, N, is greater than 15 times K. The expected ratio is about 10 times K. While the regression requirements may approach those of direct use, having once prepared the equations, the computational requirements of optimization are reduced to the point where an interactive process becomes a reality.

DIRECT USE BY ANALYZER

FIGURE OF MERIT =

(DIRECT USE)
(REGRESSION ANALYSIS)

| | UPPER | LOWER | FACTOR |
|--|---------------------|-----------------------|--------------------------|
| | 10 (N + 3) | $\frac{5}{2} (N + 3)$ | CALLS/START |
| | N | \sqrt{N} | STARTS/PROBLEM |
| | NK | $\sqrt{N} K$ | NO. OF PROBLEMS |
| | 10 N ³ K | 5 N ² K | PRODUCT |
| REGRESSION ANALYSIS UPPER $\frac{N^3}{6} + N^2 + \frac{11 N}{2} + 1 \rightarrow \frac{N^3}{6}$ | 60 K | $\frac{15 K}{N}$ | GEOMETRIC MEAN = 10 K |
| LOWER $3 \left(\frac{N^2}{2} + \frac{3 N}{2} + 1 \right) \rightarrow \frac{3 N^2}{2}$ | $\frac{20 NK}{3}$ | $\frac{5 K}{3}$ | |

FIGURE OF MERIT =

$$\frac{(\text{DIRECT USE})}{(\text{REGRESSION ANALYSIS})}$$

PERFORMANCE INDEX (OBJECTIVE FUNCTION)

A weighted sum of squares of the dependent variables is the form selected for the performance index, or objective function, because of its flexibility. Even with single objectives, it is usually the magnitude that is to be minimized, as opposed to a minimization in the algebraic sense. Multiple objectives are ideally combined on a sum-of-squares basis since often they are mutually exclusive and the user's value function is generally elliptic. Vibration is one of the key items considered in helicopter design. The quantity to be minimized is the vector sum of the real and imaginary components of the hub forces and moments as they are transmitted throughout the airframe, as well as the vibratory stresses in the rotor blades themselves. Tradeoffs among the importance of the various objectives and vibration levels at various points in the airframe can be readily accomplished by varying the weighting factors. Constraints can also be accommodated as penalty functions by introducing bias levels.

o WEIGHTED SUM OF SQUARES

o SINGLE OBJECTIVE

o MULTIPLE OBJECTIVES

o VIBRATION

o TRADEOFFS

o CONSTRAINTS

PERFORMANCE INDEX EQUATIONS

The form of the performance index to be minimized, PI, is shown. The weighting factors, W_h , and bias levels, B_h , are provided as real time user inputs so that tradeoffs can be conducted in an interactive mode. The dependent variables Y_h are calculated from the polynomial approximating equations. The first and second gradients with respect to each of the design variables are calculated directly from the coefficients of the approximating equations. Quantities to be maximized are given a negative weighting factor.

Constraints are accommodated as penalty functions by setting the bias value, B_h , equal to the constraint value. It is usually necessary to start with a small weighting factor and then increase it to move as close to the constraint value as desired. For "greater than" or "less than" constraints, W_h is zero when the constraint is not violated and positive or negative, as appropriate, when it is violated.

$$PI = \sum_h W_h (Y_h - B_h)^2$$

$$W_h, B_h = \text{USER INPUTS}$$

$$Y_h = f(x_1, x_2, \dots, x_n)$$

GRADIENTS

$$\nabla PI(f) = \frac{\partial PI}{\partial x_f} = 2 \sum_h W_h (Y_h - B_h) \frac{\partial Y_h}{\partial x_f}$$

$$\nabla^2 PI(f, g) = \frac{\partial^2 PI}{\partial x_g \partial x_f} = 2 \sum_h W_h \left[(Y_h - B_h) \frac{\partial^2 Y_h}{\partial x_g \partial x_f} + \frac{\partial Y_h}{\partial x_g} \cdot \frac{\partial Y_h}{\partial x_f} \right]$$

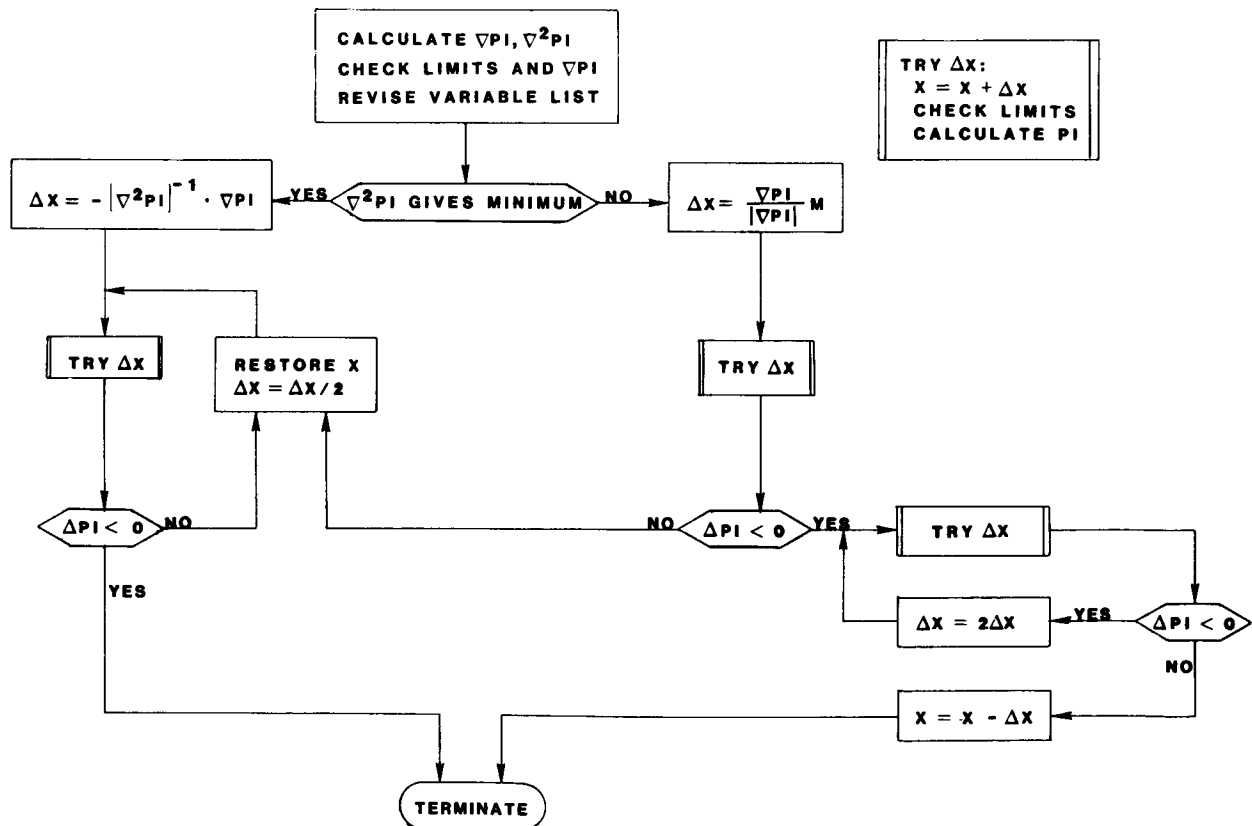
BASIC SEARCH STRATEGY

The basic search strategy that constitutes each iteration of the optimization loop is shown. The first step is to calculate the gradients at the current design point from the approximating equation coefficients and determine which of the design variables are within limits or would move within limits in reducing the performance index, PI. The next step is to determine whether or not the stationary point described by the second gradient is a minimum.

If the stationary point is a minimum, the Newton-Raphson algorithm calculates the changes in the design variables, ΔX , to approach it. The "Try ΔX " subroutine constrains the design variables to remain within limits and calculates the new value of PI using the approximating equations. Because of system non-linearities, PI may increase instead of decrease. If so, a loop is entered that decreases ΔX until PI decreases or a count is exceeded. In the latter case, an alternate search strategy (not shown) is entered.

If the second gradient does not describe a minimum, a modified "steepest gradient" ΔX is calculated. (M is a scaling constant that is modified in accordance with the curvature of the PI surface.) If that ΔX does not decrease PI, the loop on the left is entered to try smaller magnitudes. If ΔX does reduce PI, the loop on the right is entered to increase the magnitude of ΔX until PI no longer decreases.

This basic iteration cycle is repeated until the decrease in PI is less than a given convergence limit.



PROGRAM IMPLEMENTATION

The concepts just described have been implemented on a DEC20 time-sharing system in BASIC. The user calls the file that contains the approximating equation coefficients for the problem of interest and goes to work. Commands are used to initiate the many options and capabilities available in the program. We have applied it to a number of design problems, one of which will be described in another presentation. Performance has been good. In one problem involving seven design variables and seven dependent variables, the average amount of CPU time to find a minimum of the performance index from any start point was under four seconds.

Several kinds of output are available to help the user gain insight into the relationships involved in the problems. Sensitivities, tradeoffs, and contour plots are but three examples. The latter two are practical because of the rapidity with which the conditions at any design point can be calculated using the approximating equations.

o DEC20 TIME SHARE - BASIC

o INTERACTIVE PROCESSING

o 4 SECONDS OF CPU PER SEARCH

o AUXILIARY CAPABILITIES

- SENSITIVITIES

- TRADEOFFS

- CONTOUR PLOTS

SENSITIVITIES

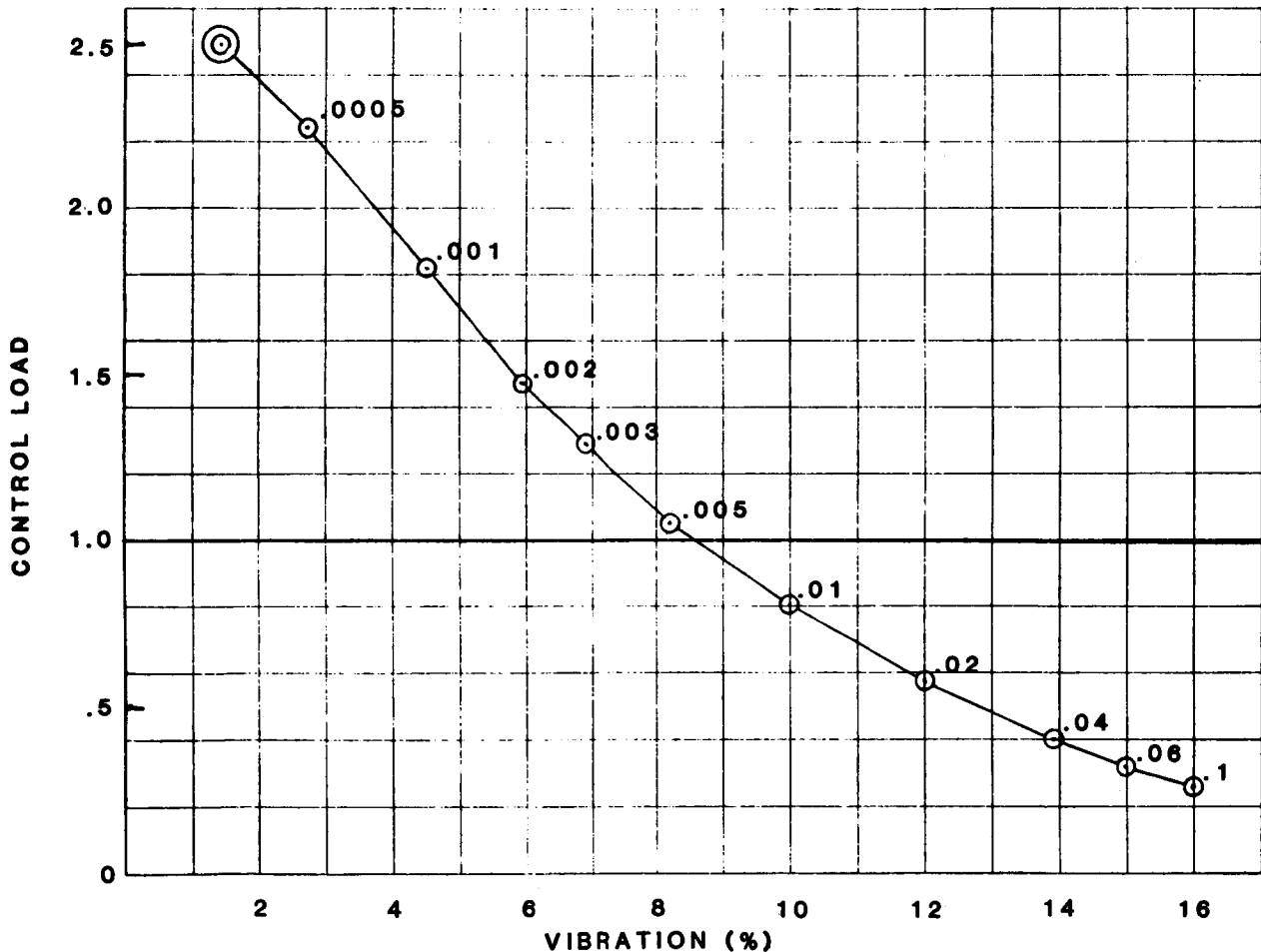
This shows a table of the first derivatives of each of the dependent variables, down the left (rotor power, maximum and minimum angle of attack, blade bending moment, hub shear force and pitching moment, and control load), with respect to each of the design variables, across the top (blade bending frequency and mode, torsion mode, retention frequency, sweep angle, blade twist, and torsion frequency). The first and second derivatives of the performance index at any design point and for any set of weighting factors can also be tabulated.

| DEPENDENT VARIABLES | DESIGN VARIABLES | | | | | | | |
|---------------------|------------------|--------|--------|--------|--------|--------|--------|--------|
| | BF | BMD | TMD | RF | SWP | TWST | TF | |
| | HP | 0.103 | -0.007 | 0.274 | -0.010 | 0.010 | 0.248 | -0.119 |
| | AMAX | 0.013 | -0.029 | -0.029 | 0.031 | 0.214 | -0.478 | 0.466 |
| | AMIN | 0.370 | 0.207 | -0.514 | 0.000 | -1.334 | 1.431 | -1.321 |
| | BBM | -2.424 | -0.012 | 0.387 | 3.694 | 0.483 | 0.156 | -1.047 |
| | THS | 0.278 | 0.993 | -0.002 | 2.323 | 1.428 | -0.341 | -0.115 |
| | PM | -6.739 | 1.601 | 1.346 | 2.587 | 0.181 | -0.339 | 2.046 |
| | PHL | 0.468 | 0.000 | -0.258 | -0.095 | 6.672 | -0.583 | -0.518 |

TRADEOFF STUDY

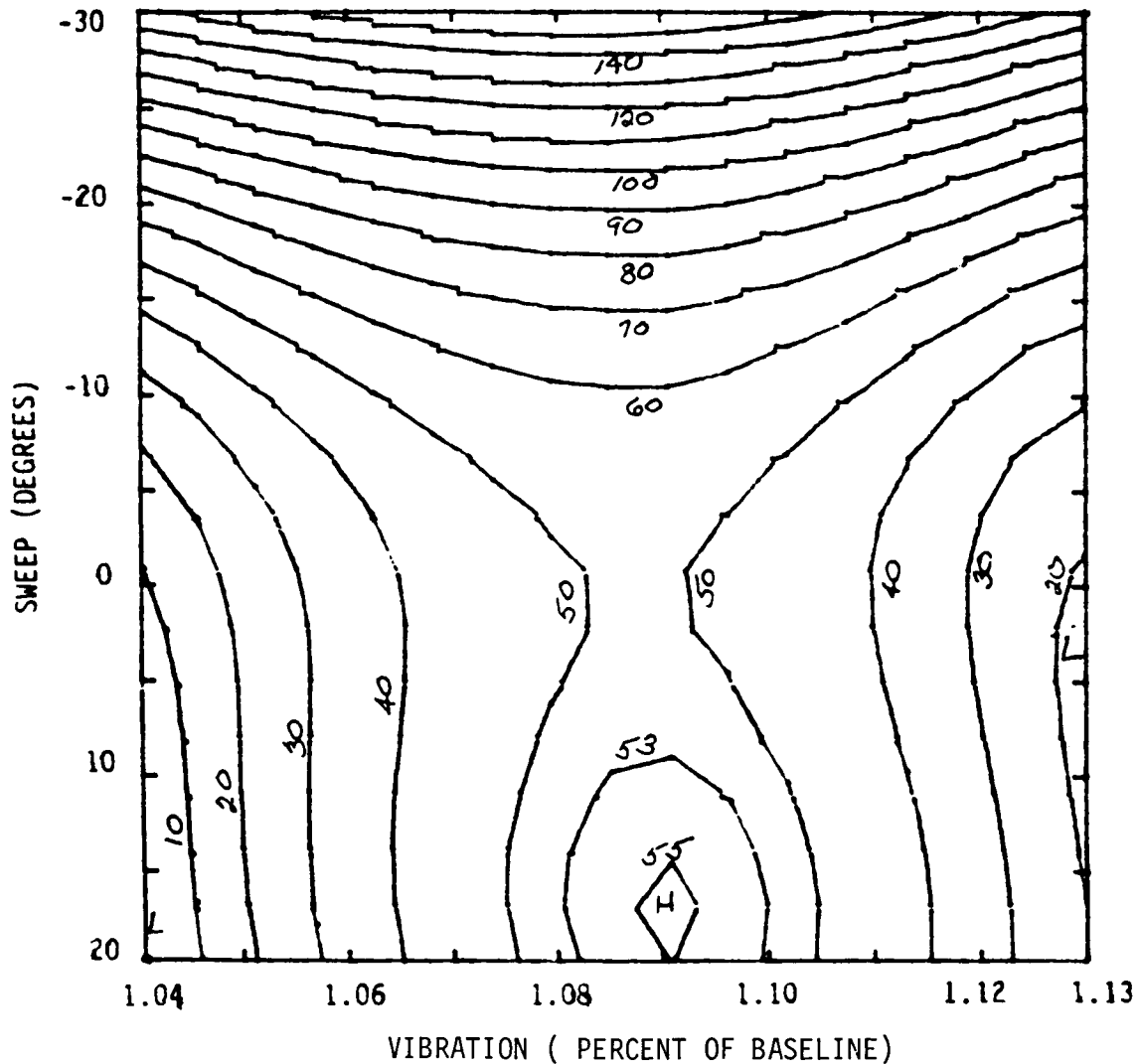
An example of a tradeoff study is a rotor design problem that was concerned with vibration. The optimization process was started with all weighting factors except those on vibration terms equal to zero. A minimum was found where the vibration level was only 1.4% of the baseline value. However, the pitch horn load was 2.4 times the baseline value and was considered too high. The weighting factor on pitch horn load was then increased and optimization was repeated. By doing this a number of times, the curve below was generated. The double circle denotes the initial design point and the weighting factor is given at each optimization point.

This shows that pitch horn load can be decreased below the baseline value while still retaining a vibration level of less than 9%. CPU time was not measured, but the total time was less than ten minutes.



CONTOUR PLOTS

Contour plots can be generated that show any dependent variable or the performance index with any set of weighting factors as a function of any two of the design variables. This example is from the seven-variable rotor design problem and shows vibration level. It helps to explain some of the multiple minima that were found. There is a saddle point near the center and a ridge that goes from top to bottom. If the optimization process is started anywhere to the left of that ridge, it goes to the minimum at the lower left. Otherwise, it goes to the minimum near the right center.



VALUE OF REGRESSION ANALYSIS

Our experience to date has convinced us of the value of regression analysis in the design optimization process. One obvious advantage is the broadening of the choice of search strategies made possible by the simple approximating equations and their derivatives. The search strategy just described is by no means the best that can be achieved, but it has proven its worth.

The relative ease of doing tradeoffs among the design criteria means that answers will be found to questions that would be ignored in a more complex world. And some of those answers will be worthwhile.

Perhaps the greatest benefit is the interactive learning that can now take place. Answers lead to more questions, their answers, and then more questions. However, if it takes a day, or even a few hours, for an answer to come back, the whole thought process may be lost. The history of engineering design activities is full of examples of the benefits of an interactive process vs a batch process, not simply in reducing the cost of the design process, but in improving the quality of the resulting design.

o CHOICE OF SEARCH STRATEGIES

o TRADEOFF STUDIES

o INTERACTIVE LEARNING

A ROTOR OPTIMIZATION USING
REGRESSION ANALYSIS

N. Giansante
Kaman Aerospace Corporation
Bloomfield, Connecticut

PRECEDING PAGE BLANK NOT FILMED

KAMAN REGRESSION, OPTIMIZATION, AND SENSITIVITY PROCEDURE

The design and development of present helicopter rotors is subject to the many design variables and their interactions that affect rotor operation. Until recently, selection of rotor design variables to achieve specified rotor operational qualities has been a costly, time consuming, repetitive task. For the past several years, Kaman Aerospace Corporation has successfully applied multiple linear regression analysis, coupled with optimization and sensitivity procedures, in the analytical design of rotor systems. Figure 1 presents the basic steps in the regression, optimization, and sensitivity analyses used at Kaman Aerospace Corporation.

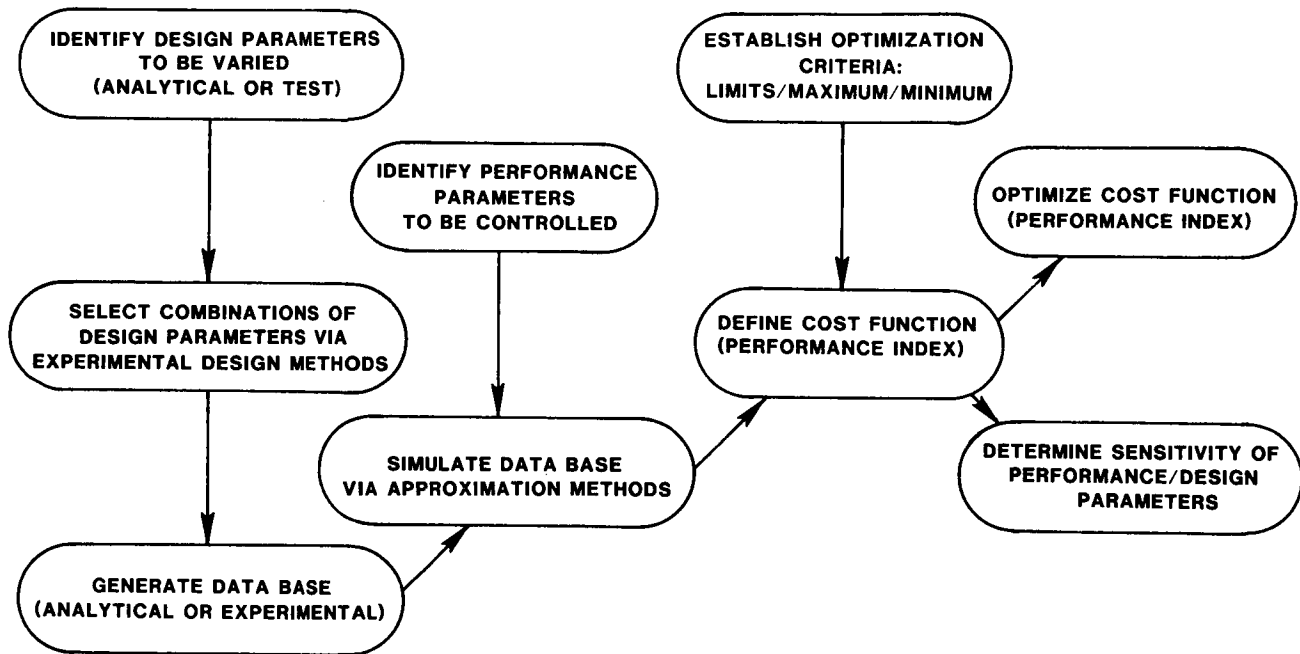


Figure 1

ROTOR DESIGN OPTIMIZATION FOR PERFORMANCE

The problem which was analyzed was a rotor design optimization for performance. The helicopter configuration studied was an RSRA type airframe with the rotor characteristics listed in Figure 2. The optimization problem, as presented in Figure 2, was to minimize the rotor power required at hover while maintaining a maximum speed of 160 knots and a maneuver capability of 1.5g at 120 knots with an installed power of 1740 HP.

PROBLEM:

MINIMIZE POWER REQUIRED AT HOVER

MAINTAIN V_{MAX} OF 160 KNOTS

MANEUVER CAPABILITY 1.5g AT 120 KNOTS

INSTALLED POWER OF 1740 HP

CONFIGURATION: RSRA AIRFRAME

| | |
|---------------------|-----------------|
| GROSS WEIGHT | 18400 LB |
| ROTOR RADIUS | 27 FT |
| ROTOR RPM | 256 |
| BLADE CHORD | 25.5 IN. |

Figure 2

BASIC PROCEDURE

The basic procedure for the regression, optimization, and sensitivity analysis is shown in Figure 3. The analysis starts with the selection and allowable ranges of design variables. A general form of the approximating equations is established, followed by a design of experiments to select vectors of design variables for entry into the aeroelastic loads analyses. At each flight condition the aeroelastic analysis is used to develop a data base of rotor operational qualities as a function of the design variables. Using the data base, the multiple linear regression equations for horsepower are developed and used subsequently in Kaman's optimization program, KAOPT, and in the sensitivity study. The analysis technique is not limited to the use of the optimization program, KAOPT. Any suitable optimization program may be used in the analysis.

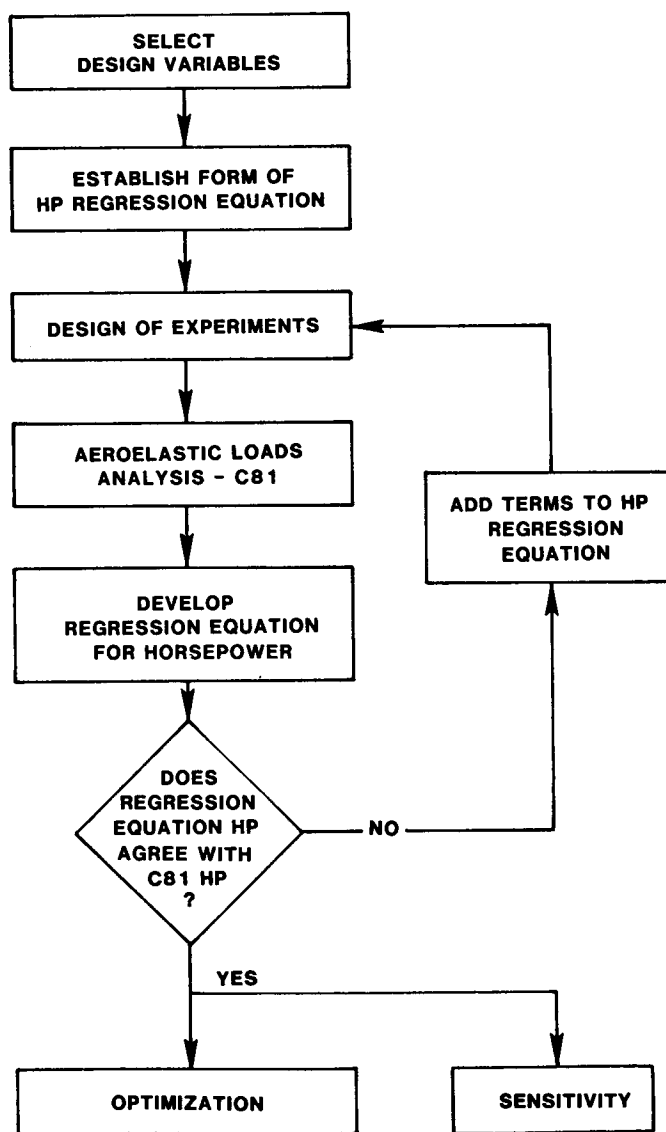


Figure 3

PERFORMANCE OPTIMIZATION DESIGN VARIABLES

The design variables and the levels of these variables used in developing the multiple linear regression equations for rotor horsepower are presented in Figure 4. The range of variables was selected to encompass all realistic rotor designs. Experience in optimizing other flight conditions, or reasonably close design variations of the rotor, or availability of experimental data may aid in estimating the range of variables within which the optimum is likely to occur.

| DESIGN VARIABLES | LEVELS OF DESIGN VARIABLES |
|-----------------------------|---|
| SWEEP ANGLE* | 20°, 0°, -20°, -30° |
| BUILT-IN TWIST | -8°, -12°, -14°, -16° |
| TAPER RATIO | 1.1:1, 2:1, 3:1 |
| PERCENT TIP TAPER | 15%, 25%, 50% |

*** SWEEP ANGLE + = FORWARD**

Figure 4

FORM OF REGRESSION EQUATION FOR PERFORMANCE OPTIMIZATION

The general form of the horsepower equation used for performance optimization is given in Figure 5. The equation is second order in the design variables and contains first order interactions among the design variables. Experience has shown that this form of analytical model is capable of accurately predicting rotor horsepower.

$$\begin{aligned}
 \text{HP} = & a_0 + a_1 x_1 + a_2 x_2 + a_3 x_3 + a_4 x_4 \\
 & + a_{11} x_1^2 + a_{22} x_2^2 + a_{33} x_3^2 + a_{44} x_4^2 \\
 & + a_{12} x_1 x_2 + a_{13} x_1 x_3 + a_{14} x_1 x_4 \\
 & + a_{23} x_2 x_3 + a_{24} x_2 x_4 + a_{34} x_3 x_4 \\
 \\
 \text{HP} = & a_0 + \sum_{i=1}^n a_i x_i + \sum_{i=1}^n a_{ii} x_i^2 + \sum_{i=1}^{n-1} \sum_{j=i+1}^n a_{ij} x_i x_j
 \end{aligned}$$

| | | |
|---------------------------|---|------------------|
| $x_1 =$ SWEEP ANGLE | } | DESIGN VARIABLES |
| $x_2 =$ BUILT-IN TWIST | | |
| $x_3 =$ TAPER RATIO | | |
| $x_4 =$ PERCENT TIP TAPER | | |

Figure 5

DESIGN OF EXPERIMENTS -
MATRIX OF CONDITIONS FOR PERFORMANCE ANALYSIS

A design of experiments was developed to select vectors of design variables from the total design space to be used in the aeroelastic loads analysis. A data base of rotor operational qualities was established using the matrix of conditions shown in Figure 6. The data points were selected randomly and were carefully screened from a statistical viewpoint. Thus, the chance of accounting for the effects of each of the variables was maximized over the design space within the number of analytical cases run in the aeroelastic loads program.

| X ₁ SWEEP X ₂ TWIST | | 20° | | | | 0° | | | | -20° | | | | -30° | | | |
|--|-------|-----|------|------|------|-----|------|------|------|------|------|------|------|------|------|------|------|
| | | -8° | -10° | -12° | -16° | -8° | -10° | -12° | -16° | -8° | -10° | -12° | -16° | -8° | -10° | -12° | -16° |
| X ₃ TAPER RATIO X ₄ % TAPER | 1:1:1 | | | 14 | | 6 | | | 25 | | | | 30 | | | | |
| | | | 19 | | | | 22 | | | | 28 | | | 32 | | | 2 |
| | | | | | 21 | | | | | 11 | | | | | 3 | | |
| | 2:1 | 17 | | | | | | 26 | | | | 15 | | | | 36 | |
| | | | | 18 | | | 23 | | | | | | 31 | | | | 13 |
| | | | | | 8 | | | | | | 29 | | | 33 | | | |
| | 3:1 | | 7 | | | 5 | | 4 | | | | 9 | | | 1 | | |
| | | | | | 20 | | | | 27 | 12 | | | | | | 10 | |
| | | 16 | | | | | 24 | | | | | | | 34 | | | 35 |

Figure 6

COEFFICIENTS FOR HORSEPOWER REGRESSION EQUATIONS

Using a stepwise multiple linear regression analysis, the approximating equations for rotor horsepower were developed for each flight condition. The coefficients of the horsepower equations are given in Figure 7. Also shown are the Multiple Correlation Coefficient (M.C.C) and the Standard Error of the Estimate (S.E.E.) for each flight condition. The M.C.C. and the S.E.E. are statistical measures of the fit of the regression equations within the domain of the data.

| COEFFICIENT | VARIABLE | HOVER | 80 KNOTS | 160 KNOTS |
|-------------|----------|---------|----------|-----------|
| a_0 | | 1975.08 | 1038.84 | 2054.88 |
| a_1 | S | --- | --- | - 1.31 |
| a_2 | T | 12.13 | 18.89 | 44.88 |
| a_3 | TR | - 77.59 | -27.60 | -27.88 |
| a_4 | %T | --- | -11.32 | --- |
| a_{11} | S^2 | - 0.067 | - 0.04 | - 0.08 |
| a_{22} | T^2 | --- | 0.74 | 2.078 |
| a_{33} | TR^2 | 19.43 | 5.45 | --- |
| a_{44} | $\%T^2$ | --- | 62.81 | 140.25 |
| a_{12} | S,T | --- | - .01 | - 0.10 |
| a_{13} | S,TR | --- | --- | --- |
| a_{14} | S,%T | --- | --- | .61 |
| a_{23} | T,TR | 1.26 | - .29 | - 1.84 |
| a_{24} | T,%T | - 7.00 | --- | 9.12 |
| a_{34} | TR,%T | -106.88 | -38.14 | --- |
| * M.C.C. | | .987 | .982 | .978 |
| ***S.E.E. | | 11.7 | 4.7 | 9.1 |

* M.C.C. - Multiple Correlation Coefficient

***S.E.E. - Standard Error of the Estimate

Figure 7

HORSEPOWER COMPARISON - REGRESSION EQUATIONS AND C81

In order to evaluate the predictive capability of the regression equations, several cases were run on the aeroelastic loads program, C81, using combinations of design variables not used in developing the original data base. Figure 8 presents the results of these additional cases compared to results obtained using the regression equation. The correlation between the two sets of data is excellent, giving confidence in the predictive capability of the analytical model over the total design space.

| x_1 SWEEP | x_2 BUILT IN TWIST | x_3 TAPER RATIO | x_4 % TIP TAPER | V = 160 KNOTS | | V = 80 KNOTS | | V = 0 KNOTS | |
|----------------|-------------------------------|-------------------------|-------------------------|--------------------|-------------|--------------------|-------------|--------------------|-------------|
| | | | | REGRESSION (HP) | C81 (HP) | REGRESSION (HP) | C81 (HP) | REGRESSION (HP) | C81 (HP) |
| - 20° | - 13° | 2.5:1 | 30% | 1753.65 | 1776.25 | 849.69 | 853.12 | 1624.21 | 1618.44 |
| - 30° | - 9° | 2.5:1 | 30% | 1712.66 | 1715.82 | 838.76 | 839.81 | 1643.57 | 1629.31 |
| - 30° | - 13° | 2.5:1 | 30% | 1711.29 | 1714.56 | 830.20 | 829.73 | 1590.81 | 1581.85 |
| - 20° | - 9° | 2.5:1 | 30% | 1750.94 | 1752.02 | 857.88 | 861.98 | 1676.96 | 1678.20 |
| 20° | - 13° | 2.5:1 | 30% | 1761.53 | 1768.76 | 854.52 | 852.32 | 1624.21 | 1618.01 |
| 20° | - 9° | 2.5:1 | 30% | 1742.53 | 1748.47 | 861.22 | 862.08 | 1676.96 | 1677.67 |
| - 30° | - 13° | 1.5:1 | 30% | 1715.24 | 1715.92 | 843.64 | 839.34 | 1639.15 | 1616.54 |
| - 30° | - 9° | 1.5:1 | 30% | 1723.97 | 1724.64 | 853.37 | 848.83 | 1686.86 | 1662.44 |
| - 20° | - 13° | 1.5:1 | 30% | 1757.60 | 1776.04 | 863.13 | 865.69 | 1672.55 | 1662.93 |
| - 20° | - 9° | 1.5:1 | 30% | 1762.26 | 1760.44 | 872.50 | 875.68 | 1720.26 | 1720.64 |
| 20° | - 9° | 1.5:1 | 30% | 1753.85 | 1755.93 | 875.84 | 875.93 | 1720.26 | 1719.92 |
| 20° | - 13° | 1.5:1 | 30% | 1765.49 | 1767.46 | 867.96 | 865.14 | 1672.55 | 1662.34 |

Figure 8

MINIMUM HOVER POWER WITH CONSTRAINTS

Results of the optimization process are shown in Figure 9. The equations for horsepower, developed by the regression analysis, were used in the optimization program, KAOPT, to derive an optimum rotor based on minimum hover horsepower as a criterion, with horsepower constraints at flight speeds of 120 and 160 knots and a 1.5g maneuver capability at 120 knots.

Two local minima were found, depending upon the value of sweep used to start the solution. This result emphasizes the need to start the solution at several points in the design space to achieve the optimum design.

The horsepower obtained from the regression equations for each of the flight conditions for the two local minima is shown in Figure 9. Also shown, in parentheses, is the horsepower obtained for the two local minima using the C81 aeroelastic loads analysis. The correlation between the two sets of horsepower is excellent.

| | LOCAL MINIMA | |
|----------------------|--------------|--------------|
| | POINT 1 | POINT 2 |
| SWEEP | -30° | +20° |
| TWIST | -15.8 | -10.4 |
| TAPER | 3:1 | 3:1 |
| PERCENT TAPER | 50% | 44% |

| CONDITION | HORSEPOWER | | | |
|------------------|-------------|---------------|-------------|---------------|
| | KAOPT | C81 | KAOPT | C81 |
| HOVER | 1501 | (1509) | 1616 | (1601) |
| 120 KNOTS | 1613 | (1626) | 1684 | (1688) |
| 160 KNOTS | 1740 | (1744) | 1740 | (1744) |

Figure 9

ALTERNATE DESIGNS

The original regression equations for horsepower and the optimization program, KAOPT, were used to extend the problem and determine the power required at hover if the design constraints are altered to minimize power at 120 knots or 160 knots, or minimize installed power, respectively. The power requirements for the alternate designs are compared to the baseline design in Figure 10. The original regression equations were used, but the objective functions and constraints were altered for each of the minimizations. The use of regression equations accommodates easily and efficiently the multiplicity of conditions required in a rotor design optimization study.

| | HOVER | 120 KNOTS | 160 KNOTS |
|--------------------------|-------------|-------------|-------------|
| BASELINE | 1501 | 1613 | 1740 |
| MINIMUM AT HOVER | 1498 | 1615 | 1744 |
| MINIMUM AT 120 | 1573 | 1508 | 1809 |
| MINIMUM AT 160 | 1576 | 1735 | 1698 |
| MINIMUM INSTALLED | 1559 | 1698 | 1698 |

Figure 10

SENSITIVITY - HORSEPOWER VERSUS TWIST AT 160 KNOTS

One of the primary advantages of using regression analysis is that the resulting approximation equations can be used rapidly and efficiently to perform sensitivity studies. An example of the results of such a study is shown in Figure 11. Horsepower is presented as a function of taper ratio and twist for two combinations of sweep and percent tip taper. Plots of this type, which can be obtained readily from the approximating equations, provide an understanding of the effects the independent variables have on rotor performance.

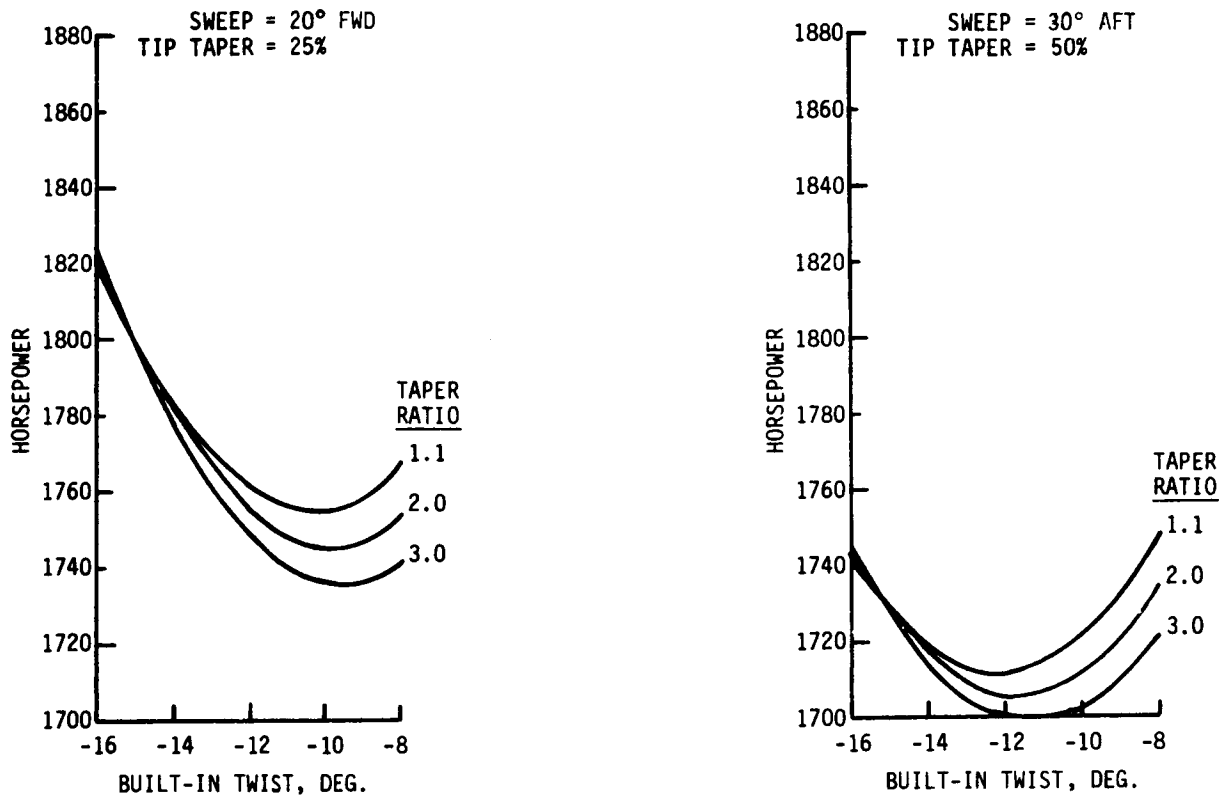


Figure 11

CONCLUSIONS

- Approximating equations can be developed rapidly for a multiplicity of objective and constraint functions and optimizations can be performed in a rapid and cost effective manner.
- The number and/or range of design variables can be increased by expanding the data base and developing approximating functions to reflect the expanded design space.
- The order of the approximating equations can be expanded easily to improve correlation between analyzer results and the approximating equations.
- Gradients of the approximating equations can be calculated easily and these gradients are smooth functions reducing the risk of numerical problems in the optimization.
- The use of approximating functions allows the problem to be started easily and rapidly from various initial designs to enhance the probability of finding a global optimum.
- The approximating equations are independent of the analysis or optimization codes used.
- The approximating equations can be developed using analytical or experimental data.
- Sensitivity and tradeoff studies can be accomplished at minimal cost.

N87-11756

**OPTIMIZATION OF HELICOPTER ROTOR BLADE
DESIGN FOR MINIMUM VIBRATION**

**M. W. Davis
United Technologies Research Center
East Hartford, Connecticut**

PRECEDING PAGE BLANK NOT FILMED

INTRODUCTION

The optimization approach discussed herein is part of an ongoing effort to develop a general automated procedure for rotor blade design. This procedure can be used to determine the necessary geometric, structural, and material properties of a rotor system to achieve desired design objectives relating to vibration, stress, and aerodynamic performance. This paper concentrates on the approach used for helicopter vibration. Based on analytical studies performed at the United Technologies Research Center (UTRC), a simplified vibration analysis has been developed to be used in conjunction with a forced response analysis in the optimization process. This simplified analysis improves the efficiency of the design process significantly. Results of applying this approach to the design of an existing rotor blade model will be presented.

ROTOR BLADE DESIGN OPTIMIZATION APPROACH

As shown in Figure 1, the approach for rotor blade design has been formulated as several separate component optimization problems concerned with areas such as vibration, stress, and aerodynamic performance. Appropriate constraint functions are formulated to account for the influence of design changes in areas other than those of primary concern for a given problem. After gaining experience with each component problem, the goal is to develop a completely integrated approach to optimize on several design considerations simultaneously. Based on experience with the individual optimization problems, it will be possible to better formulate an integrated and efficient overall approach. Furthermore, experience will be gained as to the design variables having the largest impact on each individual problem, the tradeoffs to be expected between various design considerations, and the capability to meet specified design criteria for a given problem.

- **Develop generic procedure applicable to all design considerations**

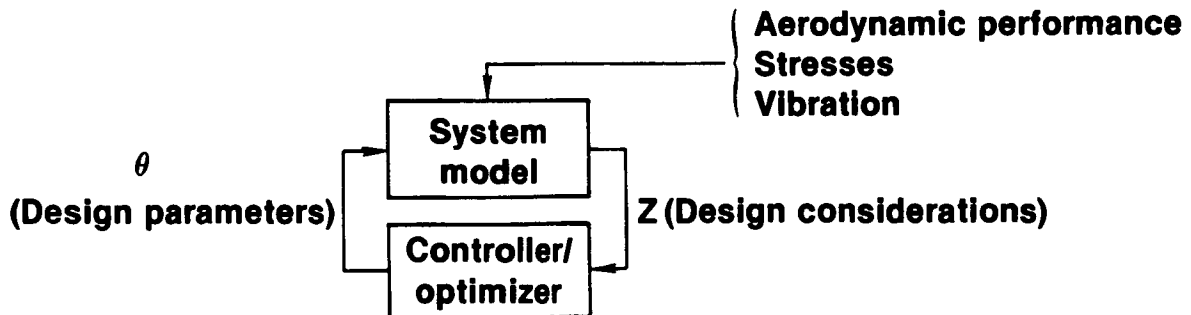


Figure 1

GENERAL DESIGN PARAMETERS AND CONSIDERATIONS

Figure 2 shows potential design parameters that might be used for one of the three component optimization problems shown in the previous figure. These include blade geometrical properties, primarily associated with aerodynamic performance; material properties, generally associated with blade stress; and structural properties, associated with vibration and stresses. Figure 2 also shows general considerations that must be accounted for in the overall design problem and therefore in each of the component problems. Depending on the problem being studied, these considerations may be used as objective functions to be optimized by appropriate selection of the design variables, as constraint functions to be satisfied, or as parameters to be monitored during the design sequence. In this paper, the vibration problem is of primary importance, and the design parameters used are mass and bending stiffnesses at radial stations along the blade.

- | • Typical parameters | • Typical considerations |
|--|---|
| <ul style="list-style-type: none">• Rotor radius• Chord• Twist• Airfoil• Sweep• Modal frequencies• Mode shapes• Mass• EI• GJ• CG axis• Elastic axis• Elastic limit• Endurance limit• Materials | <ul style="list-style-type: none">• Hover figure of merit• Cruise efficiency• Rotor flap inertia• Blade weight• Vibrations• Fatigue stresses• Steady stresses |

Figure 2

APPROACH FOR VIBRATION

Figure 3 outlines the approach to be used for helicopter vibration. In order to achieve the computer efficiency required of any useful design optimization tool, a simplified vibration analysis is used to develop the vibration parameters or criteria to be optimized. While the automated closed-loop design procedure can be formulated by using a forced response aeroelastic rotor analysis, the proposed optimization procedure uses a simplified analysis based on modal characteristics of the blade for the primary or inner loop. Since modal analyses are on the order of twenty times faster than forced response analyses, the potential savings in time is significant for the many iterations that may be required by any constrained optimization program. The forced response analysis G400 (Ref. 1) is then used to verify the vibration characteristics of the new blade design in the outer optimization loop, where closed-loop optimization can also be performed.

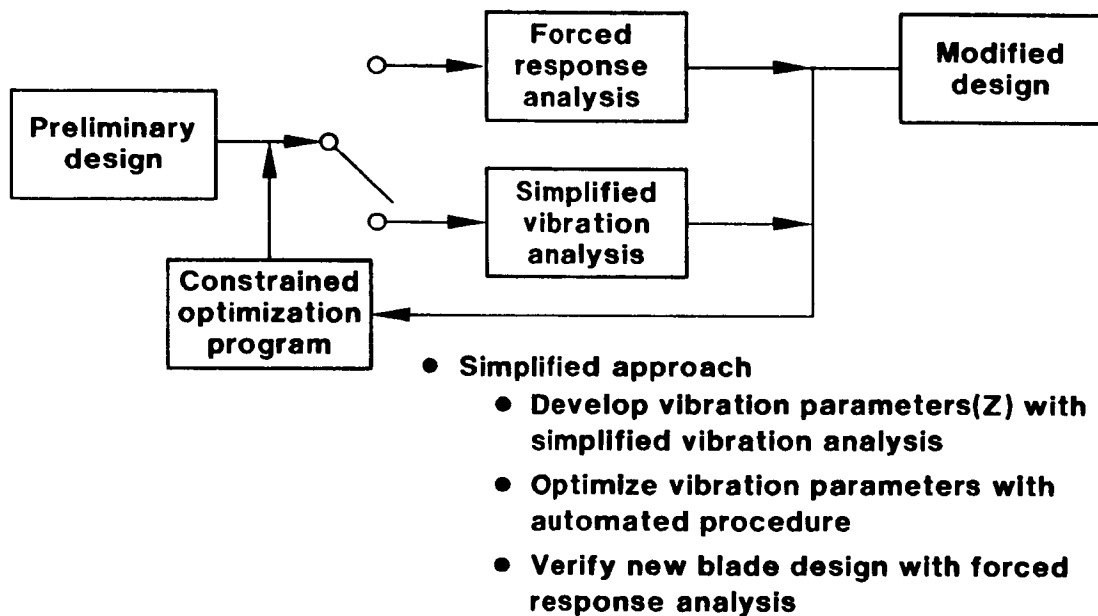
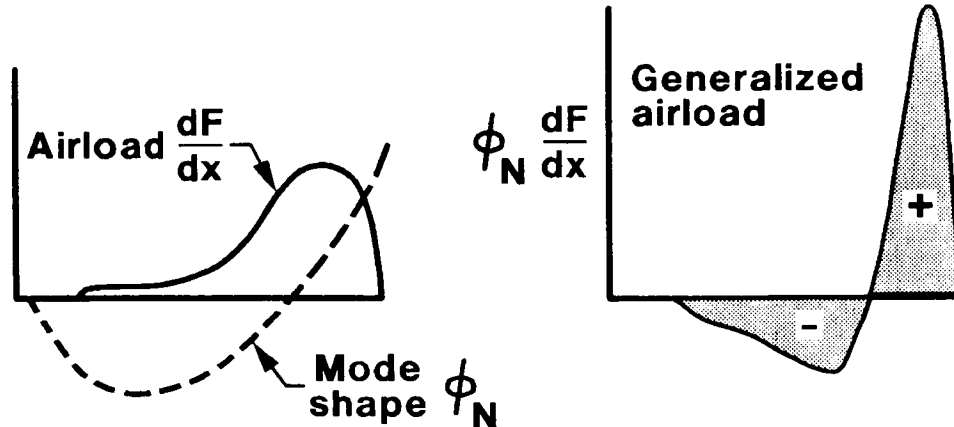


Figure 3

SIMPLIFIED ANALYSIS FOR VIBRATION

The simplified vibration analysis is based on the assumption that appropriate modal parameters can be defined that indirectly relate vibration characteristics to changes in blade design. Traditionally, frequency placement has been used to minimize vibration response. In recent studies at the United Technologies Research Center (UTRC) (Refs. 2 and 3), shaping of blade modes has also been shown to be important, and associated parameters have been identified as indicators of rotor blade sensitivity to vibratory airloads. In particular, it has been predicted that vibration can be reduced by minimizing certain weighted modal integrals. This is presented conceptually in Figure 4, where modal shaping is used to orthogonalize the Nth mode shape relative to the airloading distribution. In the simplified approach used for vibration, polynomial approximations to the airload distribution are used as weightings in the modal integrals. Mode shaping is accomplished by driving these generalized airloads to zero to desensitize the blade to vibratory airloading. In general, quadratic and/or cubic weighting terms are used to approximate airload distributions encountered in high speed flight conditions.

MODAL SHAPING DESIGN CONCEPT



- Desensitize blade to vibratory airloads by shaping of critical modes:

$$\text{Generalized airload} = \int \phi_N \frac{dF}{dx} dx \approx \int \phi_N \sum_j X_j^i dx \rightarrow 0$$

Figure 4

AUTOMATED DESIGN PROCEDURE USING THE SIMPLIFIED ANALYSIS

Figure 5 shows a more detailed schematic of the inner optimization loop shown in Figure 3. A blade eigensolution analysis (El59) is used to calculate blade frequencies and mode shapes for a given set of design variables. This information and the assumed airload distributions are used to calculate the appropriate modal integrals and the difference between the actual and optimum modal frequencies. Frequency placement and modal shaping are accomplished by simultaneously driving these parameters to zero via minimization of a quadratic performance index that consists of the weighted sum of the squares of each vibration parameter. The weighting matrix W_z is used to reflect the relative importance of each vibration parameter. The constrained optimization program used for the results presented in this paper is COPES/CONMIN (Refs. 4 and 5), which is based on the Method of Feasible Directions (Ref. 6). This program minimizes the performance index in an iterative manner. At each step, it attempts to satisfy all specified constraints, which may be either explicit or implicit functions of the design variables. As shown by the dashed line in Figure 5, blade frequencies and modal integrals can also be included as constraints rather than added to the performance index. Based on gradient and functional information for the objective and constraint functions, COPES/CONMIN calculates necessary changes in the design variables to further reduce the performance index at the current iteration. The necessary gradients are calculated by finite differences.

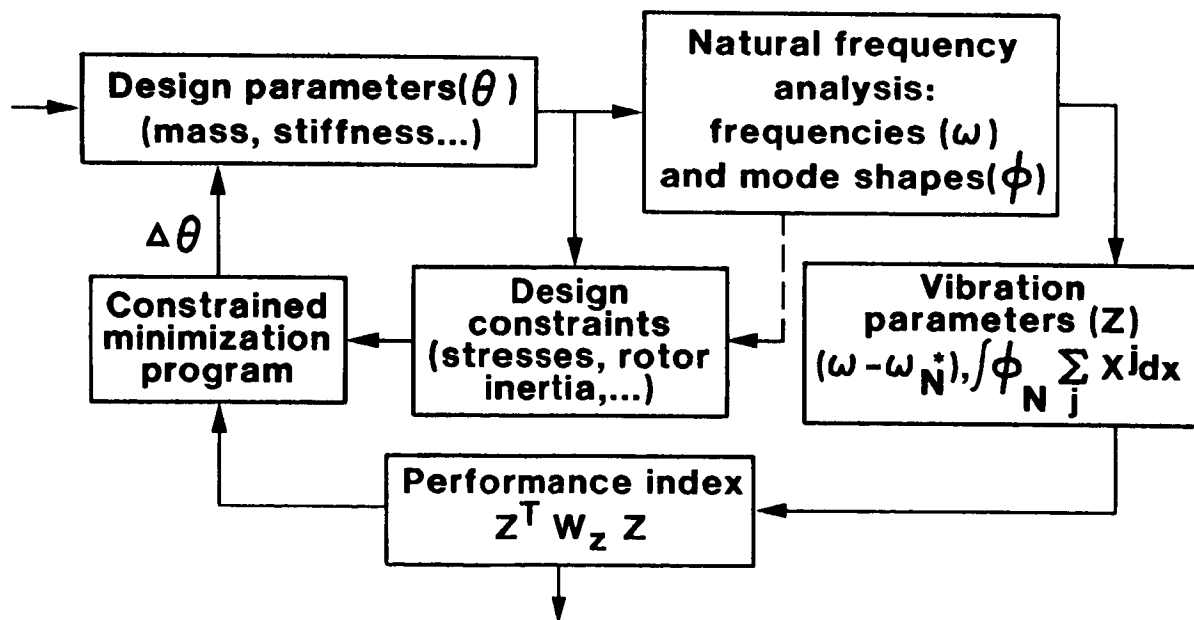


Figure 5

SAMPLE 6 X 30 DESIGN PROBLEM

Figure 6 shows the design variables to be used and the vibration parameters to be considered for reducing vibration by the approach outlined above. The problem is based on an articulated rotor operating at a steady 160 kt flight condition. Thirty (30) design variables are used in the frequency placement and modal shaping of three selected modes. The design variables consist of the flatwise and edgewise bending stiffnesses and the mass at each of ten (10) spanwise blade stations. An optimum frequency and modal integral are specified for each mode to give a total of six (6) vibration parameters to be driven to zero. The forced response analysis G400 has been used to identify the key modes and the associated frequency placement and modal shaping criteria for the articulated rotor investigated. The three modes selected are the first and second elastic flatwise modes and the first elastic edgewise mode. Recent analytical studies at UTRC have shown these modes to be of particular importance for this articulated rotor (Ref. 3). Although torsion frequencies and mode shapes are also important, no active frequency placement or modal shaping of torsional modes are attempted in this preliminary study. The modal integral used for each mode includes a cubic weighting function of the blade spanwise location (x) to approximate the airloading for this high speed flight condition.

Articulated rotor 160 kt

● 6 vibration design considerations

| Frequencies | Modal integrals |
|---------------|-------------------------|
| ω_{1F} | $\int \phi_{1F} x^3 dx$ |
| ω_{2F} | $\int \phi_{2F} x^3 dx$ |
| ω_{1E} | $\int \phi_{1E} x^3 dx$ |

● 30 spanwise design variables

- 10 masses
- 10 flatwise stiffnesses
- 10 edgewise stiffnesses

Figure 6

RESULTS FOR 6 X 30 DESIGN PROBLEM

Results for recent analytical studies at UTRC (Ref. 3) indicate the potential for reduced vibration response in this articulated rotor if the first elastic flatwise and edgewise frequencies can be tuned to the range of 3.2 to 3.5/rev and of 5.5 to 5.7/rev, respectively. These studies also showed shaping of the first and second elastic flatwise modes to be of prime importance. Thus, the objectives of this design problem are to meet the specified frequency criteria and to drive the first two flatwise modal integrals with cubic weighting (Fig. 6) to zero. The second flatwise frequency and the first edgewise modal integral are monitored but not included in the performance index. Other than practical upper and lower bounds on each design variable, no constraints are placed on the design space. Thus, bounds are placed on the mass at each radial blade station, but no attempt is made to achieve the lightest blade possible. The baseline blade is based on an existing production rotor blade. Figure 7 indicates the success of the automated design procedure in placing the first flatwise and edgewise frequencies at their desired values. Furthermore, the first two flatwise modal integrals are reduced by over 98 percent. As added benefits, the second flatwise frequency is driven away from 5/rev and the first edgewise modal integral is reduced by over 95 percent. However, the final design results in a 20 percent increase in blade weight.

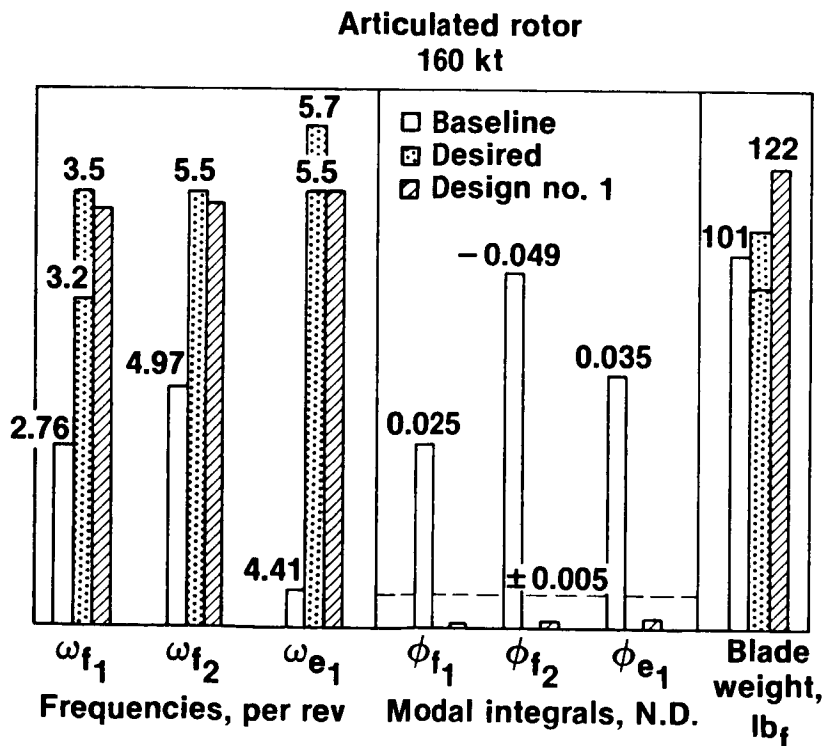


Figure 7

RESULTS OF BLADE WEIGHT MINIMIZATION

While the first design case demonstrates the capability to achieve significant changes in blade modal properties, the final blade weight is too high. Therefore, the automated designer is used to redesign the blade to minimize weight while maintaining essentially the same modal properties shown in Figure 7. In this design problem, blade weight is added to the performance index used above. Furthermore, constraints of ± 0.005 are applied to the first two flatwise modal integrals to ensure that the minimum values shown in Figure 7 are maintained. Note that this constraint corresponds to the dashed line shown in Figure 7. Design No. 1, achieved above, is used as the preliminary design for optimization. As shown in Figure 8, the automated designer met all the specified criteria on the primary vibration parameters while reducing the blade weight of Design No. 2 to 104 lb, which is only 3 percent heavier than the baseline blade. Once again, appropriate lower bounds have been placed on the mass design variables. These results are achieved in one computer run, which requires only 11.5 CPU minutes on a UNIVAC 1100 machine.

Articulated rotor 160 kt

| | ω_{1f} | ω_{1e} | ϕ_{1f} | ϕ_{2f} | Blade weight |
|--------------|---------------|---------------|-----------------|-----------------|--------------|
| Baseline | 2.76 | 4.41 | 0.0253 | - 0.0489 | 101 |
| Design no. 1 | 3.44 | 5.51 | 0.0009 | - 0.0025 | 122 |
| Design no. 2 | 3.40 | 5.78 | 0.0050 | - 0.0029 | 104 |
| Desired | 3.2 — 3.5 | 5.5 — 5.7 | 0.0 ± 0.005 | 0.0 ± 0.005 | — |

Figure 8

MODIFIED MASS DISTRIBUTION FOR 6 X 30 DESIGN PROBLEM

Figure 9 shows the final mass distribution for Design No. 2, which was used for the results presented above. Also shown in this figure is the distribution for the baseline production blade. The cross-hatched region represents blade root end hardware which has not been modified. While the blade weights for both the production blade and Design No. 2 are about the same, the mass distributions are significantly different. The automated designer has shifted almost 15 lb from mid-span to the outer 25 percent of the blade. This is required to achieve the substantial increase specified in the first flatwise natural frequency. As an added benefit, the increased mass outboard also improves rotor auto-rotation characteristics.

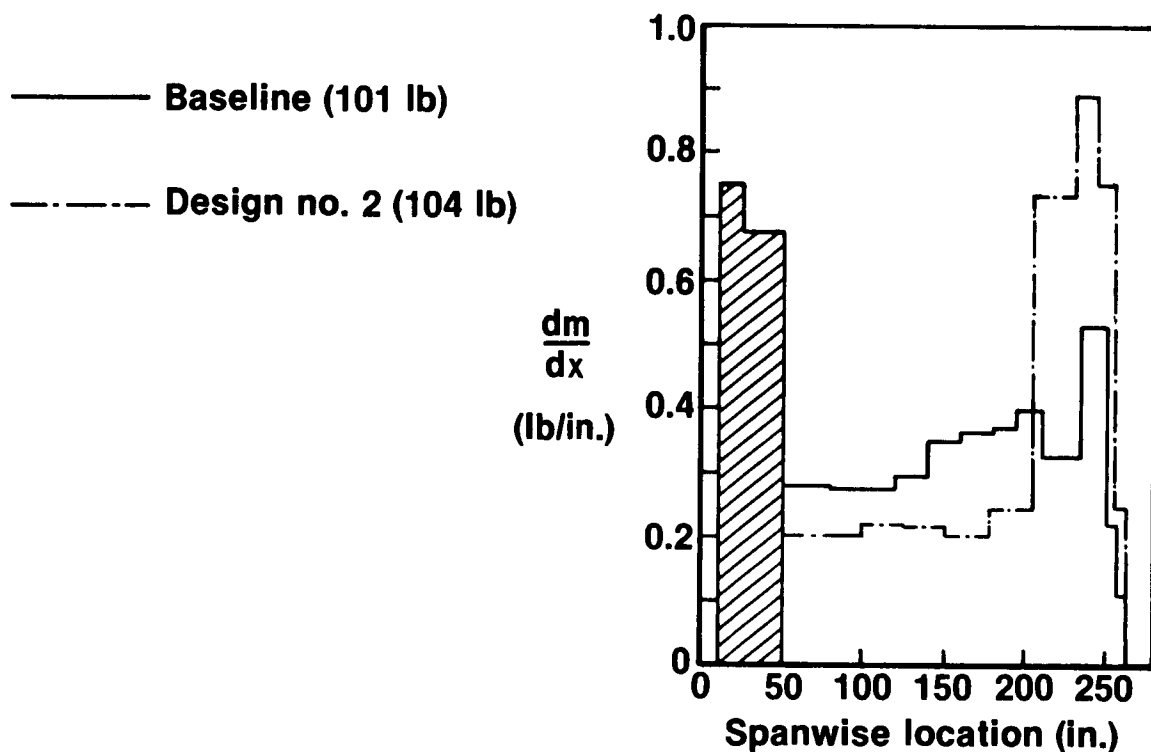


Figure 9

MODIFIED EDGEWISE STIFFNESS FOR 6 X 30 PROBLEM

Figure 10 compares the final edgewise stiffness along the blade span for Design No. 2 to that of the baseline production helicopter. The cross-hatched region represents the invariant root end hardware. As indicated, about a 40 percent increase in edgewise stiffness across most of the blade span is required to achieve the high frequency specified for the first elastic edgewise mode. Although not shown, changes made by the automated designer in flatwise stiffness along the blade span are insignificant, since flatwise frequency and mode shape requirements are accomplished through changes in the spanwise mass distribution.

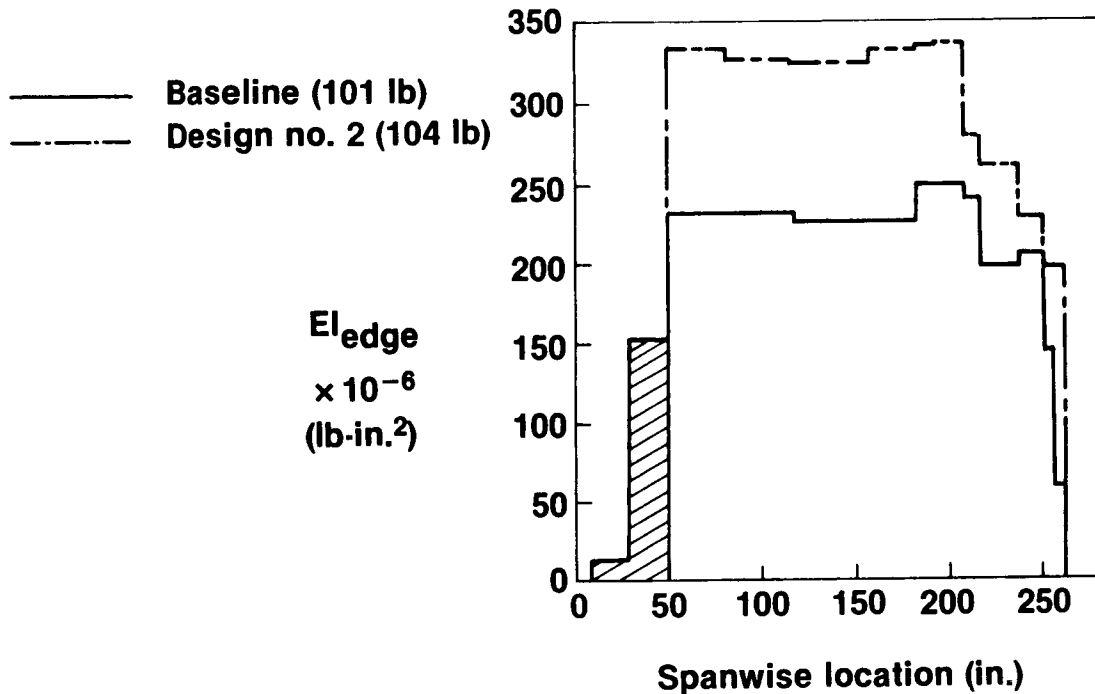


Figure 10

PREDICTED VIBRATORY HUB LOADS

Figure 11 compares the vibratory hub loads (fixed system) predicted by the forced response analysis G400 for the baseline blade and for Design No. 2. The two inplane shears have been reduced by over 65 percent and the vertical shear by 20 percent. The vibratory hub moments are shown only for reference, since the hub moments make an insignificant contribution to fuselage vibration for this articulated rotor. Since the two inplane shears have been previously identified as primary contributors to fuselage vibration in this rotorcraft (Ref. 3), the particular frequencies and modal integrals shown in Figure 6 were selected to reduce the response of these two components.

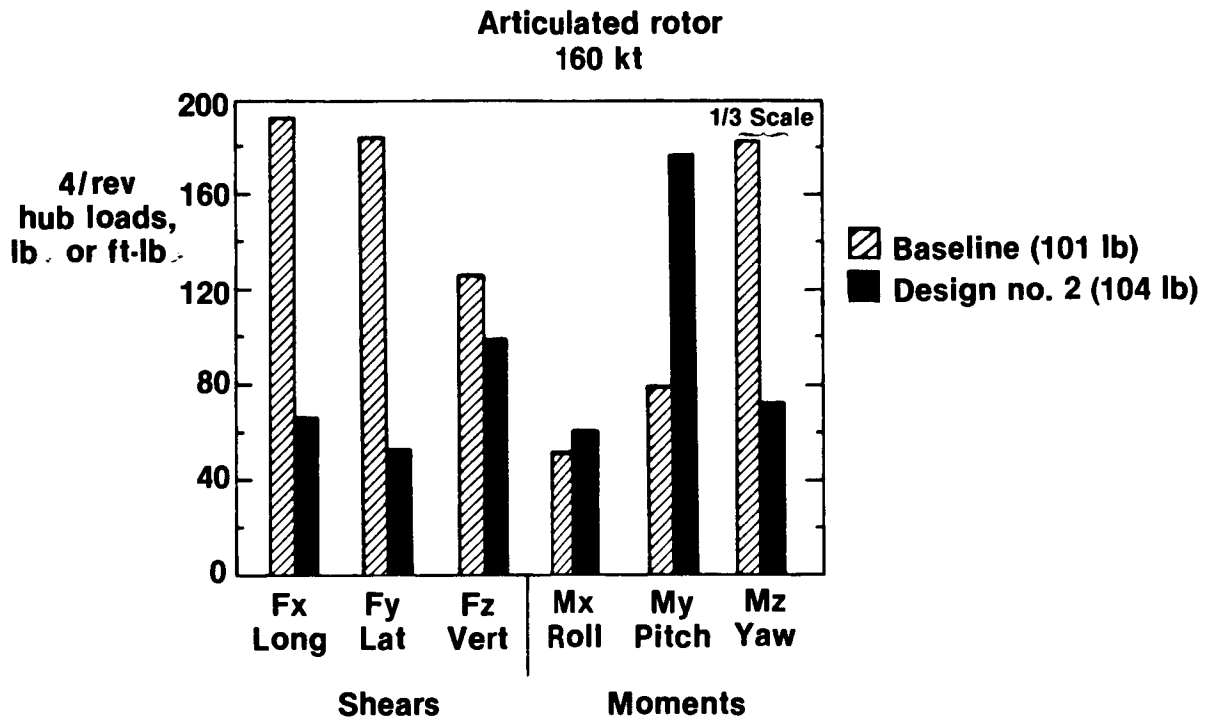


Figure 11

PREDICTED FUSELAGE VIBRATIONS

Figure 12 shows the predicted 4/rev vibrations in the cockpit and cabin for the baseline design and Design No. 2. As a result of frequency placement and modal shaping to reduce the inplane and vertical hub shears, reductions in vibration on the order of 50 percent have been achieved at all components except pilot seat vertical. The low baseline value of this component has been maintained.

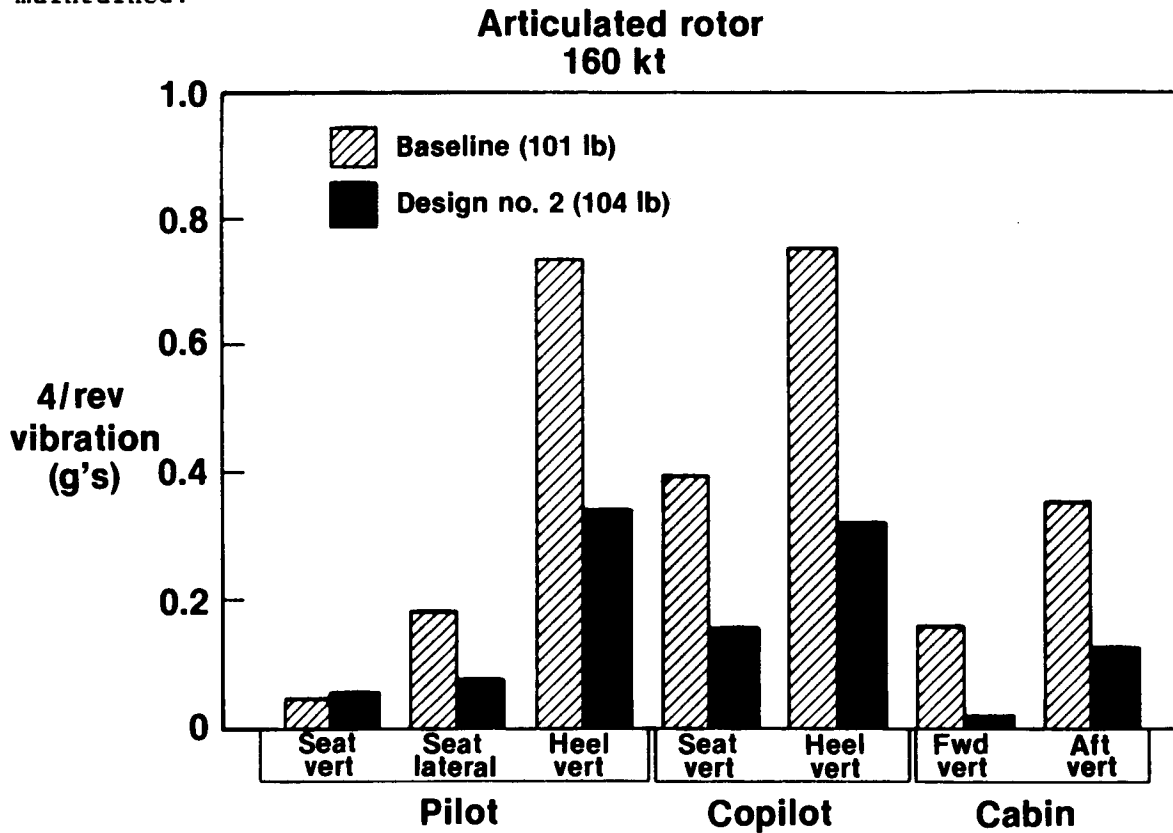


Figure 12

PREDICTED VIBRATORY STRESSES

Figure 13 shows the blade spanwise 1/2 peak-to-peak vibratory stresses predicted for both the baseline and Design No. 2. Significant reductions in flatwise and edgewise bending stresses and in torsional stress have been achieved all along the blade span. Reductions of nearly 50 percent have been achieved at all the critical stress areas (outboard flatwise, midspan edgewise, and inboard torsional) despite the lack of stress constraints and stress terms in the performance index. This indicates that reductions can be achieved in both fuselage vibration and blade stresses when blade frequencies and mode shapes are appropriately tailored.

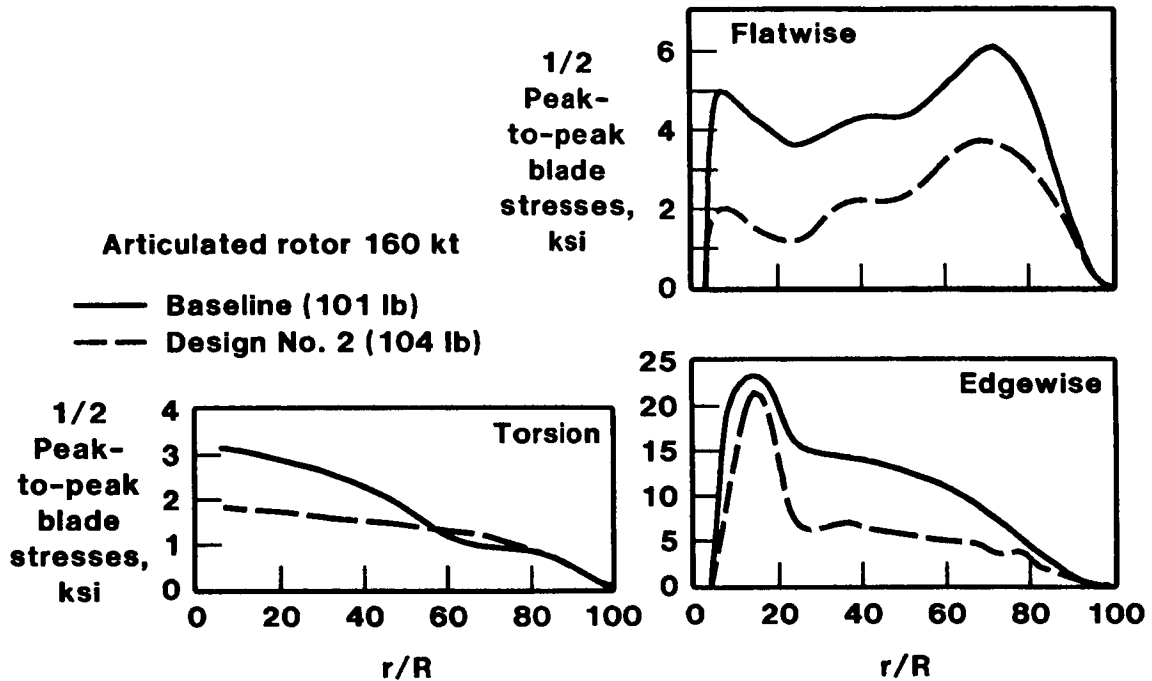


Figure 13

CONCLUDING REMARKS

This paper has outlined a simplified approach for minimizing vibration in a rotorcraft. Rather than using a forced response analysis for the bulk of the design optimization process, a modal analysis has been used to calculate key vibration parameters that have been identified as being indicative of blade sensitivity to vibratory airloading. These parameters are based on blade modal frequencies and generalized airload integrals. By driving these modal parameters to zero, it is possible to place frequencies and to tailor mode shapes for reduced vibration in the fuselage. The forced response aeroelastic analysis G400 has been used to identify the key modes and associated frequency placement and modal shaping criteria for the articulated rotor investigated. The forced response analysis has also been used to verify the vibration characteristics of new blade designs. This approach of using both modal and forced response analyses for the optimization of blade structural properties has predicted reductions in fuselage vibration on the order of 50 percent in a computationally efficient manner. An added benefit of appropriate modal tailoring is the reduction of blade stresses along the entire blade span. The results of applying this approach indicate that blade modal properties can be changed to achieve significant improvements in both fuselage vibration and blade stress. Furthermore, these changes in modal properties can be achieved with practical blade designs and without significant weight penalties. While these preliminary results are not yet substantiated by experiment, they demonstrate the application of optimization techniques to existing methodology. Optimization studies will be continued and expanded to include aerodynamic considerations in the design process.

REFERENCES

1. Bielawa, R. L.: Aeorelastic Analysis for Helicopter Rotors with Blade Appended Pendulum Absorbers - Program User's Manual. NASA CR-165896, June 1982.
2. Taylor, R. B.: Helicopter Vibration Reduction by Rotor Blade Modal Shaping. Presented at the 38th Annual Forum of the American Helicopter Society, Anaheim CA, May 4-7, 1982.
3. Taylor, R. B.: Helicopter Rotor Blade Design for Minimum Vibration. UTRC Report R83-915783-27, United Technology Research Center, December 1983.
4. Madsen, L. E.; and G. N. Vanderplaats: Copes--A Fortran Control Program for Engineering Synthesis. Naval Postgraduate School, Report No. NPS69-81-003, March 1982.
5. Vanderplaats, G. N.: Conmin--A Fortran Program for Constrained Function Minimization; User's Manual. NASA TM X-62282, August 1982.
6. Vanderplaats, G. N.; and F. Moses: Structural Optimization by Methods of Feasible Directions. Computers and Structures, Vol. 3, 1973, pp. 739-755.

C-2

APPLICATION OF NUMERICAL OPTIMIZATION
TO ROTOR AERODYNAMIC DESIGN

W. A. Pleasants III and T. J. Wiggins
Applied Technology Laboratory
Ft. Eustis, Virginia

PRECEDING PAGE BLANK NOT FILMED

ADVANCED DESIGN REQUIREMENTS

The concept formulation for the Army family of light rotorcraft (LHX) has resulted in greatly increased demands for accurate projections of rotary wing technology to support independent government preliminary design trade-off studies. The concept formulation process is presented in detail in reference 1. Figure 1 shows the diversity of requirements which must be addressed in rotor design for LHX. This paper will present the experience gained in the implementation and application of existing optimization and analysis methods to rotor aerodynamic design. The objective of the optimization effort was to obtain major reductions in the calendar time and man-hours required to predict advanced rotor performance for the multiple design points of advanced Army aircraft concepts. While typical results of optimization will be presented, the paper will concentrate on program structure and approach, analysis and optimization problems, and areas requiring additional effort.

- INCREASED SPEED
- HIGH ALTITUDE, HOT DAY ENVIRONMENT
- EXTENDED RANGE
- AIR-TO-AIR COMBAT
- COMMONALITY OF DYNAMIC COMPONENTS

Figure 1

PROGRAM STRUCTURE AND APPROACH

Figure 2 illustrates the basic program structure obtained by combining the FRANOP/CONMIN optimization codes of references 2 and 3 with the Bell Helicopter A7906 hover code of reference 4 and the forward-flight code of reference 5. A preliminary design level weights analysis and simple representation of engine performance were added to allow evaluation of rotor design on the total helicopter design. Modular design of the computer program was an important consideration in developing the optimization code. Experience was first gained with the optimizer using simple, low cost analysis methods. As simple analysis methods were replaced with the more complex methods, the range of design variables, constraints, and objective function was expanded and considerations for overall aircraft design were added. The ability to easily add to or modify the objective functions, constraints, or even the basic analysis was of critical importance in responding to rapidly changing design requirements. In addition, the modular structure will allow the future use of alternate optimization codes with minimal impact on the remainder of the code. No attempt to use approximate analysis or other approaches for increased efficiency was attempted as computer costs were a secondary concern to manpower available to implement the analysis.

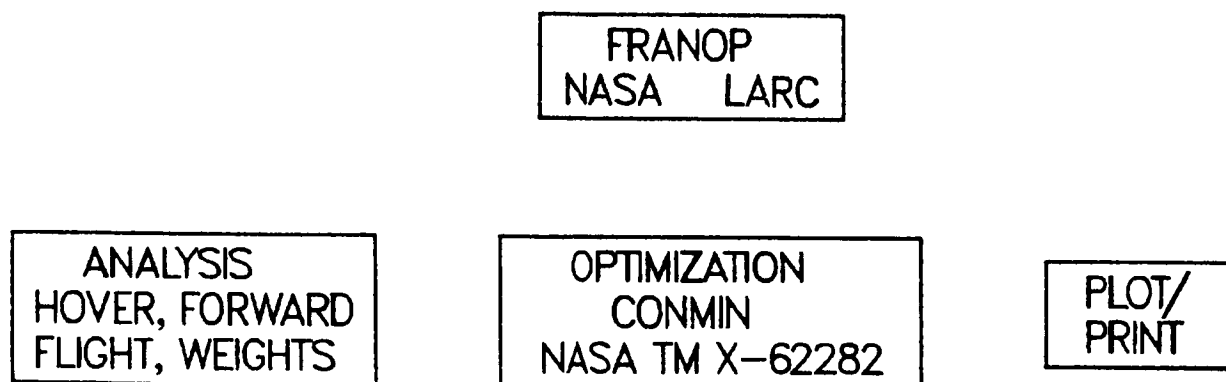


Figure 2

THE OPTIMIZATION PROBLEM

In general, the optimization problem may be given as:

$$F(X) \rightarrow \min$$

subject to

$$g_j(X) < 0 \quad 1 < j < m$$

where X is a vector of design variables, $F(X)$ is an objective function to be minimized, and $g(X)$ are constraint equations. In addition, CONMIN allows side constraints, or upper and lower limits, to be imposed on the design variables. The typical design problem has a well-defined design requirement which leads to an optimum design. The Army concept formulation process requires an optimization process which is responsive to rapidly changing and widely varying design requirements. Figure 3 shows the options now available for design variables, objective functions and constraints. Objective functions, design variables, and constraints may be selected in any meaningful combination. While some design variables are obviously redundant, care must also be exercised in selection of design variables so that they are compatible with the problem. Selection of design variables to which the objective function is insensitive can result in large amounts of computer time expended for very little benefit.

$$F(x) \rightarrow \text{MINIMUM}$$

$$\text{SUBJECT TO } G_j(x) < 0 \quad 1 < j < m$$

DESIGN VARIABLES

- LINEAR TWIST
- RADIUS
- TIP SPEED
- EQUIVALENT CHORD
- LINEAR TAPER RATIO
- RADIAL STATION AT WHICH TAPER BEGINS
- LOCAL TWIST
- LOCAL CHORD
- LOCAL AIRFOIL

OBJECTIVE FUNCTION

- ENGINE SIZE
- L/D
- DYNAMIC SYSTEM WEIGHT
- FUEL WEIGHT

CONSTRAINTS

- STALL CRITERIA
- ENGINE SIZE

Figure 3

PROGRAM CONTROL

The Framework for Analysis and Optimization Problems (FRANOP) computer code provides the general purpose framework used in implementing the optimization problem described here. The primary functions of FRANOP are tabulated in figure 4. From the viewpoint of a user who is interested in using existing optimization methods to provide better and faster solutions to existing design problems, FRANOP has several features worthy of note. First, the ability to conduct single point analysis was found to be highly useful in the implementation of analysis additions and/or modifications. The ability to conduct sensitivity analysis was found to be useful in defining the exact behavior of the objective function problem areas for the optimizer. Finally, it was found in most cases that the output of the optimizer alone was inadequate to fully understand the design process. FRANOP can be easily modified to provide for tabulation of any desired output from the analysis. This output provides an excellent compromise between "being buried in paper" and operating with a "black box" for which the user has only the input and final answers.

FRAMEWORK FOR ANALYSIS AND OPTIMIZATION PROBLEMS (FRANOP)

- SINGLE POINT ANALYSIS
- SENSITIVITY ANALYSIS
- OPTIMIZATION
- TABULATION & OUTPUT OF DATA

Figure 4

ANALYSIS

The functions of the analysis section of the optimization program are shown in figure 5. In developing the analysis section of the optimization program, two constraints were imposed. First, the optimization program would use existing rotor performance methods with minimum changes. Second, the interface between the optimization routines and performance methods would have maximum flexibility in selection of design variables, design conditions, objective functions, and constraints. This flexibility was found to be necessary to investigate widely varying design requirements, but it places a greater requirement on the user to select reasonable design variables and objective functions. Selection of design variables which have minimal impact on the objective function or which result in unrealistic designs can waste large amounts of computer time.

OPTIMIZATION ANALYSIS FUNCTIONS

- INTERFACE BETWEEN OPTIMIZER AND PERFORMANCE METHODS
- ONE TIME PERFORMANCE METHOD INPUT
- DESIGN VARIABLE SELECTION
- OBJECTIVE FUNCTION AND CONSTRAINT DEFINITION
- SELECTION AND EVALUATION OF DESIGN CONDITIONS
(HOVER,CRUISE,MANEUVER)

Figure 5

PERFORMANCE METHODS

The major characteristics of the performance methods selected are shown in figure 6. These methods are generally well correlated for existing and developmental rotor designs and flight conditions. Availability of program documentation, ease of modification and integration with the optimizer correlation data base, and sensitivity to the desired design variables were the primary factors in selecting the analysis methods. For example, representation of the rotor wake in hover is necessary to obtain realistic sensitivities of performance to nonlinear twist. Also, rotor design is a compromise between a number of possible design conditions and can strongly drive other areas of the rotorcraft design. Preliminary design level weights prediction and engine representation were incorporated to allow best overall system design as opposed to optimum isolated rotor design for a single point.

A7906 HOVER ANALYSIS

- LIFTING SURFACE ANALYSIS
- CIRCULATION COUPLED WAKE
- VERTICAL DRAG CALCULATION OPTION
- WELL CORRELATED

ROTOR FORWARD FLIGHT ANALYSIS

- STRIP ANALYSIS METHOD
- RIGID BLADE
- TRIM LIFT AND DRAG
- ROTOR WAKE NOT DIRECTLY INCLUDED
- CORRELATED FOR CRUISE AND MANEUVER

WEIGHTS ANALYSIS

- PARAMETRIC PRELIMINARY DESIGN LEVEL
- ROTOR, ENGINE, DRIVE SYSTEM, FLIGHT CONTROLS AND FUEL SYSTEM

ENGINE CHARACTERISTICS

- POWER AND FUEL FLOW

Figure 6

ANALYSIS PROBLEMS

The major problems encountered in implementation of the analysis portion of the optimization code were the failure of the performance methods to converge near the boundaries of the rotor operational envelope shown in figure 7 and the fact that for some combinations of design variables, there will be no answer and the analysis methods will diverge. Considerable effort was devoted to providing more efficient and stable rotor trim methods. It was also found necessary to deal with occasional near failures of the analysis to converge. In those cases the analysis was close to trim but had the potential to distort partial derivatives. A much less obvious problem with the analysis methods was that the optimization could lead to designs well outside the correlation base of the performance methods. In this case, the user must then carefully consider the validity and level of confidence in the optimization results.

ROTOR THRUST LIMIT

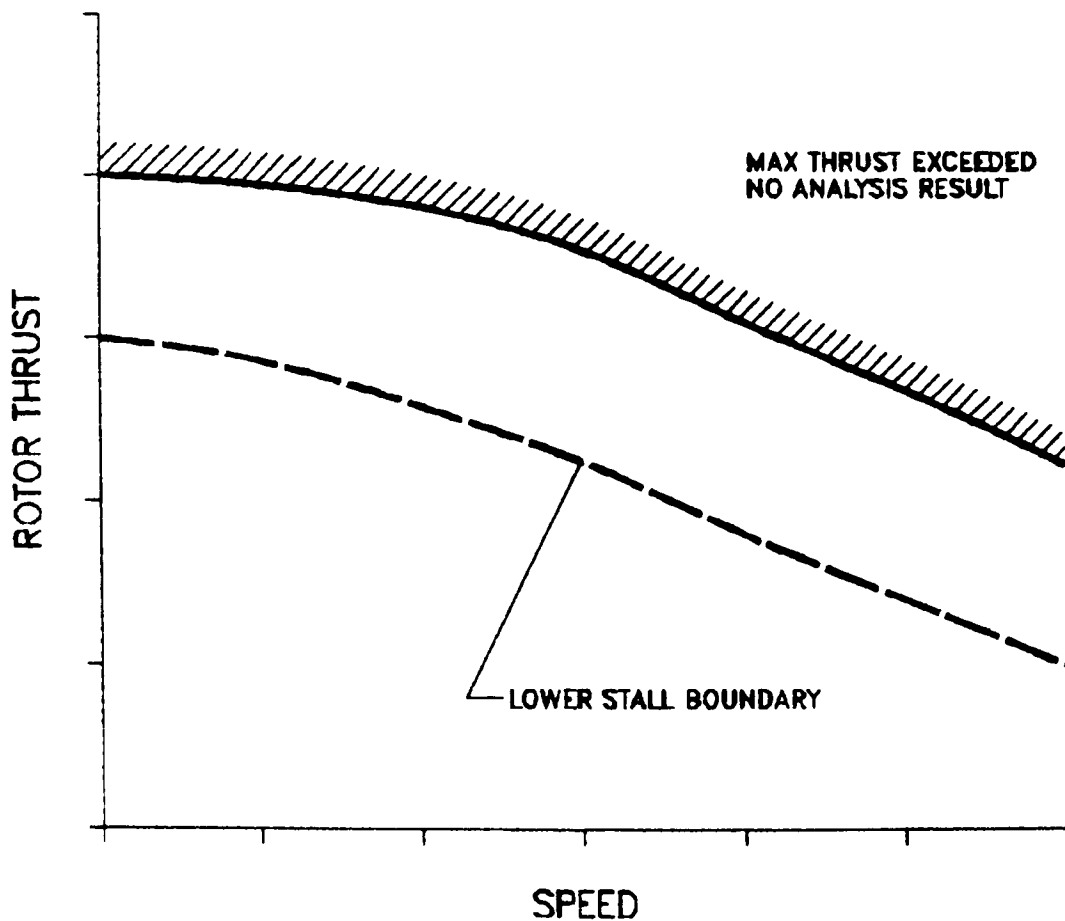


Figure 7

OPTIMIZATION PROBLEMS

Figure 8 summarizes the major problem areas with the optimizer from the viewpoint of the user. Scaling of design variables and/or finite difference objective function gradients was generally necessary for efficient optimization. It was necessary to modify the optimizer to increase flexibility in dealing with scaling. The objective functions used in this effort exhibited widely varying sensitivity to the design variables. Near an optimum the objective function often had a wide region of the design space where little change took place. It was often desirable to conduct sensitivity analysis to illustrate the overall behavior of the objective function. Optimizer output was generally adequate to monitor the overall optimization process but was not adequate to monitor the overall design process. Iteration histories of key analysis outputs during the optimization process were a major help in eliminating the feeling that the user is dependent on a "black box." Finally, finite difference derivatives must be taken with increments in design variables sufficiently large to insure that partial derivatives are outside the "noise" level of the analysis. Optimization program defaults were found to yield unsatisfactory finite difference derivatives in many cases.

- SCALING
- LACK OF FLEXIBILITY
- SENSITIVITY OF OBJECTIVE FUNCTIONS TO DESIGN VARIABLES
- OUTPUT
- FINITE DIFFERENCE DERIVATIVES

Figure 8

ROTOR DESIGN

Figure 9 illustrates some typical sensitivities obtained in attempting to design a rotor for improved performance over a range of design conditions. Note that different design conditions do tend to yield the same optimum and thus rotor design is often a compromise between a number of different conditions. Also note that the objective function may be very insensitive to a specific design variable near the optimum. Optimizer response to this condition is frequently the failure to converge on a single optimum when started from different conditions.

OBJECTIVE FUNCTION SENSITIVITY

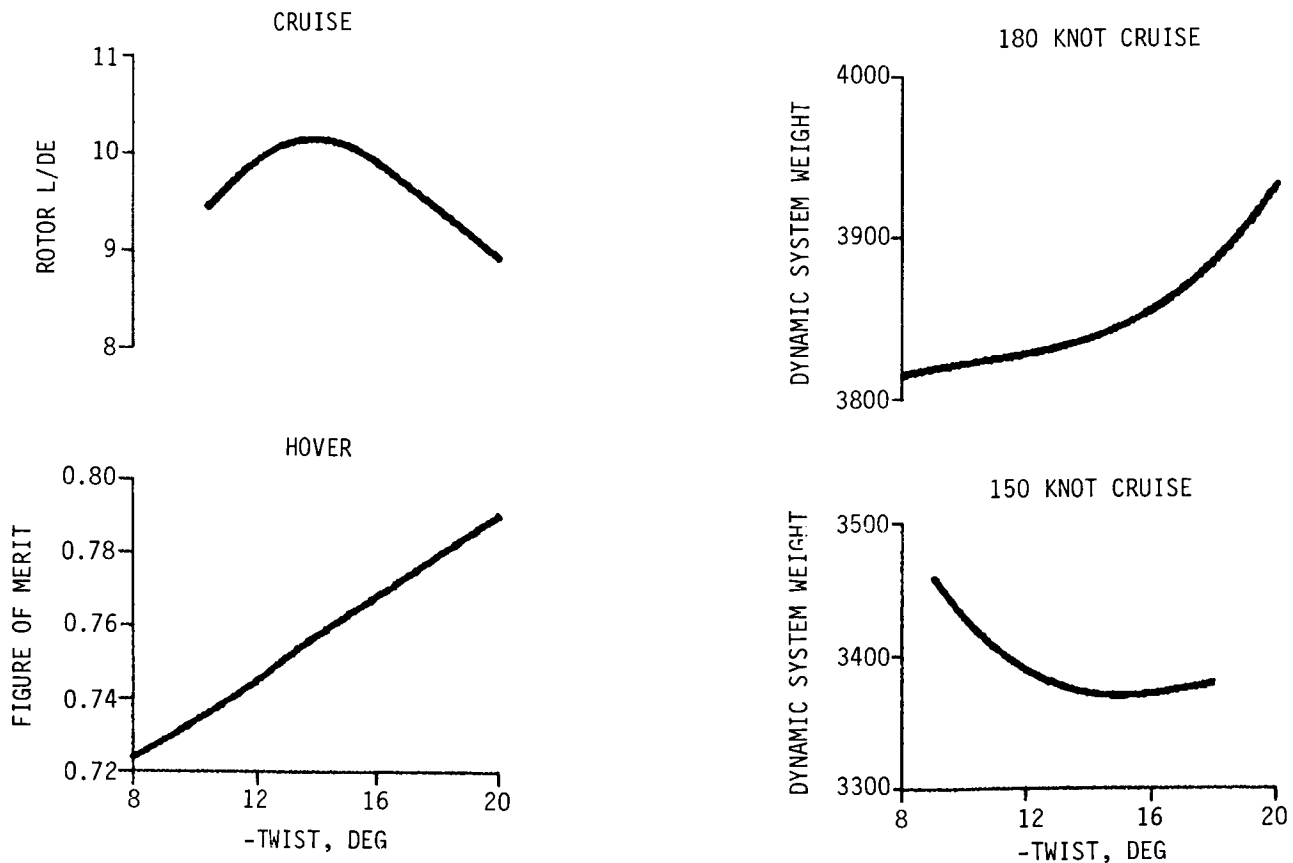
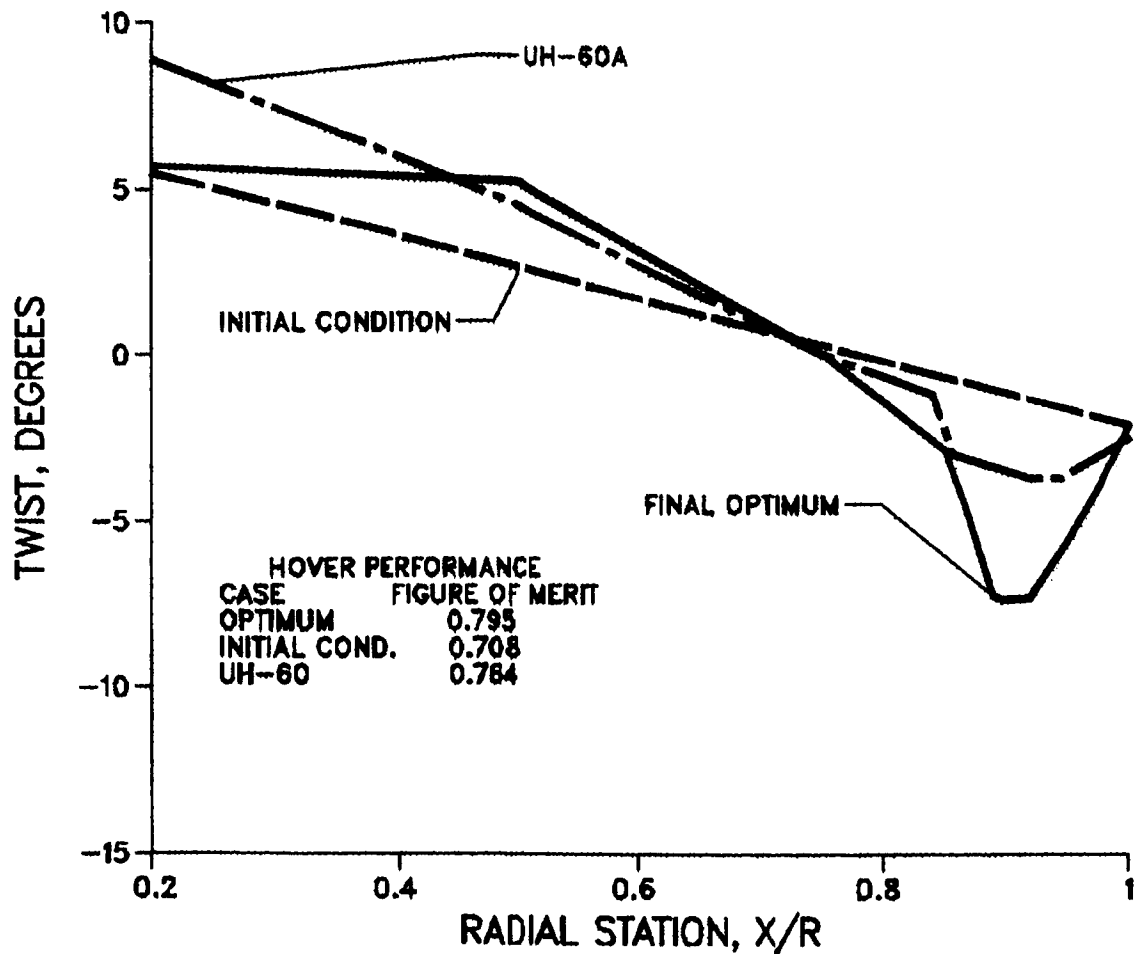


Figure 9

HOVER OPTIMIZATION

Figure 10 shows the results of two hover optimizations. Figure 10a illustrates a nonlinear twist optimization based on the UH-60 rotor chord, radius, and airfoils. Starting from a -10° linear twist, the optimizer produced a nonlinear twist characteristic of the UH-60, but with improved performance. Additional effort would be required to determine if the analysis results were valid and the rotor could be built. Note that highly nonlinear behavior of the rotor twist was represented with a relatively small number of design variables. This was accomplished through the use of a combination of linear and nonlinear interpolation methods which reduce the required number of design variables from fifteen to six. This approach was also used to reduce the number of design variables required to represent airfoil distributions and chord as a function of radius. Figure 10b illustrates a second hover optimization. Note that if the objective function is insensitive to a particular design variable, the optimizer used tends to leave it at the initial value.

HOVER DESIGN

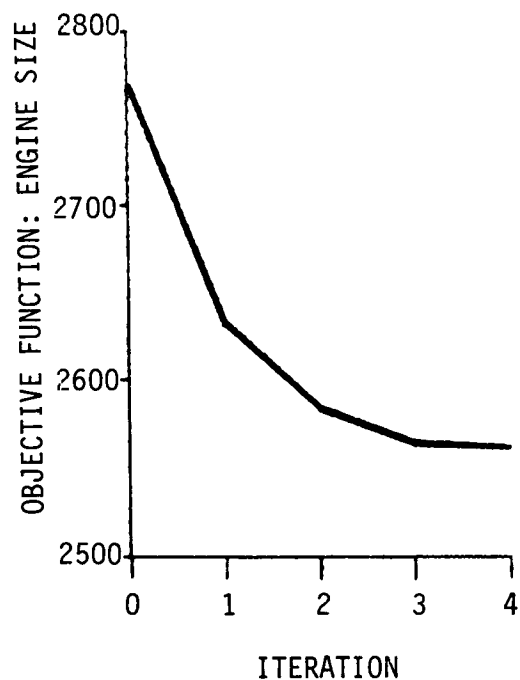
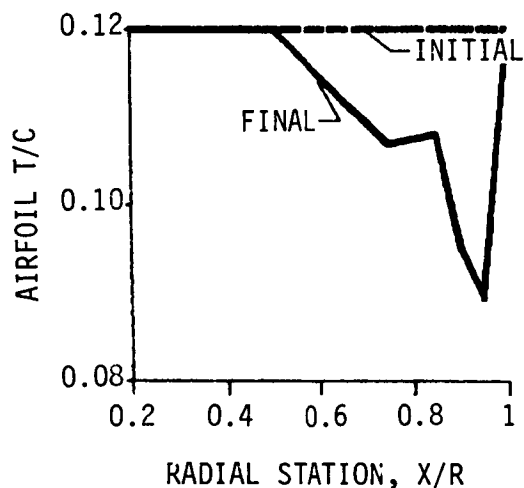


(a)
Figure 10

HOVER OPTIMIZATION

| VARIABLE | INITIAL | FINAL |
|----------|---------|-------|
| TWIST | -17.0 | -25.0 |
| TAPER | 0.760 | 0.507 |

NOTE: TWIST LOWER LIMIT IS -25 DEG



(b)
Figure 10

SUSTAINED MANEUVER

Figure 11 shows the results of a rotor design optimized for a 1.5 g sustained load factor maneuver. A total of eleven design variables were used together with a rotor stall criteria constraint. The optimizer revealed a minimum in two to three iterations, as was typically the case. The initial condition was chosen to be near or to violate the stall criteria constraint. Note that the optimizer moved chord, tip speed, and airfoil thickness (t/c) in a direction which would increase the lift capability of the rotor.

| VARIABLE | INITIAL | FINAL |
|-----------|---------|-------|
| RADIUS | 26.8 | 27.0 |
| TWIST | -18.0 | -21.1 |
| TIP SPEED | 725. | 735. |
| CHORD | 1.74 | 1.77 |

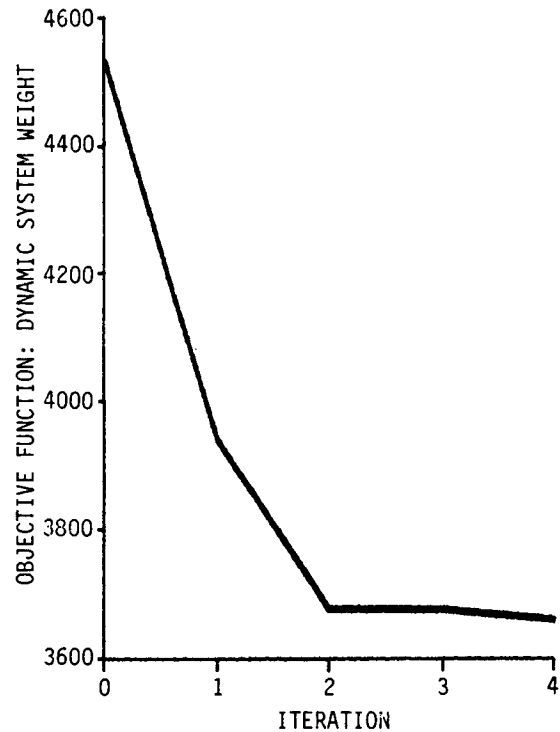
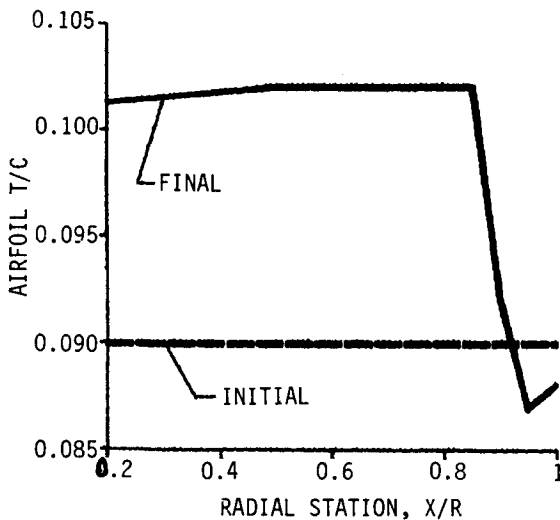


Figure 11

HIGH SPEED CRUISE

Figure 12 shows the results of a rotor optimization for a 180-knot cruise. Design variables, constraints and objective functions were identical to those used for the problem shown in Figure 11. The optimizer effectively revealed a minimum in three iterations, although an additional five iterations were forced to explore behavior of the optimizer. Oscillations in the objective function after the third iteration were more directly related to performance method convergence than to improved design. Movement of the design variables was in a direction which tailored the rotor to the high Mach number conditions. Also note that hover, cruise, and maneuver design conditions do not generally produce compatible designs and it may be necessary to consider all design points simultaneously to produce a design representing the best compromise between all requirements.

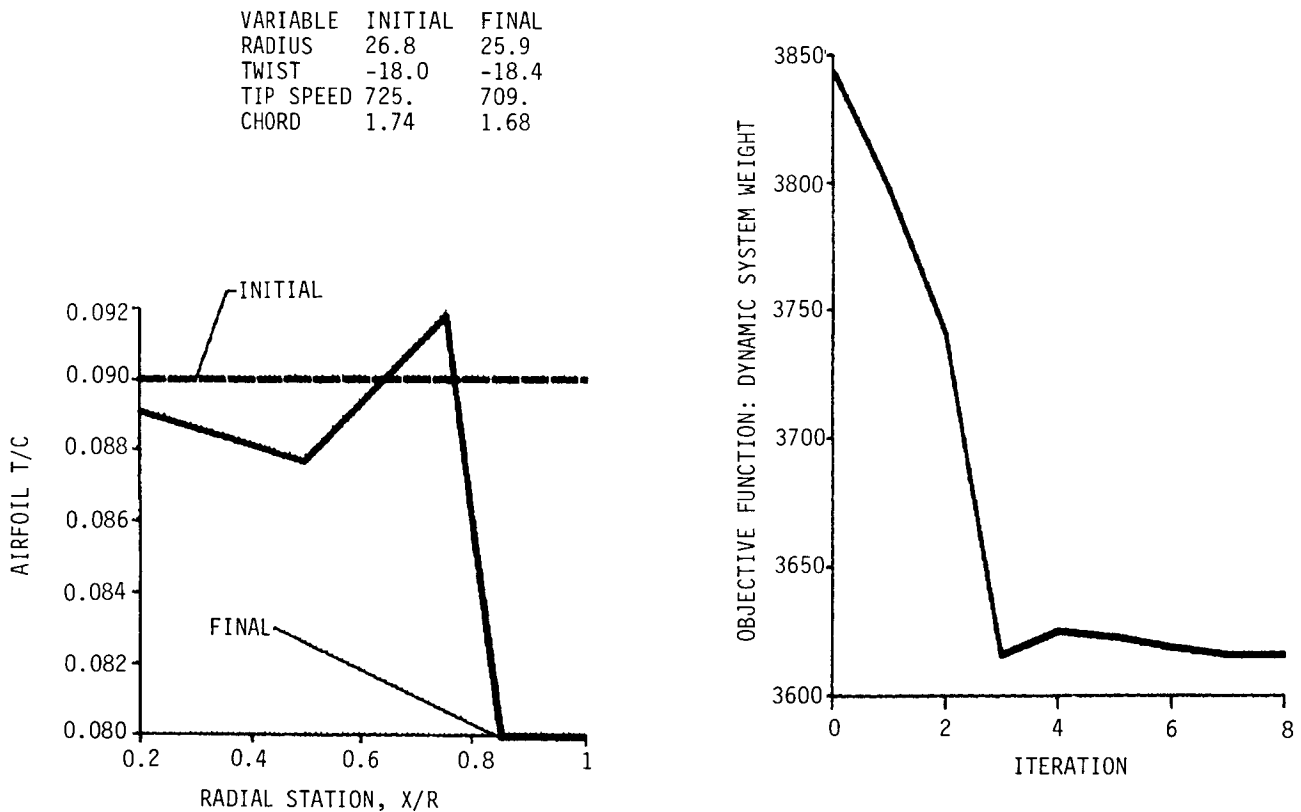


Figure 12

CONCLUSIONS

Based on initial results obtained from the performance optimization code discussed in this paper, a number of observations can be made regarding the utility of optimization codes in supporting design of rotors for improved performance.

1. The primary objective of improving the productivity and responsiveness of current design methods can be met.
2. The use of optimization allows the designer to consider a wider range of design variables in a greatly compressed time period.
3. Optimization requires the user to carefully define his problem to avoid unproductive use of computer resources.
4. Optimization will increase the burden on the analyst to validate designs and to improve the accuracy of analysis methods.
5. Direct calculation of finite difference derivatives by the optimizer was not prohibitive for this application but was expensive. Approximate analysis in some form would be considered to improve program response time.
6. Program development is not complete and will continue to evolve to integrate new analysis methods, design problems, and alternate optimizer options.

REFERENCES

1. Singley, G. T. III, "Army Light Family of Rotorcraft (LHX) Concept Formulation," AIAA-83-2552, October 1983.
2. "FRANOPP - Framework for Analysis and Optimization Problems - User's Manual," NASA CR-165653, 1981.
3. Vanderplaats, G. N., "CONMIN - A Fortran Program for Constrained Function Minimization, Users Manual," NASA TM X-62282, 1973.
4. Kocurek, J. David, et al, "Hover Performance Methodology at Bell Helicopter Textron," Presented at the 36th Annual Forum of the American Helicopter Society, Washington, D.C., May 1980.
5. Groff, T.E., "Vehicle Rotor Program," Vitro Laboratories, Silver Springs, MD, May, 1968.

N87-11758

AEROELASTIC/AERODYNAMIC OPTIMIZATION
OF
HIGH SPEED HELICOPTER/COMPOUND ROTOR

L. R. Sutton
Applied Technology Laboratory
U.S. Army Research and Technology Lab (AVSCOM)
Fort Eustis, VA
and
R. L. Bennett
Bell Helicopter Textron Inc.
Fort Worth, TX

PRECEDING PAGE BLANK NOT FILMED

HELICOPTER FUSELAGE VIBRATION PROBLEM

The helicopter fuselage vibration problem is one of the major challenges facing the helicopter industry. Excessive vibration can have an adverse effect on crew and passenger comfort as well as limiting the component's service life. In order for a single analysis to predict correctly the fuselage environment, it must be multi-disciplinary to cover the rotor aerodynamics, rotor dynamics, fuselage dynamics, and flight mechanics of the helicopter.

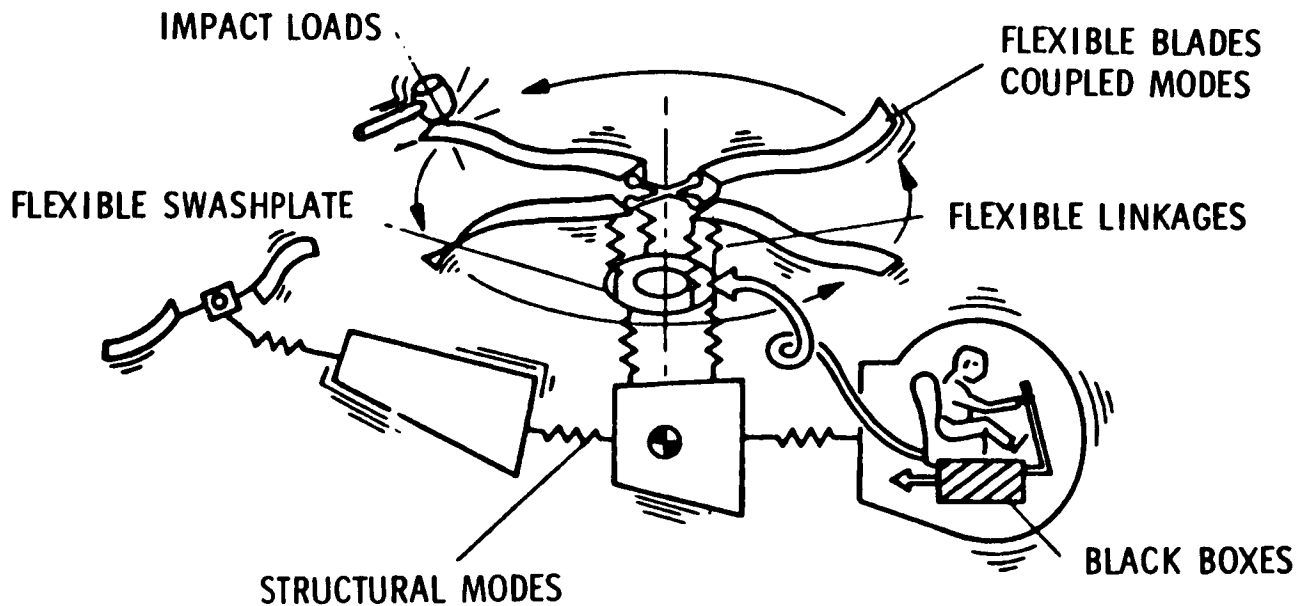


Figure 1

EFFECTS OF FUSELAGE VIBRATIONS

Reducing the fuselage vibrations has been a continuing goal of the helicopter technical community. The fuselage vibration level has a direct impact on the fiscal, physical, and psychological acceptance of the helicopter. Being able to eliminate or significantly reduce (without cost, weight, or complexity penalties) fuselage vibrations would enhance the acceptance of the next generation helicopters.

- COMPONENT FATIGUE
- CREW AND PASSENGER COMFORT
- PERFORMANCE LIMITATIONS
- WEAPON DELIVERY ACCURACY

Figure 2

SOURCE OF EXTERNAL AIR LOADS

For the typical helicopter configuration, the relative wind produced by the helicopter's forward velocity is parallel to the plane of the rotor. For the airplane propellor, the flow is perpendicular to the rotor plane. The parallel flow affects the relative wind velocity components perpendicular to and along the leading edge of the blade. The harmonic variation in the flow is the primary source of the oscillatory aerodynamic forces acting on the rotor blade.

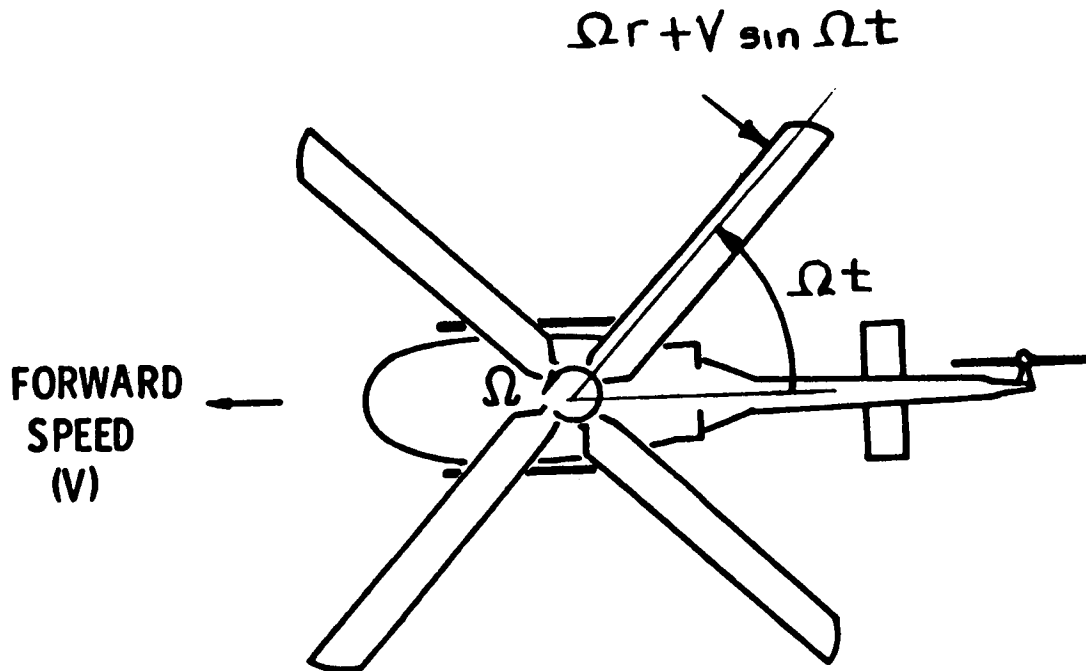
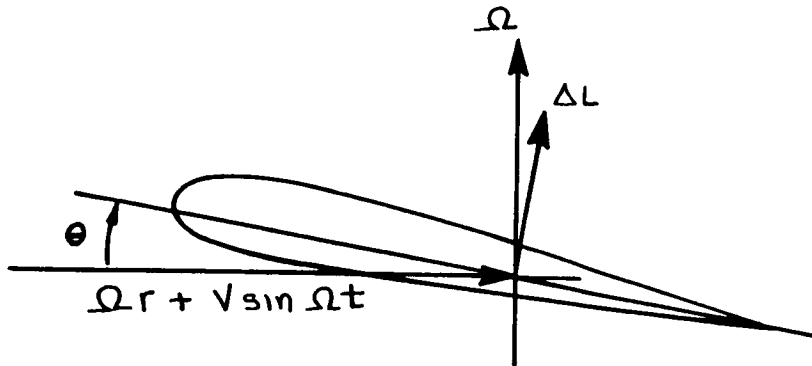


Figure 3

SOURCE OF PERIODIC AIR LOADS

The simple harmonic variation in flow perpendicular to the leading edge has the same frequency as the rotation speed of the rotor. However, this periodic flow variation produces periodic aerodynamic forces at integer multiples of the rotation speed.



$$\begin{aligned}
 \Delta L &\approx q a \theta \Delta H = a \theta \Delta H \left\{ \frac{1}{2} \rho (\Omega r + V \sin \Omega t)^2 \right\} \\
 &= \frac{1}{2} \rho a \theta \Delta H \left\{ \Omega^2 r^2 + 2 V \Omega r \sin \Omega t + V^2 \sin^2 \Omega t \right\} \\
 &= \frac{1}{2} \rho a \theta \Delta H \left\{ \Omega^2 r^2 + 2 V \Omega r \sin \Omega t + V^2 \left(\frac{1}{2} - \frac{\cos 2 \Omega t}{2} \right) \right\} \\
 &= \frac{1}{2} \rho a \theta \Delta H \left\{ \underbrace{\Omega^2 r^2 + \frac{V^2}{2}}_{\text{Steady}} + \underbrace{2 V \Omega r \sin \Omega t}_{1/\text{Rev}} - \underbrace{\frac{V^2}{2} \cos 2 \Omega t}_{2/\text{Rev}} \right\}
 \end{aligned}$$

Figure 4

TYPICAL AIRFOIL ENVIRONMENT

The forward velocity of the helicopter, when coupled with the rotational velocity of the rotor, produces significant changes in the flow environment of the airfoil. In hover, the typical rotor tip speed is approximately 700 ft/sec for all azimuth locations. However, if the helicopter has a forward velocity of 140 knots, then the advancing tip will encounter a local tangential velocity of 936 ft/sec or a Mach 0.84. One-half revolution later the tip will have a velocity of 464 ft/sec. For the control of the helicopter, it is necessary to change the geometric pitch of the blade as a function of the blade's azimuthal location. These changes in geometric pitch produce a related change in blade aerodynamic angle of attack. The changes in local Mach number when coupled with the changing angle of attack produce a complex flow environment for the helicopter rotor blade airfoil.

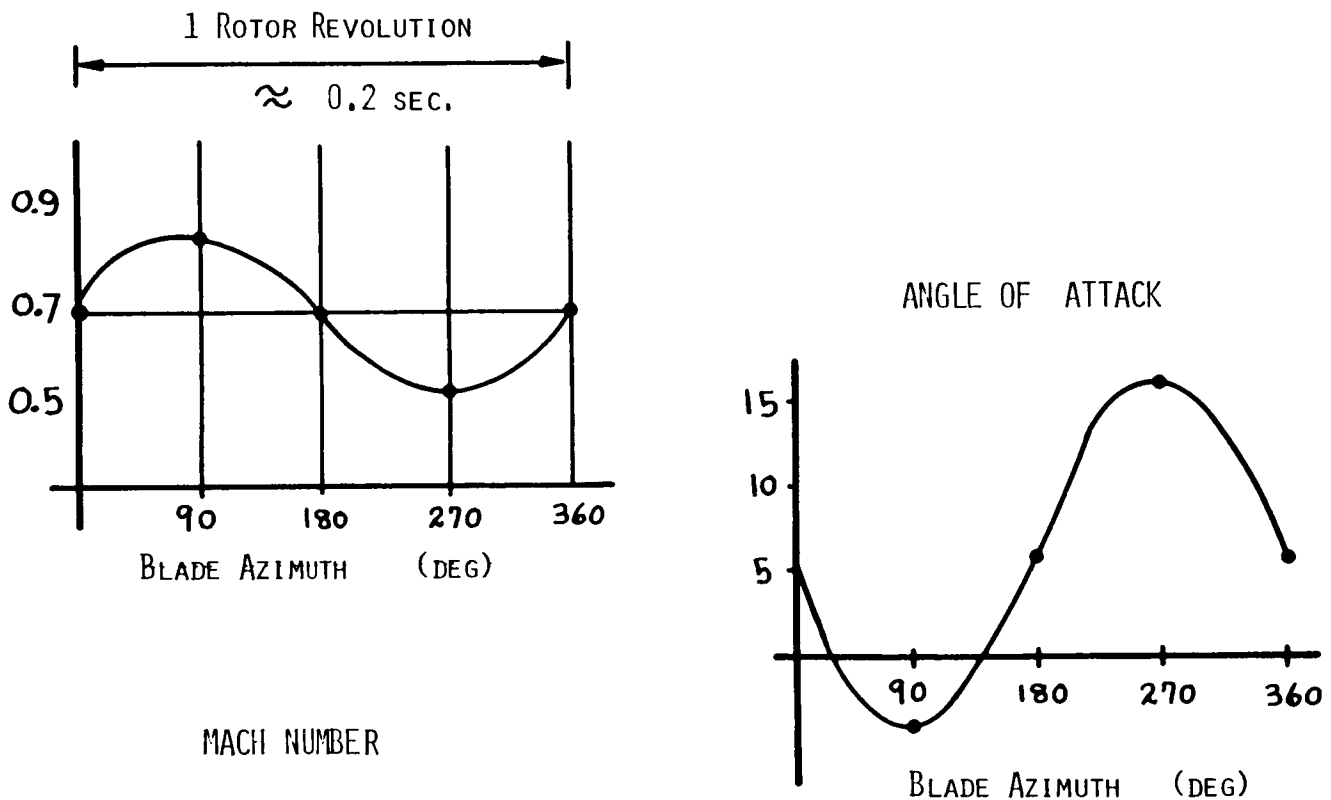


Figure 5

TYPICAL AIRFOIL CHARACTERISTICS

The variations in local blade Mach number and angle of attack when coupled with the airfoil characteristics introduce nonlinearities that are a major component in the behavior of the helicopter. It is not at all uncommon for the advancing tip Mach number to be above the drag divergence Mach number; and one-half revolution later for the retreating blade to be in the stalled flow region.

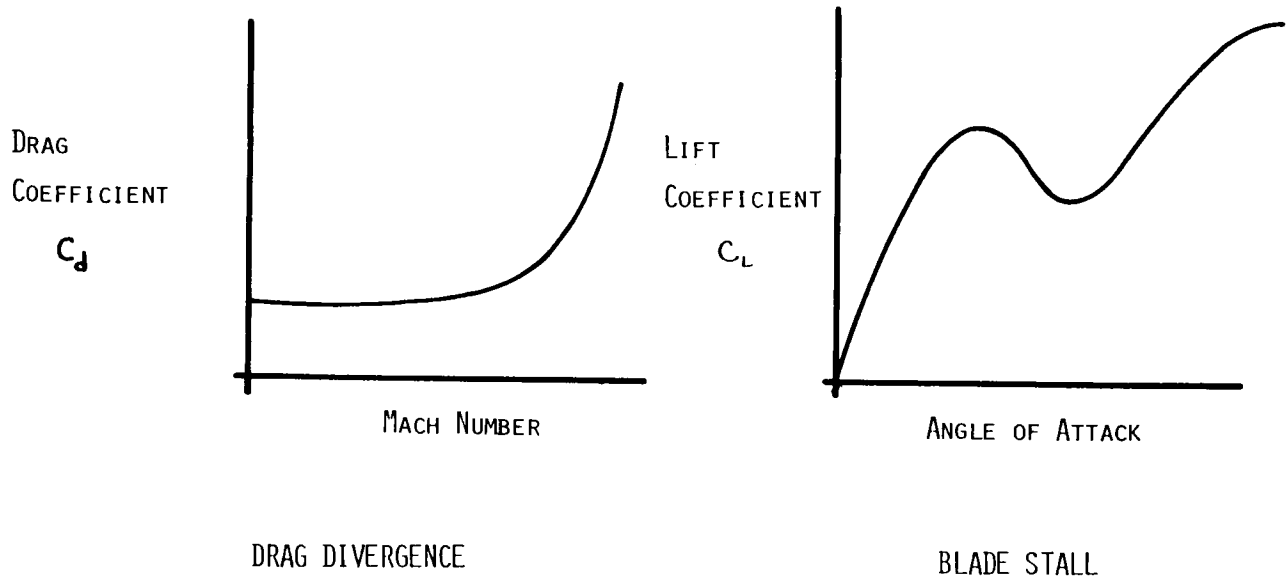
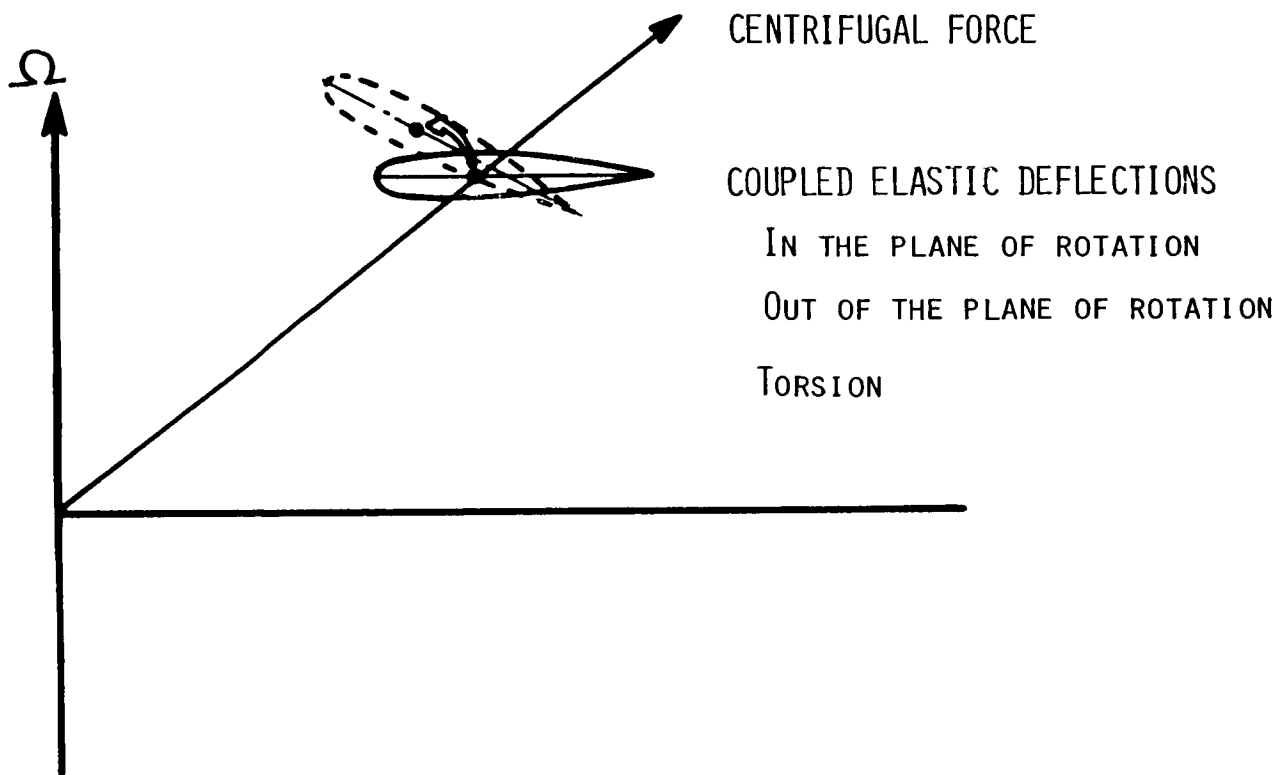


Figure 6

ROTOR DYNAMICS

The dynamic behavior of the rotor blade is influenced by the centrifugal force field as it combines with the elastic deflections (in the plane of rotation, out of the plane of rotation, and elastic torsion). The centrifugal force at the hub can be an order of magnitude greater than the gross weight of the helicopter. Finite element techniques are used to calculate the coupled natural frequencies as a function of the blades built in geometric twist, collective pitch, and rotation speed. The centrifugal force has more influence on the out of plane modes than on the inplane modes. Coupled modes are calculated for various combination boundary conditions at the interface between the blade and the mast.



TENSION BEAM ANALYSIS

Figure 7

ROTOR BLADE FREQUENCY

The aeroelastic response of the helicopter rotor blade is governed by the separation of the aerodynamic forcing function frequencies (at integer multiples of the rotation speed) from the coupled natural frequencies. The "fan plot" shows this relationship in addition to identifying the nominal operating RPM band for the rotor. Depending on the number of blades and the blade boundary conditions at the hub, certain modes respond only at selected forcing function frequencies.

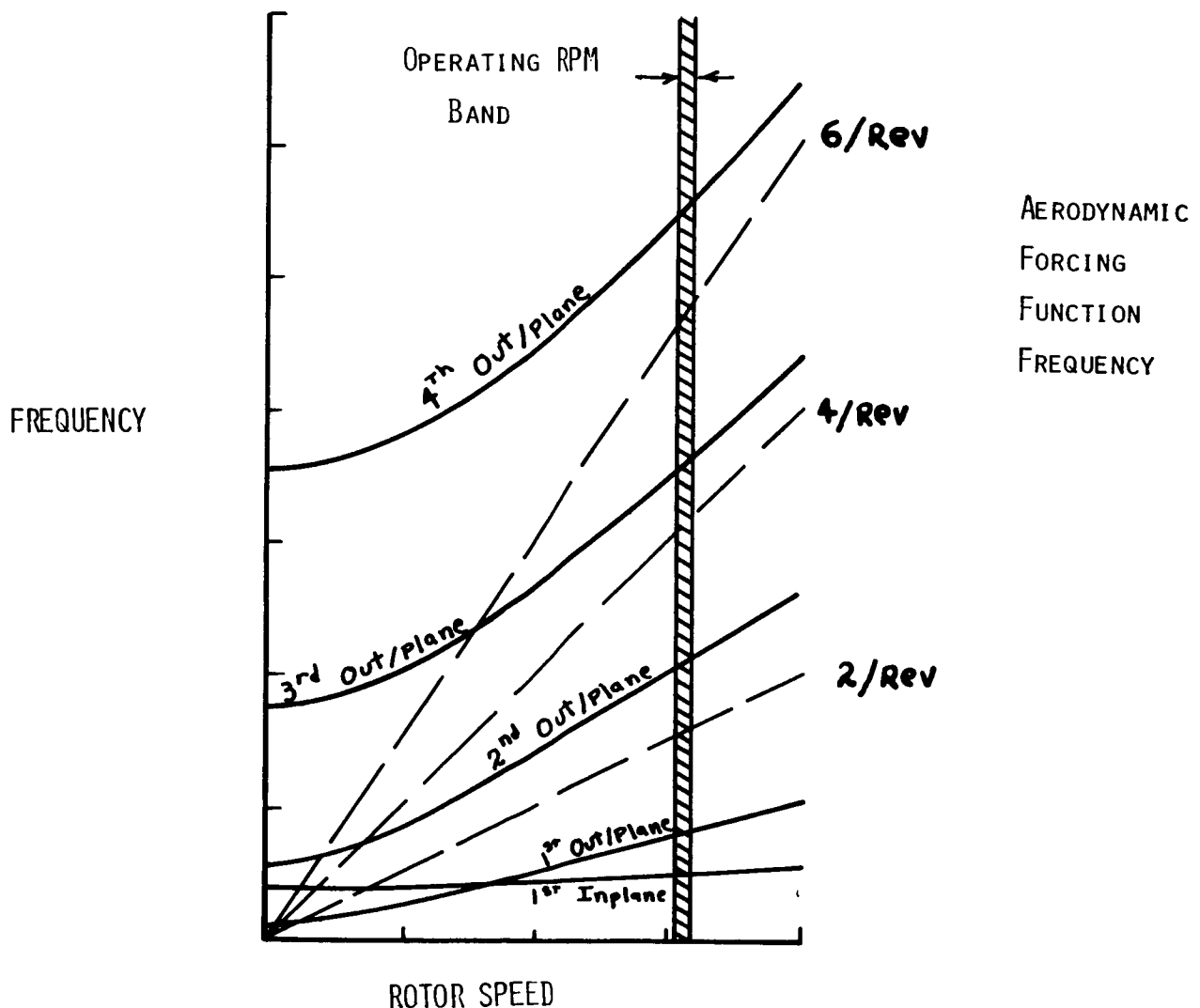
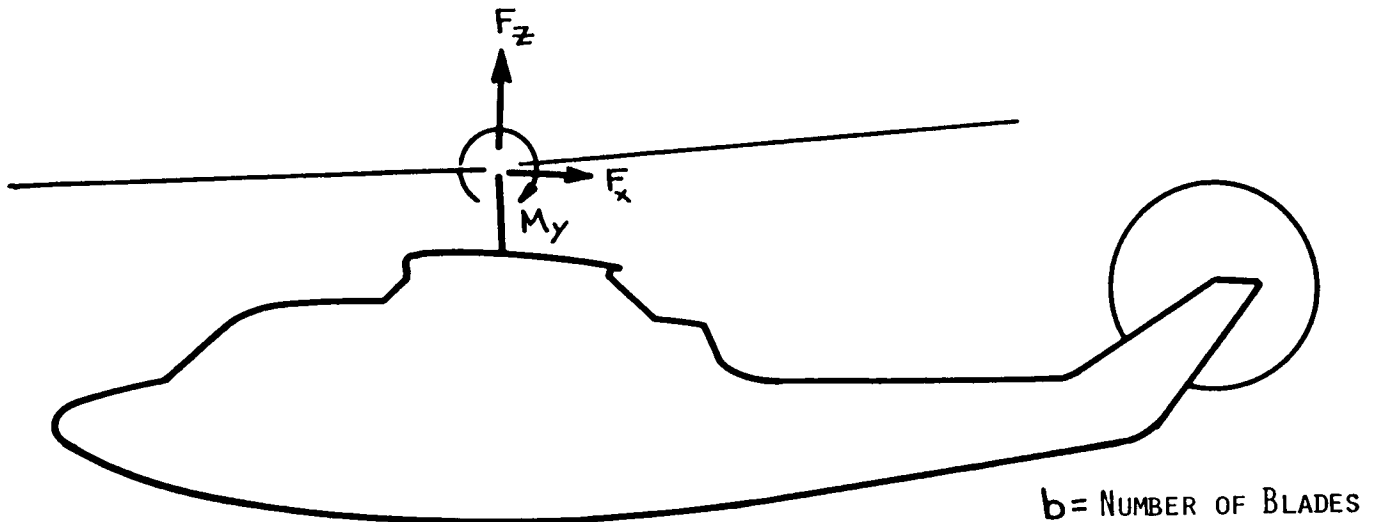


Figure 8

ROTOR FORCES TRANSMITTED TO FUSELAGE

The large oscillatory aerodynamic forces acting on the blades are summed together at the top of the mast to form the forces and moments that are transferred to the fuselage. The unique property of this summing action is that the forces and moments transferred from the rotor to the fuselage occur at frequencies formed by multiplying the number of blades and the rotor speed. Thus a two-bladed rotor turning at 300 rpm (5 Hz) will excite the fuselage at 10 Hz, 20 Hz, 30 Hz, etc. while a four-bladed rotor would excite the fuselage at 20 Hz, 40 Hz, etc.



$$F_x = \sum_{n=1}^{\infty} a_n \sin(nb\Omega t + \phi'_{nb})$$

$$F_z = \sum_{n=1}^{\infty} c_n \sin(nb\Omega t + \phi''_{nb})$$

$$M_y = \sum_{n=1}^{\infty} d_n \sin(nb\Omega t + \phi'''_{nb})$$

Figure 9

FUSELAGE DYNAMICS

The forces and moments transferred from the rotor to the fuselage occur at frequencies near the natural frequencies of the elastic fuselage. This proximity has given rise to various vibration attenuation devices that are often added to the helicopter after the design is complete. These after-the-fact additions are expensive in terms of cost and weight.

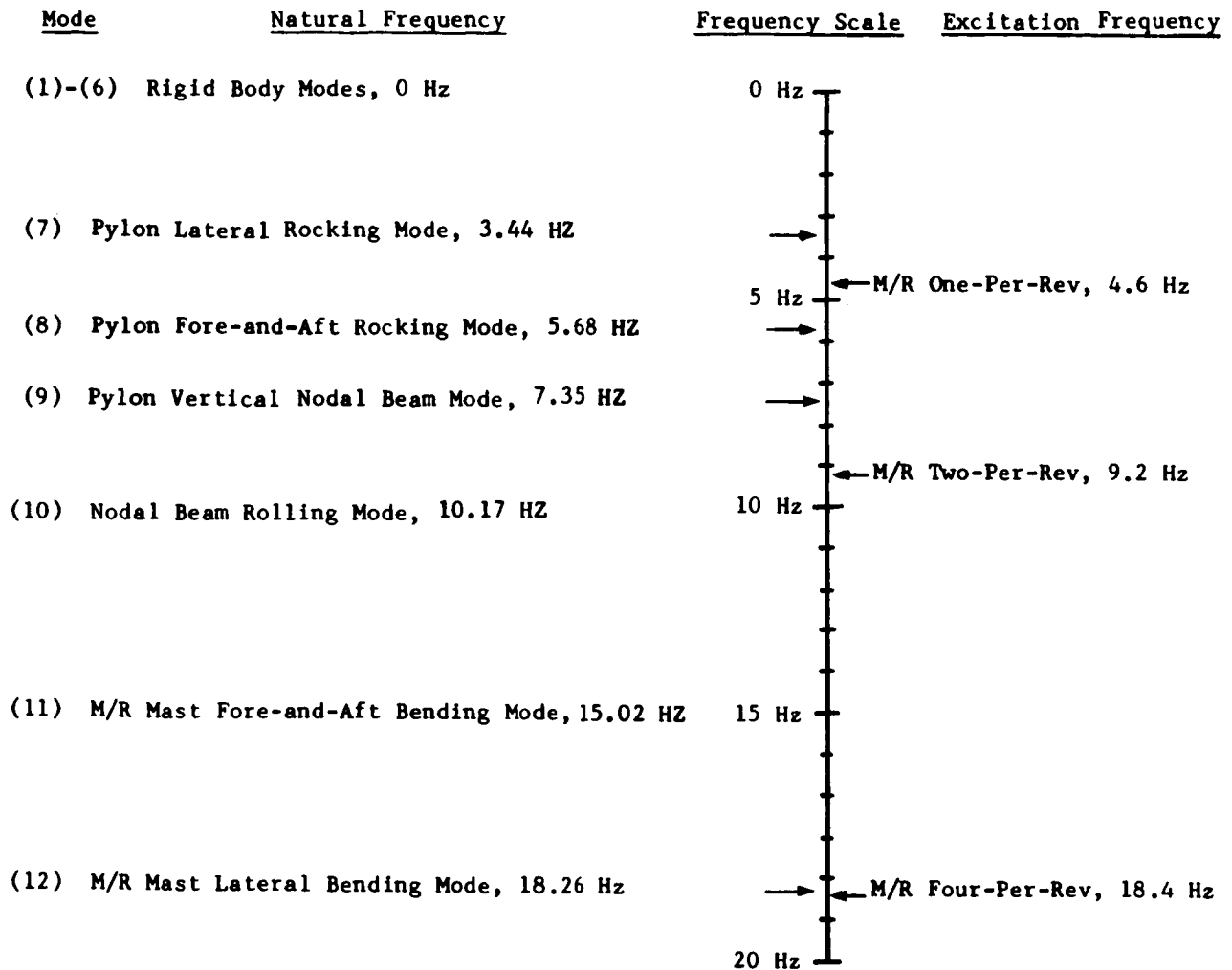


Figure 10

ANALYTICAL MODEL

The analytical model used during the helicopter rotor design must contain very detailed mathematical representations of the dynamic and aerodynamic components. For the airfoils, aerodynamic characteristics tabular data tables are used to store the lift, drag, and pitching moments as a function of Mach number and angle of attack. The Mach number range must go from 0.0 to 1.0, and the angle of attack table must contain entries from -180 degrees to +180 degrees. The rotor and fuselage dynamic model is based on the modal method of structural analysis. The flight mechanics model contains 10 rigid body degrees of freedom--six for the fuselage and two angles to locate the tip path plane for two rotors. Numerical integration is used to obtain the aeroelastic response of the coupled rotor/fuselage system.

ROTOR AERO

20 RADIAL SEGMENTS

TABULAR DATA FOR $C_L(\alpha, M)$, $C_D(\alpha, M)$, $C_m(\alpha, M)$

ROTOR DYNAMICS

FINITE ELEMENT / MODAL REPRESENTATION

TENSION BEAM ANALYSIS

FUSELAGE DYNAMICS

FINITE ELEMENT / MODAL REPRESENTATION

FLIGHT MECHANICS

10 RIGID BODY DEGREES OF FREEDOM

AEROELASTIC ANALYSIS

TIME HISTORY INTEGRATION OF

COUPLED ROTOR / FUSELAGE

MODAL EQUATIONS

Figure 11

CLASSICAL ROUTES FOR VIBRATION REDUCTIONS

Several routes have been advanced for reducing fuselage vibrations. Certain configurations have the potential for reducing fuselage vibrations--the tilt rotor reconfigures itself for improved aerodynamic performance and reduced vibrations. The active systems have a stringent demand for reliability since they can be in the primary control channels. Several passive systems add weight and are sensitive to changes in rotor speed.

- CONFIGURATION

- TILT ROTOR
- COMPOUND
- COAXIAL ROTOR

- ACTIVE SYSTEMS

- HIGHER HARMONIC CONTROLS
- MODAL SUPPRESSOR

- PASSIVE SYSTEM

- ABSORBERS
- ISOLATORS
- AEROELASTICALLY CONFORMABLE ROTOR

Figure 12

PROGRAM OBJECTIVES

In October of 1983, the Applied Technology Laboratory of the U.S. Army Research and Technology Lab awarded Bell Helicopter Textron Inc. a contract to demonstrate the feasibility and assess the impact of using optimization in the rotor design process. Particular emphasis will be placed on designing rotors for minimum fuselage vibrations. The resulting computer program will have to incorporate state-of-the-art technology modules and an efficient nonlinear programming algorithm.

DEMONSTRATE THE FEASIBILITY

&

ASSESS THE IMPACT OF

USING OPTIMIZATION

IN THE

ROTOR DESIGN PROCESS

Figure 13

PROGRAM PHASES

The three year program is divided into four phases. Bell Helicopter has recently completed the first phase which is the development of the approach for the Rotor Design Optimization Computer Program (RDOCP). In addition to merely developing another computer program, the RDOCP will be used to design fully optimized rotors and a resulting rotor design will be tested in the Transonic Dynamics Tunnel at NASA Langley.

- I. DEVELOPMENT APPROACH

- II. DESIGN AND DEVELOPMENT OF DESIGN
 OPTIMIZATION METHOD

- III. USE OF PROGRAM

- IV. EXPERIMENTAL VERIFICATIONS

Figure 14

DEVELOPMENT OF APPROACH

In the development of the approach, the first task was to examine, in detail, the current rotor design process used at Bell Helicopter Textron. The examination was conducted without regard for analytical methods or computer programs, but rather to identify the flow of information in the design process. The results of the examination were converted to the standard nonlinear programming problem by stating the key design variables (blade mass and stiffness distribution, etc.) and the major aerodynamic, dynamic, and handling qualities constraints. These led to the definitions of the approach and the required software.

TASKS

- EXAMINATION OF CURRENT ROTOR DESIGN PROCESS
- FORMALIZATION OF ROTOR DESIGN OPTIMIZATION ANALYSIS
- DEFINITION OF APPROACH FOR THE ROTOR DESIGN OPTIMIZATION COMPUTER PROGRAM (RDOCP)
- DEFINITION OF REQUIRED SOFTWARE
- SUMMARY BRIEFING

Figure 15

REQUIREMENTS FOR THE ROTOR DESIGN OPTIMIZATION ANALYSIS

Since the design of a rotor system is a multidisciplinary task, the first requirement for RDOCP is generally in terms of technical modules. It must be able to calculate the externally applied rotor airloads as well as the resulting forced response of the coupled rotor fuselage system. Finally the program must be very carefully developed in terms of user considerations if it is to receive widespread acceptance.

- GENERALITY
- FUSELAGE FORCED RESPONSE
- ROTOR EXCITATION
- ROTOR RESPONSE
- USER CONSIDERATIONS

Figure 16

ENGINEERING MODULES

RDOCP is being structured to permit the independent variables from the NLP to be used by the rotor modal analysis and/or the forced response analysis. Fuselage modal data from a finite element analysis will be used to represent the fuselage dynamic properties; however the fuselage modal analysis will not be included within the optimization process. Results passed to the sensitivity analysis will be used to reduce the computer demands.

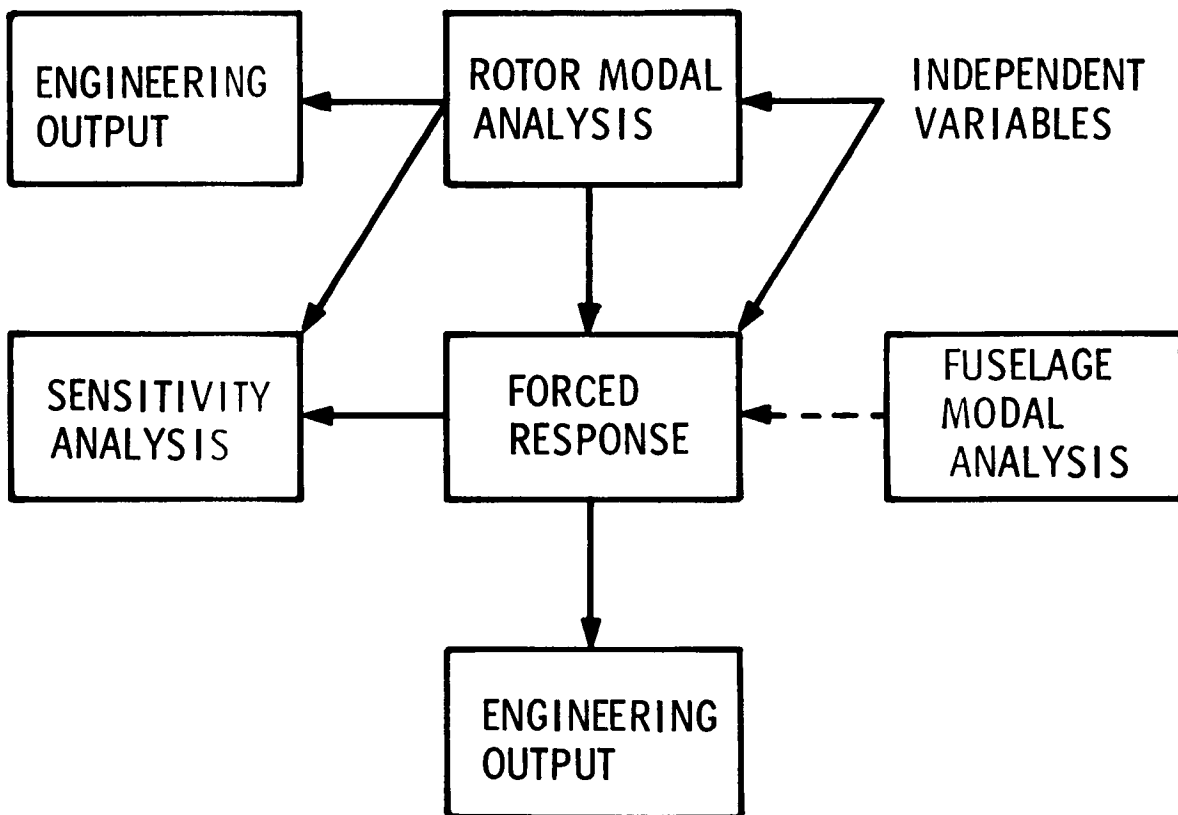


Figure 17

MODULES FOR RDOCP

The Rotor Design Optimization Computer Program will contain three major modules. The executive module will serve as the interface between the user and the technical modules. The technical modules will be existing validated engineering analyses. The Rotorcraft Flight Simulation Program C81 will be used to calculate the forced response. Rotor modal data required during the optimization process will be generated by the Myklestad analysis. RDOCP will not contain a specific NLP but will be sufficiently general so that it can be combined with any NLP.

- EXECUTIVE ROUTINE

- TECHNICAL MODULES
 - ROTOR MODAL ANALYSIS
 - FUSELAGE MODAL ANALYSIS
 - COUPLED ROTOR / FUSELAGE FORCED
RESPONSE ANALYSIS

- NONLINEAR PROGRAMMING ALGORITHM

Figure 18

EXECUTIVE ROUTINE

Bell Helicopter Textron must develop an executive routine for RDOCP to serve as the interface between the engineering user and the technical modules. The executive must accept a wide range of objective function formulations, constraints and bounds. In addition, it must control the flow of data between the technical modules.

- STATEMENT OF ENGINEERING PROBLEM
- ROTOR MODAL ANALYSIS INFORMATION
- FUSELAGE MODAL ANALYSIS INFORMATION
- FORCED RESPONSE ANALYSIS INFORMATION
- NLP DATA
- DIAGNOSTIC OUTPUT CONTROL

Figure 19

N87-11759

THE STRUCTURAL OPTIMIZATION OF A SPREADER BAR
FOR TWIN LIFT HELICOPTER OPERATIONS

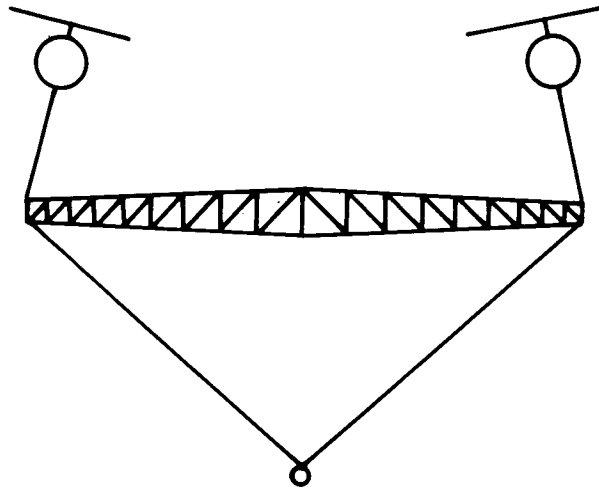
Alan Dobyns
Sikorsky Aircraft
Stratford, Connecticut

TWIN LIFT SPREADER BAR OPTIMIZATION STUDY

An optimization study has been performed to develop a minimum weight spreader bar to allow two helicopters to lift the same payload. With this arrangement, the maximum payload that can be lifted is almost doubled without the expense of designing and building a new helicopter. The concept has had some limited use by civil helicopter operators using small helicopters and has been demonstrated in large scale by two CH-54's which successfully lifted a total load of 20 tons (see figure).

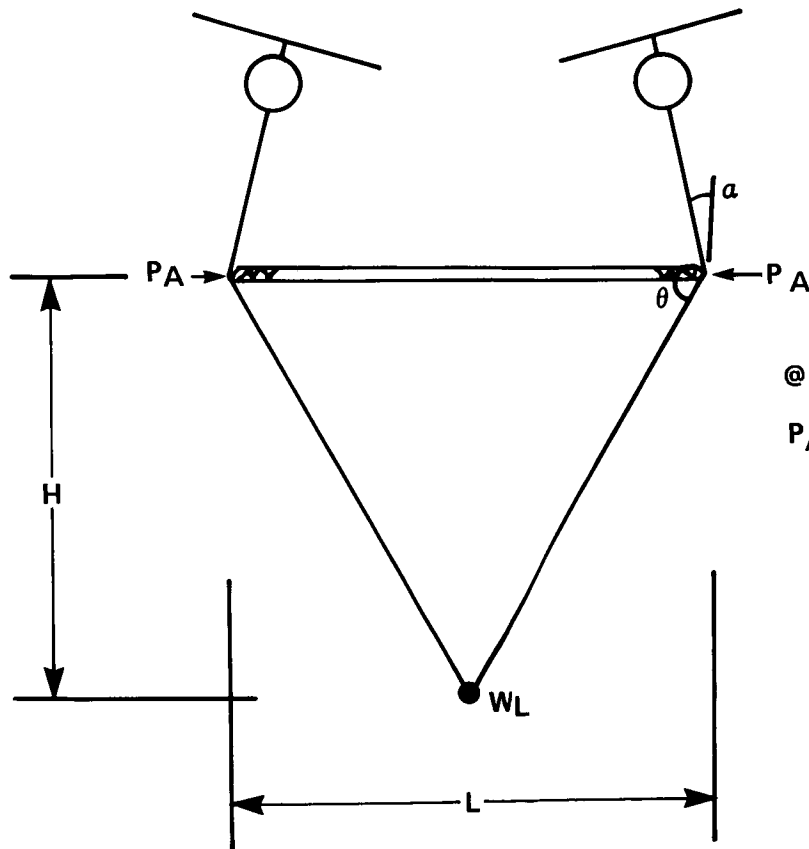
To this point, rather heavy available beams or tower structures have been used for the spreader bar. Since the weight of the bar not only detracts from payload but also adds to the logistics problem, there are more than the usual incentives to minimize weight. Since the design requirement is for classic beam column with uniform side loads resulting from bar weight and aerodynamic drag, the design problem is particularly amenable to optimization.

A study has been performed at Sikorsky to establish the minimum weight for a spreader bar sized to carry a load equal to the capacity of two Army BLACK HAWK helicopters. Toward this end, a computer program was written to analyze the spreader bar deflections and stresses and coupled to the NASA developed CONMIN optimization routines.



SPREADER BAR GEOMETRY

The payload (W_L) is suspended below the spreader bar by cables (called the bridle) so that the axial load in the bar is easily calculated from the cable geometry. A maximum cant angle of the vertical cables (α) of 15° was used in the study.



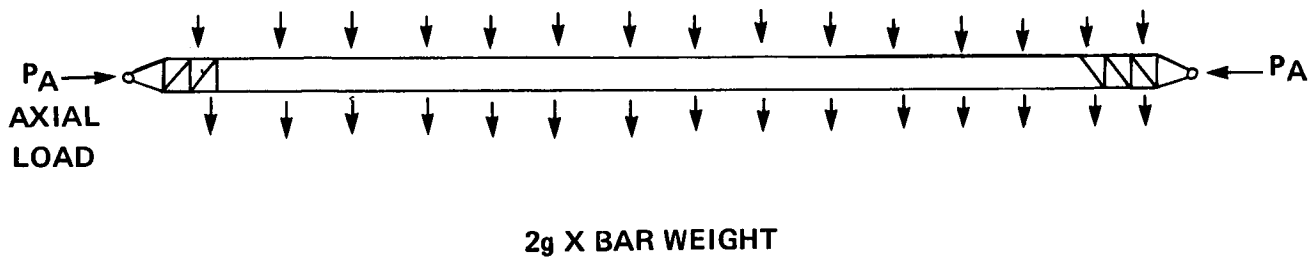
@ 2g X 1.5 SAFETY FACTOR

$$P_A = \frac{3 \cdot W_L \cdot L}{4 H} + \frac{3 W_L}{2} \tan \alpha$$

LOADS ON SPREADER BAR

The spreader bar is loaded by an axial load due to the cable angles, by drag loads due to rotor downwash and bar forward velocity and by maneuvering load factors on the bar weight.

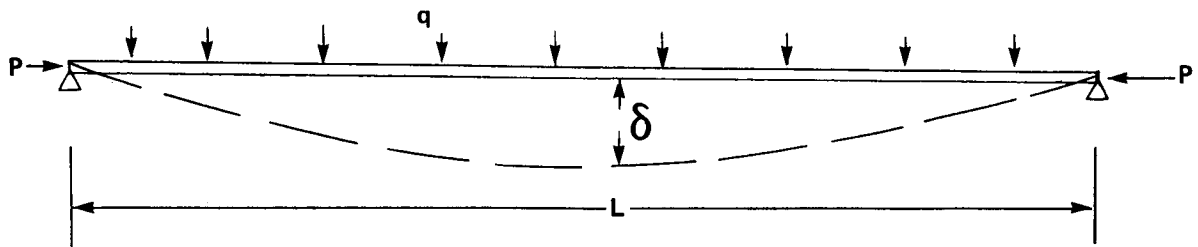
DRAG LOAD DUE TO ROTOR DOWNWASH AND FORWARD VELOCITY



BEAM COLUMN ANALYSIS

The combined normal and axial loads make the spreader bar truss a beam column. The bending moment and normal deflection are magnified in a beam column so that as the axial load approaches the critical column buckling load, the moment and deflection approach infinity. The equations for deflection and moment for a uniform beam column are shown below.

BEAM WITH COMBINED NORMAL AND AXIAL LOADS



- $M_{MAX} = q j^2 \left(1 - \sec \frac{L}{2j} \right)$

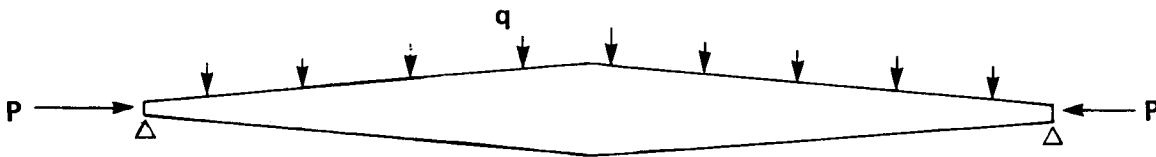
- $j = \sqrt{\frac{EI}{P}}$

- $\delta = \frac{5qL^4}{384 EI} \cdot \frac{1}{(1 - P/P_{CR})}$

- UNIFORM BEAMS ONLY

NEWMARK'S BEAM COLUMN ANALYSIS

For a tapered beam column, no closed-form equations are available to calculate the deflections and moments and an iterative method must be used. Newmark's method (Ref. (1)), which is a modification of the old Hardy-Cross method, was used for calculating moments and deflections. As shown below, an initial deflection is assumed based on the deflection due to the normal load times a magnification factor derived from the buckling load. The axial loads are then applied and the increase in moments and deflections are calculated at several points along the beam. The new deflection is compared to the previous assumed deflection. If the two deflections are not within one percent of each other, another iteration is made using the last deflection as the starting point. Iterations continue until convergence is achieved.



● NON-UNIFORM BEAM COLUMN ANALYSIS.

● ASSUME DEFLECTED SHAPE ---- $P \times \delta$

- CALCULATE MOMENTS
- CALCULATE NEW DEFLECTION
- CHECK FOR CONVERGENCE
- RESULTS-DEFLECTION & MOMENTS

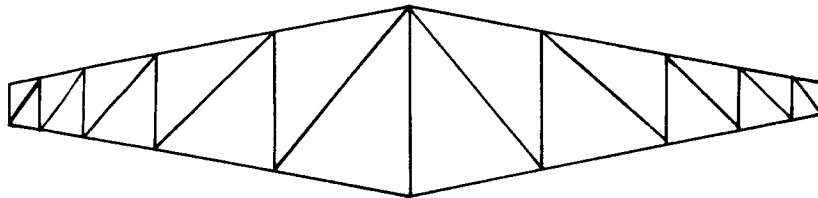
TRUSS DESIGN CONSTRAINTS

Strength constraints considered in the truss optimization included overall column buckling, cap stress, cap crippling or local buckling, and cap buckling as a column between bays. The overall column buckling constraint can never become critical because as a result of the beam column effects the bending moment approaches infinity as the axial load nears the column buckling load. Constraints were placed on the D/τ and L/ρ ratios for the cap, cross and diagonal members so that the final design would not be susceptible to ground handling damage. A constraint was also placed on the maximum center deflection, mainly to keep the truss from becoming too flexible, which could result in vibration problems.

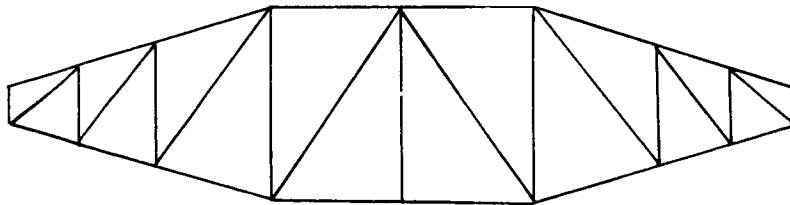
- CAP STRESS - $\sigma = \frac{MY}{I} + P/A$
- CAP CRIPPLING - LOCAL BUCKLING
- CAP BUCKLING BETWEEN BAYS
- CENTER DEFLECTION - $\delta/L < .00166$
- CAP AND DIAGONAL $D/\tau < 50$
- CAP AND DIAGONAL $L/\rho < 60$
- COLUMN BUCKLING

TYPES OF TRUSS ANALYZED

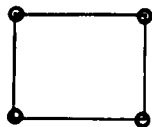
For the optimization study, both constant taper and uniform center section trusses were studied with both triangular and square cross sections. Design variables considered in the optimization were center and end width; cap, cross, and diagonal thickness and diameter; and diagonal angle. The NASA Ames developed CONMIN optimization subroutines (Ref. (2)) were used to find the optimum design, along with the NASA Langley developed FRANOPP control and plotting routines (Ref. (3)). CONMIN uses a feasible direction optimization method based on Zoutendijk's method to solve a constrained optimization problem. CONMIN is easy to use and has proved to be very well suited to structural optimization problems. FRANOPP was used as a control program to allow contour plotting of the design variables versus constraint or objective function values. This allows the analyst to view the design space and gain insight into the problem being optimized.



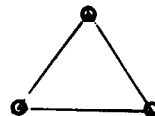
CONSTANT TAPER



UNIFORM CENTER SECTION



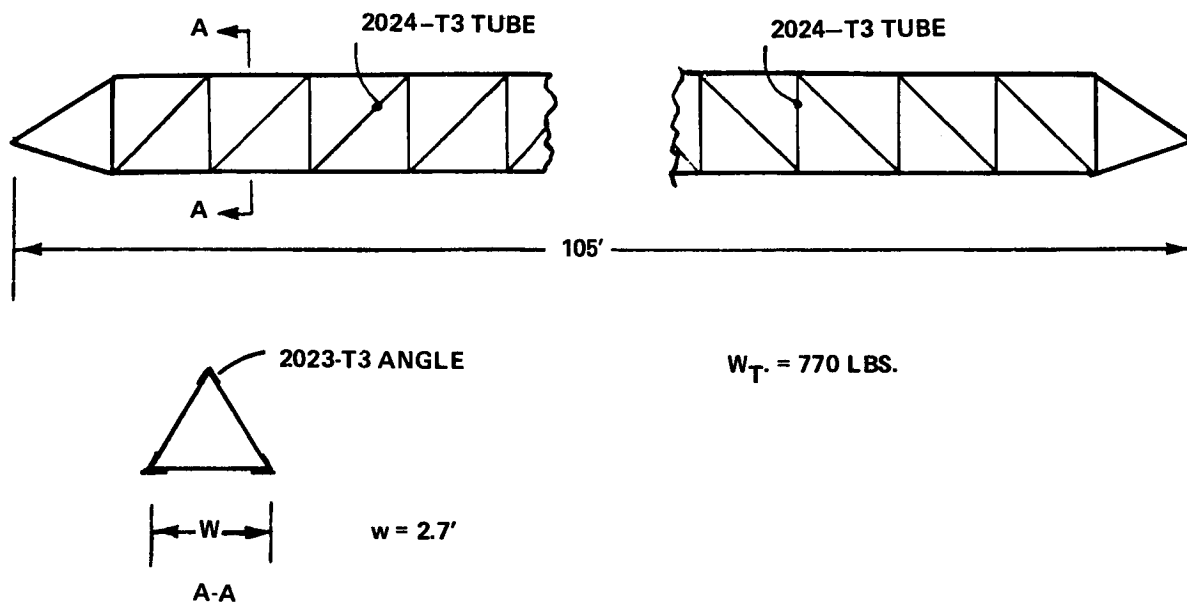
**SQUARE CROSS
SECTION**



**TRIANGULAR
CROSS SECTION**

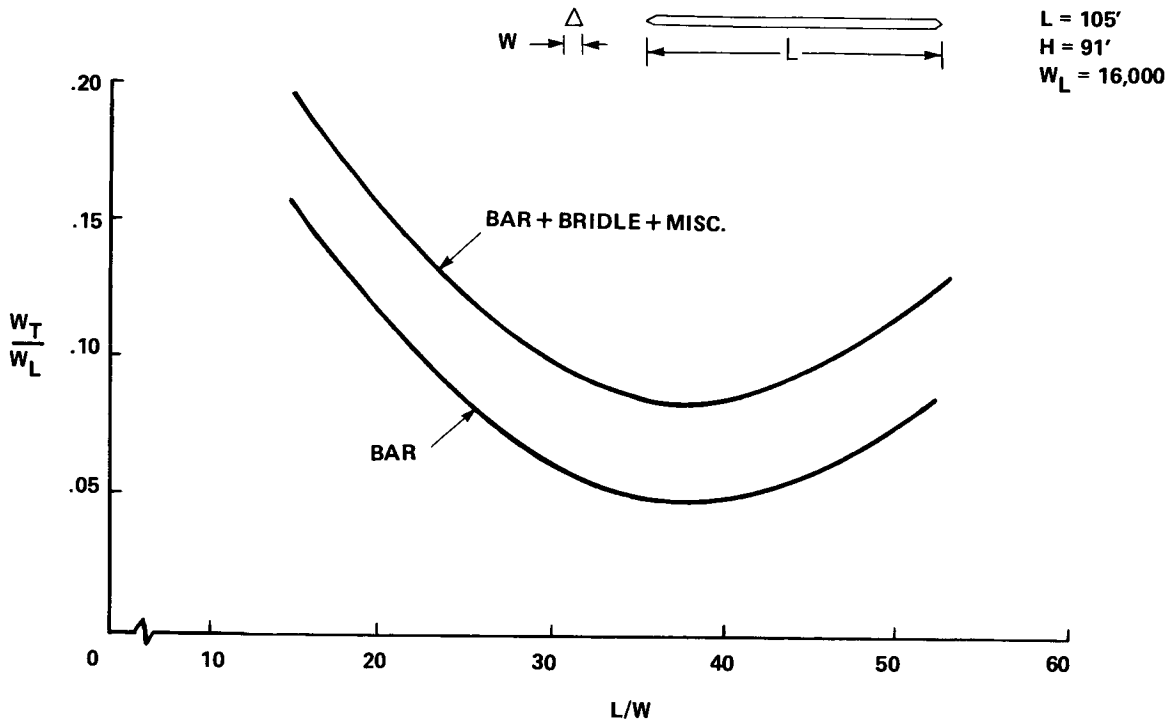
BLACK HAWK SPREADER BAR

A uniform triangular spreader bar optimized for the BLACK HAWK helicopter weighed 770 lb. The design consisted of aluminum angles for the cap members and aluminum tubes for the cross and diagonal members. A tapered truss was used as the initial design but the program consistently removed the taper, resulting in the uniform truss shown. The program was also run with constraints on the center and end widths to force the program to produce a tapered truss, which resulted in heavier designs than the uniform truss shown below.



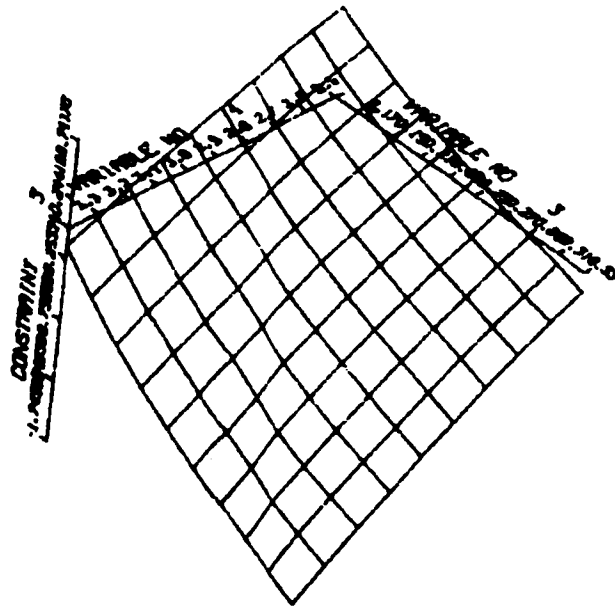
BAR ASPECT RATIO STUDY

A study was performed to find the optimum bar length to width ratio by constraining the truss width at center span and allowing the program to optimize the end width. For L/W ratios less than 36, tapered trusses resulted, while L/W ratios greater than 36 resulted in uniform trusses.



CONTOUR PLOT OF DESIGN SPACE

A contour plot of the effect of varying cap thickness (variable No. 1) and cap diameter (variable No. 3) on the cap buckling constraint (constraint No. 3) is shown below. The FRANOPP control program allows plotting of any one or two variables against the objective function or any constraint, which is very useful in gaining insight about the design space. While the example shown below is relatively linear, a more highly non-linear problem would be difficult to understand from simply examining the series of designs produced by CONMIN. Several plots of the design space are worth a thousand numbers, to paraphrase the popular saying.



CONCLUSIONS

An optimization study has been conducted to design a minimum weight spreader bar to lift a payload with two helicopters. The spreader bar, which is loaded as a beam-column, was optimized using the CONMIN optimization subroutines to obtain a minimum weight design for the given constraints. A uniform, triangular truss structure was found to be the minimum weight design for this application.

REFERENCES

1. Timoshenko, S.P., Gere, G.N., "Theory of Elastic Stability", McGraw Hill, New York, 1961.
2. Vanderplaats, G.N., "CONMIN: A Fortran Program for Constrained Function Minimization: User's Manual", NASA TM X-62282, August 1973.
3. Riley, K.M., "FRANOP - Framework for Analysis and Optimization Problems - User's Guide", NASA CR-165653, January 1981.

N87 - 11760

MULTIOBJECTIVE OPTIMIZATION TECHNIQUES FOR STRUCTURAL DESIGN

S. S. Rao
San Diego State University
San Diego, CA

INTRODUCTION

The multiobjective programming techniques are important in the design of complex structural systems whose quality depends generally on a number of different and often conflicting objective functions which cannot be combined into a single design objective. The applicability of multiobjective optimization techniques is studied with reference to simple design problems. Specifically, the parameter optimization of a cantilever beam with a tip mass and a three-degree-of-freedom vibration isolation system and the trajectory optimization of a cantilever beam are considered. The solutions of these multicriteria design problems are attempted by using global criterion, utility function, game theory, goal programming, goal attainment, bounded objective function, and lexicographic methods. It has been observed that the game theory approach required the maximum computational effort, but it yielded better optimum solutions with proper balance of the various objective functions in all the cases.

PROBLEM STATEMENT

Single objective optimization problem:

$$\begin{aligned} &\text{Minimize } f(\vec{X}) \\ &\text{subject to} \\ &g_j(\vec{X}) \leq 0, \quad j = 1, 2, \dots, m \\ &\text{where} \end{aligned}$$

$$\vec{X} = \begin{Bmatrix} x_1 \\ x_2 \\ \vdots \\ x_n \end{Bmatrix}$$

Multiobjective optimization problem:

$$\begin{aligned} &\text{Minimize } \vec{f}(\vec{X}) \\ &\text{subject to} \\ &g_j(\vec{X}) \leq 0, \quad j = 1, 2, \dots, m \\ &\text{with} \\ &\vec{f}(\vec{X}) = \{ f_1(\vec{X}) \quad f_2(\vec{X}) \quad \dots \quad f_k(\vec{X}) \}^T \end{aligned}$$

BRIEF OUTLINE OF TECHNIQUES

All the multiobjective optimization techniques considered in this work make use of a single objective optimization routine. In the global criterion method, a preselected global criterion, constructed in terms of the various objective functions, is minimized. The utility function method tries to maximize the combined or overall utility function. The game theory approach is similar to finding the equilibrium state when several players, having different goals, try to find their optimal strategies simultaneously. The goal programming procedure involves the minimization of the deviations from preset goals for the various objective functions. The goal attainment method is similar to the goal programming method except that certain weights are also associated with different objectives. In the bounded objective function method, an objective function is minimized by placing bounds on the remaining objective functions. The lexicographic method minimizes the objective functions sequentially starting from the most important one.

GAME THEORY APPROACH

In this method, each objective function is associated with a player who tries to minimize his own objective. All the players are assumed to be equally intelligent and the problem can be solved either as a non-cooperative or as a cooperative game (fig. 1). The cooperative game theory is used in the present work. In this figure, N denotes the Nash equilibrium point in a non-cooperative game and the arc AB represents the set of pareto-optimal points. Along the arc AB, the contours of f_1 and f_2 meet tangentially and our interest is to pick one point on AB using some supercriterion.

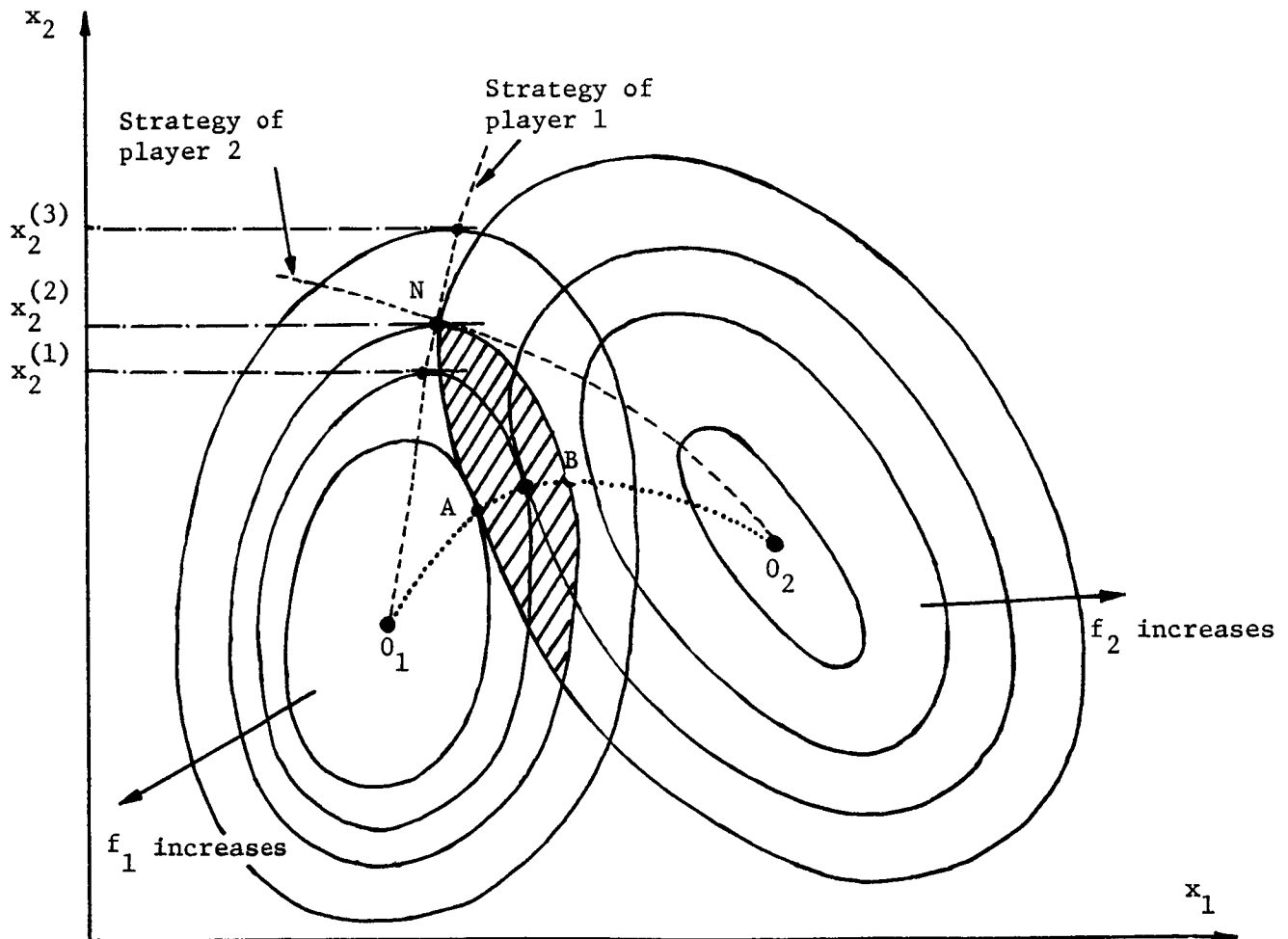


Figure 1

EXAMPLE 1: PARAMETER OPTIMIZATION OF A CANTILEVER BEAM WITH END MASS

The optimum design of the cantilever beam shown in figure 2 is considered with the cross sectional dimensions b , d , and h as the design variables. The minimization of the structural mass, the maximization of the natural frequency of vibration, and the minimization of the fatigue damage in time T are taken as the design objectives. The base of the beam is assumed to be subjected to a Gaussian white noise excitation. The material properties and the geometric parameters are treated as random variables. The constraints are expressed as follows:

$$\begin{aligned} g_1: & P[(\text{maximum stress induced in beam in } 0 \leq t \leq T) \geq S_y] \leq p_1 \\ g_2: & P[(\text{maximum acceleration of end mass in } 0 \leq t \leq T) \geq A] \leq p_2 \\ g_3: & P[(\text{flange buckling stress}) \geq S_y] \leq p_3 \\ g_4: & P[(\text{web buckling stress}) \geq S_y] \leq p_4 \\ g_5: & P[b \geq \frac{\ell}{10}] \leq p_5 \\ g_6: & P[d \geq \frac{\ell}{10}] \leq p_6 \\ g_7: & \sigma_{F_1} \leq \bar{k}_1 F_1 \\ g_8, g_9, g_{10}: & b, d, h \geq 0 \end{aligned}$$

It was observed that game theory approach required the maximum computational effort but yielded a better optimum solution.

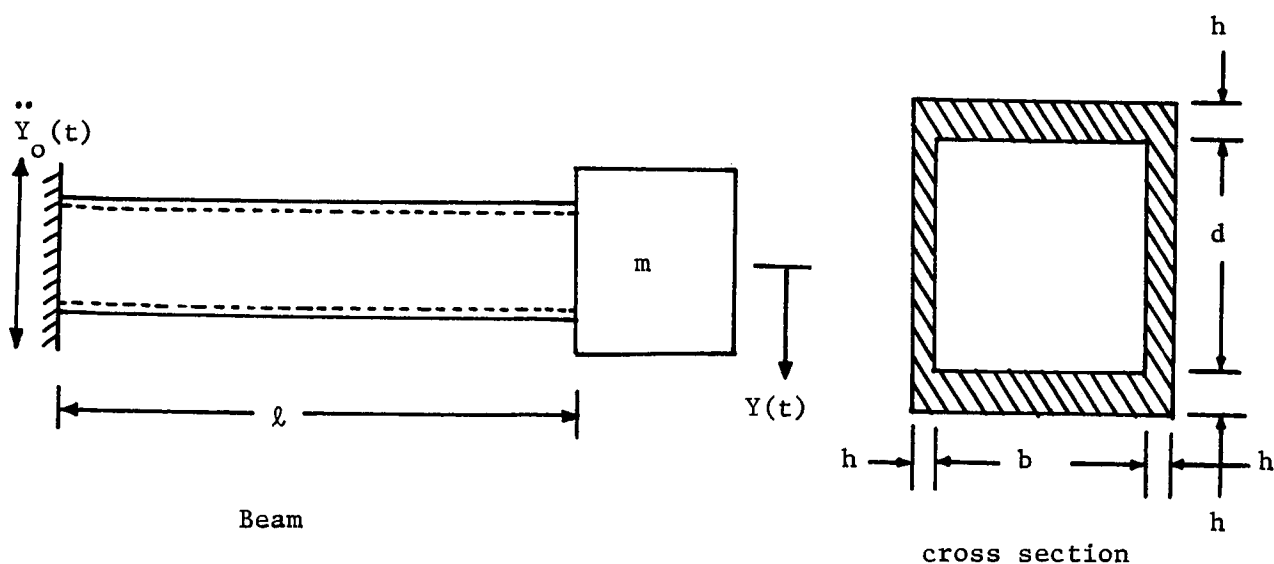


Figure 2

EXAMPLE 2: PARAMETER OPTIMIZATION OF A VIBRATION ISOLATION SYSTEM

In the three-degree-of-freedom vibration isolation system shown in figure 3, $z_o(t)$ represents the base excitation. The equations of motion are given by

$$[m] \ddot{\vec{Z}}(t) + [c] \dot{\vec{Z}}(t) + [k] \vec{Z}(t) = \vec{k}_o z_o(t) + \vec{c}_o \dot{z}_o(t)$$

These equations can be solved for $\vec{Z}(t)$ for any specified $z_o(t)$ and the initial conditions. The spring stiffnesses and the damping constants are taken as design variables so that $\vec{X} = \{k_1 \ c_1 \ k_2 \ c_2 \ k_3 \ c_3\}^T$. Two objective functions are considered as

$$f_1(\vec{X}) = \int_0^T [z_o(t) - z_3(t)]^2 dt = \text{integrated value of square of relative displacement}$$

$$f_2(\vec{X}) = \int_0^T [k_3(z_2 - z_3) + c_3(z_2 - z_3)]^2 dt = \text{integrated value of square of force transmitted to main mass}$$

Upper and lower bounds are placed on the design variables during the solution process. As in the case of example 1, here also the game theory approach yielded a more balanced optimum solution but involved more computational effort.

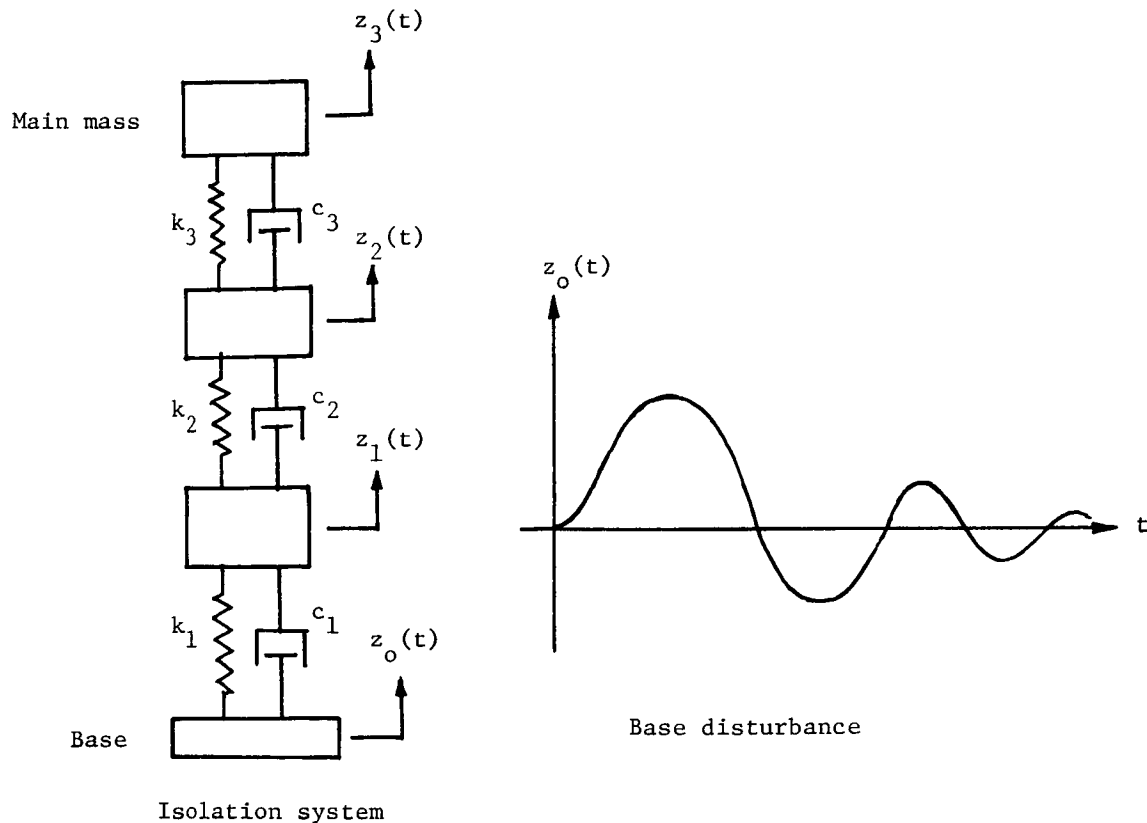


Figure 3

EXAMPLE 3: TRAJECTORY OPTIMIZATION OF A CANTILEVER BEAM

The tapered beam shown in figure 4 is considered by treating $u(x)$ as the control variable. The problem is stated as follows.

Find an admissible control $u(x)$ which causes the generation of a state trajectory as

$$y_1'(x) = y_2(x)$$

$$y_2'(x) = - \frac{M(x)}{E I(u(x))}$$

$$[y_1(x) = y(x), y_2(x) = y'(x)]$$

and minimizes the performance measures

$$J_1(u(x)) = \int_0^{\ell} [\alpha y_1^2(x) + \beta y_2^2(x)] dx$$

$$J_2(u(x)) = \int_0^{\ell} \gamma A(u(x)) dx$$

subject to

$$\sigma(x) \leq \sigma_o, \quad 0 \leq x \leq \ell$$

$$y(x) \leq \Delta, \quad 0 \leq x \leq \ell$$

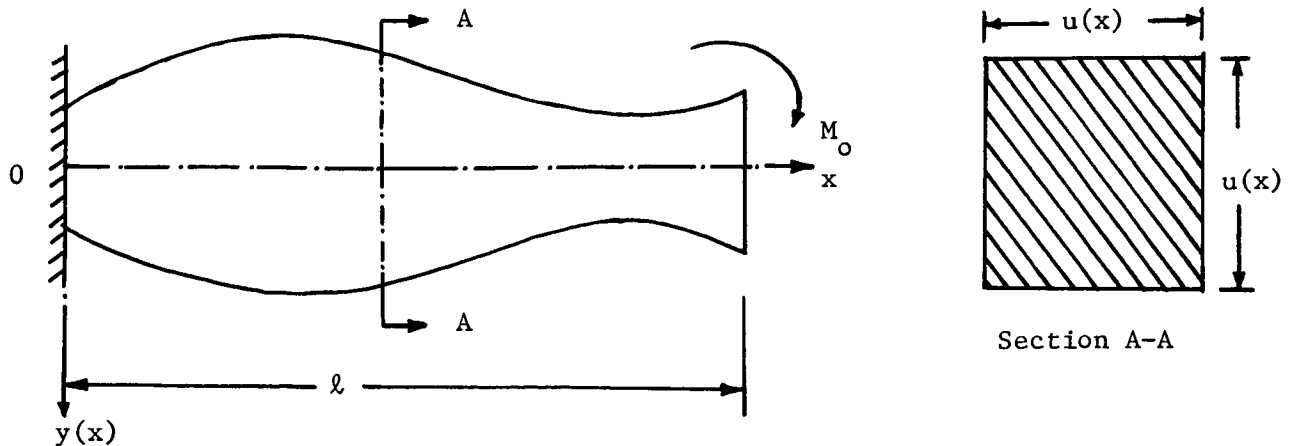


Figure 4

CONCLUSIONS

The present study reveals that several multiobjective optimization techniques can be used for the optimal design of structures. The quality of the final solution depends on the method used for solution. The game theory approach appears to be promising, but more work is to be done in improving the method from the point of view of computational efficiency. It will be worthwhile to conduct a comparative study of the various multiobjective optimization techniques in the context of more complex structural design problems.

SYMBOLS AND ABBREVIATIONS

| | |
|-------------------------|--|
| A | specified acceleration |
| b | width of beam |
| c_i | damping constant of i th damper |
| $[c]$ | damping matrix |
| d | depth of beam |
| f | objective function |
| f_j | j th objective function |
| \vec{f} | vector of objective functions |
| F_j | j th normalized objective function |
| g_j | j th inequality constraint |
| h | wall thickness |
| J_i | i th performance measure |
| k | number of objective functions |
| k_i | stiffness of i th spring |
| k_1 | constant |
| $[k]$ | stiffness matrix |
| l | length of beam |
| m | number of constraints; mass |
| m_i | value of i th mass |
| $M(x)$ | bending moment |
| $[m]$ | mass matrix |
| n | number of design variables |
| p_i | specified probability |
| $P[...]$ | probability of occurrence of the event [...] |
| S_y | yield stress |
| t | time |
| T | duration of load application; transpose when used as a superscript |
| $u(x)$ | control variable |
| x_i | i th design variable |
| \vec{x} | vector of design variables |
| $z_i(t)$ | displacement of i th mass |
| $z_0(t)$ | base displacement |
| α, β, γ | constants |
| σ | stress |
| Δ | permissible deflection |

N87-11761

IDEAS, A MULTIDISCIPLINARY COMPUTER-AIDED CONCEPTUAL
DESIGN SYSTEM FOR SPACECRAFT

Melvin J. Ferebee, Jr.
NASA Langley Research Center
Hampton, Virginia

INTRODUCTION

During the conceptual development of advanced aerospace vehicles, many compromises must be considered to balance economy and performance of the total system. Subsystem tradeoffs may need to be made in order to satisfy system-sensitive attributes. Due to the increasingly complex nature of aerospace systems, these trade studies have become more difficult and time-consuming to complete and involve interactions of ever-larger numbers of subsystems, components, and performance parameters. The current advances of computer-aided synthesis, modeling and analysis techniques have greatly helped in the evaluation of competing design concepts.

Langley Research Center's Space Systems Division is currently engaged in trade studies for a variety of systems which include advanced ground-launched space transportation systems, space-based orbital transfer vehicles, large space antenna concepts and space stations. The need for engineering analysis tools to aid in the rapid synthesis and evaluation of spacecraft has led to the development of the Interactive Design and Evaluation of Advanced Spacecraft (IDEAS) computer-aided design system. The IDEAS system has been used to perform trade studies of competing technologies and requirements in order to pinpoint possible beneficial areas for research and development.

This paper is intended to present IDEAS as a multidisciplinary tool for the analysis of advanced space systems. The capabilities of IDEAS are highlighted by results from previous studies. These capabilities range from model generation and structural and thermal analysis to subsystem synthesis and performance analysis.

IDEAS FUNCTIONAL DESCRIPTION

The Interactive Design and Evaluation of Advanced Spacecraft (IDEAS) Computer-Aided Design and Analysis System functional methodology is shown in Figure 1. It consists of 40 program modules linked together by an efficient data management system. The system is divided into two distinct disciplines: interactive graphics and interactive computing. The interactive graphics are the graphical representations of concept models and data on the interactive terminal, and the interactive computing of the actual multidisciplinary analysis programs available to the user. The design process begins with the creation of a three-dimensional geometry model for concept visualization and verification. An analysis model must then be created for input into the analysis programs. The models could be finite-element, finite-difference, or other mathematical representations of the system. Mass properties are generated also for input into analysis programs. The spacecraft subsystems are synthesized for a total systems concept definition. The model can then be analyzed using various tools under the IDEAS system.

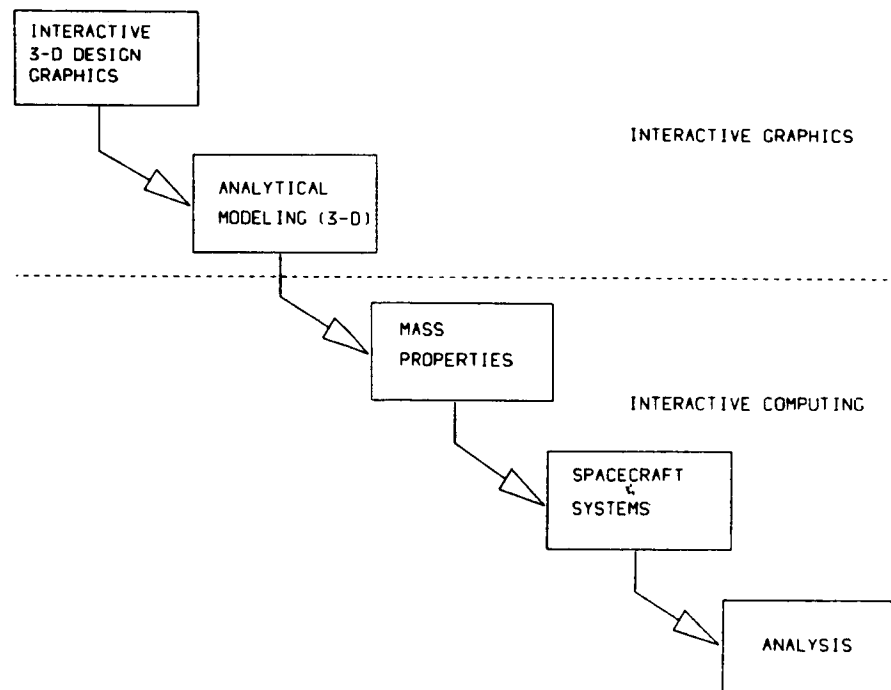


Figure 1. Spacecraft Computer-Aided Design

ORIGINAL PAGE IS
OF POOR QUALITY

GEOMETRY MODELING

An important step in the initial modeling of a space system concept is the visualization of the proposed system to be modeled. Figure 2 shows some initial versions of space station concepts. The geometry models were generated using a solid modeling geometry generator under development at NASA. Through the use of various primitive geometric entities, such as cylinders, cones, rectangles, and volumes of revolution, combined with rotation, translation and boolean operations, an analyst can model a concept in order to determine form-and-fit criterion, concept feasibility, and functionality. By refining the concept at the geometry level, one may save time and effort due to the fact that there are no analytical models created. Through the use of more powerful commercial geometry display software, such as MOVIE.BYU, the models could be placed into realistic views, such as in orbit, there could be a light source representative of the Sun, shadows could be cast onto the model, and shadow information could be extracted for use in thermal analysis.

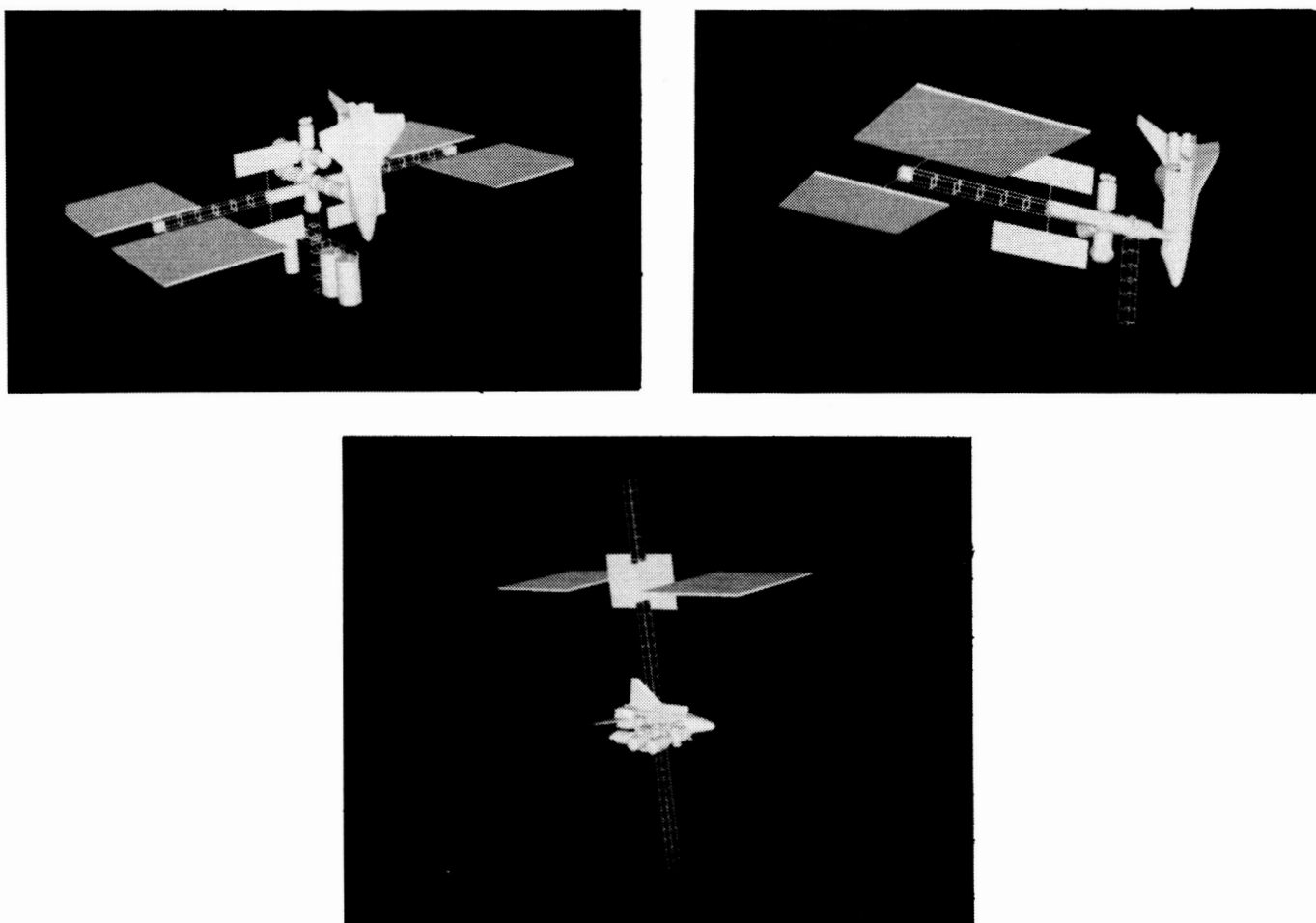


Figure 2. Space Station Concepts

STRUCTURE SYNTHESIZATION

The approach in IDEAS is to use strict mathematical relations to automatically generate a finite-element model of the repeating structural members in complex truss-like structures (for any user-specified size, shape, and lattice density). The interconnecting truss hardware masses and sizes are computed as a function of the structural member diameter and their masses distributed at appropriate nodal points in the truss finite-element model. Additional structural appendages are then added to the truss using the appendage synthesizer programs. Figure 3 shows the lattice-type structures currently being supported with a structure synthesizer. In general, the synthesizers create and output the masses of the structural components, the masses of the reflective mesh systems in the case of antenna design, and the mass of the total system. Also, the center of gravity and mass moment of inertia tensors are computed. Appendage synthesizers are used to design and add structural appendages to a repeated structural system. The process results in an updated structural model and updated mass/inertia properties for the entire spacecraft. The elements used in the design of the structural members are a mass-efficient isogrid, a relatively stiff triangular strut, tension cables, and three- and four-noded elements (Ref. 1).

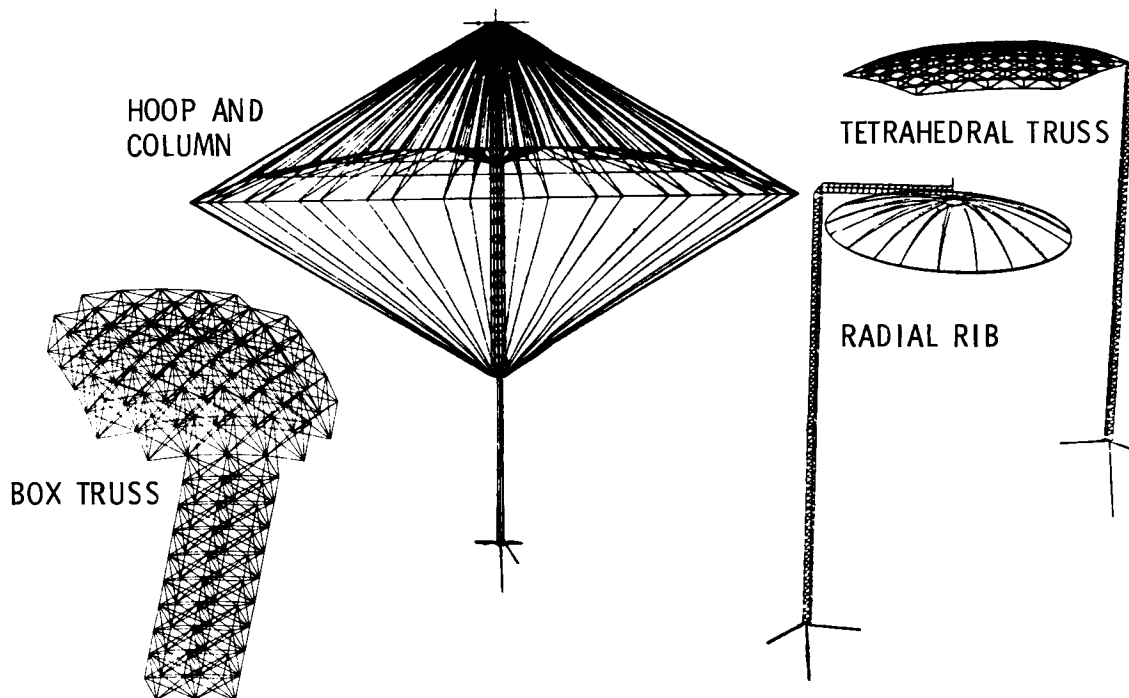
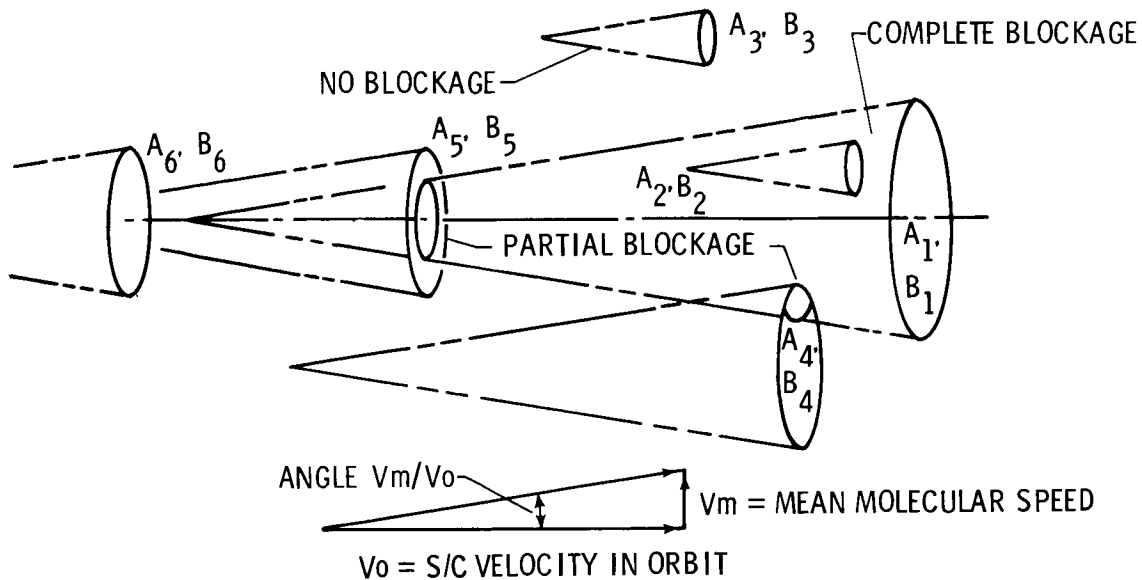


Figure 3. Antenna Structural Concepts

DRAG AREA COMPUTATIONS

Another labor-saving feature incorporated into the IDEAS system is the automated computation of effective drag areas for lattice structures both with and without a porous mesh, and the generation of an aerodynamic drag area model for rigid-body controllability analyses. In single discipline analyses, the structural analyst may have no need for these areas and the aerodynamicist is sometimes faced with the task of generating these data for various structural elements and orientations from design drawings. The atmospheric drag area approximation approach is illustrated in Figure 4. Each node, which consists of the intersection of several members at various orientations, is reduced from the finite-element model to an equivalent solid structural area normal to the spacecraft velocity vector. The blockage effects of upstream areas on downstream areas are factored in the solution. Also, in the case of a porous mesh, the effects of a variable transmissibility mesh can be superimposed onto the solution. Solid areas of external supporting subsystems, such as solar arrays, are included (Ref. 2).



EACH NODE POINT REDUCED TO EQUIVALENT CIRCULAR AREA
 EACH AREA HAS A BLOCKAGE FACTOR, B ($= 1$ IF SOLID)
 MASKING AREAS REDUCED IN PROPORTION TO DOWNSTREAM DISTANCE
 DRAG IS FUNCTION OF MASKED AREA TIMES BLOCKAGE FACTOR

Figure 4. Drag Area Computation

FINITE-ELEMENT MODELING OF DEPLOYING STRUCTURES

Limited research effort has been devoted to the important areas of deployment, kinematic, and kinetic analyses of large space systems. The spacecraft undergoes large changes in inertia (see Fig. 5) and center of gravity locations that may affect spacecraft stability and influence rigid-body control design. The capability to generate finite-element models of these structures as they undergo deployment is a prerequisite to conducting stability and stress analyses. The application of mathematical synthesization techniques to describe the deploying structure offers a rapid, effective means for generating the needed finite-element models at any stage of deployment (Ref. 3).

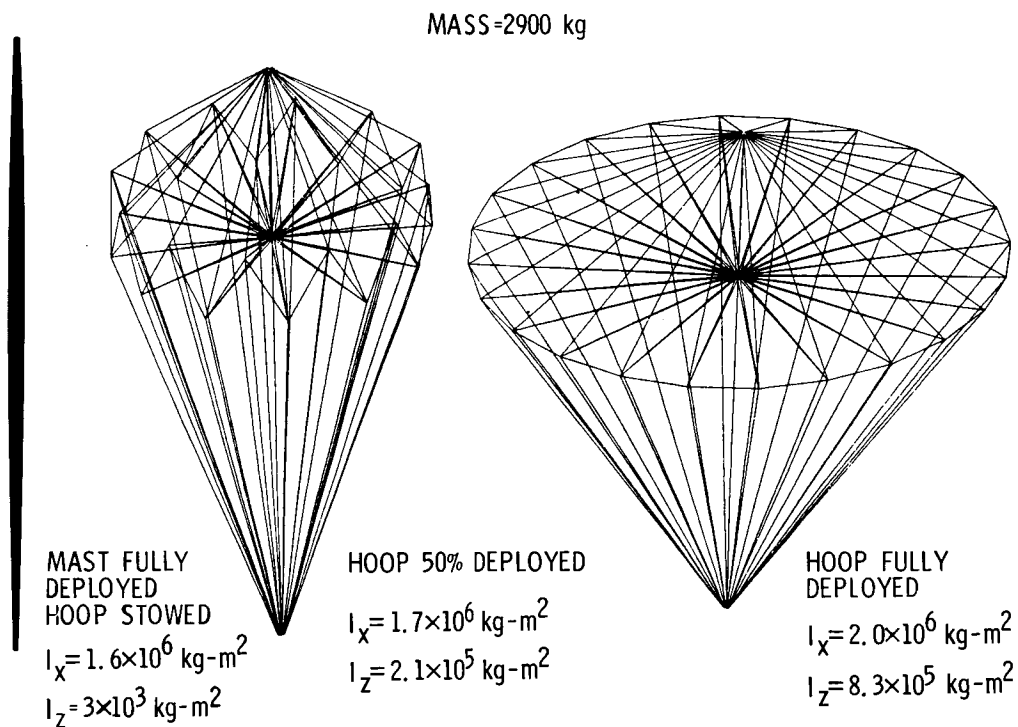


Figure 5. IDEAS Deployment Analysis Module

RIGID-BODY CONTROLLABILITY ANALYSIS

The Rigid-Body Control Dynamics (RCD) module calculates the on-orbit environmental forces and maneuver forces, and their corresponding torques on the spacecraft at user-specified circular orbital altitudes, spacecraft orientation, and mission duration. It then determines momentum storage and desaturation requirements, control system sizing criteria, and propellant requirements for stationkeeping, altitude control, and user-specified maneuvers. The principal features of RCD are shown in Figure 6. The total torque and force time histories are analyzed to determine cyclic momentum for momentum exchange system sizing and desaturation requirements. Momentum desaturation requirements are met using reaction control system (RCS) thrusters. RCS requirements for stationkeeping are also determined (Ref. 2).

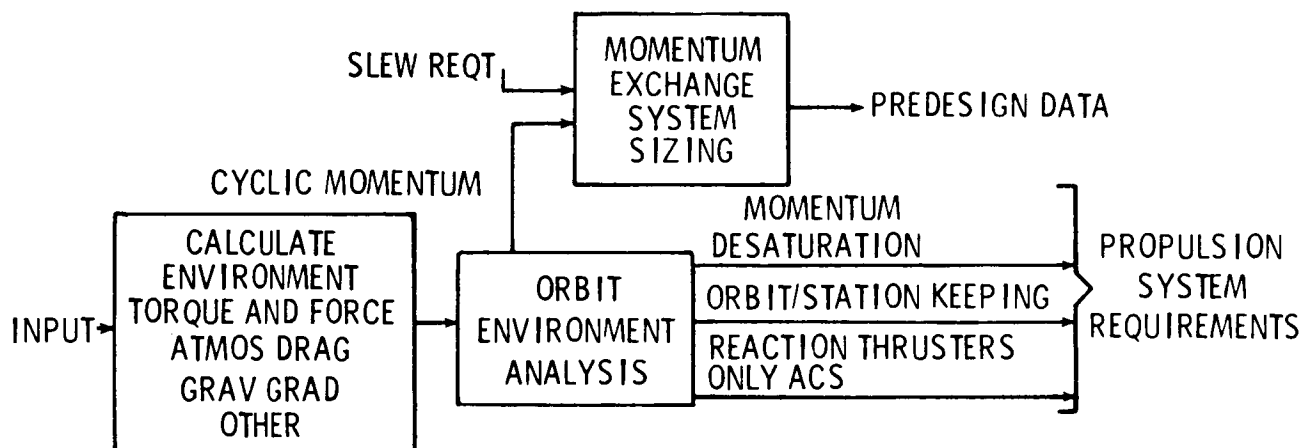


Figure 6. Rigid-Body Control Dynamics Module (RCD)

ALTERNATE CONFIGURATION ANALYSIS OF A MANNED ORBITING SPACE STATION

ORIGINAL PAGE IS
OF POOR QUALITY

A primary criterion for evaluating space station concepts is the on-orbit controllability of the space station itself. Due to the modular design of all space station concepts, the controllability of the station will vary during its evolutionary buildup phase. This is because the center of pressure, center of mass, moments and products of inertia, and aerodynamic drag areas are continuously changing. Research is under way to determine the force, torque and controller torque for several generic space station configurations. Time histories such as those in Figure 7 are used to size control moment gyroscopes and propellant storage facilities on the station. The forces are caused by three factors: aerodynamic drag, gravity gradient, and solar pressure. These histories are also used to determine the relative merits of various configurations flying at various orientations.

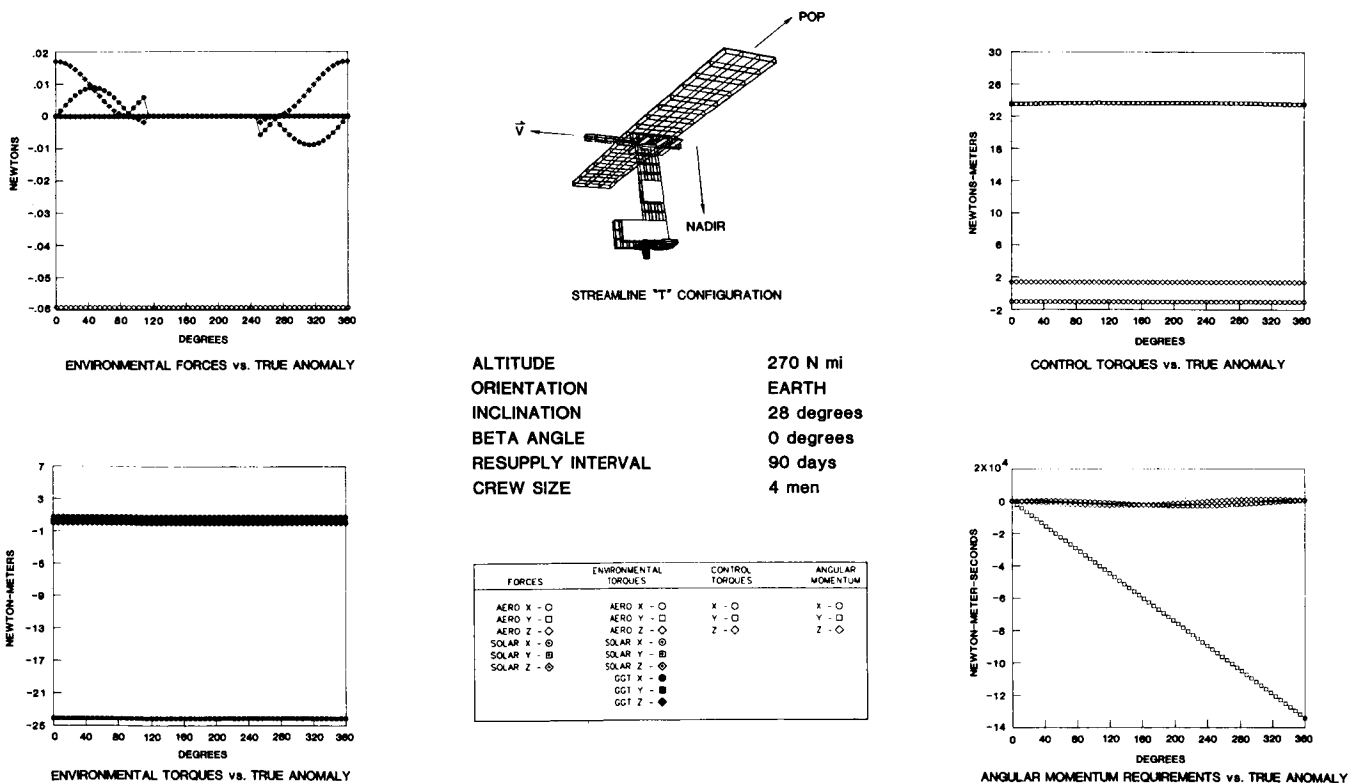


Figure 7. Controllability Analysis of Manned Space Station Configuration

INTERACTIVE THERMAL ANALYSIS

The finite-element model files can be transferred automatically to the Thermal Analyzer Program in order to calculate the transient temperature response for each structural member at a given position in the spacecraft orbit. Heat sources are solar radiation, Earth albedo, and Earth thermal radiation. The balance between absorption of energy from the elements out into deep space is used to determine the transient thermal response. Earth shadowing is included. Three major assumptions are made in this type of analysis. First, each element is considered to be an isothermal element. Secondly, the radiation exchanges between structural members are neglected due to small radiation view factors. Finally, structural member-to-member shadowing is neglected. Input into this module consists of the model geometry, thermal characteristics of all materials used in the structure and the position in the orbit where the thermal analysis begins and ends. Output yields elemental temperatures and heating rate time histories shown in Figure 8 (Refs. 4 and 5).

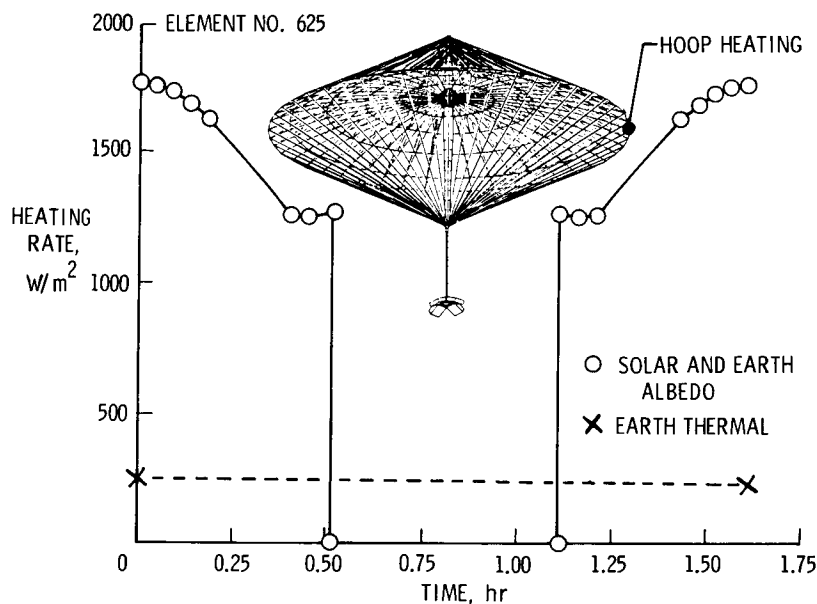


Figure 8. Hoop Column Antenna Heating Rates

THERMAL ANALYSIS OF LATTICE STRUCTURED SPACECRAFT

Selection of materials for use in the various concepts is an extremely important criterion in concept selection. Thermally induced loads are important contributors to the structural soundness of any concept. Analyses have been performed in order to determine the feasibility of two candidate materials for lattice-structured spacecraft. Figure 9 shows orbital temperature ranges for both aluminum and graphite epoxy as used in lattice-type structures designed to perform in equatorial orbits. In this case, aluminum members are colder throughout the orbit due to low absorptivity to emissivity ratio when compared to the absorptivity to emissivity ratio of graphite epoxy. In the Earth's shadow, the graphite epoxy exhibits faster cooling due to low thermal inertia. Using results such as these, it can be determined just what materials can be used for various missions (Ref. 5).

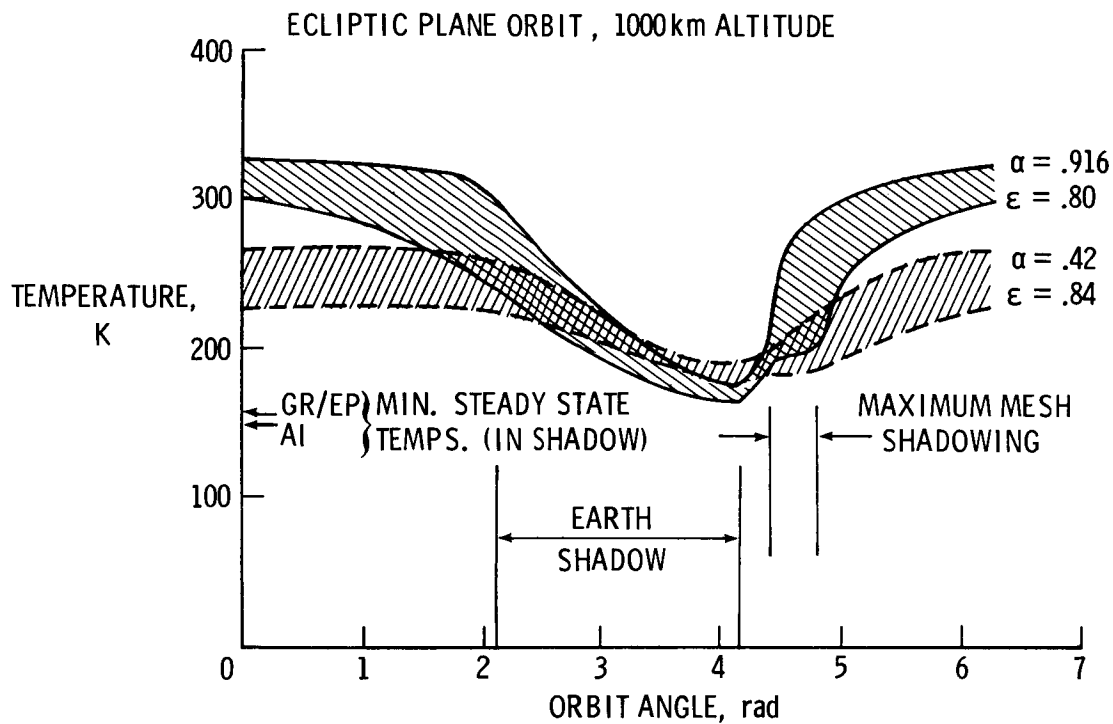


Figure 9. Orbital Temperature Ranges

STATIC STRUCTURAL LOADING ANALYSIS

A static loading analysis of a concept consists of two parts. First, a computation of all the environmental and spacecraft-induced loads must be performed. The loading sources are from thermal loading, gravity gradient loading, atmospheric drag, static thrust, and in the case of tension/compression structures, loads induced by structure pretension. With the loads identified, a static, linear structural analysis can be executed in order to obtain stresses and deflections. The second half of the analysis consists of graphically presenting the stress data in the form of applied axial loads. With this information, the analyst can interactively redesign specific elements that are identified as having potential stress problems. Figure 10 shows histograms of element loads experienced in a tetrahedral truss antenna dish structure. The top graphs represent the number of elements experiencing a range of both tensile and compressive loads due to all environmental effects. The bottom graphs represent the loads experienced by thermal effects only.

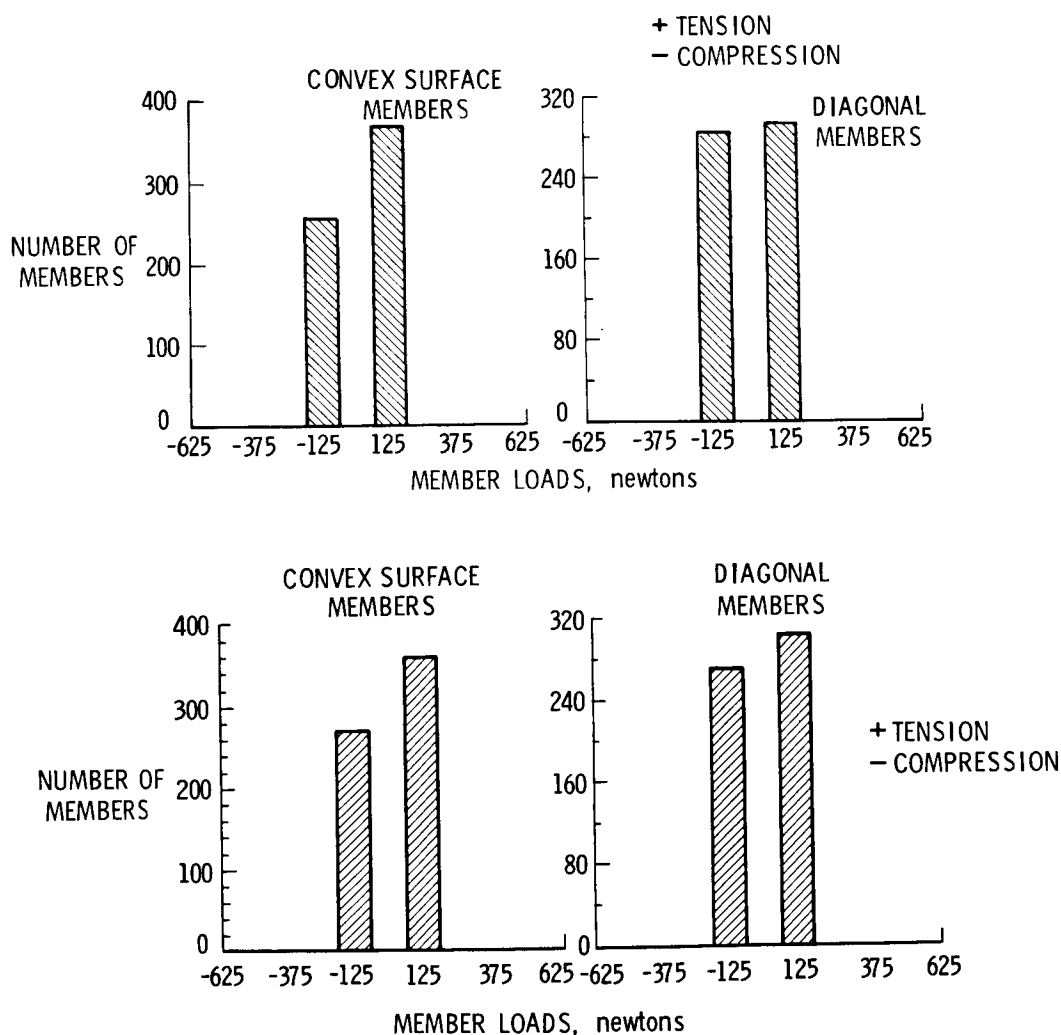


Figure 10. Microwave Radiometer Spacecraft Structural Member Loads

SURFACE ACCURACY COMPUTATIONS ON ANTENNA CONCEPTS

An important criterion in the analysis of large aperture space antennas is the performance of the antenna reflective surface. The reflective surface, mesh-like in composition, is usually fastened onto the antenna structure; therefore, structural deflections will tend to affect the surface roughness of the mesh. The surface accuracy module is designed to determine the rms surface roughness, defocus information and boresight offset information by utilizing the results of the static structural analysis in terms of nodal deflections. The surface roughness is determined and is just a parameter measuring the degree of roughness. It does not account for the errors in manufacturing and costing considerations. (See fig. 11.)

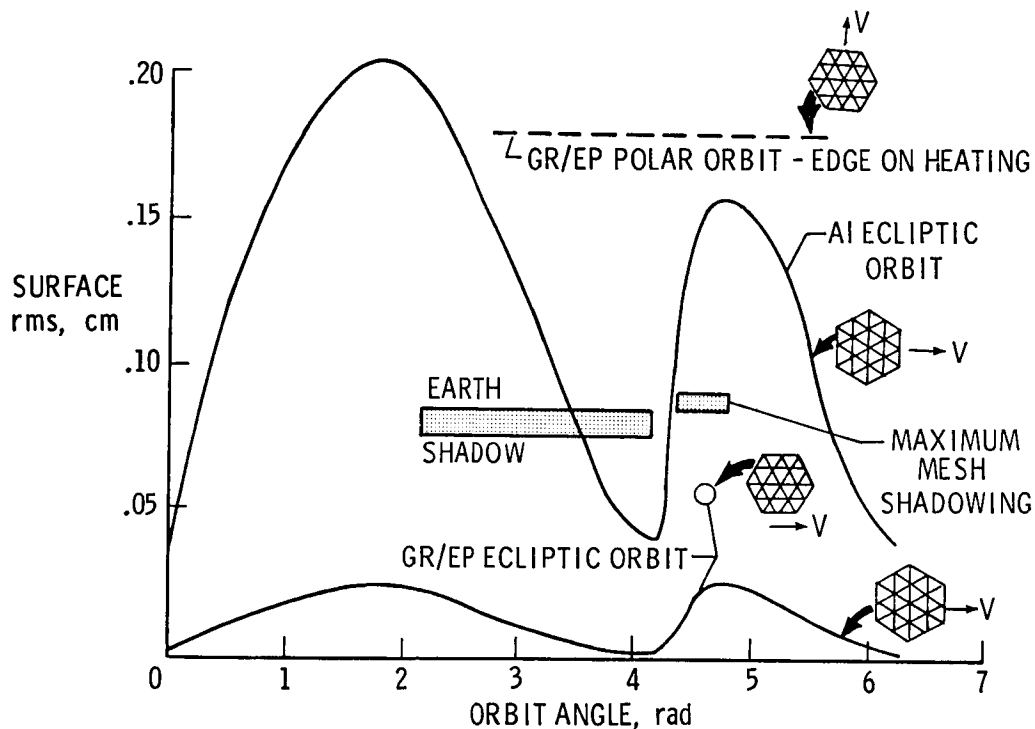


Figure 11. Surface Distortion Variations

DYNAMIC STRUCTURAL ANALYSIS

In the determination of the flexible body controllability, the natural frequencies of the structure must be determined. The finite-element model used throughout IDEAS can now be input into the structural analysis program for a linear dynamic analysis. Figure 12 shows one mode of vibration for the contiguous box truss structure used for Earth sciences missions and its correlation with an independent analysis using the NASTRAN structural analyzer. A design criterion for this type of structure was to increase the frequency of the first mode of vibration of the offset feed mast in order to match the frequency of the first mode of vibration of the reflective dish structure. These mode shapes and frequencies are also used in the dynamic response analysis of these types of structures (Ref. 6).

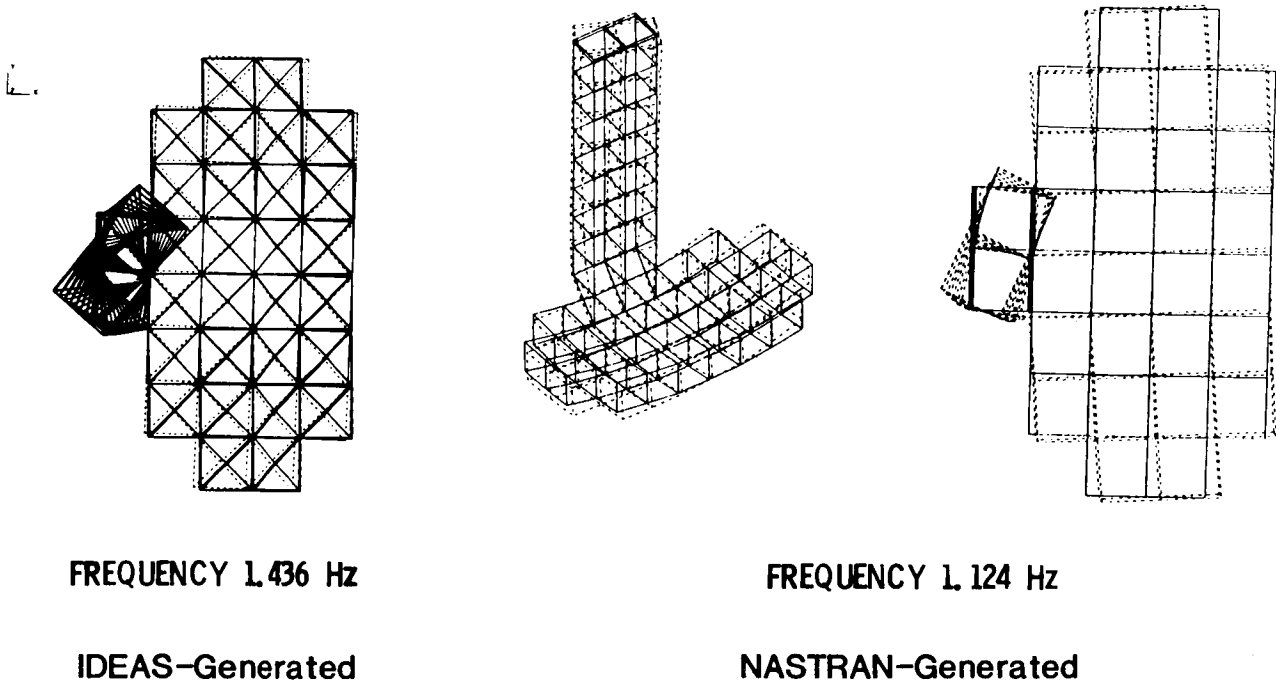


Figure 12. Vibrational Mode

DYNAMIC RESPONSE ANALYSIS OF LARGE SPACE ANTENNA

The dynamic response and structural loading of individual concepts of large space antenna are compared to reveal the relative merits and deficiencies of each system. Recommendations for system improvement can be made based on information obtained from this analysis. The nodal deflection responses of the individual concepts, such as those in Figure 13, illustrate the flexible nature of large structures. Utilizing natural frequency information extracted in the dynamic structural analysis, a concept can be subjected to proposed operational environments and the effects on structural displacement and member structural loads can be examined. The operational environments are modeled through the use of reaction control jets imparting an impulse of a specific magnitude and duration. Also, structural damping coefficients are taken into account in the analysis. The results of the analysis consist of excited modes, changes in structural surface roughness and nodal excursion (Ref. 7).

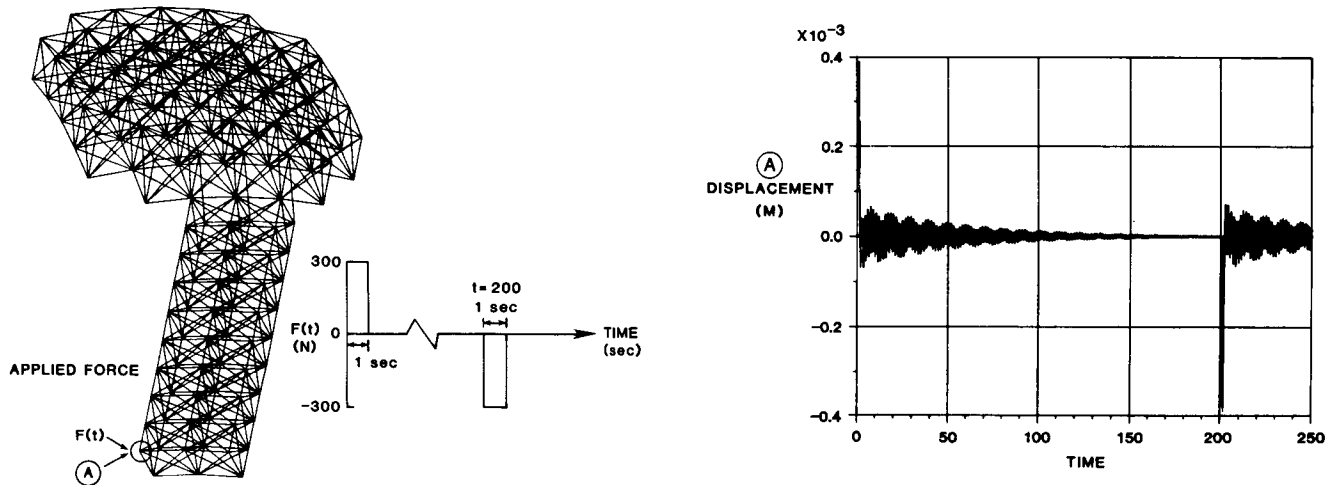


Figure 13. Box Truss Feed Mast Nodal Deflection Response

SUBSYSTEM SYNTHESIS

In addition to candidate system tradeoffs, the individual subsystems must be synthesized and their performance evaluated. The Subsystem Synthesis model allows a user to input mission parameters and payload support criteria in order to generate seven subsystems and their individual performance requirements. The functional methodology is shown in Figure 14. The subsystems are synthesized by selecting individual subsystem component parts from an equipment database. This database, consisting of some 2500 component parts, is sectioned into five subsystems: stabilization and control, propulsion, data processing and instrumentation, communications, and electrical power subsystems. The structural and thermal subsystems are not created through the use of database entries because the shape, size, volume, and power requirements of the total systems are unknown until the other five systems are defined. Output is in the form of total system and subsystem performance data and an assembly listing of all components selected from the database (Ref. 7).

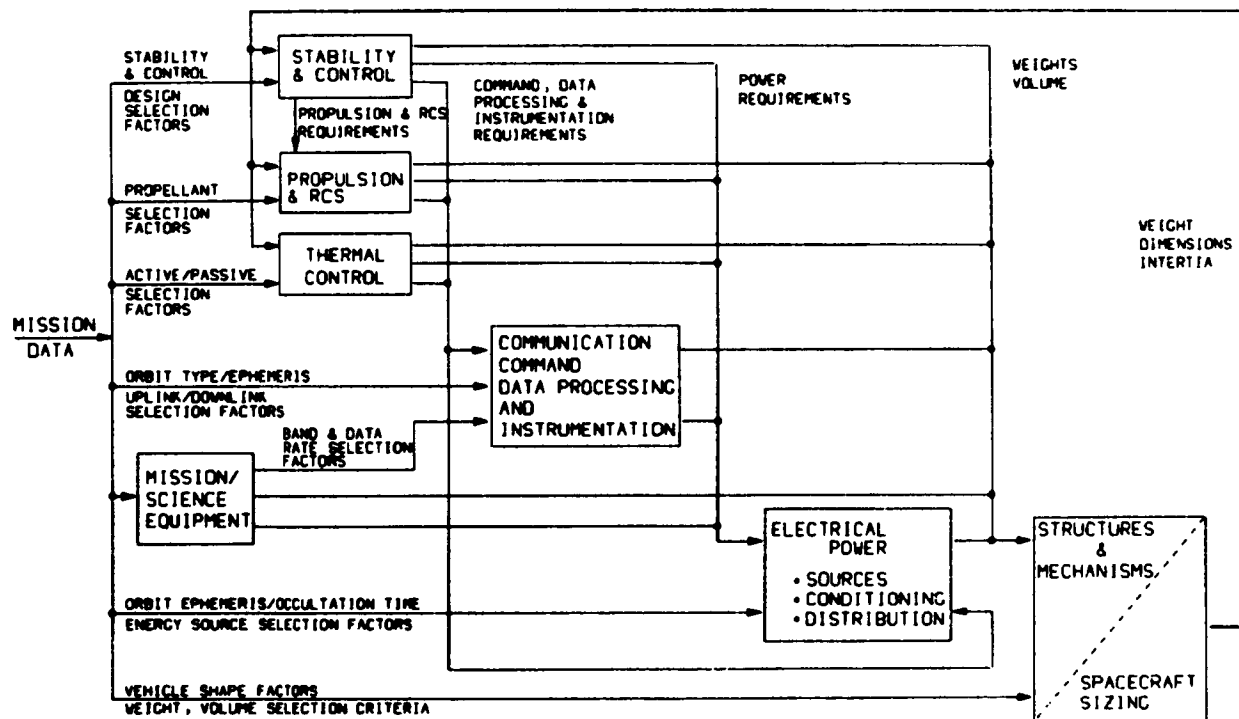


Figure 14. Spacecraft Subsystem Design

ENVIRONMENTAL CONTROL AND LIFE SUPPORT SYSTEM (ECLSS) COMPUTER-AIDED TECHNOLOGY ASSESSMENT PROGRAM

In the case of manned space flight, the ECLSS system candidates must be modeled and evaluated. The ECLSS Technology Assessment Program (Fig. 15) receives three forms of inputs: mission requirements and consumption rates, the candidate subsystems to be evaluated, and the criterion to which the evaluation is to be based. Mission inputs include mission duration, resupply interval, and crew size. Consumption rates include metabolic rates, water usage rates, and waste production rates. Various options are available in each of the ECLSS subsystems. For instance, air revitalization can be achieved through either stored gas or water electrolysis. Other methods of air revitalization could be used in conjunction with other subsystem options in order to determine overall ECLSS system performance. The output yields three results. First, the resupply and consumables requirements are determined. Second, overall ECLSS system performance is quantified and finally, the life cycle costs for all candidate systems are computed (Ref. 8).

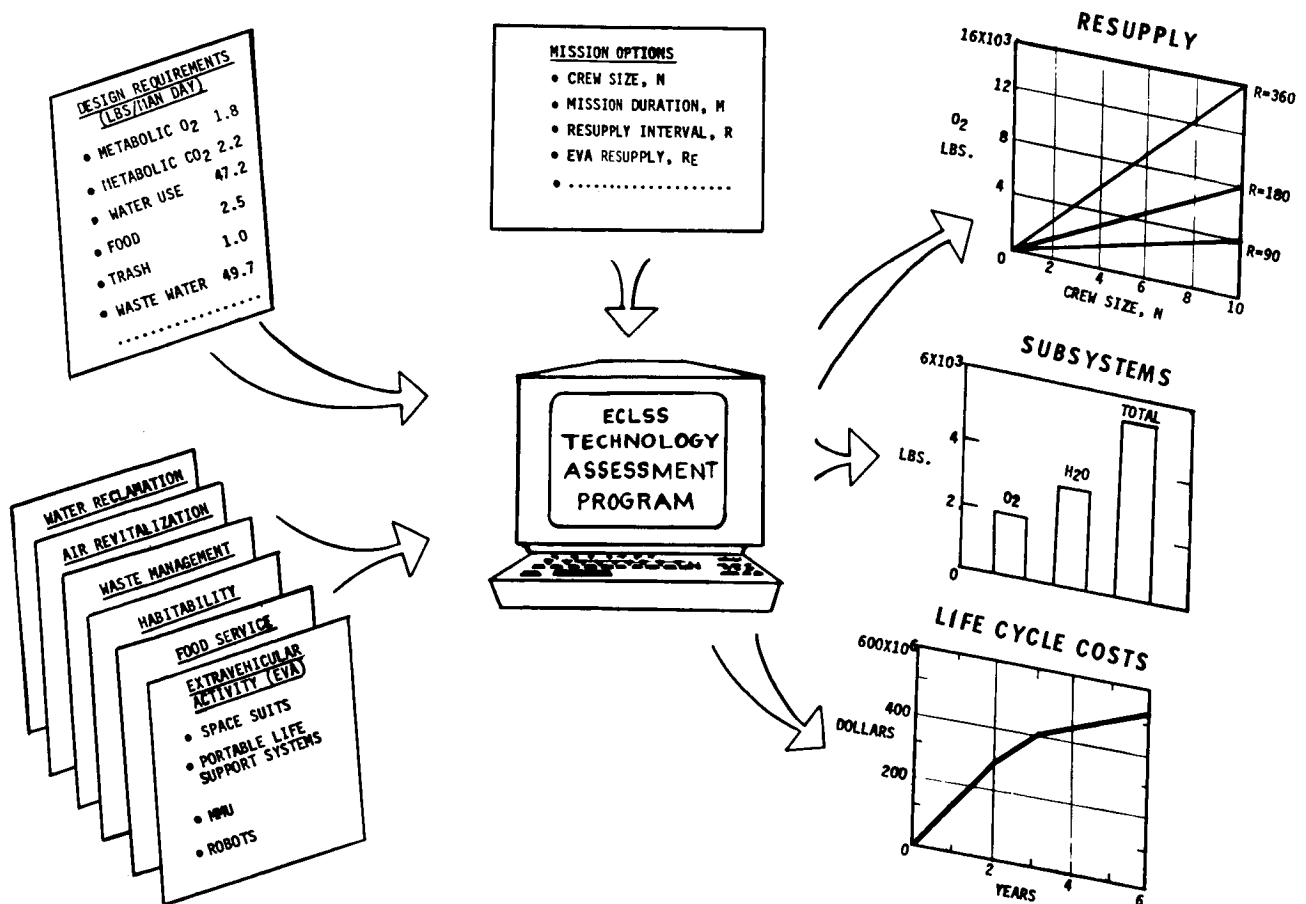


Figure 15. Environmental Control and Life Support System (ECLSS) Computer-Aided Technology Assessment Program

PROPOSED DEVELOPMENTS FOR IDEAS

IDEAS, as it now stands, is a system designed to provide a user with a good first-order analysis of a multiplicity of candidate designs in rapid fashion. It is recognized that IDEAS can be further improved with the items listed in Figure 16. Near-term developments include the vibration and dynamic loading analysis capabilities, kinematic and kinetic analysis capabilities, thermal analysis of structures including radiation view factors and thermal interelement conduction, and the analysis of the performance of thermal radiator (heat pipe) systems. Far-term improvements for IDEAS as well as for computer-aided design will include the constant maintenance of the spacecraft subsystem database, the incorporation of second-order analysis capabilities in structural analysis, thermal analysis and flexible-body controls, the simulation/emulation of spacecraft subsystems, and the cost/reliability/risk analysis capability of the various space systems.

STRUCTURAL DYNAMICS

- Improve and Refine Vibration and Dynamic Loading Analyses

DEPLOYMENT ANALYSIS

- Improve Kinetic and Kinematic Analyses

THERMAL ANALYSIS

- Include Interelement Shadowing and Conduction, Radiation View Factors and Area Structures
- Heat Pipe Performance

SUBSYSTEM ANALYSIS

- Update Subsystem Data Base
- Incorporate ECLSS Design Algorithms into Subsystem Synthesis Module

ADDITIONAL ANALYSES

- Second-Order Analysis in Following Areas:
 - Structural Analysis
 - Thermal Analysis
 - Controls
- Cost/Reliability/Risk Analysis
- Subsystem Simulation/Emulation

Figure 16. Proposed Developments for IDEAS

OPTIMIZATION ISSUES IN MULTIDISCIPLINARY INTERACTIVE DESIGN

In this type of design process, one finds many needs for the optimization of the space system design. In the area of rigid-body controllability, the determination of a concept's natural orientation in flight (that is, the principal axis of inertia is aligned with the local vertical of the spacecraft) will aid in the determination of the desired orientation of the spacecraft as well as where the thrusters can be placed. Also, in thermal analysis of these structures, the worst-case altitude for thermal distortion is usually determined by trial and error. Research is required in this area in order to more accurately predict the points in orbit where thermal effects on a structure are at a maximum. Finally, the environmental control/life support subsystem performance algorithms should be incorporated into the subsystem synthesis program so that a total systems concept could be synthesized and optimized. (See fig. 17.)

SPACECRAFT CONTROLLABILITY

- Preferred Orientation

Determination of Attitude Minimizing Control Torques

THERMAL ANALYSIS

- Determination of Worst Case Attitude for Max. Stress, Max. Distortion

SUBSYSTEM PERFORMANCE

- Incorporation of ECLSS Algorithms into Subsystem Performance Module

Figure 17. Optimization Issues

CONCLUDING REMARKS

ORIGINAL PAGE IS
OF POOR QUALITY

The Interactive Design and Evaluation of Advanced Spacecraft computer-aided design and analysis system is a multidisciplinary tool for use in the evaluation of competing concepts of advanced space systems on a conceptual level. Figure 18 shows the capabilities of the system. A user can interactively create a model, assign mass/inertia properties, synthesize the corresponding subsystems and perform structural, thermal, and environmental analyses rapidly. The time to perform a complete systems analysis usually requires 1 man-month. Because of the rapidity of the design/evaluation process, many concepts can be evaluated. The capabilities of the system have been demonstrated with results of studies performed on large space antennae and manned space stations. Optimization issues have been identified and plans for updating the system have been recommended.

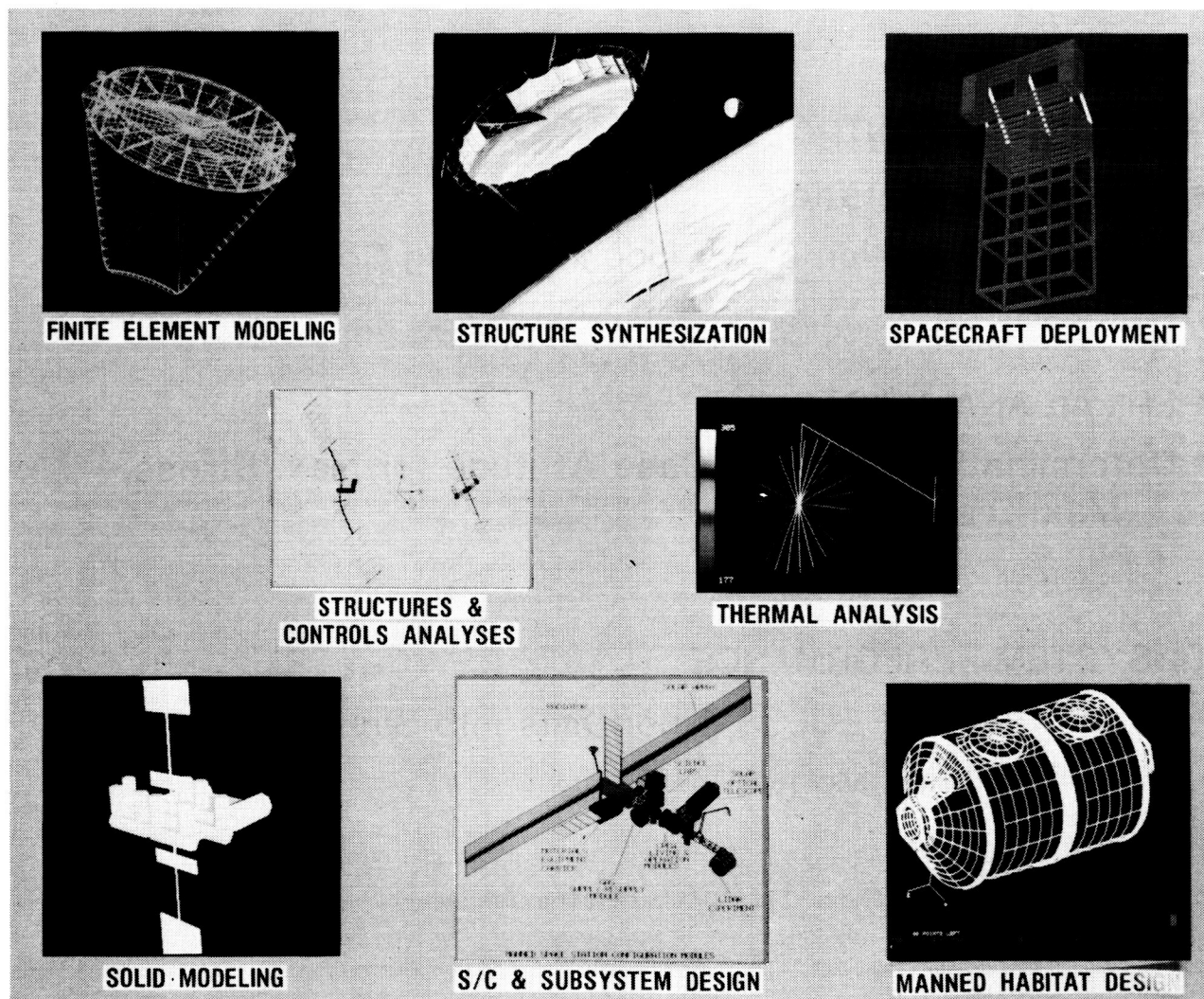


Figure 18. IDEAS Capabilities

REFERENCES

1. Garrett, L. B.: Mathematical Synthesization of Complex Structures. Computer-Aided Geometry Modeling, NASA CP-2272, 1984, p.389.
2. Garrett, L. B.: Interactive Design and Analysis of Future Large Spacecraft Concepts. NASA TP-1937, December 1981.
3. Garrett, L. B. and Ferebee, M. J., Jr.: Comparative Analysis of Large Antenna Spacecraft Using the IDEAS System. AIAA Paper No. 83-0798-CP, May 1983.
4. Wright, R. L. and DeRyder D. D.: Orbital Thermal Analysis of Lattice Structured Spacecraft Using Color Video Display Techniques. NASA TM-85640, June 1983.
5. Garrett, L. B.: Thermal Modeling and Analysis of Structurally Complex Spacecraft Using the IDEAS System. AIAA Paper No. 83-1459, June 1983.
6. Wright, R. L., DeRyder, D. D., Ferebee, M. J., Jr., and Smith J. C.: Interactive Analysis of a Large Aperature Earth Observations Satellite. SAWE Paper No. 1556, May 1983.
7. Ferebee, M. J., Jr., Garrett, L. B., and Farmer, J. T.: Interactive Systems Analysis of a Land Mobile Satellite System. AIAA Paper No. 83-0219, January 1983.
8. Hall, J. B., Sage, K. H., and Pickett, S. J.,: Manned Space Station Environmental Control and Life Support System (ECLSS) Computer-Aided Technology Assessment Program. Presented at the Fourteenth Annual Intersociety Conference on Environmental Systems (ICES), San Diego, California, July 16-18, 1984.

N87-11762

MICROCOMPUTER DESIGN AND ANALYSIS OF THE CABLE CATENARY
LARGE SPACE ANTENNA SYSTEM

W. AKLE
TRW
REDONDO BEACH, CALIFORNIA

PRECEDING PAGE BLANK NOT FILMED

SYSTEM ENGINEERING AT THE CROSSROAD

For those of us who experienced the challenge of opening space to the post-Apollo overspecialization, the 1980's promise a return to a more personal involvement in the systems we are creating. The personal computer is offering us, individually, an almost unlimited engineering data base, computing power, and availability. It is now practical to generate integrated solutions to preliminary, system level multidisciplinary problems with a small engineering team.

This paper describes one attempt to meet this challenge in the area of Integrated System Design of Large Spacecraft (ISDLS).

| | | |
|-----------------|---------------------------------------|--|
| UP TO 1950's | THE DESIGN ENGINEER AS A 'HERO' | <ul style="list-style-type: none">• SLIDE RULES AND FAST AIRPLANES• ONE-MAN DESIGNS |
| 1970's | AGE OF SPECIALIZATION | <ul style="list-style-type: none">• FORTRAN/NASTRAN• MOON LANDING• MASS ENGINEERING AND SPECIALIZATION |
| 1984 | ENGINEERING IN TRANSITION | <ul style="list-style-type: none">• OPERATIONAL STS• 3RD GENERATION PERSONAL COMPUTERS |
| 1990's | THE 'COMPLEAT' SYSTEM ENGINEER? | <ul style="list-style-type: none">• INTERACTIVE CREATIVITY: INTUITION FOLLOWED BY PROOF |

Figure 1

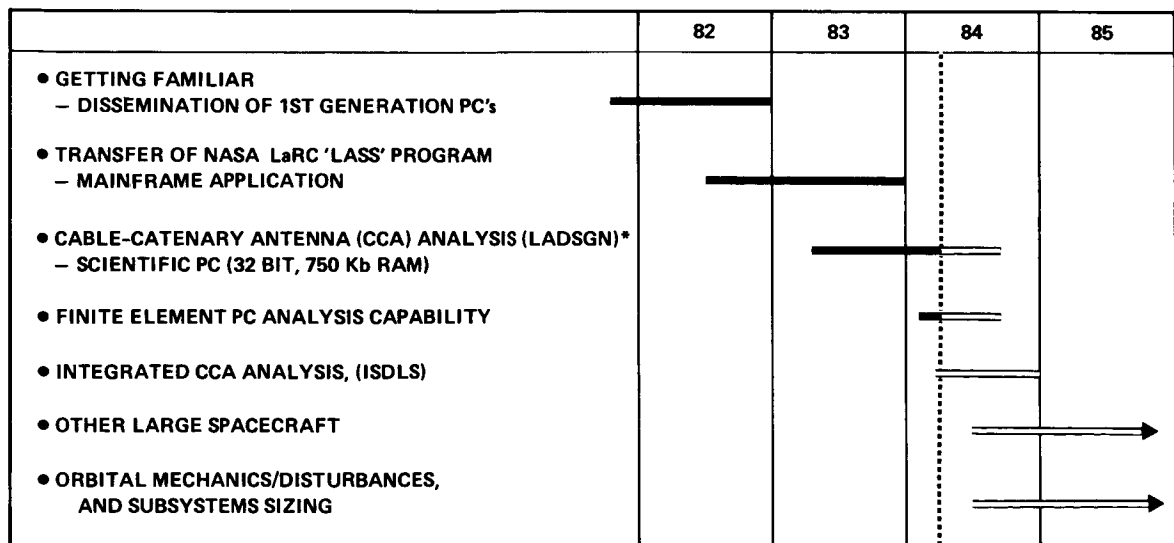
DEVELOPMENT OF SYSTEM DESIGN ANALYSIS CAPABILITY

As part of its productivity effort, TRW provided personal computers (PC) to its system engineers as they became available. This encouraged learning of personal programming and PC.

Since the early 1970's, NASA LaRC had been developing the "dream" program to integrate total preliminary spacecraft system design. One program, Large Advanced Space Systems (LASS), based on mainframe computers, was highly successful in many applications. Some of the LASS capability was implemented in 1983 on the TRW time-share system.

The convergence of a) LASS methodology, b) the emerging familiarity with PC's, and c) availability of low cost, 32 bit scientific PC's has led TRW system engineers to start developing the PC-based Integrated System Design of Large Spacecraft (ISDLS).

Plan - Integrated System Design of Large Spacecraft



*LADSGN: LARGE ANTENNAS DESIGN

Figure 2

THIRD GENERATION SCIENTIFIC PC

The shift from mainframe implementation of "LASS" to implementing Large Antenna Design (LADSGN) occurred when we became aware of the capacity of the latest PC's.

As an example, in our work we are using the Hewlett-Packard Series 200 (HP9816). Its use was prompted by the fact that it was accessible and had capacity well in excess of our predicted needs. Compared to timeshare programming methodology, the results were almost instantaneous, allowing fast familiarization, debugging and program build-up.

One drawback is that the disk operating system and the powerful HPL language are not transportable. For wide personal use, a simple language, such as BASIC, though slower may be more universal.


- 
- | | |
|--|--|
| • PERSONAL CONTROL | – USER IS THE PROGRAMMER RAPID CHANGES AND UPDATES |
| • SPEED (32 BIT MICRO PROCESSORS) | – EXTENSIVE LOOPING AND SIMPLE CONVERGENCE ANALYSIS |
| • CAPACITY (3/4 Mb RAM; 15 Mb DISC) | – ALLOWS EXTENSIVE PROGRAM OVERHEAD FOR EASIER MAINTENANCE: PROMPTS, ANNOTATIONS... |
| • COST (LESS THAN \$8K) | – DEDICATED PC CAN FOLLOW THE JOB FOR COLLOCATIONS |

Figure 3

DATA BASE - CORE OF INTEGRATED SYSTEM ANALYSIS

The system design engineer generating PC programs to solve unique problems is doing the peripheral technical work required by ISDLS. With the advent of large capacity PC's it is natural to want to couple some of these programs together.

The key to achieving "linkage" between various programs is a common data base. The ISDLS program follows this simple technique. **Because a large memory storage** capability is available, there is no need to cut corners in data base allocations. What is required is to make such an allocation, with room for growth.

Once this data base is identified, productive work can start with one program, and expand as time and demands dictate.

An added advantage is the ability to make rapid changes to the conceptual design modeling and analysis.

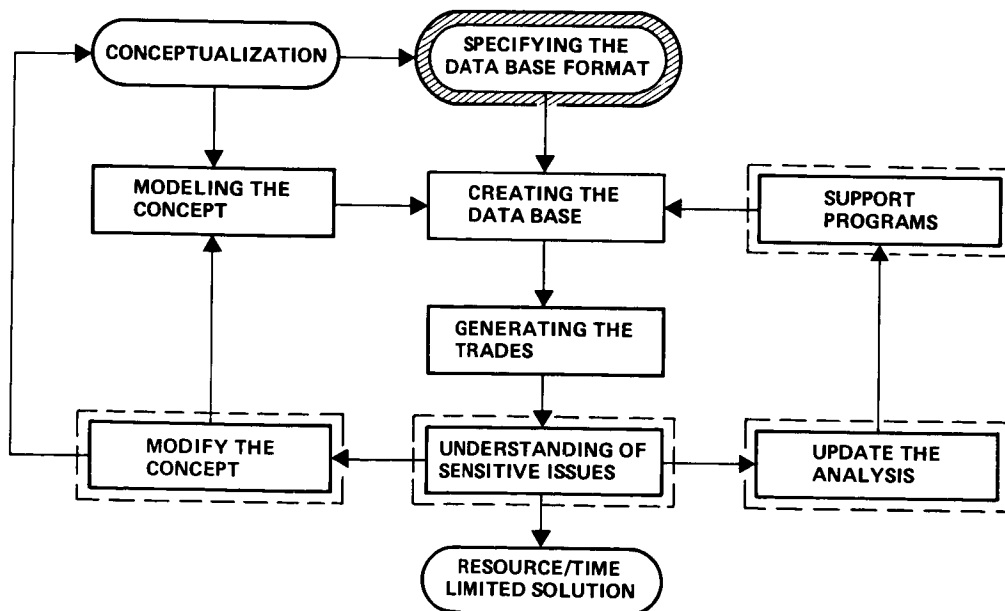


Figure 4

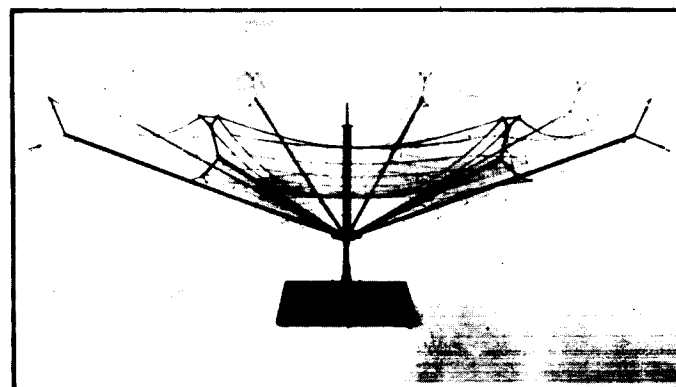
THE CABLE CATENARY ANTENNA (CCA)
LARGE ANTENNA DESIGN (LADSGN) PROGRAM

The CCA has been under development by TRW since the late 1960's. It is adaptable to very large diameters (over 1000 ft) while still remaining compatible with an STS system launch. The figure shows a 10 ft working model of the CCA.

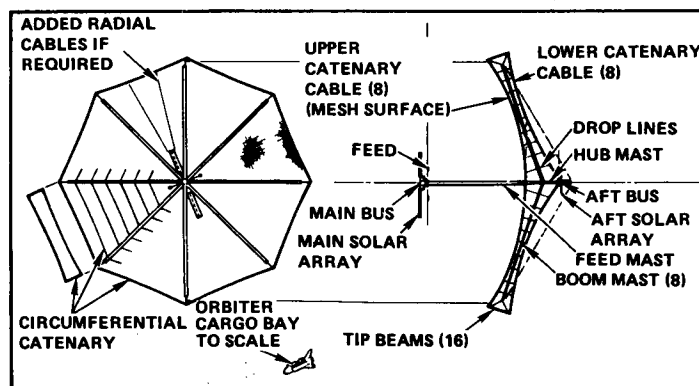
Its main elements are:

- 8 radial deployable booms
- A deployable hub and a feed support mast
- Balanced (front and back) radial and circumferential catenary cabling (this concept has no interfering cabling in the antenna's operational field)
- Drop lines to maintain the catenaries' front and back shades
- An RF reflecting mesh supported on the front catenaries

Also shown is a typical satellite configuration in which subsystem buses and solar array are integrated.



CABLE CATENARY ANTENNA, 10-FOOT SCALE MODEL



TYPICAL SATELLITE CONFIGURATION - CABLE CATENARY ANTENNA

Figure 5

STS COMPATIBILITY IS INTEGRATED INTO THE LADSGN PROGRAM

As an example of the integrated system level analysis capability of LADSGN, physical constraints stowage analysis is performed within the program.

Allocations may be made in the LADSGN internal default parameters (IDP) for the following:

- STS lift capability
- OTV weight and length as a function of spacecraft weight
- Space allowance for STS CCTV, EVA, and spacecraft buses

LADSGN attempts to maintain CCA weight, length, and diameter within these limits.

OTV: Orbital Transfer Vehicle
EVA: Extra Vehicular Activity
CCTV: Closed Circuit TV

Cable Catenary Antenna Spacecraft Stowage Concept in the STS

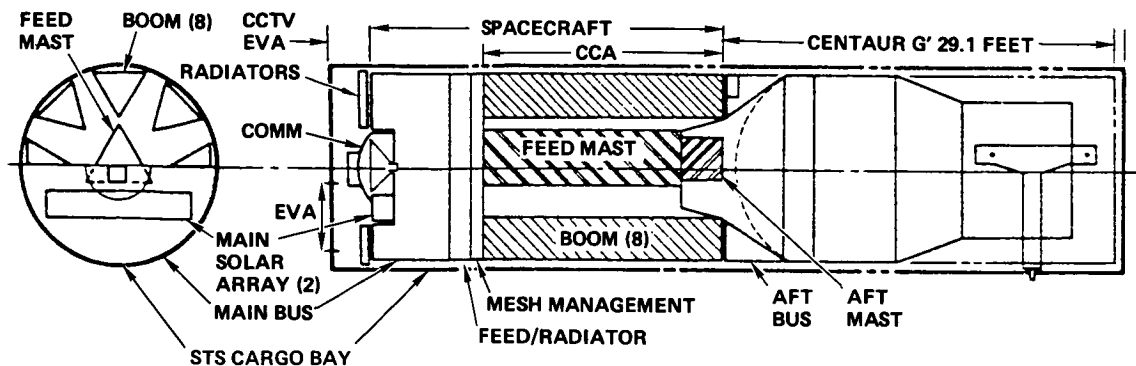


Figure 6

PROGRAM STRUCTURE

Several features are built in LADSGN to make it "friendly" to the user-programmer.

Use of Internal Default Parameters (IDP) achieves one of the program goals:

1. Inputs are reduced to the major trade variables.
2. Specialized parameters (material properties, mesh design, ...) are preset. They can be modified easily if so desired.

To be easily reprogrammable, each analytical step is self contained; the equations and IDP's are written in "English." Optimization is achieved by looping through the steps. This technique requires more program lines but is easily understood by a non-programmer.

| INPUTS | INTERNAL DEFAULT PARAMETERS (IDP) | MAJOR CONVERGENCE LOOPS | OUTPUT |
|---|---|--|--|
| <ul style="list-style-type: none">• ANTENNA TYPE• DIAMETER• F/D RATIO• RF FREQUENCY• SURFACE ACCURACY• 1ST DYNAMIC MODE• POINTING• OPTIMIZE LENGTH OR WEIGHT | <ul style="list-style-type: none">• ANTENNA MIN NUMBER OF GORES CABLING SIZE AND LOADS, MESH SIZING AND LOADS• STRUCTURES MATERIALS PROPERTIES TUBING MIN t, D, D/t COLUMN L/P RANGE• MECHANICAL STOWAGE PARAMETER, PRELOADS | <ul style="list-style-type: none">• BOOMS MAST<ul style="list-style-type: none">– LONGERON BUCKLING– CRIPPLING– MAST BUCKLING– STOWED LENGTH– STOWED WEIGHT• FEED/HUB MAST (REPEAT ABOVE) | <ul style="list-style-type: none">• DATA STORAGE<ul style="list-style-type: none">– INPUTS– MASS PROPERTIES• PRINTOUT• GRAPHICS |
| | | <div>TIME TO PERFORM:</div> <ul style="list-style-type: none">• LESS THAN 5 SEC | <ul style="list-style-type: none">• PRINTOUT 1 MIN• GRAPHICS 5 MIN |

(PROGRAM LADSGN: 37 K BYTES, 869 LINES).

Figure 7

LADSGN PROGRAM LOGIC

LADSGN logic diagram also illustrates the extensive use of loops and analysis modules.

For the CCA the total analysis is first done for the boom masts and then repeated for the feed-hub mast.

After convergence is achieved, full mass properties are derived and all data is stored in the common data base.

A detailed printout and graphics plot complete the output.

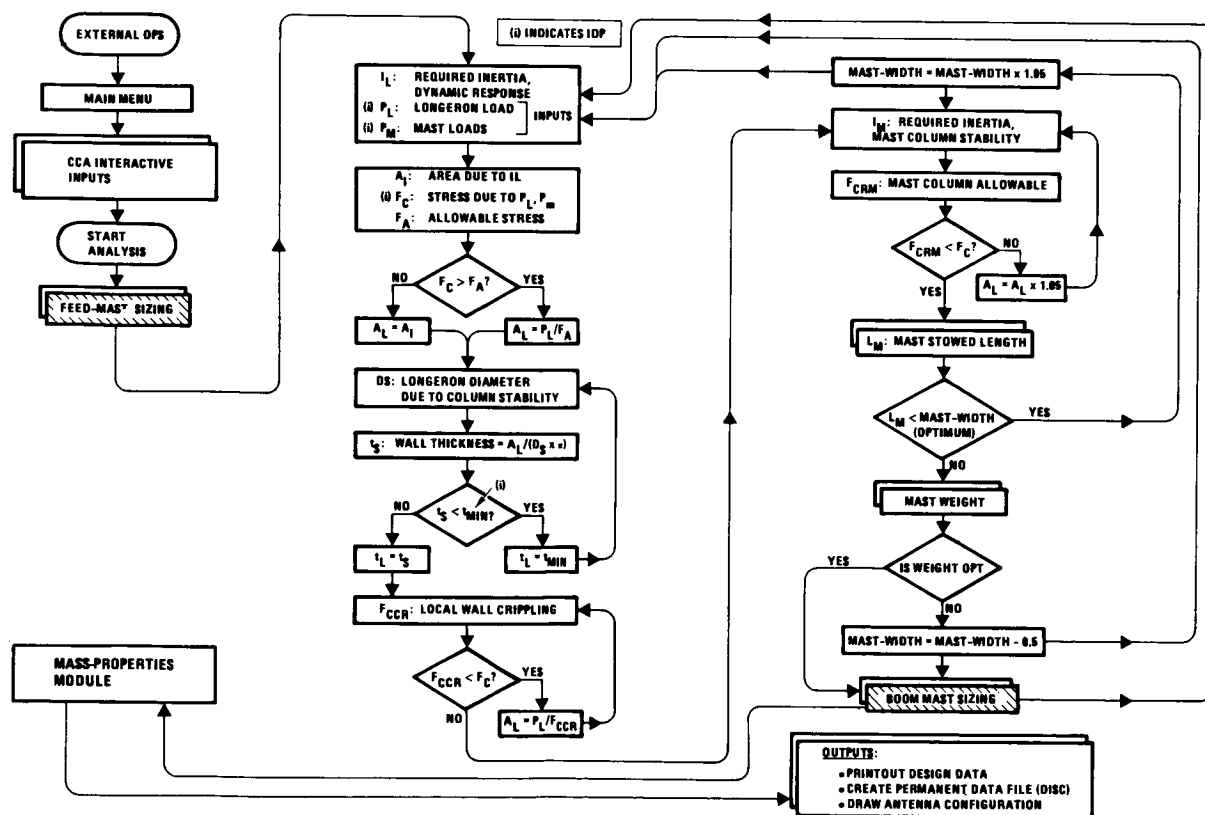


Figure 8

LADSGN PRINTOUT

The printout provides all the design and analysis data required to detail "draft" the structure as well as carry the analysis to other programs.

Critical design conditions and weights are identified to sensitize the user to the configuration "drivers."

ORIGINAL PAGE IS
OF POOR QUALITY

```
09:31:58 20 Oct 1983
'LADSGN' PROGRAM ,Wade AKLE , VERSION 1.1

***** CABLE-CATENARY ANTENNA SIZING ANALYSIS *****
ANTENNA DIAMETER (Ft)= 100
FOCAL LENGTH/DIAMETER (F/D) = .6
OPERATING RF FREQUENCY (GHz)= 2
SURFACE ACCURACY (WAVELENGTH/MAX ERROR)= 16
MAIN ELEMENT STRUCTURAL RESPONSE (Hz)= .1
OPERATING RF WAVELENGTH (Ft)= .5
NUMBER OF GORES = 14
OFF-POINTING ANGLE FROM NADIR (Deg)= 8
=====
MASTS SIZED TO OPTIMIZE WEIGHT, WITHIN MAX ALLOWED WIDTH

===== FEED MAST DESIGN DATA OUTPUT:
MAST DESIGNED BY LONGERON BUCKLING DUE TO GENERAL
COMPRESSIVE MAST LOADS (Lb)= 1700
MATERIAL ALLOWABLE STRESS IS CRITICAL!

MAST DEPLOYED LENGTH (Ft)= 67
MAST STOWED LENGTH (Ft)= 2.6
MAST BAY WIDTH=BAY HEIGHT (Ft)= 1
NUMBER OF BAYS = 67

LONGERON DIAMETER (Ft)= .0289
LONGERON THICKNESS(Ft)= .00140

CANISTER WEIGHT (Lb)= 19.0
LONGERON WEIGHT (Lb)= 15.4
BATTENS WEIGHT (Lb)= 7.7
DIAGONALS WEIGHT (Lb)= 4.4
JOINTS WEIGHT (Lb)= 22.1
MECHANISM WEIGHT (Lb)= 12.0
===== TOTAL MAST WEIGHT (Lb)= 80

===== CATENARY BOOM-MAST DESIGN DATA OUTPUT:
MAST DESIGNED BY LONGERON BUCKLING DUE TO GENERAL
COMPRESSIVE MAST LOADS (Lb)= 1269
MATERIAL ALLOWABLE STRESS IS CRITICAL!

MAST DEPLOYED LENGTH (Ft)= 50
MAST STOWED LENGTH (Ft)= 1.9
MAST BAY WIDTH=BAY HEIGHT (Ft)= 1
NUMBER OF BAYS = 50

LONGERON DIAMETER (Ft)= .0251
LONGERON THICKNESS(Ft)= .00239

CANISTER WEIGHT (Lb)= 19.0
LONGERON WEIGHT (Lb)= 4.8
BATTENS WEIGHT (Lb)= 2.4
DIAGONALS WEIGHT (Lb)= 2.5
JOINTS WEIGHT (Lb)= 16.5
MECHANISM WEIGHT (Lb)= 12.0
===== TOTAL MAST WEIGHT (Lb)= 57

***** CABLE-CATENARY ANTENNA MASS PROPERTIES *****
ANTENNA MESH MESH WEIGHT (Lb)= 19
RADIAL CATENARIES WEIGHT = 12
CIRCUMFERENTIAL CATENARIES= 2
TIP MASTS WEIGHT = 81
MECHANISMS WEIGHT = 7
-----
TOTAL ANTENNA WEIGHT (Lb)= 664.
ANTENNA CG FROM PARABOLA APEX (Ft)= +7.0

ANTENNA INERTIA (PERPENDICULAR TO AXIS) (Lb-Ft^2)=+6.01E+05
ANTENNA INERTIA (PARALLEL TO AXIS) (Lb-Ft^2)=+7.27E+05
ANTENNA CROSS INERTIA (Lb-Ft^2)=+0.00E+00
OFF-POINTING ANGLE FROM NADIR (Deg)= 8.0
```

Figure 9

LADSGN INTEGRATED GRAPHICS OUTPUT

Graphics output summarizes the results and provides for an accurate drawing of the specified antenna.

ORIGINAL PAGE IS
OF POOR QUALITY

Cable Catenary Antenna Design Output

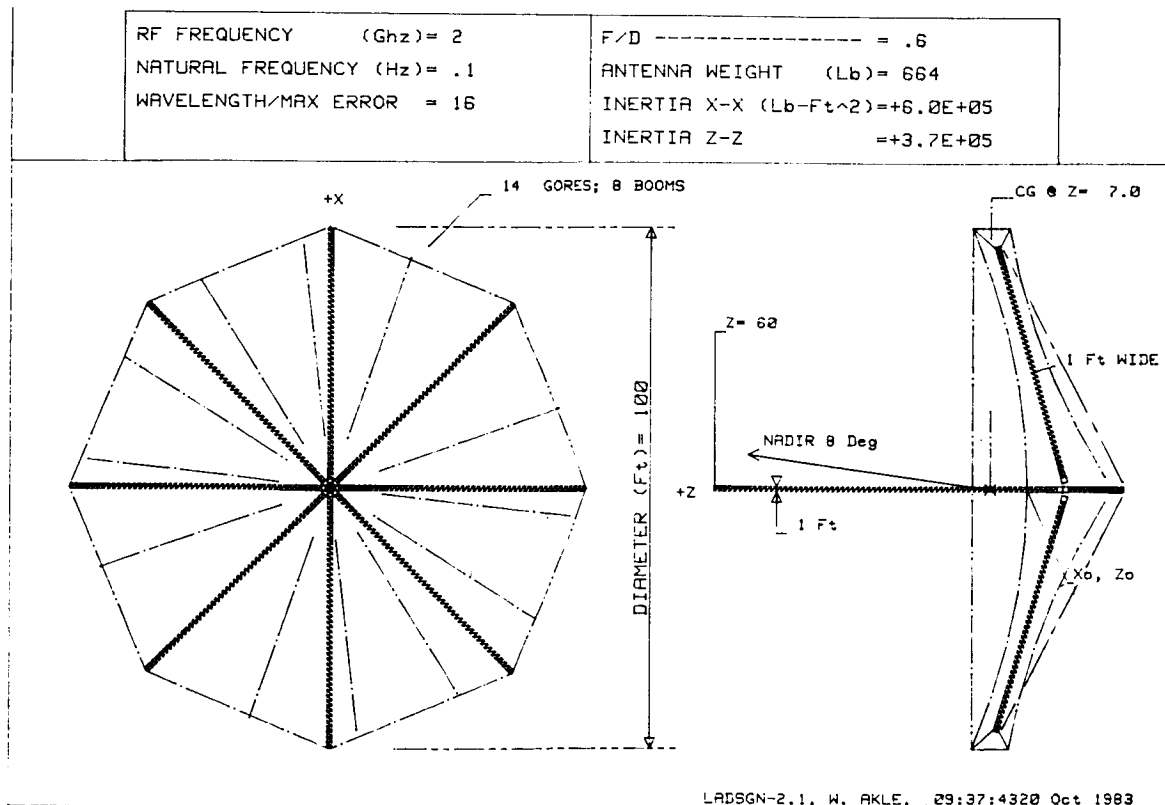


Figure 10

CCA TRADES USING 'LADSGN'

The power of interactive personal programs resides in their ability to produce system trades over a wide range of selected parameters.

In a matter of a couple of hours, many types of system trades can be generated.

The PC usefulness resides not only in the amount of data generated, but more meaningfully, in sensitizing the user to the critical elements of his design (and his program).

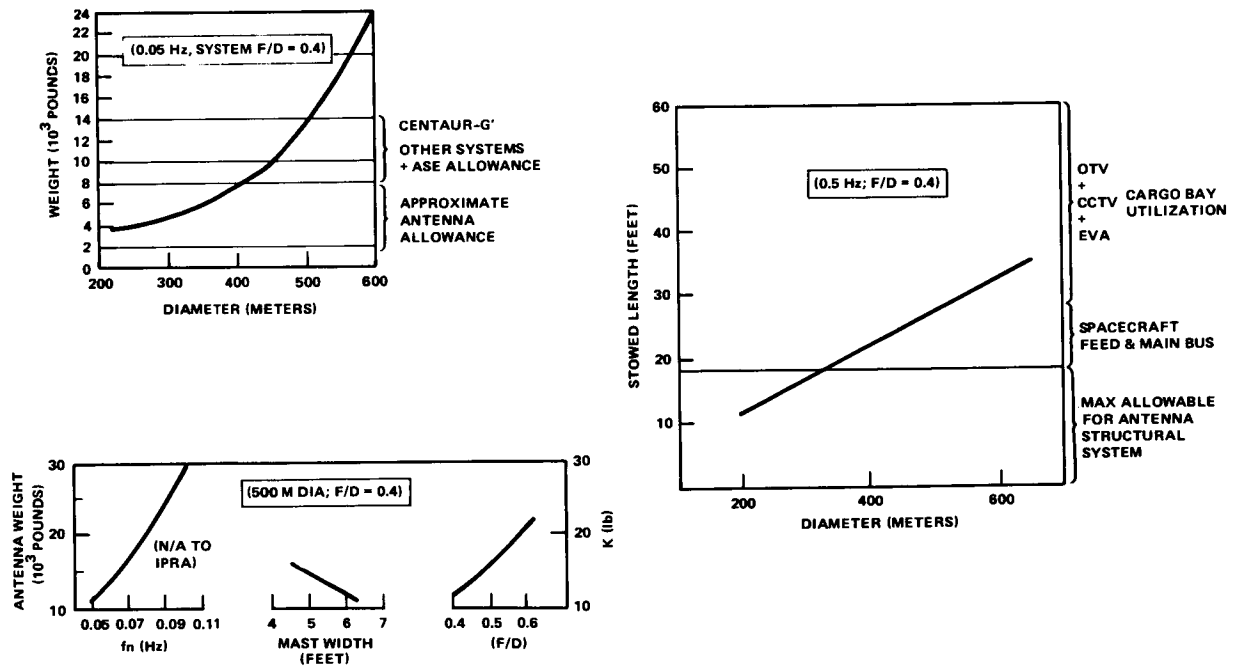


Figure 11

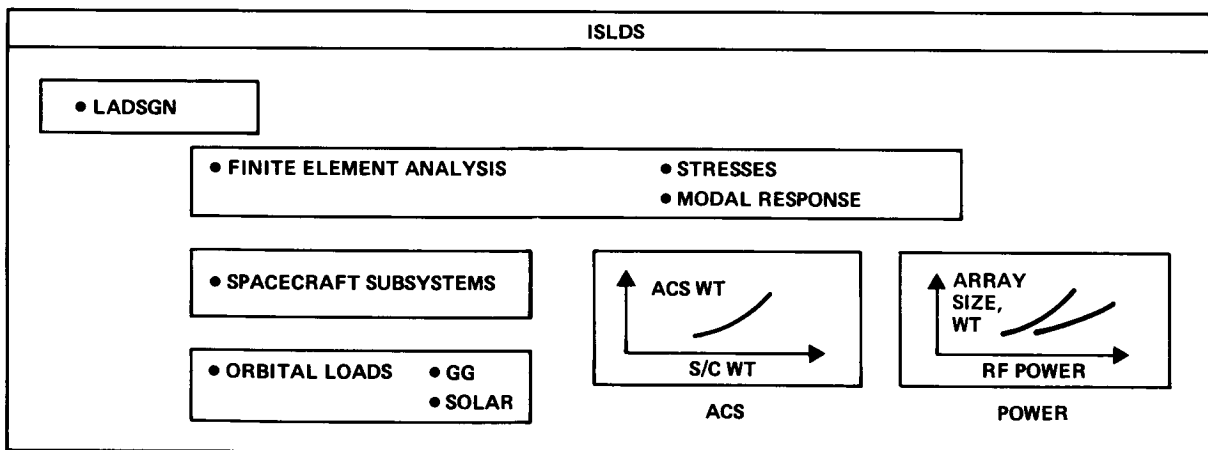
THE NEXT STEP

In 1984, the plan is to expand the LADSGN cable catenary antenna by integrating three features:

- Finite element capability to provide stress and model data
- Spacecraft subsystems sizing as a function of orbit, pointing, and RF power requirements (an extensive data base and individual programs exist, and will be integrated)
- Integration of available PC-based orbital transfers and perturbation programs.

As LADSGN expands it will become the basis for ISDLS.

Integrated System Design of Large Spacecraft



TYPICAL APPLICATIONS:

- MOBIL SAT
- DIRECT VOICE BROADCAST
- ANTENNA FLIGHT EXPERIMENT
- VLBI

Figure 12

BIBLIOGRAPHY

1. Garrett, L. Bernard: Interactive Design and Analysis of Future Large Spacecraft Concepts. NASA TP-1937, 1981.

N87-11763

DESIGN OPTIMIZATION OF THE 34-METER DSN-NCP ANTENNAS

Roy Levy
Jet Propulsion Laboratory
Pasadena, California

C-3

*

NEW 34-METER ANTENNA STRUCTURE CONFIGURATION

The new NASA Deep Space Network (DSN) 34-m-diameter azimuth-elevation (Az-El) antenna structure (fig. 1) is an example of an essentially computer-automated design. In addition to pivotal computer Lagrange multiplier design optimization software, much of the associated pre- and post-processing was also performed by computer.

The construction of one of these antennas at Goldstone, California, is well advanced and will be completed this summer. A second installation is in progress in Australia. Both antennas will be used primarily for spacecraft tracking and will operate in the 8.5-GHz, 3.5-cm (1.4-in.) wavelength microwave frequency.

The alidade rotates in azimuth on a wheel-and-track horizontal bearing. It supports the elevation bearings and the drives of a tipping structure that rotates in elevation. The tipping structure contains the microwave-reflecting surface panels, a backup structure to which the panels connect, an elevation wheel that holds the backup structure, a feed cone, and a subreflector-supporting quadripod. The surface panels, subreflector, and feed cone are the essential microwave components and the purpose of the remaining structures is to support, steer, and hold these three components in precise alignment. We will consider here only the design of the backup and elevation wheel portions of the tipping structure, which are by far the most complex structural components.

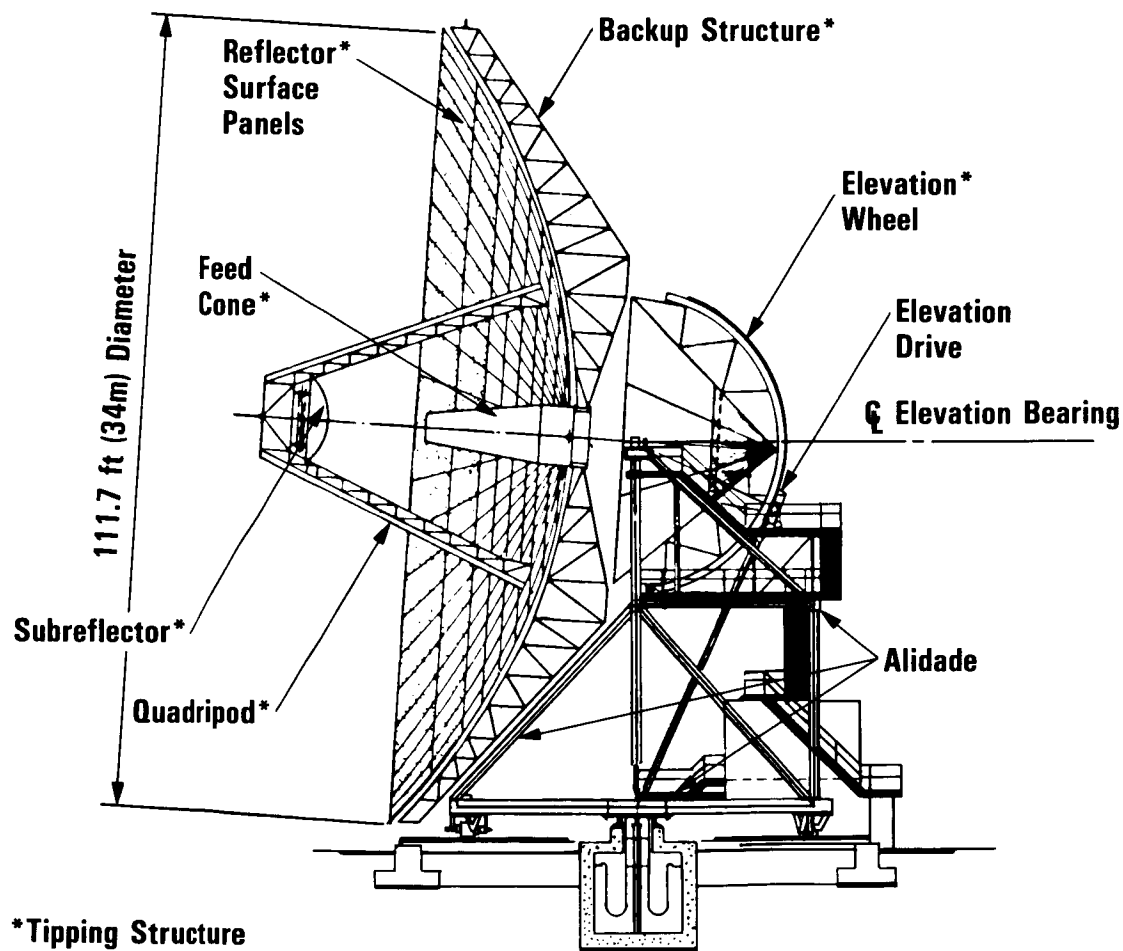


Figure 1

BACKUP STRUCTURE FRAMING

The backup structural framing is shown in fig. 2. It is highly modular and consists of 24 main radial rib trusses, 24 secondary radial rib trusses, 12 circumferential hoop trusses, and some added bracing.

The surface panels, which are parasitic and support only their own weight and local tributary surface loads, are attached at four corners by adjustable connectors to the top nodes of the rib trusses. The backup structure is supported by the elevation wheel at eight attachment points.

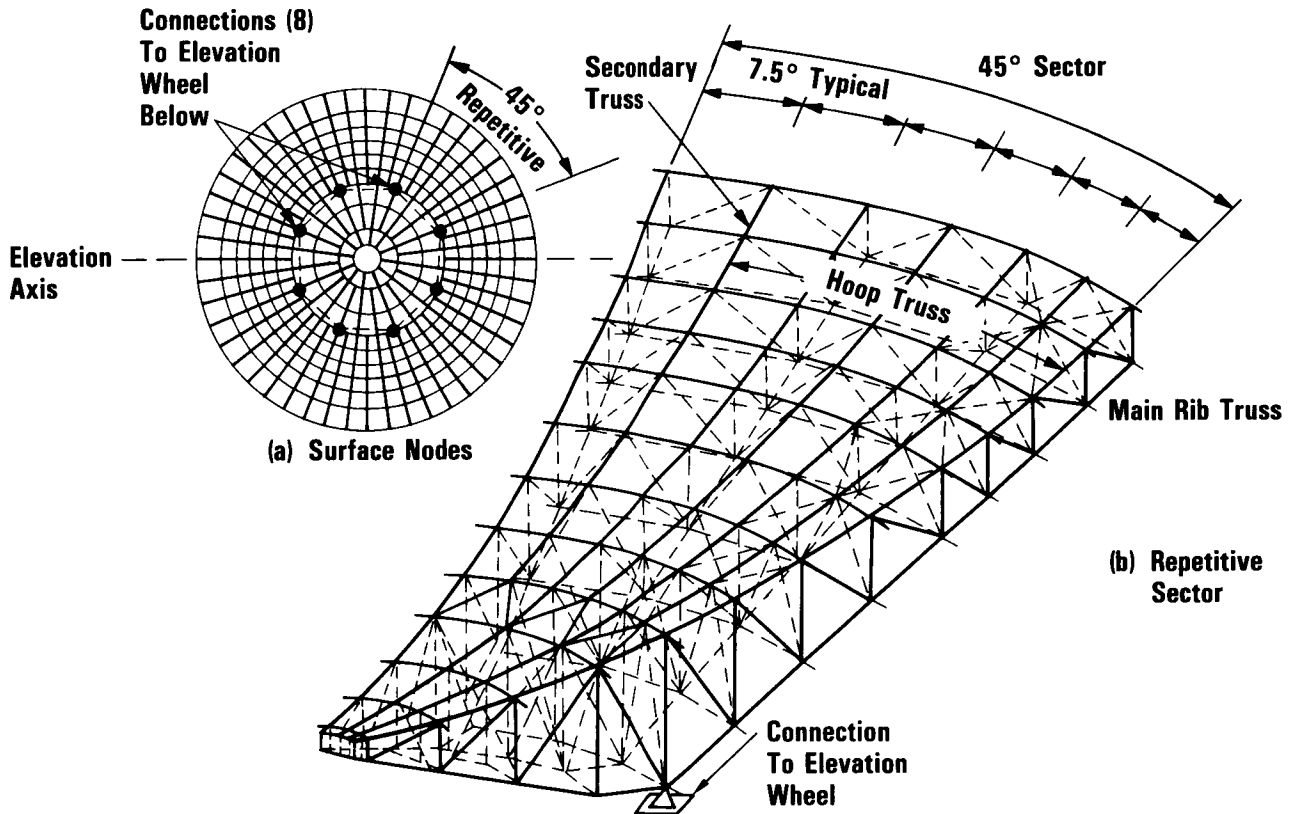


Figure 2

ELEVATION WHEEL

The elevation wheel in fig. 3 provides the eight-point support for the backup structure. Its essential features, in addition to providing the eight attachment points, are the large radius elevation bull gear, which is driven by a pinion from the alidade; the elevation tie box beam, which spans between elevation bearings; and the counterweight, which balances the eccentricity of the weight with respect to the elevation axis.

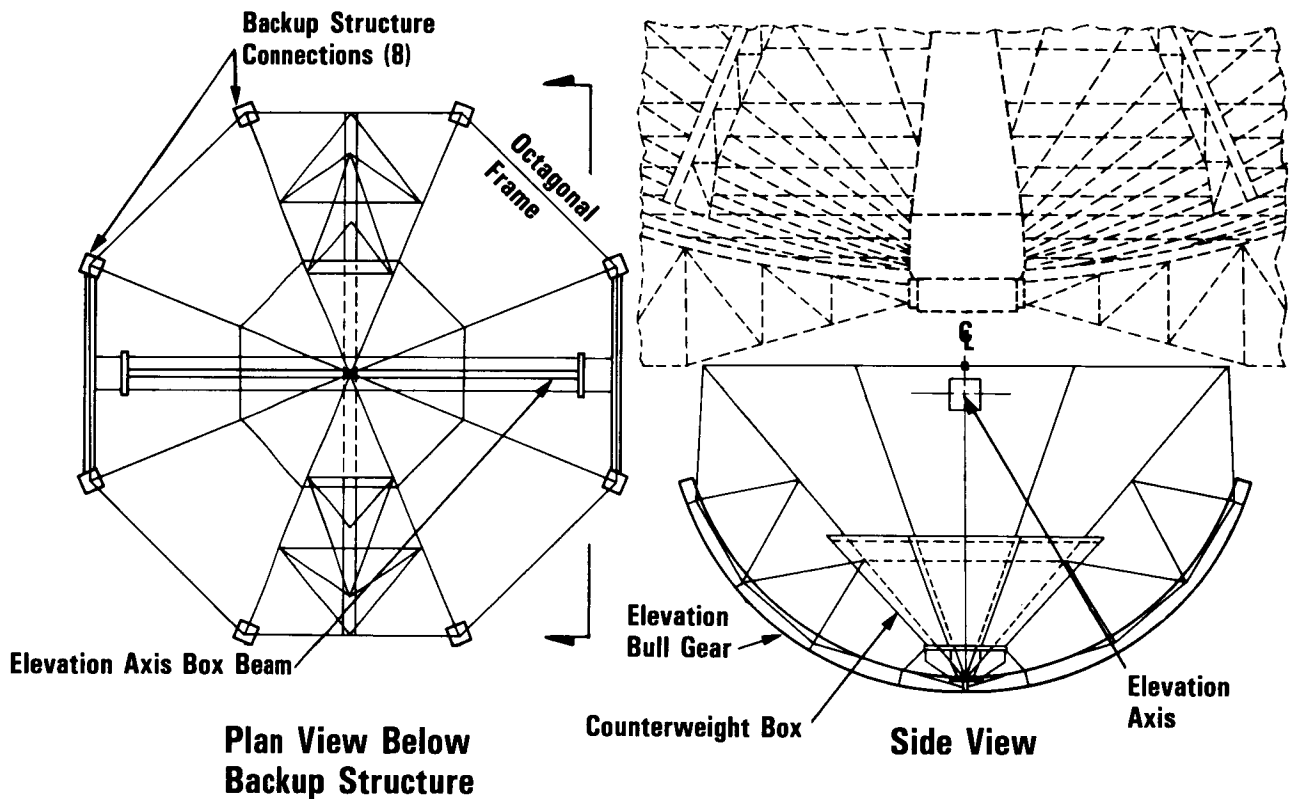


Figure 3

ANTENNA DESIGN PROBLEM

Figure 4 shows how the traditional formulation of the optimization problem is specifically applied to the design of the tipping structure. The constraints are based on microwave performance requirements and these tend to be so restrictive that constraints on member stresses only occasionally influence member size selection. Consequently it is both efficient and adequate to treat stress as a side constraint by means of a fully stressed design algorithm.

The microwave pathlength and pointing errors will be discussed subsequently. The best-fit surface is an alternative paraboloid found from least-squares analysis which minimizes the residual mean square pathlength error. The rigging angle (ref. 1) is the elevation angle at which the surface panels are field-adjusted to a near-perfect configuration. The antenna structure is presumed to be in perfect alignment at the rigging angle.

- **Objective: Minimize structure weight**
- **Primary constraints:**
 - **Root mean square microwave pathlength error (from best-fit surface)**
 - **Boresight pointing error**
- **Secondary constraints:**
 - **Stress, buckling, commercially available structural shapes, design variable groups**
- **Loading conditions**
 - **Gravity (horizon to zenith elevation change in gravity vector-w.r.t. rigging angle)**
 - **Wind (variable antenna elevations, wind azimuths)**

Figure 4

MICROWAVE PATHLENGTH ERROR

The geometric ray tracing on fig. 5 illustrates the pathlength-error-type constraint. The pathlength is the distance from the aperture plane to the surface and then, after reflection, from the surface to the focal point. The error is the difference between the pathlength of an ideal ray reflected from a perfect surface and the pathlength of a ray reflected from a deformed surface. It can be shown (ref. 2) that half the pathlength error at any point is the projection of the deformation vector on the surface normal times the direction cosine with respect to the focal axis. In practice the perfect surface reference for the pathlength error is actually an alternative paraboloid that is least-squares best fit to the deformed surface. The best fitting parabola is defined by up to six parameters, e.g., the three translations in the directions of Cartesian axes, a change in focal length, and the two rotations about the axes in the plane parallel to the aperture plane.

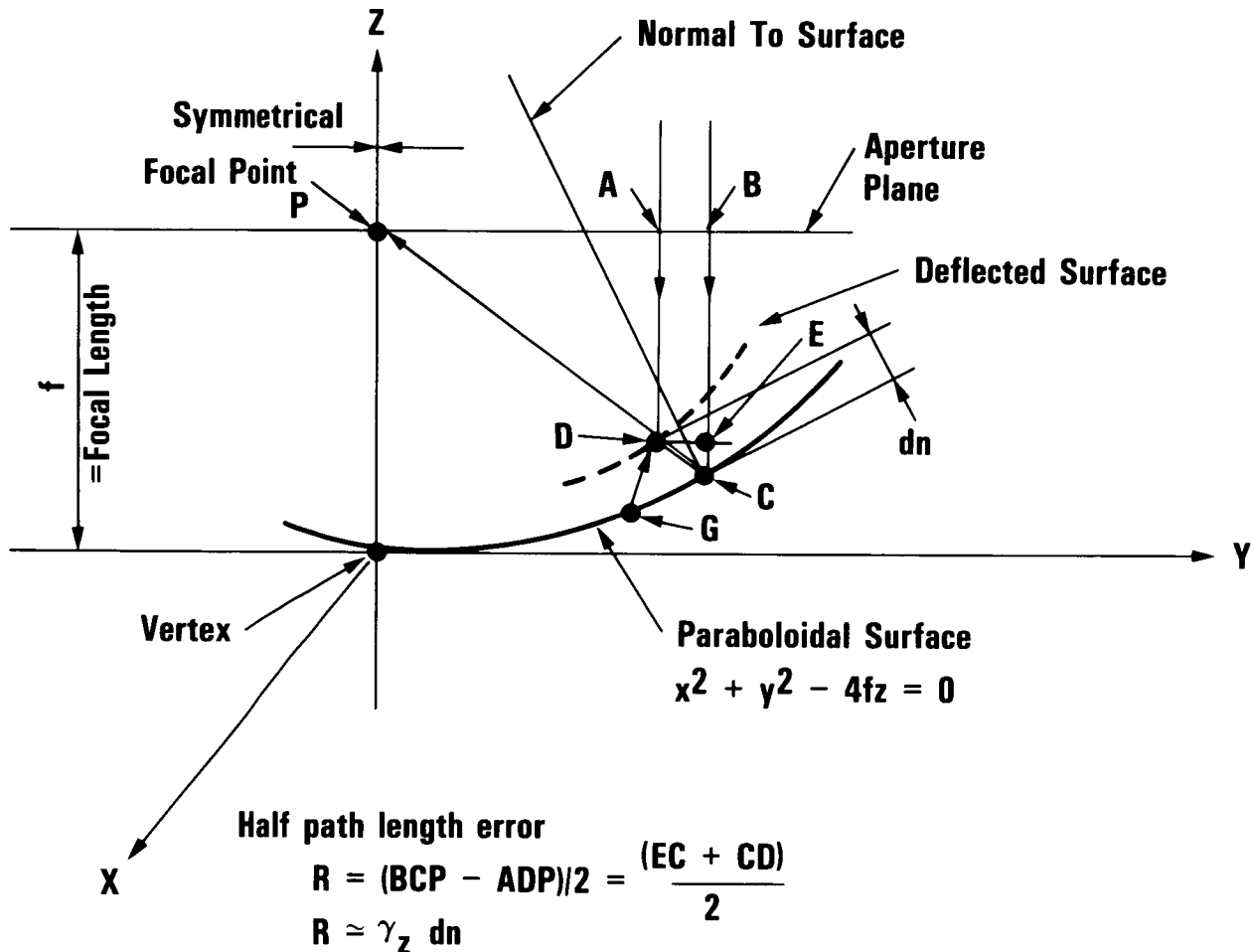


Figure 5

BORESIGHT POINTING ERROR

Five independent structure compliance terms are entailed in the computation (ref. 3) of the pointing error in conjunction with microwave optics parameters. The compliances are identified on fig. 6. The lateral vertex shift and paraboloid axis rotation terms are associated with the best fitting surface. These two terms and the subreflector lateral translation usually tend to dominate the error calculation.

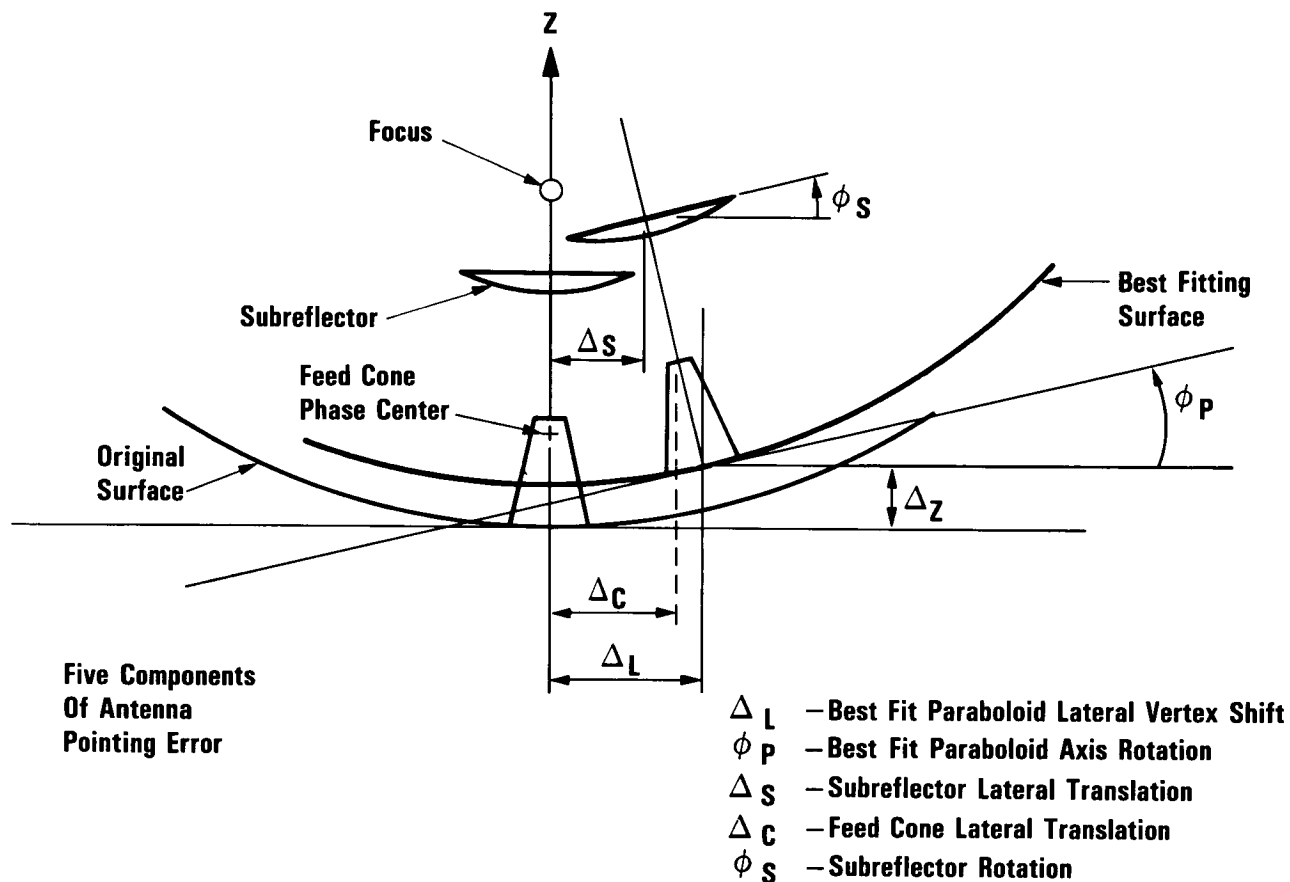


Figure 6

CONSTRAINTS

Figure 7 outlines how the pathlength or pointing error constraints are formulated using the familiar virtual work expression. The design variables are actually groups of bar or plate elements assembled so that all members of the same group are required to have the same area (for bar groups) or thickness (for plate groups). One type of virtual loading is constructed for pathlength error constraints (ref. 1) and another related type is constructed for pointing error constraints (ref. 3). Both of these depend upon the deviations from the best fitting paraboloid. The gravity virtual loading also incorporates the difference in loading from the rigging angle to the extreme operating elevation angles. The constraint ratio defined in this figure is a convenient measure of how well the design satisfies a particular constraint. Ratios less than unity indicate a satisfied constraint and those greater indicate violations.

- Virtual work formulation for primary constraints
- The virtual work of the i th bar for the j th constraint is:

$$C_{ij} = \frac{S_{ir} U_{ik} L_i}{A_i E_i}$$

S_{ir} = Stress resultant for real load r

U_{ik} = Stress resultant for virtual load k

The virtual load is a specially constructed vector for each pathlength or pointing constraint

L_i, A_i, E_i = Length, Area, Young's Modulus

C_j = Actual value of j th constraint (pathlength or pointing)
= Sum of virtual work of individual members

Thus $C_j = \sum_i C_{ij}$

- | | | |
|---|---|--|
| <ul style="list-style-type: none"> ● Constraint equation ● Constraint ratio | } | $C_j^* = \text{Prespecified upper limit constraint}$ |
| $G_j = C_j - C_j^* \leq 0.0$ | | |
| $D_j = \frac{C_j}{C_j^*} \leq 1.0$ | | |

Figure 7

DESIGN PROCEDURE

Figure 8 refers to the familiar optimality criteria design method (ref. 4) in conjunction with Lagrange multipliers (ref. 5). Details of specific formulations used for the present project are given in ref. 6. A variation here is the member selection from discrete tables of commercially available structural shapes. Minimum member sizes are established for each bar design variable to be the smallest commercial size to meet tension or buckling stress requirements (ref. 7). However, in the optimality criteria design for performance constraints, a continuous spectrum of available sizes is assumed. The final member size selection uses the larger of either the nearest commercially available member size or the minimum size. Plate member thicknesses can also be selected from a list of commercially available thicknesses. We have compared designs derived this way with designs that assumed a completely continuous available size spectrum and found the differences to be of no practical significance.

- Find the Lagrange multipliers λ_j for $j=1,...,M$ from the solution of simultaneous nonlinear equations:

$$\lambda_j G_j = 0; \quad \lambda_j \geq 0$$

- Optimality criteria provides the design variables as

$$A_i^2 = \sum \lambda_j \frac{S_{ij} U_{ik}}{E_i}$$

- Design variable selection is also subject to side constraints:
 - Tension and buckling stress allowables for all real loads
 - Move limits
 - Specified maximum, minimum sizes
 - Linking groups
 - Exclusion from redesign
 - Discrete set of commercially available structural shapes

Figure 8

COMMERCIAL SHAPE TABLE

An excerpt from one of the commercial shape tables used in antenna design is shown in fig. 9. The first three columns of the table describe the shape, the area, and the radius of gyration. The remaining columns contain allowable compressive loads for various span lengths. A minimum shape is obtained by proceeding down the column of the first shorter span length until a shape with a load capacity larger than required is found. The buckling formula with the actual span is used to test the capacity of this shape. If the capacity is inadequate, the next lower shape is tested. Because the rows of the table are arranged in order of increasing area, this procedure reveals the lightest shape to sustain the load. A number of tables can be specified for the computer program and the selection of designated design variables can be directed to specific tables. There is an option to omit reference to any table, which allows a continuous size selection for that design variable.

| | | | L=98" P = 33.0 k | | | | | | |
|-----|---------------------|-------|----------------------|--------------|------|------|------|------|------|
| | | | *****LOAD TABLE***** | | | | | | |
| NO. | HANDBOOK SHAPE | AREA | RAD | SPAN LENGTHS | | | | | |
| | | | | 25. | 50. | 75. | 100. | 125. | 150. |
| 1) | SQTU-1.0X1.0X.083 | .304 | .370 | 7.9 | 4.8 | .0 | .0 | .0 | .0 |
| 2) | SQTU-1.25X 1.0X.120 | .542 | .465 | 14.9 | 11.6 | 6.0 | .0 | .0 | .0 |
| 3) | SQTU-1.5X1.5X.12 | .660 | .560 | 18.7 | 15.6 | 10.5 | 5.9 | .0 | .0 |
| 4) | SQTU-1.5X1.5X.18 | .950 | .540 | 26.8 | 22.0 | 14.1 | 7.9 | .0 | .0 |
| 5) | SQTU-2.0X2.0X.14 | 1.000 | .750 | 29.3 | 26.1 | 22.3 | 16.1 | 10.3 | 7.1 |
| 6) | SQTU-2.5X2.5X.12 | 1.140 | .970 | 34.2 | 31.5 | 28.5 | 25.0 | 19.6 | 13.6 |
| 7) | SQTU-2.0X2.0X.19 P | 1.270 | .720 | 37.1 | 32.8 | 27.7 | 18.8 | 12.1 | .0 |
| 8) | SQTU-3.0X3.0X.12 | 32.5 | 1.350 1.150 | 40.9 | 38.4 | 35.5 | 32.2 | 28.6 | 22.7 |
| 9) | SQTU-2.0X2.0X.25 | 20.9 | 1.590 .690 | 46.3 | 40.6 | 33.7 | 21.7 | 13.9 | .0 |
| 10) | SQTJ-2.5X2.5X.19 | 36.5 | 1.670 .950 | 50.0 | 46.0 | 41.4 | 36.1 | 27.6 | 19.2 |
| 11) | SQTU-3.5X3.5X.12 | 1.790 | 1.370 | 54.8 | 52.0 | 49.0 | 45.6 | 41.8 | 37.8 |
| 12) | SQTU-4.0X4.0X.12 | 1.820 | 1.570 | 56.0 | 53.6 | 51.0 | 48.1 | 45.0 | 41.6 |
| 13) | SQTU-3.0X3.0X.19 | 2.020 | 1.130 | 61.2 | 57.3 | 52.9 | 47.9 | 42.3 | 32.8 |
| 14) | SQTU-2.5X2.5X.25 | 2.150 | .920 | 64.2 | 58.9 | 52.7 | 45.6 | 33.3 | 23.1 |
| 15) | SQTU-3.5X3.5X.19 | 2.390 | 1.340 | 73.0 | 69.3 | 65.1 | 60.4 | 55.3 | 49.7 |

Figure 9

TIPPING STRUCTURE DESIGN FLOW

Figure 10 shows the flow of the engineering problem from model generation through design to detailing. Because our windloading specifications impose hurricane wind speeds for survival and lower speeds for meeting performance constraints, the higher speed loading is used for design and the allowable performance constraint is increased accordingly. However, as a design simplification, wind and gravity loadings are treated independently so that the minimum sizes found by the computer program are not necessarily adequate. Consequently a post-processor program is used to make the appropriate combinations of the stress resultants for gravity, wind, snow, or ice loadings and to verify or adjust the final design using the same member resistance criteria specifications as the design program. If this process or other changes made by the engineering review are considered to be sufficiently extensive, a return could be made to the design program for another analysis.

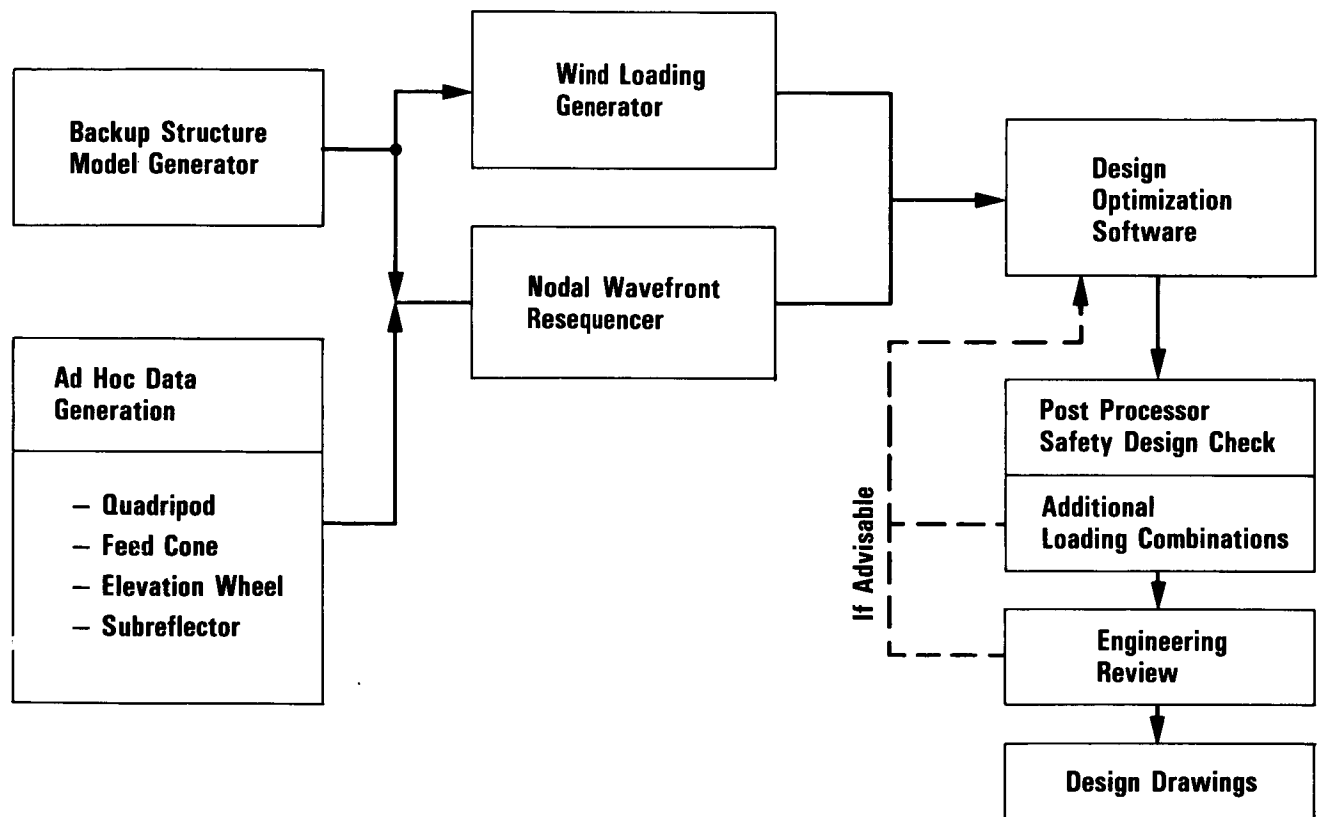


Figure 10

TIPPING STRUCTURE COMPUTER MODEL

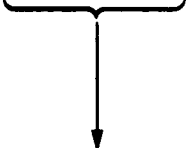
Until recently the problem size statistics for the 34-m antenna tipping structure shown in fig. 11 represented the largest problem processed by our design software. However, a current project which is to extend the three 64-m DSN antennas to 70 m exceeds all of these sizes.

The constraints shown here are actually more restrictive than those used for design of the 34-m antennas under construction, and are from a recent investigation for enhancement of performance at shorter microwave wavelengths. The nine performance constraints shown in the table were selected for this design as those most likely to become controlling. The gravity loading constraints are for the worst condition, which occurs at either zenith or horizon antenna elevations. Gravity errors become significantly lower at elevations close to the rigging angle. The rigging angle selection here is automated to make the pathlength errors equal at zenith and horizon. Another choice for rigging angle would be to minimize the weighted average pathlength error over the elevation range of a known trajectory spacecraft mission (ref. 8).

● Problem size

| | | | |
|---------------------------------|-------------|-------------------------|-------------|
| Nodes | 1145 | Rod members | 3900 |
| Degrees of freedom (dof) | 3400 | Plates | 90 |
| Matrix wavefront, dof | 220 | Design variables | 190 |

Performance constraints

| Condition | | | 1/2 Pathlength RMS, Ins | Pointing Arc Secs |
|---|------------------|------------|----------------------------|----------------------|
| Gravity-Worst Case: Horizon to Zenith | | | 0.0065 | 75.0 |
| 30 MPH Wind  | Elevation | Yaw | | |
| | 0 | 120 | 0.0130 | 30.0 |
| | 60 | 180 | 0.0130 | 30.0 |
| | 90 | 90 | 0.0130 | 30.0 |
| | 90 | 180 | None | 30.0 |

● Stress and buckling constraints

- 1) 70 MPH wind at any orientation
- 2) 100 MPH wind at zenith elevation, any azimuth

Figure 11

CONSTRAINT RATIO DESIGN HISTORY

The six cycles of constraint ratio histories shown on fig. 12 are actually six cycles of analysis and five of design. The initial design, except for a few improving changes in topology and arrangement, is essentially the design previously selected for the new antennas. Therefore, the starting point is a reasonably good one because it is a previously optimized basis. However, because of the desire for performance improvement, none of the constraints was satisfied at the beginning. Had the starting design been a more primitive one, the initial constraint ratios would have been even larger and the improvement from first to last cycles might have appeared more pronounced. The windloading pathlength and pointing constraint ratios both progress relatively smoothly to their final values of unity or less. The gravity constraint ratios progress more erratically; the pathlength error constraint, after a rapid improvement at Cycle 3, makes a violating side step at cycle four and from then on is well-behaved; the pointing error constraint is significantly violated at Cycle 2, but then becomes benign.

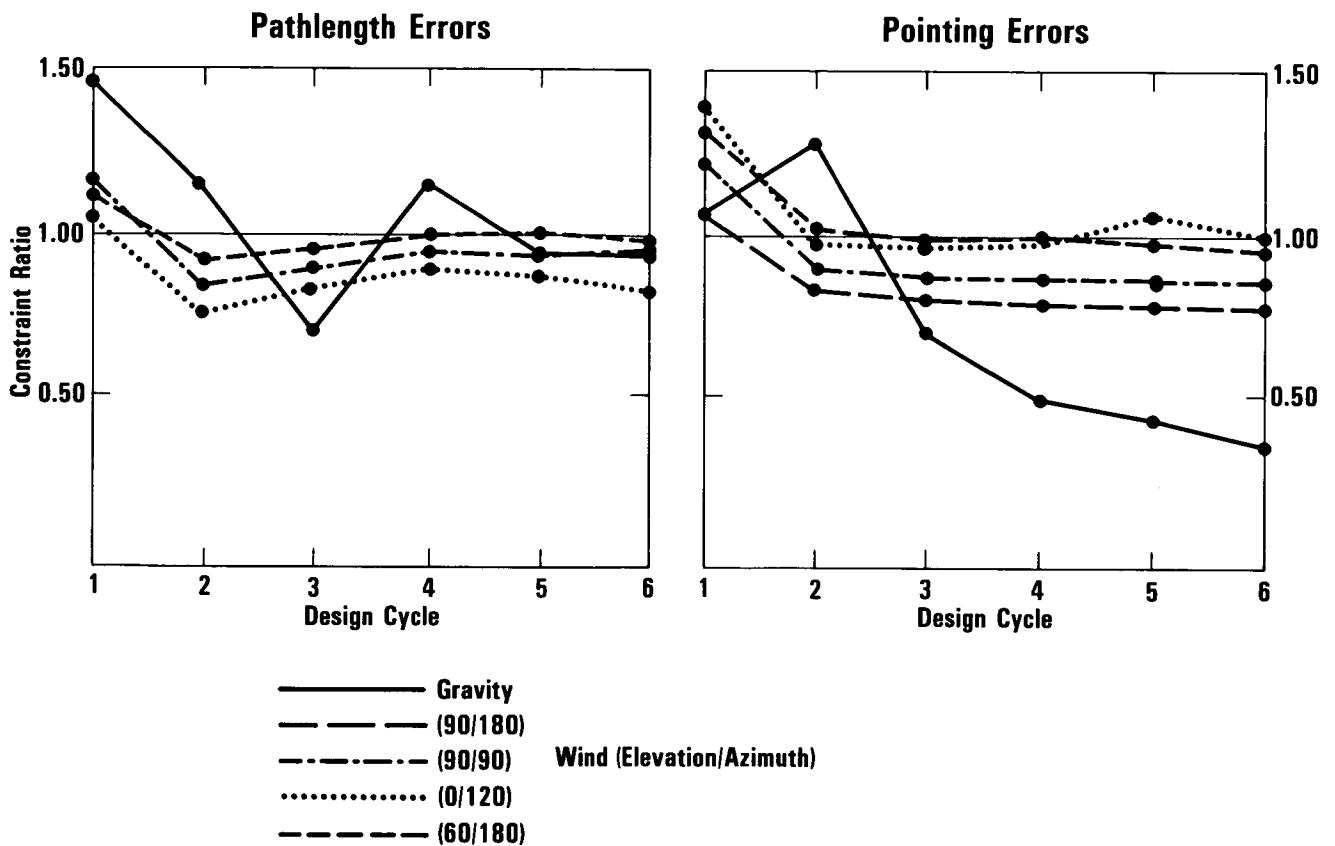


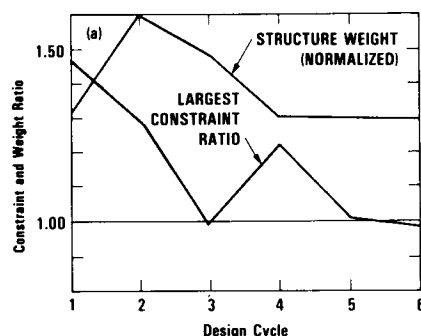
Figure 12

COMPUTER DESIGN SUMMARY

The progress of the structure weight, shown on fig. 13, could be responsible for some of the erratic gravity constraint behavior. The weight does not stabilize until Cycle 4 and this could affect the gravity constraint because the design algorithms always assume that the external loading is invariant from one cycle to the next. Even when the total weight does not change between adjacent cycles, the gravity design could be affected because of changes in the distribution of weight. The weight graph shown indicates a successful design because the final weight is about the same as the starting one and all nine initially violating constraint ratios have become feasible by the last cycle.

The run time breakdown tabulation on this figure shows how little the requirement for design optimization in each cycle adds to the time for traditional computer analysis. Nevertheless, design optimization in itself calls for multiple analysis cycles. The fact that only 2% of the cycle time is used for the actual design algorithm reflects the inherent efficiency of the optimality criteria method. The 24% of the cycle time used to process the virtual loadings represents an additional computer effort that is associated with the requirement for design and with the antenna formulation. Furthermore, any other design method not based upon a virtual work formulation could require at least the equivalent effort to establish sensitivity coefficients for the design variables.

● Weight and controlling constraint ratio



● Run time breakdown

| | Cpu Secs*/Cycle | Percent |
|---|-----------------|------------|
| Matrix Decomposition | 209 | 60 |
| Load-displacement Analysis | 40 | 12 |
| Stress Analysis | 5 | 1 |
| Pathlength, Pointing Error Analysis | 4 | 1 |
| <u>Analysis Subtotal</u> | <u>258</u> | <u>74</u> |
| Pathlength and Pointing Error Virtual Load Processing | 83 | 24 |
| Design (Lagrange Multipliers, Optimality Criteria) | 7 | 2 |
| <u>Design Subtotal</u> | <u>90</u> | <u>26</u> |
| Total | 348 | 100 |

*UNIVAC-1100/81

Figure 13

SUMMARY

The summary shown in fig. 14 is almost self-explanatory. Reflective symmetry, proposed in the last item, could provide a significant reduction of the computer effort. Almost all Az-El antennas have a vertical plane of symmetry and a half-structure model would be adequate to design for gravity loadings and all wind loadings with 0 (or 180) deg wind azimuth. Although the analysis for winds from the side could be synthesized by first decomposing these loads and then processing independent half-structure models with appropriate displacement boundary constraints, this in itself is not sufficient for design. The methods of reflective symmetry make it possible to use a half-structure model both for analysis and design. The approach currently under development is to automate matrix decomposition with symmetric and anti-symmetric boundary constraints, to operate on decomposed loading vectors, and to synthesize the virtual work of the un-modelled "phantom" half-structure. Although two stiffness matrix decompositions are required, each should require much less than the time for the full structure stiffness matrix. Our current 70-m antenna extension project model has over 6000 degrees of freedom in the half structure. Even with the most modern and largest capacity computer hardware, the time and cost to process several design cycles with a stiffness matrix of about 12,000 degrees of freedom with a wavefront of about 500 make the savings through reflective symmetry and the half-structure model seem attractive.

- **Large antenna structure automated design satisfies pathlength and pointing error constraints**
- **Simultaneous design treats a spectrum of gravity and wind loadings**
- **Members chosen from commercial shape tables satisfy:**
 - **Performance constraints at operational conditions**
 - **Stress and buckling requirements at extreme environmental conditions**
- **Per cycle computer time for design is a modest fraction of the time for analysis. Therefore a complete design can take less than 10 times the time for conventional single analysis cycle**
- **For a future reduction of computer effort**
 - **Use the principles of reflective symmetry and load decomposition on a half-structure model**

Figure 14

REFERENCES

1. Levy, R., and Melosh, R.J., "Computer Design of Antenna Reflectors," Journal of the Structural Division, Proc. ASCE 99(ST-11), Proc. Paper 10178, pp. 2269-2285, November 1973.
2. Utku, S., and Barondess, S.M., "Computation of Weighted Root-Mean-Square of Pathlength Changes Caused by the Deformation and Imperfections of Rotational Paraboloidal Antennas," Technical Memorandum 33-118, Jet Propulsion Laboratory, Pasadena, Calif., March 1963.
3. Levy, R., "Optimization of Antenna Structure Design," Eighth Conference Electronic Computation (ASCE), Houston, Texas, February 1983.
4. Berke, L., and Khot, N., "Use of Optimality Criteria Methods for Large Scale Systems," AGARD Lecture Series No. 70, On Structural Optimization, Hampton, Va., pp. 1-29, October 1974.
5. Khot, N., Berke, L., and Venkayya, V., "Comparison of Optimality Criteria Algorithms for Minimum Weight Design of Structures," AIAA Journal, Vol. 17, No. 2, pp. 182-190.
6. Levy, R., and Parzynski, W., "Optimality Criteria Solution Strategies in Multiple Constraint Design Optimization," AIAA Journal Vol. 20, No. 5, pp. 708-715.
7. "Guide for Design of Steel Transmission Towers," ASCE Manual and Report on Engineering Practice, No. 52, 1971.
8. Levy, R., "Antenna Bias Rigging for Performance Objective," IEEE Mechanical Engineering in Radar Symposium, Wash. D.C., Nov. 8-10, 1977.

N 87 - 11764

POST AND A RANDOM-WALK SEARCH MODE

James A. Martin
NASA Langley Research Center
Hampton, Virginia

TOPICS

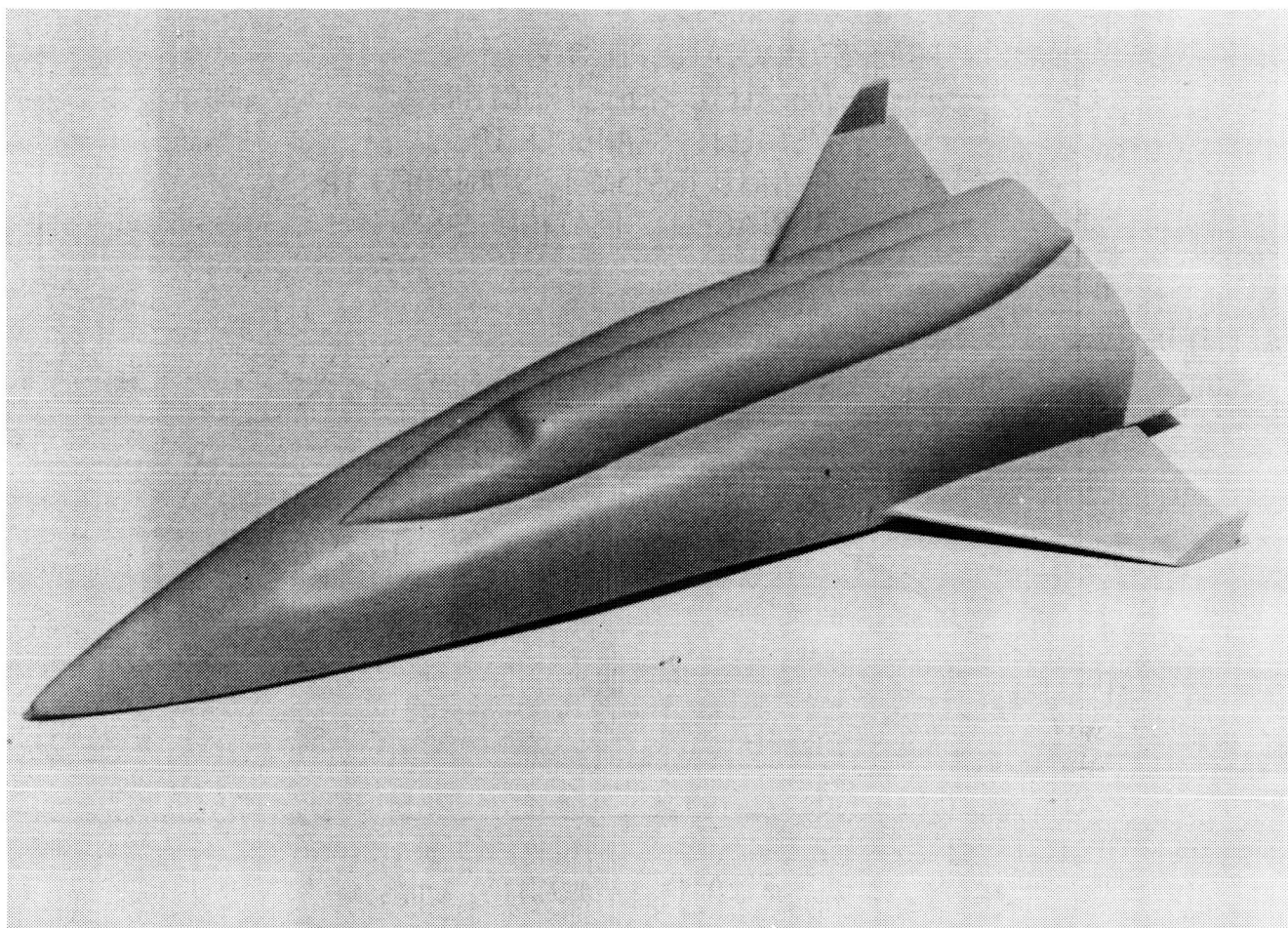
Multidisciplinary analysis often requires optimization of nonlinear systems that are subject to constraints. Trajectory optimization is one example of this situation. The Program to Optimize Simulated Trajectories (POST) (ref. 1) has been used successfully for a number of problems. The purpose of this report is to describe POST and a new optimization approach that has been incorporated into it. Typical uses of POST will also be illustrated. The projected-gradient approach to optimization is the preferred option in POST and will be discussed. A new approach to optimization, the random-walk approach, will be described, and results with the random-walk approach will be presented.

- TYPICAL USES OF POST
- PROJECTED-GRADIENT APPROACH TO OPTIMIZATION
- RANDOM WALK APPROACH TO OPTIMIZATION
- RANDOM-WALK RESULTS

ORIGINAL PAGE IS
OF POOR QUALITY

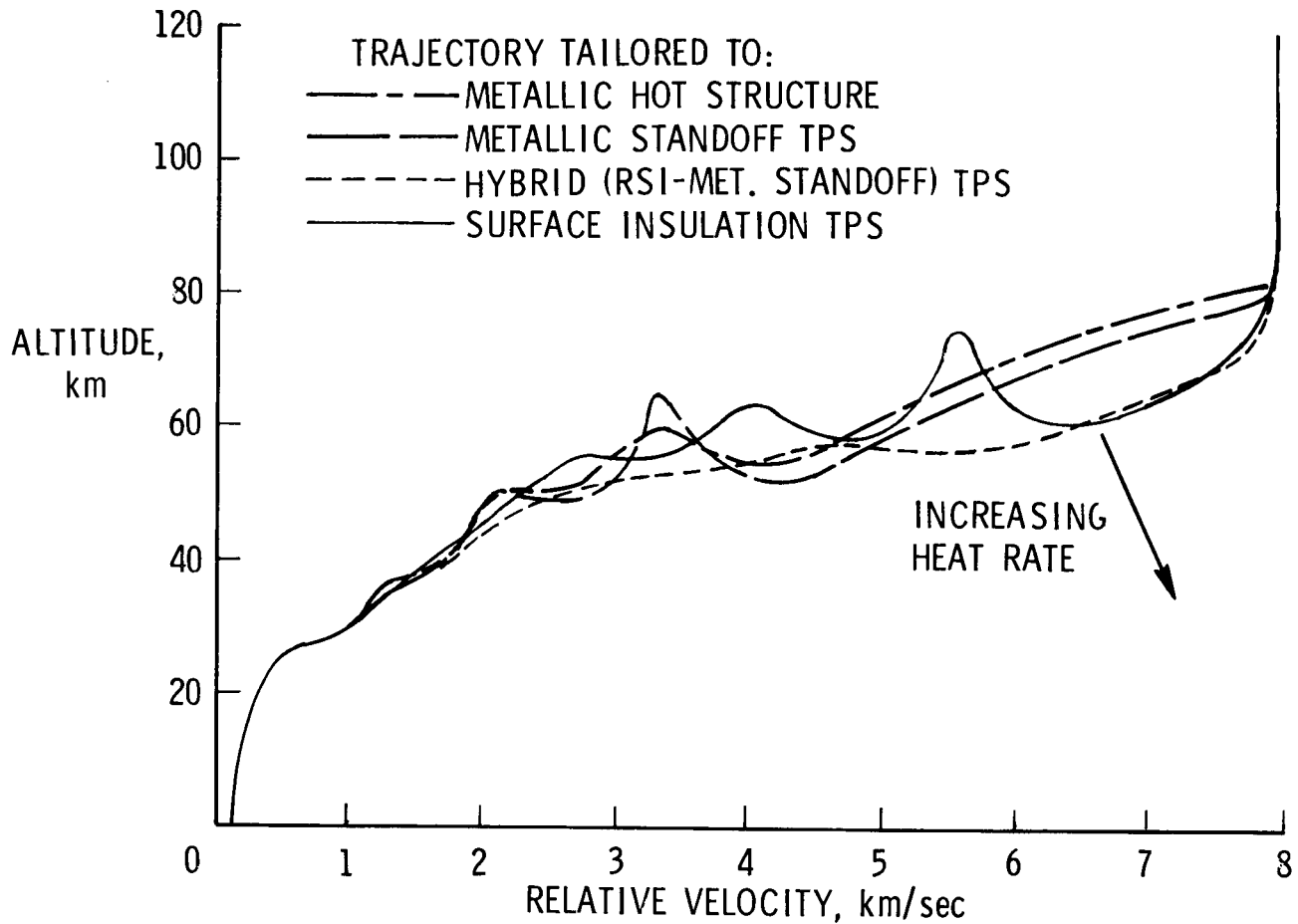
CONFIGURATION FOR ENTRY TRAJECTORIES

The configuration illustrated was developed for advanced Earth-to-orbit studies and has been used for assessing entry trajectories (ref. 2). The configuration is typical of a control-configured vehicle. Rather than provide aerodynamic surfaces large enough for aerodynamic stability, smaller aerodynamic surfaces are designed to provide a high degree of control authority, and artificial stability augmentation is used.



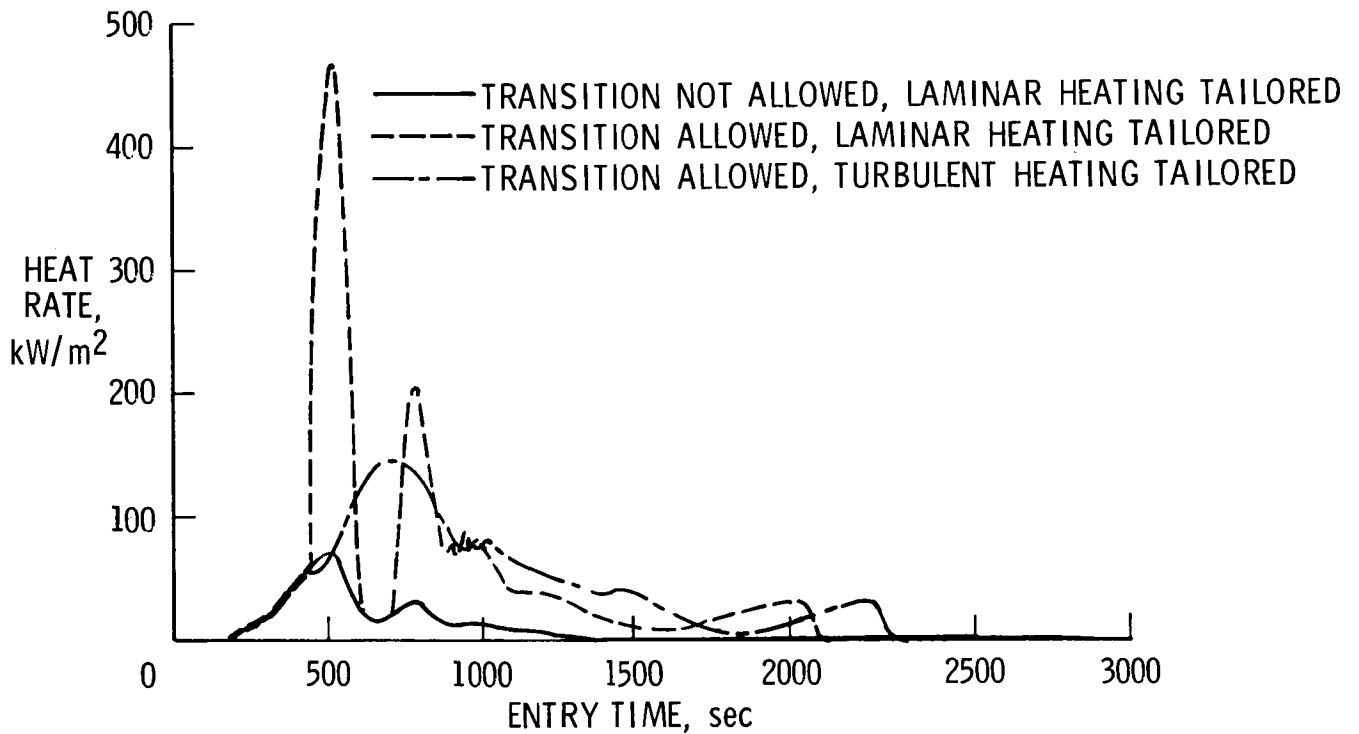
TYPICAL ENTRY TRAJECTORIES

Entry trajectories have been optimized using POST. The trajectories shown (ref. 2) illustrate how the optimum trajectory shifts as the type of thermal protection system (TPS) varies, changing the allowed maximum heat rate. The higher-heat-rate trajectories dip further into the dense atmosphere initially, which reduces the heat load.



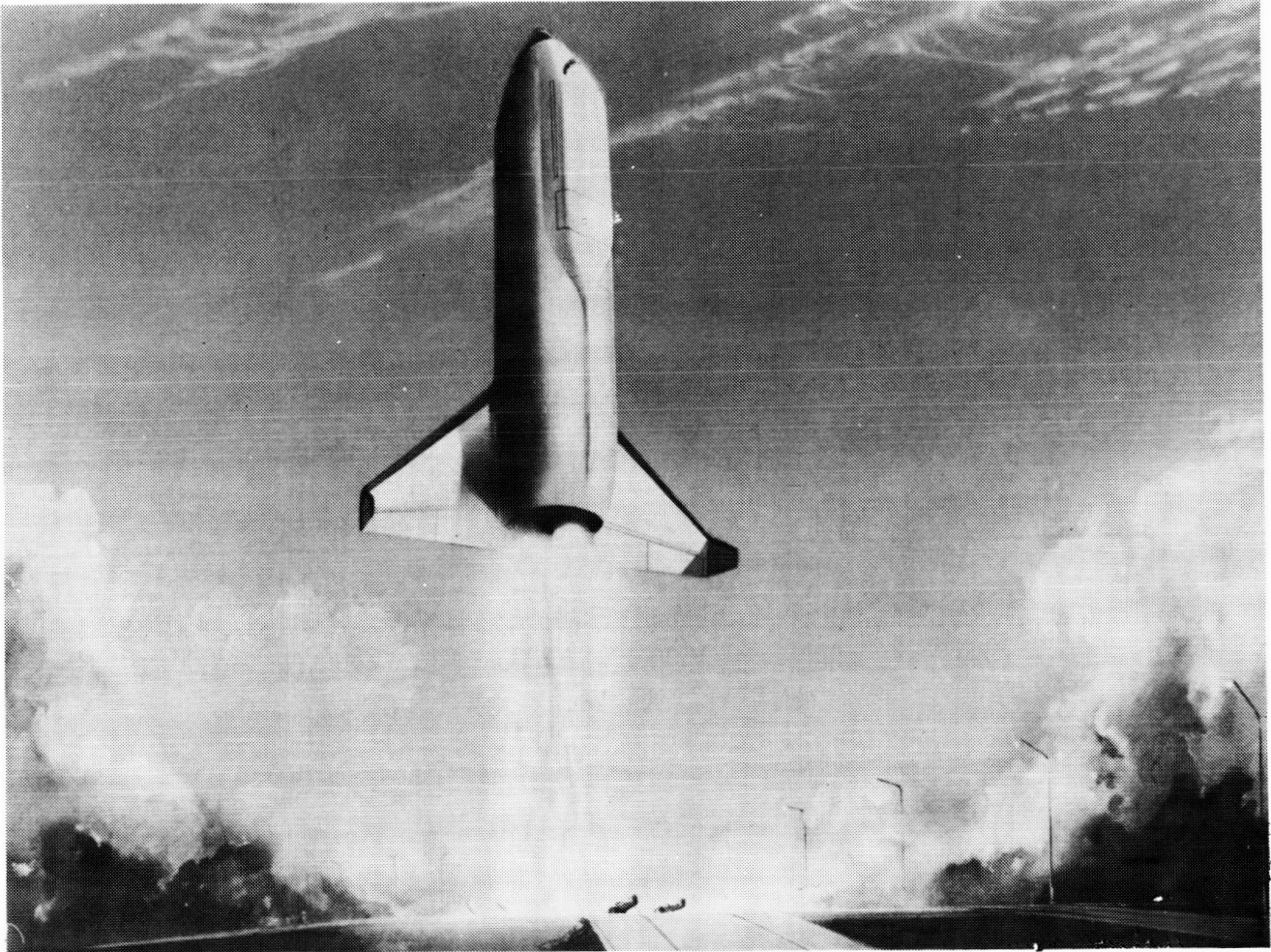
EFFECT OF TURBULENCE ON ENTRY HEATING

The trajectories shown (ref. 2) illustrate how the entry trajectory must be tailored to the condition of the boundary layer. If there is only laminar heating, the heat rate is quite low. If transition is allowed and turbulent heating exists, the heating rate is very high unless the trajectory is tailored to account for the different heating.



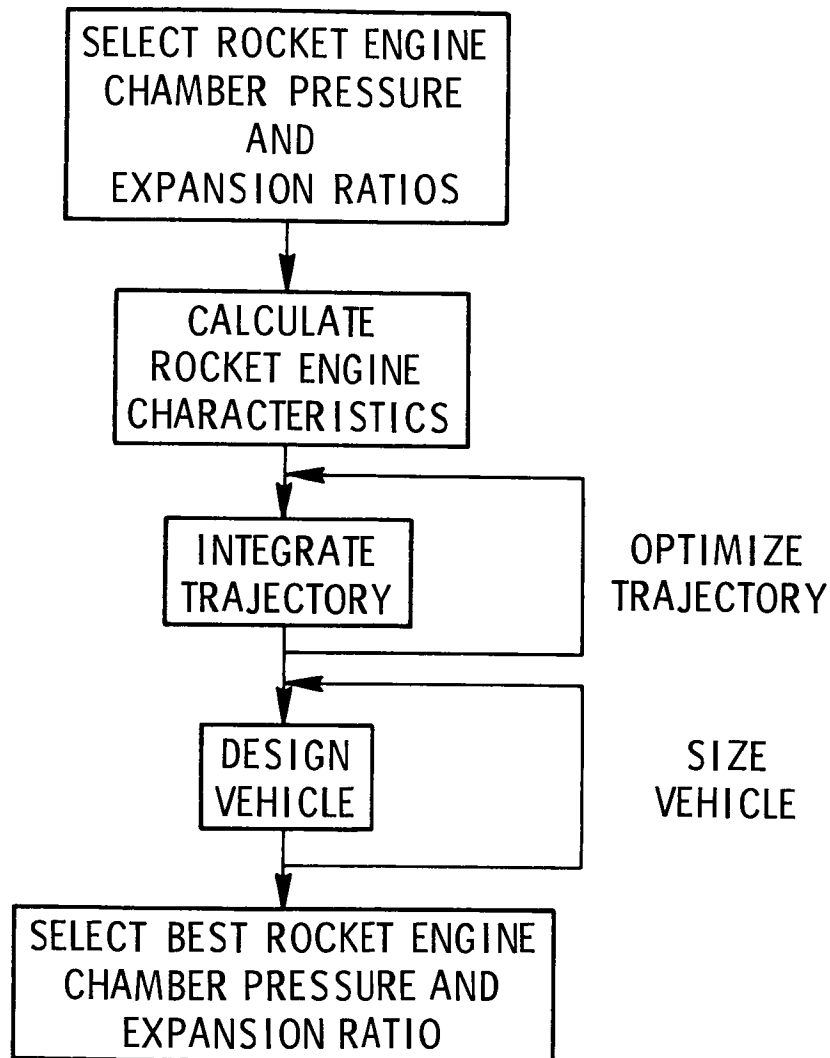
LIFTOFF OF ADVANCED EARTH-TO-ORBIT VEHICLE

Ascent trajectories for advanced Earth-to-orbit vehicles have been optimized with POST. Single-stage vehicles, such as the one shown (ref. 3), have been studied, as well as staged systems. Horizontal takeoff and airbreathing concepts have also been considered. The ascent trajectories often include targetting to a particular insertion orbit and constraints on acceleration, normal force, and dynamic pressure.



APPROACH FOR ROCKET ENGINE OPTIMIZATION

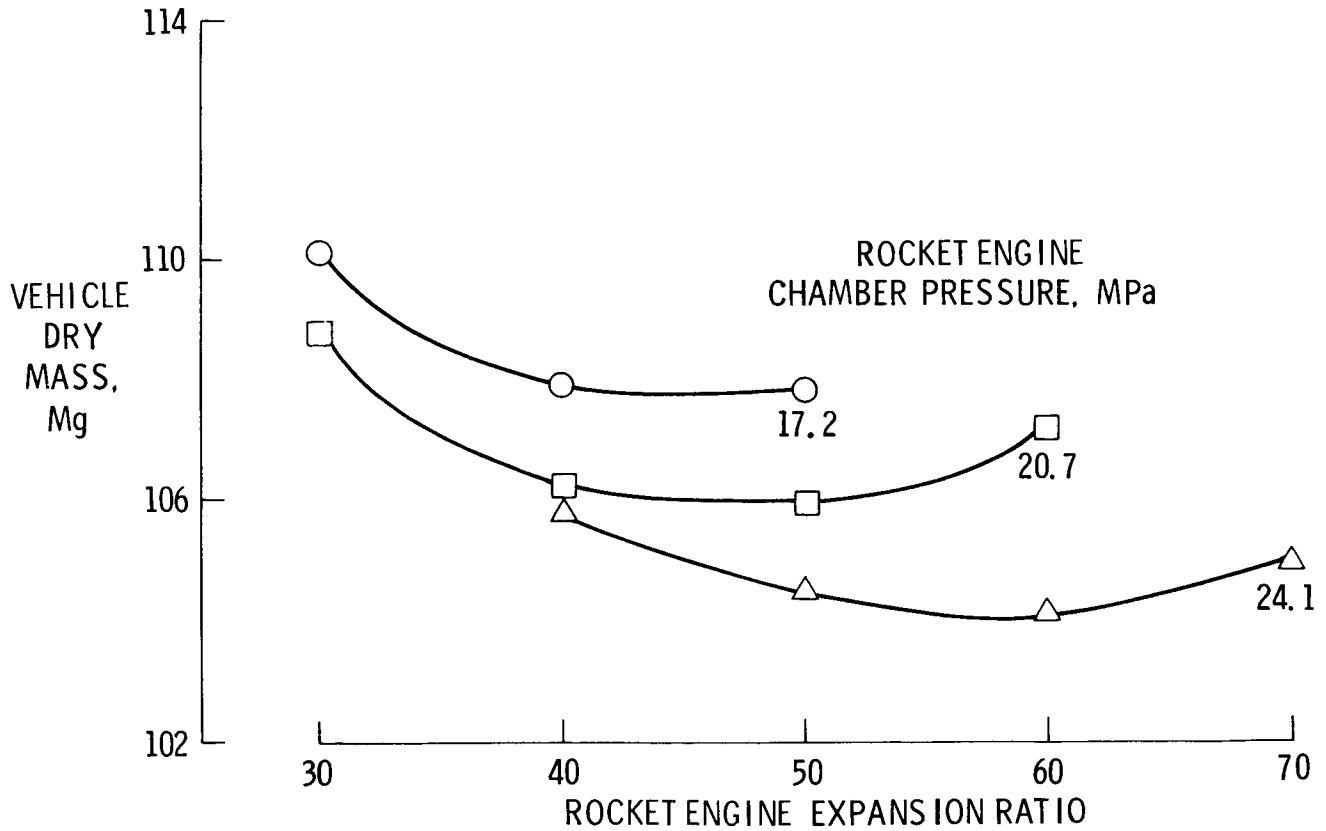
In a recent study to select optimum rocket engine chamber pressure and expansion ratio (ref. 4), POST was used together with rocket engine design programs and vehicle design and sizing programs. Although the trajectory was optimized internally, the rocket engine chamber pressure and expansion ratio could only be optimized parametrically.



ROCKET ENGINE OPTIMIZATION

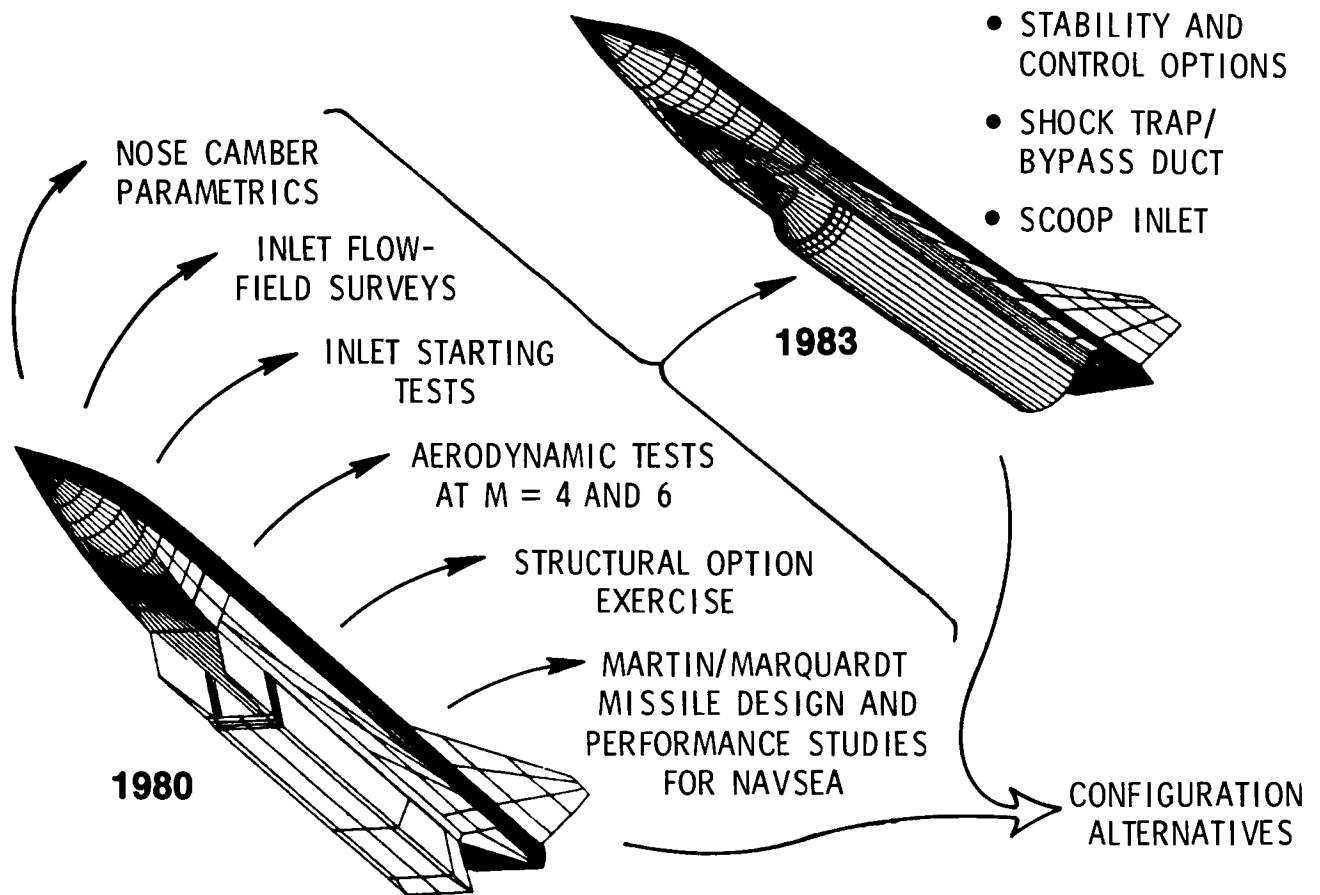
Results of the parametric optimization of the rocket engine chamber pressure and expansion ratio are shown (ref. 4). If vehicle dry mass is the parameter to be minimized, the optimum rocket engine would have a chamber pressure of 24.1 MPa and an expansion ratio of 60. The parametric results also provide vehicle gross mass and inputs for cost estimating so that the optimum engine could be selected on a cost basis.

SINGLE-STAGE-TO-ORBIT VEHICLE



HYSAM CONFIGURATION DEVELOPMENT

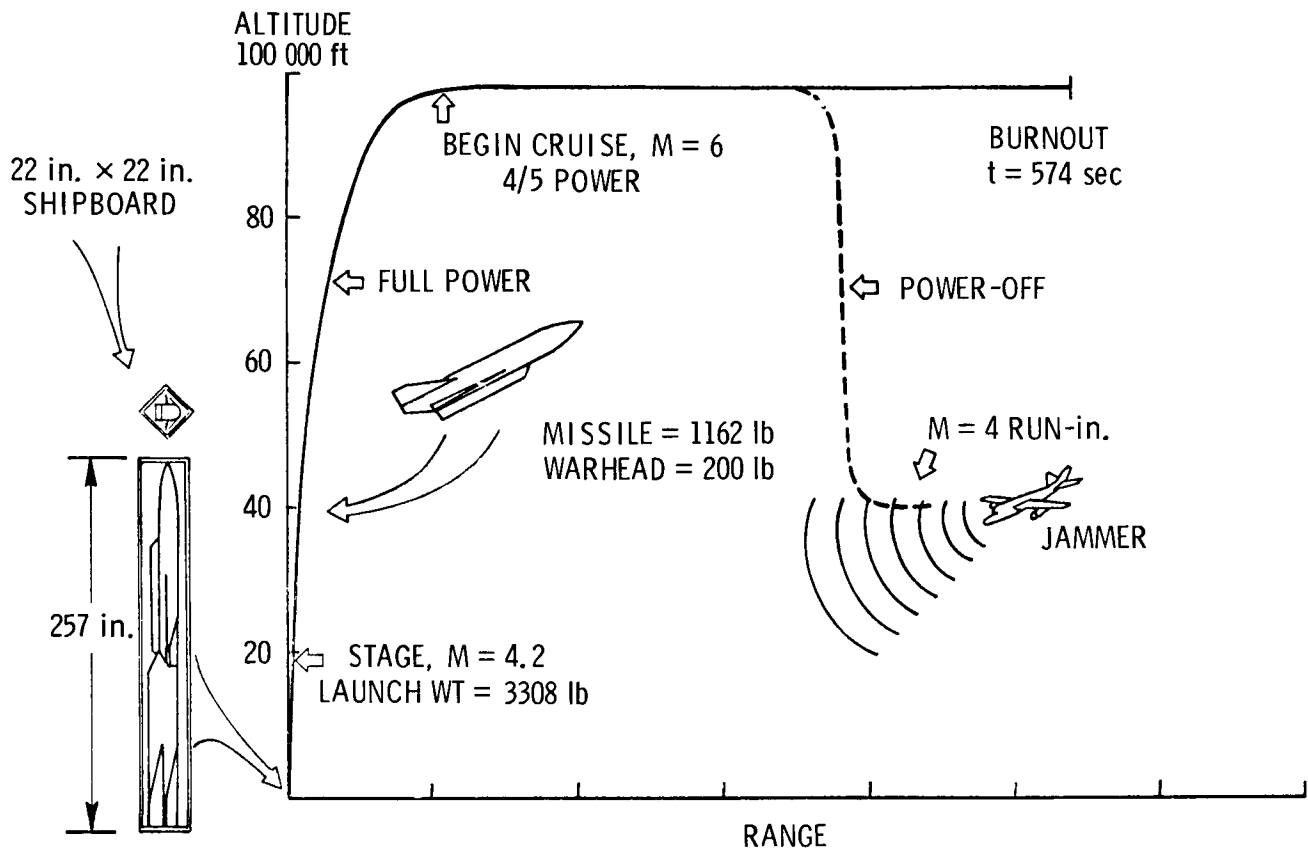
A program has been under way to develop a hypersonic surface-to-air missile (HYSAM). Some of the configuration development work that has taken place is illustrated (ref. 5).



HYSAM TRAJECTORY FOR FLEET DEFENSE

A typical HYSAM trajectory (ref. 5) is shown. The HYSAM trajectories are considerably different from Earth-to-orbit vehicle trajectories, but POST has been used successfully in both applications.

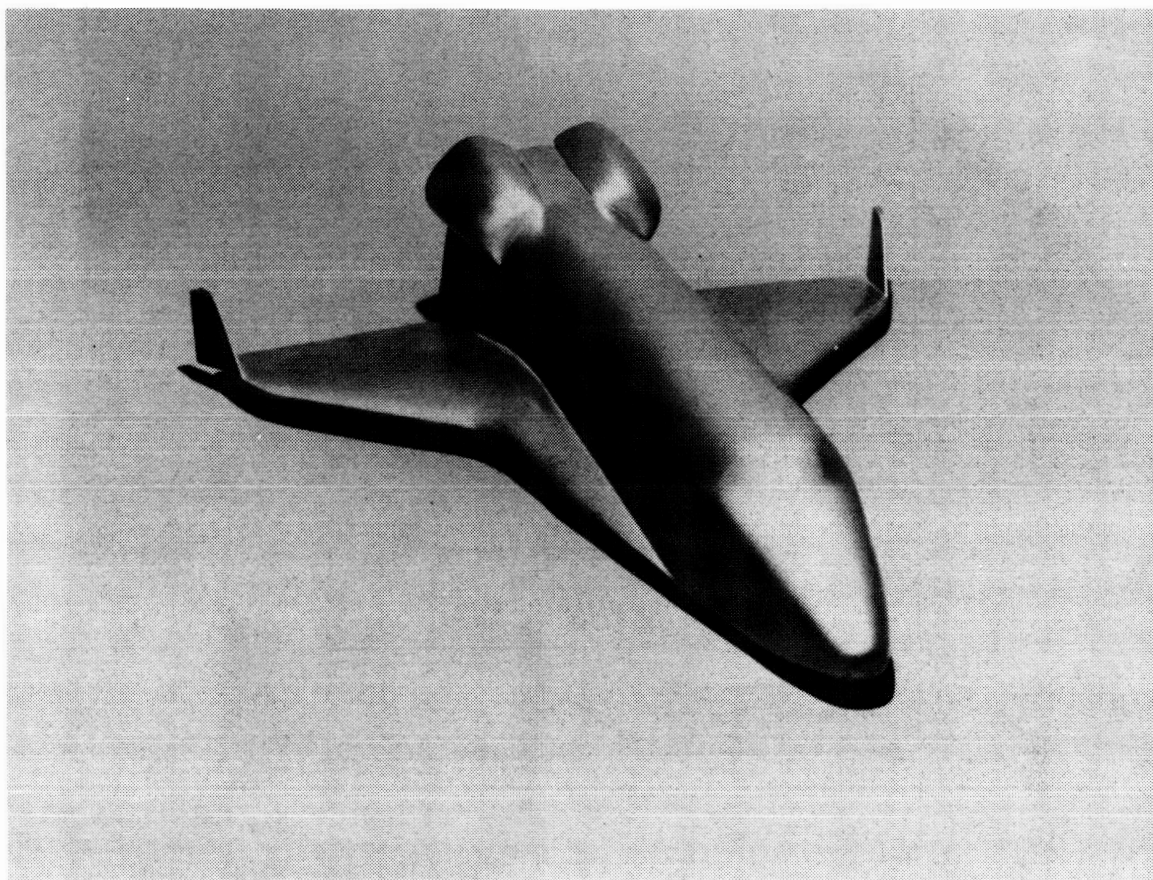
(SCRAMJET ENGINE-HYDROCARBON FUEL-150 in. MISSILE)



ORIGINAL PAGE IS
OF POOR QUALITY

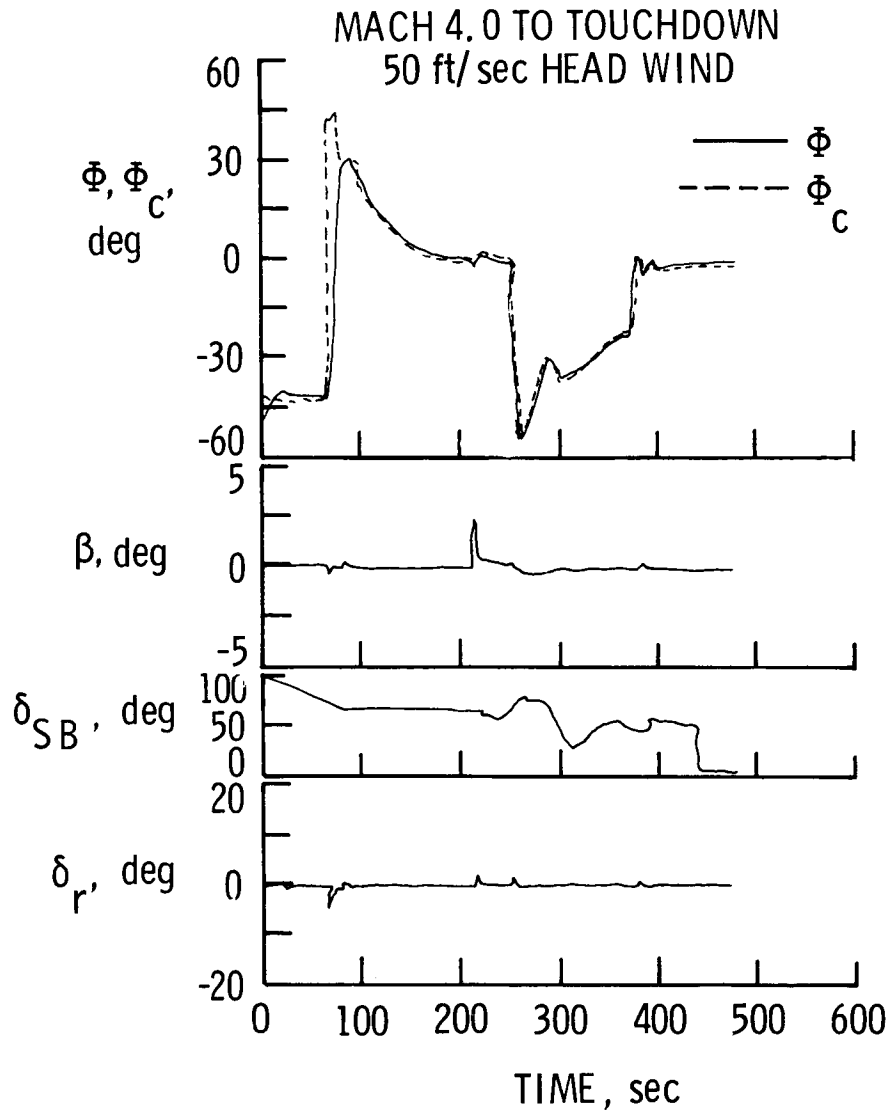
SPACE SHUTTLE ORBITER WITH TIP-FIN CONTROLLERS

The control-configured-vehicle approach appears to be useful for advanced Earth-to-orbit vehicles. To help develop the technology, a program has been under way to investigate using tip fins in place of the center vertical tail on the Space Shuttle orbiter (ref. 6).



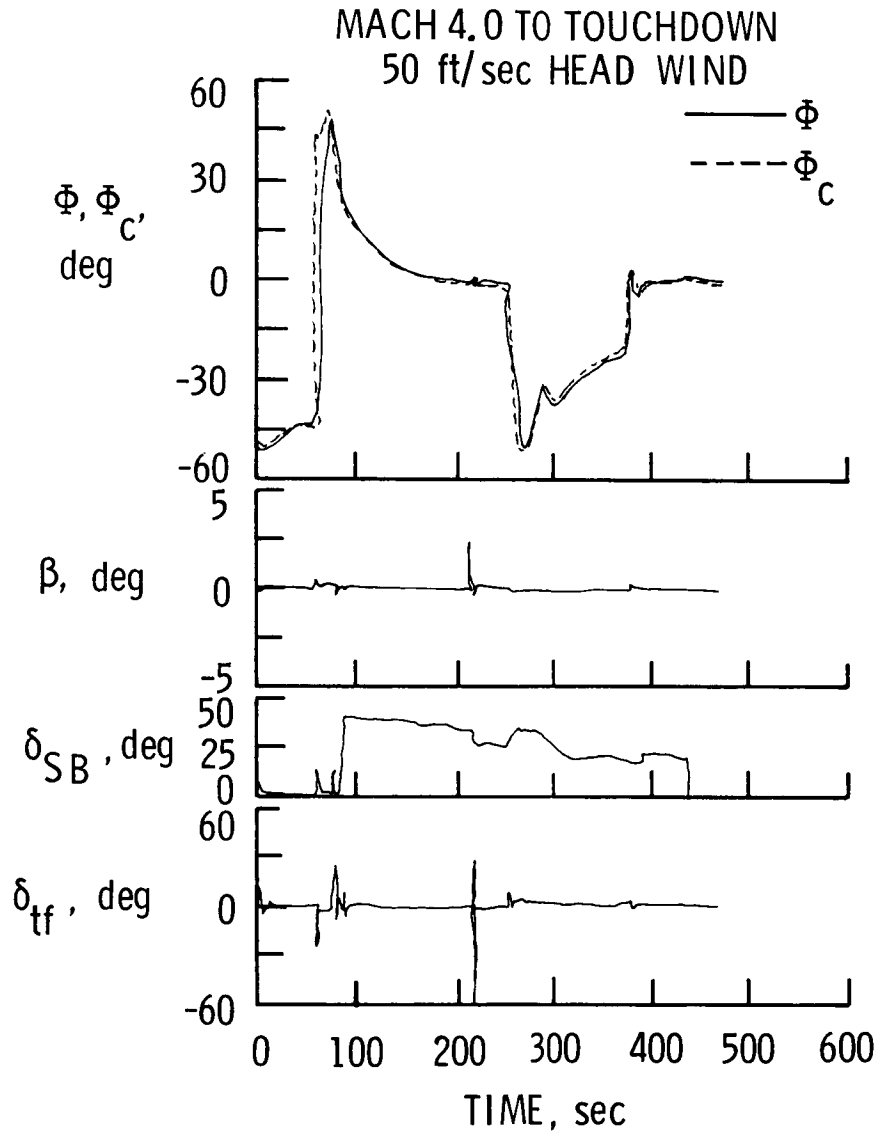
RESPONSE OF SHUTTLE

As part of the investigation of the Space Shuttle Orbiter with tip fins, the six-degree-of-freedom version of POST was used to study the response of the orbiter along various trajectories. This figure (ref. 6) is for the existing Shuttle orbiter and shows the response to a 50 ft/sec head wind for a Mach number of 4.0 to touchdown.



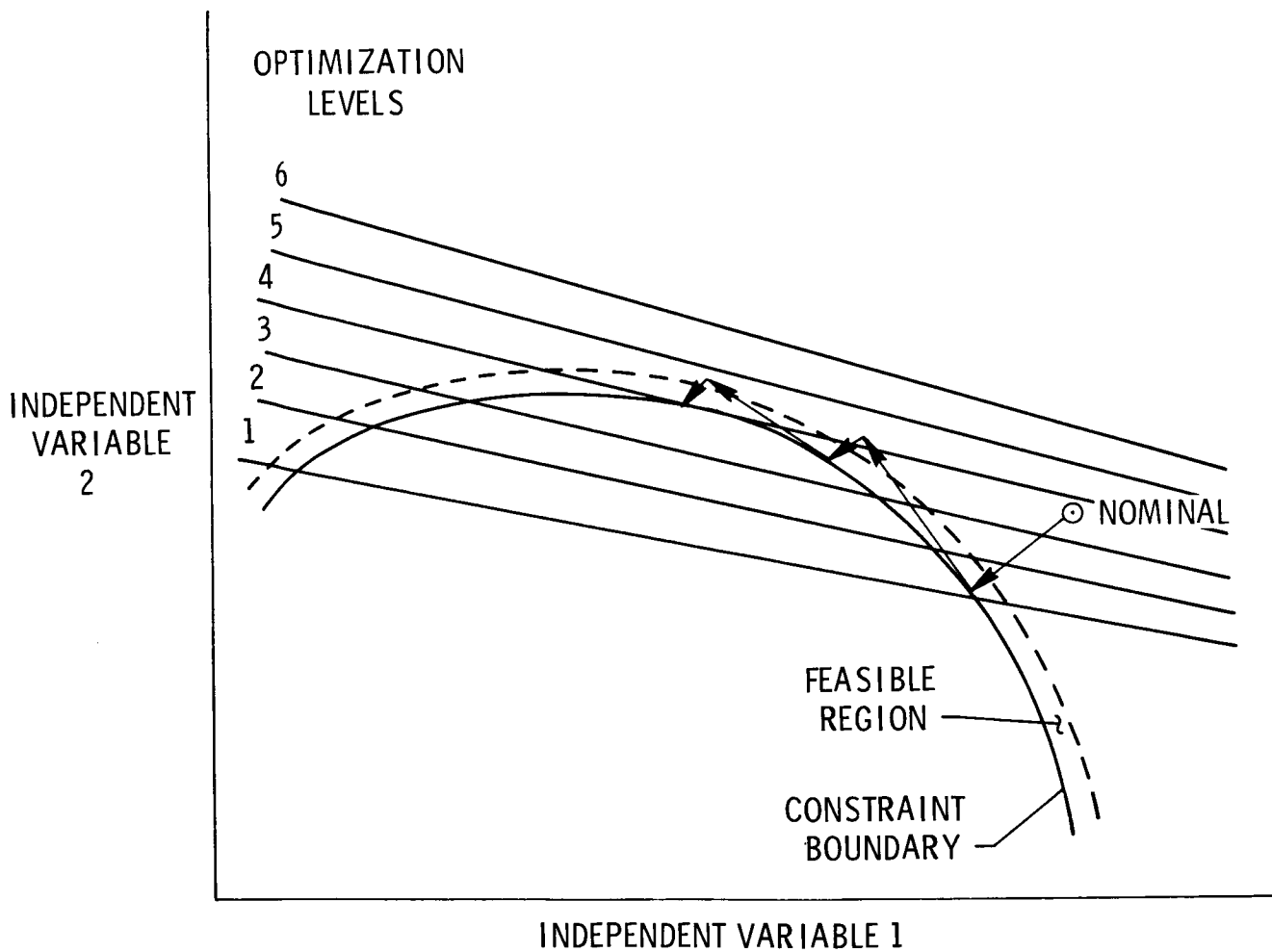
RESPONSE OF SHUTTLE WITH TIP FINS

The figure is different from the previous figure only in that the Shuttle has tip fins instead of the central vertical fin (ref. 6). The differences in response are used to evaluate the merits of the configuration change. Changes in the guidance system logic have also been evaluated.



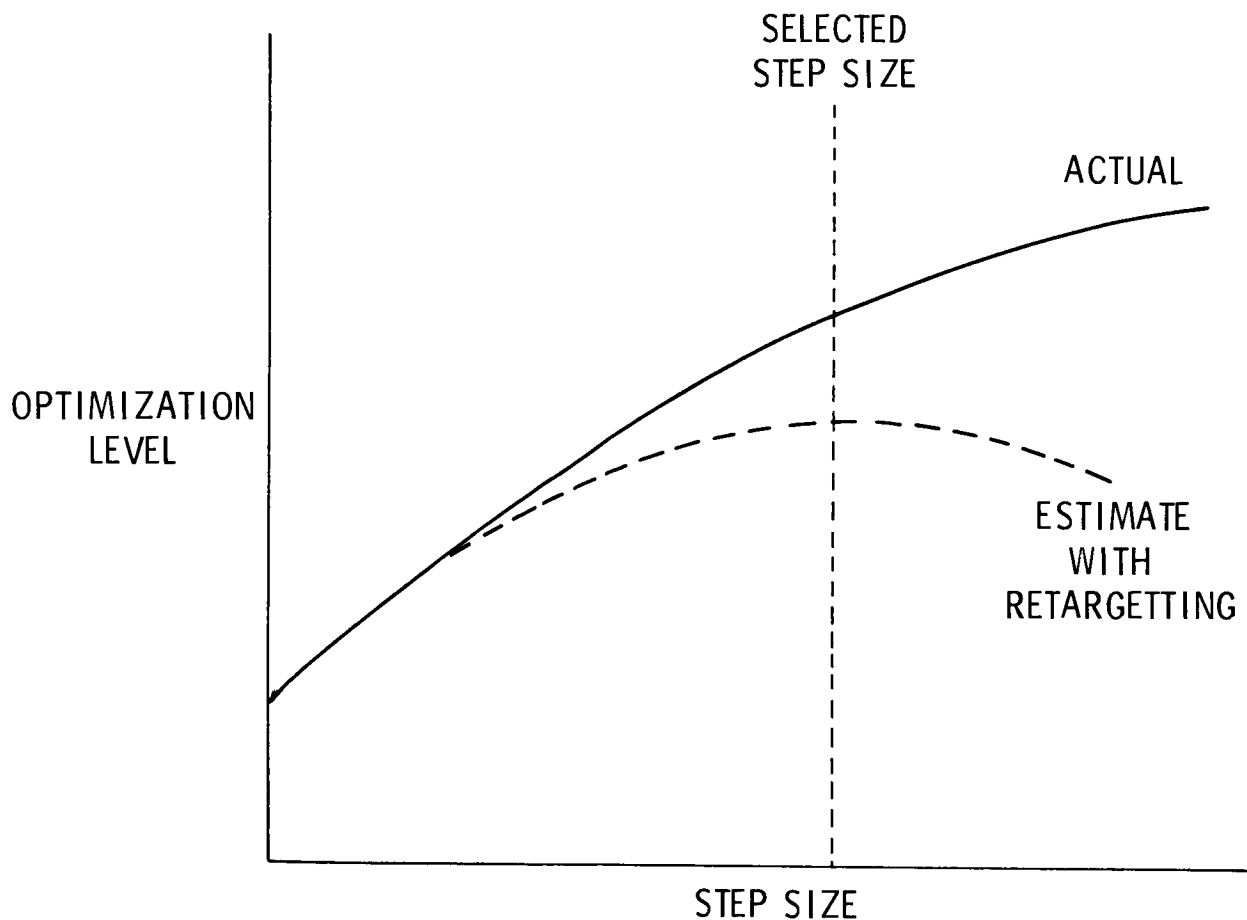
PROJECTED-GRADIENT OPTIMIZATION

This figure illustrates the projected gradient approach to optimization (ref. 1), which is the preferred option. The problem is to find the point with the highest optimization level subject to the constraint boundary. A feasible region is defined, within which the constraint errors are small enough that the trajectory can be considered meaningful. An initial guess or nominal solution may be outside the feasible region, as illustrated. In this case, the scheme tries to satisfy the constraints or target in a manner that changes the independent variables a minimum amount. Once targetted, the scheme tries to increase the optimization level along the constraint boundary. Because of nonlinearities, the direction of search leaves the constraint boundary so that a retargetting phase takes place based on the gradient information at the beginning of the optimization phase.



OPTIMIZATION STEP SIZE

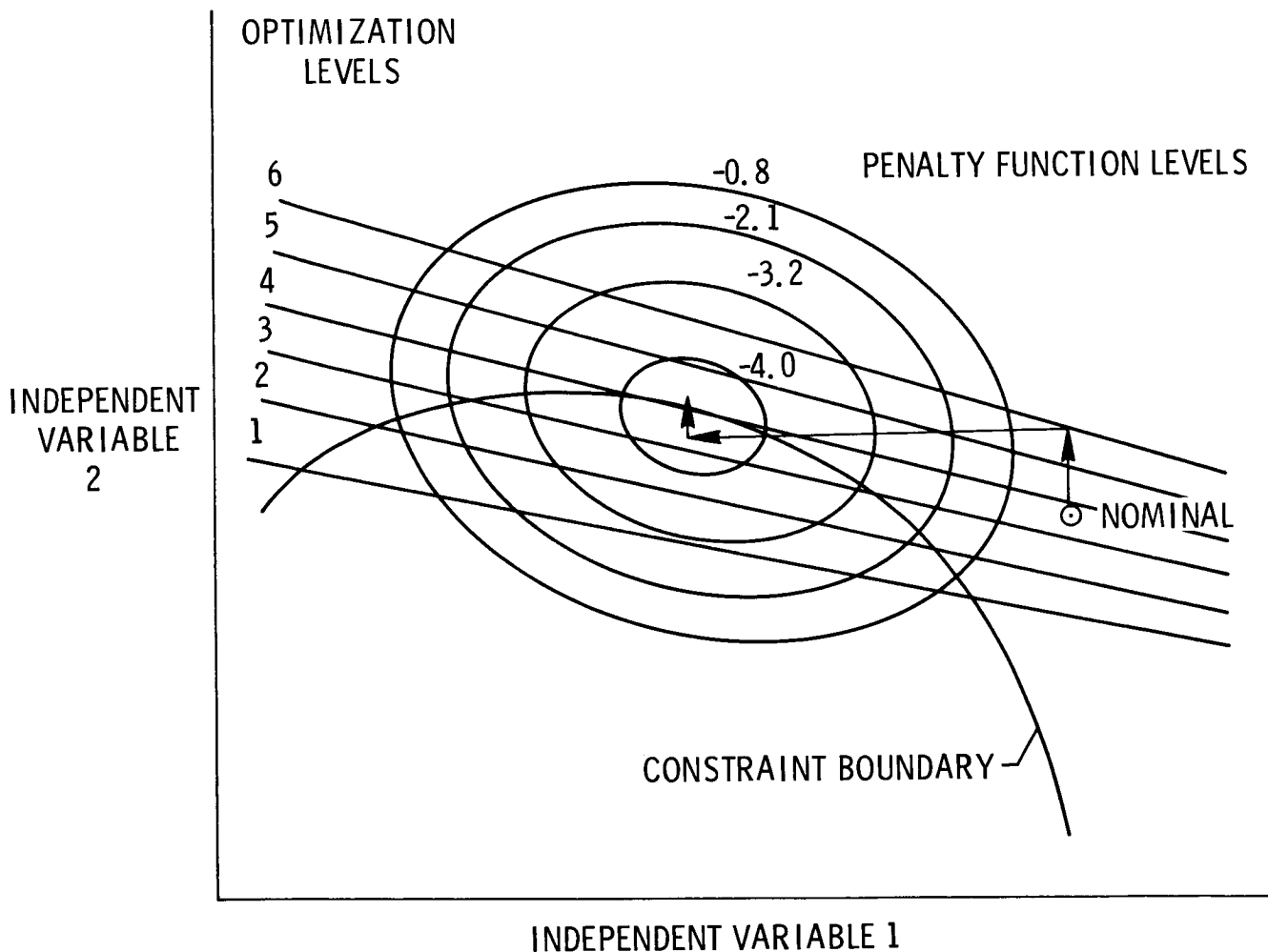
The step size must be selected for the optimization phase of the projected-gradient scheme. The actual optimization level may continue to increase for very large steps, but the constraint errors would probably be unacceptable. The approach used by POST is to estimate what the optimization level will be after retargetting. The step size is then selected to maximize the retargetted optimization level.



RANDOM WALK OPTIMIZATION

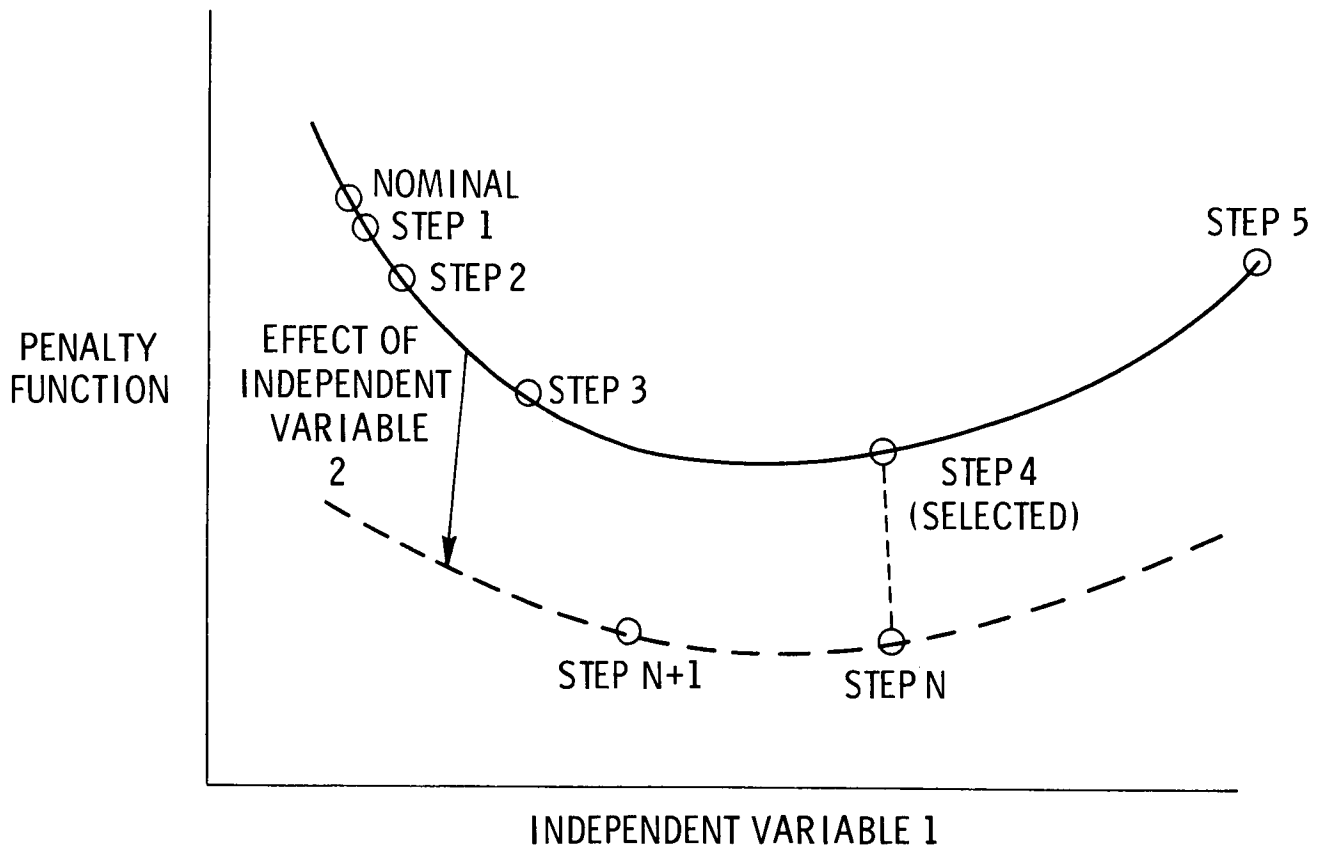
Although the projected-gradient approach has been used very successfully in POST, occasional problems occur. For example, a trajectory might crash or otherwise fail to reach a normal termination. For these infrequent but important cases, an approach has been incorporated into POST which is almost foolproof in the sense that if a nominal trajectory can be improved it will be.

This figure illustrates the random-walk approach to optimization. A penalty function is constructed from the optimization index and the sum of the constraint errors squared. The random-walk approach is to vary one independent variable at a time. If an improvement in the penalty function level occurs, the new point is used for the search in the next direction.



RANDOM-WALK STEP SIZE

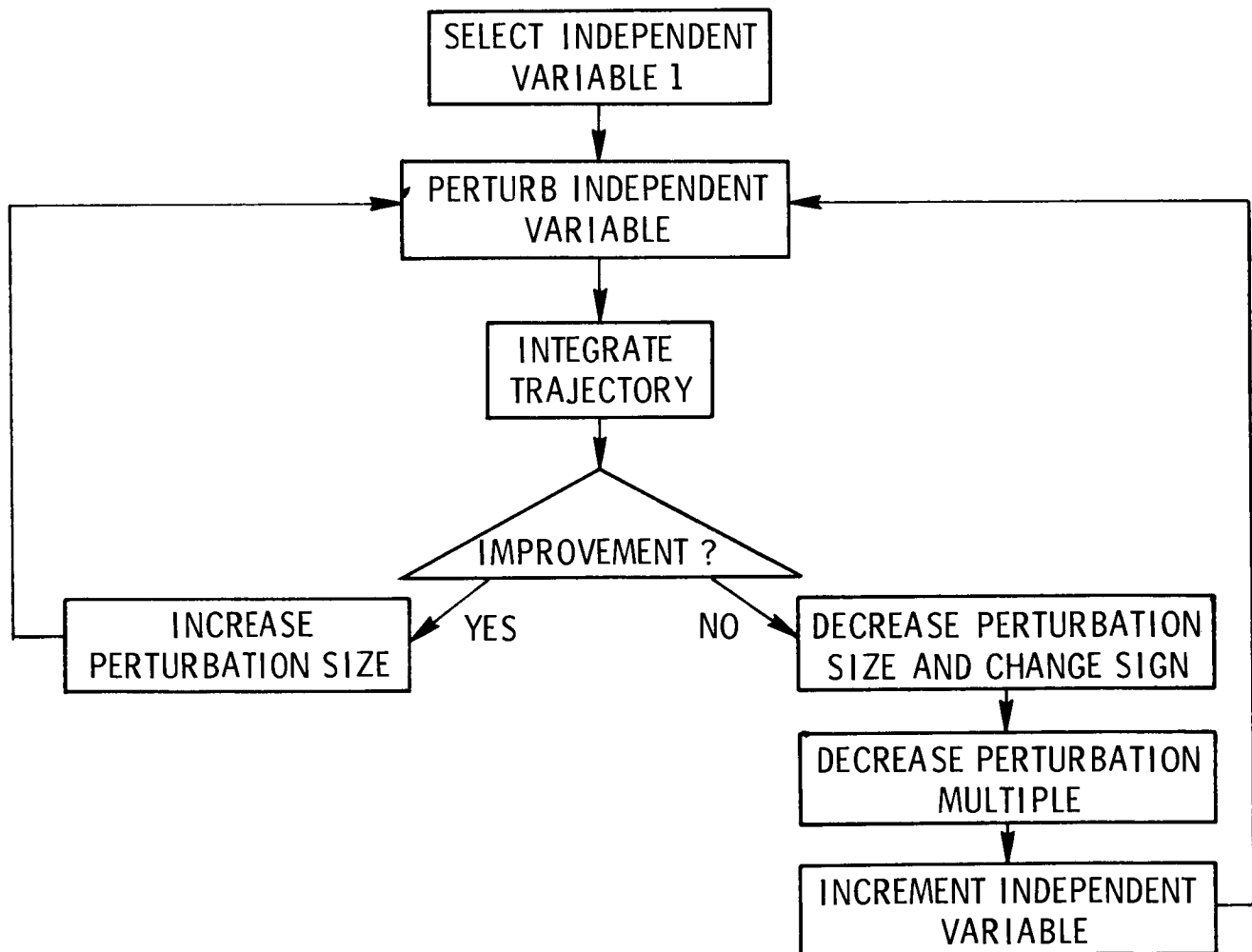
The random-walk step size starts with a small value. If a step is successful, the next step is larger. Once a step is unsuccessful, the scheme moves to the next independent variable. When the scheme returns to the first independent variable, the step direction is reversed and the step size is reduced.



RANDOM-WALK LOGIC

The logic for the random-walk scheme is mostly fairly straightforward. The first independent variable is perturbed a small amount. If the penalty function is reduced, the perturbation size is increased and another step is taken. When the step fails to reduce the penalty function, the step size is reduced and the sign is reversed. The next independent variable is then perturbed.

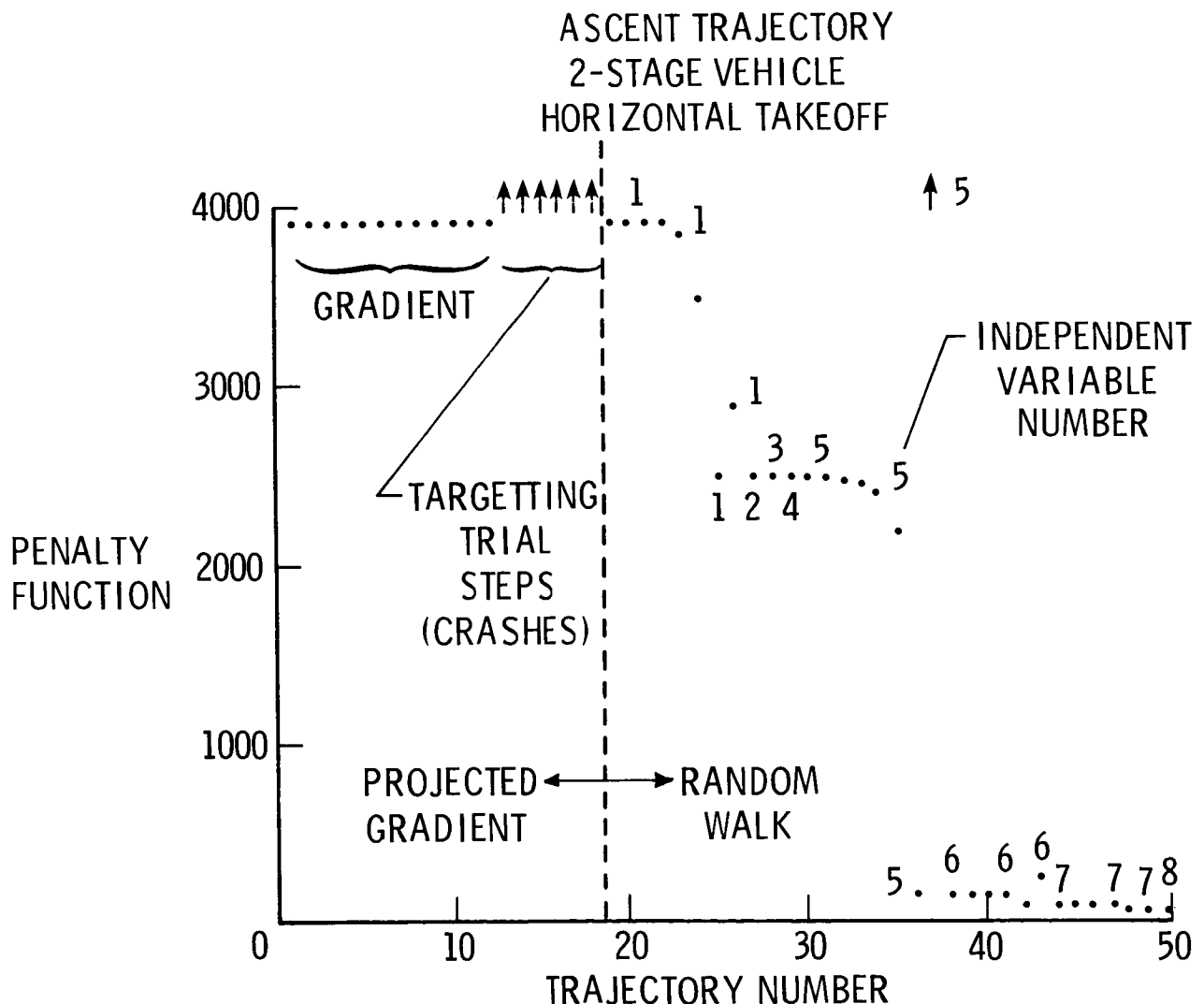
The increase or decrease of the perturbation magnitude is controlled by a perturbation multiplier for each independent variable. The perturbation multiplier is initially set at 5.0 so that the steps initially grow by more than two orders of magnitude in three steps. Since the initial perturbation is often several orders of magnitude smaller than the change needed to find the solution, such large changes are useful. Each time the direction of search in an independent variable changes sign, the perturbation multiple is reduced by raising it to the 0.7 power. This method allows closer examination of the region near the optimum, yet large steps can still be taken when needed.



INITIAL OPTIMIZATION RESULTS

Typical results of a case in which the random-walk method was used are shown. The projected gradient method was used first. The first 12 trajectories were required to get the gradient. The next six trajectories were attempts to target the errors, and all six crashed. Each time a trial step crashes, the step size is reduced by an order of magnitude. In this case, with a reduction of five orders of magnitude in the step size and the crash of the sixth trajectory, the selected search direction is apparently not a good choice.

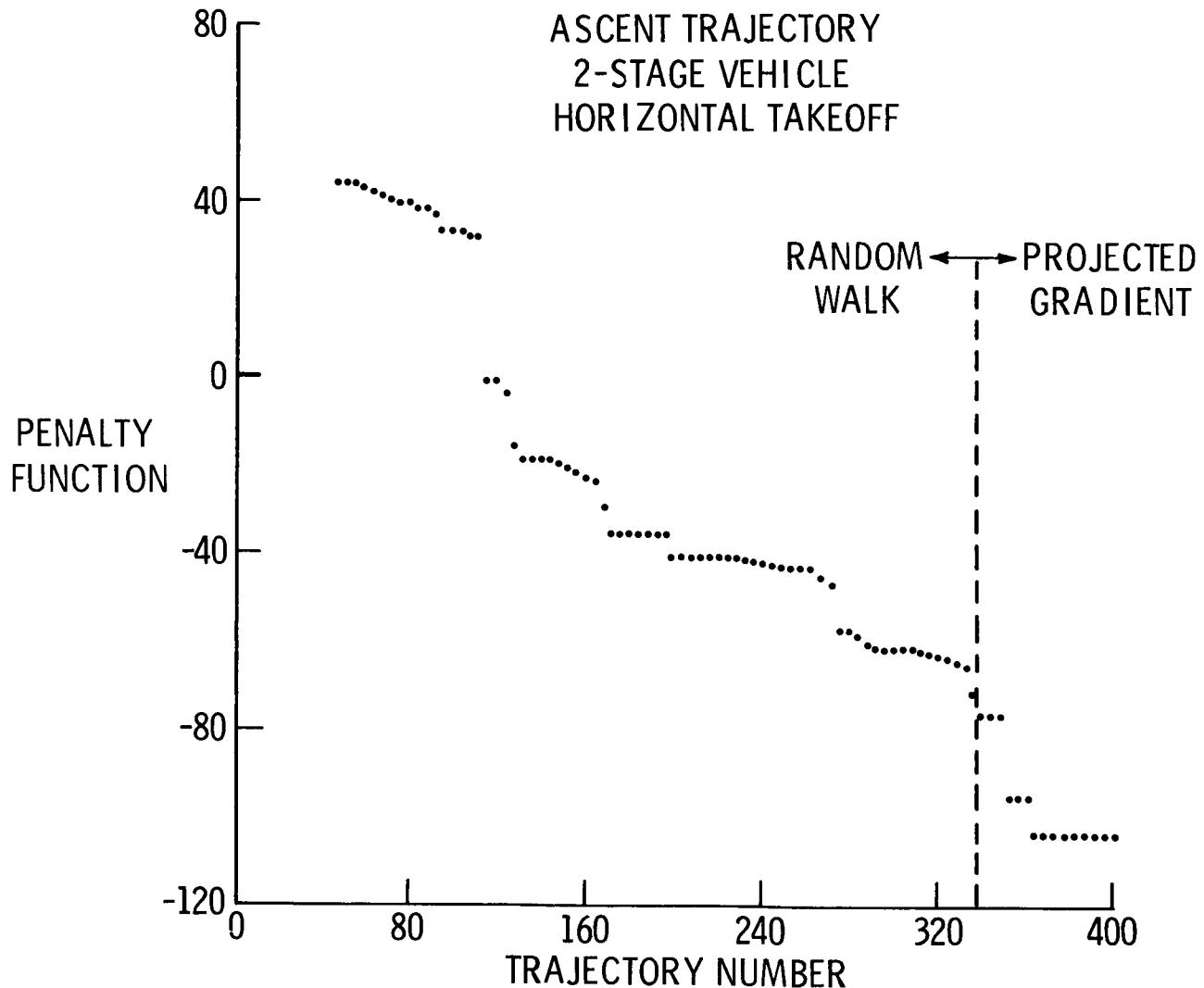
The random-walk method was used when it became obvious that the projected gradient method was having trouble. After seven trajectories with steps in the first independent variable, the penalty function was reduced by about one third. Perturbations in independent variables 2, 3, and 4 were not helpful. Six trajectories with independent variable 5 perturbed reduced the penalty function dramatically.



FINAL OPTIMIZATION RESULTS

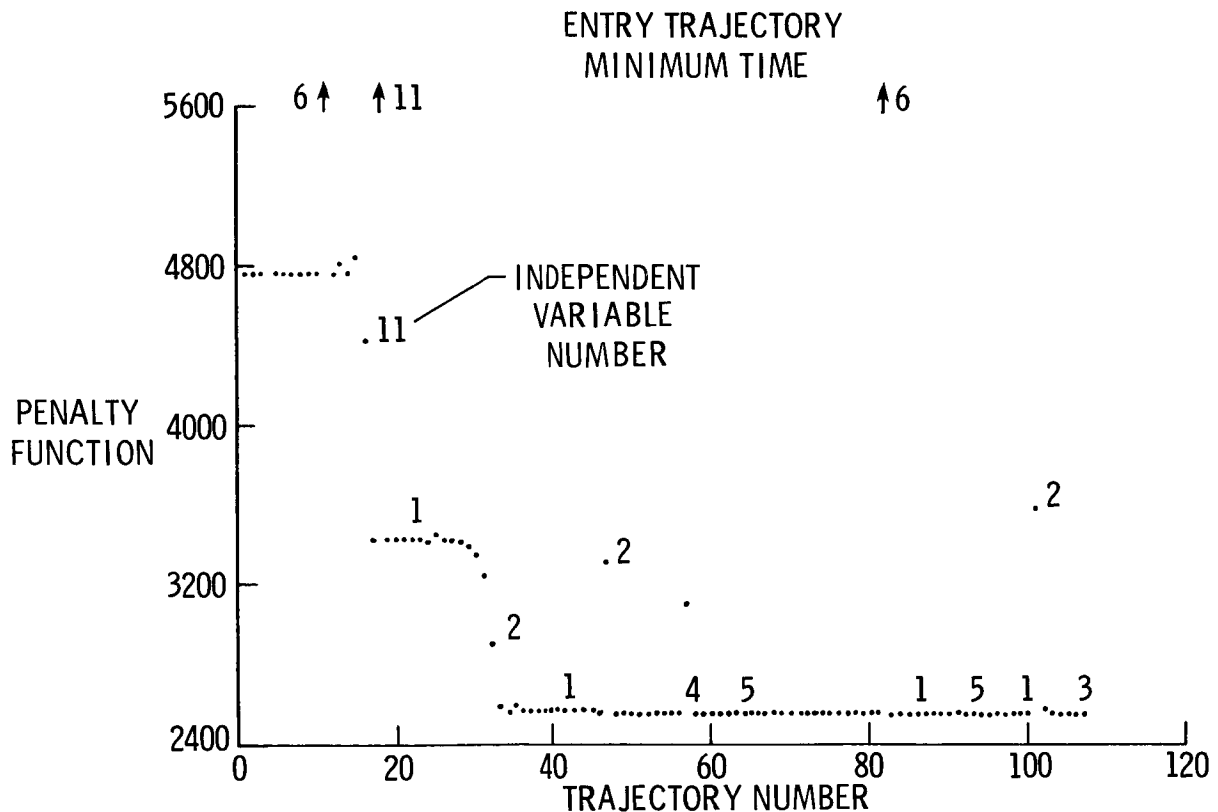
This figure shows the continuation of the case shown in the previous figure. The penalty function scale is expanded, and only the best of each four trajectories is shown. The random-walk method was used for about 300 trajectories, and some improvement was still being found.

The projected-gradient method was used at the end. Two iterations quickly reduced the errors to acceptable levels, and further optimization iterations made improvements that are not evident with the scale of the figure. Actually, the projected-gradient method probably could have been used successfully much sooner and would have solved the problem more efficiently.



RANDOM-WALK RESULTS

Another example of use of the random-walk method is shown in this figure. Independent variable 6 provides some insight into the random-walk results. Trajectories 7 through 10 were improved minimally by perturbations of independent variable 6, and trajectory 11 resulted in a large increase in the penalty function. Trajectory 39 was a perturbation of independent variable 6 in the negative direction which did not reduce the penalty function. Trajectories 77 through 81 again resulted in minimal improvements in the penalty function followed by a large increase on trajectory 82. Cases like this indicate a strong nonlinearity. Up to a certain point, there is little effect of changing independent variable 6, but beyond that point the results are significantly affected. This kind of behavior can lead to problems for gradient methods if the gradient is calculated where the slope is shallow and steps are taken beyond the point where the change is significant. In the random-walk approach, there is not much improvement from independent variable 6, but the nonlinearity does not cause the method to fail. Changes in independent variables 11 and 2 provide most of the improvement.



CONCLUSIONS

Experience with POST at a number of organizations around the country indicates that it is an excellent program for trajectory optimization problems. Also, the projected-gradient scheme used in POST can be used for problems other than trajectory problems which require optimization of non-linear systems subject to constraints. Despite the usefulness of the projected-gradient scheme in most problems, there are occasional situations when using it will be difficult. For these situations, a random-walk approach has been developed which offers a nearly foolproof solution to most difficulties that might be encountered.

- POST IS RECOMMENDED FOR TRAJECTORY OPTIMIZATION PROBLEMS
- THE PROJECTED-GRADIENT SCHEME IN POST IS RECOMMENDED FOR ALL NON-LINEAR OPTIMIZATION, NOT JUST TRAJECTORIES
- THE RANDOM-WALK APPROACH OFFERS A NEARLY FOOLPROOF SOLUTION TO MOST DIFFICULTIES ENCOUNTERED BY THE PROJECTED-GRADIENT SCHEME

References

1. Brauer, G. L.; Cornick, D. E.; and Stevenson, R.: Capabilities and Applications of the Program to Optimize Simulated Trajectories. NASA CR-2770, Feb. 1977.
2. Wurster, K. E.: An Assessment of the Impact of Transition on Advanced Winged Entry Vehicle Thermal Protection System Mass. AIAA Paper No. 81-1090, presented at the AIAA 16th Thermophysics Conference, Palo Alto, CA, June 23-25, 1981.
3. Calouri, V. A.; Conrad, R. J.; Jenkins, J. C.: Technology Requirements for Future Earth-to-Geosynchronous Orbit Transportation Systems. NASA CR-3265, April 1980.
4. Martin, J. A.: Hydrocarbon Rocket Engines for Earth-to-Orbit Vehicles. Journal of Spacecraft and Rockets, Vol. 20, No. 3, May-June 1983, pp. 249-256.
5. Hunt, J. L.; et al: Design and Performance Sensitivities of a Dual-Mode Scramjet Missile with Otto Fuel, Silane, and RJ-5 Pilots. Presented at the 1983 JANNAF Propulsion Meeting, Monterey, CA, February 14-18, 1983.
6. Powell, R. W.; and Freeman, Delma C., Jr.: Evaluation of the Aerodynamic Control of the Space Shuttle Orbiter with Tip-Fin Controllers. AIAA Paper No. 84-0488, presented at the AIAA 22nd Aerospace Sciences Meeting, Reno, NV, January 9-12, 1984.

ACKNOWLEDGEMENTS

Examples presented were provided by James L. Hunt, J. Chris Naftel, Richard W. Powell, Kathryn E. Wurster. Their cooperation is appreciated.

N87-11765

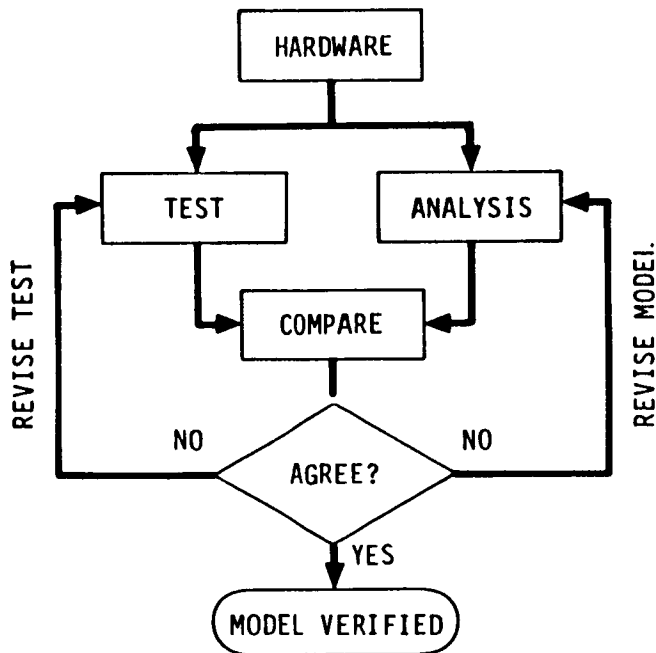
COMPONENT TESTING
FOR DYNAMIC MODEL VERIFICATION

T.K. Hasselman and Jon D. Chrostowski
Engineering Mechanics Associates, Inc.
Palos Verdes Estates, California

PRECEDING PAGE BLANK NOT FILMED

DYNAMIC MODEL VERIFICATION

Dynamic model verification is the process whereby an analytical model of a dynamic system is compared with experimental data, adjusted if necessary to bring it into agreement with the data, and then qualified for future use in predicting system response in a different dynamic environment. There are various ways to conduct model verification. The approach taken here employs Bayesian statistical parameter estimation. Unlike "curve fitting," whose objective is to minimize the difference between some analytical function and a given quantity of test data (or "curve"), Bayesian estimation attempts also to minimize the difference between the parameter values of that function (the model) and their initial estimates, in a least squares sense. The objectives of dynamic model verification, therefore, are to produce a model which (1) is in agreement with test data, (2) will assist in the interpretation of test data, (3) can be used to help verify a design, (4) will reliably predict performance, and (5) in the case of space structures, will facilitate dynamic control. (See fig. 1.)



OBJECTIVES

- MATCH ANALYSIS AND TEST
- INTERPRET DATA
- VERIFY DESIGN
- PREDICT PERFORMANCE
 - IMPEDANCE
 - DISPLACEMENT
 - LOADS
 - FATIGUE
 - ETC.
- FACILITATE CONTROL

Figure 1

RELATIONSHIP TO SYSTEM IDENTIFICATION

As a practical matter, system identification is synonymous with statistical estimation, whether it be nonparametric regression analysis or sequential parameter estimation. Some degree of uncertainty is always present in real data. Statistical methods are useful in managing this uncertainty. Statistical estimation may be divided into two categories, parametric and nonparametric. The parametric form assumes that a model configuration is given; the nonparametric form does not. Parametric system identification can be further divided into two categories, Bayesian and non-Bayesian. The Bayesian form assumes some prior knowledge of the parameter values; the non-Bayesian form does not. Since model verification implies the existence of a prior model, including knowledge of its parameter values, the Bayesian form of parameter estimation is well suited for it. As will be shown, Bayesian parameter estimation not only "tunes" the model to match the data but also provides a means of assessing the confidence in new parameter estimates and response predictions. (See fig. 2.)

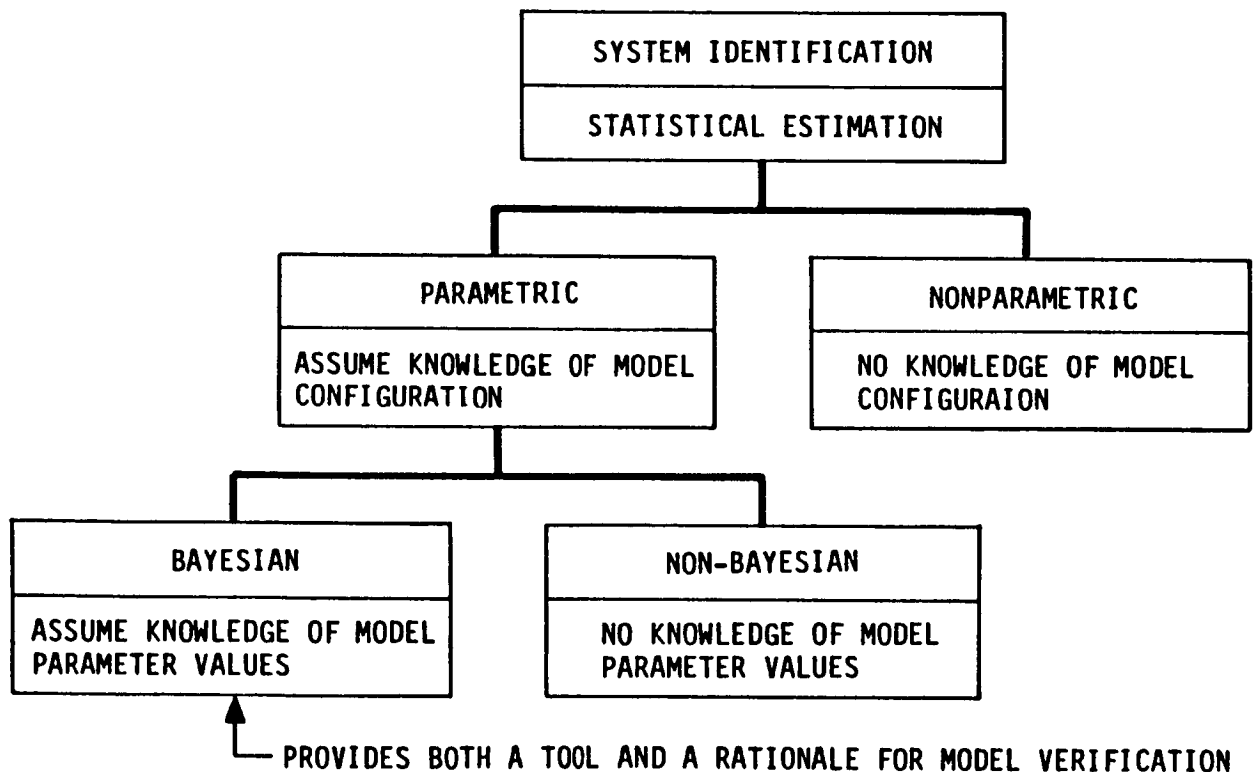


Figure 2

MODEL VERIFICATION PLANNING

An explicit model verification plan is essential to successful model verification. It should precede the writing of a test plan because it establishes the requirements for instrumentation, calibration, measurement accuracy, data acquisition and data processing. The plan should begin by defining the physical system under consideration and its behavior of interest. It should define the model and the test in the terms listed in fig. 3. The scope of the test should be consistent with the scope of the model; i.e., the test should be capable of revealing those characteristics of the model which influence the behavior of interest. While it may not be possible or practical to establish complete criteria for model verification at the outset, provision should be made for evaluating model limitations after the fact. The evaluation should address the degree to which the verified model is true to the physical system (fidelity) and the degree of confidence one may associate with response predictions obtained from it.

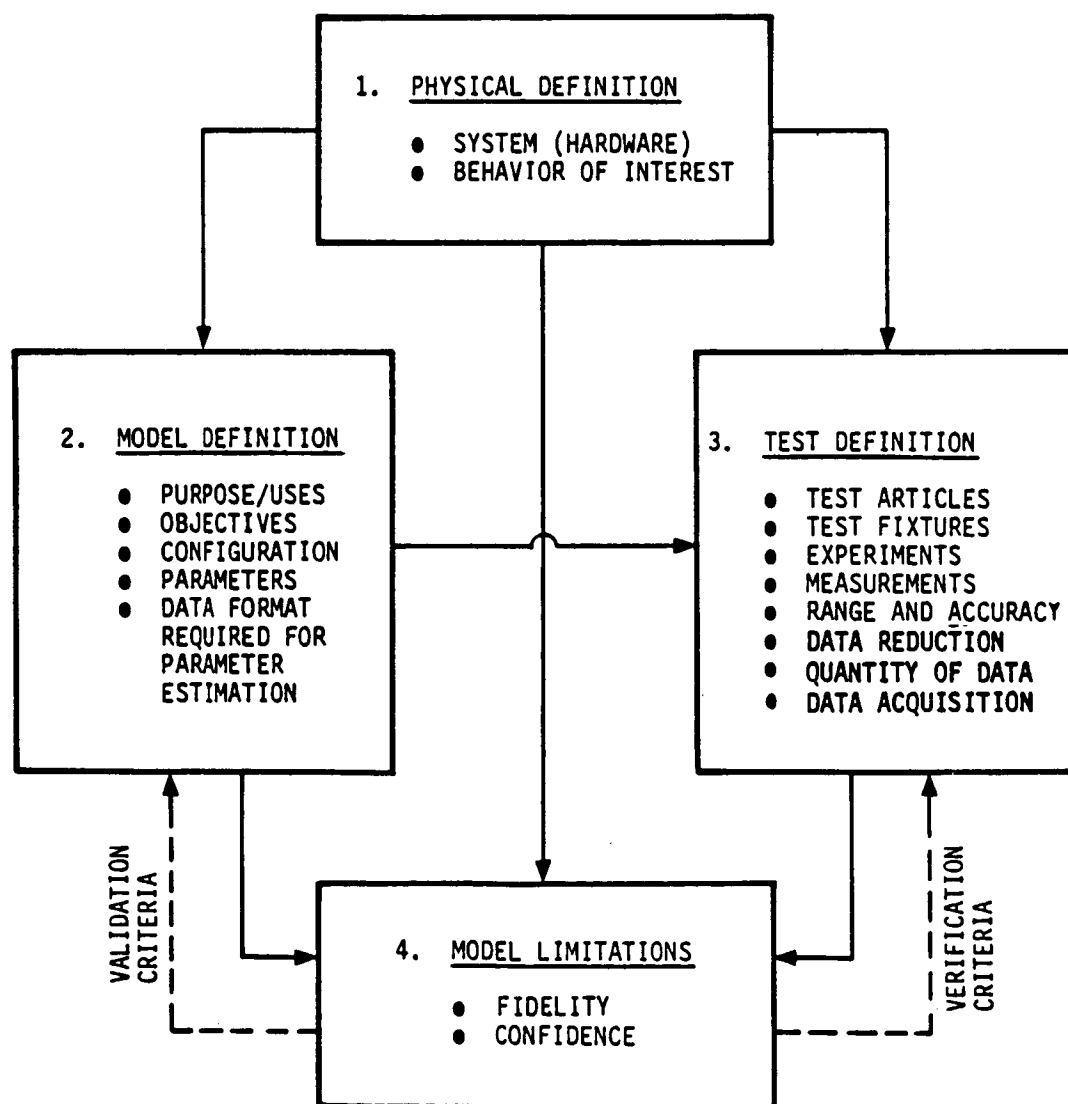


Figure 3

STRATEGY CONSIDERATIONS

When a dynamic model must replicate the behavior of a complex physical system responding to various sources of excitation, a strategy will be needed to carry out the model verification. The military principle of "divide and conquer" is helpful in formulating such a strategy. Component testing offers one avenue of simplification. Direct measurement (e.g. of mass or stiffness) is always preferable to indirect parameter estimation, and should be employed wherever possible. Software capabilities and computational limitations dictate the primary constraints on parameter estimation, as indicated in fig. 4. Grouping and sequencing procedures may be employed to achieve successful model verification within these constraints.

COMPONENT TESTING

- DIRECT MEASUREMENT
- PARAMETER ESTIMATION

SOFTWARE CAPABILITY

- MODELING CAPABILITY
- NUMBER OF PARAMETERS ESTIMATED
- TYPE OF DATA INPUT
- NUMBER OF DATA POINTS PROCESSED

COMPUTATIONAL LIMITATIONS

- RESPONSE/PARAMETER SENSITIVITY
- NUMERICAL CONDITIONING
- COMPUTATION EFFORT AND COST

GROUPING

- MODEL PARAMETER SUBSETS
- TEST DATA SUBSETS

SEQUENCING

- BY COMPONENTS
- BY MODEL PARAMETER SUBSETS
- BY MEASUREMENT CHANNELS
- BY FREQUENCY BANDS

Figure 4

RECENT EXPERIENCE
VIBRATION TESTING OF A CANTELEVER BEAM WITH DISCRETE DAMPER

The foregoing principles of model verification planning and strategy development are currently being applied to a structure which resembles a cantilever beam, with discrete damping and stiffness elements attached to its free end (fig. 5). The beam is nearly axi-symmetric and exhibits closely spaced pairs of modes perpendicular to its axis. It is suspended vertically with a double compound pendulum damper near its lower end. The damper consists of a pendulous weight immersed in silicone damping fluid. The mathematical model is comprised of two components: a modal representation of the beam itself, extracted from a 500 degree-of-freedom finite element model, and a lumped-mass model of the damper. Testing consisted of single-point random vibration, from which complex frequency response and coherence functions were obtained at several stations along the beam.

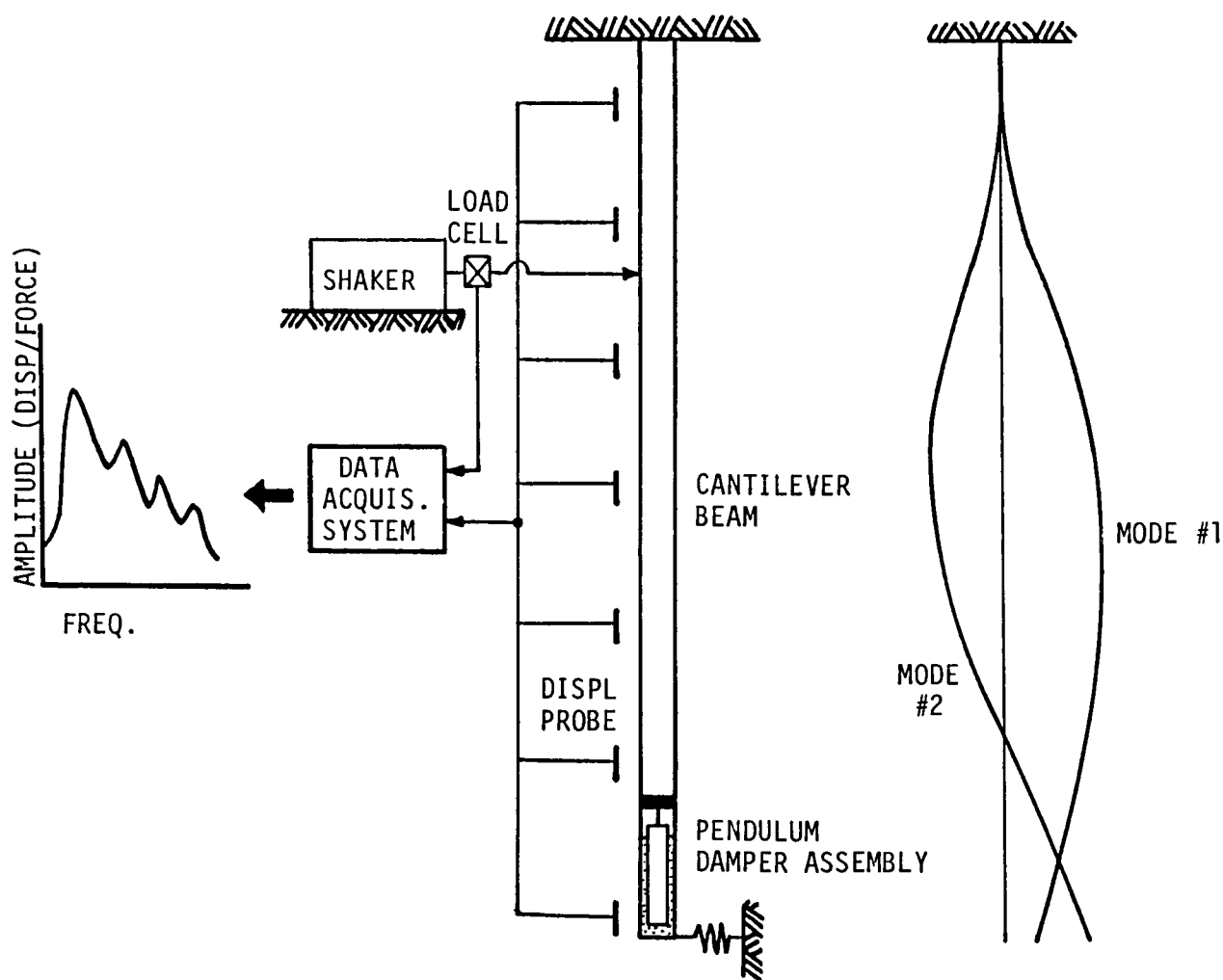


Figure 5

COMPONENT TESTING OF DISCRETE DAMPER

One of the objectives of this model verification effort was to determine the damping characteristics of the discrete damper itself. Anticipating that it might be difficult to extract this information from vibration testing of the complete beam assembly, available data from earlier component tests performed on the damper alone were processed. The component vibration tests consisted of rigidly securing the damper housing to a carriage that was free to move back and forth on rails. Broad-band random excitation was applied to the carriage by a shaker, and the resulting acceleration of the carriage was measured. Load cells in the clamps securing the damper housing measured the force applied to the housing. The data were Fourier analyzed to obtain the complex frequency response of force divided by acceleration, i.e. an effective mass. The pendulum damper was modeled with two degrees of freedom, as shown in fig. 6.

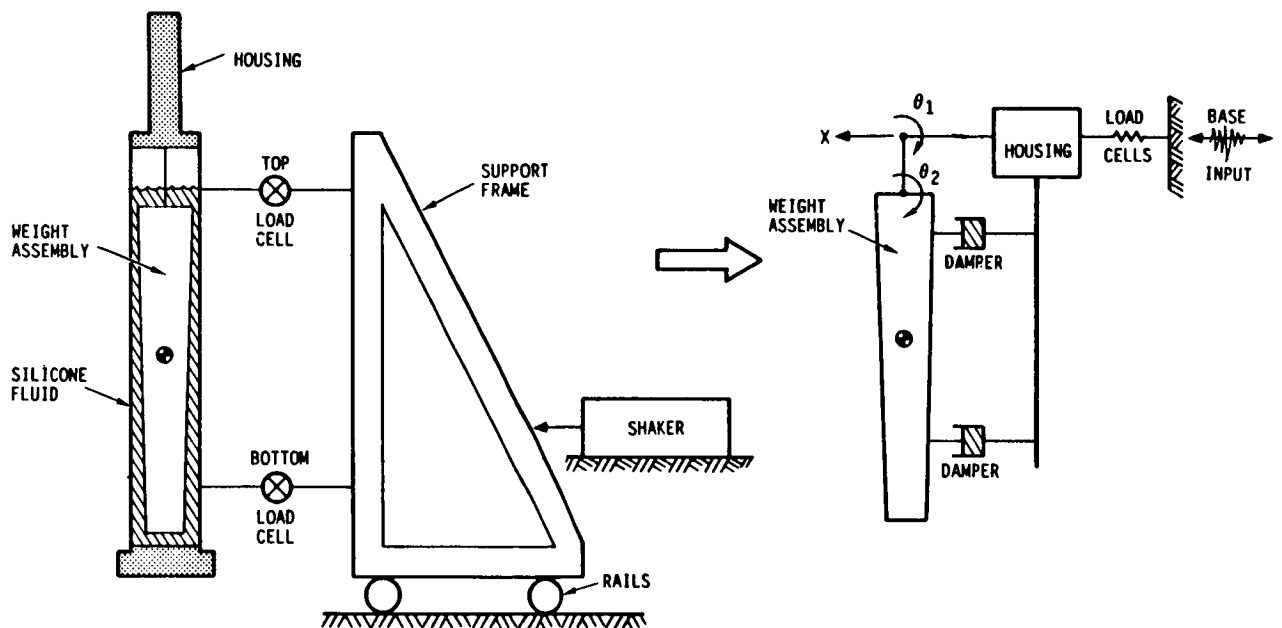


Figure 6

COMPARISON OF PREDICTED AND MEASURED RESPONSE - DISCRETE DAMPER

Initial estimates of the damping constants for the pendulum damper were inferred from "snap-back" tests on the beam assembly. These estimates proved to be grossly in error as evidenced by the comparison of "prior model" and "test data" response shown below. A modified version of the MOVER computer program (ref. 1) was then used to estimate lateral and rotational damping coefficients C_L and C_R , an equivalent representation of the two dashpots shown in the preceding figure. A subsequent attempt was made to estimate a possible rotational stiffness, K_R , which might arise from fluid sloshing at the frequency of the second pendulum mode. No significant estimate of K_R was obtained; however, the estimated values of C_L and C_R were approximately the same in both cases. These estimates produced the response curve labeled "revised model" in fig. 7. It matched the data points quite well.

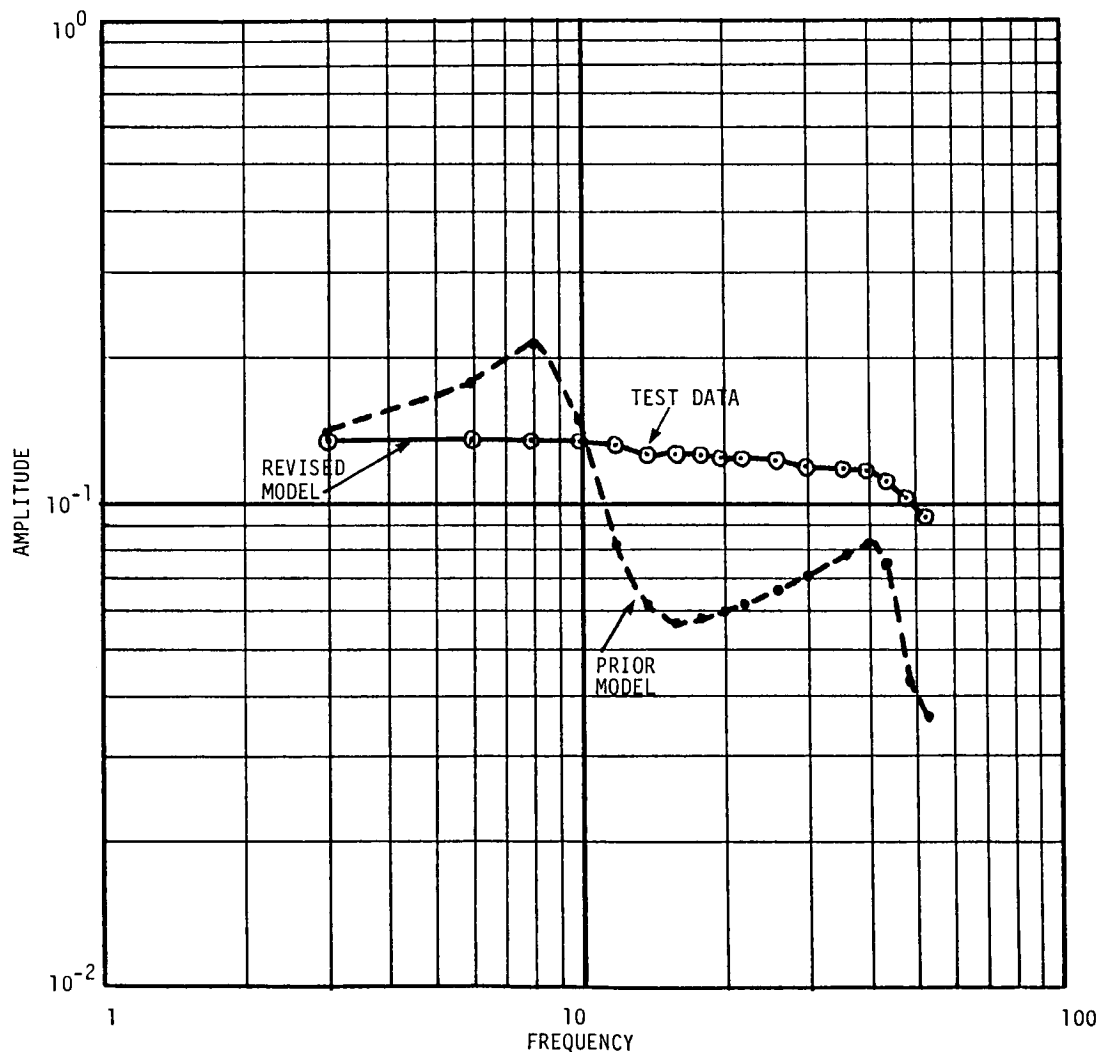


Figure 7

PARAMETER ESTIMATES - DISCRETE DAMPER

A summary of the parameter estimates for C_L , C_R and K_R is shown in fig. 8. The prior estimates are shown along with the revised estimates. In addition to each set of estimates, the standard deviations and correlation matrix of each estimate are shown. Standard deviations of the initial estimates were assumed to be arbitrarily large, with no correlation. Standard deviations of the revised estimates indicate the statistical significance of those estimates. Of the three, only C_L was estimated with a satisfactory degree of confidence. The estimated values of C_L and C_R resulted in the first mode of the damper being overcritically damped (approximately 400% of the critical damping) and the second mode having about 50% of critical damping. The revised estimate of K_R was rejected in favor of the prior estimate, $K_R=0$.

| PRIOR | | | | | |
|---------------------|--------------------|-----------------------|-----------------------|------|------|
| PARAMETER SYMBOL | ESTIMATED VALUE | STANDARD DEVIATION | CORRELATION MATRIX | | |
| C_L | .140 | 31.6 | 1.0 | .0 | .0 |
| C_R | .140 | 31.6 | | 1.0 | .0 |
| K_R | .0 | 3.16 | | | 1.0 |
| REVISED | | | | | |
| C_L | 3.787 | .444 | 1.0 | .406 | .171 |
| C_R | .537 | .800 | | 1.0 | .069 |
| K_R | .492 | 2.914 | | | 1.0 |

Figure 8

COMPARISON OF PREDICTED AND MEASURED RESPONSE - BEAM ASSEMBLY

The estimates of C_L and C_R obtained from the foregoing component test and parameter estimation were then used in a model of the beam assembly to generate a frequency response function representing displacement response at the lower end of the beam divided by the force input measured by the load cell (fig. 5). The discrete damper model was coupled to the modal model of the beam, wherein each mode was nominally assumed to have 0.5% damping (one-half of one percent). The corresponding results labeled "prior model" are shown in fig. 9 in comparison with data points actually used in subsequent parameter estimation. A total of 24 mass, stiffness and damping parameters was estimated in three groups, each associated with a pair of orthogonal modes perpendicular to the beam axis. Data from three distinct frequency bands were used in the estimation, which produced the results labeled "revised model" in the figure. As can be seen, the revised model fits the data reasonably well except in the vicinity of the third resonance. This is where the effect of a poor estimate of C_R for the pendulum damper would be expected to appear. Efforts are continuing to improve upon this estimate.

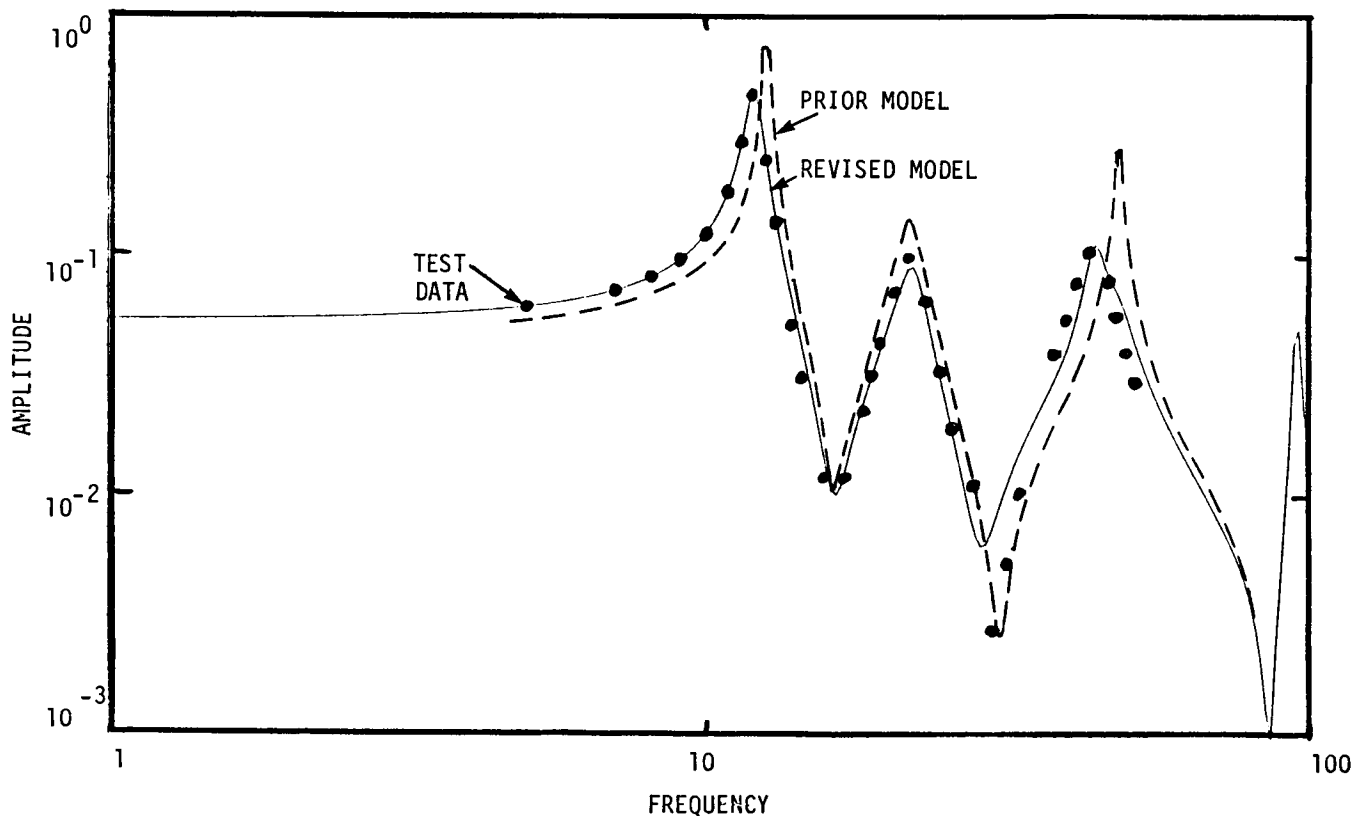


Figure 9

PARAMETER ESTIMATES - CANTILEVER BEAM

The modal mass, stiffness and damping estimates for the first pair of modes of the cantilever beam are shown in fig. 10. The mass parameters are denoted by m_{11} , m_{12} , and m_{22} representing the two modal masses and the corresponding coupling term for the first pair of modes. The stiffness parameters are likewise denoted by k_{11} , k_{12} , and k_{22} . They are normalized parameters, having been divided by circular frequency squared. The modal damping parameters, denoted by c_{11} and c_{22} , have been normalized such that unit value represents 0.5% modal damping. Standard deviations and the corresponding correlation matrix for each set of estimated values are shown as before. Three sets of estimates are included: (a) the prior estimate, (b) a revised estimate using data at only the first four frequencies, and (c) a second revised estimate using the first as a prior and data at the next eight frequencies spanning the first resonance. Data from six probes (fig. 5) were used, two near the upper end (orthogonal directions), two near the middle and two at the lower end. Excitation was applied separately in the two orthogonal directions during testing. A correlation matrix for the prior set of estimates was assumed on the basis of rather limited experience (e.g. ref. 2). In some cases, the assumed correlation coefficients proved to be incorrect, as revealed in subsequent estimates. This matter is presently under investigation. It is of interest to note the progression of increasing confidence (smaller standard deviation) as sequential estimation occurs. As one would expect, estimates of the damping parameters were very weak until data spanning the resonant peak were processed. One may also take note of the high degree of correlation among estimates of the modal mass and stiffness parameters. Estimates of the damping parameters tend to be uncorrelated with estimates of mass and stiffness.

A. PRIOR

| PARAMETER SYMBOL | ESTIMATED VALUE | STANDARD DEVIATION | CORRELATION MATRIX | | | | | | | |
|---------------------|--------------------|-----------------------|-----------------------|-----|-----------|-----|-----|-----|-----|-----|
| m_{11} | 1.0 | 0.2 | 1.0 | .0 | .95 | .90 | .0 | .90 | .0 | .0 |
| m_{12} | 0.0 | 0.2 | | 1.0 | .0 | .0 | .0 | .0 | .0 | .0 |
| m_{22} | 1.0 | 0.2 | | | 1.0 | .90 | .0 | .90 | .0 | .0 |
| k_{11} | 1.0 | 0.3 | | | | 1.0 | .0 | .95 | .0 | .0 |
| k_{12} | 0.0 | 0.15 | | | | | 1.0 | .0 | .0 | .0 |
| k_{22} | 1.0 | 0.3 | | | SYMMETRIC | | | 1.0 | .0 | .0 |
| c_{11} | 1.0 | 1.0 | | | | | | | 1.0 | .0 |
| c_{22} | 1.0 | 1.0 | | | | | | | | 1.0 |

Figure 10

B. REVISED (1)

| PARAMETER SYMBOL | ESTIMATED VALUE | STANDARD DEVIATION | CORRELATION MATRIX | | | | | | | |
|---------------------|--------------------|-----------------------|-----------------------|-------|------|-------|-------|-------|-------|-------|
| m ₁₁ | 1.150 | .045 | 1.0 | -.234 | .213 | .504 | -.240 | -.041 | -.011 | .004 |
| m ₁₂ | .000 | .046 | | 1.0 | .166 | -.134 | .609 | .107 | -.003 | .004 |
| m ₂₂ | 1.141 | .054 | | | 1.0 | .411 | -.204 | .009 | -.035 | .011 |
| k ₁₁ | .973 | .043 | | | | 1.0 | -.788 | -.796 | -.077 | .022 |
| k ₁₂ | .016 | .030 | | | | | 1.0 | .768 | .066 | -.018 |
| k ₂₂ | .986 | .046 | | | | | | 1.0 | .066 | -.022 |
| c ₁₁ | .858 | .574 | | | | | | | 1.0 | -.442 |
| c ₂₂ | 1.735 | .668 | | | | | | | | 1.0 |

C. REVISED (2)

| PARAMETER SYMBOL | ESTIMATED VALUE | STANDARD DEVIATION | CORRELATION MATRIX | | | | | | | |
|---------------------|--------------------|-----------------------|-----------------------|-------|-------|-------|-------|-------|-------|-------|
| m ₁₁ | 1.150 | .025 | 1.0 | -.860 | -.872 | .992 | -.852 | -.854 | -.144 | -.398 |
| m ₁₂ | -.002 | .016 | | 1.0 | .849 | -.859 | .992 | .836 | -.145 | .368 |
| m ₂₂ | 1.117 | .028 | | | 1.0 | -.878 | .851 | .989 | -.092 | .304 |
| k ₁₁ | .990 | .021 | | | | 1.0 | -.861 | -.874 | .149 | -.496 |
| k ₁₂ | -.171 | .013 | | | | | 1.0 | .851 | -.153 | .329 |
| k ₂₂ | .951 | .024 | | | | | | 1.0 | -.122 | .265 |
| c ₁₁ | 2.248 | .102 | | | | | | | 1.0 | -.509 |
| c ₂₂ | 2.456 | .144 | | | | | | | | 1.0 |

Figure 10
(continued)

EVALUATION OF RESULTS

The progress of a model verification effort must be continuously monitored to assure acceptable results. Quantities available for critical evaluation include the items listed in fig. 11. Experience has shown that if an incorrect model is being used in the parameter estimation, the estimates may not converge, or they may converge to unreasonable values. Both the parameter values themselves and the corresponding eigenvalues and eigenvectors (for a linear model) should be recorded during the iterative process of parameter estimation. This record often provides insight to problems (e.g. failure to converge) which arise. The statistical significance of parameter estimates should be evaluated before accepting the results. If a partial set of parameter estimates from one estimation is used in a subsequent estimation involving different parameters, the estimates of the partial set should be uncorrelated from the remainder of that set. When evaluating predicted response, one should consider the confidence limits on predicted response, in addition to how well it matches a particular set of data.

PARAMETER ESTIMATES

- NUMERICAL CONVERGENCE OF PARAMETER ESTIMATES
- REASONABLENESS OF PARAMETER ESTIMATES
- REASONABLENESS OF CORRESPONDING EIGENVALUES AND EIGENVECTORS
- STATISTICAL SIGNIFICANCE OF PARAMETER ESTIMATES
- CORRELATION AMONG PARAMETER ESTIMATES

PREDICTED RESPONSE

- RMS ERROR BETWEEN PREDICTED AND MEASURED RESPONSE
- CONFIDENCE LIMITS ON PREDICTED RESPONSE

Figure 11

CONCLUSIONS

Dynamic model verification is a multi-disciplined task involving analysis, testing, parameter estimation, and most importantly, an overall plan which coordinates these efforts. Parameter estimation (or system identification, as some would call it) is only a part of the process. Bayesian parameter estimation, however, is a valuable tool, greatly facilitating the "marriage" of analytical and experimental data bases. (See fig. 12.)

Model verification is not an easy task. Ironically, while Bayesian estimation adds a new dimension of capability for accomplishing this task, it seems at times to make it even more difficult. But that is only because it reveals weaknesses in the model or the data which might otherwise escape unnoticed. In a very important sense, it holds the analyst more accountable by demanding a higher degree of model fidelity to the physical system, and measurable confidence in the final results.

DYNAMIC MODEL VERIFICATION SHOULD INCLUDE THE FOLLOWING ELEMENTS:

1. AN INITIAL PLAN WHICH COORDINATES MODELING, TESTING AND SUBSEQUENT PARAMETER ESTIMATION IN SUCH A WAY THAT SUFFICIENT DATA ARE OBTAINED TO ESTIMATE THE DESIRED MODEL PARAMETERS.
2. A STRATEGY FOR PARAMETER ESTIMATION THAT ENABLES MODELS OF COMPLEX SYSTEMS TO BE VERIFIED WITHIN THE LIMITATIONS OF AVAILABLE SOFTWARE AND NUMERICAL COMPUTATION.
3. A FINAL EVALUATION OF MODEL LIMITATIONS, BASED ON THE RESULTS OF PARAMETER ESTIMATION, AND INHERENT LIMITATIONS OF ANALYSIS AND TEST WHICH ARE OTHERWISE KNOWN.

Figure 12

REFERENCES

1. Chrostowski, J.D., Evensen, D.A., and Hasselman, T.K., "Model Verification of Mixed Dynamic Systems," ASME Journal of Mechanical Design, Vol. 100, April 1978.
2. Hasselman, T.K., "Structural Uncertainty in Dynamic Analysis," Paper 811049, Transactions of the Society of Automotive Engineers, 1982.

N87-11766

DUAL STRUCTURAL-CONTROL OPTIMIZATION OF
LARGE SPACE STRUCTURES

Achille Messac and James Turner

The Charles Stark Draper Laboratory, Inc.
Cambridge, Massachusetts

PRECEDING PAGE BLANK NOT FILMED

Abstract

This paper proposes a new approach for solving dual structural-control optimization problems for high-order flexible space structures where reduced-order structural models are employed. For a given initial structural design, a quadratic control cost is minimized subject to a constant-mass constraint. The sensitivity of the optimal control cost with respect to the structural design variables is then determined and used to obtain successive structural redesigns using a constrained gradient optimization algorithm. This process is repeated until the constrained control cost sensitivity becomes negligible. A numerical example is presented which demonstrates that this new approach effectively addresses the problem of dual optimization for potentially very high-order structures.

I Introduction

One important variable which determines the cost of transporting a payload to orbit is its total mass. Consequently, at the structural design stage, a strong effort is made to optimize the structure for the mission at hand. Minimum mass and maximum structural eigenvalues constitute the two most frequently used structural optimization criteria (Refs. 1-7). The resulting structure is generally highly flexible and often requires active control (Refs. 8-12). As a result, subsequent to the structural design, the control engineer attempts to determine the optimal control strategy necessary to accomplish the mission.

Traditionally, the problems of optimal structural design and optimal control design are solved with little or no interaction. As a result, the "global design" is not optimal. In an effort to overcome this situation, we present in this paper a new method for simultaneously optimizing the structural and control design. A key feature of the proposed method is the use of a reduced-order model for the equations of motion. A numerical solution for the problem of optimal spacecraft slewing maneuvers of a structurally optimal spacecraft is presented.

This dual optimization problem has previously been considered by Hale (Refs. 13, 14) for problems involving simple structures. The main difficulty encountered in the formulation of Hale's algorithm is the relatively high order of the resulting non-linear two-point boundary value problem (TPBVP) which must be solved at each stage of the iterative redesign procedure; indeed the order of the resulting system is more than four times the order of the mass or stiffness matrix. Moreover, the

problems associated with handling high dimensional systems are the primary reason for the relatively limited scope of the applications of the different methods proposed to date.

The new approach we present in this paper follows a drastically different path in the derivation of the necessary conditions for the joint structural-control optimization. The problem is formulated in modal rather than physical space. As a result, the order of the TPBVP is dictated no longer by the complexity of the structure (order of the mass and stiffness matrices) but rather by the number of structural modes which participate in the dynamic excitation of the spacecraft. In most practical applications, the total number of such modes rarely exceeds a dozen.

Specifically, we seek the optimal structural design that enables the slewing maneuver and vibration suppression of the spacecraft to be performed optimally while keeping the total mass constant. The appropriate techniques for obtaining an optimal minimum-mass structure are considered in another paper (Ref. 15).

II Generic Problem Statement

We wish to determine the structural design that minimizes the following performance index

$$J = \frac{1}{2} x_f^T S(d) x_f + \frac{1}{2} \int_0^{t_f} [x^T Q(d) x + u^T R u] dt \quad (1)$$

subject to a linear time-invariant equation

$$\dot{x}(t) = A(d)x(t) + B(d)u(t) \quad (2)$$

where the total mass m_T and initial state x_0 are given. In the above equation d is the design variable vector, t_f and x_f are the final time and final state respectively, $x(t)$ is the state vector, $u(t)$ is the

control force vector, S and Q are real positive semi-definite matrices, R is a real positive definite matrix, and S , Q , and R are defined in Appendix A.

To obtain Eq. (2) we first derive the appropriate set of governing second-order ordinary differential equations of the form

$$M(d)\ddot{w}(t) + K(d)w(t) = E(d)u(t) \quad (3)$$

where $M(d)$ and $K(d)$ represent the $(N \times N)$ symmetric mass and stiffness matrices, $w(t)$ is a generalized coordinate vector for the elastic and rigid-body motions, and $E(d)$ is an $(N \times N_C)$ control influence matrix which determines the point of application of the generalized control forces numbering N_C . Equation (3) is transformed to modal coordinates by carrying out an eigenvalue analysis and normalizing the modes ϕ such that $\phi^T M \phi = I$ and $\phi^T K \phi = \Lambda$. By retaining only those modes - numbering $N_m < N$ - which significantly participate in the dynamic response of the structure, a reduced-order state space model of the form of Eq. (2) is obtained by defining

$$A = \begin{bmatrix} 0 & -\Lambda \\ I & 0 \end{bmatrix} \quad (4)$$

$$B = \begin{bmatrix} \phi^T E \\ 0 \end{bmatrix} \quad (5)$$

$$x^T = \{ \dot{\eta}^T, \eta^T \} \quad (6)$$

where A and B are of order $(2N_m \times 2N_m)$ and $(2N_m \times N_C)$ respectively, η is a vector of modal coordinates, and I is an identity matrix.

III Optimization Problem Solution

A. Optimal Control Design

The necessary conditions for an optimal control solution can be shown to satisfy (Ref. 9)

$$\begin{pmatrix} \dot{x} \\ \dot{\lambda} \end{pmatrix} = D \begin{pmatrix} x \\ \lambda \end{pmatrix} \quad (7)$$

and

$$u = -R^{-1} B^T \lambda$$

where λ is the costate vector,

$$D = \begin{bmatrix} A & -BR^{-1}B^T \\ -Q & -A^T \end{bmatrix}$$

and the boundary conditions are

$$\lambda(t_f) = Sx(t_f) \quad (9)$$

$$x(t_0) = x_0 \quad (10)$$

Through some simple manipulations it can be shown that

$$\lambda(0) = Hx_0 \quad (11)$$

where

$$H = -H_A^{-1} H_B \quad (12)$$

and

$$H_A = -S\Psi_{21} + \Psi_{22} \quad (13)$$

$$H_B = -S\Psi_{11} + \Psi_{12} \quad (14)$$

with Ψ defined as

$$\Psi = e^{Dt_f} = \begin{bmatrix} \overbrace{\Psi_{11}}^{2m} & \overbrace{\Psi_{12}}^{2m} \\ \Psi_{21} & \Psi_{22} \end{bmatrix} \begin{matrix} \} 2m \\ \} 2m \end{matrix} \quad (15)$$

Moreover, from Ref. 11, it can be shown that the cost of Eq. (1) can be written as

$$J(d) = \frac{1}{2} x_o^T H(d) x_o \quad (16)$$

B. Iterative Structural Redesigns

So far, we have determined the optimal control cost associated with a given set of design variables d . We now present the numerical scheme which is used to minimize the control cost by iteratively refining d .

We first express the constant mass requirement as $p^T d = m_T$, where d is the design variable vector, m_T the given total mass, and p a vector of structural parameters. More specifically, in terms of changes in the design variables Δd , the constant mass constraint follows as

$$p^T \Delta d = 0 \quad (17)$$

In order to establish a constrained optimization algorithm which takes into account Eq. (17), we first determine the normalized gradient vector $\alpha = -\frac{\partial J}{\partial d} / \left\| \frac{\partial J}{\partial d} \right\|$ (Appendix B) where $\|*\|$ denotes the Euclidian norm (see Figure 1). We subsequently make use of the Orthogonal Projection Theorem (Ref. 16) which states that the projection of the vector α onto the surface of constant mass represents the direction of greatest decrease in J which also satisfies Eq. (17). As a result, the desired change in the design variable vector, to within a multiplicative constant c , becomes

$$\Delta d = c \left\{ \alpha - \frac{\alpha^T p}{p^T p} p \right\} \quad (18)$$

The performance index partial derivatives are listed in Appendix B.

From a geometrical point of view, the above equation clearly states that when $\alpha^T p = \|\alpha\| \cdot \|p\|$, the gradient vector α is orthogonal to the constant-mass-constraint plane and $\Delta d = 0$; thus no further improvement can be made and a minimum has been reached (see Figure 1). On the other hand, when $\alpha^T p = 0$, the gradient vector lies in the constant mass plane and Eq. (18) requires $\Delta d = c\alpha$; thus great improvement can be made.

In order to monitor progress towards the optimum dual design, the following convergence parameter is defined:

$$\beta = \frac{|\alpha^T p|}{||\alpha|| \cdot ||p||}$$

which is equal to 0 for the worst possible design and 1 for the optimal design where $|*|$ denotes absolute value.

The constant c in Eq. (18) can be chosen in the beginning of the optimization process such that a given small fraction of the total design mass is displaced. Examination of Eq. (18) reveals the desirable property that the norm of Δd decreases monotonically as the optimal design is being approached. Once c is chosen, the following step sizes are then automatically determined. The dually optimal design is reached when the parameter β satisfies the inequality $|1-\beta| < \epsilon_1$, where ϵ_1 is user specified.

IV Illustrative Example

A. Structural Model

The example problem analyzed in this paper consists of a linear structure which has the following characteristics (see Figure 2):

- 20 extensional finite elements of equal length
- 21 nodal displacements which coincide with the lumped masses
- uniform mass density $\rho = 100 \text{ kg/m}^3$
- uniform Young's modulus $E = 800 \text{ N/m}^2$
- equal initial cross-sectional areas which constitute the design parameters (see Fig. 2)
- length $\ell = 3\text{m}$
- a control force applied to the left-most structural node (see Figure 2).

This structure has been selected because it offers two desirable features. First, in order to verify the ability of the proposed approach to optimize higher order structures through reduced-order modelling, it was deemed necessary to analyze a structure which is composed of more than 15 elements. (Clearly this objective has been met.) Second, the structure is simple enough to allow physical interpretation of the results.

B. Optimal vs. Non-Optimal Dynamic Response

In the control problem considered here, it is desired to perform a rest-to-rest maneuver where the rigid body modal displacement takes on the initial value of 30.0 and the final value of 0.0 in 2 seconds (Figure 3). As shown in Figure 3, the optimal control performance is greatly improved through successive iterative structural redesigns, where the "optimal" control design of the initial structure is contrasted to that of the final - optimal - structure. There are two salient features of the dynamic response. First, the peak values of these time-varying quantities are significantly higher in the case of the non-optimal structural design. In particular, the optimal design requires a peak control force 3.4 times lower, and the resulting elastic deflection is 3.07 and 4.96 times lower for the first and second mode, respectively. Second, the optimal dynamic responses are typically smoother in the case of the optimal structural design.

C. Control Cost Decrease

As previously stated, each step of the redesign process is responsible for a decremental change in the control cost J at each redesign stage. Figure 4 clearly depicts the expected monotonic decrease in J : 83% from the initial to final structural design in 45 iterations. Clearly, this represents a dramatic decrease in the optimal cost. At a value

of the convergence parameter β of 0.95, the optimal design was considered reached, in order to prevent the last design variable from vanishing. It is anticipated that further gains in system performance can be achieved by: i) allowing the total mass to be a design variable; ii) allowing the elements of the control weighting matrices S , Q , and R to be design variables (Appendix A); and iii) allowing the sensor and actuator locations to be design variables. However, these extensions are not considered here.

D. Consequences of Mode Shape Derivatives

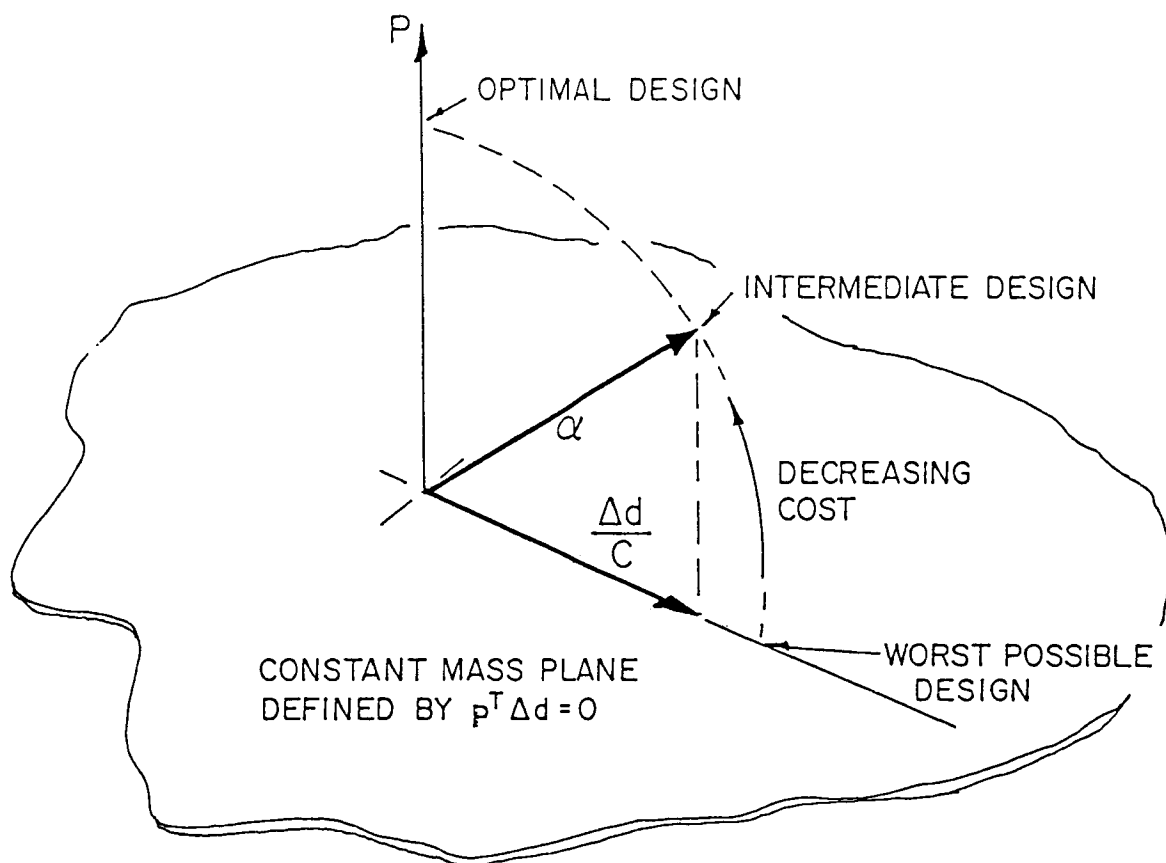
Often, in structural analyses involving the variations of eigenvalues and eigenvectors, the structural designer only accounts for the changes in the eigenvalues. While in many cases such action is acceptable, in many others the omission of the eigenvector sensitivities leads to erroneous results. Unfortunately, the problem dealt with in this paper belongs to the latter class of problems. To see this we refer to Figure 5, where we observe that the first eigenvalues which participate in the dynamic response increase (see Figure 6). Furthermore, we make the important observation that the eigenvector nodal displacements which are close to the point of application of the force decrease, while the others increase. (We recall that the force vector is applied to the left; see Figure 2.) Physically, the smaller nodal displacement at the force application point leads to reduced structural excitation (Ref. 15).

We finally note that the effect of the mode shape sensitivity is contained in the control influence coefficient matrix B (see Eq. (5)), and thus conclude that the eigenvalue derivative alone will not capture the ingredients necessary for convergence toward the global optimum.

The basic algorithm is formulated in Figure 7.

V Conclusion

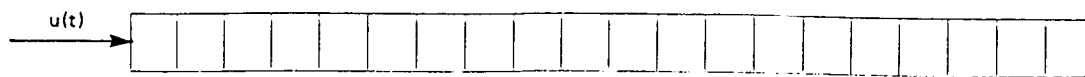
In this paper we present an approach for solving a dual structural-control problem which involves high-order structures through a reduced-order model. The validity of the theory developed is demonstrated by using a structural model of 20 finite elements. The significant findings of this paper are: i) the use of reduced-order models has a tremendous impact on the computer time required in the optimization process and may be necessary in the optimization of high-order structures; ii) the implementation of a constant mass optimization leads to a dramatic decrease in the control cost; iii) the use of mode shape derivatives is required for convergence towards the global optimum; and iv) the use of the eigenvalue and eigenvector extrapolation formulas of Appendix B makes the reduced-order model formulation a practical numerical technique (indeed, the exact eigen solution was computed only three times during the optimization process).



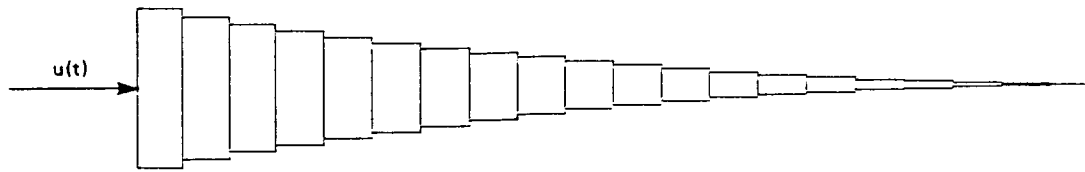
α = NEGATIVE OF NORMALIZED COST GRADIENT VECTOR

$$\Delta d = c \left(\alpha - \frac{\alpha^T p}{p^T p} p \right)$$

Figure 1. Gradient vector with respect to the constant-mass plane.



INITIAL DESIGN



FINAL DESIGN

- BOTH DESIGNS HAVE EQUAL TOTAL MASS
- $u(t)$ = CONTROL FORCE

Figure 2. Initial vs. final structural design.

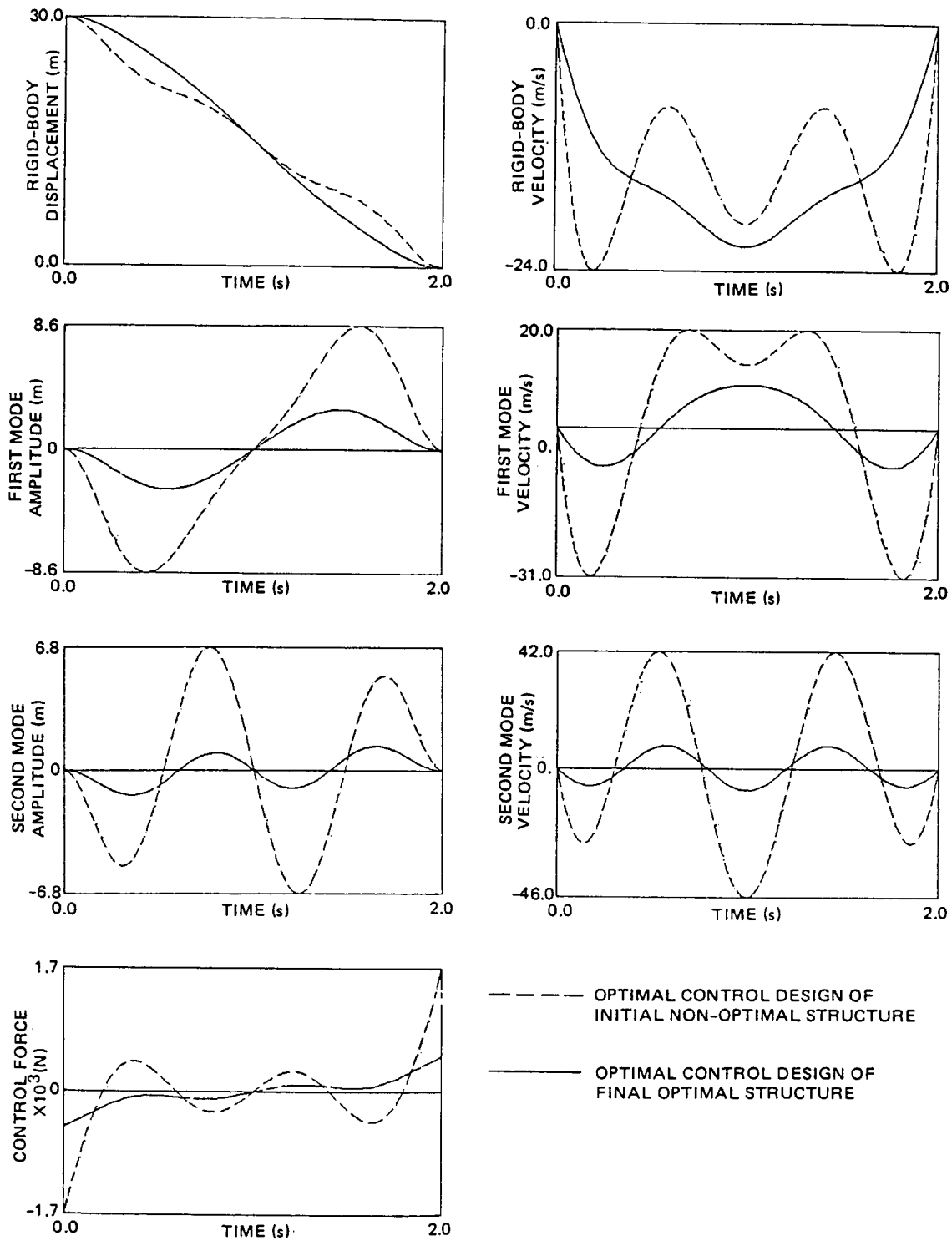


Figure 3. Optimal control design of initial vs. final (optimal) structural design.

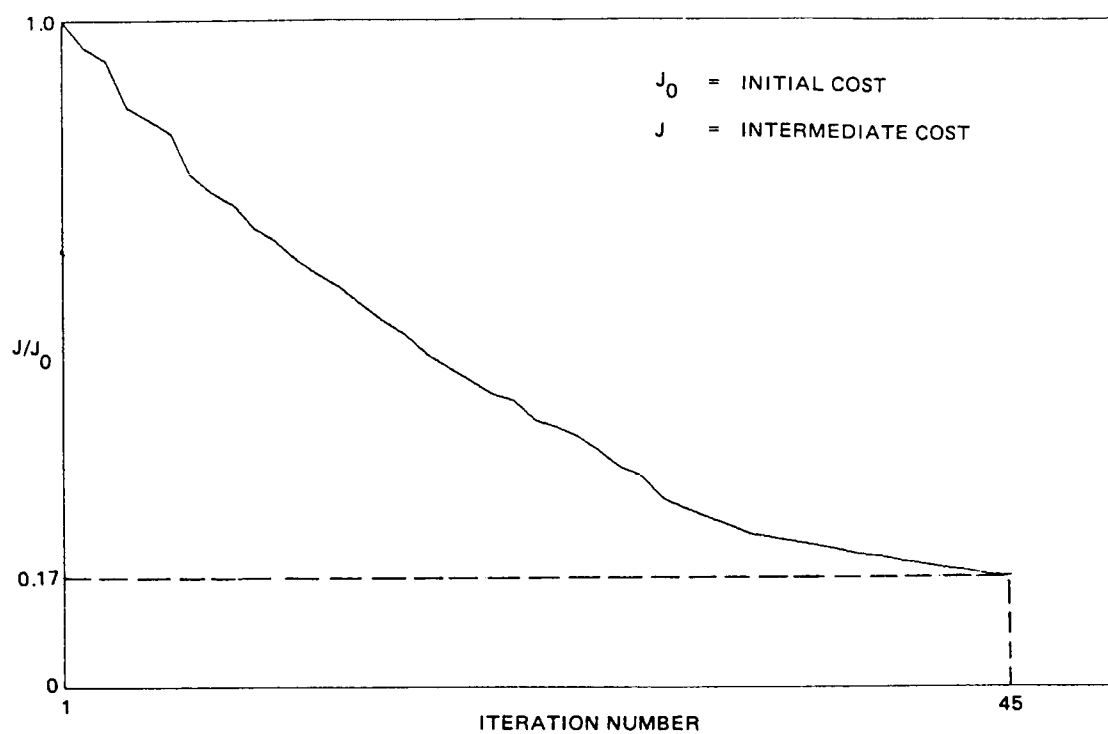
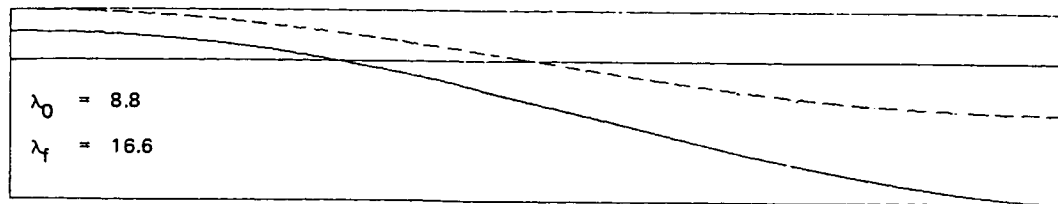
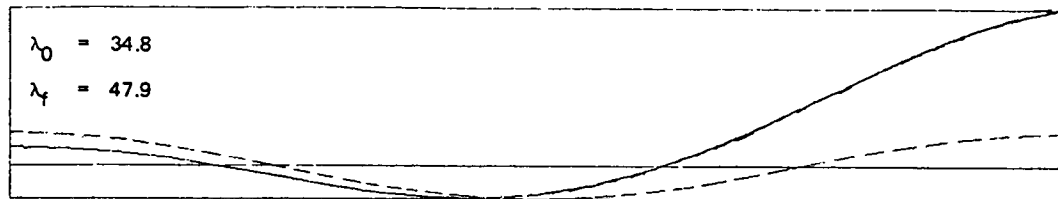


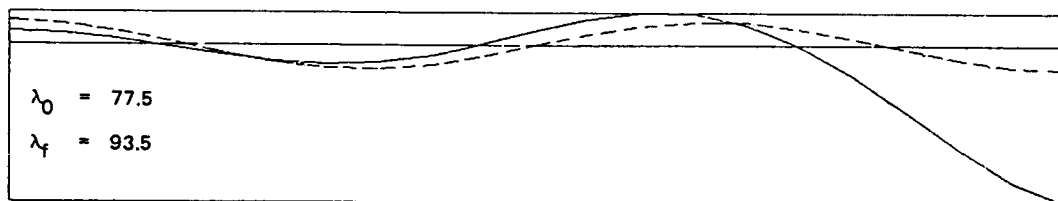
Figure 4. Monotonic decrease of optimal control cost during the "dual" optimization process.



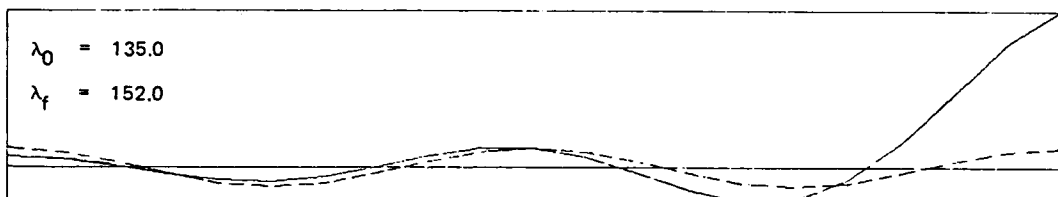
FIRST MODE



SECOND MODE



THIRD MODE



FOURTH MODE

----- INITIAL STRUCTURAL MODE SHAPE

———— FINAL OPTIMAL MODE SHAPE

λ_0 = INITIAL EIGENVALUES (rad/s)²

λ_f = FINAL EIGENVALUES (rad/s)²

The modes are normalized such that $\phi^T M \phi = 1$.

Figure 5. Initial vs. final eigenstructure.

| Structural Spectrum $(\frac{\text{rad}}{\text{s}})^2$ | | |
|---|---------|---------|
| Mode # | Initial | Optimal |
| 1 | 0.0 | 0.0 |
| 2 | 8.8 | 16.6 |
| 3 | 34.8 | 47.9 |
| 4 | 77.5 | 93.5 |
| 5 | 135.0 | 152.0 |
| 6 | 208.0 | 223.0 |
| 7 | 293.0 | 306.0 |
| 8 | 388.0 | 398.0 |
| 9 | 491.0 | 498.0 |
| 10 | 600.0 | 603.0 |
| 11 | 711.0 | 711.0 |
| 12 | 822.0 | 818.0 |
| 13 | 931.0 | 923.0 |
| 14 | 1034.0 | 1023.0 |
| 15 | 1129.0 | 1115.0 |
| 16 | 1214.0 | 1198.0 |
| 17 | 1286.0 | 1269.0 |
| 18 | 1345.0 | 1328.0 |
| 19 | 1387.0 | 1374.0 |
| 20 | 1413.0 | 1405.0 |
| 21 | 1422.0 | 1422.0 |

| Structural Designs | | |
|--------------------|---------|---------|
| Design Par. # | Initial | Optimal |
| 1 | 0.1451 | 0.405 |
| 2 | 0.1451 | 0.363 |
| 3 | 0.1451 | 0.326 |
| 4 | 0.1451 | 0.291 |
| 5 | 0.1451 | 0.258 |
| 6 | 0.1451 | 0.227 |
| 7 | 0.1451 | 0.198 |
| 8 | 0.1451 | 0.171 |
| 9 | 0.1451 | 0.146 |
| 10 | 0.1451 | 0.122 |
| 11 | 0.1451 | 0.101 |
| 12 | 0.1451 | 0.082 |
| 13 | 0.1451 | 0.065 |
| 14 | 0.1451 | 0.050 |
| 15 | 0.1451 | 0.037 |
| 16 | 0.1451 | 0.026 |
| 17 | 0.1451 | 0.017 |
| 18 | 0.1451 | 0.010 |
| 19 | 0.1451 | 0.005 |
| 20 | 0.1451 | 0.002 |

Figure 6. Structural spectrum and structural design parameters for the initial and final (optimal) design.

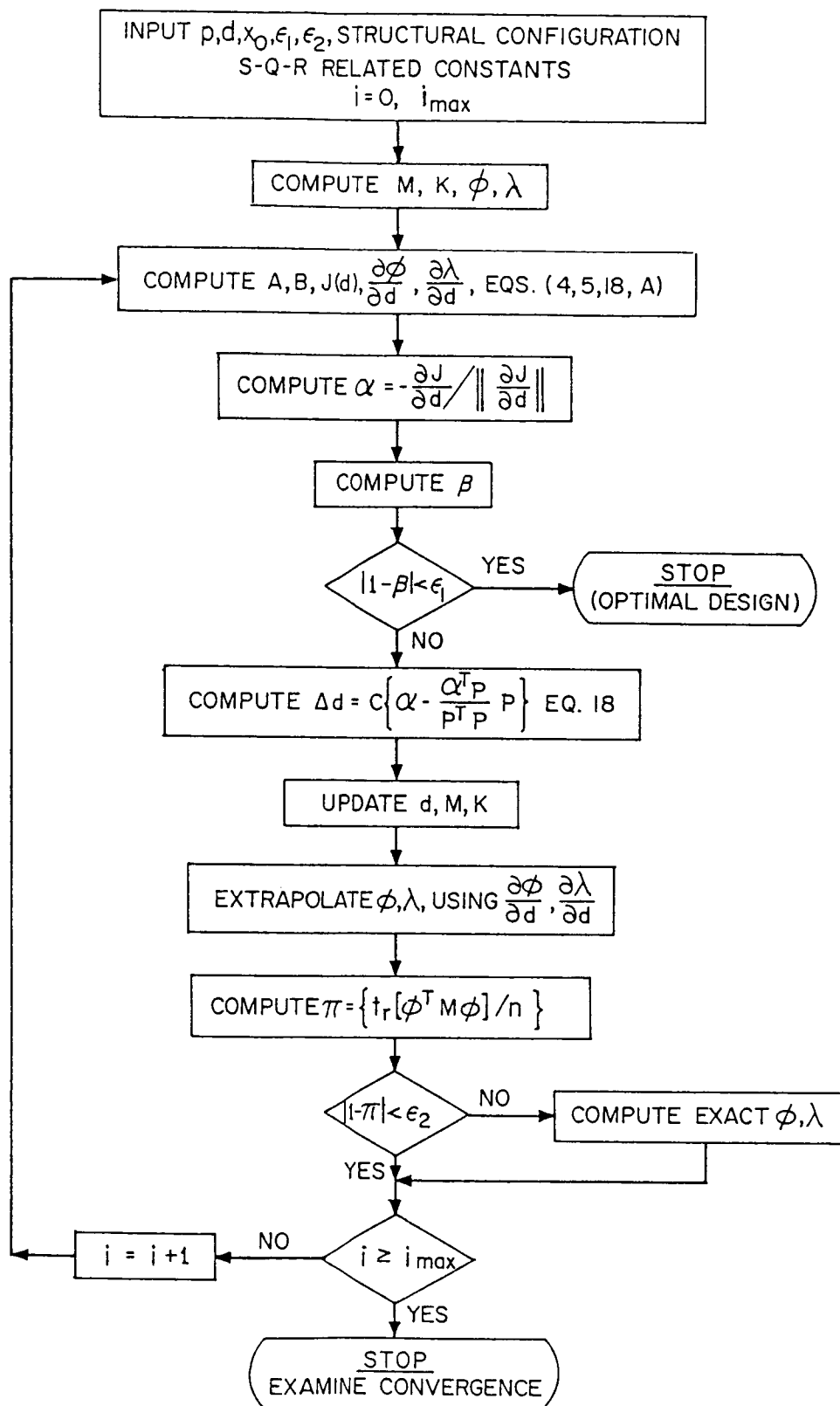


Figure 7. Differential correction algorithm.

REFERENCES

1. Pierson, B.L., "A Survey of Optimal Structural Design Under Dynamic Constraints," International Journal For Numerical Methods in Engineering, Vol. 4, pp. 491-499, 1972.
2. Sheu, C.Y., and W. Prager, "Recent Developments in Optimal Structural Design," Applied Mechanics, Rev. 21, pp. 985-992, 1968.
3. Turner, M.J., "Design of Minimum-Mass Structures With Specified Natural Frequencies," AIAA Journal, 5, pp. 406-412, 1967.
4. McIntosh, S.C., and F.E. Eastep, "Design of Minimum-Mass Structure With Specified Stiffness Properties," Vol. 6, No. 5, AIAA Journal, pp. 962-964, 1968.
5. Bellagamba, L., and T.Y. Yang, "Minimum-Mass Truss Structure With Constraints on Fundamental Natural Frequency," Vol. 19, No. 11, AIAA Journal, pp. 1452-1458 (AIAA 81-4295).
6. Carmichael, D.G., "Structural Modelling and Optimization," Ellis Horwood, Ltd., Halsted Press: a division of John Wiley & Sons, 1981.
7. Morris, A.J., Editor, "Foundations of Structural Optimization: A Unified Approach," John Wiley & Sons, Ltd., 1982.
8. Turner, J.D., and H.M. Chun, "Optimal Feedback Control of a Flexible Spacecraft During a Large Angle Rotational Maneuver," presented as Paper No. 82-1589 at the AIAA Guidance and Control Conference, San Diego, CA, August 9-12, 1982.
9. Turner, J.D., and H.M. Chun, "Optimal Distributed Control of a Flexible Spacecraft Using Control Rate Penalties in the Controller Design," presented as Paper No. 82-1438 at the AIAA Guidance and Control Conference, San Diego, CA, August 9-12, 1982.
10. Kirk, D.E., "Optimal Control Theory, An Introduction," Prentice-Hall, Inc., 1970.
11. Kwakernaak, H., and R. Sivan, "Linear Optimal Control Systems," John Wiley & Sons, Inc., 1972.
12. Meirovitch, L., and H. Oz, "Modal-Space Control of Distributed Gyroscopic Systems," Journal of Guidance and Control, Vol. 3, No. 2, pp. 140-150, 1980.

13. Hale, A.L., R.J. Lisowski, and W.E. Dahl, "Optimizing Both the Structure and the Control of Maneuvering Flexible Spacecraft," presented as Paper No. 83-377 at the AAS/AIAA Astrodynamics Specialist Conference, Lake Placid, NY, August 22-25, 1983.
14. Hale, A.L., and R.J. Lisowski, "Optimal Simultaneous Structural and Control Design of Maneuvering Flexible Spacecraft," presented at the Fourth VPI & SU/AIAA Symposium on Dynamics and Control of Large Space Structures, Blacksburg, VA, June 6-8, 1983.
15. Messac, A., J. Turner, "Optimal Minimum-Mass Structural-Control Design of Large Space Structures," AIAA Specialist Dynamics Conference, Palm Springs, CA, May 17 & 18, 1984.
16. Brogan, B.R., "Modern Control Theory," Quantum Publishers, Inc., 1974.
17. Brewer, W.J., "Kronecker Products and Matrix Calculus in System Theory," IEEE Transactions on Circuits, Vol. CAS-25, No. 9, pp. 772-781, September 1978.
18. Fox, R.L., and M.P. Kapoor, "Rate of Change of Eigenvalues and Eigenvectors," AIAA Journal, Vol. 6, No. 12, PP. 2426-2429, December 1968.
19. Nelson, B.R., "Simplified Calculation of Eigenvector Derivatives," AIAA Journal, Vol. 14, No. 9, pp. 1201-1205, September 1976.

APPENDIX A

CONTROL PENALTY MATRICES S, Q, AND R

The matrices S, Q, and R define the weights imposed on the final state, the intermediate states, and the control, respectively (see Eq. (1)).

Motivated by the desire to minimize the sum of the square of the physical nodal displacements and velocities, we write

$$\begin{aligned} \mathbf{w}^T \mathbf{w} &\approx (\phi \eta)^T (\phi \eta) \\ &\approx \eta^T [\phi^T \phi] \eta \end{aligned} \tag{A-1}$$

where modal truncation has already taken place, \mathbf{w} is defined by Eq. (3), and

$$\dot{\mathbf{w}}^T \dot{\mathbf{w}} \approx \dot{\eta}^T [\phi^T \phi] \dot{\eta} \tag{A-2}$$

We further let

$$\Theta = [\phi^T \phi]$$

and recall that

$$\mathbf{x}^T = \{ \dot{\eta}^T, \eta^T \} \tag{A-3}$$

As a result, the form of the matrix Q which has resulted in desirable dynamic responses is given by

$$Q = \begin{bmatrix} \theta_1 & 0 \\ 0 & \theta_2 \end{bmatrix} \quad (A-4)$$

where

$$[\theta_1]_{ij} = \begin{cases} 5[\theta]_{ij} & \text{for any } i \text{ or } j = 1 \text{ (rigid-body velocity)} \\ 0.1[\theta]_{ij} & \text{for any } i \text{ or } j > 1 \text{ (flexible-body velocity)} \end{cases}$$

$$[\theta_2]_{ij} = \begin{cases} [\theta]_{ij} & \text{for any } i \text{ or } j = 1 \text{ (rigid-body displacement)} \\ 0.01[\theta]_{ij} & \text{for any } i \text{ or } j \text{ greater than } 2 \text{ (flexible-body displacement)} \end{cases}$$

and $[\theta]_{ij}$ denotes the ij -th element of " θ ". The matrix S was chosen to be equal to 10^9 times the matrix Q . Finally, the control penalty matrix has one entry equal to 0.5.

APPENDIX B

PERFORMANCE INDEX GRADIENT

The partial derivatives of $J(d)$ in Eq. (16) with respect to the i -th design variable follow as

$$\partial J / \partial d_i = (1/2) x_0^T (\partial H / \partial d_i) x_0 \quad (B-1)$$

where

$$\partial H / \partial d_i = H_A^{-1} (\partial H_A / \partial d_i) H_A^{-1} H_B - H_A^{-1} (\partial H_B / \partial d_i) \quad (B-2)$$

$$\partial H_A / \partial d_i = -(\partial S / \partial d_i) \Psi_{21} - S(\partial \Psi_{21} / \partial d_i) + \partial \Psi_{22} / \partial d_i \quad (B-3)$$

$$\partial H_B / \partial d_i = -(\partial S / \partial d_i) \Psi_{11} - S(\partial \Psi_{11} / \partial d_i) + \partial \Psi_{12} / \partial d_i \quad (B-4)$$

The partial derivatives for the state transition matrix of Eq. (15) with respect to the i -th design variable can be expressed as (Ref. 17)

$$\partial \Psi / \partial d_i = e^{\Gamma} \int_0^1 e^{-\Gamma \sigma} [\partial \Gamma / \partial d_i] e^{\Gamma \sigma} d\sigma \quad (B-5)$$

$$= \begin{bmatrix} \partial \Psi_{11} / \partial d_i & \partial \Psi_{12} / \partial d_i \\ \partial \Psi_{21} / \partial d_i & \partial \Psi_{22} / \partial d_i \end{bmatrix} \begin{matrix} \} 2 N_m \\ \} 2 N_m \end{matrix}$$

$\underbrace{\hspace{4em}}$
 $2 N_m$

$\underbrace{\hspace{4em}}$
 $2 N_m$

where

$$\partial \Gamma / \partial d_i = \begin{bmatrix} \partial(A t_f) / \partial d_i & -\partial(B R^{-1} B^T t_f) / \partial d_i \\ -\partial(Q t_f) / \partial d_i & -\partial(A^T t_f) / \partial d_i \end{bmatrix} \quad (B-6)$$

and

$$\Gamma = D t_f$$

$$\partial A / \partial d_i = \begin{bmatrix} 0 & -\partial \Lambda / \partial d_i \\ 0 & 0 \end{bmatrix} \quad (B-7)$$

$$\partial B / \partial d_i = \begin{bmatrix} \partial(\phi^T E) / \partial d_i \\ 0 \end{bmatrix} \quad (B-8)$$

It is understood that the chain rule is to be applied to produce the appropriate expressions in Eqs. (B-6) and (B-8).

The structural eigenvalue and eigenvector partials required in Eqs. (B-6 - B-8) follow as (Ref. 18)

$$\partial \lambda_j / \partial d_i = \underline{\phi}_j^T [\partial K / \partial d_i - \lambda_j (\partial M / \partial d_i)] \underline{\phi}_j \quad (B-9)$$

$$\partial \underline{\phi}_j / \partial d_i = \sum_{\substack{k=1 \\ k \neq j}}^n a_{k \rightarrow k} \underline{\phi}_k + a_{j \rightarrow j} \underline{\phi}_j \quad (B-10)$$

$$a_r = \begin{cases} \frac{\phi_r^T}{\lambda_r} \left[\partial K / \partial d_i - \lambda_k (\partial M / \partial d_i) \right] \frac{\phi_k}{(\lambda_k - \lambda_r)} , & r \neq k \\ \frac{\phi_r^T}{\lambda_r} \left[\partial M / \partial d_i \right] \phi_r / 2 , & r = k \end{cases} \quad (B-11)$$

Since the calculation of the structural eigen solution and associated partials is costly, we use the following analytic continuation formulas for extrapolating these important quantities.

$$\lambda_j(d + \Delta d) \approx \lambda_j(d) + \sum_{j=1}^n (\partial \lambda_j / \partial d_i) \Delta d_j \quad (B-12)$$

$$\phi_j(d + \Delta d) \approx \phi_j(d) + \sum_{j=1}^n (\partial \phi_j / \partial d_i) \Delta d_j \quad (B-13)$$

where Δd is the current differential correction vector for the design variables. The partial derivatives of λ_j and ϕ_j are then produced by substituting the results of Eqs. (B-12) and (B-13) into Eqs. (B-9) through (B-11). In order to monitor the validity of the first-order extrapolation formulas above we test the following inequality:

$$\left| \text{TRACE} (\phi^T M \phi) / N_m - 1 \right| = \begin{cases} < \epsilon_2 & \text{use Eqs. (B-12) and (B-13)} \\ \geq \epsilon_2 & \text{compute the exact solution for } \phi \text{ and } \lambda \end{cases}$$

where ϵ_2 is user specified.

STATE TRANSITION MATRIX SENSITIVITY CALCULATION

To efficiently compute the state transition matrix partial derivatives of Eq. (B-5), we first express the matrix $\Gamma = Dt_f$ in terms of the following right and left eigenvector description:

$$\Gamma R = R\gamma, \quad \Gamma^T L = L\gamma, \quad L^T R = I \quad (B-14)$$

$$\Gamma = R\gamma L^T$$

where R and L denote the right and left modal matrices, respectively, leading to

$$e^{\Gamma\sigma} = R e^{\gamma\sigma} L^T \quad (B-15)$$

$$e^{-\Gamma\sigma} = R e^{-\gamma\sigma} L^T \quad (B-16)$$

Introducing the expressions above into Eq. (B-5) we find

$$\partial\Psi/\partial d_i = R e^{\Gamma} H_i L^T \quad (B-17)$$

where

$$H_i = \int_0^1 e^{-\gamma\sigma} G_i e^{\gamma\sigma} d\sigma \quad (B-18)$$

$$G_i = L^T (\partial\Gamma/\partial d_i) R \quad (B-19)$$

The pq-th term of Eq. (B-18) can further be written as

$$[H_i]_{pq} = \int_0^1 [G_i]_{pq} e^{(\gamma_q - \gamma_p)\sigma} d\sigma \quad (B-20)$$

or, upon carrying out the integral above analytically we find

$$[H_i]_{pq} = \begin{cases} [G_i]_{pq} (e^{(\gamma_q - \gamma_p)} - 1) / (\gamma_q - \gamma_p) & , \quad q \neq p \\ [G_i]_{pq} & , \quad q = p \end{cases} \quad (B-21)$$

The important feature of the calculation above is that one set of right and left eigenvectors produces the sensitivity partials for all the design variables.

N87-11767

STRUCTURAL OPTIMIZATION WITH CONSTRAINTS
ON TRANSIENTS RESPONSE

Robert Reiss
Howard University
Washington, D.C. 20059

BACKGROUND

An exceptionally elegant method for structural optimization with constraints on the static response has been presented by Shield and Prager (ref. 1). Their derivation of the optimality condition was facilitated by a reformulation of the structural elasticity equations in terms of what was then a new variational principle, the principle of stationary mutual potential energy. Their optimality condition relates the design variable to an appropriately defined "mutual strain energy." An alternative but related approach, based upon the principle of stationary mutual complementary energy, was presented by N.C. Huang (ref. 2).

The simplicity of these principles lies in the facts that the energy functionals are stationary at the solution to the field equations and that their stationary value is proportional to the quantity to be optimized.

PRINCIPLE OF STATIONARY MUTUAL POTENTIAL ENERGY

The mutual potential energy functional ϕ is expressed in Eq. (1) for a beam in flexure. Here u and \bar{u} are deflections, $p(x)$ and $\bar{p}(x)$ are distributed loads, and $S(x)$ is the bending stiffness. The displacements \bar{u} and u are required only to be kinematically admissible. Under these conditions, ϕ is stationary over all admissible u and \bar{u} if and only if u and \bar{u} are the true deflections under p and \bar{p} , respectively.

If \bar{p} is a unit point load centered at $x=y$, then the stationary value of ϕ is proportional to $u(y)$. The stationary condition for u over all admissible designs S is, therefore, also the stationary condition for ϕ .

$$\phi \{ u, \bar{u} ; S \} = \frac{1}{2} \int S u'' \bar{u}'' dx - \frac{1}{2} \int (p \bar{u} + \bar{p} u) dx \quad (1)$$

$$\delta \phi = 0 \iff \text{field equations}$$

$$\delta \phi = 0, \bar{p} = \delta(x-y) \Rightarrow u(y) = -2\phi$$

$$\delta_S u = 0 \iff \delta_S \phi = 0$$

PRINCIPLE OF STATIONARY MUTUAL COMPLEMENTARY ENERGY

The mutual complementary energy ψ is defined in Eq.(2) for a beam with bending stiffness $S(x)$. Here, M and \bar{M} are bending moments statically admissible with the loads p and \bar{p} , respectively. The principle of stationary mutual complementary energy states that ψ is stationary if and only if M and \bar{M} are the true bending moments corresponding to the loads p and \bar{p} .

Again, if \bar{p} is a unit concentrated force acting at $x=y$, then the stationary value of ψ is $1/2 u(y)$. Once again, therefore, the condition that $u(y)$ is stationary over all designs S is also the stationary condition for ψ

$$\psi \{M, \bar{M}; S\} = \frac{1}{2} \int S^{-1} M \bar{M} dx \quad (2)$$

$$\delta\psi = 0 \iff \text{field equations}$$

$$\delta\psi = 0, \bar{p} = \delta(x-y) \implies u(y) = 2\psi$$

$$\delta_S u = 0 \iff \delta_S \psi = 0$$

A STATIONARY FUNCTIONAL OF DISPLACEMENTS

The energy-like functional (3) is written specifically for a vibrating rod fixed at $x=0$ and acted upon by tip forces $F(t)$ and $\bar{F}(t)$. Here, u and \bar{u} are the respective kinematically admissible axial displacements, $S(x)$ is the cross-sectional area, u' and \dot{u} are, respectively, the spatial and temporal derivatives of the axial displacement, and c is the wave speed of propagation. The symbol $*$ denotes the convolution integral in time.

If the rod is initially at rest, then ϕ is stationary if and only if u and \bar{u} are the actual displacements induced by the tip forces F and \bar{F} , respectively. Furthermore, if \bar{F} is the unit impulse force, then the stationary value of the functional ϕ is proportional to the tip displacement $u(L,t)$.

It should be observed that for the special case $u = \bar{u}$, ϕ reduces to Gurtin's functional (ref. 3) which is the transient counterpart to the principle of stationary potential energy.

$$2\phi = \int S u' * \bar{u}' dx + c^{-2} \int S \dot{u} * \dot{\bar{u}} dx - F(t) * \bar{u}(L,t) - \bar{F}(t) * u(L,t) \quad (3)$$

$$\delta\phi = 0 \iff \text{field equations}$$

$$\delta\phi = 0, \bar{F}(t) = \delta(t) \implies u(L,t) = -2\phi$$

$$\delta_S u(L,t) = 0 \iff \delta_S \phi = 0$$

A STATIONARY FUNCTIONAL OF STRESSES

Analogous to the mutual complementary energy functional, Ψ (Eq. (4)) is also a functional of the generalized stresses, which are, for rods, the axial forces N and \bar{N} . Unlike the foregoing, however, these generalized stresses are not required to meet any field equations of constraint; they must only be compatible with the static boundary conditions, that is, $N(L,t) = F(t)$ and $\bar{N}(L,t) = \bar{F}(t)$. It may easily be shown that Ψ is stationary if and only if N and \bar{N} are the true axial forces due to the tip forces F and \bar{F} , respectively.

Moreover, if \bar{F} is the unit impulse force, then the stationary value of Ψ is exactly half of the tip displacement $u(L,t)$.

$$2\Psi = \int s^{-1} \{ c^2 g * N' * \bar{N}' + N * \bar{N} \} dx \quad (4)$$

$$g(t) \equiv t$$

$$\delta\Psi = 0 \iff \text{field equations}$$

$$\delta\Psi = 0, \bar{F}(t) = \delta(t) \implies u(L,t) = 2\Psi$$

$$\delta_S u(L,t) = 0 \iff \delta_S \Psi = 0$$

DESIGN DERIVATIVE OF THE RESPONSE: APPLICATION OF VARIATIONAL PRINCIPLES

Since the stationary value of the functionals Φ and Ψ is proportional to the response u , the variation $\delta_S u$ induced by the small design change δS is obtained by treating Φ and Ψ as explicit functionals of the axial stiffness S . The power of this formulation is that the implicit dependence of the functionals on S through the kinematic arguments (Eq. (3)) or static arguments (Eq. (4)) is necessarily ignored.

In Eq.(5), \bar{u} is the axial response due to a unit impulse force applied to the tip of the rod. Likewise, in Eq.(6), \bar{N} is the axial force due to the same impulsive force. Equations (5) and (6) provide alternative explicit representations for the variation of the response in terms of the variation in axial stiffness.

$$\begin{aligned}\delta_S u &= - 2 \delta_S \Phi(u, \bar{u}; S) \\ &= - \int \{ u' \bar{u}' + c^{-2} \dot{u} \dot{\bar{u}} \} \delta S dx\end{aligned}\tag{5}$$

$$\begin{aligned}\delta_S u &= 2 \delta_S \Psi(N, \bar{N}; S) \\ &= - \int S^{-2} \{ c^2 g_{*N}' \bar{N}' + N \bar{N} \} \delta S dx\end{aligned}\tag{6}$$

DESIGN DERIVATIVE OF THE RESPONSE:
APPLICATION OF GREEN'S FUNCTIONAL

To the extent that Green's function is stiffness dependent, it is a functional of the design. In what follows, $G(x,y,t;S)$ is the response of a bar with axial stiffness $S(x)$ to a unit impulse force $\delta(t)$ applied at the location $x=y$. Assuming the bar is initially at rest, G satisfies Eq. (7a) and boundary conditions (7b). The displacement $u(y,t)$, due to a driving force $F(t)$ applied to the tip of the rod, is given by Eq. (8).

It is evident, upon taking the variation of u with respect to the stiffness (Eq. (9)), that $\delta_S u$ is known if $\delta_S G$ is known. The latter can be explicitly found by convoluting the variation of the field equation (7a) with G and integrating the result by parts over the entire beam. The result, which is expressed in (10), is substituted into (9) to obtain (11). Apart from notational differences, Eqs. (11) and (5) are identical.

$$g * (SG')' - c^{-2}SG = -g\delta(x-y) \quad (7a)$$

$$G(0,y,t;S) = 0 \quad (7b)$$

$$S(L)G'(L,y,t;S) = 0$$

$$u(y,t) = F * G(L,y,t;S) \quad (8)$$

$$\delta_S u(y,t) = F * \delta_S G(L,y,t;S) \quad (9)$$

$$\begin{aligned} \delta G(y,Z) = - \int \{ G'(x,z,t;S) * G'(x,y,t;S) + \\ + c^{-2} \dot{G}(x,z,t;S) * \dot{G}(x,y,t;S) \} \delta S(x) dx \end{aligned} \quad (10)$$

$$\delta u = - \int [G' * u' + c^{-2} \dot{G} * \dot{u}] \delta S dx \quad (11)$$

OPTIMALITY CRITERION

Now that the response variation is known explicitly in terms of the design variable (Eq. (11)), it is a straightforward matter to develop conditions of optimality. For example, if T is the time at the maximum tip deflection, then the necessary condition for the tip deflection $u(L,T)$ to be a minimum for a specified total mass (12) is given by (13). Similarly, if the mean square tip deflection during the time interval $0 < t < T$ is identified as the cost functional (14), then the optimality condition is given by equation (15). The constants μ and ν appearing in (13) and (15), respectively, are Lagrange multipliers which are determined from the specified total mass condition.

It is obvious that finding an exact solution to the optimality condition (13) and field equations for the transient response of a rod initially at rest to a tip force $F(t)$ is extremely difficult. However, for the special case of an instantaneously applied constant force (16), it can be shown that the optimum design is a uniform one, which incidentally is also the optimum design for the corresponding static problem.

$$\delta \int S(x) dx = 0 \quad (12)$$

$$c^{-2} \dot{G}(x,L,T) * \dot{u}(x,T) + G'(x,L,T) * u'(x,T) = \mu \quad (13)$$

$$\delta \int_0^T u^2(L,t) dt = 0 \quad (14)$$

$$\int_0^T u(L,t) \{ c^{-2} \dot{G}(x,L,t) * \dot{u}(x,t) + G'(x,L,t) * u'(x,t) \} dt = \nu \quad (15)$$

$$\begin{aligned} F(t) &= 0 & t < 0 \\ &= F & t \geq 0 \end{aligned} \quad (16)$$

ABSTRACT LINEAR STRUCTURAL DYNAMICS

Let u, σ and ϵ denote, respectively, the displacement, generalized stress and generalized strain of a rod, beam, frame, plate or shell structure. Then the field equations can be symbolically written in the form (17). Here T and T^* are adjoint linear operators, $E(S)$ a linear stiffness operator and $M(S)$ a linear mass operator. Adjoined to (17) are mixed boundary conditions (18), where B, B^*, γ and γ^* are appropriately defined linear operators. Specific examples as well as a detailed discussion of these operators can be found in Refs. 4 and 5. In (18), $\partial\Omega_1$ and $\partial\Omega_2$ are complementary subsets of the boundary of the structure.

It can be shown that the design derivative $\delta_S u$ is given by (19) where (\cdot, \cdot) denotes the bilinear form which is an L_2 inner product in the spatial variable and a convolution integral in time. Also, G is the Green's function for the structure. Equation (19) may be used as the starting point in the development of optimality conditions for transient problems.

$$\begin{aligned} Tu &= \epsilon && \text{strain - displacement} \\ E\epsilon &= \sigma && \text{stress - strain} \\ T^*\sigma + M\ddot{u} &= p && \text{equation of motion} \end{aligned} \tag{17}$$

$$\begin{aligned} B\gamma u &= g && \text{on } \partial\Omega_1 \times [0, \infty) \\ B^*\gamma^*ETu &= h && \text{on } \partial\Omega_2 \times [0, \infty) \end{aligned} \tag{18}$$

$$\begin{aligned} \delta_S u &= - (T u, \frac{\partial E}{\partial S} \delta S T G) \\ &\quad - (\dot{u}, \frac{\partial M}{\partial S} \delta S \dot{G}) \end{aligned} \tag{19}$$

REFERENCES

1. Shield, R.T.; and Prager, W.: Optimal Structural Design for Given Deflection. ZAMP, vol. 21, 1970, pp. 513-523.
2. Huang, N.C.: On the Principle of Stationary Mutual Complementary Energy and Its Applications to Structural Design. ZAMP, vol. 22, 1971, pp. 608-620.
3. Gurtin, M.E.: Variational Principles for Linear Elastodynamics. Archive, Rational Mechanics and Analysis, vol. 16, 1964, pp. 34-50.
4. Oden, J.T. ; and Reddy, J.N.: Variational Methods in Theoretical Mechanics. Springer-Verlag, Berlin, 1976.
5. Reiss, R.: and Haug, E.J.: Extremum Principles for Linear Initial-Value Problems of Mathematical Physics. Int. J. Engrg. Sci., vol. 16, 1978, pp. 231-250.

C-4

N87 - 11768

OPTIMIZATION APPLICATIONS IN AIRCRAFT ENGINE DESIGN AND TEST

**T. K. Pratt
Pratt & Whitney Engineering Division
United Technologies Corporation
E. Hartford, CT 06108**

PRECEDING PAGE BLANK NOT FILMED

OPTIMIZATION APPLICATIONS SUPPORT MANY MULTIDISCIPLINARY PROJECTS THROUGHOUT UTC

As shown in Figure 1, optimization projects have been undertaken throughout UTC for many years. The first major effort at Pratt & Whitney Engineering Division - Connecticut Operations (PWEDCO) has been the ongoing STAEBL (Structural Tailoring of Engine BLades) program, sponsored by NASA since 1980 [1, 2]. Phase 1 demonstrated the structural optimization of two fan blades of advanced construction for minimum weight and cost. Among the multidisciplinary spin-offs from the STAEBL program are the structural optimization of compressor blades, rotor cases and shafts, and the aerodynamic optimization of compressor blades. As a result of interdivisional symposia, joint optimization efforts such as the aerodynamic optimization of turbo-prop blades at Hamilton Standard (HSD), helicopter rotor blades at United Technologies Research Center (UTRC), and flexbeams and twin lift spreader bars at Sikorsky were supported at other UTC divisions.

Optimization techniques have also been applied to the interactive evaluation of test data. Real-time compressor vane optimization programs were developed for rig testing at Pratt & Whitney Engineering Division - Florida Operations (PWEDFO) [3], and later applied to both engine and rig testing at PWEDCO.

Current and projected efforts include the STAT (Structural Tailoring of Advanced Turboprops) program sponsored by NASA, preliminary engine design, and the optimization of manufacturing facilities.

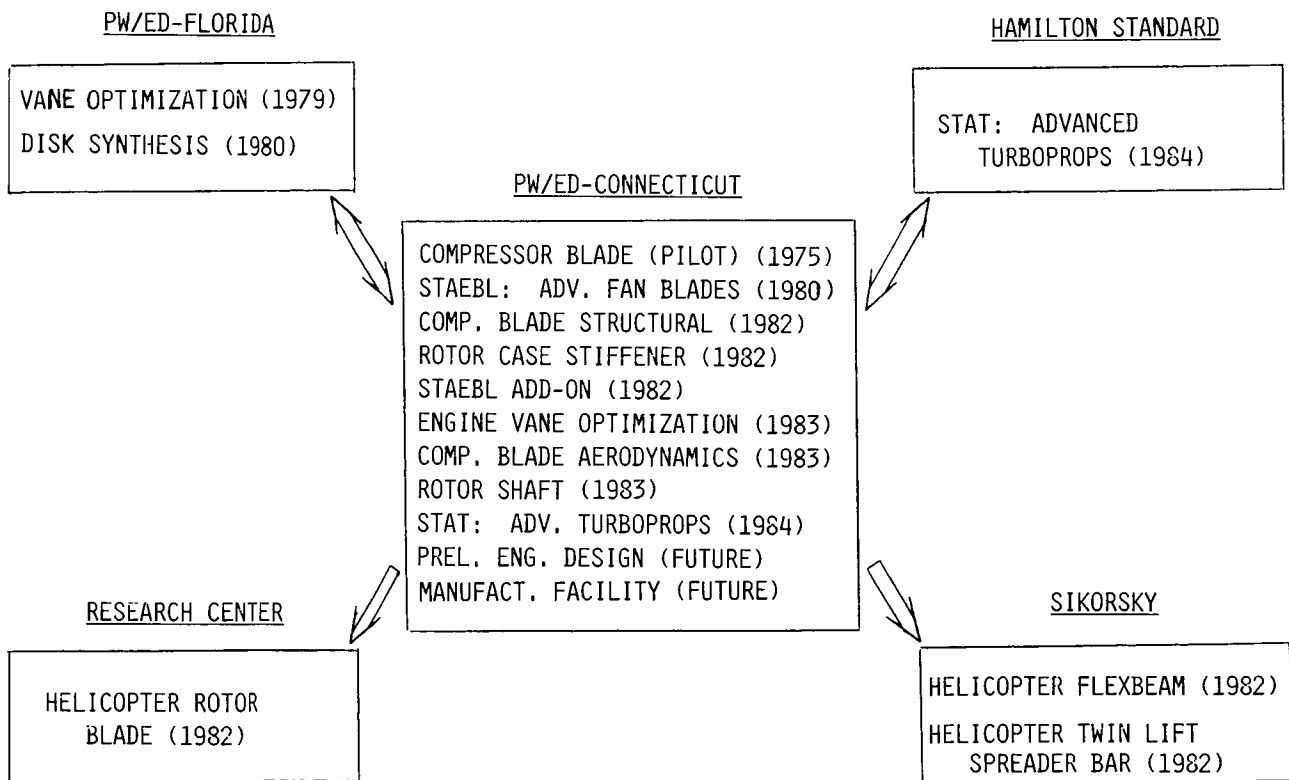
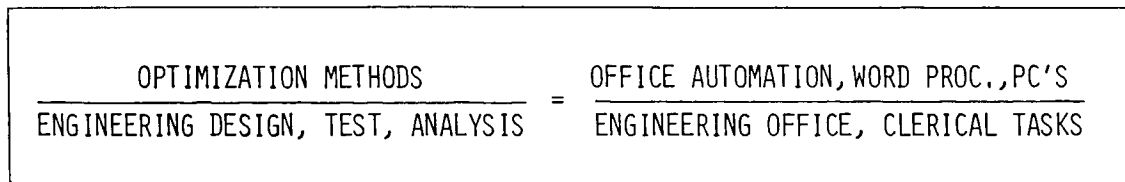


Figure 1

OPTIMIZATION METHODS INCREASE ENGINEERING SOPHISTICATION AND EFFICIENCY

Productivity and efficiency are of paramount importance in today's increasingly competitive engineering and manufacturing environments. With the advent of word processors, personal computers, and electronic networking, many repetitive engineering office and clerical tasks are being automated. In an analogous fashion many difficult but repetitive engineering design, testing, and analytical tasks are also being automated and optimized using commercially available hardware and software programs. In addition to increasing efficiency, optimization programs are especially useful for design improvement since more design variables, trade-off studies, and sophisticated analyses can be incorporated into the design process.

The automation of these engineering procedures has been made possible by the widespread use of CAD (Computer Aided Design) techniques in which the computer provides rapid analyses of proposed designs and the design engineer makes the trade-off decisions. As shown in Figure 2, a logical extension of CAD is fully automated design in which the computer also makes the design decisions. In automated optimal design, the task is twofold: first, find a feasible design, and second, determine an optimal design. With computer power improving every year, it is now possible to use these automated optimization procedures to produce correct designs the first time.



- OPTIMIZATION CAN BE THOUGHT OF AS "DESIGN IMPROVEMENT":
CAD → AUTOMATED DESIGN → AUTOMATED OPTIMAL DESIGN
- IDEALLY, OPTIMIZATION TECHNIQUES SHOULD AUTOMATICALLY BE
PART OF ENGINEERING DESIGN, TESTING, AND ANALYTICAL PROCEDURES

Figure 2

METHOD OF FEASIBLE DIRECTIONS DETERMINES SOLUTION OF CONSTRAINED MINIMIZATION PROBLEM

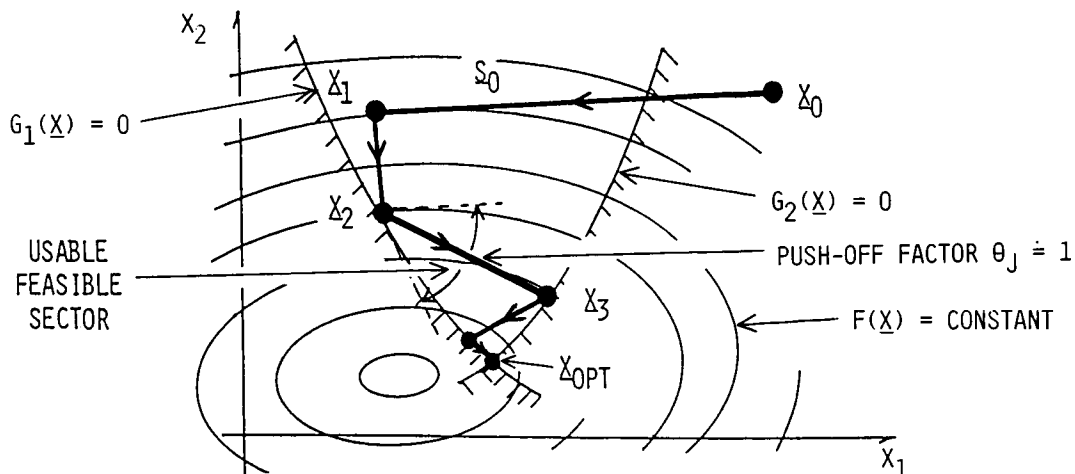
All the optimization problems in Figure 1 were formulated as the following type of nonlinear constrained minimization problem: determine design variables $\underline{x} = (x_1, \dots, x_n)$ which minimize the objective function $f(\underline{x})$ while satisfying constraints $g_i(\underline{x}) < 0, i = 1, \dots, m$. This problem can be solved directly using the method of feasible directions by generating a sequence of one-dimensional line searches, $x_{i+1} = x_i + \alpha s_i, i = 1, \dots, p$, as shown in Figure 3. For reasonably smooth functions, the sequence $[x_i]$ converges to x_{opt} , provided an optimal feasible solution exists. The push-off factor θ_j is used in conjunction with Zoutendijk's method [4] to determine the orientation of the new search direction s_i within the usable feasible sector (i.e., the union of all search vectors that reduce the objective function without violating any currently active constraints).

COPES/CONMIN (Control Program for Engineering Synthesis/CONstrained MINimization) [5, 6] is a very versatile, robust, and widely distributed program, developed under NASA sponsorship by Dr. G. N. Vanderplaats (Naval Postgraduate School), that has been used to solve constrained and unconstrained minimization problems for many practical applications involving continuous functions as well as discrete test data. Recently, Dr. Vanderplaats has developed the ADS (Automated Design Synthesis) [7] general purpose optimization package to permit the user to choose from among a broad spectrum of optimization algorithms (including CONMIN and a generalized reduced gradient method).

MINIMIZE $F(\underline{X})$

SUCH THAT $G_I(\underline{X}) \leq 0, I = 1, \dots, M$

$$\underline{X}_{I+1} = \underline{X}_I + \alpha \underline{S}_I, I = 0, 1, \dots, P$$



● COPES/CONMIN AND ADS PROGRAMS (DR. G. N. VANDERPLAATS)

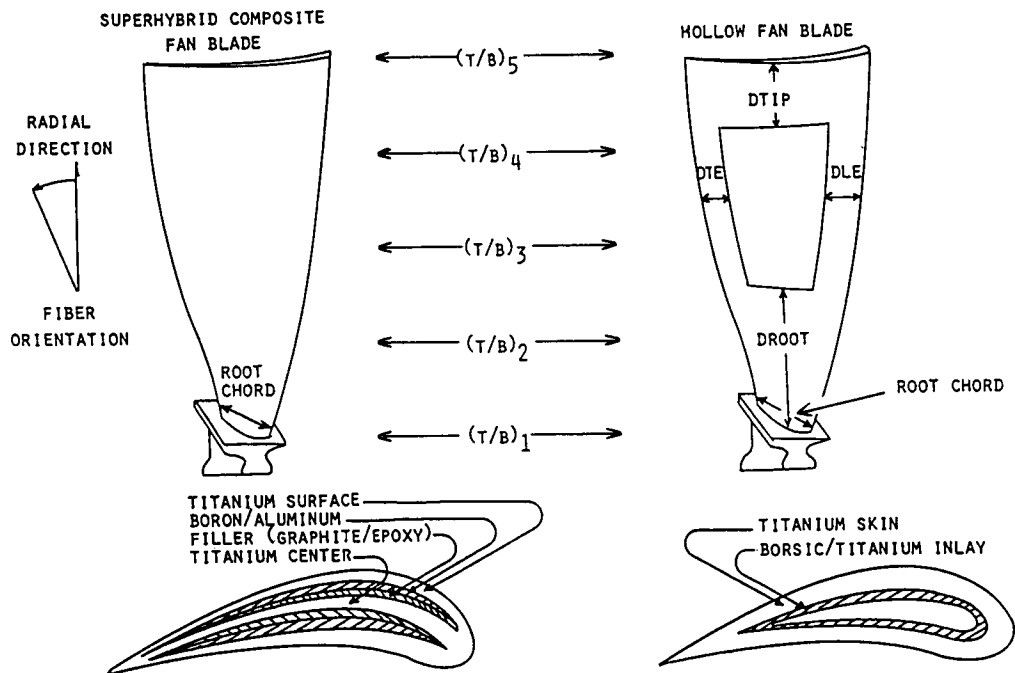
Figure 3

STAEBL PROGRAM DEMONSTRATED ON TWO ADVANCED FAN BLADES

The optimal design of shroudless fan blades represented a significant application of optimization methods to a complex engineering design problem at Pratt & Whitney. Although the blade design process had been previously automated, it was still necessary for an engineer to remain in the design loop in order to make changes to the design variables before re-running the vibration, stress, flutter, and foreign object damage (FOD) programs. Because of the complex nature of blade resonances due to engine order excitation levels, it was generally sufficient to determine a feasible blade, one that was usually not optimized for weight or cost. On occasion it was necessary to accept blades with resonance margin violations (i.e., critical frequencies within the operating range) if it appeared that additional experience-based hand iterations would not produce a feasible design.

In STAEBL, two fan blades of advanced internal construction (shown in Figure 4) were optimized for direct operating cost (a weighted sum of relative engine weight, manufacturing cost and maintenance cost) while satisfying constraints on resonance, flutter, root stress, FOD, etc. The design variables for both blades included thickness-to-chord ratios, root chord, and composite material thicknesses, as well as fiber orientation angles for the superhybrid composite blade, and location and size of the cavity for the hollow blade.

● DESIGN VARIABLES:



● OBJECTIVE FUNCTION: DIRECT OPERATING COST

● CONSTRAINTS: RESONANCE MARGIN, FLUTTER, F.O.D., ROOT STRESS

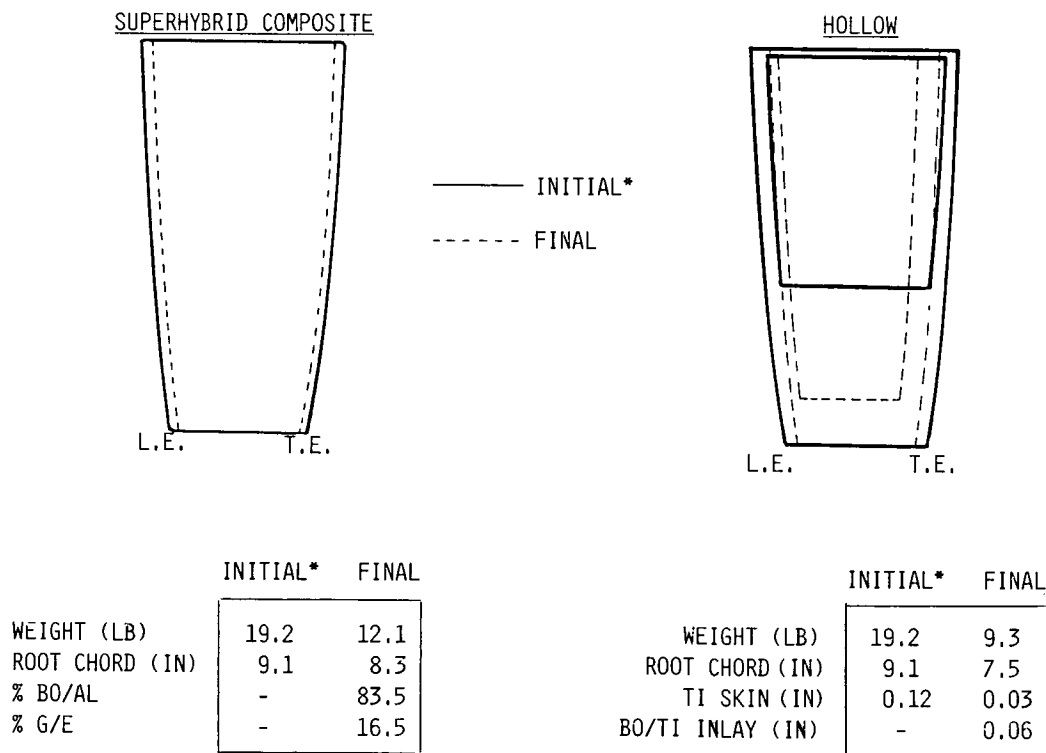
Figure 4

TAILORING OF EXTERNAL GEOMETRY AND INTERNAL CONSTRUCTION REDUCED WEIGHT AND COST

The structural optimization problems for the superhybrid composite and hollow fan blades were of moderate size, with 11 and 13 design variables, respectively; each had 68 constraints. The reference blade was a 19.2 lb hollow shroudless fan blade developed for the E³ (Energy Efficient Engine) project sponsored by NASA. The initial design for each problem was similar to the reference blade. As shown in Figure 5, significant weight decreases were obtained for both optimized blades by reducing root chord, introducing composite materials, and, for the hollow blade, enlarging and extending the cavity.

Using the COPES/CONMIN program, the optimization procedure for each blade converged after 13-15 iterations, or roughly 1 hour CPU time on an IBM 3081 computer. Each final blade configuration was limited by several active constraints that restricted further design improvement. These optimal feasible designs also were re-analyzed using a refined finite element program. Correction factors based upon any discrepancies were applied to the constraints, and each blade was then re-optimized. This procedure converged for the superhybrid composite blade, but no convergence was obtained for the hollow blade because of incompatibilities between the approximate and refined analyses.

In Phase II of the STAEBL program, a NASTRAN-compatible 2-D finite element plate vibration model and an approximate large deflection local FOD model replaced 1-D beam analyses in order to obtain closer agreement between the approximate and refined analyses.



* REFERENCE: NASA E³ FAN BLADE

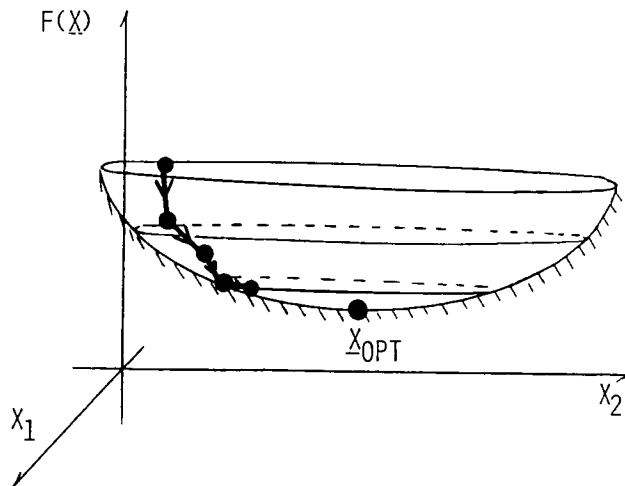
Figure 5

SCALED GRADIENTS ELIMINATE CONVERGENCE PROBLEMS

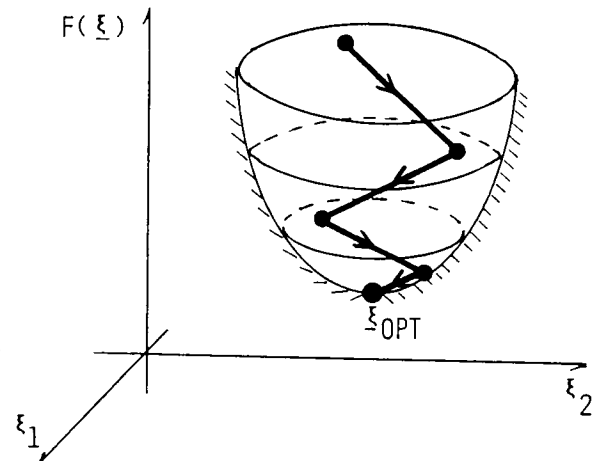
Proper scaling of design variables is important in many engineering optimization applications. Ideally, the independent variables should be balanced so that the components of the gradient of the objective function with respect to the design variables are all within roughly the same order of magnitude. If the design surfaces are stretched in the direction of one or more design variables, as illustrated in Figure 6a, then gradient-based methods using steepest descent or conjugate gradient algorithms can easily be biased in favor of the design variables with the largest gradient components. If certain design variables are ignored during the search, then the methods can converge prematurely to non-optimal solutions, as indicated in Figure 6a. For properly balanced cases, as in Figure 6b, it is expected that nearly all design variables will be changed during each iteration.

For most problems, scaling is successfully achieved by dividing each design variable by its initial value, i.e., $\xi_i = x_i/x_i^0$, $i = 1, \dots, n$. This normalization can be updated with current values every 1-5 iterations, especially if there have been significant changes among the design variables.

$$\xi_I = X_I/X_I^0, \quad \left(\partial F/\partial \xi_I\right) = X_I^0 \left(\partial F/\partial X_I\right), \quad I = 1, \dots, N$$



A) UNSCALED: SEARCH MAY TERMINATE PREMATURELY



B) SCALED: ALL RELEVANT DESIGN VARIABLES CHANGE ALONG EACH SEARCH DIRECTION

Figure 6

COMPONENTS OF SCALED GRADIENT ARE ALL WITHIN SAME
ORDER OF MAGNITUDE FOR HOLLOW FAN BLADE

In several applications (e.g., blade structural, blade aerodynamic, and rotor shaft optimization), improper scaling produced misleading results. For example, when no scaling was used in the STAEBL hollow fan blade analysis, d_{root} (the distance of the hollow section from the root) was virtually unchanged from its initial value after 13 iterations. Subsequent analysis confirmed, however, that a larger hollow section would both substantially reduce weight and not violate any constraints. A check of the objective function gradient in Figure 7 revealed the problem. The gradient component associated with t_{Ti} (the titanium skin thickness) was two orders of magnitude larger than the component associated with d_{root} . As a result most of the optimization program effort was focused on optimizing t_{Ti} , to the neglect of d_{root} .

When this problem was scaled, however, by dividing each design variable by its value on the previous iteration, all objective function gradient components were within the same order of magnitude. All design variables changed during each line search. Consequently, after 9 iterations, d_{root} had been reduced from 9.0 in. to 4.88 in., and the program converged. Since 3 constraints were active, the final design was easily confirmed to be an optimal feasible point.

| DESIGN VARIABLE | INITIAL VALUE (INCHES) | I TH COMPONENT OF GRADIENT OF OBJECTIVE FUNCTION | |
|-------------------------|------------------------------|--|--|
| | | UNSCALED $\frac{\partial f}{\partial x_i}$ | SCALED $\frac{\partial f}{\partial \xi_i}$ |
| $x_1 = T_{\text{ROOT}}$ | 0.875 | 0.460 | 0.403 |
| $x_2 = T_{\text{TIP}}$ | 0.334 | 0.140 | 0.047 |
| $x_3 = D_{\text{ROOT}}$ | 9.650 | 0.027 | 0.260 |
| $x_4 = T_{\text{TI}}$ | 0.120 | 2.700 | 0.324 |

SAME
ORDER

- UNSCALED: AFTER 13 ITERATIONS, D_{ROOT} UNCHANGED AND PROGRAM DID NOT CONVERGE.
- SCALED: AFTER 9 ITERATIONS, D_{ROOT} REDUCED TO 4.88 IN. AND PROGRAM CONVERGED.

Figure 7

CONSTRAINT THICKNESS AND PUSH-OFF FACTOR USE SIMULTANEOUSLY ACTIVE CONSTRAINTS TO ELIMINATE ZIGZAGGING

From a theoretical standpoint, most optimization strategies and programs will obtain optimal feasible solutions for a wide variety of problems. For large industrial applications, where CPU time is important and function calls are expensive, the superior program is one that obtains a solution in the fewest number of function evaluations. In addition, the program should be robust enough to recognize and recover from such convergence problems as zigzagging (i.e., bouncing between alternately active constraints), and skidding (i.e., re-encountering the same active constraint on successive iterations).

The COPES/CONMIN program has several adjustable parameters that can be fine tuned for individual problems and are effective in accelerating convergence. The push-off factor θ_j determines the rebound angle within the usable feasible sector and ranges from aggressive directions nearly tangent to active constraints ($\theta_j \approx 0$) to cautious directions nearly tangent to level surfaces of the objective function ($\theta_j \gg 1$). The intermediate value $\theta_j = 1$ nearly "bisects" the usable feasible sector. For nearly linear problems, aggressive values of θ_j will reduce the objective function most rapidly, but may also encounter skidding. Overly cautious values of θ_j can lead to zigzagging and larger CPU times.

Another parameter, CT, the constraint thickness parameter, performs several tasks to reduce CPU time. First, by adding constraint thickness, the program can come close to a constraint rather than waste time determining its position exactly. In addition, zigzagging can be avoided as shown in Figure 8. If two alternately active constraints become simultaneously active because of their increased thickness, then a new search direction will proceed down the "trough" formed by these constraints and obtain a substantial reduction in the objective function.

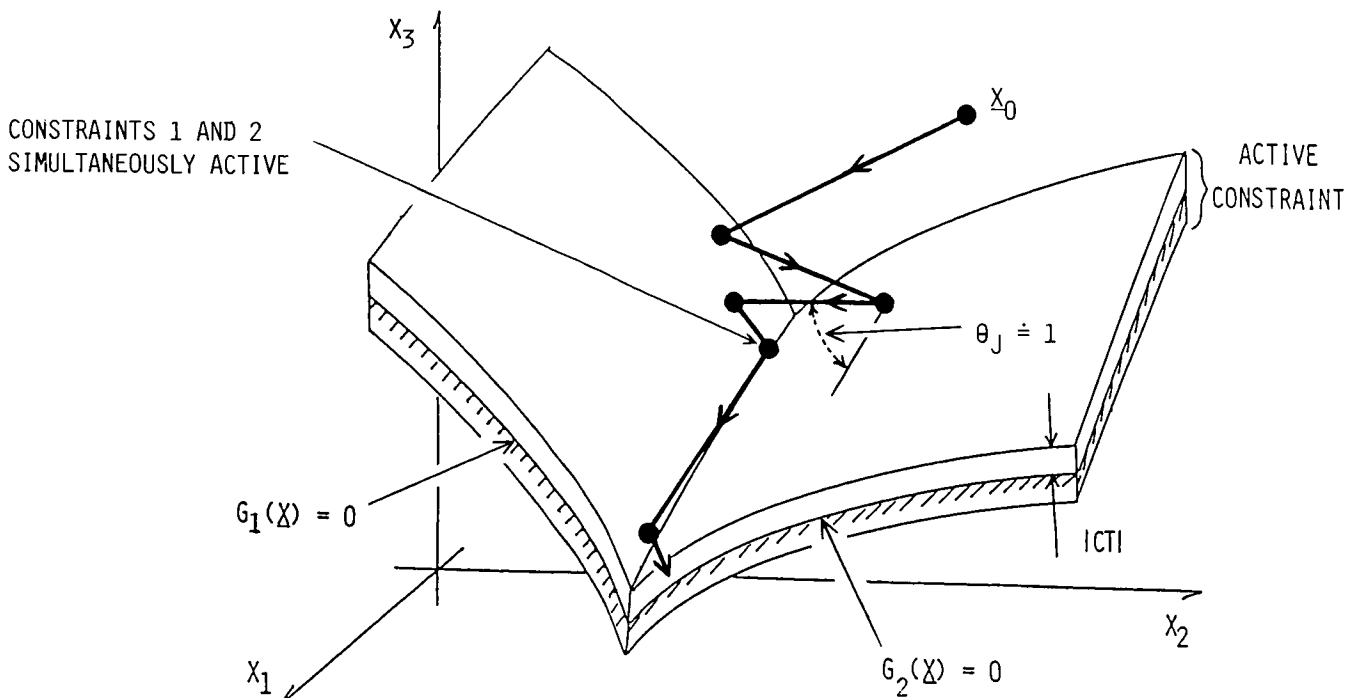


Figure 8

PROPER SELECTION OF CONSTRAINT THICKNESS AND PUSH-OFF FACTOR ACCELERATES CONVERGENCE FOR DISK OPTIMIZATION

Compressor disks are among the most critical components of an aircraft engine; the failure and rupture of a disk can lead to serious containment problems for the engine case. In order to provide a large margin of safety, disks are designed to be strong and durable, with special resistance to high cycle fatigue. On the other hand, any reduction in disk weight permits a reduction in related components and can provide significant savings in overall engine weight. In a joint effort between PWEDFO [8] and PWEDCO, an optimization program was developed to design minimum weight disks that satisfy constraints on profile geometry, stress, burst margin, etc.

As shown in Figure 9, the initial disk configuration was chosen to be unrealistically bulky to insure feasibility of the initial design, in order to accelerate convergence. The performance of the optimization procedure was significantly affected by the choice of search parameters. For a push-off factor $\theta_j = 0.3$, zigzagging between constraints 5 and 7 (which both measured slopes along the disk profile) was evident during iterations 4-18. At iteration 19, both of these constraints were simultaneously active, and a large decrease was obtained for the objective function. Convergence was not achieved until 61 iterations. When a more aggressive value $\theta_j = 0.1$ was taken, zigzagging was minimized, and convergence was achieved in only 34 iterations.

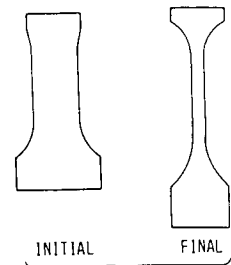
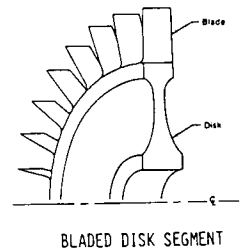
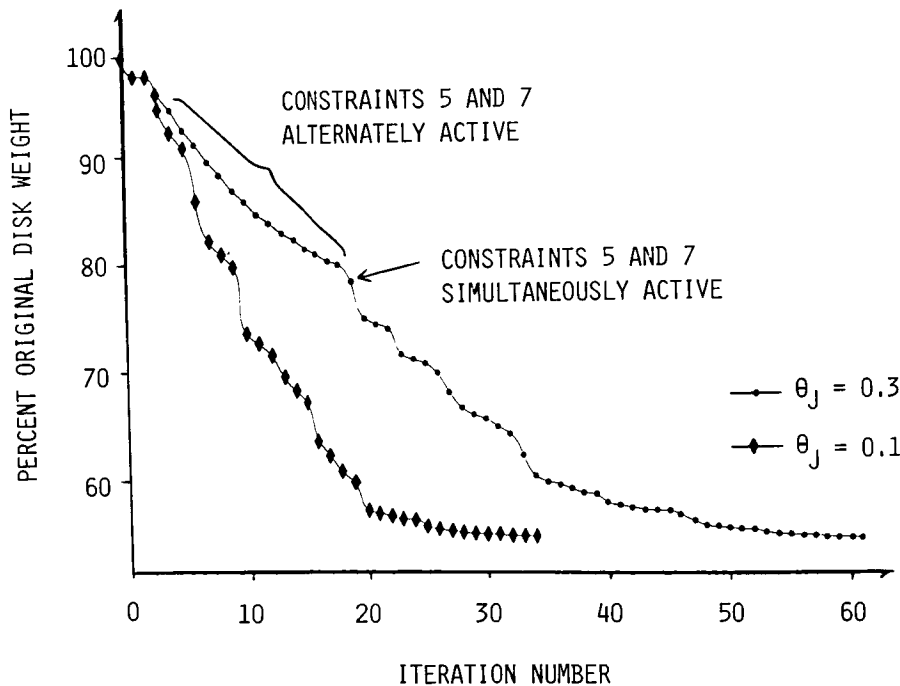


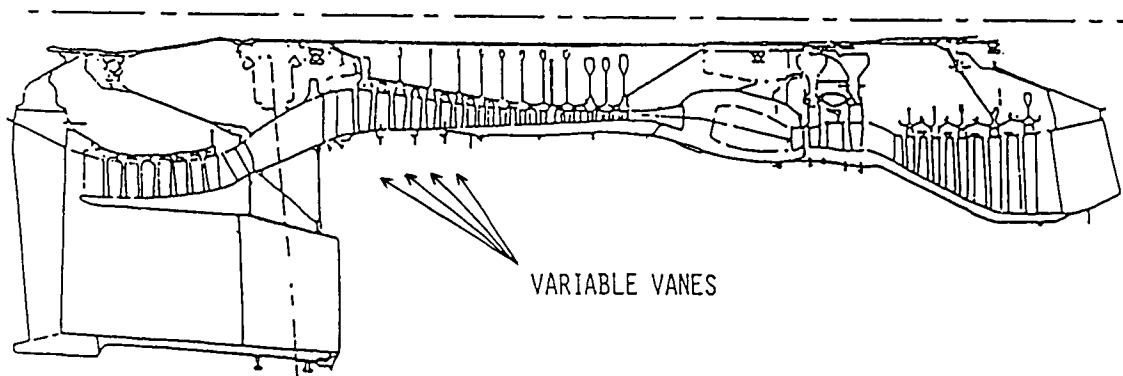
Figure 9

AUTOMATED TESTING PROCEDURE FOR VANE OPTIMIZATION

Engine and rig testing is a time-consuming and expensive process. For example, high by-pass ratio turbofans running at full power can consume several thousand gallons of fuel per hour. It is an inexact science, dependent upon events such as weather, instrumentation, and mechanical failures over which there is little or no control. The rewards, however, are substantial, e.g. an improvement of only 0.1% in TSFC (Thrust Specific Fuel Consumption) can provide significant yearly savings in airline fleet fuel costs.

Variable compressor vanes can be adjusted to improve TSFC (or alternatively, compressor or turbine efficiencies) at various power settings. As shown in Figure 10, a compressor generally has 3-5 variable vanes which can be moved individually during the test. Standard analytical techniques have been previously applied. For example, the vane angles can be set sequentially from the rear to the front of the engine. This technique, however, does not model interactive effects, especially the strong coupling between the first (inlet guide vane) and last vanes. Statistical tests (e.g., partial or full factorial) have also been utilized. The disadvantage of this approach is that the settings must be established prior to test, and unnecessary data may be collected in regions far from optimal vane settings.

The approximate optimization option [9] in COPES/CONMIN can be used to analyze test data. By using it interactively in real time during a test, the vane setting procedure can be automated using a directed search. Another advantage is that side constraints can be imposed for maximum and minimum vane angles, and behavior constraints can be imposed for minimum compressor and turbine efficiencies, maximum corrected fuel flow, etc.



- PERFORMANCES OF ADVANCED ENGINES AND RIGS OPTIMIZED IN A TEST CELL BY VARYING VANE SETTINGS
- USED APPROXIMATE OPTIMIZATION OPTION OF COPES/CONMIN TO PREDICT TEST VANE SETTINGS INTERACTIVELY IN REAL TIME

Figure 10

OPTIMUM VANE SETTINGS CORRESPOND TO CONSTRAINED
MINIMUM OF QUADRATIC FIT THROUGH TEST DATA

The solution procedure can be illustrated graphically for 2 unknown vane angles as follows. Suppose TSFC and efficiency values are known for several different vane settings. After a smooth surface is fit through these points, the COPES/CONMIN program can easily determine the constrained minimum point, as shown in Figure 11. The engine or rig is then run with vane angles set at these new predicted optimum settings, another TSFC point is appended to the data, and a new optimum is determined from a surface fit to these new data. When two successive optima agree within an accepted tolerance level, the iterative procedure has converged. The order of the surface fit is either linear or quadratic, depending upon the number of data points that are available. If there are more data points than unknown coefficients for the surface fit, then a least squares fit, with recent data points weighted more heavily than previous points, is used to approximate the data.

The approximate optimization procedure is usually successful whenever analytical functions and test data can be approximated locally by linear or quadratic functions. It is especially effective when there is a relatively small number (<8) of design variables. Another advantage is that the approximate method usually requires far fewer function calls than the "exact" method.

A starting procedure is normally used to generate the first few points. For vane optimization, an initial approximation to the gradient is usually obtained by incrementing, in turn, each vane angle from the nominal settings. During the optimization, move limits restrict the search to a neighborhood of the previous optimum, as shown in Figure 11. As more data points are determined, the move limits are increased. For sequential unconstrained linear optimization, it is imperative to have move limits; otherwise the search would be unbounded. In this case, the next optimum is usually located at one of the "corners" of the "search rectangle".

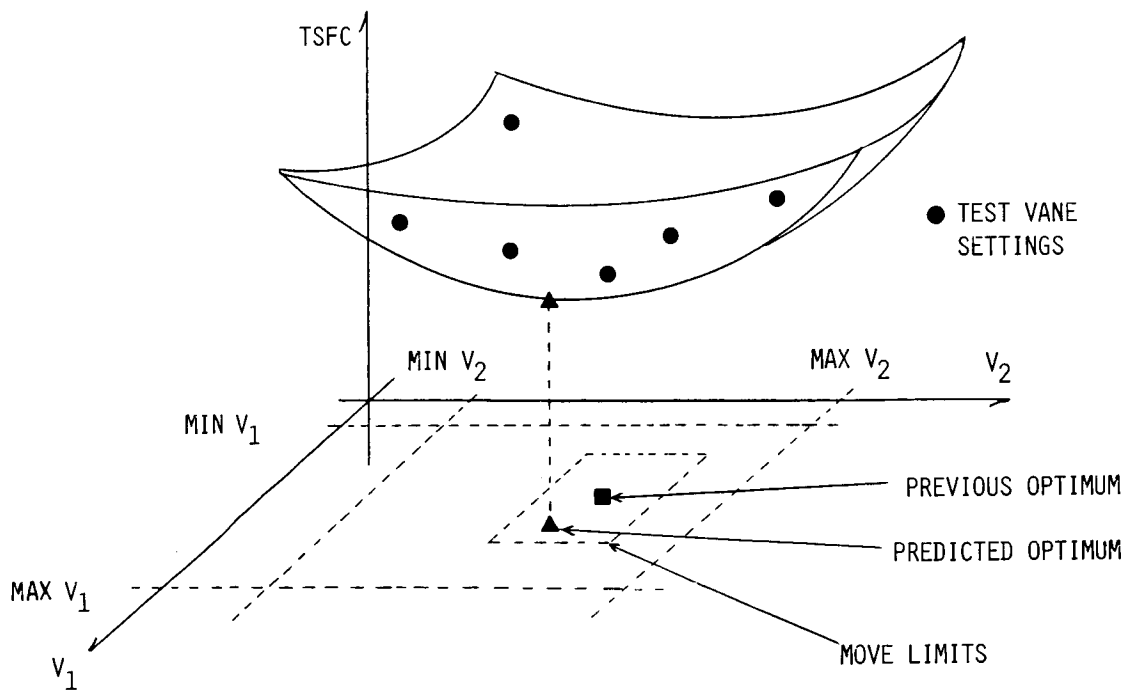


Figure 11

APPROXIMATE OPTIMIZATION ANALYSES BECOME INCREASINGLY ACCURATE AS HIGH ORDER TERMS ADDED

The objective function and constraints associated with the test data are approximated with truncated Taylor series. For example, a quadratic approximation for the objective function about the nominal design \underline{x}_0 is given by

$$f(\underline{x}) \approx f(\underline{x}_0) + \nabla f(\underline{x}_0) \cdot (\underline{x} - \underline{x}_0) + \frac{1}{2} (\underline{x} - \underline{x}_0)^T \cdot \underline{H}(\underline{x}_0) \cdot (\underline{x} - \underline{x}_0) \quad (12.1)$$

where components of the gradient vector and Hessian matrix (assumed symmetric), respectively, are given by

$$[\nabla f]_i = \partial f / \partial x_i \quad i = 1, \dots, n \quad (12.2)$$

$$[\underline{H}]_{ij} = \partial^2 f / \partial x_i \partial x_j \quad i, j = 1, \dots, n \quad (12.3)$$

The number of unknowns in (12.1) is $1 + n + n(n+1)/2$, or $1 + 2n$ if only the diagonal terms in the Hessian matrix are used. As more data points become available, the approximations shown in Figure 12 for the optimization problem progress from linear to leading order quadratic (diagonal Hessian terms) to the full quadratic expansion (including all cross product terms). For vane optimization problems, the diagonal Hessian approximation usually includes sufficient curvature effects in order to determine an optimum.

Accuracy of the approximate optimization method is dependent upon the nonsingularity of the matrix used to calculate the unknown coefficients in the Taylor series (12.1). During engine and rig tests at PWEDCO, the condition number of this coefficient matrix is monitored continuously to insure the integrity of the calculations.

- OBJECTIVE FUNCTION AND CONSTRAINTS FIT BY LINEAR AND QUADRATIC POLYNOMIALS (TRUNCATED TAYLOR SERIES):

$$f(\underline{x}) \approx f(\underline{x}_0) + \nabla f(\underline{x}_0) \cdot (\underline{x} - \underline{x}_0) + \frac{1}{2} (\underline{x} - \underline{x}_0)^T \cdot \underline{H}(\underline{x}_0) \cdot (\underline{x} - \underline{x}_0)$$

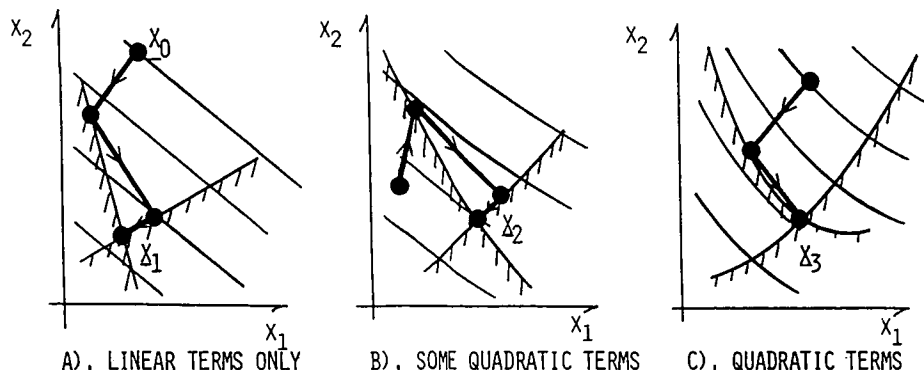
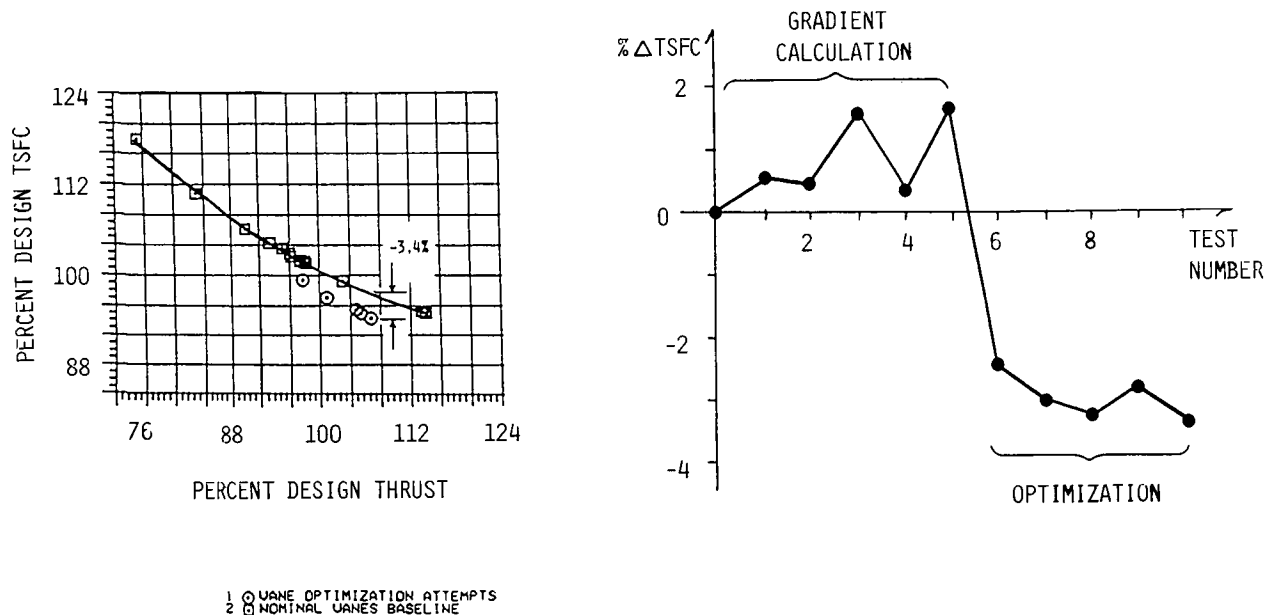


Figure 12

AUTOMATED VANE OPTIMIZATION TEST PROGRAM FOR ADVANCED COMMERCIAL ENGINE REDUCED TSFC 3.4% AT LOW POWER

Results of an actual test in which 5 vane angle settings were determined in order to minimize TSFC at low power for an advanced commercial engine are shown in Figure 13. The first 5 test points were used to calculate the finite difference approximation to the gradient. The next 3 points each produced significant reductions in TSFC. After the 10th test point, the diagonal terms of the Hessian were available, and testing was completed soon thereafter with a substantial net TSFC improvement of 3.4%. Since nearly every data point showed marked improvement over its predecessor during the optimization portion of the test, there was much positive feedback and reinforcement among the test engineers, test stand operators, and analytical support staff. In addition, the optimization procedure predicted points very rapidly in an interactive mode. Since it takes 3-5 minutes for engine performance parameters to stabilize whenever new vane settings are made, there is even ample time to run alternate analyses.

As in any real time testing environment a lack of repeatability and a variety of experimental errors adversely affected the optimization procedure. For example, there were dead-band and hysteresis errors in the real time stator control mechanism that actually set the vane angles. Instrumentation errors were especially significant at cruise power settings, since the engine was well-balanced and TSFC was relatively insensitive to small changes in vane settings. Numerical convergence of the optimization scheme is rare in these tests. The iterations are usually terminated when there is a consensus among test and analytical personnel that any relative improvement in results would be below the threshold of experimental error.



● CONVERGENCE PROBLEMS DUE TO EXPERIMENTAL ERRORS

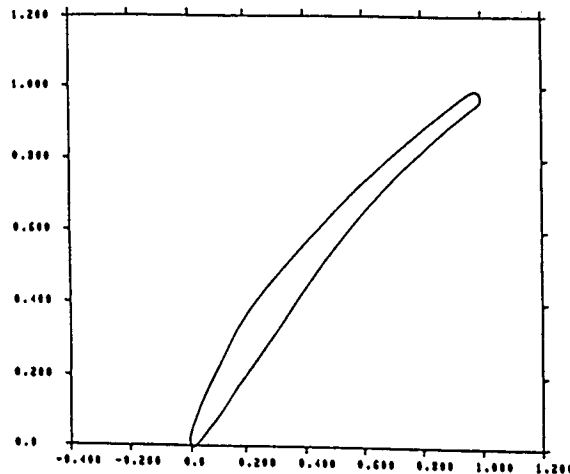
Figure 13

AUTOMATED COMPRESSOR BLADE DESIGN SYSTEM OPTIMIZES AERODYNAMICS

In designing compressor blades at PWEDCO, separate analyses are generally run by the Aerodynamics Group (who desire thin, streamlined, high-performing shapes) and the Structures Group (who desire strong, durable shapes). There is, however, an overall iterative loop between the groups as new designs are analyzed separately and passed back and forth until an acceptable compromise is reached. Most of the structural analysis programs for blade design (e.g., vibration, stress, foreign object damage, etc.) have long been linked together into an automated design system. As a result of the STAEBL program, the structural optimization of blade design is now becoming more and more commonplace. Similarly, the aerodynamic blade design programs have also been unified into an automated system, and a preliminary attempt has been made to optimize the process. As shown in Figure 14, several geometric design variables are determined in order to minimize loss at the aerodynamic design point while satisfying restrictions on the location of the flow separation point at various power settings.

As in the compressor blade structural optimization, this aerodynamic optimization procedure will perform the arduous, repetitive tasks associated with designing optimal feasible blades. Since this process must be repeated several times for each new build during the ongoing development of a new compressor, an automated optimization program will give the aerodynamicist more time to analyze results and investigate innovative designs.

● GEOMETRIC DESIGN VARIABLES:



● OBJECTIVE FUNCTION: MINIMIZE LOSS AT AERODYNAMIC DESIGN POINT

● CONSTRAINTS: LOCATION OF FLOW SEPARATION POINT FOR VARIOUS POWER SETTINGS

Figure 14

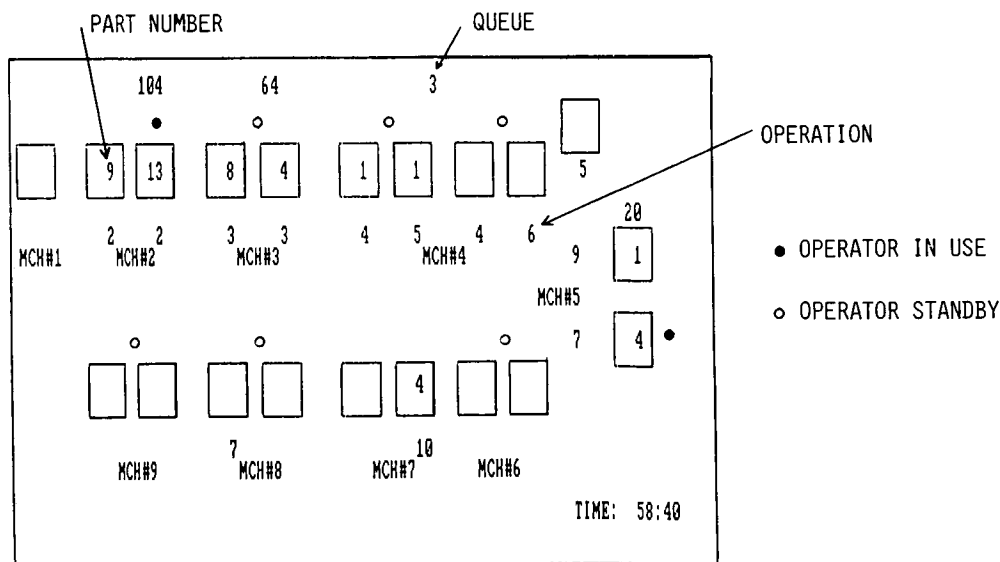
APPROXIMATE OPTIMIZATION TECHNIQUES CAN BE USED TO REDUCE COST AND INVENTORY FOR MANUFACTURING FACILITY

Another new area at Pratt & Whitney for the application of optimization methods is in the Manufacturing Division. Recently much attention has been focused upon the tremendous cost and inventories associated with production processes. In an attempt to reduce end product costs, much effort will be expended over the next few years in order to modernize and streamline manufacturing operations. Many analytical techniques developed previously for engineering applications can now be adapted to manufacturing applications.

A pilot effort is currently under way to optimize performance and minimize total cost associated with a small prototype manufacturing facility, shown in Figure 15, that is dedicated to the production of sets of similar types of parts. Programs such as GPSS (General Purpose Simulation System) [10] are available for simulating the operation of such a facility. By including different types of machines, machine operators, tasks, part numbers, lot sizes, and queues, a GPSS simulation can sequence through a time history of events during a production cycle.

A representative optimization problem would be to determine the proper lot sizes for part groups to minimize the total cost (e.g., capital equipment, personnel, set-up, and holding costs) and work-in-process while still meeting production schedule and not exceeding machine capacity. An optimization program such as COPES/CONMIN or ADS can be coupled with GPSS in order to determine the optimal configuration of the facility. Because GPSS is not written in FORTRAN and uses integer design variables, however, the approximate optimization option of COPES/CONMIN will probably be used in an iterative manner to analyze discrete sets of previously generated data.

● DESIGN VARIABLES:



● OBJECTIVE FUNCTION: MINIMIZE TOTAL COST, WORK-IN-PROCESS

● CONSTRAINTS: PRODUCTION SCHEDULE, MACHINE CAPACITY

Figure 15

CONCLUSIONS

Starting with the NASA-sponsored STAEBL program, optimization methods based primarily upon the versatile program COPES/CONMIN have been introduced over the past few years to a broad spectrum of engineering problems in structural optimization, engine design, engine test, and more recently, manufacturing processes. By automating design and testing processes, many repetitive and costly trade-off studies have been replaced by optimization procedures. Rather than taking engineers and designers "out of the loop," optimization has, in fact, put them more in control by providing sophisticated search techniques. The ultimate decision whether to accept or reject an optimal feasible design still rests with the analyst. Feedback obtained from this decision process has been invaluable since it can be incorporated into the optimization procedure to make it "more intelligent." On several occasions, optimization procedures have produced novel designs, such as the nonsymmetric placement of rotor case stiffener rings, not anticipated by engineering designers. In another case, a particularly difficult resonance constraint could not be satisfied using hand iterations for a compressor blade; when the STAEBL program was applied to the problem, a feasible solution was obtained in just two iterations.

Finally, the multidisciplinary nature of optimization has fostered applications in many diverse areas throughout Pratt & Whitney and UTC in general. Initial reluctance on behalf of some groups has usually been overcome by a few demonstration cases, using programs with which they are familiar. Educational courses and symposia have also been very useful in exchanging ideas about this emerging and important discipline in the workplace. (See fig. 16.)

- EFFICIENT OPTIMIZATION METHODS ARE INCREASINGLY BEING APPLIED TO PROBLEMS IN ENGINEERING DESIGN AND TESTING.
- STRUCTURAL OPTIMIZATION CAN PROVIDE ACCEPTABLE DESIGNS EVEN IF STANDARD ENGINEERING DESIGN METHODS AND INTUITION FAIL.
- THERE IS SUBSTANTIAL AND GROWING INTEREST IN SHARING THE RESULTS AND BENEFITS OF THIS TECHNOLOGY THROUGHOUT UTC.

Figure 16

REFERENCES

1. Platt, C.E., T.K. Pratt, and K.W. Brown, "Structural Tailoring of Engine Blades (STAEBL)," NASA CR-167949, 1982.
2. Brown, K.W., T.K. Pratt, and C.C. Chamis, "Structural Tailoring of Engine Blades (STAEBL)," Proc. AIAA/ASME/ASCE/AHS 24th Structures, Structural Dynamics, and Materials Conference, Lake Tahoe, Nevada, May 1982, pp. 79-88.
3. Garberoglio, J.E., J.O. Song, W.E. Boudreaux, "Optimization of Compressor Vane and Bleed Settings," ASME Paper 82-GT-81, ASME Gas Turbine Conference, London, England, April 1982.
4. Zoutendijk, C.G., Methods of Feasible Directions, Elsevier, Amsterdam, 1960.
5. Madsen, L.E., and G.N. Vanderplaats, "COPES - A FORTRAN Control Program for Engineering Synthesis," NPS 69-81-003, Naval Postgraduate School, Monterey, CA, March 1982.
6. Vanderplaats, G.N., "CONMIN - A FORTRAN Program for Constrained Function Minimization: User's Manual," NASA TM X-62282, August 1973.
7. Vanderplaats, G.N., K. Sugimoto, and C.M. Sprague, "ADS-1: A New General Purpose Optimization Program," AIAA/ASME/ASCE/AHS 24th Structures, Structural Dynamics, and Materials Conference, Lake Tahoe, Nevada, May 1982, pp. 117-123.
8. Song, J.O., and R.E. Lee, "Application of Optimization to Aircraft Engine Disk Synthesis," Proc. International Symposium on Optimum Structural Design, University of Arizona, Tucson, Arizona, Oct. 1981.
9. Vanderplaats, G.N., "Efficient Algorithm for Numerical Airfoil Optimization," AIAA Journal of Aircraft, Vol. 16, No. 12, Dec. 1979, pp. 842-847.
10. Henriksen, J.O., and R.C. Crain, "GPSS-H User's Manual," 2nd Ed., Wolverine Software Corp., 1983.

ON OPTIMAL DESIGN FOR THE BLADE-ROOT/HUB
INTERFACE IN JET ENGINES[†]

Noboru Kikuchi and John E. Taylor
The University of Michigan
Ann Arbor, Michigan

[†]The work described herein was supported via NASA Grant NAG3-388.

OPTIMAL DESIGN FOR THE BLADE-ROOT/HUB INTERFACE

Figure 1 shows two major problems identified with the design of the blade-root/hub interface. The first is the so-called friction contact problem which has two special features: unilateral contact and Coulomb's friction. One of the difficulties in this problem is that the portions of contact and sticking/sliding surfaces are not known *a priori*.

The second is the shape optimization problem which is characterized either by the minimization of the maximum contact pressure or by the minimization of the equivalent stress on the boundary. Design variables are the shapes of the blade-root and the hub. It is noted that friction contact and shape optimization problems are strongly coupled in the present design problem.

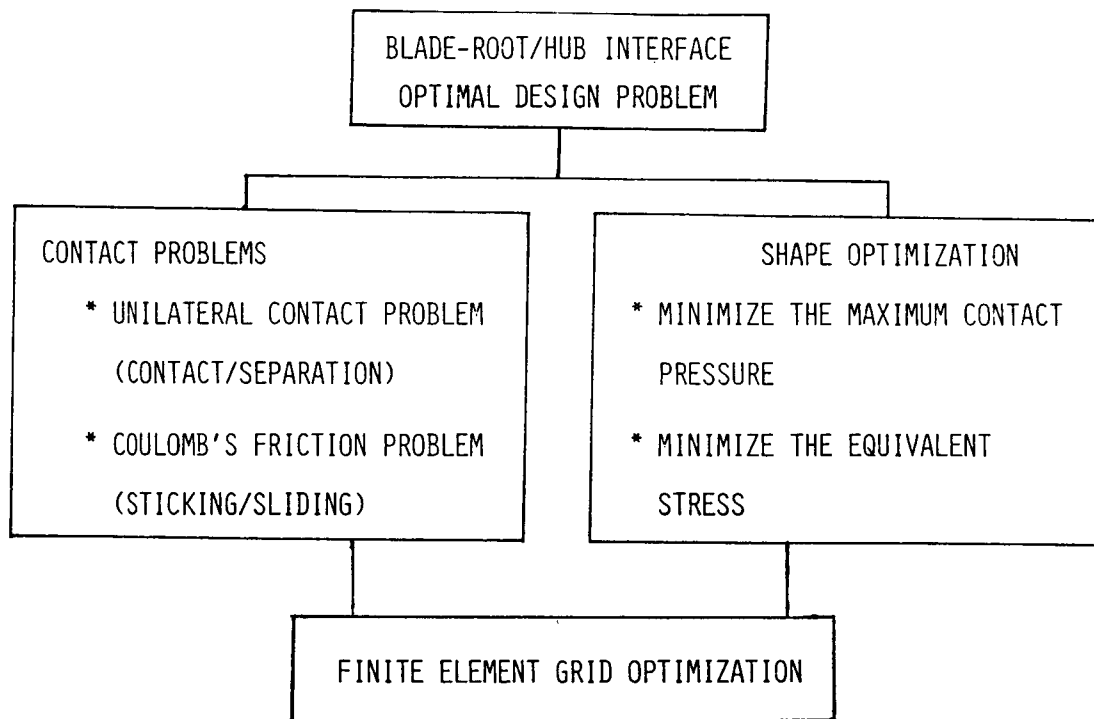


Figure 1

UNILATERAL CONTACT PROBLEMS

If the initial gap between two elastic bodies is given by $g_0(s)$ and the relative displacement of two bodies is denoted by $\tilde{u}_R(s)$, the kinematic contact condition along a possible contact surface (which should contain the true contact surface) is expressed by $\tilde{u}_R \cdot \tilde{N} - g_0 \leq 0$ (shown in Fig. 2) where \tilde{N} is the unit vector inward normal to the "master" surface $\tilde{\Gamma}^m$. This means that the relative normal displacement $\tilde{u}_R \cdot \tilde{N}$ cannot exceed the initial gap g_0 of two surfaces. The corresponding stress condition is given by $p \leq 0$, where p is the contact pressure normal to the surface. Since unilateral contact is considered, p cannot be positive. The switching condition of these is represented by $p(\tilde{u}_R \cdot \tilde{N} - g_0) = 0$. That is, if two bodies separate, then $p=0$ while $\tilde{u}_R \cdot \tilde{N} - g_0 < 0$. On the other hand, $p < 0$ and $\tilde{u}_R \cdot \tilde{N} - g_0 = 0$ if the two bodies are in contact.

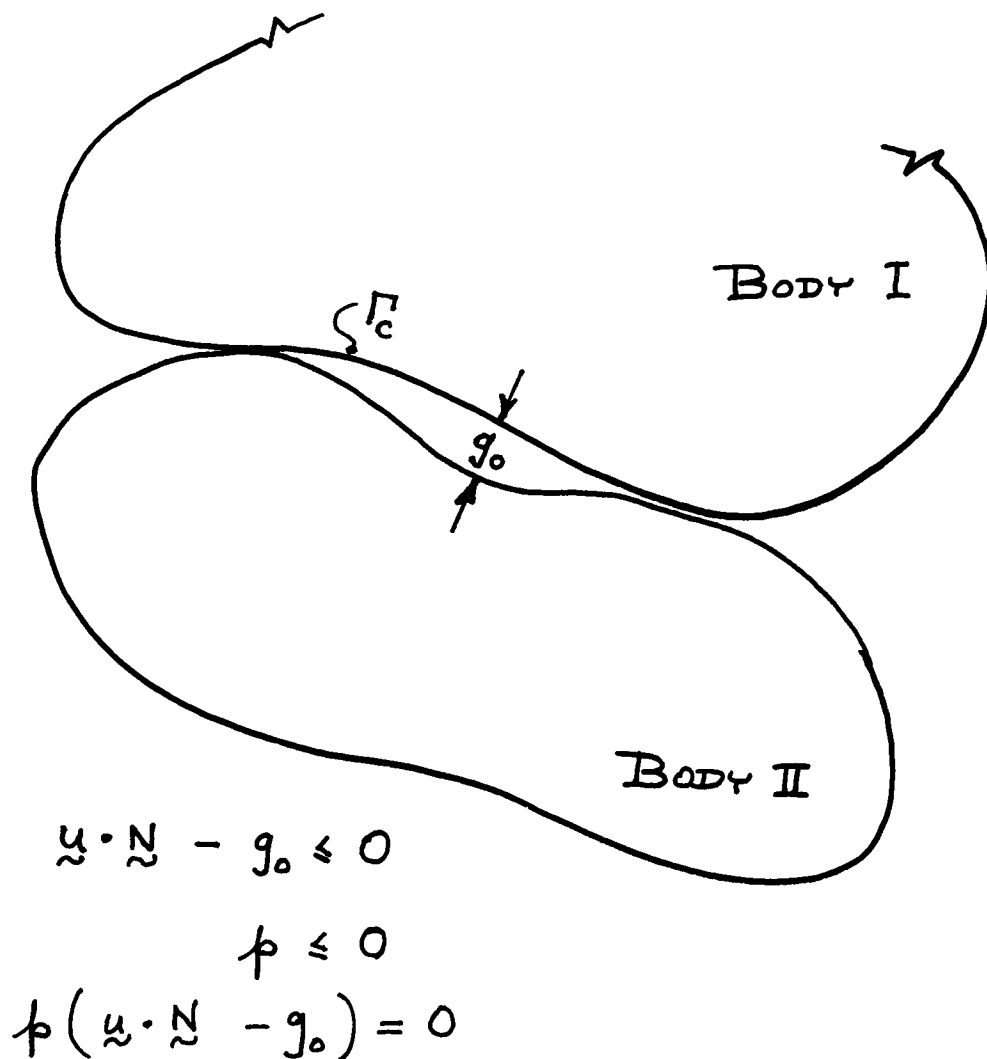


Figure 2

COULOMB'S FRICTION PROBLEMS

Figure 3 shows Coulomb's friction law which can be idealized by a spring-slider model. Since the work done by the friction stresses due to Coulomb's friction law yields a non-differentiable functional $\int_{\Gamma} (-\mu p) |\dot{v}_{RT}| d\Gamma$ where μ is the coefficient of friction and $|\dot{v}_{RT}|$ is the magnitude of the relative tangential displacement, this has to be approximated by a differentiable one $\int_{\Gamma} (-\mu p) \phi_{\epsilon}(\dot{v}_{RT}) d\Gamma$ using a nonlinear function ϕ_{ϵ} and a parameter ϵ such that $\phi_{\epsilon}(\dot{v}_{RT}) \rightarrow |\dot{v}_{RT}|$ as $\epsilon \rightarrow 0$.

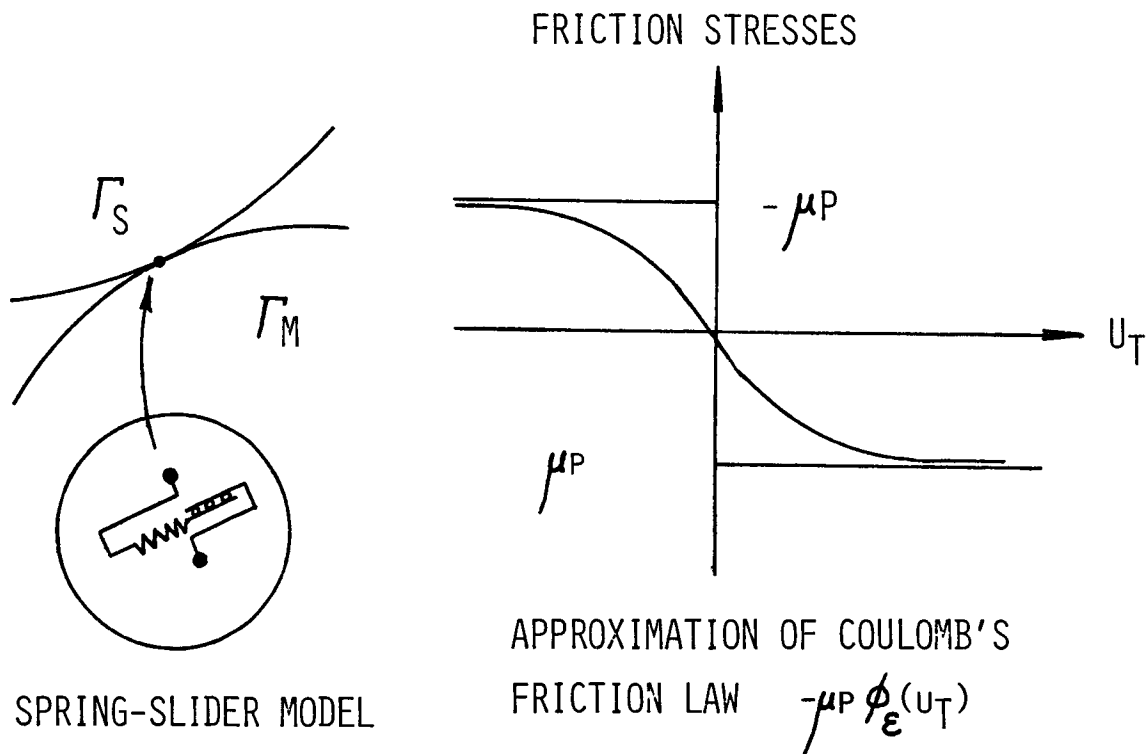


Figure 3

FORMULATION FOR CONTACT GAP DESIGN PROBLEM

We consider the contact between two elastic bodies as represented in Figure 2, including an account of friction and slip as indicated in Figure 3. The design problem calls for the determination of optimal gap g_0 , where g_0 represents the initial (before loading) gap between the bodies. The design is to be determined according to a criterion on the contact pressure p , namely to minimize the maximum pressure:

$$\text{Min } [\max_{x \in \Gamma_c} -p]$$

subject to:

(equilibrium problem statement) (P1)

$$\tilde{u} \cdot \tilde{N} - g_0 \leq 0$$

$$p \leq 0$$

$$p(\tilde{u} \cdot \tilde{N} - g_0) = 0; \quad \int_{\Gamma_c} g_0 d\Gamma - G \leq 0$$

This is interpreted into the form:

$$\text{Min } (\beta)$$

$$g_0$$

subject to:

$$-p - \beta \leq 0$$

$$p \leq 0; \quad \int_{\Gamma_c} g_0 d\Gamma - G \leq 0$$

$$\int_{\Omega} \sigma_{ij}(\tilde{u})_{ij}(\tilde{v} - \tilde{u}) d\Omega - \int_{\Gamma_c} p(\tilde{v} - \tilde{u}) \cdot \tilde{N} d\Gamma \quad (P2)$$

$$+ \int_{\Gamma_c} -\mu p(|\tilde{v}_T| - |\tilde{u}_T|) d\Gamma$$

$$- \int_{\Omega} \tilde{f} \cdot (\tilde{v} - \tilde{u}) d\Omega - \int_{\Gamma_F} \tilde{t} \cdot (\tilde{v} - \tilde{u}) d\Gamma \geq 0 \quad \forall \tilde{v}$$

$$\int_{\Gamma_c} (q - p)(\tilde{u} \cdot \tilde{N} - g_0) d\Gamma \geq 0 \quad \forall q \text{ s.t. } q \leq 0$$

In this virtual displacement statement of the equilibrium problem, u represents the actual displacement field while v symbolizes any displacement within the admissible set. The optimal solution, say p^*, g_0^*, u^* , must satisfy the following necessary conditions associated with problem (P2) (Γ_{CD} identifies intervals where $g_0^* \neq g_0$):

$$p = -\beta \quad \text{on } \Gamma_{CD}$$

$$-p > -\beta \quad \text{on } (\Gamma_c - \Gamma_{CD})$$

$$\int_{\Gamma_c} g_0 d\Gamma - G = 0$$

$$p(\tilde{u} \cdot \tilde{N} - g_0) = 0 \quad \text{on } \Gamma_c$$

SHAPE OPTIMIZATION

Another shape design problem, shown in Figure 4, involves rather large scale shape modification in order to reduce the maximum values of local criteria such as von Mises' equivalent stress, the maximum shear stress, or the maximum principal stress. The optimal design problem is then represented by:

$$\min_{\Gamma} [\max_{s \in \Gamma} |f(u)|]$$

subject to equilibrium equations and the gap constraint, where $f(u)$ is a local criterion evaluated at the solution u . It is noted that this problem strongly depends on the design of gap of two bodies. Indeed, if the contact pressure generates large bending moment, any kind of local criterion dramatically increases at the valley of blade-roots.

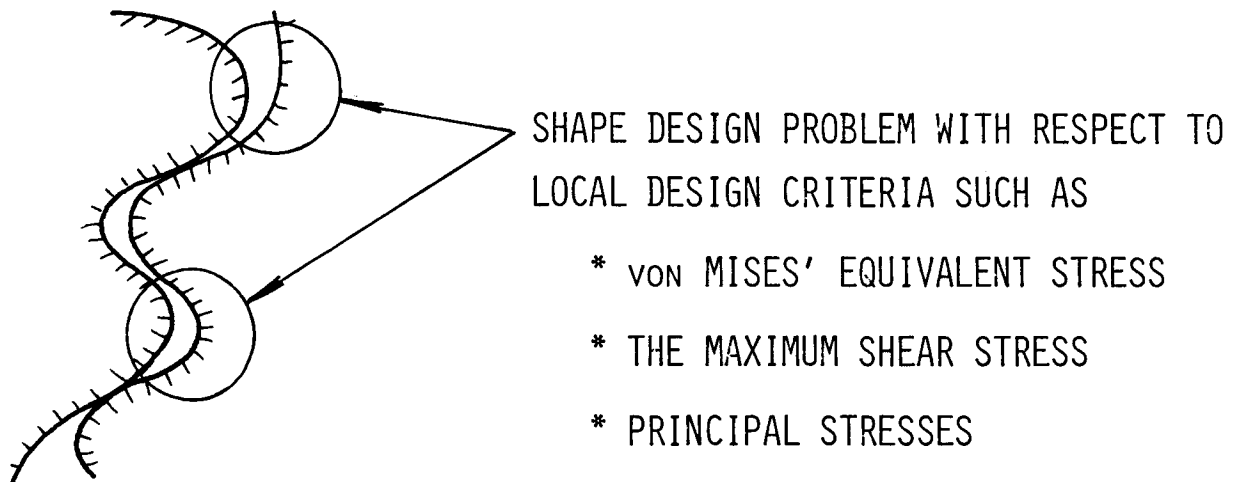


Figure 4

FINITE ELEMENT DISCRETIZATION AND GRID OPTIMIZATION

To analyze the design problems described above, finite element approximations are introduced. An important fact is that the final (optimal) shape by the optimal design problem is affected by the quality of finite element approximations. Almost all optimality criteria are represented by the stress tensor which is not approximated well by finite element methods. To overcome this difficulty the present study introduces the finite element grid optimization algorithm. An example of this application is shown in Figure 5.

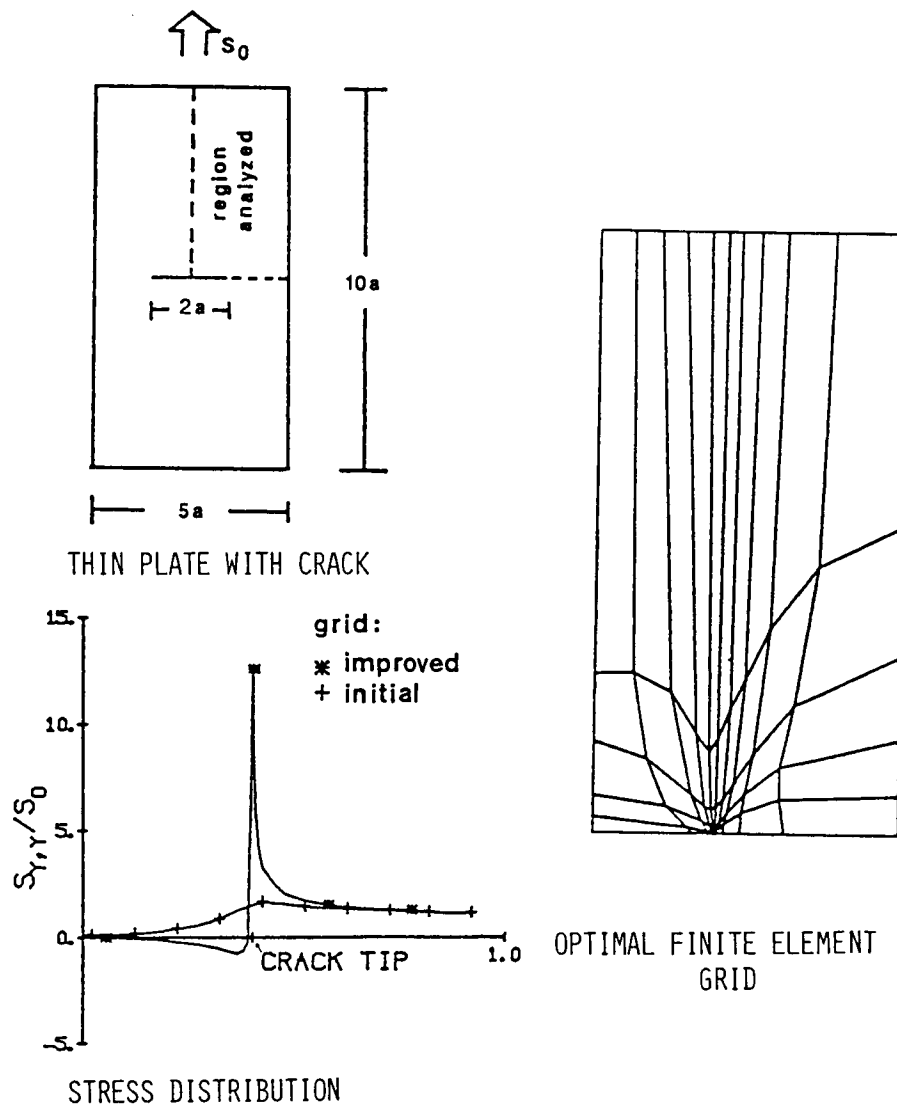


Figure 5

IMPLEMENTATION

Using optimality criterion methods, we shall solve the shape design problem of the blade-root/hub interface. Figure 6 shows a flow chart of the algorithm applied in the present study. For a given shape of blade-root valley, the optimal design problem for the initial gap between two bodies is solved. After determining the gap, the valley shape is now subject to design to reduce the maximum value of a local criterion with a fixed gap. Since the gap design problem is not independent of the shape of the valley part of blade-roots, we have to iterate the above procedure until both design changes become sufficiently small.

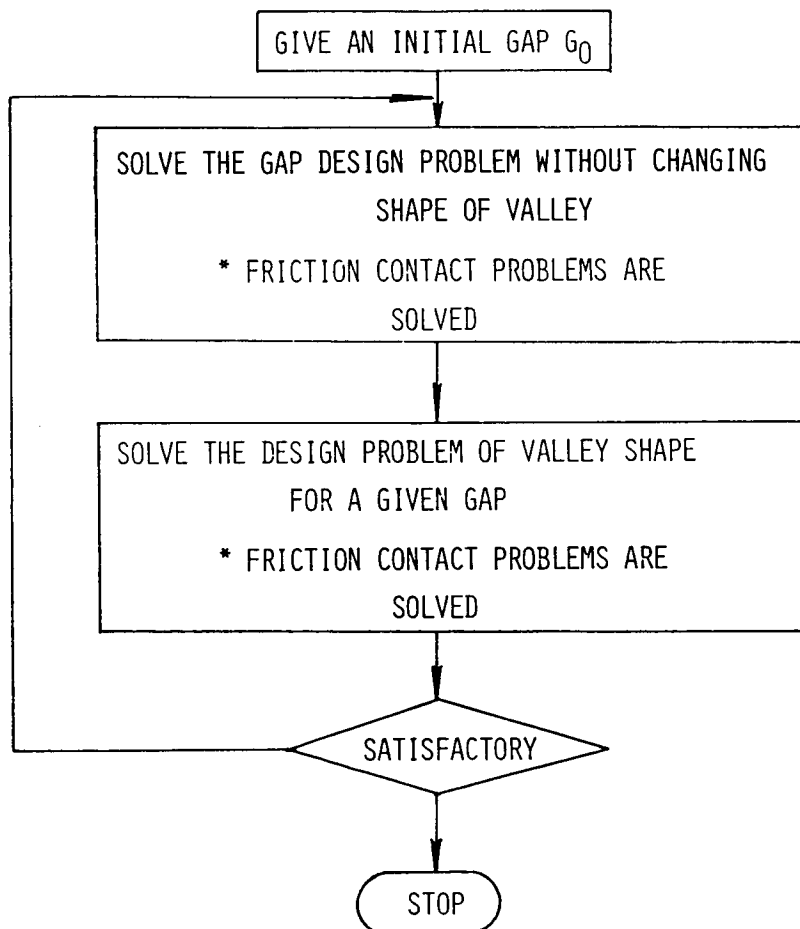


Figure 6

EXAMPLES - FRICTION CONTACT PROBLEMS

Figure 7 shows an example of friction contact problems solved by the penalty-regularity method. The unilateral contact condition $\underline{u}_R \cdot \underline{N} - g_0 \leq 0$ is resolved by the exterior penalty method. In this case if ϵ is the penalty parameter and is a sufficiently small number, then the boundary condition on a possible contact surface becomes $p_\epsilon = -(\underline{u}_R \cdot \underline{N} - g_0)^+ / \epsilon$ where p_ϵ is an approximation of the contact pressure and a function h^+ means h if $h > 0$ and zero if $h \leq 0$. The boundary condition in the tangential direction due to Coulomb's friction law is regularized by a differentiable one using an approximation of the absolute function. That is, a differentiable function ϕ_ϵ is introduced to have a smooth friction law. This method is called the regularity method. Convergence of an iterative method to solve the system of non-linear equations obtained by a finite element approximation, is achieved within seven to ten iterations.

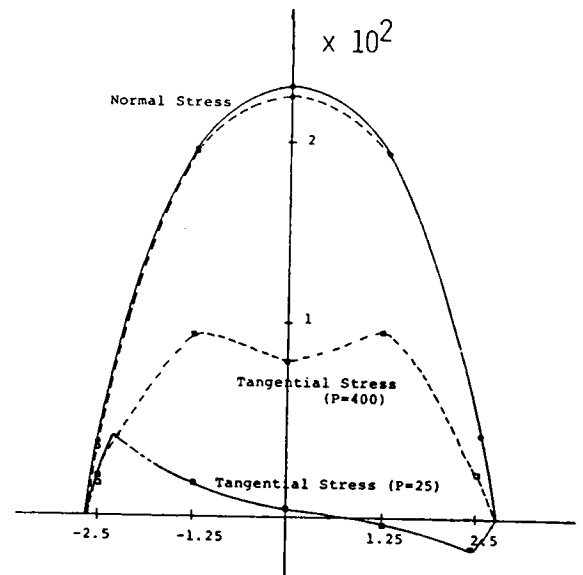
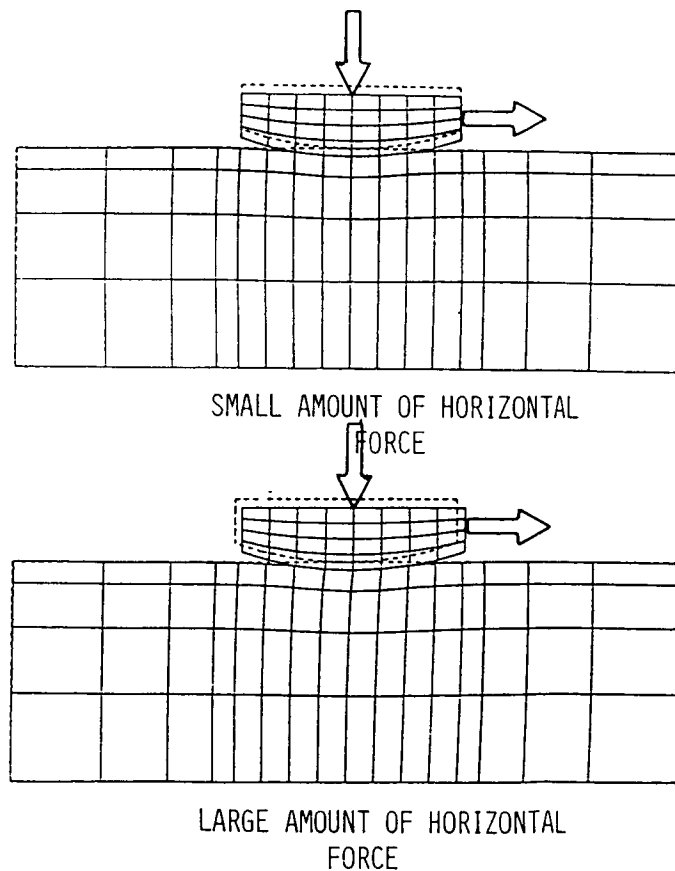


Figure 7

EXAMPLES - SHAPE OPTIMIZATION

Figure 8 shows an example of shape optimization problems. A thin linearly elastic plate is under a tension field, and the upper surface of the plate is designed to reduce the value of the maximum shear stress under the constraint on the volume of the plate. The design on the left hand side is obtained without using the finite element grid optimization routine and a smoothing scheme of the design surface. The design on the right hand side is obtained using these additional capabilities. The results show that the grid optimization and the smoothing scheme are very helpful to obtain a smooth design.

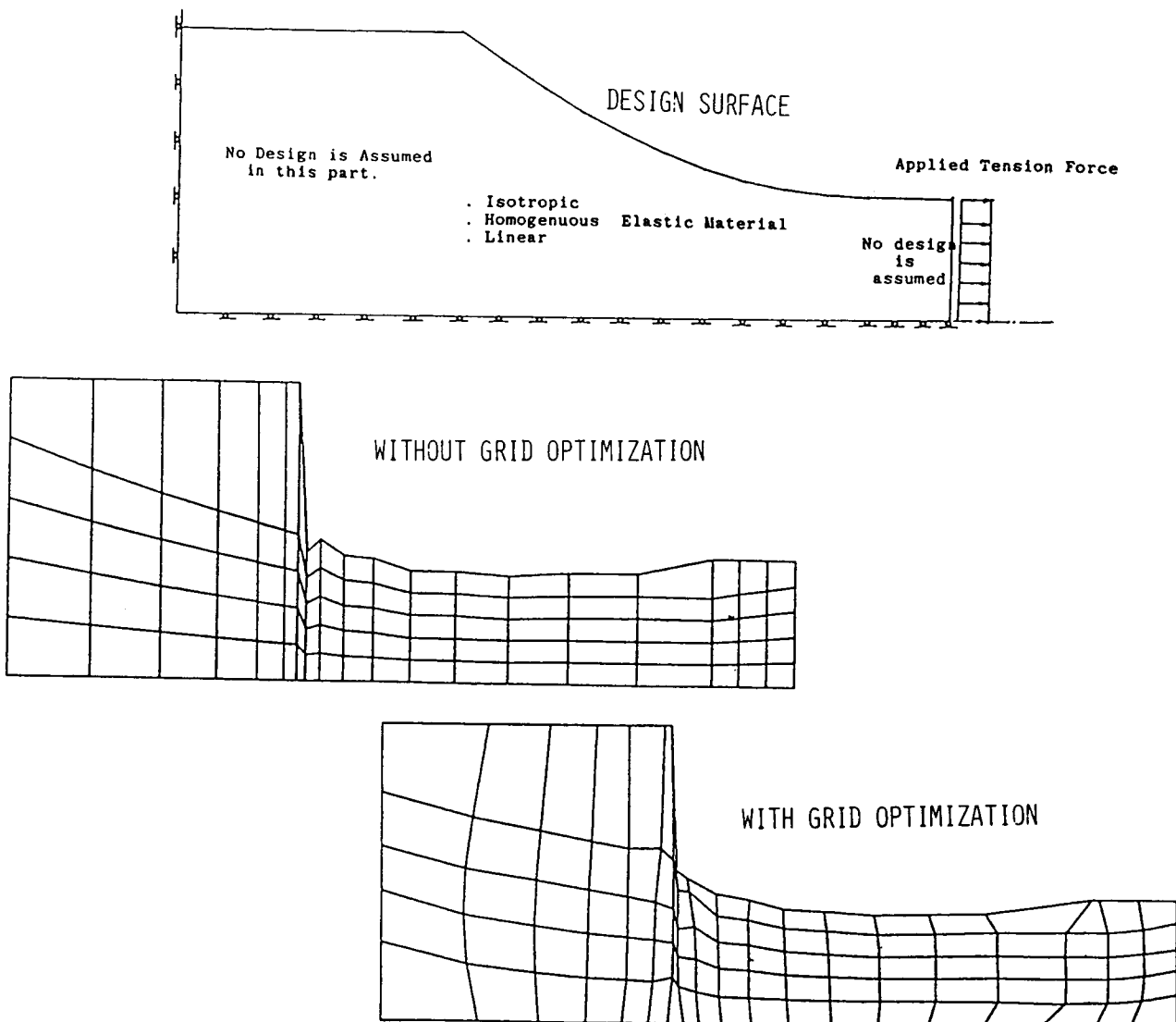


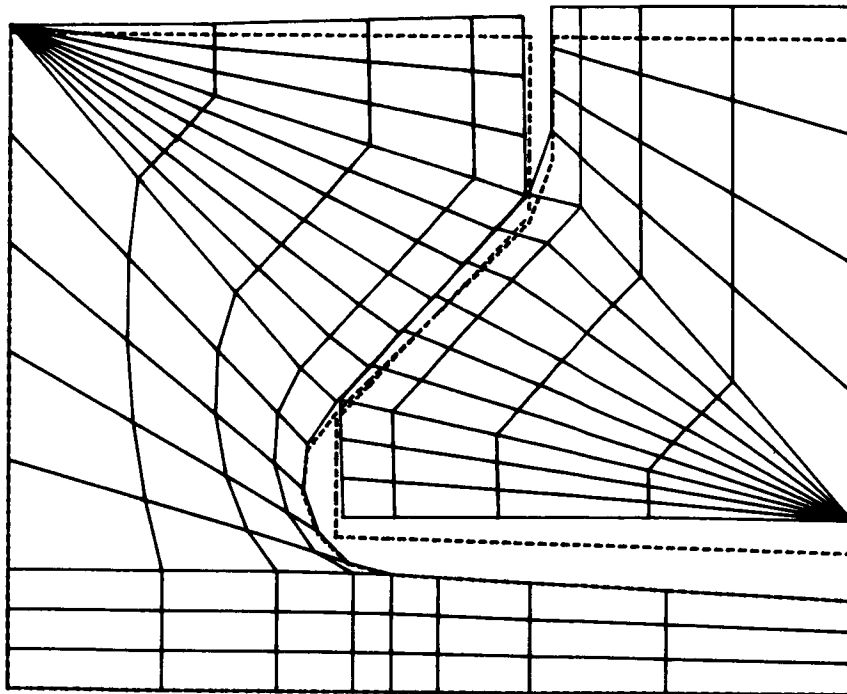
Figure 8

THE BLADE-ROOT/HUB

EXAMPLE - DESIGN OF INTERFACE

Figure 9 shows a model problem of a design of the blade-root/hub interface. Design of shape is combined with the algorithm for solving friction contact problems, although the grid optimization routine is not interfaced in the present example.

ORIGINAL AND DEFORMED SYSTEM



3000 rpm

Total 10 iterations

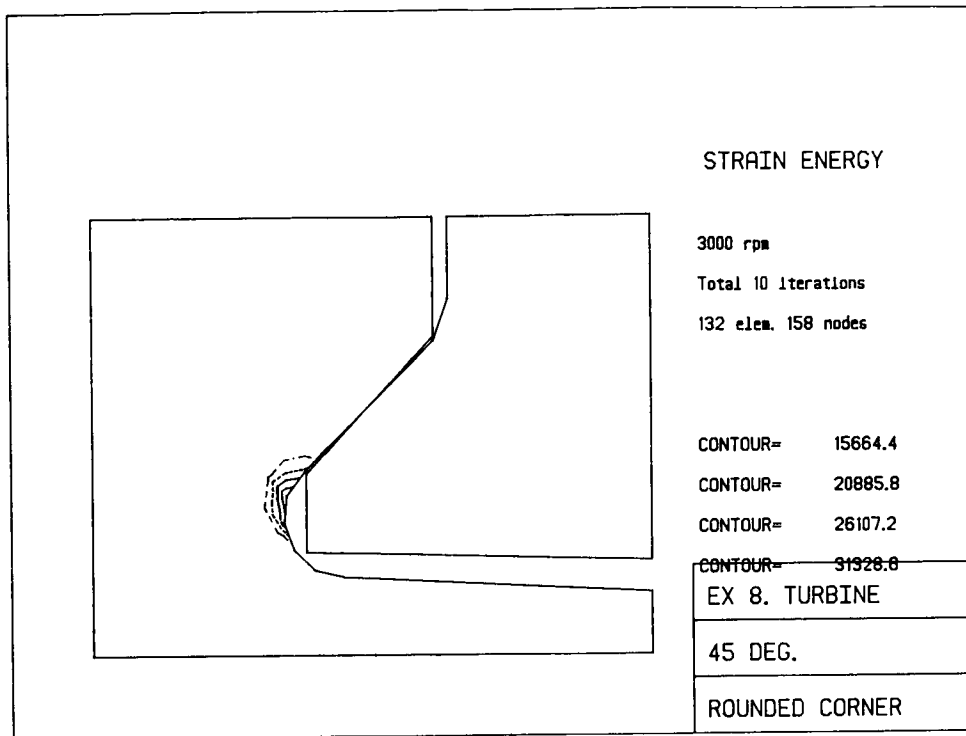
132 elem. 158 nodes

EX 8. TURBINE

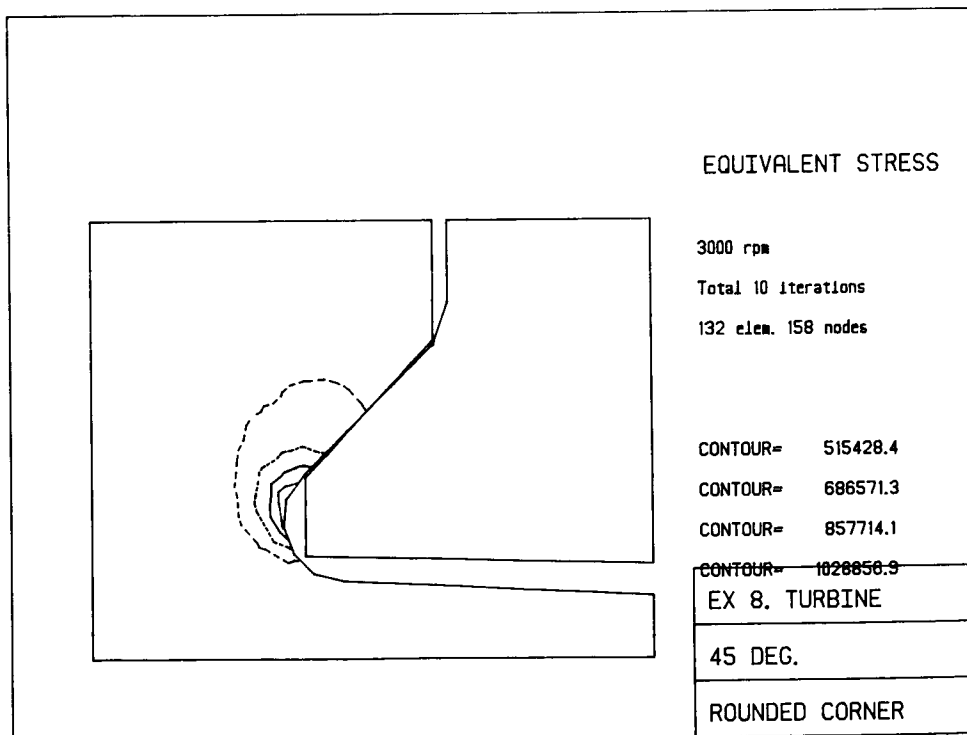
45 DEG.

ROUNDED CORNER

(a)
Figure 9

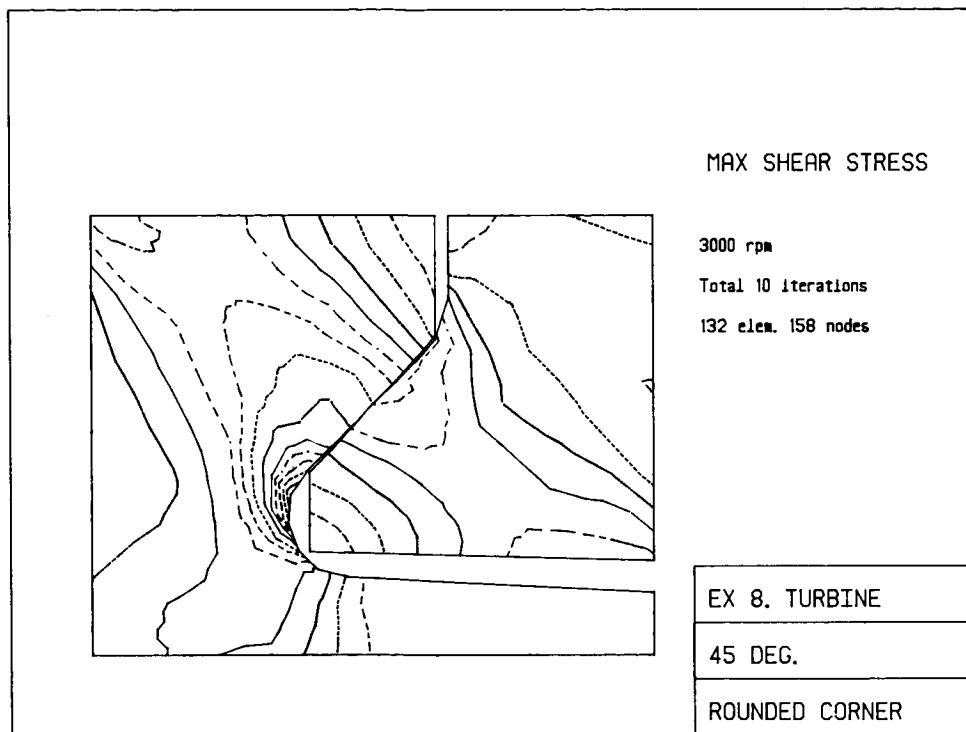


(b)

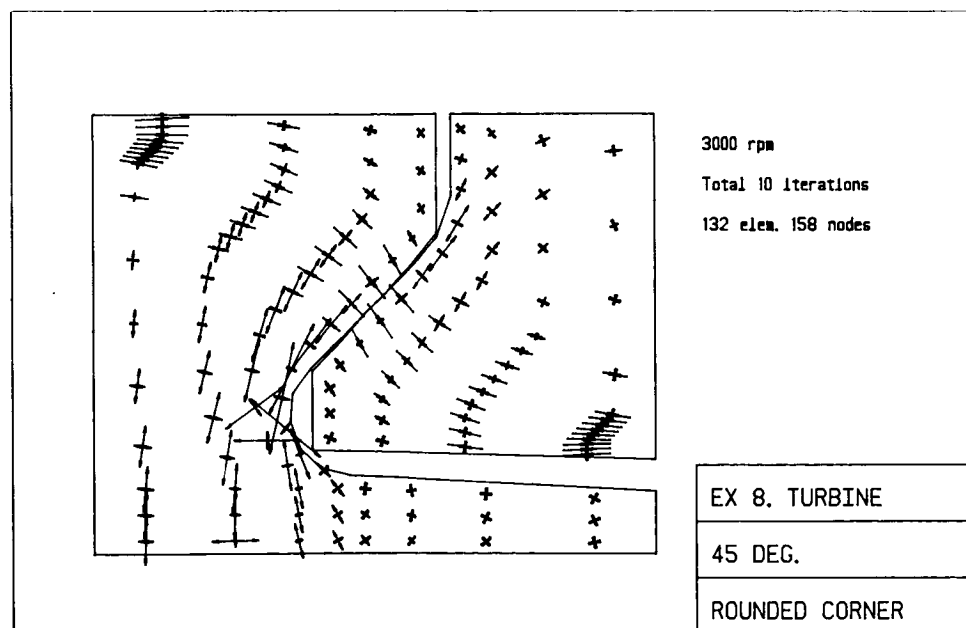


(c)

Figure 9.- Continued.



(d)



(e)

Figure 9.- Concluded.

FURTHER DEVELOPMENT

We have analyzed the optimal shape design problem of blade-root/hub interface by dividing the original problem into several parts for the friction contact and shape optimization problems. Furthermore, the finite element grid design problem is also defined in order to improve the quality of approximations. The future studies are to make use of combinations of these segments. Especially, combination of the shape and gap design problems is the next subject to be studied. After this, the grid optimization routine must be interfaced into the means for solution (see Figure 10).

ACKNOWLEDGEMENTS

The present work is performed jointly with Dr. A. R. Diaz (responsible for developments in the grid optimization scheme), Mr. T. Ting, and Mr. K. Y. Chung (performed programming and obtained results for the sample problems). The authors express their appreciation to them.

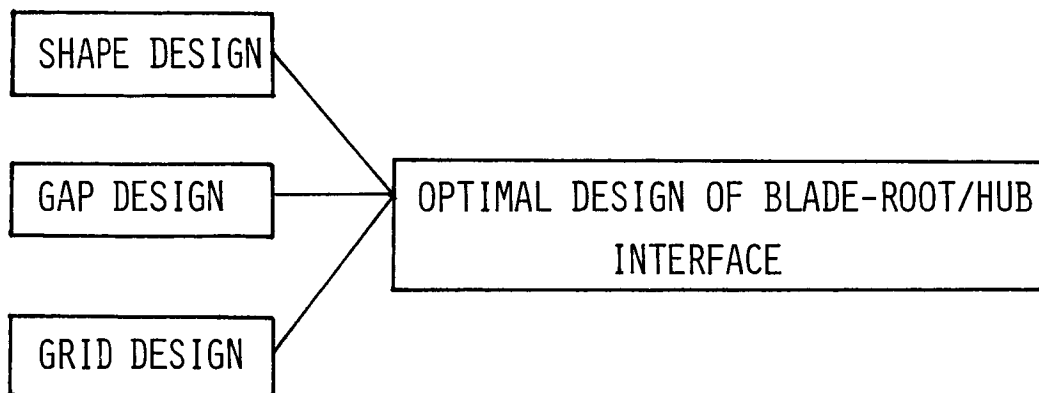


Figure 10

N87-11770

PROBLEMS IN LARGE-SCALE STRUCTURAL OPTIMIZATION

Jasbir S. Arora
University of Iowa
Iowa City, Iowa

and

Ashok D. Belegundu
GMI Engineering & Management Institute
Flint, Michigan

1. INTRODUCTION

During the year 1979, it was observed that the methods of structural optimization were not being utilized in the industry as extensively as expected. About 20 years of extensive research on methods of structural optimization had been conducted by that time. Several researchers had demonstrated applications of optimization methods on various classes of problems. It was disappointing to find that the general engineering design community was not taking advantage of the advanced technology. Therefore, it was decided to determine reasons for this lack of interest. The first observation was that some designers had tried optimization methodology without success. There was a general feeling in the community that optimization methods could be used only by the experts. The second serious problem was that general purpose software that could handle each designer's cost and constraint functions was not available for the solution of engineering design problems. A major reason was that it was not known which method would be most suitable for engineering design applications. Therefore, there was a need to conduct a comprehensive study to evaluate various available methods with a particular regard to their suitability for structural design optimization problems. Such a study was started in 1979 and completed by the middle of 1982. Results of this study are presented in this paper. Throughout the paper, reference is made to structural optimization problems. However, the discussion is applicable to the design of mechanical as well as other complex engineering systems.

It is somewhat satisfying to see the use of optimization methodology being accelerated in the recent past. For example, some real world applications of optimization methods were presented at the recent Euromech Colloquium [1], 18th Midwestern Mechanics Conference [2], International Symposium on Optimum Structural Design [3], and the 11th IFIP Conference on System Modelling and Optimization [4]. More effort is beginning to be spent on software development. For example, the incorporation of design sensitivity analysis into MSC/NASTRAN [5], IDESIGN program [6], OPT package [7], and many other special purpose programs [8-12] have been developed in the recent past. However, substantial effort needs to be expended in these areas to fully realize the potential of optimization methods.

In this paper, a general design optimization model for large complex systems is defined. Major features of the model that challenge various optimization algorithms are discussed. Requirements of a model optimization algorithm are identified. Objectives of the study of various algorithms are defined and a basis for conducting such a study is developed. Primal as well as transformation methods are analytically studied and a unified viewpoint of various methods is presented. Several numerical examples are solved using different methods to study their performance. Conclusions drawn from the study are presented and discussed. Areas of future research in nonlinear programming as well as structural optimization are identified and discussed.

2. DESIGN OPTIMIZATION MODEL FOR LARGE SYSTEMS

In this section, a general design optimization model and its features are presented and discussed.

2.1 Design Optimization Model

Let $b \in R^n$ be a vector of design parameters. Then a general design optimization problem is defined as follows:

$$\min f(b); \quad b \in S \quad (2.1)$$

where the constraint set S is a subset of R^n defined as

$$S = \{b: g_i(b) = 0, i = 1 \text{ to } m'; g_i(b) \leq 0, i = (m' + 1) \text{ to } m\} \quad (2.2)$$

It is assumed that the functions $f(b)$ and $g_i(b)$ are at least continuously differentiable. In appearance, the model defined in Eqs. (2.1) and (2.2) is identical to the standard nonlinear programming problem. However, there is one very important difference. The difference is that some of the functions $f(b)$ and $g_i(b)$ are implicit functions of design variables b . That is, the explicit form of these functions in terms of the design variables is not known. The functions can usually be evaluated only after a large, complex analysis problem has been solved.

There are several classes of engineering design problems that can be represented [13] by the model defined in Eqs. (2.1) and (2.2). For example, minimum weight structural design problems with stress, displacement, buckling load, natural frequency, and other constraints under static as well as dynamic loads; mechanical system design optimization; fail-safe optimal structural design problems; kinematic synthesis; and optimal design of large systems with substructures can be represented by the model. In addition, there are many problems of optimal shape design of systems or subsystems that are represented by the model.

With the above definition of the design optimization model, we are in a position to define what is meant by large-scale optimization problems. Of course, the obvious definition is that the numbers of design variables and/or constraints are large. Typically, $n \geq 25$ and/or $m \geq 100$. However, in engineering design, the problem can be classified as a large-scale problem even if n and m are not very large. The reason for this is that the analysis model can be so large that it can take hours of CPU time on a fast computer to calculate functions and their gradients. This is true for problems that require large dimensional finite element models to accurately predict response of the system. For transient dynamic response problems, even smaller-degree-of-freedom models can consume a large amount of CPU time. Therefore, we will classify any engineering design problem to be of large scale if $n \geq 25$ and/or $m \geq 100$, or if it has implicit functions that require a large amount of CPU time to compute function values.

2.2 Major Difficulties

The most prominent difficulty with problems of engineering design is the implicit nature of the functions. As noted, evaluation of the functions can require an enormous amount of computational effort. In addition, the evaluation of gradients of such functions requires not only additional computational effort, but also computer programming effort. For each class of problems, special programs must be developed to evaluate functions and their gradients. These programs can be very large, needing advanced database management and software development concepts. Depending on the type of problem, this process may require several man-years of effort.

Another difficulty with problems of engineering design is that, in general, the problem cannot be shown to be convex. In fact, engineering design problems are characterized by the presence of multiple local minima. This means that several starting designs must be tried and the problem optimized each time in the hope of obtaining a better design. This can be a tedious and time-consuming process.

Software for design optimization is either not available or tedious to use. Most of the existing programs are not interactive. They do not allow any user control over the iterative process. Graphics capability is almost unheard of in design optimization software. In addition, many of the programs have no proven global convergence properties. In this regard, it must be observed that the engineering design community has not developed algorithms and software based on strict global convergence theory. Global convergence is an indication of the reliability and robustness of an algorithm. Use of globally convergent algorithms in engineering design will require less adjustment of various parameters and consequently, less expertise in optimization theory on the part of the general user. More attention should be paid to this aspect in engineering design applications.

3. MODEL DESIGN OPTIMIZATION ALGORITHM

In this section, we describe a model algorithm for engineering design optimization. We must strive to develop such an algorithm in the future. Most existing algorithms can be described by the following iterative prescription:

$$b^{(k+1)} = b^{(k)} + \alpha_k p^{(k)}; k = 0, 1, 2, \dots \quad (3.1)$$

where k is the iteration number, $p^{(k)}$ is a direction of desirable move in the design space, α_k is a step length along the direction $p^{(k)}$, and $b^{(0)}$ is an initial design estimate.

An obvious requirement of an algorithm for large scale optimization is that it must be efficient. Efficiency of an algorithm can be improved in two ways: (i) by reducing the total number of iterations, and (ii) by reducing the computing time per iteration. With regard to reducing the total number of iterations, it is desirable for an algorithm to have a superlinear or quadratic rate of convergence. Many methods incorporate quasi-Newton updates for Hessian matrix of the Lagrangian function into their algorithm to achieve a superlinear rate of convergence. The basic idea here is that with the curvature information for the Lagrange function incorporated into an algorithm, a better direction of design improvement is obtained, thus accelerating the rate of convergence.

With regard to reducing computing time per iteration, calculations for $p^{(k)}$ and α_k should be as efficient as possible. Efficiency of calculations for the direction vector $p^{(k)}$ in engineering design applications can be substantially improved if active set strategies are used in an algorithm. The reason for this is that with active set strategies, gradients of only a subset of the constraints are needed. This results in significant savings because of the implicit nature of the functions. Note, however, that use of an active set strategy should not destroy any global convergence properties that the algorithm may have.

Another very important calculation at each design iteration is to determine the step size α_k . Many methods calculate step size by minimizing a descent function along the direction $p^{(k)}$. The descent function is usually constructed using the functions of the problem. To find α_k , therefore, a search must be performed along the direction $p^{(k)}$, which requires an evaluation of functions. Since many functions are implicit in engineering design, an evaluation of the exact α_k can require an enormous amount of calculations. Thus, approximate strategies must be developed to calculate the step length, or perhaps the use of a descent function and the associated line search should be avoided altogether.

The problem of determination of a step length, however, is more involved than it appears. It turns out that global convergence of an algorithm is assured through the requirement that a descent function must reduce in value at each iteration. This is assured by calculating the proper step length. Since global convergence is a 'must' for an algorithm that has to be applied to problems of engineering design, it does not seem possible to avoid a one-dimensional search for computing the step length.

The algorithm to be used in engineering design environment must treat the general optimization problem defined in Eqs. (2.1) and (2.2). In other words, equality constraints must also be treated. No assumptions regarding the form of the functions of the problem (i.e., linear, posinomial, separable) should be made.

Finally, the user should not be required to select too many parameters related to the optimization algorithm. The general user is usually not an expert in optimization theory, so he will not know how to select the parameters. In addition, he cannot be expected to fix any failures of the algorithm. Therefore, a good algorithm should be self correcting. If failure does occur, the user should be given some indication of where the trouble may have occurred and how to fix it. In summary, then, the model algorithm must be generally applicable, efficient, globally convergent, and easy to use, and must incorporate active set strategy.

4. PURPOSE OF THE STUDY

A natural question now arises: which of the existing methods is/are most suitable for solving (2.1)? Unfortunately, very few comparative studies have been done in optimal design of structural systems. The emphasis has been on studying one particular method by solving a variety of problems without considering how it compares with other existing methods. As a result, we now have several algorithms whose relative performance is not properly understood.

A few studies have been conducted in the field of mathematical programming (MP). However, it may not be possible to correlate the performance of an algorithm on MP problems with its performance on structural optimization problems. The reason is that the MP problems do not possess many of the difficulties present in the structural problem. The first comprehensive study in the field of mathematical programming was conducted by Colville [14]. Since then, other comparative studies have been conducted by Stocker [15], Himmelblau [16], Biggs [17], Schittkowski [18], Miele et al. [19], and a few others. The study of Sandgren and Ragsdell [20] is based on a solution of some problems in engineering design. However, the

problems chosen are of the MP type: explicit functions, small dimension ($n + m \leq 51 + \text{bounds}$). Problems with multiple local minima are not considered.

In structural optimization, far less information is available on the relative merits of algorithms. De Silva and Grant [21] have compared penalty function techniques by solving a planar truss problem. Their study, however, considered only Sequential Unconstrained Minimization Techniques (SUMT's). Carpenter and Smith [22] have also studied SUMT's for solving structural design problems. Their emphasis is on studying the unconstrained minimization algorithms used in SUMT's and comparing the use of finite difference versus analytical computation of gradients. In the second study by Carpenter and Smith [23], which is fairly comprehensive, the method of sequential linear programming, a feasible directions method, and SUMT's are considered. Trusses and plates are used as test problems. The main conclusion reached by these authors is that the sequential linear programming method is more efficient than both the SUMT's and the method of feasible directions. However, this conclusion is questionable because the gradient of the penalty function in SUMT's is computed inefficiently [22] and not by the efficient technique recommended by Belegundu and Arora [24]. Use of the technique in Ref. 22 will make SUMT's more competitive in the study. Furthermore, multiplier methods are not included in that study.

The present study differs from previous studies because the difficulties posed by problem (2.1) are addressed, a number of recently developed algorithms are included, both theoretical as well as numerical aspects are considered, and some relatively large scale problems are solved. Aims of the study are to identify strengths and weaknesses of a method and to develop a unified viewpoint for the NLP methods.

5. ANALYTICAL EVALUATION OF NONLINEAR PROGRAMMING METHODS

In Section 3, essential features that an algorithm should possess for structural optimization were presented. In this section, we will examine how existing methods measure up to the stated requirements. Specifically, the following basis is used to study each method. (1) The presence of implicit functions makes problem (2.1) different from an MP problem. It is therefore examined whether a given method is especially suited for handling such implicit functions. (2) The geometrical significance of the direction vector $p^{(k)}$ in Eq. (3.1) is studied to bring out similarities and differences between methods. (3) The global convergence properties of a method are studied. (4) It is examined whether the method uses an active set strategy. Further, it is determined whether any global convergence properties that the method possesses are valid with the use of an active set strategy. (5) It is examined whether the method uses the W matrix (which is a positive definite approximation to the Hessian of the Lagrangian function), or if not, whether it is possible to incorporate this matrix into the method. Use of such a method leads to superlinear convergence.

Various gradient-based NLP methods can be grouped under primal methods and transformation methods. By a primal method of solution, we mean a method that works directly on the original problem given in (2.1). In primal methods, the direction vector $p^{(k)}$ at the k th iteration is determined by an expression of the form

$$W^{(k)} p^{(k)} = \mu_0 N^0 + \sum_{i \in I_k} \mu_i N^i \quad (5.1)$$

where μ_0 and μ_i are scalars (Lagrange multipliers), N^0 and N^i are gradients of the cost and constraint functions, respectively, matrix $W^{(k)}$ was defined earlier, and I_k is the active constraint set. It is evident from (5.1) that computing $p^{(k)}$ requires computing the gradient vectors N^i of individual functions that are in the set I_k .

Transformation methods are based on solving (2.1) by reformulating it as a sequence of unconstrained minimizations. In this class of methods, the design is updated during an unconstrained minimization, and $p^{(k)}$ is obtained by an expression of the form

$$W^{(k)} p^{(k)} = - \nabla \phi(b^{(k)}, \theta^{(k)}) \quad (5.2)$$

where $W^{(k)}$ is a known matrix and $\theta^{(k)}$ is a vector of known parameters. In (5.2), even though ϕ depends on the functions g_i for $i \in I_k$, computing $\nabla \phi$ does not require computing the gradients N^i of individual constraint functions. This is desirable for structural optimization problems and is discussed in more detail in Refs. 24 and 25. As a result, we conclude that transformation methods possess a special structure to handle implicit functions and primal methods do not. Therefore, the classification into primal and transformation methods is intimately related to the structure of the structural optimization problem.

5.1 Primal Methods

Recursive QP Methods

Recursive quadratic programming (RQP) methods have been recently developed [26-34]. They are gaining popularity due to their strong convergence characteristics. The basic idea behind RQP methods is to develop Newton-like algorithms for constrained optimization. This results in the iterative solution of the QP:

$$\begin{aligned} \min \quad & N^0 p + 1/2 p^T W p \\ \text{s.t.} \quad & N^i p + g_i = 0, \quad i \in I_1 \\ \text{and} \quad & N^i p + g_i \leq 0, \quad i \in I_2 \end{aligned} \quad (5.3)$$

where W , N^0 , N^i , and g_i are all evaluated at $b^{(k)}$, and I_1 and I_2 are active sets associated with the equality and inequality constraints, respectively. Once p is obtained from (5.3), a step length is estimated along p by minimizing a descent function.

A relatively straightforward calculation shows [34] that the solution p of (5.3) can be expressed as

$$p = -p^1 + p^2 \quad (5.4)$$

where p^1 is a vector obtained by projecting the cost gradient into the tangent hyperplane to the active constraints, and p^2 is a vector normal to this hyperplane. The p^1 and p^2 directions are shown in Fig. 1. The vectors p^1 and p^2 are orthogonal (relative to the W matrix). From Fig. 1, we see that $-p^1$ is a cost

reduction step while p^2 is a constraint correction step. Thus, the p -vector in RQP methods tries to achieve a simultaneous reduction in cost and constraint violations. So far, two globally convergent RQP algorithms have been developed. One is by Han [29] in 1977 and the other by Pshenichny [30] in 1978.

Han's Algorithm: No active set strategy is used [29]. The QP in (5.3) solved at each iteration includes all m constraints of the original problem. This is needed to ensure that p is a continuous function of the design variable. The fact is used to prove global convergence of the algorithm. The algorithm is unsuitable for structural optimization due to the enormous computation involved. However, Han obtains superlinear convergence by taking W to be a positive definite approximation to $\nabla^2 L$, where L is the Lagrangian function. Powell [32], who has implemented a modified form of Han's algorithm, has generated W using a quasi-Newton update.

Pshenichny's Algorithm: Global convergence has been proved using an active set strategy [30]. This algorithm has been successfully used for structural design problems [34]. Pshenichny, however, ignores the possibility of using second order information in the W -matrix. He takes W as an identity matrix. We can therefore accelerate Pshenichny's method by taking W to be a positive definite approximation to $\nabla^2 L$.

RQP methods possess a common drawback. The step length α is determined by minimizing a descent function of the form $\theta(b) = f(b) + rF(b)$, where $F(b)$ is some penalty function that measures the amount of infeasibility of design b . The difficulty is that the scalar r tends to become large during the iterative process. This results in small step size because of greater emphasis on constraint feasibility.

Gradient Projection Methods

The gradient projection method was first developed by Rosen [35] in 1961. Feasible directions methods that were developed earlier (in 1960 [36]) involved

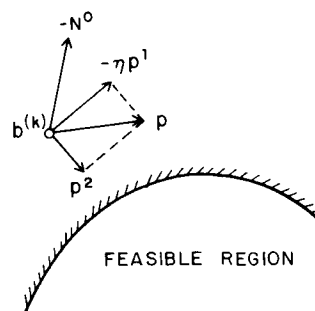


Figure 1. p^1 and p^2 Vectors

solving an LP or QP subproblem at each iteration. However, if the cost of function and gradient evaluations was small compared to that of solving a linear program, then feasible direction methods could become expensive to use. Rosen was thus motivated to develop a method in which the direction vector could be obtained in a closed form rather than by solving an LP or QP subproblem. Thus, in contrast with feasible directions methods, the gradient projection method uses a direction vector which is not the best but is much easier to compute. It was noted in Section 2 that function and gradient evaluations in structural optimization are enormously expensive. Because of this, it is better to solve a relatively inexpensive LP or QP subproblem and obtain the best possible improvement in design, rather than implement the gradient projection philosophy.

An analysis of the gradient projection methods helps to view the method in terms of the p^1 and p^2 steps discussed in connection with RQP methods. First, a $-p^1$ step is taken from a feasible design $b^{(k)}$. Let α be the step size in this direction. Then, a new design $b^{(k,1)} = b^{(k)} + \alpha p^1$ is obtained, which is in general infeasible (Fig. 2). Now, a sequence of p^2 steps, or 'correction' steps, is taken to obtain a new feasible design, $b^{(k+1)}$.

Because of sudden changes in the active set, the gradient projection method has not been proved to be globally convergent. Further, modifying the method to make it globally convergent would destroy the basic simplicity of the method. Another disadvantage is that it is difficult to maintain descent. Thus, it may happen that upon returning to the feasible region, $f(b^{(k+1)}) > f(b^{(k)})$. In this case, a smaller step α has to be chosen from the previous feasible design $b^{(k)}$, and the correction procedure has to be re-initiated. This 'orthogonal iteration' can be quite expensive. Moreover, the correction procedure needs special care to ensure that a solution exists. Finally, though a W-matrix can be incorporated into the method in calculating p^1 and p^2 , it is computationally difficult to maintain quasi-Newton updates because of the complicated logic involved.

Reduced Gradient Methods

Reduced gradient methods are based on the simple variable elimination technique developed by Wolfe [37] in 1967. The idea is to use the constraints satisfied at equality at the current point to eliminate some of the variables. The problem then becomes unconstrained in the remaining variables.

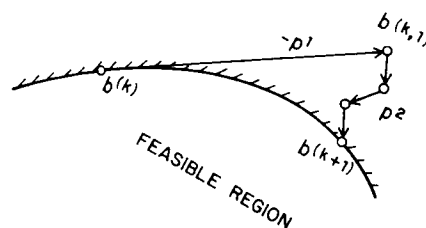


Figure 2. Gradient Projection Method

There is, however, some confusion in both the mathematical programming literature as well as the structural optimization literature on the relative merits and demerits of the reduced gradient methods. For example, the reduced gradient method has been declared superior to the gradient projection method [20,38], whereas these two methods are considered to be essentially the same in Ref. 39. The confusion arises when studying reduced gradient methods in the context of solving inequality constrained problems. Some researchers convert the inequality constrained problem to an equality constrained one by adding nonnegative slack variables, while others adopt an active-set strategy. It turns out that if an active-set strategy is used, the reduced gradient method becomes essentially the same as the gradient projection method. On the other hand, if the inequality constrained problem is converted to an equality constrained problem, then the reduced gradient method behaves quite differently from the gradient projection method. In this case, the reduced gradient method is more efficient than the gradient projection method and can also be shown to be globally convergent (unlike the gradient projection method). Unfortunately, the inequality constrained problem in structural optimization has to be solved using an active-set strategy. The reason for this is that the addition of slack variables to convert inequalities in equalities implies that all constraints are active and hence have to be differentiated. This is ruled out in large-scale structural optimization because of enormous computation and storage of information involved. Therefore, when solving structural optimization problems we need not differentiate between gradient projection and reduced gradient methods.

Method of Bard and Greenstadt

Though this method assumes convexity of the problem (which cannot be assumed for the structural problem) it is briefly examined here because it casts further light on the p^1 and p^2 directions discussed earlier.

It was noted that the direction p (Fig. 1) tries to reduce both cost and constraint violation. There is thus no single-purpose goal for selecting step size along p . Bard and Greenstadt [40] were therefore motivated to decompose p into two directions; s^1 and s^2 maximizes the Lagrangian. They then consider an algorithm in which these steps are taken alternately. The attraction of this algorithm is that in making each step, the aim of either minimizing or maximizing the Lagrangian is well defined. As a result, step size selection along each step is not a difficulty. It turns out that the s^1 and s^2 directions are identical to the p^1 and p^2 directions discussed earlier.

We therefore see that the p^1 and p^2 steps form the backbone of the primal methods discussed above. The aims of these different methods are shown in Fig. 3. The geometrical similarity between these methods is tied into common difficulties with step size selection, maintaining descent and global convergence.

Feasible Directions Methods

The idea behind these methods is to move from one feasible design to an improved feasible design. This is in contrast to the 'exterior point' methods studied above which iterate through the infeasible region. Feasible directions methods solve an LP or QP subproblem which yields an 'improving feasible direction', d . The vector d satisfies the conditions $N^0 T d < 0$ and $N^i T d < 0$ for $i \in I_k$. Such a direction d is shown in Fig. 4. The solution of the LP or QP

subproblem to determine d also involves certain user-supplied parameters, θ_i , called the 'push-off' factors (Fig. 4). The greater the value of θ_i , the greater the direction is pushed away from the i th constraint boundary into the feasible region.

Evidently, the direction vector used in feasible directions methods is conceptually different from the p^1 and p^2 directions of earlier methods. Some feasible directions methods are proved to be globally convergent and also use an active set strategy. Zoutendijk's ϵ -perturbation algorithm [36] and an algorithm by Polak [41,42] are in this category. On the other hand, Topkis and Vienott's algorithm [43] is globally convergent but does not use an active set, which makes it inapplicable to structural design problems.

Theoretically, therefore, feasible directions methods are quite attractive. Computationally, however, there are certain major difficulties. First, a constrained line search has to be performed. Second, it is clear that a good

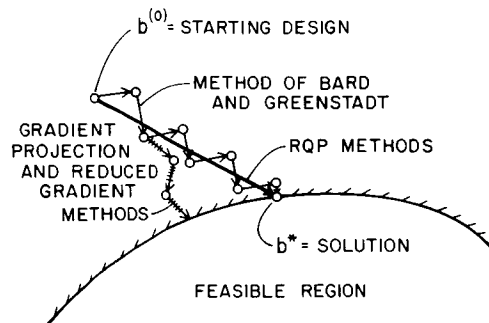


Figure 3. The Aims of Different Methods

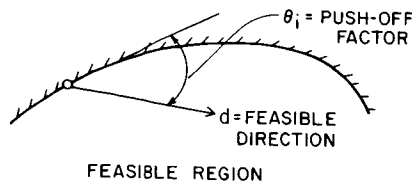


Figure 4. Feasible Direction

choice of push-off factors θ_i at a current design $b^{(k)}$ requires information about the curvature of the constraint functions. Since the curvature is different at different points, no initial choice of θ_i can, in general, be made to obtain rapid convergence. Note that if θ_i are too small, then the design iterations constantly hit the constraint boundary, slowing down convergence. One may possibly infer from this that feasible directions methods will work best in an interactive mode.

In existing feasible directions methods, no curvature information is used, and hence only linear convergence can be expected. In defining the QP subproblem, a normalization constraint of the form $1/2d^T d \leq 1$ is used. It is suggested instead to use the constraint

$$1/2d^T W d \leq 1 \quad (5.5)$$

where W is the usual quasi-Newton approximation to $\nabla^2 L$. Use of curvature information in W can be expected to accelerate convergence, and perhaps alleviate the difficulty in choosing appropriate values for the push-off factors. This, at any rate, needs to be investigated.

Sequential LP Methods

In these methods, an LP subproblem is obtained by linearizing the cost and constraint functions about the current design and imposing a linear step size constraint. The LP subproblem at each iteration is

$$\begin{aligned} \min \quad & N^0 p \\ \text{s.t.} \quad & N^1 p + g_1 = 0, \quad i \in I_1 \\ & N^1 p + g_i \leq 0, \quad i \in I_2 \\ \text{and} \quad & |p_j| \leq \xi_j, \quad j = 1 \text{ to } n \end{aligned} \quad (5.6)$$

where p is the direction vector, I_1 and I_2 are active sets associated with the equality and inequality constraints, respectively, and ξ_j are move limits input by the user. These methods are known to researchers in structural optimization, but are not used by researchers in mathematical programming.

Major difficulties with this type of method are listed below.

(1) The step size constraint $|p_j| \leq \xi_j$, $j = 1, \dots, n$, causes difficulty in identifying a descent function. The descent function used in RQP methods does not serve as a descent function in (5.6), as may be verified. Absence of a descent function makes it difficult to estimate step size and to prove global convergence.

(2) Referring to Fig. 5, we notice that if ξ_j in (5.6) are chosen too small, then no solution may exist for the subproblem. On the other hand, if ξ_j is large, then p may become large. A step size control along p then becomes necessary. Unfortunately, this is difficult in view of (1) above.

These difficulties and the fact that only linear convergence is possible (since no curvature information is involved) make sequential LP methods inferior compared to RQP methods. The reason is that function and gradient calculations

require much more computation than solving an LP or QP subproblem in structural optimization. Thus, one may as well solve a QP instead of an LP and use a method that is superlinearly and globally convergent.

Other Primal Methods

We will briefly comment on other primal methods. Optimality criteria methods have been used for structural optimization [44,45]. These methods are based on iterative techniques for solving the nonlinear set of necessary conditions. A major difficulty with the methods is that a descent towards the optimum can not be maintained. Therefore global convergence of the methods can not be proved.

There are other projection methods that have been developed in the MP literature [46]. These are iterative techniques based on a combination of active set selection and projection concepts. The techniques have not been used for structural optimization.

There are other methods that involve solving a sequence of nonlinear subproblems [47]. The subproblem has a nonlinear objective function (the Lagrangian) and linear constraint approximations. Such methods are not suitable for structural optimization because (i) they are not globally convergent, and (ii) they require more computational effort.

5.2 Transformation Methods

The term 'transformation method' is used to describe any method that solves the constrained optimization problem by transforming it into one or more unconstrained optimization problems. Transformation methods include exterior and interior penalty function methods as well as augmented Lagrangian or multiplier methods.

Many of the constraint functions in optimal structural design are implicit functions of design variables. This implicit nature of the constraint functions makes it expensive to calculate their gradients. Transformation methods essentially collapse all constraints of the design problem into one equivalent functional constraint [48] which serves as a penalty term for the transformation methods. This is in contrast to primal methods, as discussed in Section 5.1.

There are three classes of transformation methods that have usually been discussed in the literature: the penalty function (exterior), the barrier (or interior penalty) function, and the multiplier (augmented Lagrangian) methods.

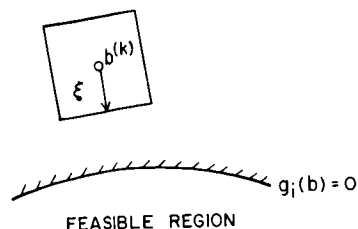


Figure 5. No Solution Exists to LP Problem

The penalty and barrier methods have been referred to as Sequential Unconstrained Minimization Techniques (SUMT's) by Fiacco and McCormick [49].

All transformation methods convert the constrained problem (2.1) into an unconstrained problem for the 'transformation function'

$$\phi(b, r) = f(b) + P(g(b), r) \quad (5.7)$$

where r , is a vector of controlling parameters and P is a real-valued function whose action of imposing the penalty is controlled by r . The local minimum of $\phi(b, r)$ at the k th iteration is denoted by $b^{(k)}$. The idea of transformation methods is very attractive because efficient unconstrained algorithms (e.g., Davidon-Fletcher-Powell method) [38] can be used to completely solve the constrained problem. It is shown that the idea of transformation methods is also very attractive for design problems in which implicit constraints must be treated.

SUMT's

The most popular penalty function is the quadratic function given by

$$P(g(b), r) = r \sum_{i=1}^{m'} [g_i(b)]^2 + r \sum_{i=m'+1}^m [g_i^+(b)]^2 \quad (5.8)$$

where r is a scalar parameter and $g_i^+(b) = \max(0, g_i(b))$. The inverse and log barrier functions are also quite popular [49]. The barrier methods, however, are not applicable to problems having nonlinear equality constraints. It can be shown that as $r^{(k)} \rightarrow \infty$, $b^{(k)} \rightarrow b^*$, where b^* is a solution of the constrained problem.

SUMT's possess a number of undesirable properties. The weaknesses are most serious when r is large. When r is large, the penalty and barrier functions tend to be ill-behaved near the boundary of the constraint set where the optimum points usually lie. There is also the problem of selecting the sequence $\{r^{(k)}\}$. The choice of $r^{(1)}$ and the rate at which $r^{(k)}$ tends to infinity can seriously affect the computational effort to find a solution. Furthermore, the Hessian matrix of the unconstrained function becomes ill-continued as $r \rightarrow \infty$ [38]. In spite of these difficulties, these methods have been used quite extensively for structural optimization. For barrier methods, Schmit and co-workers [50] and Haftka and co-workers [51] have used certain 'extended-barrier functions' which are free from weaknesses possessed by conventional barrier methods.

Multiplier Methods

The multiplier methods have been developed in the recent literature to alleviate some of the difficulties with SUMT's. In multiplier methods, there is no need for the controlling parameters r to go to infinity. As a result, the transformation function ϕ has good conditioning with no singularities. Furthermore, multiplier methods (like SUMT's) are globally convergent and have been proved to possess faster rates of convergence than SUMT's [52].

In multiplier methods, the penalty function is given as

$$P(g(b), r, \theta) = \frac{1}{2} \sum_{i=1}^{m'} r_i [g_i(b) + \theta_i]^2 + \frac{1}{2} \sum_{i=m'+1}^m r_i [(g_i(b) + \theta_i)^+]^2 \quad (5.9)$$

where θ_i and $r_i > 0$ are parameters associated with the i th constraint. The Lagrange multiplier μ_i associated with the i th constraint is given by $\mu_i = r_i \theta_i$.

If $\theta_i = 0$ and $r_i = r$, then (5.9) reduces to the well-known quadratic loss function given in (5.8) where convergence can be forced by letting $r \rightarrow \infty$. However, the objective of multiplier method is to keep each r_i finite. Furthermore, if $b(\theta)$ is obtained by minimizing $\phi(g(b)r, \theta)$, then the aim of choosing θ_i is such that

$$g_i(b(\theta)) \rightarrow 0 \text{ for } 1 \leq i \leq m' \text{ and } \max(-\theta_i, g_i(b(\theta))) \rightarrow 0 \text{ for } m'+1 \leq i \leq m \quad (5.10)$$

Powell [53] and Hestenes [54] have independently suggested a modified Newton formula for changing θ_i to satisfy (5.10). This method is especially attractive for large scale problems because of its simplicity. A second-order Newton method can also be used for changing θ_i . The idea behind selecting r_i is to make sure that the constraint violations are improved. This is done by suitably increasing the values of r_i . Details regarding changes in θ_i and r_i are given in Ref. 25. The increases in parameters r_i are especially significant because they lead to a practical method for enforcing global convergence. This fact is borne out by test results.

The geometrical significance of multiplier methods can be best understood by the following result derived by Powell [53]. He showed that minimizing $\phi(b, r, \theta)$ to obtain $b(\theta)$ is equivalent to solving the problem

$$\begin{aligned} \min \quad & f(b) \\ \text{s.t.} \quad & g_i(b) = g_i(b(\theta)), \quad i = 1 \text{ to } m' \\ \text{and} \quad & g_i(b) \leq \max(-\theta_i, g_i(b(\theta))), \quad i = (m' + 1) \text{ to } m \end{aligned} \quad (5.11)$$

From (5.11), the aim of changing θ in (5.10) also becomes clear. The iterative process is shown in Fig. 6.

The problem associated with step size calculations in primal methods to force convergence is not present in transformation methods. Transformation methods are more reliable as a result, and numerical results confirm this fact. In multiplier methods, the strategy for increasing r_i to ensure a monotonic reduction in the convergence parameter turns out to be an outstanding feature.

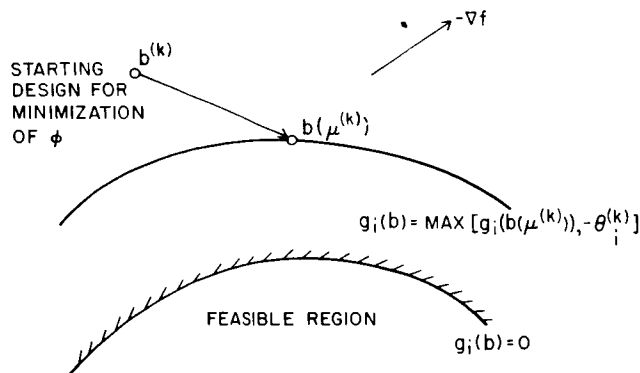


Figure 6. Direction Vector in Multiplier Methods

It has been shown [55] that Newton's formula to change θ leads to an arbitrarily fast rate of linear convergence by making r_i sufficiently large. Furthermore, the second-order formula to change θ leads to a superlinear rate of convergence. However, transformation methods require a series of unconstrained minimizations, which is quite expensive. This latter fact also raises a question about the level of approximation that needs to be maintained for each minimization.

Both SUMT's and multiplier methods use active set strategies. In penalty methods based on (5.8), an inequality constraint $g_i < 0$ need not be considered for evaluating ϕ or $\nabla\phi$. Similarly in multiplier methods, there is no need to consider an inequality constraint g_i for which $g_i + \theta_i < 0$.

More details about the methods can be found in Refs. 24, 46, and 56.

6. NUMERICAL EVALUATION OF PROMISING NLP ALGORITHMS FOR LARGE SCALE STRUCTURAL OPTIMIZATION

6.1 Test Problems

Most of the test problems are obtained from structural optimization literature. The twelve test problems include design of plane trusses as well as plane frames. In these problems, the cost function to be minimized is the weight of the structure. The constraints correspond to limits on stresses, displacements, and lowest natural frequency. The stress constraints are obtained from the AISC specifications [57]. Also, different cross-sectional shapes are used. Thus, the problems have a variety of cost and constraint functions. The problems are of different sizes; the number of design variables ranges from 3 to 47 and the number of constraints ranges from 3 to 252. A list of the test problems together with the number of design variables and constraints for each problem is given in Table 1. Detailed data and figures can be found in Refs. 46 and 58.

Table 1. PROBLEMS IN STUDY

| NO. | PROBLEM DESCRIPTION | n | m |
|-----|------------------------------|----|-----|
| 1 | ROSEN-SUZUKI (ref. 59) | 4 | 3 |
| 2 | SPRING | 3 | 7 |
| 3 | 3-BAR TRUSS | 3 | 19 |
| 4 | 10-BAR TRUSS-CASE 1A | 10 | 28 |
| 5 | 10-BAR TRUSS-CASE 1B | 10 | 28 |
| 6 | 10-BAR TRUSS-CASE 2A | 20 | 38 |
| 7 | 10-BAR TRUSS-CASE 2B | 20 | 39 |
| 8 | 1-BAY, 2-STORY FRAME-CASE 1A | 16 | 84 |
| 9 | 1-BAY, 2-STORY FRAME-CASE 1B | 16 | 85 |
| 10 | 47-BAR TRUSS | 47 | 134 |
| 11 | 2-BAY, 6-STORY FRAME | 36 | 252 |
| 12 | 200-BAR TRUSS | 29 | 116 |

6.2 Evaluation Criteria

The choice of criteria to be used for evaluating codes based on their performance on test problems is a difficult issue. One approach that has been

used in the past is to solve a variety of test problems and then simply present summary statistics. In recent years, other approaches have been developed in mathematical programming [18,20,60,61]. Minkoff's paper [61] presents an excellent discussion of the considerations involved in developing evaluation criteria.

Unfortunately, the criteria that have been developed in mathematical programming cannot be directly used in structural optimization because of certain complications in the latter class of problems. One reason is that often the optimum solution b^* cannot be precisely calculated. A second complication in structural optimization is that, for some large scale problems, it is generally not possible to run a program to "completion" because of the excessive amount of computing costs as well as the difficulty of obtaining an optimum. One approach that may be followed is to run each code for a fixed amount of time and then compare the final solutions. Another complication in comparing codes is the presence of a large number of local minima in structural problems. For example, a code which is highly sensitive to local minima will converge to the local minima nearest a starting design. In spite of such difficulties, it may be possible to combine various reliability measures such as accuracy, efficiency, global convergence, finding a global minimum, into one single criterion. However, there is an arbitrary aspect to combining these criteria.

The evaluation criteria that have been used in the present work to analyze test results are as follows:

(1) Accuracy: The value of the cost function at the final design (which is required to be feasible) is compared. This criterion has been chosen because it is of great significance to the designer.

(2) Reliability: A reliable code is expected to give a feasible solution. The solution need not be an exact optimum. For example, a code may give accurate solutions for some problems but may fail to give feasible solutions on others. Such a code is labelled unreliable.

(3) Efficiency: Total computing time is used as a measure of the efficiency of a code.

The three criteria above are not combined in any manner. Thus, no effort is made to identify the "best" code. A code is simply labelled as accurate, reliable, and/or efficient. It is up to the reader to judge the best method based on his or her viewpoint.

Every optimization algorithm has a set of parameters that have to be selected before execution. In this work, an effort has been made to select near-optimum values for these parameters to compare different methods at their "best." Colville [14] has also used this approach. One drawback of this approach is that it depends on the familiarity the testers have with the codes. Furthermore, all gradient calculations have been done analytically. Finally, the convergence criterion of the desired solution has been set between 1% and 0.1% for most problems. The convergence criterion is measured differently in some codes, but is generally a reflection of the accuracy with which the Kuhn-Tucker conditions are satisfied. It is well known that no optimization code exists today that can obtain more accurate solutions for most structural problems with reasonable computational effort. Moreover, in design practice, a tolerance of 1% or less is entirely satisfactory. Therefore, variations of the convergence criteria (for each problem) have not been carried out in this study.

6.3 Codes of Study

The codes that are described below are based on the theory and algorithms presented earlier. These codes are run on a set of test problems and the results are discussed in the next section. Each code is given a name and these names are used in all discussions.

- (1) CONMIM: This code has been developed by Vanderplaats and is based on a feasible directions method. References 62 and 63 may be consulted for further details.
- (2) OPTDYN: This code has been developed by Bhatti and Polak [43] and is based on the feasible directions method.
- (3) LINRM: This code has been developed by the authors and is based on the recursive quadratic programming method of Pshenichny [30,34].
- (4) GRP-UI: This code has been developed by the authors [64]. It is based on a gradient projection algorithm and usually requires modification of the step size parameter after a few iterations.
- (5) SUMT: This code has been programmed by the authors and is based on the exterior quadratic penalty function.
- (6) M-3: This is a multiplier code developed by the authors and is based on Powell's algorithm [25,56].
- (7) M-4: This is a multiplier code developed by the authors. M-4 differs from M-3 in the way in which the Lagrange multipliers are updated [25,56].
- (8) M-5: This is a multiplier code developed by the authors and is based on Fletcher's algorithm [25,56].

The first four codes are based on the primal methods and the last four are based on the transformation methods.

6.4 Results

Each of the eight codes in Section 6.3 is used to solve the twelve problems in Table 1 (except for OPTDYN, which is not run on the last three problems in Table 1 because of computer storage restrictions). For each run, iteration histories of the cost function, constraint violations, and convergence parameter are recorded. Also, total computing time, number of function and gradient evaluations, optimum cost, and description of active constraints at the optimum are noted. The list of active constraints is useful in examining whether different codes converged to different local minima. The detailed information can be found in Ref. 46. Here, summary results and a few detailed results are presented to substantiate the conclusions.

First, let us discuss the accuracy as measured by the cost function value at the final design of each code. Table 2 presents the optimum (final) cost for each problem and code. It is clearly evident that OPTDYN is the most inaccurate, and performance on problems 7, 8 and 9 is 'unacceptable'. The second thing we notice is that the final costs obtained from LINRM are consistently higher than for the other codes, except for problem 11 (2-bay, 6-story frame). CONMIN, GRP-UI, SUMT,

M-3, M-4 and M-5 have very nearly the same accuracy for problems 1 to 10. GRP-UI and SUMT are inaccurate on problem 11, and CONMIN is inaccurate on problem 12 (200-bar truss). Therefore, the main conclusions regarding accuracy are that OPTDYN is the most inaccurate, LINRM is inaccurate, and the rest are comparable.

Consider now Tables 3, 4 and 5 which may be used to examine efficiency. In Table 3, computing times for problems 1-3 are not given because the number of function and gradient evaluations (FE and GE) is more significant because of the small size of the problems. Note that total computing time is used to measure the inefficiency of a code. However, FE and GE counts are also provided. It is evident that CONMIN and GRP-UI are the most efficient. The four transformation codes, on the other hand, are the most inefficient. LINRM and OPTDYN fall in between.

Table 2. COMPARISON OF OPTIMUM COST FUNCTION VALUES

| NO. | CONMIN | OPTDYN | LINRM | GRP-UI | SUMT | M-3 | M-4 | M-5 |
|-----|--------|--------|--------|--------|--------|--------|--------|--------|
| 1 | 56.15 | 56.01 | 56.0 | 56.0 | 56.0 | 56.0 | 56.0 | 56.0 |
| 2 | FAILS | .01543 | .01543 | FAILS | .01470 | .01273 | .01272 | .01283 |
| 3 | 21.05 | 20.54 | 20.54 | 20.54 | 20.53 | 20.53 | 20.53 | 20.54 |
| 4 | 5563 | 5472 | 6429 | 5727 | 5932 | 5719 | 11280 | 5725 |
| 5 | 5607 | 5711 | 6965 | 5810 | 5921 | 6072 | 6011 | 6173 |
| 6 | 4793 | 9436 | 6151 | 5077 | 5070 | 4898 | 5057 | 5211 |
| 7 | 4982 | 15570 | 5907 | 5350 | 4774 | 4978 | 4988 | 4876 |
| 8 | 6529 | 13220 | 8122 | 6646 | 6464 | 6460 | 6493 | 6511 |
| 9 | 7333 | 25771 | 8122 | 7302 | 7300 | 7316 | 8493 | 7593 |
| 10 | 3723 | ---- | 4307 | 3779 | 3784 | 3880 | 3775 | 3740 |
| 11 | FAILS | ---- | 22832 | 35380 | 34072 | 26616 | FAILS | 24445 |
| 12 | 348000 | ---- | 33315 | FAILS | 27564 | 266600 | 266654 | 26262 |

Table 3. COMPARISON OF COMPUTING TIME (SEC)

| NO. | CONMIN | OPTDYN | LINRM | GRP-UI | SUMT | M-3 | M-4 | M-5 |
|-----|--------|--------|--------|--------|--------|--------|--------|--------|
| 4 | 10.7 | 37.2 | 7.1 | 24.7 | 65.0 | 106.0 | 71.4 | 46.2 |
| 5 | 7.3 | 43.0 | 11.0 | 23.2 | 66.0 | 109.0 | 52.1 | 61.0 |
| 6 | 12.9 | 41.0 | 17.7 | 17.4 | 86.0 | 76.0 | 68.0 | 89.0 |
| 7 | 23.0 | 95.0 | 42.9 | 26.2 | 101.0 | 289.0 | 143.0 | 146.0 |
| 8 | 20.7 | 88.0 | 81.0 | 29.5 | 95.0 | 148.0 | 182.0 | 139.0 |
| 9 | 51.0 | 185.0 | 81.0 | 41.8 | 148.0 | 221.0 | 431.0 | 207.0 |
| 10 | 45.5 | ---- | 77.0 | 31.5 | 150.0 | 159.0 | 186.0 | 186.0 |
| 11 | FAILS | ---- | 330.0 | 148.0 | 248.0 | 230.0 | FAILS | 301.0 |
| 12 | 333.0 | ---- | 1582.0 | FAILS | 1400.0 | 1524.0 | 1543.0 | 1556.0 |

It may also be noted that SUMT is as efficient as the multiplier methods for structural optimization problems. On MP problems, however, it is well known that SUMT is significantly less efficient compared to multiplier methods. This is also noticed for problem 1 in the present study. We conclude that SUMT is not as inefficient (compared to multiplier methods) on structural problems as on MP problems.

As for reliability (measured by the ability of a code to obtain a feasible design), we see that CONMIN fails on problems 2 and 11, and GRP-UI fails on problems 2 and 12. Among transformation methods, M-4 fails in problem 11. LINRM, SUMT, M-3 and M-5 are reliable.

6.5 Discussion of Results

The analytical study presented earlier helps to explain results obtained in Section 6.4. First, note that transformation codes are slower (in computing time) than primal codes. This is primarily due to the unconstrained minimizations. Primal methods work with direct approximations to the functions and are consequently faster.

Second, the most efficient codes, CONMIN and GRP-UI, are also the most unreliable. LINRM, SUMT, M-3 and M-5 are the most reliable but are far less efficient. It is interesting to note that LINRM, SUMT, M-3 and M-5 are all proved to be globally convergent in theory (convergent from any starting design), whereas CONMIN and GRP-UI are not. Thus, we see that the globally convergent algorithms have proved to be more reliable. However, they are not very efficient. Upon further consider-

Table 4. COMPARISON OF FUNCTION EVALUATIONS

| NO. | CONMIN | OPTDYN | LINRM | GRP-UI | SUMT | M-3 | M-4 | M-5 |
|-----|--------|--------|-------|--------|------|------|------|------|
| 1 | 40 | 506 | 91 | 45 | 191 | 67 | 72 | 64 |
| 2 | -- | 522 | 188 | -- | 1604 | 1010 | 1605 | 1605 |
| 3 | 46 | 400 | 56 | 45 | 85 | 68 | 72 | 71 |
| 4 | 132 | 716 | 39 | 50 | 1200 | 2000 | 1218 | 854 |
| 5 | 95 | 722 | 101 | 50 | 1200 | 2000 | 800 | 1488 |
| 6 | 162 | 425 | 201 | 40 | 1320 | 1093 | 929 | 1200 |
| 7 | 152 | 323 | 201 | 40 | 551 | 1645 | 832 | 842 |
| 8 | 151 | 453 | 213 | 65 | 567 | 880 | 971 | 926 |
| 9 | 187 | 335 | 213 | 80 | 367 | 547 | 1189 | 556 |
| 10 | 129 | -- | 201 | 20 | 526 | 651 | 600 | 600 |
| 11 | -- | -- | 750 | 70 | 600 | 572 | -- | 495 |
| 12 | 139 | -- | 601 | -- | 600 | 750 | 750 | 750 |

Table 5. COMPARISON OF GRADIENT EVALUATIONS

| NO. | CONMIN | OPTDYN | LINRM | GRP-UI | SUMT | M-3 | M-4 | M-5 |
|-----|--------|--------|-------|--------|------|------|------|------|
| 1 | 13 | 144 | 19 | 45 | 130 | 51 | 54 | 52 |
| 2 | -- | 115 | 50 | -- | 1192 | 1805 | 2365 | 2691 |
| 3 | 14 | 201 | 26 | 45 | 65 | 59 | 66 | 64 |
| 4 | 45 | 95 | 20 | 50 | 1168 | 1979 | 1214 | 796 |
| 5 | 22 | 95 | 50 | 50 | 1185 | 1997 | 798 | 593 |
| 6 | 39 | 97 | 100 | 40 | 938 | 932 | 864 | 1179 |
| 7 | 37 | 95 | 100 | 40 | 493 | 1601 | 693 | 613 |
| 8 | 37 | 88 | 100 | 65 | 454 | 681 | 816 | 572 |
| 9 | 46 | 92 | 100 | 80 | 268 | 394 | 730 | 361 |
| 10 | 30 | -- | 100 | 20 | 286 | 141 | 387 | 398 |
| 11 | -- | -- | 154 | 70 | 120 | 216 | -- | 307 |
| 12 | 46 | -- | 200 | -- | 301 | 441 | 456 | 435 |

ation, this is not surprising, because in globally convergent algorithms, the step size is determined to reduce the value of a descent function [56]. It leads to a conservative choice of step size and slows down the rate of convergence. This probably means that no code can be both efficient and reliable at the same time. Hybrid codes are therefore suggested in which we first use an efficient code and then switch over to a reliable code [56].

In Section 6.4, it was noticed that LINRM is less accurate than the other codes (except OPTDYN). This is clearly evident from Table 3. This is interesting because the convergence parameter in LINRM is close to zero for all the problems. This indicates that the Kuhn-Tucker necessary conditions [38] are satisfied. Since LINRM is based on a descent algorithm, it is reasonable to assume that a local minimum is obtained. Upon closer examination of the results, it is noticed that the step size used in LINRM is considerably smaller than in other codes. This is primarily because the scalar r becomes too large (see Section 5.2 on RQP methods). Because of this, LINRM is more sensitive to local minima than other codes. It simply converges to a local minimum nearest the starting design, which may be far from the global minimum. This is shown conceptually in Fig. 7 in reference to an unconstrained minimization problem. In Fig. 7, a code that is initiated from $b^{(0)}$ will generally miss the local minimum b^* and converge to b^{**} , unless it takes extremely small steps. The reliability of LINRM to converge to a local minimum makes it a good code. However, its maximum potential lies in hybrid methods. In such methods, a large-step algorithm is first used to "jump" over some of the nearest local minima. Then a switch is made to LINRM.

7. PROBLEMS NEEDING ATTENTION

Considering analytical as well as numerical aspects, we conclude that global convergence is expensive to enforce. However, globally convergent algorithms are

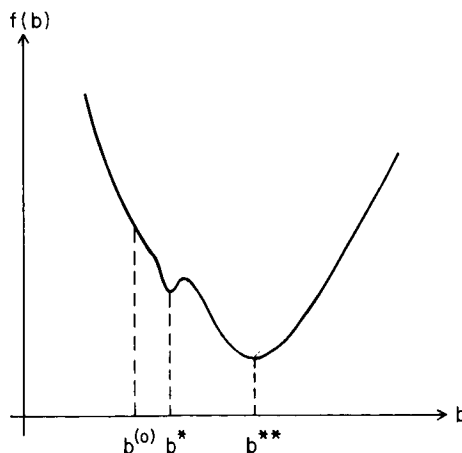


Figure 7. Step Size and Sensitivity to Local Minimum

reliable and therefore extremely attractive in the general design environment. Our goal should then be to make globally convergent algorithms more efficient. In particular, better descent functions in RQP methods and use of approximations (while maintaining convergence) in transformation methods should be investigated. Second-order information in Pshenichny's RQP algorithm and feasible directions methods must be incorporated. Further, the level of approximation at each unconstrained minimization in transformation methods needs further attention.

The difficulty in achieving both efficiency and reliability motivates the use of hybrid methods. We may first run a large-step algorithm to bring the design near an optimum in relatively few iterations. A switch can then be made to a reliable algorithm for terminal convergence. Also, initial use of large-step codes will prevent the design from converging to a poor local minimum far off from the global minimum.

Finally, there are ways in which a study of this nature can be improved. Specifically, use of a larger number of codes representing each method, wider variety of test problems (mixed element problems, dynamic problems) and different starting points. The evaluation criteria for engineering design problems can also be refined.

REFERENCES

1. Eschenauer, H. and Olhoff, N. (Eds.), Optimization Methods in Structural Design, Proceedings of the Euromech Colloquium 164, University of Siegen, FRG, October 12-14, 1982.
2. Arora, J.S., Benedict, R.L., Liu, Y.K. and Patel, V.C. (Eds.), Developments in Mechanics, Vol. 12, Proceedings of the 18th Midwestern Mechanics Conference, The University of Iowa, Iowa City, Iowa, May 16-18, 1983.
3. Gallagher, R.H., et al (Eds.), Proceedings of the International Symposium on Optimum Structural Design, University of Arizona, Tucson, AZ, Oct. 19-22, 1981.
4. Thoft-Christensen, P. (Ed.), System Modelling and Optimization, Abstracts of the 11th Conference, International Federation for Information Processing, Technical University of Denmark, Copenhagen, Denmark, July 25-29, 1983.
5. Lahey, R.S., "Implementing Design Sensitivity Analysis in MSC/NASTRAN," Developments in Mechanics 12, Proceedings of the 18th Midwestern Mechanics Conference, The University of Iowa, Iowa City, Iowa, May 16-18, 1983.
6. Arora, J.S. and Liu, W.B., "Interactive Design Optimization of Systems: IDESIGN User's Manual", Department of Civil Engineering, The University of Iowa, Iowa City, Iowa, March 1983.
7. Ragsdell, K.M., OPT Package, Design Optimization Laboratory, University of Arizona, Tucson, AZ, 1976.
8. Fleury, C. Ramanathan, R.K., Salana, M., and Schmit, L.A., Jr., "ACCESS Computer Program for Synthesis of Large Structural Systems", Proceedings of the International Symposium on Optimum Structural Design, University of Arizona, Tucson, AZ, October 1981.

9. Sobieski, J., "From Black-Box to a Programming System: Remarks on Implementation and Application of Optimization Methods", Proceedings of the NATO Advanced Studies Institute on Structural Optimization, Sart-Tilman, Belgium, 1980.
10. Bennett, J.A. and Nelson, M.R., "An Optimization Capability for Automotive Structures", SAE Transactions, Vol. 88, 1979, pp. 3236-3243.
11. Nguyen, D.T., Arora, J.S. and Belegundu, A.D., "Design Optimization Codes for Structures: DOCS Computer Program", J. of Aircraft, Vol. 20, No. 9, September 1983, pp. 817-824.
12. Haftka, R.T. and Prasad, B., "Programs for Analysis and Resizing of Complex Structures (PARS)", Computers and Structures, Vol. 10, Nos. 1 and 2, March 1979, pp. 323-330.
13. Haug, E.J. and Arora, J.S., Applied Optimal Design: Mechanical and Structural Systems, Wiley-Interscience, New York, 1979.
14. Colville, A.R., "A Comparative Study of Nonlinear Programming Codes", Tech. Rep. No. 320-2949, IBM New York Scientific Center, June 1968.
15. Stocker, D.C., "A Comparative Study of Nonlinear Programming Codes", M.S. Thesis, The University of Texas, Austin, Texas, 1969.
16. Himmelblau, D.M., Applied Nonlinear Programming, McGraw-Hill, New York, 1972.
17. Biggs, M.C., "Constrained Minimization Using Recursive, Equality Quadratic Programming", in Numerical Methods for Nonlinear Optimization, F.A. Lootsma (Ed.), Academic Press, London, 1972.
18. Schittkowski, K., "A Numerical Comparison of 13 Nonlinear Programming Codes With Randomly Generated Test Problems", in Numerical Optimization of Dynamic Systems, L.C.W. Dixon and G.P. Szego (Eds.), North-Holland Publishing Co., 1980.
19. Miele, A., Tietze, J.L. and Levy, A.V., "Comparison of Several Gradient Algorithms for Mathematical Programming Problems", Aero-Astronautics Report No. 94, Rice University, 1972.
20. Sandgren, E. and Ragsdell, K.M., "The Utility of Nonlinear Programming Algorithms: A Comparative Study - Parts I and II", Journal of Mechanical Design, Vol. 102, July 1980, pp. 540-552.
21. DeSilva, B.M.E. and Grant, G.N.C., "Comparison of Some Penalty Function Based Optimization Procedures for the Synthesis of a Planar Truss", International Journal for Numerical Methods in Engineering, Vol. 7, No. 2, 1973, pp. 155-173.
22. Carpenter, W.C. and Smith, E.A., "Computational Efficiency in Structural Optimization", Engineering Optimization, 1975, Vol. 1, pp. 169-188.

23. Carpenter, W.C. and Smith, E.A., "Computational Efficiency of Nonlinear Programming Methods on a Class of Structural Problems", International Journal for Numerical Methods in Engineering, Vol. 11, 1977, pp. 1203-1223.
24. Belegundu, A.D. and Arora, J.S., "Potential of Transformation Methods in Optimal Design", AIAA Journal, Vol. 19, No. 10, pp. 1372-1374, 1981.
25. Belegundu, A.D. and Arora, J.S., "A Computational Study of Transformation Methods for Optimal Design", AIAA Journal, Vol. 22, No. 4, pp. 535-542, 1984.
26. Han, S.P., "Superlinearly Convergent Variable Metric Methods for General Nonlinear Programming", Mathematical Programming, Vol. 11, 1976, pp. 263-282.
27. Polak, E. and Tits, A.L., "A Recursive Quadratic Programming Algorithm for Semi-Infinite Optimization Problems", Memorandum No. UCB/ERLM80/50, Electronic Research Laboratory, The University of California, Berkeley, September 1980.
28. Powell, M.J.D., "The Convergence of Variable Metric Methods for Nonlinearly Constrained Optimization Calculations", in Nonlinear Programming 3, O.L. Mangasarian, R.R. Meyer and S.M. Robinson, (Eds.), Academic Press, 1978, pp. 27-63.
29. Han, S.P., "A Globally Convergent Method for Nonlinear Programming", Journal Optimization Theory Applications, Vol. 22, 1977, pp. 297-309.
30. Pshenichny, B.N. and Danilin, Y.M., Numerical Methods in Extremal Problems, Mir Publishers, Moscow, 1978.
31. Wilson, R.B., "A Simple Algorithm for Concave Programming", Ph.D. Dissertation, Graduate School of Business Administration, Harvard University, Boston, 1963.
32. Powell, M.J.D., "A Fast Algorithm for Nonlinearly Constrained Optimization Calculations", presented at the 1977 Dundee Conference on Numerical Analysis.
33. Chao, N., Fennes, S.J. and Westerberg, A.W., "Application of a Reduced Quadratic Programming Technique to Optimal Structural Design", Proceedings of the International Symposium on Optimum Structural Design, held at The University of Arizona, Tuscon, Arizona, October 19-22, 1981.
34. Belegundu, A.D. and Arora, J.S., "A Recursive Quadratic Programming Method with Active Set Strategy for Structural Optimization", International Journal for Numerical Methods in Engineering, Vol. 20, pp. 803-816, 1984.
35. Rosen, J.B., "The Gradient Projection Method for Nonlinear Programming, Part II. Nonlinear Constraints", Journal of the Society for Industrial and Appl. Math., Vol. 9, 1961, pp. 514-532.
36. Zoutendijk, G., Methods of Feasible Directions, Elsevier, Amsterdam, 1960.
37. Wolfe, P., "Methods of Nonlinear Programming", Chapter 6 of Nonlinear Programming, J. Abadie, (Ed.), North-Holland Publishing Company, Amsterdam, 1970.

38. Luengerger, D.G., Introduction to Linear and Nonlinear Programming, Addison-Wesley Publishing Co., Reading, Massachusetts, 1973.
39. Sargeant, R.W.H., "Numerical Methods for Constrained Optimization", P.E. Gill and W. Murray (Eds.), Academic Press, 1974.
40. Bard, Y. and Greenstadt, J.L., "A Modified Newton Method for Optimization with Equality Constraints", in Optimization, R. Fletcher, (Ed.), Academic Press, London and New York, 1969.
41. Gonzaga, G., Polak, E., and Trahan, R., "An Improved Algorithm for Problems with Functional Inequality Constraints", Memorandum No. UCB/ERLM 78/56, Electronics Research Laboratory, University of California, Berkeley, September 1977.
42. Bhatti, M.A., Polak, E. and Pister, K.S., "OPTDYN - A General Purpose Optimization Program for Problems With or Without Dynamic Constraints", Rep. No. UCB/EERC-79/16, University of California, Berkeley, July 1979.
43. Topkis, D.M. and Vienott, A.F., Jr., "On the Convergence of Some Feasible Direction Algorithms for Nonlinear Programming", J. SIAM Control 5, 2, May 1967, pp. 268-279.
44. Dobbs, M.W. and Nelson, R.B., "Application of Optimality Criteria to Automated Structural Design", AIAA Journal, 14, 10, October 1976, pp. 1436-1443.
45. Khot, N.S., Berke, L. and Venkayya, V.B., "Comparison of Optimality Criteria Algorithms for Minimum Weight Design of Structures", presented at the AIAA/ASME/SAE 19th Structures, Structural Dynamics and Materials Conference, Bethesda, MD, April 1978, pp. 37-46.
46. Belegundu, A.D. and Arora, J.S., "A Study of Mathematical Programming Methods for Structural Optimization", Technical Report No. CAD-SS-82.5, Division of Materials Engineering, The University of Iowa, Iowa City, Iowa, August 1982.
47. Rosen, J.B. and Kreuser, J., "A Gradient Projection Algorithm for Nonlinear Constraints", in Numerical Methods for Nonlinear Optimization, F.A. Lootsma (Ed.), Academic Press, London, 1972, pp. 297-300.
48. Arora, J.S., Haug, E.J. and Rajan, S.D., "Efficient Constraint Treatment in Structural Optimization", Paper 80-501, ASCE National Convention, Hollywood, Florida, October 1980.
49. Fiacco, A.V. and McCormick, G.P., "Nonlinear Programming: Sequential Unconstrained Minimization Techniques", John Wiley and Sons, Inc., 1968.
50. Cassis, J.H. and Schmit, L.A., "On Implementation of the Extended Interior Penalty Function", Int. J. for Numerical Methods in Engineering, Vol. 10, 1976, pp. 3-23.
51. Prasad, B. and Haftka, R.T., "A Cubic Extended Interior Panalty Function for Structural Optimization", Int. J. for Numerical Methods in Engineering, Vol. 14, No. 9, 1979, pp. 1107-1126.

52. Bertsekas, D.P., "Multiplier Methods: A Survey", Automatica, vol. 12, 1976, pp. 133-145.
53. Powell, M.J.D., "A Method for Nonlinear Constraints in Minimization Problems", in Optimization, R. Fletcher (Ed.), Chapter 19, Academic Press, London and New York, 1969.
54. Hestenes, M.R., "Multiplier and Gradient Methods", J. Opt. Theory Appl., 4, 1969, pp. 303-320.
55. Fletcher, R., "An Ideal Penalty Function for Constrained Optimization", J. Inst. Maths. Applics., 15, 1975, pp. 319-342.
56. Belegundu, A.D. and Arora, J.S., "A Study of Mathematical Programming Methods for Structural Optimization - Part I: Theory", Accepted by International Journal for Numerical Methods in Engineering, 1983.
57. American Institute of Steel Construction, Manual of Steel Construction, Seventh Edition, 1973.
58. Belegundu, A.D. and Arora, J.S., "A Study of Mathematical Programming Methods for Structural Optimization - Part II: Numerical Results", Accepted by International Journal for Numerical Methods in Engineering, 1984.
59. Rosen, J.B. and Suzuki, S., "Construction of Nonlinear Programming Test Problem", Communications of Association for Computing Machinery, Vol. 8, p. 113, 1965.
60. Miele, A., Gonzalez, S. and Wu, A.K., On Testing Algorithms for Mathematical Programming Problems, Aero-Astronautics Report No. 134, Rice University, 1976.
61. Minkoff, M., "Methods for Evaluating Nonlinear Programming Software", in Nonlinear Programming 4, O.L. Mangasarian, R.R. Meyer, and S.M. Robinson (Eds.), Academic Press, 1981.
62. Vanderplaats, G.N. and Moses, F., "Structural Optimization by Methods of Feasible Directions", Computers and Structures, Vol. 3, 1973, pp. 739-755.
63. Vanderplaats, G.N., CONMIN - A Fortran Program for Constrained Function Minimization User's Manual, NASA TM X-62282, August 1973.
64. Arora, J.S. and Sohoni, V.N., "A General Purpose Nonlinear Programming Code GRP Projection Method", Technical Report No. 41, College of Engineering, University of Iowa, Iowa City, Iowa, June 1978.

ACKNOWLEDGEMENT

This research is supported
by the NSF Grant CEE 82-13851

N87-11771

STRUCTURAL OPTIMIZATION OF
LARGE OCEAN-GOING STRUCTURES

Owen F. Hughes
Naval Architecture Department
University of New South Wales
Sydney, Australia

Introduction

Ocean-going vehicles and platforms are among the largest structures in the world and are subjected to relatively harsh conditions of motions and loads. Some of them, such as semi-submersible platforms, are a relatively new type of structure and hence there is no formal, well evolved and established structural design code as there is for more traditional structures.

These structures are costly and, because of the smaller waterplane area compared to a ship, they are much more weight sensitive, especially if they utilize vertically tensioned mooring for better seakeeping. Hence there is a paramount need to reduce both cost and weight and to achieve an optimum tradeoff between them, while at the same time providing the required degree of reliability, damage tolerance and maintainability. The structural design of warships is even more complex, involving tradeoffs in the structure's vertical center of gravity as well as in weight and cost. In the past the only way of coping with such challenging structural design tasks was to develop a design code for each particular type of structure. But the availability of computers and the methods of structural analysis and structural optimization that computers have made possible have provided the opportunity to develop more rationally or scientifically based methods of design - in essence, design from first principles. This requires not only the coupling of finite element analysis and optimization, but also the synthesis of these with limit state analysis, reliability and damage tolerance. The earliest and strongest efforts to achieve this have occurred in the field of aircraft and aerospace structures, and much progress has been made.

More recently, efforts have also been made to develop a design method of this type for ships and other ocean structures (ref. 1). One of the many advantages of a rationally based design method is versatility; it can be used for structures that have widely differing purposes, measures of merit, shapes and sizes - which is, of course, the *raison d'être* of this conference. Hence the purpose of this paper is to describe a rationally based design method that has been developed within the field of ocean structures, in order that persons dealing with other types of structure can judge whether and to what extent its various features may be useful for those other types. Also, even though some features may not be applicable they might stimulate some useful ideas.

Basic Design Method

In any large structure it is possible to distinguish three levels of structural design. Concept design deals with the topology and overall geometry of the structure; preliminary design establishes the structural dimensions of all principal structural members; and detail design is concerned with local aspects such as joints, openings, and reinforcements. Overall structural geometry is generally determined by overall design requirements rather than by structural requirements, while detail design is largely guided and constrained by fabrication methods and requirements. Also, since local structural details are numerous and basically

similar among various structures they lend themselves to standardization and to design from handbooks and structural codes. Thus, it is in preliminary design that the structural designer has the largest number of significant decisions and options, and the greatest scope for optimizing the structure so that it best fulfills the objectives and satisfies all of the various constraints and requirements. Therefore the design method described herein is for preliminary design only.

Fig. 1 shows the methodology and the seven essential aspects of rationally based preliminary structural design. Of course the steps could be further subdivided and/or grouped differently, but the basic scheme is applicable to nearly all structures, and all seven aspects are essential for true rationally based design. But it is also necessary that they be balanced and integrated. "Balanced" means that each aspect should be developed to the level of detail and capability that is appropriate for preliminary design; no more and no less. Some special care is required to achieve this balance. For example, one of the great advantages of the finite element method is its ability to portray local stress concentrations by using a fine mesh. But preliminary design deals only with principal members and it has to model the entire structure; hence a fine mesh representation, although appealing because it gives more complete information (and also "looks better" graphically) is not appropriate for this phase of design. The basic problem is a lack of correspondence between the analysis variables (element thicknesses) and the design variables (web heights, flange widths, stiffener sizes and spacings, in addition to thicknesses).

A mismatch can also occur in the choice of the optimization method. For example, most penalty function and gradient methods are best suited for finding a "field optimum", as occurs when there are only a few constraints and all are non-linear. But for each principal member in a large structure there are dozens of constraints, and the above methods become too slow. Moreover, they also become inappropriate because all of these constraints overlap and partly eclipse each other, and the optimum invariably lies at an intersection of constraints rather than in a "hollow" formed by one or two constraints.

In addition to being balanced (dealing with the same information) the various aspects must also share that information easily and efficiently. Therefore, the computer program that implements the design method must have a well organized and well documented database.

Although the basic method of Fig. 1 applies to nearly all structures, the first 3 aspects will differ in content for different types of structure because the loads, the types of principal members, and the possible limit states of those members will all be different. Hence for maximum versatility these aspects of the program should be modular, to permit their adaptation or substitution.

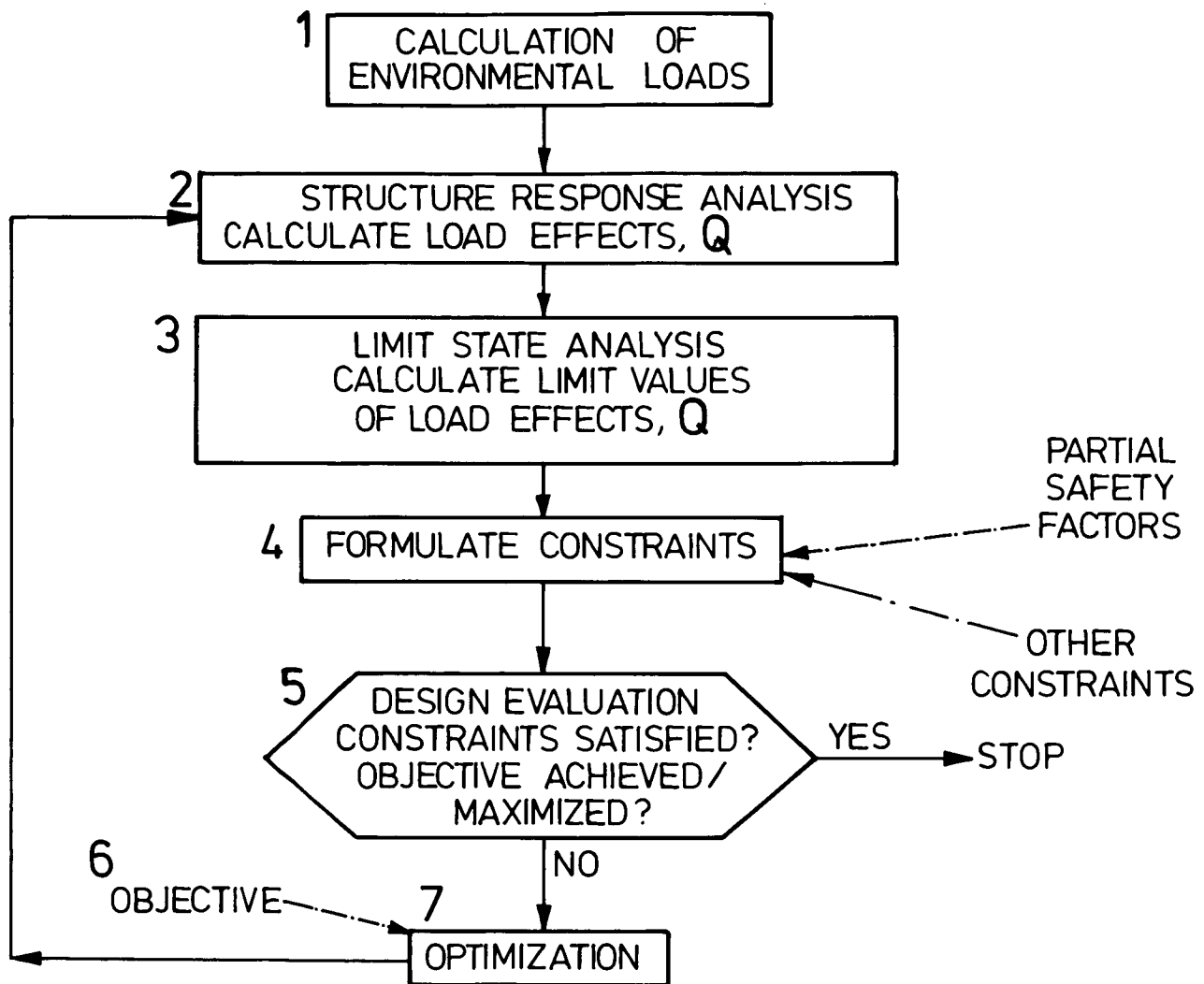


Figure 1

Method for rationality based on preliminary structural design

The method of Fig. 1 has been implemented in a computer program known as MAESTRO*. The program is modular, corresponding to the boxes shown in the figure, and the response analysis has been further subdivided to permit substructuring. A common database is used for storing and sharing information among the modules. These features have helped to make the program versatile. For example, as shown in refs. 2, 3 and 4, MAESTRO has been applied successfully to a box girder bridge, to commercial ships and to warships, even though these three classes of structure have totally different purposes (and measures of merit) and substantial differences in loads, in the proportions, complexity and stiffness of the structure, in operating requirements and in many other aspects. A design study involving a semi-submersible platform will be published in the near future. As noted earlier, the basic methodology applies to an even wider variety of structures, such as road and rail vehicles and aircraft. For these further applications the program would, of course, require some modification, but because of its modular structure it is definitely capable of such adaptation and extension.

The remainder of this paper consists of a brief description of how the basic aspects of Fig. 1 have been implemented in MAESTRO. The seventh aspect - optimization - is not discussed here because it is covered fully in the paper by Mistree, Shupe and Hughes (ref. 5). The paper concludes with a brief summary of the use of MAESTRO for the structural optimization of a 96000 ton tanker.

1. Calculation of External Loads

Because of the new and rather unusual geometry of semi-submersibles and other ocean platforms there are no empirically derived and time-tested expressions for design loads as there are for ships, bridges and aircraft. Therefore during the past ten years or so several computer programs have been developed for calculating these loads from first principles, most often by means of source distributions. Some examples are SPLASHD, WAMLOS, AQWA and MATTHEW. In the development of MAESTRO the intention has been to eventually interface one of these with the MAESTRO load module. Therefore the latter is largely passive, accepting whatever loads the designer inputs (as obtained from the empirical expressions and methods). The only loads that are calculated and applied automatically are the hydrostatic loads due to immersion, as in a ship's hull.

2. Response Analysis

The method for the response analysis is, of course, the finite element method. For a ship the overall structure is essentially a box girder (the "hull girder") and it is possible to begin the analysis with a segment of the hull girder. But for structures of more complex topology, such as ocean platforms, the response analysis must deal with the complete structure. To attempt to begin at any lower level would introduce unacceptable levels of uncertainty in relation to boundary conditions - both loads and restraints.

* Method for Aalysis, Evaluation and STRuctural Optimization

In MAESTRO the structural modeling is divided into three levels: modules, strakes and principal members, as shown in Fig. 2. A *module* is any structure, or portion of structure, consisting of frames and plating and having one direction or axis (regarded as "lengthwise") along which the transverse frames are evenly spaced and are orthogonal to that axis. In a very general sense a module is "tubular", but it need not be prismatic and the cross section may be of any shape whatever, open or closed. In Fig. 2 the drilling tower, deck, column segments and pontoon are all modules. Other examples are segments of a ship hull (Fig. 3) or aircraft fuselage or wing (Fig. 4).

As shown in Fig. 2 a *strake* is a lengthwise row of stiffened panels and frame segments and, optionally, a girder along either edge. Each strake can have linear taper and/or twist along its length, and hence the overall module can have a pronounced change in its cross sectional shape; it need not be prismatic. A strake can be either flat or cylindrical, and the panel stiffeners can be either longitudinal or transverse.

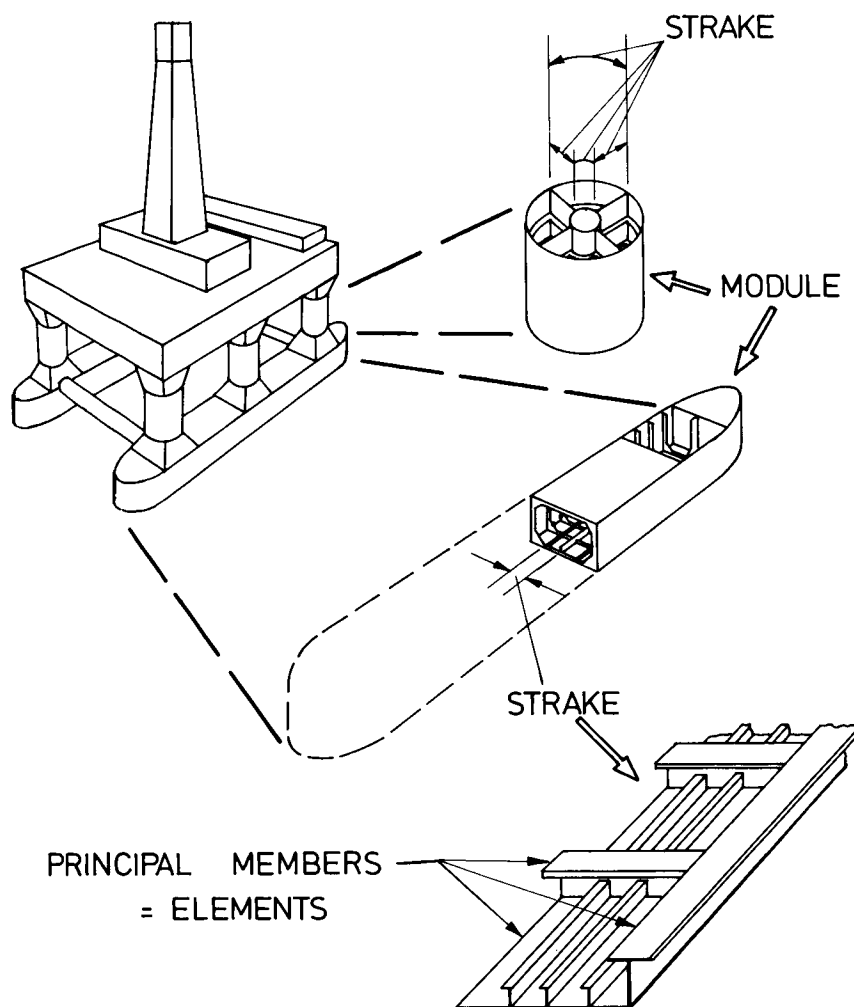
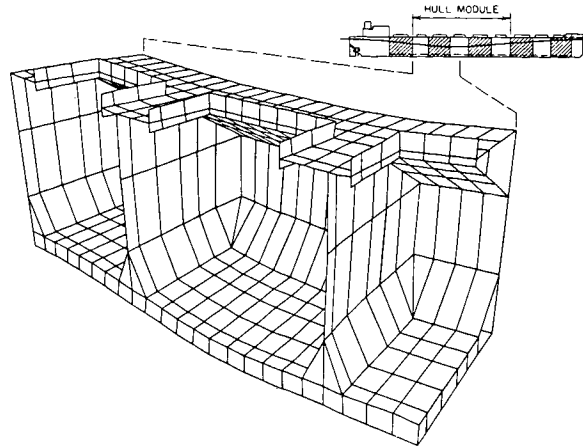


Figure 2

Subdivision of structure



NOTE: This figure is an example of a MAESTRO-produced deflection plot, using the hidden line removal option and a deflection exaggeration factor of 50.

Figure 3

MAESTRO model of a bulk carrier (1 module)

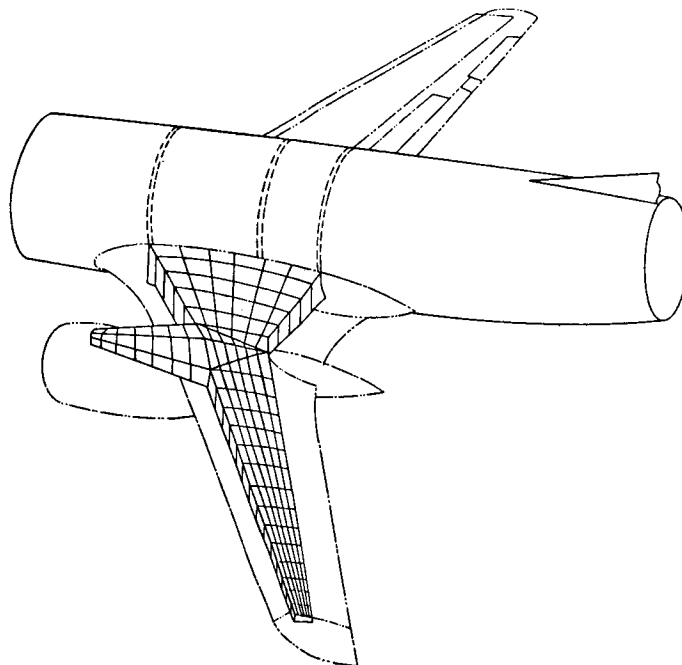


Figure 4

MAESTRO model of a 737 wing (4 modules)

As mentioned earlier, preliminary structural design is not concerned with local details but rather with the dimensions of the principal members. In order to have a balance and a good interface between the response analysis and the optimization, the finite elements in MAESTRO correspond precisely to the principal members. The elements are therefore relatively large; e.g. a complete panel from one deck to another and from one frame to the next, as shown in Fig. 5, or a corresponding segment of a transverse frame or longitudinal girder. Figure 6 shows the subdivision into elements for a typical semi-submersible platform.

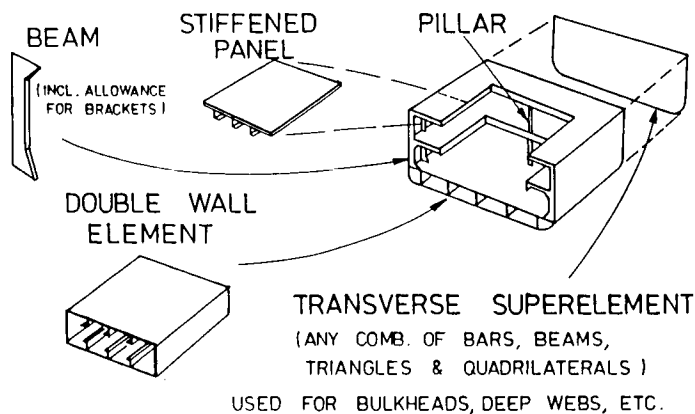


Figure 5

Typical elements in MAESTRO

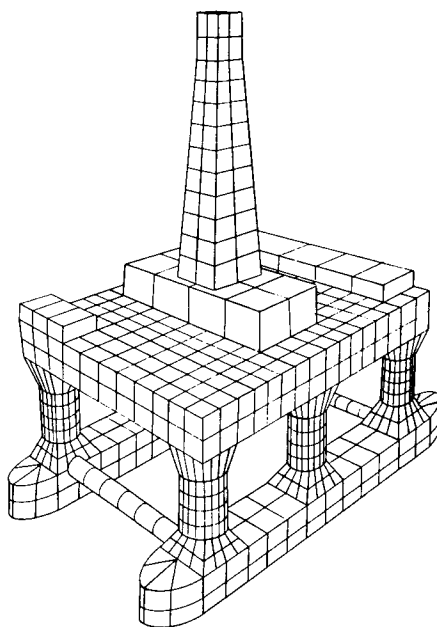


Figure 6

MAESTRO model of a semi-submersible platform (12 modules)

The elements in MAESTRO have been carefully defined in order to provide the degree of accuracy that is required (and no more). For example the beam element accounts for the effects of transverse shear, end rigidity due to brackets, and elastic angular deformation of joints; also it can represent either an ordinary beam or a beam attached to plating, with the plating acting as a flange. For large brackets, bulkheads, and other principal members of nonstandard geometry the element representing the member is constructed as a "superelement"; i.e. it is built up of smaller elements and then static condensation is used to eliminate all internal nodes, keeping only those that are needed for attachment to other principal members. Figure 7 illustrates this for a large bracket.

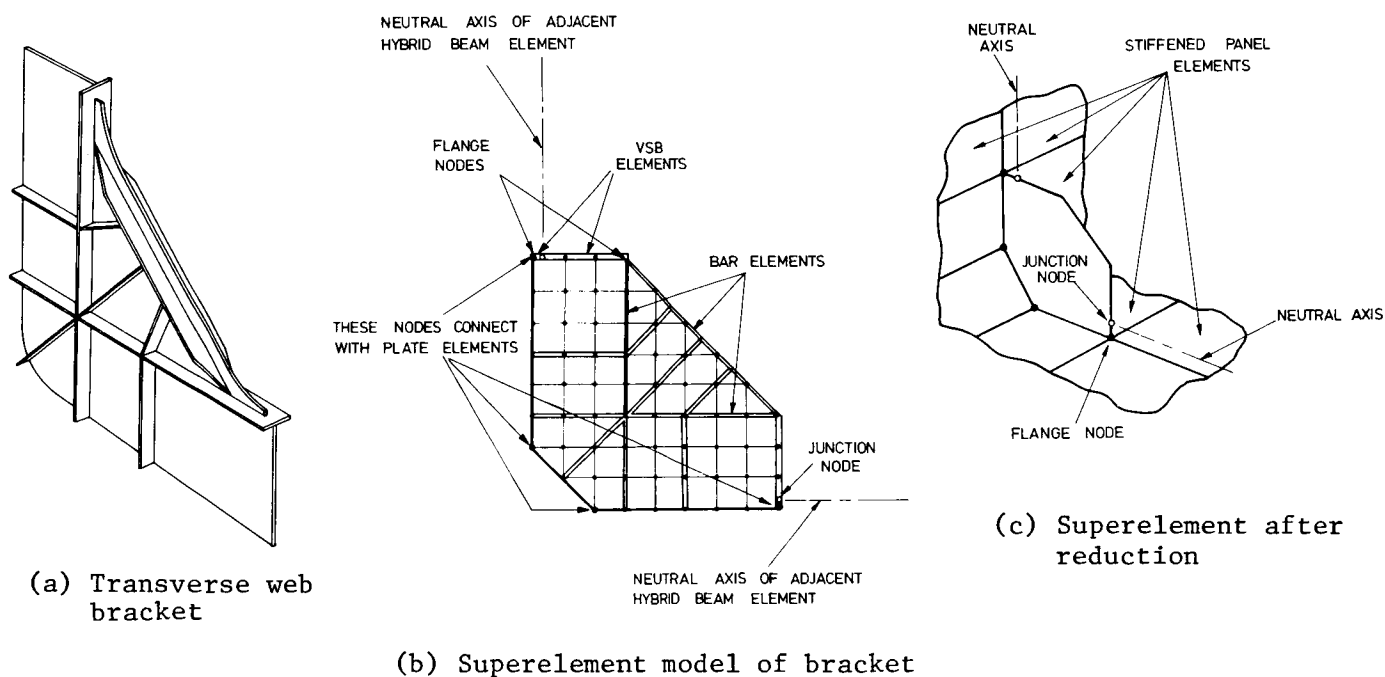


Figure 7

Reduction of superelement

Figure 8 shows the design variables in a typical strake. These values are constant over the length of the strake. If the strake is nonprismatic (tapered and/or twisted) the values will be determined by the combination or "envelope" of lowest safety margins over the length of the strake. If it is desired to have a change in a design variable within a module length (e.g. a change of plate thickness) then two (or more) in-line strakes are used instead of one.

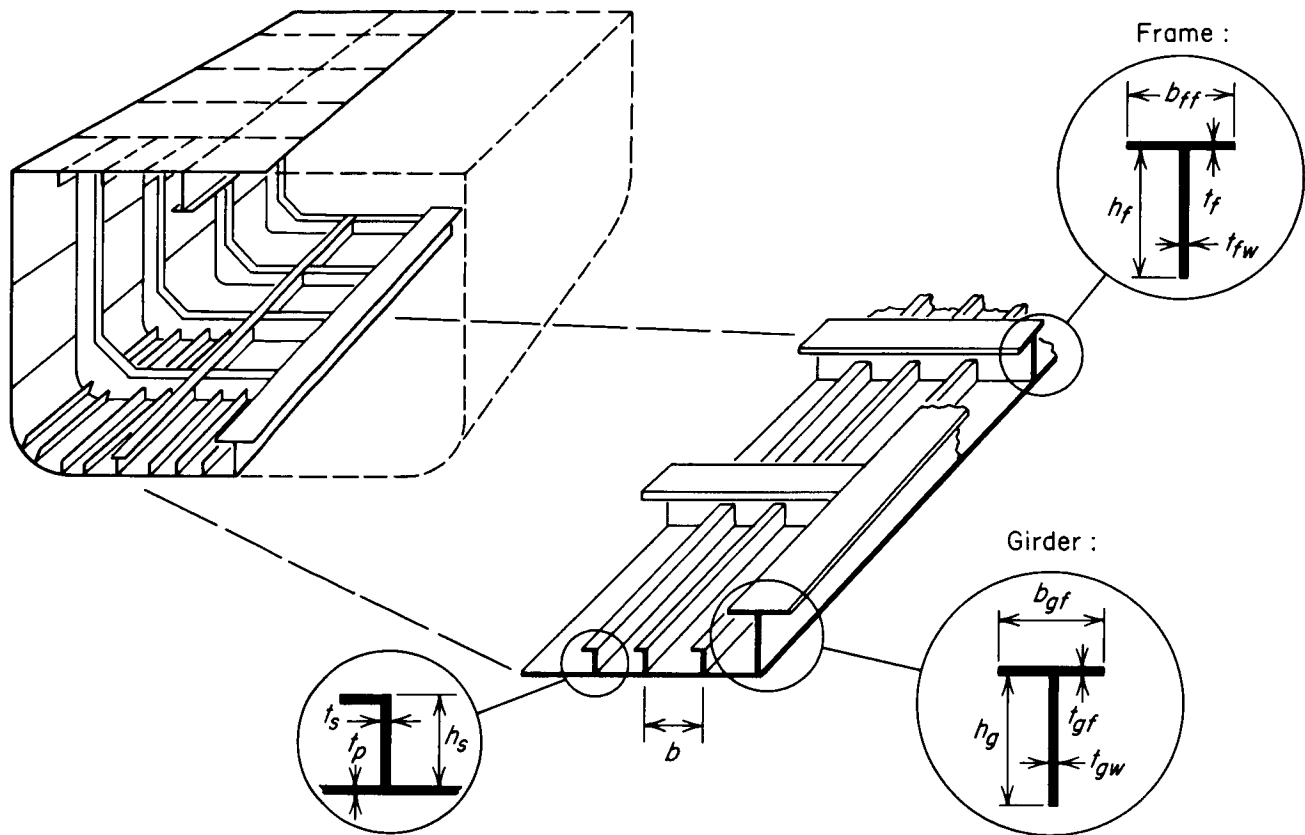


Figure 8

Example of a strake, showing design variables

Through the use of strakes, a module can contain any number of lengthwise webs, bulkheads, floors, decks, etc. Through the use of superelements a module may also contain any number of transverse brackets, webs, diaphragms and bulkheads. Openings are created by deleting elements; openings smaller than a panel element are ignored. Fig. 9 illustrates how strakes, superelements and modules can be combined to represent quite complex structures, in this case a naval frigate.

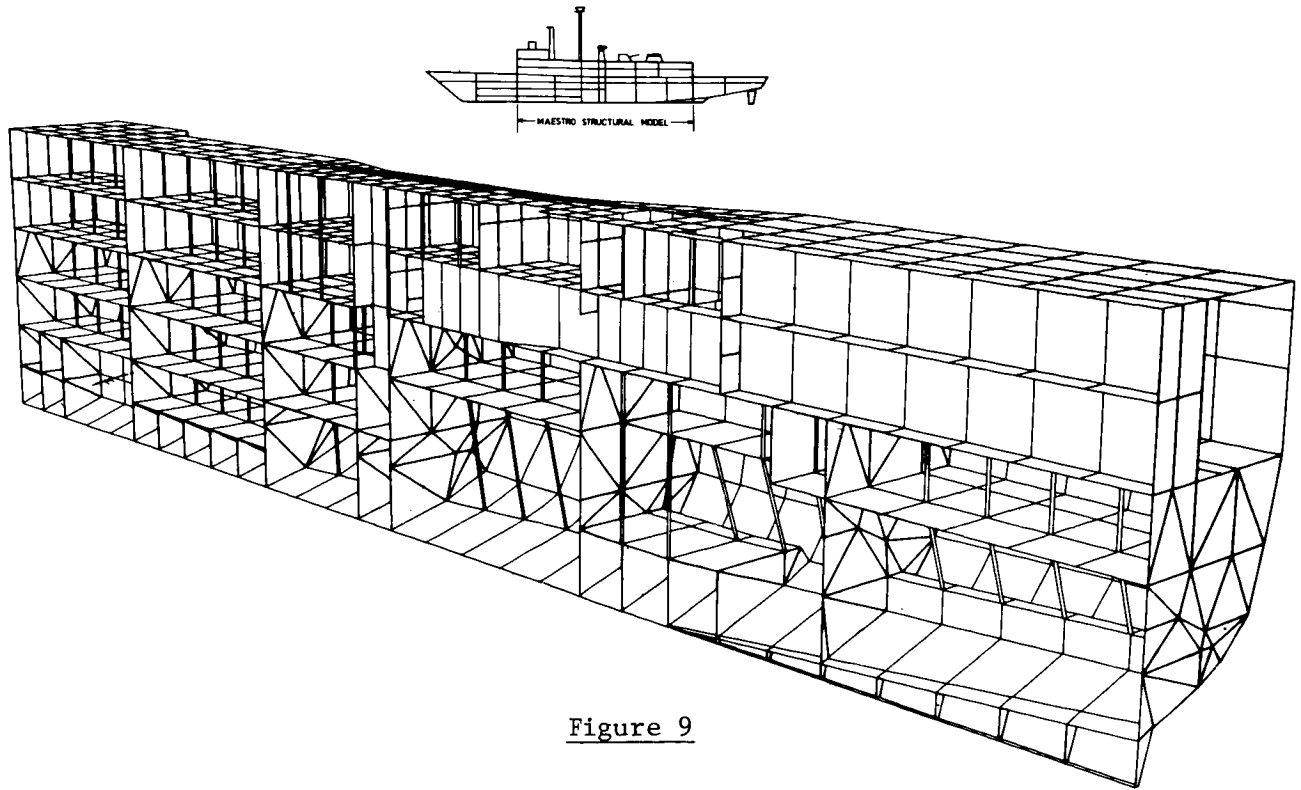


Figure 9

MAESTRO model of a frigate (5 modules)

3. Limit State Analysis

A limit state is any undesirable condition that a structure might possibly reach, and the limit values, Q_L , are the values of the load effects Q at which that condition would be reached. There are two types of limit state analyses, corresponding to the two levels of limit states: those involving only individual members (strake level) and those involving several members (module level). Fig. 10 shows an example of the latter: collapse of the transverse framing of a tanker. For this limit state MAESTRO uses a simplified (and conservative) form of plastic frame analysis.

For the member limit states MAESTRO contains a library of subroutines, each of which calculates the limit values Q_L for a particular mode of failure, using approximate engineering algorithms appropriate to each mode. The limit state library currently contains algorithms for 33 member limit states: 12 for a stiffened panel, 6 for a girder segment and 15 for a transverse frame segment. The theory underlying the algorithms is presented fully in ref. 1. The limit state library is modular, allowing the addition of new subroutines to deal with new limit states, as might arise from different geometry (e.g. sandwich panels) or new materials (e.g. fiber-reinforced plastics). In most cases the limit states are a nonlinear function of the design variables \mathbf{X} ; let us denote this nonlinear dependency as $Q_L(\mathbf{X})$. The various algorithms deal with the nonlinearity algebraically, in a "strength of materials" fashion; nonlinear finite element analysis would be computationally prohibitive because of the large number of members and load combinations.

1. HULL MODULE FAILURE

I.E. MULTI-MEMBER FAILURE

MUST ACCOUNT FOR :

- INTERACTIONS BETWEEN MEMBERS
- COMBINED FAILURE MODES $\left\{ \begin{array}{l} \text{INSTABILITY} \\ \text{YIELD} \end{array} \right.$

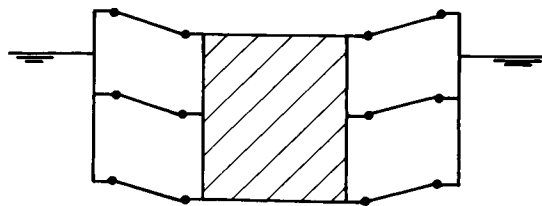


Figure 10 Example of failure at module level

Besides structural failure, there are other ways in which a member or a module can become unfit, especially the latter. For example, there may be limits on the overall deflection of a module, as occurs in a wing. Fatigue is a cumulative phenomenon that imposes a limit on the magnitude of the cyclic stress in the upper and lower "flanges" of the module when it flexes as a beam, as shown in Fig. 11 for a ship. In both cases the load effect $Q(\mathbf{X})$ (deflection, module flexural stress) is a function of the design variables of *all* of the members, not just one, and the limit value $Q_L(\mathbf{X})$ does not coincide with any single physical event.

4. Formulation of Constraints

(a) Reliability-based Strength Constraints

Having calculated both the load effects Q and the limit values $Q_L(\mathbf{X})$ in all of the members and for all loadcases, the program then formulates the constraints. These are of the form

$$\gamma_0 Q(\mathbf{X}) \leq Q_L(\mathbf{X}) \quad (1)$$

in which the parentheses indicate functional dependence, which is often nonlinear. The total safety factor γ_0 is a product of various partial safety factors which account for

- (1) the degree of seriousness of the limit state
- (2) the probability of the relevant loads
- (3) the degree of uncertainty in the associated load effects
- (4) the degree of uncertainty in the associated limit values

In MAESTRO the partial safety factors are part of the input data, and the actual values are obtained from an appropriate reliability-based code, as already exist for many classes of structure and are being developed for others.

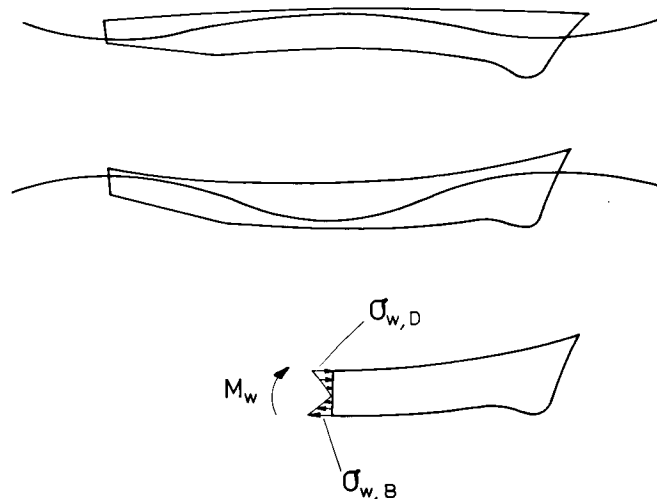


Figure 11 Limit state for fatigue (allowable cyclic stress for a given design load)

(b) Other (Non-strength-related) Constraints

As illustrated in Fig. 12, besides the strength constraints there are many others arising from functional, local and fabrication requirements. These differ widely from one structure to the next, and the MAESTRO program allows the designer to specify any number of them, of any type and in any combination, either for individual strakes or for an entire module. In the tanker example to be presented subsequently, there were approximately 550 strength-related constraints and about 450 other constraints, giving a total of about 1000 constraints.

5. Evaluation of Current Design

In each cycle of the overall design process of Fig. 1, the formulation of the strength-related constraints involves a thorough search for the lowest margin for each of the 33 limit states in each strake; i.e. the largest difference between the left and right hand sides of eq. (1). Within each strake the calculations are repeated bay by bay, and for each loadcase in turn, and a complete record is kept of the values of the lowest margins, the corresponding location and loadcase, and the values of the relevant load effects. If requested, the program prints this information in an orderly tabular format, in various optional levels of detail. Thus as the optimization proceeds the designer can monitor the process as closely as he wishes. This feature also means that MAESTRO can be used for the comprehensive evaluation of a given design or of an existing structure - perhaps after some damage or some modification, either real or projected.

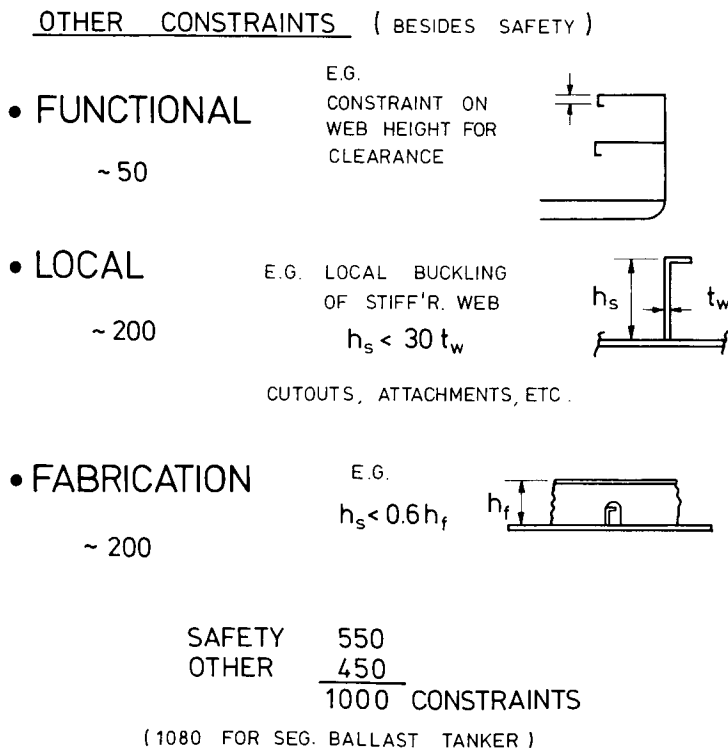


Figure 12

Other (non-strength-related) constraints

6. Measure of Merit

In MAESTRO the measure of merit may be any function of the design variables - linear or nonlinear, single or multiple. For example, it may be any desired combination of weight, cost and vertical center of gravity (VCG). This particular combination is illustrated in Fig. 13. The curved surface represents the combined and net effect of all of the constraints. It is actually an irregular surface - it is the outer envelope of all of the many individual constraints, each of which is itself a surface consisting of the lowest possible combinations of weight, VCG, and cost which just satisfy the requirements of that particular constraint. In different regions of the design space different constraints are the outermost or "active" constraints. Any point in the design space that does not penetrate below this surface is a feasible design (such as point A) and any point actually on the surface is an optimum design (point B). The surface indicates what sort of tradeoffs are available to the designer.

For example, the weight would be lower in a more intricate - and costlier - design (point C) but the extent to which this option is followed may depend on the ratio between the weight savings and the extra cost. Because of its flexibility in regard to measures of merit, the program can be used for a wide variety of tradeoff studies. As mentioned earlier the optimization aspects of the program are covered in ref. 5.

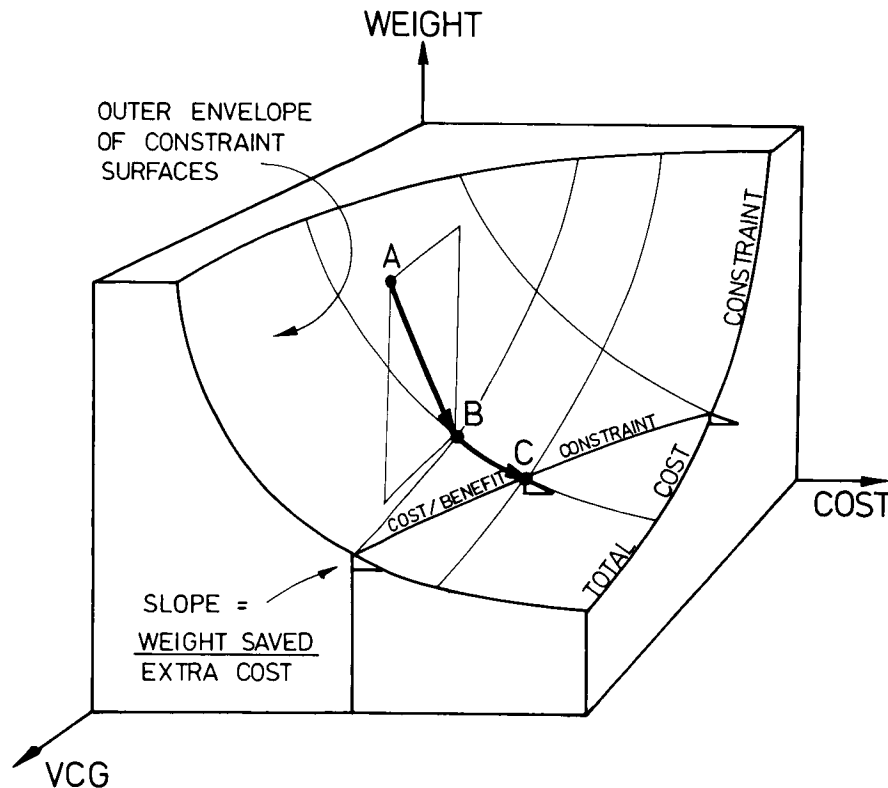


Figure 13

Multiobjective optimization

Example

By way of example, this section briefly summarizes the results of an optimum design of a 96000 ton tanker, on the basis of least life-cycle cost. Details are given in ref. 3. Because one of the main purposes of this study was to assess the economic benefits of rationally based design, all of the design specifications (principal dimensions, geometry, loads, etc.) were the same as for an actual, rule-based, manually produced design. As explained in ref. 3 special steps were taken to avoid any bias in favour of MAESTRO and to remove the rather uncertain question of corrosion allowance from the comparison. In rationally based design there is a clear distinction between steel that is required for adequate strength and steel that is provided in order to allow for corrosion. MAESTRO provides only the former; the latter must be added on after the optimization.

The transverse section of the basis ship is shown in Fig. 14. For the three cargo tank lengths which comprised the MAESTRO structural model the cost of the basis design was 9708 cost units, and the structural weight (which is automatically calculated by MAESTRO) was 8050 tons. As mentioned earlier, the initial scantlings for MAESTRO are completely arbitrary and so in this case, in order to provide a direct and graphic comparison between the rule-based design and the MAESTRO design, the scantlings of the former were used as the initial scantlings for MAESTRO.

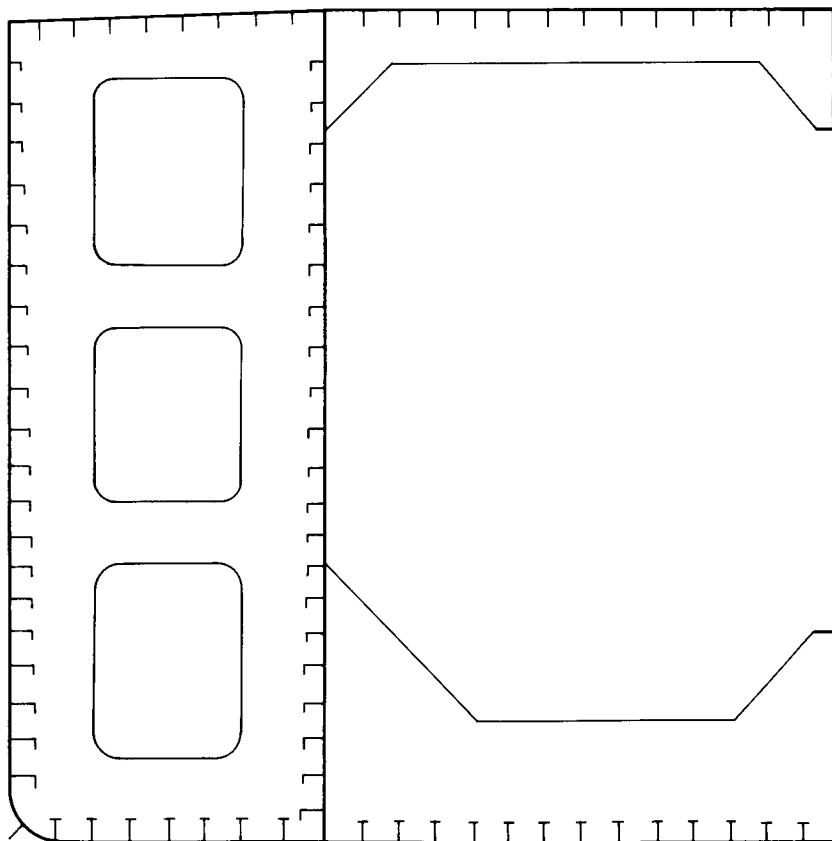


Figure 14

Basis ship: 96000 dwt tanker

The performance of MAESTRO is shown in Fig. 15. The solution for the optimum design required 12 design cycles, which took about 12 minutes of computer time on an IBM 370/158. The total computing (cpu) cost was about \$130. The resulting optimum design had a total life-cycle savings (in which increased revenue from weight savings is converted to and subtracted from initial cost) of 8477 cost units, which is a 13% improvement on the basis of current practice design. The savings in initial cost was 6%, which for a tanker of this size represents a savings of the order of one million dollars.

The figure also shows two other optimization runs starting with very different initial values of the design variables: one in which they are all 3 times the basis ship values and another in which they are all 1/3 of the basis values. In both cases the program converged to the same optimum solution as before, thus demonstrating that it does not require good - or even feasible - initial values, and also showing that it achieves a global optimum.

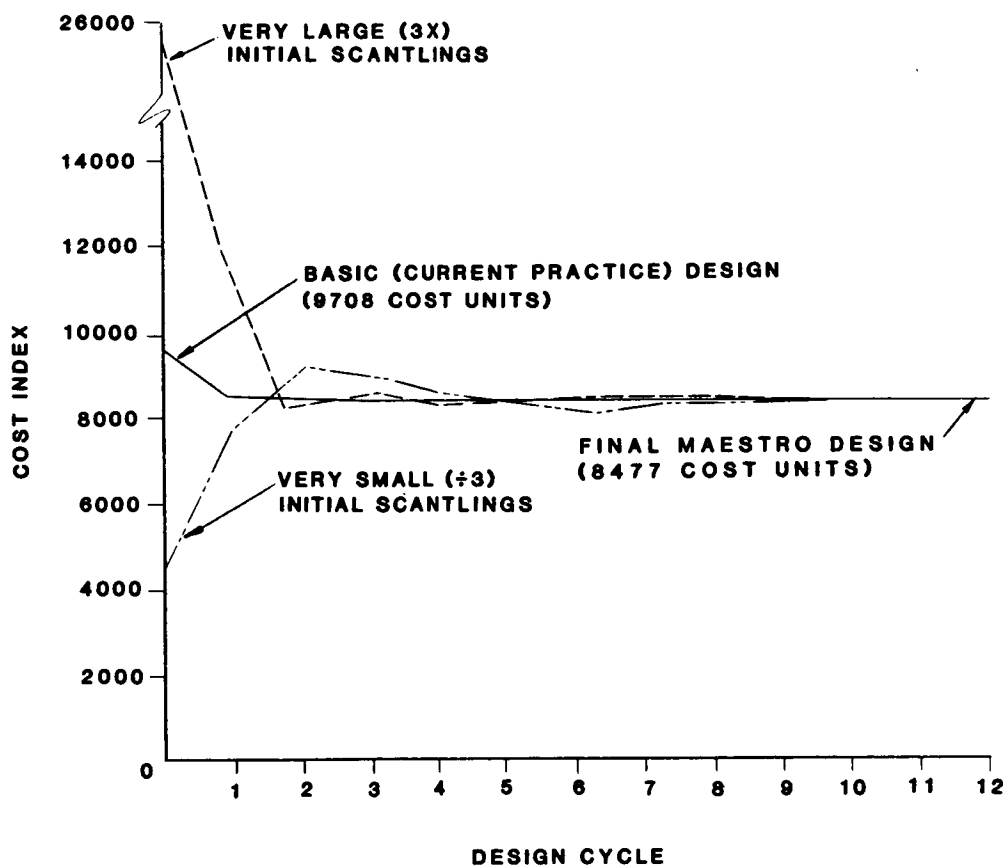


Figure 15
Results of tanker optimization

Effect of Using Standard Sections

The foregoing savings will be decreased slightly by the need to use standard plate thicknesses and standard rolled sections for the stiffeners. MAESTRO deliberately treats these design variables, and also the stiffener spacing, as continuous variables in order to avoid the enormous computation and complexity of discrete variable optimization. This also has the advantage of allowing the designer himself to decide these questions, and to do so *after* he has seen what the idealized optimum is. This is very helpful information and with it he can make a better decision as to how much standardization he wants. The standard sizes do not all have to be the next larger size; it is usually sufficient to choose the nearest size, unless this would mean decreasing all of the scantlings in a particular stiffened panel. After inserting standard sizes wherever he wishes, the designer then runs MAESTRO for one more cycle with all of these design variables fixed (a standard feature on MAESTRO). The program then automatically adjusts all other scantlings to obtain the new (and final) optimum design which has all of the standard sizes and still satisfies all of the constraints. By observing the new optimum cost the designer can immediately see how far from the idealized optimum his selection of standard sizes has taken him. In most cases the departure is small. For example, in the tanker the insertion of standard sections reduced the life-cycle savings from 13% to 11% compared to the rule-based design, which still represents a substantial savings. Moreover this guarantees that the 6% savings in initial cost is a real savings, being based on realistic limitations to standard sections.

References

1. O.F. Hughes, *Ship Structural Design*, Wiley-Interscience, 1983.
2. O.F. Hughes, F. Mistree, and J. Davies, "Automated Limit State Design of Steel Structures", *Proceedings of the Sixth Australasian Conference on the Mechanics of Structures and Materials*, Christchurch, August 1977, pp. 98-106.
3. D. Liu, O.F. Hughes, and J.E. Mahowald, "Applications of a Computer-Aided, Optimal Preliminary Ship Structural Design Method", *Trans. SNAME*, Society of Naval Architects and Engineers, 1981.
4. O.F. Hughes, "A Method for Nonlinear Optimum Design of Large Structures, and Applications to Naval Ship Design", *Int. Symp. on Optimum Structural Design*, Univ. of Arizona, Tucson, Oct. 1981.
5. F. Mistree, J.A. Shupe, and O.F. Hughes, "A Conceptual Basis for the Design of Damage Tolerant Structural Systems", *Recent Experiences in Multidisciplinary Analysis and Optimization*, NASA CP-2327, Part 2, 1984, pp. 907-942.

N87-11772

FUNDAMENTAL DIFFERENCES BETWEEN OPTIMIZATION CODE TEST PROBLEMS
AND ENGINEERING APPLICATIONS

E. D. Eason
Failure Analysis Associates
Palo Alto, California

INTRODUCTION

There are many studies in the literature comparing the performance of nonlinear programming codes applied to a wide variety of problems [1-9]. Several of these comparison studies have been conducted with real or realistic engineering problems [1-8]. In addition, there is a growing body of literature regarding the methodology of conducting comparative tests and the validity of comparative results [8,11-18]. An entire conference was devoted to this topic in 1981 [18]. A key result from all of the nonlinear optimization code comparison literature is that the relative performance of codes is highly dependent on the specific problem. Thus, if the typical engineering problem differs substantially from the type of problems that have been used for comparing optimization codes, it would not be surprising if the relative performance of codes on engineering problems did not agree with the published comparative results. The purpose of the present paper is to suggest that there is at least one fundamental difference between the problems used for testing optimization codes and the problems that engineers often need to solve; in particular, the level of precision that can be practically achieved in the numerical evaluation of the objective function, derivatives, and constraints. This difference affects the performance of optimization codes, as illustrated below by two examples.

All nonlinear constrained optimization problems can be put in the form:

$$\begin{array}{ll} \text{minimize} & f(x) \\ \text{subject to} & g(x) \geq 0 \\ & h(x) = 0 \end{array} \quad (1)$$

where the functions f , g , and h are generally nonlinear, x is a vector of variables, and g and h are generally vector functions. Within this framework one can define two general classes of nonlinear constrained minimization problems.

- Class One functions f , g , and h can be evaluated to any desired precision except as limited by the word length or precision of the computer.
- Class Two functions f , g , and h cannot be evaluated to a level of precision comparable to the word length or precision of the computer, generally for economic reasons.

In the typical Class One problem, f , g , and h are analytic functions. Examples of Class Two problems are cases where f , g , or h are the result of Monte Carlo simulation, solution of ordinary or partial differential equations (e.g. finite element analysis), numerical integration, solution of nonlinear algebraic equations, or any other iterative algorithm.

It should be apparent that many engineering problems fall into the second class, where the cost of refining the analysis beyond a few significant

digits would be prohibitive. Often convergence to within 10% in the basic analysis that evaluates f , g , or h is considered acceptable for engineering purposes, and this single-digit precision may be greater than the accuracy of modeling the real situation. A prime example is optimization requiring finite element analysis.

In the following figures the type of problem used in various code comparison studies is identified. Two limited-precision problems are presented and solved by two optimization codes over a range of precision in evaluating f and/or g . The first problem is typical of Monte Carlo simulation models, or analyses that are sensitive to rounding or truncation error. The functions contain a random noise component that may vary from one evaluation to the next. The second problem is typical of numerical integration, including ordinary differential equation initial value problems. The precision (and evaluation cost) can be varied by changing the integration step size.

ANALYSIS OF PROBLEMS GIVEN IN SELECTED SOURCES

Table 1 categorizes the test problems used in selected comparison studies. The vast majority are Class One problems where the function and constraints can be evaluated to arbitrarily high precision. Some problems have some of the features of Class Two problems in that they arose from engineering applications and they are not analytically differentiable, but they are not strictly Class Two because there are no precision limits. Only three problems are clearly in the Class Two category where the function or constraints can only be evaluated to limited precision. All of these involve solution of an ordinary differential equation. This can only be accomplished to relatively low precision if that evaluation is to be repeated many times. Two of the three Class Two problems and three of the ten problems with some Class 2 features were not used for ranking in these comparison studies because few codes could solve them. In summary, most test problems are Class One, and of those problems that are Class Two (or that have some features of Class Two), a significant fraction cannot be used for ranking because few optimization codes could solve them. This is evidence that the performance of optimization codes on the difficult Class Two problems is unknown.

| SOURCE | CLASS 1 | SOME FEATURES OF CLASS 2 | CLASS 2 |
|--------------------|--------------|------------------------------------|----------------|
| | (NUMBER) | (PROBLEM ID) | (PROBLEM ID) |
| COLVILLE (1) | 6 | C6,C8 | - |
| EASON & FENTON (2) | 8 | C6*,E9*,E11, E12 | E13*(ODE) |
| HIMMELBLAU (5) | 32 | C6,C8,H14 | H13(ODE) |
| SANDGREN (6) | 19 | C6,C8,E9*,E11, E12,S25-S27,S30* | E13*,S28*(ODE) |
| SCHITTKOWSKI (9) | 185 | - | - |
| | 250 PROBLEMS | 10 PROBLEMS | 3 PROBLEMS |

*Not used for ranking due to poor performance by most codes.

Table 1

EXAMPLE OF A CLASS TWO PROBLEM INVOLVING RANDOM NOISE

Problem 1 is a simple Type 2 test problem. The lack of precision in the evaluation of f and one of the constraint functions comes from additive random noise that is normally distributed with a mean of zero and standard deviation S . Such a situation may arise when the function and/or constraint are evaluated by Monte Carlo simulation, or when compounded round-off error strongly influences the calculated value of a function or constraint. Each time the optimizer asks for a new value of f and g , the value is slightly different for the same x because of the random noise component. By adjusting the standard deviation it is possible investigate a range of noise-to-signal ratios for the function f and the constraint g . (See fig. 1.)

PROBLEM 1 (RANDOM NOISE)

$$\text{MIN } f(x) = \sin(x_1/2) \cdot \cos x_2 + \rho_1$$

SUBJECT TO

$$x_1 \geq 0$$

$$x_2 \geq 0$$

$$2\pi - x_1 - x_2 + \rho_2 \geq 0$$

WHERE

ρ_1 AND ρ_2 ARE NORMALLY-DISTRIBUTED RANDOM
NUMBERS WITH MEAN $\mu=0$ AND STANDARD DEVIATION
 $\sigma = S$ (INPUT)

$S \equiv \text{NOISE/SIGNAL FOR } f$

$S/(2\pi) \equiv \text{NOISE/SIGNAL FOR } g$

FEASIBLE STARTING POINT: $x_1 = 4.0$, $x_2 = .2$

Figure 1

CONTOUR PLOT FOR PROBLEM 1 RANDOM NOISE

Figure 2 is a contour plot for Problem 1. The objective function is a periodic array of hills and valleys. The nominal position of the functional constraint cuts through the feasible minimum. The random noise causes the functional constraint to vary right and left and the function value to vary in and out of the plane of the paper.

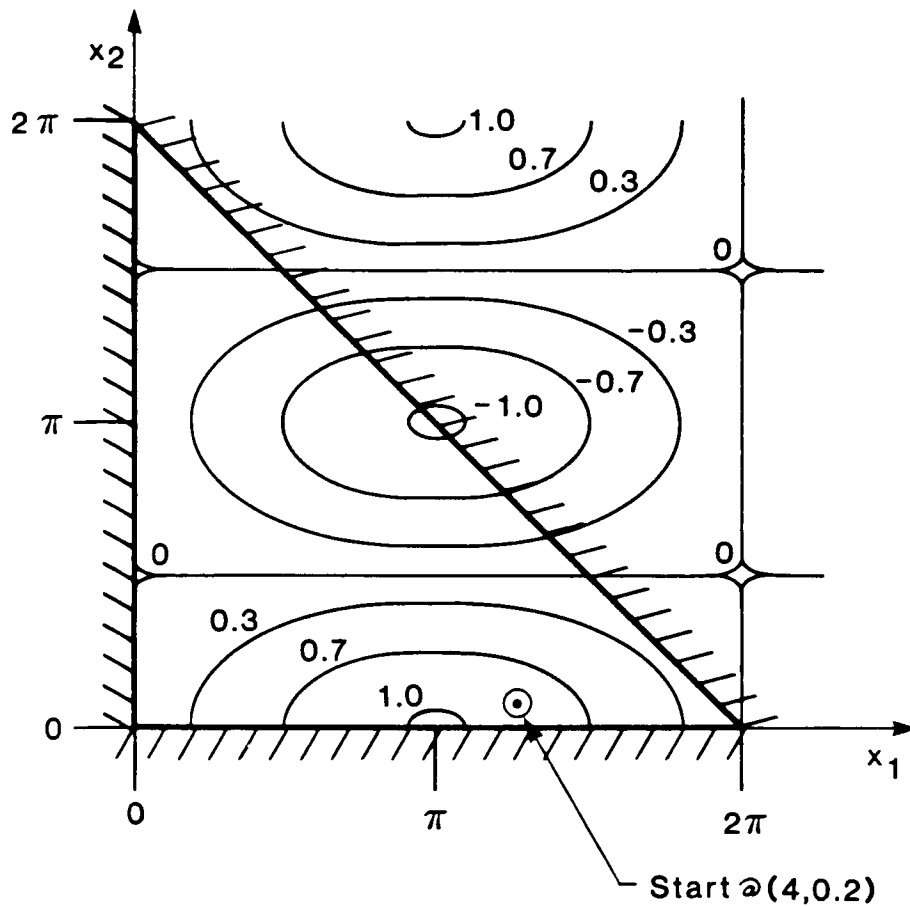


Figure 2

SOLUTIONS TO RANDOM NOISE PROBLEM

Figure 3 gives the solutions by two optimization codes to Problem 1 with a range of noise-to-signal ratios in both constraint and objective function. The numbers on the figure are the number of function evaluations to reach the corresponding relative error shown on the top scale. There are some cases (at large ratios of objective function noise-to-signal) where neither code was able to solve the problem. However, in most cases the PATPEN code, a simple Hooke & Jeeves direct search strategy [19], was able to solve the problem in 120 to 200 function evaluations. The PCON code, which is a Powell code with SUMT-type constraints [20], was very unsuccessful on this problem. PCON was able to solve only 3 of 23 cases to the same general level of error as PATPEN. In two other cases the level of error was approximately an order of magnitude greater with PCON than PATPEN. In all cases PCON required more function evaluations, sometimes substantially more, than PATPEN. The PATPEN code was well-behaved; at termination the relative error from the true solution is comparable to the noise-to-signal ratio.

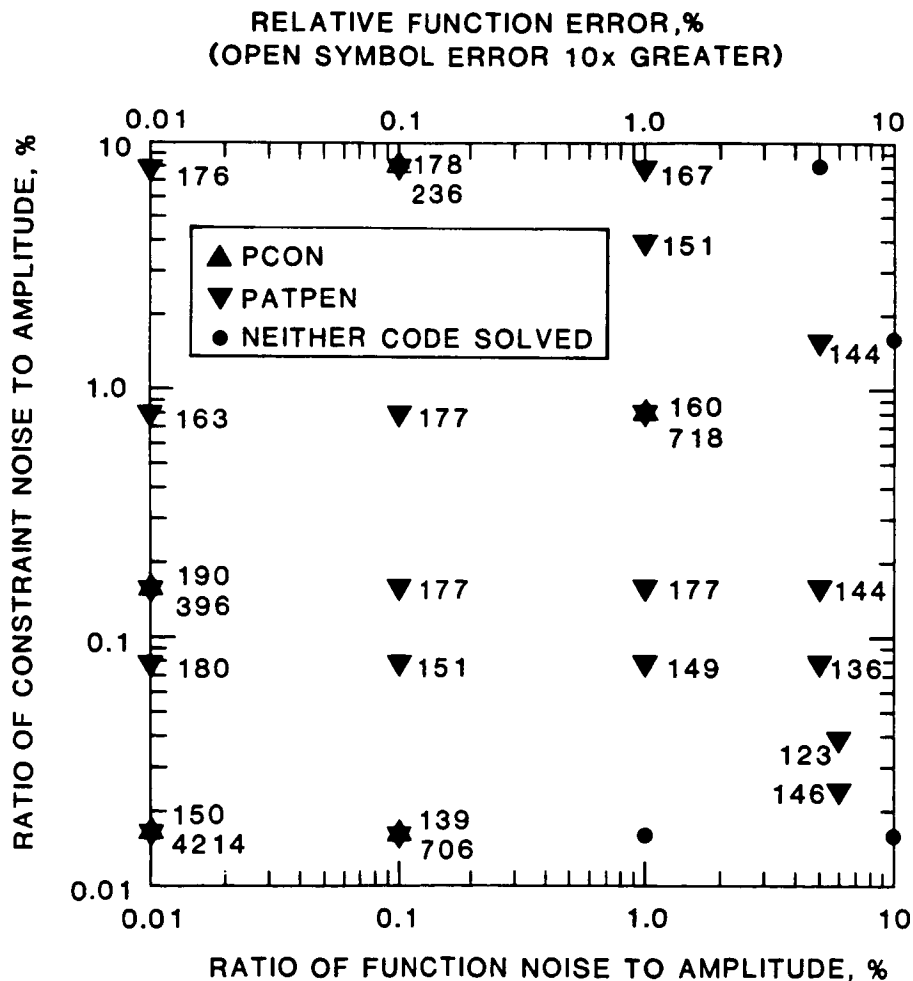


Figure 3

PROBLEM 2 OPTIMUM GEAR RATIOS

The second problem is a simulation by numerical integration of vehicle acceleration from five to one hundred miles per hour. The gear ratios are to be optimized to the torque-speed curve of the engine such that the time of the acceleration event is minimized. The expressions for the problem are given in figure 4 and the torque-speed curve is shown in figure 5. This problem is a simplified version of Problem E-13, which was one of the test problems in earlier studies (see Table 1). The objective function (time) cannot be evaluated more accurately than the time increment used in the numerical integration. There is a direct trade-off between the amount of computer effort spent in the numerical integration and the amount spent in the numerical optimization. The objective function is calculated from a discontinuous expression for acceleration that corresponds to the abrupt change from positive to negative acceleration (wind resistance) during shifts.

PROBLEM 2 (GEAR RATIO)

MIN $f(X) = T$, WHERE

$$\frac{1}{\text{CON1}} \int_0^T \text{ACC} \, dt = 95 \text{ MPH}$$

$$\text{ACC} = \begin{cases} \text{RAD} \left[\frac{(X_i) (\text{TORQUE}) - (\text{FORCE})(\text{RAD})}{(X_i)^2 (EI) + VI} \right] & \text{DURING ACCELERATION} \\ -(\text{FORCE})(\text{RAD})^2 / VI & \text{DURING SHIFTING} \end{cases}$$

SUBJECT TO

$$20 \geq X_1 \geq X_2 \geq X_3 \geq X_4 \geq X_5 \geq 2$$

$$X_1 \geq 15$$

FEASIBLE STARTING POINT: $X_1 = 15$, $X_2 = 9.05$, $X_3 = 6.14$,
 $X_4 = 4.55$, $X_5 = 3.61$

Figure 4

ENGINE CHARACTERISTIC CURVE FOR PROBLEM 2

Figure 5 corresponds to the engine torque-speed curve in the acceleration problem. The dashed line is the maximum allowable engine speed, at which a shift must occur.

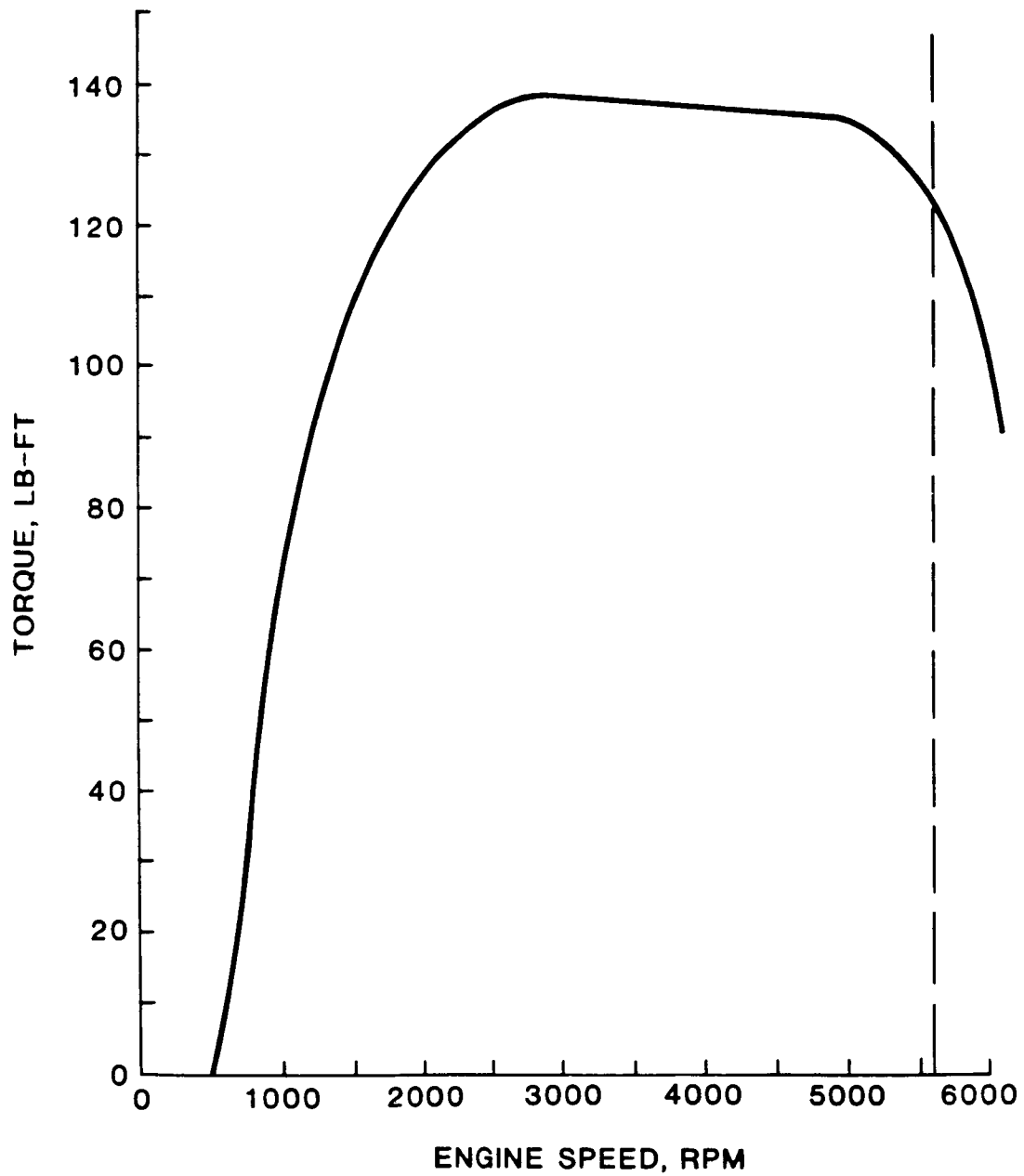


Figure 5

COMPARISON OF OPTIMAL GEAR RATIO SOLUTIONS

Table 2 shows solutions to Problem 2 at three precision levels (numerical integration time steps). The same two optimization codes are used as in Problem 1, and in some cases multiple runs are shown. The x_i are the gear ratios, f is the total elapsed time in seconds (to be minimized), and #FE is the number of function evaluations required for the solution.

At the lowest precision level the PATPEN code finds as good a solution as the PCON code in far fewer function evaluations. The x_i solutions are slightly different between the two codes, but the objective function is the same. This is indicative of the discreteness in the objective function, which can only take values at 0.1 sec steps. At the finer integration step (0.01 sec) PATPEN is still superior, requiring far fewer function evaluations to reach the improved function value of 38.53. However, at this integration precision PCON is capable of finding a slightly better solution, albeit with more than ten times as many function evaluations. At the finest integration step PCON finds a significantly better solution than PATPEN in about the same number of function evaluations, indicating that the more sophisticated code performs better when the function can be evaluated accurately. However, note that each function evaluation takes a hundred times more computation at the 0.001 sec time step compared to the 0.1 sec time step. Consequently, 330 function evaluations at 0.001 time step are as expensive as 33,000 function evaluations at 0.1 time step. Overall, the least-cost solution is to use the less sophisticated code and the larger integration step.

| INTEGRATION STEP | | x_1 | x_2 | x_3 | x_4 | x_5 | f | #FE |
|------------------|--------|-------|-------|-------|-------|-------|--------|------|
| 0.1 | PATPEN | 18.2 | 10.0 | 7.8 | 5.8 | 3.8 | 38.7 | 58 |
| | PCON | 16.5 | 11.7 | 8.3 | 5.8 | 3.8 | 38.7 | 485 |
| | | 17.7 | 13.0 | 9.3 | 6.2 | 3.8 | 38.7 | 1186 |
| 0.01 | PATPEN | 19.7 | 13.1 | 8.6 | 5.8 | 3.8 | 38.53 | 84 |
| | PCON | 19.6 | 12.0 | 8.0 | 5.8 | 3.8 | 38.53 | 509 |
| | | 19.4 | 13.9 | 9.0 | 5.9 | 3.8 | 38.51 | 935 |
| 0.001 | PATPEN | 20.0 | 12.4 | 8.5 | 5.8 | 3.8 | 38.659 | 258 |
| | PCON | 19.8 | 12.7 | 8.7 | 5.8 | 3.8 | 38.501 | 330 |

TABLE 2

DISCUSSION OF PERFORMANCE DIFFERENCES

In the random noise Problem 1, the objective function value at x_1 can be either larger or smaller than the value at x_2 depending on f_i and ρ_i (see Figure 6). If the difference $f_1 - f_2$ is small compared to the ρ_i , an optimization code may be totally confused by the random nature of the apparent gradient. Algorithms such as PCON that base their line search step length and direction on apparent gradients or an assumed quadratic functional form may take large steps in totally wrong directions because of the random component in the function. Less sophisticated algorithms such as Hooke & Jeeves [19] or Nelder & Mead simplex [21] have predetermined, relatively small search step lengths, so they do not go far in wrong directions.

An additional performance difference arises from the stopping criterion. More sophisticated codes often test for zero gradients or numerical satisfaction of Kuhn-Tucker conditions. In the presence of random noise, these conditions are unlikely to be satisfied to normal tolerance levels except by random chance, so the codes would be expected to "dither" unproductively about the minimum point. The direct search codes terminate when a better point cannot be found by reducing the step length below some minimum. Thus they seize on a low function value and quickly terminate because no smaller $f + \rho$ is likely in the immediate vicinity. One would expect such a code to return a final $f + \rho$ that is about one standard deviation below optimum f , and this is observed. In Figure 3, for example, the error in the PATPEN solution $[final(f + \rho) - f_0]/f_0$ is slightly below the true noise-to-amplitude ratio ρ/f_0 , where subscript 0 refers to the true optimum.

Problem 1 schematic

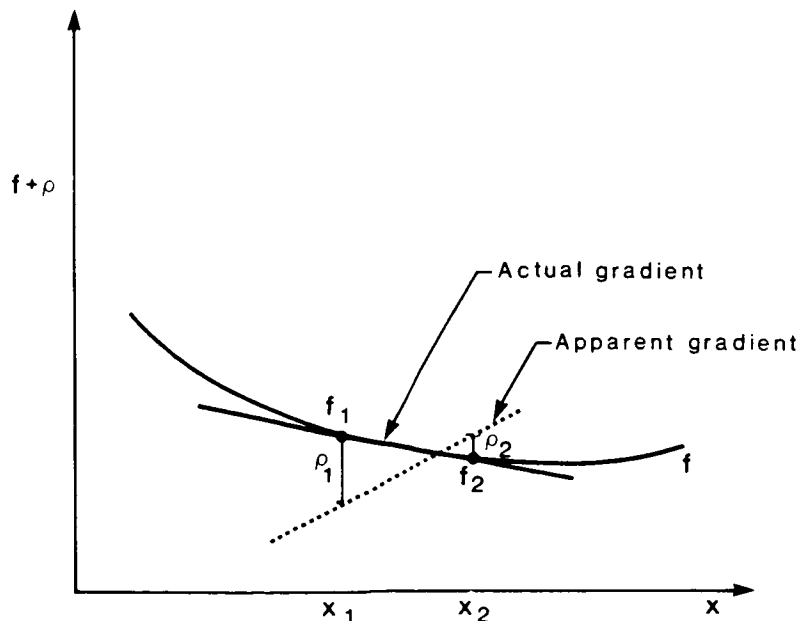


Figure 6

PERFORMANCE DIFFERENCES

In Problem 2, the principal difficulty is the discrete-valued objective function, conceptually shown for two variables in Figure 7. The minimum height difference between adjacent regions is the integration time step (0.1 to 0.001), but within each region the objective function is flat for a range in each of the variables. In the test problem it would be easy to eliminate the most obvious source of discreteness by interpolating final time at 100 mph; however, there may be other sources of discreteness in real simulation models.

On a stepwise flat objective function, codes that estimate local gradients are likely to terminate prematurely. Assumptions of quadratic form in line search strategies are also likely to be unproductive unless the minimum step length can be forced to be greater than the average size of the discrete-valued region. Direct search strategies have less problem because the step size typically starts large and reduces when no further progress occurs. Such codes will automatically terminate when their step size is reduced below the size of the discrete region.

Problem 2 schematic

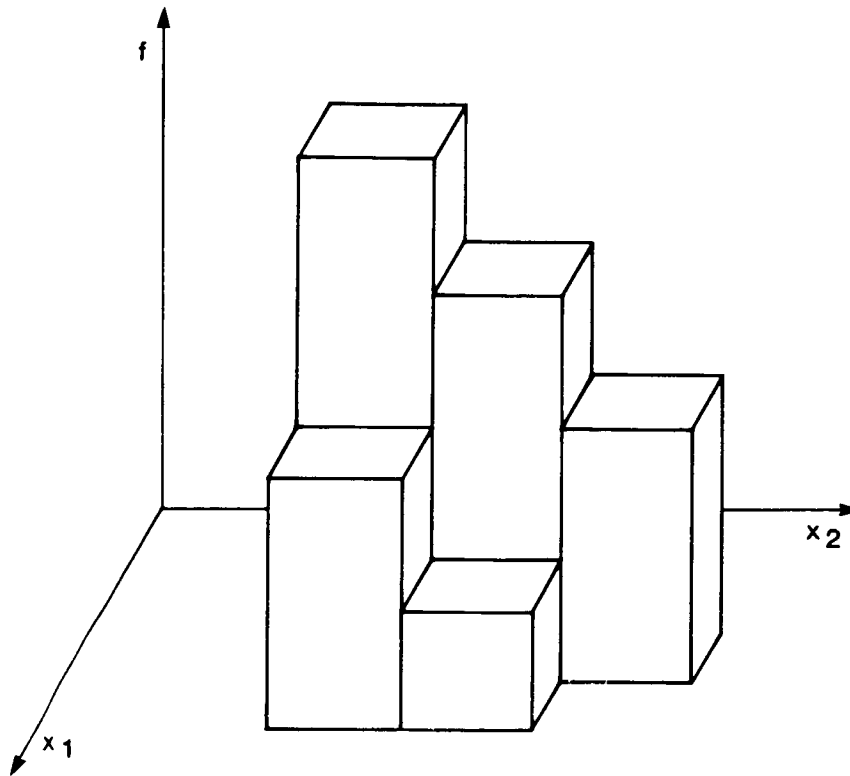


Figure 7

CONCLUSIONS

1. Two classes of optimization problem have been defined. Class One functions and constraints can be evaluated to a high precision that depends primarily on the word length of the computer. Class Two functions and/or constraints can only be evaluated to a moderate or a low level of precision for economic or modeling reasons, regardless of the computer word length.
2. Optimization codes have not been adequately tested on Class Two problems. Where those problems have been used, many codes have been unsuccessful.
3. There are very few Class Two test problems in the literature, while there are literally hundreds of Class One test problems.
4. The relative performance of two codes may be markedly different for Class One and Class Two problems. Based on the limited sample of two problems and two codes, less sophisticated direct search type codes may be less likely to be confused or to waste many function evaluations on Class Two problems. Of course, the less sophisticated codes may be unable to solve problems with many variables.
5. The analysis accuracy and minimization performance are related in a complex way that probably varies from code to code. On a problem where the analysis precision was varied over a range, the simple Hooke and Jeeves code was more efficient at low precision while the Powell code was more efficient at high precision.
6. These results are tentative and should be confirmed by generation of many more Class Two test problems and comparisons of optimization codes of interest to engineers.
7. The results suggest that a great deal more testing effort should be expended to ensure that codes being developed now do not degrade significantly in the presence of low accuracy, Type 2 Problem functions.

REFERENCES

1. Colville, A. R., "A Comparative Study on Nonlinear Programming Codes," IBM New York Scientific Center Report No. 320-2949, June 1968, summarized in Proceedings of the Princeton Symposium on Mathematical Programming, Kuhn, H. W., ed., Princeton, NJ, 1970, pp. 487-501.
2. Eason, E. D. and Fenton, R. G., "Testing and Evaluation of Numerical Methods for Design Optimization," University of Toronto Report UTME-TP 7204, September 1972.
3. Eason, E. D. and Fenton, R. G., "A Comparison of Numerical Optimization Methods for Engineering Design," Journal of Engineering for Industry, Trans. ASME Series B, Vol. 96, No. 1, February 1974, pp. 191-196.
4. Stocker, D. C., A Comparative Study of Nonlinear Programming Codes, MS Thesis, University of Texas at Austin, 1969.
5. Himmelblau, D. M., Applied Nonlinear Programming, McGraw-Hill, New York, 1972.
6. Sandgren, E., The Utility of Nonlinear Programming Algorithms, Ph.D. Thesis, Purdue University, 1977.
7. Sandgren, E., and Ragsdell, K. M., "The Utility of Nonlinear Programming Algorithms: A Comparative Study- Parts I and II," ASME Journal of Mechanical Design, Vol. 102, No. 3, July 1980, pp. 540-551.
8. Sandgren, E., "A Statistical Review of the Sandgren-Ragsdell Comparative Study," Evaluating Mathematical Programming Techniques, Lecture Note #199, Springer-Verlag, 1982, pp. 72-90.
9. Schittkowski, K., Nonlinear Programming Codes - Information, Tests, Performance, Lecture Notes in Economics and Mathematical Systems, No. 183, Springer-Verlag, New York, 1980.
10. Eason, E. D., "Validity of Colville's Time Standardization for Comparing Optimization Codes," ASME Paper No. 77-DET-116, September 1977.
11. Dembo, R. S. and Mulvey, J. M., "On the Analysis and Comparison of Mathematical Programming Algorithms and Software," Proceedings of the Bicentennial Conference on Mathematical Programming, Gaithersburg, Maryland, 1976.
12. Hillstom, K. E., "A Simulation Test Approach to the Evaluation and Comparison of Unconstrained Nonlinear Optimization Algorithms," Argonne National Laboratories Report No. ANL-76-20, 1976.
13. Nazareth, L. and Schlick, F., "The Evaluation of Unconstrained Optimization Routines," Proceedings of the Bicentennial Conference on Mathematical Programming, Gaithersburg, Maryland, December 1976.
14. Crowder, H. P., Dembo, R. S., and Mulvey, J. M., "Reporting Computational Experiments in Mathematical Programming," Mathematical Programming, Vol. 15, #3, November 1978, pp. 316-329.

15. Miele, A. and Gonzalez, S., "On the Comparative Evaluation of Algorithms for Mathematical Programming Problems," presented at Nonlinear Programming Symposium - 3, Madison, Wisconsin, July 1977.
16. Eason, E. D., "Evidence of Fundamental Difficulties in Nonlinear Optimization Code Comparisons," Evaluating Mathematical Programming Techniques, Lecture Note #199, Springer-Verlag, 1982, pp. 60-71.
17. Hoffman, K. L. and Jackson, R. H. F., "In Pursuit of a Methodology for Testing Mathematical Programming Software," Evaluating Mathematical Programming Techniques, Lecture Note #199, Springer-Verlag, 1982, pp. 60-71.
18. Mulvey, J. M. (ed), Evaluating Mathematical Programming Techniques, (Proceedings of Conference at Boulder, Colorado, 1981), Lecture Note #199, Springer-Verlag, 1982.
19. Hooke, R. and Jeeves, T. A., "'Direct Search' Solution of Numerical and Statistical Problems," Journal of the ACM, Vol. 8, No. 2, April 1961, pp. 212-229.
20. Powell, M. J. D., "An Efficient Method for Finding the Minimum of a Function of Several Variables Without Calculating Derivatives," Computer Journal, Vol. 7, No. 4, 1964, pp. 155-162.
21. Nelder, J. A. and Mead, R., "Simplex Method for Function Minimization," Computer Journal, Vol. 7, No. 4, January 1965, pp. 308-313.

A CONCEPTUAL BASIS FOR THE DESIGN OF DAMAGE-TOLERANT STRUCTURAL SYSTEMS

Farrokh Mistree
Associate Professor
Department of Mechanical Engineering
University of Houston
Houston, Texas

Jon A. Shupe
Research Assistant
Department of Mechanical Engineering
University of Houston
Houston, Texas

Owen F. Hughes
Professor
Department of Naval Architecture
University of New South Wales
Sydney, Australia

*
C-5
PRECEDING PAGE BLANK NOT FILMED

A CONCEPTUAL BASIS FOR THE DESIGN OF DAMAGE-TOLERANT STRUCTURAL SYSTEMS

ABSTRACT

We define damage-tolerant structural systems as those systems which not only have adequate intact strength to withstand initial failure but also adequate residual strength to minimize the possibility of, and hence the consequences of, further failure. The incorporation of damage tolerance cannot be done in total isolation of the function being required of the system and the costs associated with obtaining improved damage tolerance. Our approach, therefore, is to formulate multiple-objective, multi-level decision support problems the solutions of which represent a compromise between higher costs and higher damage tolerance. Multiple-objective decision support problems are easily solved in the linear domain. Our formulations, however, include both linear and nonlinear constraints and goals, which in the past, have not been considered due to the resulting complexity. In this paper we

- . present a complete discussion and description of decision support problems, including coupled DSPs and multi-level DSPs with examples
- . provide a general formulation of a design decision support problem which provides a basis for the inclusion of damage-tolerant considerations in structural design
- . identify what further research needs to be done in order to obtain information that is required but not known for solving problems using these models
- . identify what needs to be done to implement this prototype method in practice

I. INTRODUCTION AND BACKGROUND

In the past, there have been many approaches to structural design. Most approaches have been based on deterministic, "rule of thumb" formulas that resulted in overweight, over-strengthened structures. These methods were appropriate when there were no advanced analysis techniques and structure cost was a small fraction of the total cost of the project. Now, however, as structures get larger (witness several plans for steel structures in over one thousand feet of water) and computers and programs allow more complex analysis of structures, there is a need for a rational approach (as opposed to an ad hoc, random approach) that promotes optimal structural design.

Hughes et al. (1,2) have proposed a method for the design of semi-monocoque structures. The method is summarized in Figure 1. The method begins with the input of loads and other pertinent data about the structural system. An appropriate finite-element module is used to analyze the structure and output the demand on the subsystems. A limit analysis is performed on the structural system to determine if it has the capability to withstand the demands placed upon it. Appropriate constraints are then formulated and the structural system is optimized. At this point the subsystem design cycle is entered. Here, for each subsystem in turn, a limit analysis is performed, constraints are formulated, and an optimal subsystem design is derived. This cycle continues until all subsystems have been optimized. If convergence has not been reached the process continues in the system design cycle.

There are several assumptions in this design method. It is assumed that the geometry and structural materials have been previously defined and that the loads on the structure are known. Also, a "design-oriented" type of finite-element analysis for semi-monocoque structures, together with the theory and methods for the limit analysis of both the overall structure and the various substructures, is presented in (2). Thus, these items will not be discussed in this paper. The main topics for discussion are

- development of a methodology that handles multiple levels of optimization
- formulation of the optimization problems for the structural system and each of its subsystems

This will permit a designer to obtain a superior design which, ideally, will represent the best compromise between the various (and conflicting) objectives.

2. MULTI-LEVEL SYSTEM DECISION SUPPORT PROBLEMS (DSP)

Engineering systems, such as structures, are generally too complex to be handled in their entirety. This necessitates design of the overall system by first decomposing the system into subsystems. If the system is then designed in parts (sequentially), there is no guarantee that an overall optimal design will be reached. Thus, it becomes necessary to develop a methodology for the optimization of a multi-level system. The multi-level system is described as a system that contains more than one level of interaction between the system and its subsystems. The design of such a system is based on the formulation and solution of a series of problems involving decisions to be made by the designer. In this paper, the information necessary to enable a designer to formulate these decisions as Decision Support Problems (DSP) is presented. Solution of the DSPs will result in superior (or optimal) solutions. These DSPs are capable of handling multi-objective problems that contain both "hard" and "soft" information.

In this section the structure of a multi-level DSP is presented. The characteristics of Damage-Tolerant Design (DTD) are presented in Section 3. A discussion of the compromise DSP and how it is formulated is given in Section 4. Also presented are two generic DSP formulations for damage-tolerant design. Section 5 contains two case studies. The first is an example of the use of multi-level DSPs in ship design. The second case study is a coupled DSP that combines the selection of a structural material with structural design optimization.

2.1 Structure of a Multi-Level DSP

An engineering system can be represented hierarchically as in Figure 2. The hierarchical nature of system design facilitates the identification of complexity and the inter-relationships among various levels and subsystems. The relations and bonds of a hierarchical system are essential for the visualization of the system. A practical example of parent system-subsystem relationship is shown in Figure 2. A ship hull module (or compartment) is subdivided into subsystems called strakes. In turn each strake can be considered to be made up of subsystems such as plates, stiffeners, girders, and frames. It is important to note that all of the subsystems are integral parts of the parent system (hull module). This means that changes in one subsystem affect the parent system and other subsystems, as shown by the circle intersections. Thus no subsystem can be considered in isolation from the rest.

At each level of the hierarchical structure, for each subsystem, the design process involves a set of decisions which are qualified by the following assertions (3):

Design is a series of decisions.

- Some decisions can be made concurrently.
- Some decisions must be made sequentially.

Design involves multi-level decision making.

- Interaction between the various levels of subsystems exists. This interaction may be only one way or both ways.
- Interaction between the subsystems at the same level of the same parent or of different parents also exists. This interaction can be one way or both ways.

2.2 Types of Decision Support Problems (4)

In design, there are basically three ways to derive the answers to problems encountered. They are analysis, synthesis, and heuristic thinking. These may seem to be widely divergent but it is possible to integrate all three in the form of structured decision support problems. A structuring of information for the DSP is necessary to make a good decision. Since there are different types of decisions to be made, different categories of DSP exist.

They are

- Selection
- Compromise
- Coupled Selection and Compromise

Selection DSPs are appropriate for problems that involve the choice of an alternative from among several. The choice is made based on ratings given to multiple attributes and their relative importance. Compromise DSPs involve the optimization of an alternative by changing design variables optimally. Compromise is discussed further in Section 4. A coupled DSP involves the solution of a selection and a compromise DSP simultaneously. An example of a coupled problem is given in Section 5.

3. DISCUSSION OF GENERAL DAMAGE-TOLERANT DESIGN (DTD)

Since the compromise decision support problem is capable of handling multi-goal problems, it is an important tool for the design of structural systems. This stems from the fact that, in structural systems, there are always at least two important objectives that must be met to achieve a superior design. The first objective is economic efficiency and the second is technical efficiency. Several criteria can be used as measures of efficiency. Weight, for example, may be an indirect measure of both economic and technical efficiency. Reliability, stiffness, and strength are all measures of technical efficiency. Cost is a direct measure of economic efficiency and an indirect measure of technical efficiency. Therefore, there are at least two goals or objectives that must be defined and used in the design of a structure.

Damage-tolerant structures have two kinds of strength: intact strength and residual strength (5). Intact strength represents the amount by which the working load of the structure can be exceeded before it fails. Residual strength represents the strength remaining in a structure once a vital component has been rendered ineffective. A damage-tolerant structure will thus resist initial failure (due to intact strength) and will also resist further failure after initial failure (due to residual strength). Thus, intact and residual strengths are measures of technical efficiency. Also, since a failure due to residual strength would result in complete loss of the structure and thus a large financial loss, it can be said that residual strength is an indirect measure of economic efficiency. Since it may be desirable to minimize weight in a damage-tolerant structure, we have a second indirect measure of economic efficiency. Therefore, ideally, a damage-tolerant design (DTD) represents an optimal balance between the goals of technical efficiency and the goals of economic efficiency.

4. COMPROMISE DSP: DEFINITIONS AND TERMINOLOGY

The basic approach to the solution of a structural optimization problem is to formulate the design problem as a compromise DSP and to solve it using optimization techniques. These optimization techniques must allow the designer to find the values of the design variables that simultaneously satisfy the requirements on the system's capability and to achieve desired goals as far as possible. The goals can be conflicting and of different dimensions. To formulate the compromise DSP, the techniques of goal programming are used. A program capable of solving the DSP has been implemented at the University of Houston called SLIP2. The details of this program can be found in Mistree et al. (6).

The next step is to describe how these compromise problems can be formulated. First, it is important to know the components that make up the problem. They are given by Kupparaju and Mistree (7) as

- Variables - system variables
 - deviation variables
- Constraints - system constraints
 - goal constraints
- Bounds - on system variables
 - on deviation variables
- Objective - in terms of deviation variables

A generic word formulation of the compromise problem follows:

GIVEN

- A structure with given geometry and materials
- The requirements that need to be satisfied by the design for feasibility
- The goals of the design; these need to be achieved as far as possible

FIND

- The values of the system variables
- The values of the deviation variables (which indicate the extent to which the goals are achieved)

SATISFY

- System constraints: must be satisfied for feasibility
- Goal constraints: to be achieved as far as possible
- Bounds
 - Lower and upper bounds on the system variables
 - Lower and upper bounds on the deviation variables

MINIMIZE

- The difference between the required and the estimated performance of the design

4.1 System Variables and System Constraints

The generic word problem for compromise is explained with reference to Figure 3.

System variables $\underline{X} = (x_1, x_2, x_3, \dots, x_n)$

System constraints $C_i/D_i(\underline{X}) \geq R_i$ and

$$C_i(\underline{X})/D_i(\underline{X}) \geq R_i$$

System descriptors are either fixed by the specifications provided or are variable as to the need of the design. The descriptors, as the name implies, describe the state of a system completely. Since some of the descriptors are fixed parameters and do not change during the course of the design, the state of the system is dependent entirely upon a set of variable descriptors termed system variables. In general, a set of "n" design variables is represented by \underline{X} . These variables may be continuous, Boolean (1=true, 0=false), or a combination of the two, an example of which will be shown later. System variables are, by their nature, independent of the other descriptors and can be changed as required by the designer to alter the state of a system.

A system constraint is a constraint placed on the design that has to be satisfied for feasibility of the design. Mathematically, system constraints are functions of the system variables only. They are rigid and no violations are allowed. They relate the demands placed on the system $D(\underline{X})$ to the capability of the system C or $C(\underline{X})$ to meet the demand.

Now a tie-in to damage tolerance can be made. There are four categories of system constraints: catastrophic, non-catastrophic, operational, and proportionality. Catastrophic constraints deal with complete system failure, whereas non-catastrophic constraints deal with local or limited failures that could (but not necessarily) lead to complete failure. Operational constraints keep the system within bounds to ensure its operability and proportionality constraints ensure that system components can be fabricated. In generic form, for the i-th mode of failure the system constraint is

$$C_i / D_i(\underline{X}) \geq R_i \quad \text{or} \quad C_i(\underline{X}) / D_i(\underline{X}) \geq R_i$$

The difference between the two lies in the fact that the capability can be either a constant C_i (such as yield stress) or can be a function of the design variables $C_i(\underline{X})$ (such as the critical buckling stress). For the purposes of damage tolerance, the ratio of a structure's strength capability to the demand (or stresses) placed upon it will be referred to as the intact strength factor B_i . Thus, the ratio of the system capability to the demand on the system will always be constrained to be not less than a minimum safety factor R_i for the i -th mode of failure. In reality, these factors are the product of several partial safety factors, which are specified by safety authorities such as AISC, and which have been obtained on the basis of providing a satisfactory reliability level. These system constraints do not prevent the capability/demand ratio from being very large. When this happens, the design is technically, but not economically, efficient. Prevention of large ratios is the responsibility of the goal constraints as will be shown later.

4.2 Deviation Variables and Goal Constraints

Deviation variables include d_i^- which is the underachievement of the i -th goal, and d_i^+ which is the overachievement of the i -th goal.

Goal constraints are $(1/m \sum_{i=1}^m C_i(\underline{X})/D_i(\underline{X}))/S + d_1^- - d_1^+ = 1$; m represents the number of goals

$$B_{\max}/B_{\min} + d_2^- - d_2^+ = 1$$

Goal constraints represent the aspiration levels of a designer for the design. They are always expressed as equalities and relate the goals of the designer to the actual achievement of the design. It is possible that the designer's goals are inordinately high or the system constraints are much too restrictive to attain the aspired levels of achievement. The deviation variables d_i^- and d_i^+ are used to allow the designer a certain degree of latitude in making

decisions. A particular goal may either be overachieved ($d_i^+ > 0$, $d_i^- = 0$) or underachieved ($d_i^- > 0$, $d_i^+ = 0$). The two deviation variables associated with each

goal therefore relate the actual performance of the design to the desired level of performance. If there are two or more goals it is imperative that the goals are made dimensionless with all the deviation variables varying between a fixed range (e.g. 0 to 1, 0 to 10, etc.). In order to achieve this it may be necessary to scale the goal (e.g. divide the function by a suitable constant). For example

$$\frac{\text{Goal Function}}{\text{Expected Value of Function}} + d_1^- - d_1^+ = 0$$

To particularize the goal constraints to the damage tolerant case, first, let S represent a desired value for the capability/demand ratio for the structure. If S is always greater than $\min(C_i(\underline{X})/D_i(\underline{X}))$ (or B_{\min} , for short), then it is desirable for the feasible design to satisfy the following constraints:

- the average intact strength should be as close to S as possible, i. e.,

$$(1/m) \sum_{i=1}^m C_i(\underline{X})/D_i(\underline{X}) / S + d_1^- - d_1^+ = 1$$

- the difference between the highest and lowest intact strength factors, i.e.,

$$B_{\max} = \max(C_i(\underline{X})/D_i(\underline{X})) \text{ and } B_{\min} = \min(C_i(\underline{X})/D_i(\underline{X})), \text{ for } i=1,2,\dots,m,$$

should be as small as possible, i.e.,

$$B_{\max}/B_{\min} + d_2^- - d_2^+ = 1$$

These constraints ensure that the intact strength factor B for the "average" failure mode is as close to S as possible and that the spread of B is as small as possible. Note that the system constraints maintain a minimum safety factor R for each mode of failure, while the first goal constraint uses a target safety factor S that the average of the intact strengths is made to meet.

4.3 Bounds

It is necessary to place bounds on both the system variables (\underline{X}) and the deviation variables (d^- , d^+), i.e.,

$$\underline{L} \leq \underline{X} \leq \underline{U}$$

$$0 \leq d_i^- \leq 1 \text{ for all } i$$

$$0 \leq d_i^+ \leq 1 \text{ for all } i$$

These specific limits are placed on the magnitude of each of the variables. Each variable is associated with a lower and upper bound as a result of the limited capability of the system or based on the designer's judgment. If there are two or more goal constraints, it is imperative that all the deviation variables are dimensionless (or are of the same dimension) and it is desirable that they vary between a fixed range (e.g. 0 to 1). The bounds demarcate the region in which a search is to be made for a feasible solution.

4.4 Objective Function

The objective function is to minimize $Z(\underline{d}^-, \underline{d}^+)$.

The designer sets an aspiration level for each of the goals. It may be impossible to obtain a design that is up to the standards aspired to. Hence, a compromise solution has to be accepted by the designer. It is desirable, however, to obtain a design whose performance matches the aspirations as closely as possible. This is the objective of a compromise DSP solution. The difference between the goals and achievement is expressed by a combination of the appropriate deviation variables $Z(\underline{d}^-, \underline{d}^+)$. The magnitude of $Z(\underline{d}^-, \underline{d}^+)$ is an indication of the extent to which specific goals are achieved. All the goals may not be equally important to the designer. Goal programming formulations are classified either as Archimedian or preemptive based on the manner in which importance is assigned to the deviation variables. The objective or achievement function in Archimedian goal programming is

$$Z(\underline{d}^-, \underline{d}^+) = p_1 d_1^- + p_2 d_1^+ + \dots + p_{2m-1} d_m^- + p_{2m} d_m^+$$

where the weights p_1, p_2, \dots reflect the desire to achieve one goal, more than the others. In Archimedian goal programming the weights p_i are such that

$$\sum_{i=1}^{2m} p_i = 1$$

The values of these weights are often based on estimates and designer preferences. It may be difficult to come up with truly credible weights that attach more importance to one goal than the other. This often requires more information than the designer may have at hand at the time; therefore, the Archimedian may not be the best method to use. A method for determining the weights is given in Riggs (8).

In preemptive goal programming, this uncertainty is circumvented by rank ordering the goals. Goals are ranked lexicographically and a more important goal is to be satisfied as much as possible before other goals are considered. The achievement function, for instance, may look like

$$Z(\underline{d}^-, \underline{d}^+) = p_1 d_1^- + p_2 d_1^+ + p_3 d_2^- + p_4 (d_2^- + d_3^+), \text{ etc.}$$

where p_1 is much larger than p_2 which is much larger than p_3 and so on. The deviation variable d_1^- has to be minimized preemptively before d_1^+ is considered and so forth. The priorities represent rank, i.e., by how much one goal is preferred to another. No conclusions can be drawn with respect to the amount by which one goal is preferred or is more important than another. This approach is more suitable when there is less information available.

4.5 Generic Formulation of the Compromise DSP

Using the foregoing discussion as a basis, a generic compromise DSP can be created. The solution of such a DSP will represent a superior design. This

design will represent a compromise between technical and economic efficiency, i.e. the intact strength of the intact structure and cost. The mathematical formulation of the compromise DSP which includes intact strength considerations for an intact structure follows.

GIVEN

D = demand on system

C = capability of system

R_i^c, R_i = safety factor for i-th failure mode, (superscript c indicates catastrophic as opposed to non-catastrophic failure)

S^c, S = target factor of safety

m = number of catastrophic failure modes

n = number of non-catastrophic failure modes

\underline{O} = operational functions

\underline{M} = minimum profitable operational levels

\underline{F} = fabrication functions (e.g., X_i/X_j)

\underline{T} = minimum proportional sizes

\underline{X} = system design variables

\underline{d} = deviation variables

\underline{L} = lower bounds on system variables

\underline{U} = upper bounds on system variables

B = reserve strength factor

V = total weight of system

V^E = expected value of the weight

K = cost of system

K^E = expected value of the cost

Z = objective function

FIND

The values of the design variables \underline{X}

The values of the deviation variables $\underline{d}^-, \underline{d}^+$

SATISFY

System Constraints

- Catastrophic Failure Constraints

$$C_i(\underline{X})/D_i(\underline{X}) \geq R^C, i = 1, 2, \dots, m$$

- Non-catastrophic Failure Constraints

$$C_j(\underline{X})/D_j(\underline{X}) \geq R; j = 1, 2, \dots, n$$

- Operational Constraints

$$O(\underline{X}) \geq \underline{M}$$

- Fabrication Constraints

$$F(\underline{X}) \geq \underline{T}$$

Bounds on System Variables

$$\underline{L} \leq \underline{X} \leq \underline{U}$$

Goal Constraints (dimensionless)

- Catastrophic Failure Goals

$$(1/m \sum_{i=1}^m C_i(\underline{X})/D_i(\underline{X}))/S^C + d_1^- - d_1^+ = 1$$

$$B_{\max}^C/B_{\min}^C + d_2^- - d_2^+ = 1$$

- Non-catastrophic Failure Goals

$$(1/n \sum_{j=1}^n C_j(\underline{X})/D_j(\underline{X}))/S + d_3^- - d_3^+ = 1$$

$$B_{\max}/B_{\min} + d_4^- - d_4^+ = 1$$

- Weight

$$V(\underline{X})/V + d_5^- - d_5^+ = 0$$

- Cost

$$K(\underline{X})/K^E + d_6^- - d_6^+ = 0$$

Bounds on Deviation Variables

$$0 \leq d_i^- \leq 1 \text{ and } 0 \leq d_i^+ \leq 1 \text{ for } i=1,2,\dots,m.$$

MINIMIZE

$$Z(\underline{d}^-, \underline{d}^+) = p_1 d_1^- + p_2 d_1^+ + p_3 d_2^- + \dots + p_{11} d_6^- + p_{12} d_6^+$$

with

$p_i \gg p_j \gg p_k$ (Preemptive). The symbol \gg indicated preference.

or

12

$$\sum_{i=1}^{12} p_i = 1 \text{ (Archimedian)}$$

4.6 Generic Formulation of a Coupled Selection-Compromise DSP

As mentioned before, the compromise DSP can contain system variables that are real, Boolean, or a mixture of the two. The advantage of this lies in the fact that a coupled problem can be formulated and solved. A coupled problem is one that combines selection (a choice made from several alternatives by considering various attributes) and compromise. One example of a coupled problem is the inclusion of the selection of the construction material (thus establishing important material constants, such as yield strength) in the damage-tolerant design (DTD) compromise DSP. The formulation follows.

GIVEN

D = demand on system

C = capability of system

R_i^c, R_i = safety factor for i-th failure mode, (superscript c indicates catastrophic as opposed to non-catastrophic failure)

S^c , S = target factors of safety

m = number of catastrophic failure modes

n = number of non-catastrophic failure modes

\underline{O} = operational functions

\underline{M} = minimum profitable operational levels

\underline{F} = fabrication functions

\underline{T} = minimum proportional sizes

\underline{X} = system design variables

a = number of alternative materials

b = number of attributes for material selection

\underline{Y} = alternative variables (Boolean)

$Y_i = 1$ material is selected

$= 0$ material is not selected

R_{ij} = normalized rating (i-th alternative, j-th attribute)

I_j = relative importance of attribute j (normalized)

\underline{d} = deviation variables for compromise

\underline{D} = deviation variables for selection

\underline{L} = lower bounds on system variables

\underline{U} = upper bounds on system variables

V = total weight of system

V^E = expected value of the weight

K = cost of system

K^E = expected value of the cost

Z = objective function

FIND

The value of the alternative variables (selection) \underline{Y}

The values of the system (compromise) design variables \underline{X}

The values of the deviation variables $\underline{D}^-, \underline{D}^+, \underline{d}^-, \underline{d}^+$

SATISFY

Selection System Constraints - (Only one alternative is chosen.)

$$\sum_{i=1}^a Y_i = 1$$

Selection Goal Constraints - (Merit of each alternative should be as close to unity as possible.)

$$\sum_{j=1}^b (I_j R_{ij}) Y_i + D_i^- - D_i^+ = 1; \text{ there will be 'a' such constraints}$$

Compromise System Constraints

- Catastrophic Failure Constraints

$$C_i(\underline{X})/D_i(\underline{X}) \geq R_i^C; i = 1, 2, \dots, m$$

- Non-catastrophic Failure Constraints

$$C_j(\underline{X})/D_j(\underline{X}) \geq R_j; j = 1, 2, \dots, n$$

- Operational Constraints

$$\underline{Q}(\underline{X}) \geq \underline{M}$$

- Fabrication Constraints

$$\underline{F}(\underline{X}) \geq \underline{T}$$

Bounds on System Variables

$$\underline{L} \leq \underline{X} \leq \underline{U}$$

Goal Constraints - (Dimensionless)

- Catastrophic Failure Goals

$$(1/m \sum_{i=1}^m C_i (\underline{X})/D_i (\underline{X}))/S^C + d_1^- - d_1^+ = 1$$

$$B_{\max}^C/B_{\min}^C + d_2^- - d_2^+ = 1$$

-Non-catastrophic Failure Goals

$$(1/n \sum_{j=1}^n C_j (\underline{X})/D_j (\underline{X}))/S + d_3^- - d_3^+ = 1$$

$$B_{\max}/B_{\min} + d_4^- - d_4^+ = 1$$

- Weight

$$V(\underline{X})/V^E + d_5^- - d_5^+ = 0$$

- Cost

$$K(\underline{X})/K^E + d_6^- - d_6^+ = 0$$

Bounds on Deviation Variables

$$0 \leq D_i^-, D_i^+ \leq 1; \text{ for } i=1,2,\dots, a$$

$$0 \leq d_i^-, d_i^+ \leq 1; \text{ for } i=1,2,\dots, b$$

MINIMIZE

$$Z = P_1 (\underline{D}, \underline{D}^+) + P_2 (\underline{d}, \underline{d}^+)$$

where

$P_1 \gg P_2$ where \gg symbolizes preference

Such a coupled problem has been solved and the results are given in Section 5. The structural system is a three-bar truss with two loading modes. The selection problem involves three different steels with different properties. The problem is a simple one but serves to illustrate the principles involved.

4.7 Solution Algorithm

The compromise DSP for practical structures will always have

- a mix of linear and non-linear constraint functions
- some mix of equality and inequality constraints
- multiple objectives which may also be some mix of linear and non-linear functions.

This constrained multi-objective compromise DSP can be solved by the SLIP2 algorithm (6). This program has been extensively used (1,9,10,11) to design comprehensive structural systems. Its cost effectiveness has been documented in (1,12); for 22 variables, 91 constraints (29 non-linear), and 2 goals, SLIP2 used 13 seconds of CPU time on a Honeywell 6600 computer. Recently it has been used by Lyon (13), who has correctly shown the role of preemptive and Archimedian formulations, using SLIP2 in the design of large systems (in his case, the preliminary design of ships). Ittimakin (14) has implemented the SLIP2 algorithm in BASIC on an Apple II/plus microcomputer. He has shown that the algorithm can be used to solve not only DSPs but also to solve traditional linear programming and network problems, algebraic equations (any mix of linear and non-linear equations), and curve-fitting problems.

5. EXAMPLES

Two examples are presented in this section as verification of the efficacy of the design approach that has been presented in this paper. The first example is a descriptive example embodying existing software and design thought; the second example contains a math formulation that covers a more specific, albeit pathological problem. Together, they demonstrate the more important principles covered by the design method that has been described here.

The first example is based on work modified from Hughes (2). The example that has been drawn forth and applied to large problems serves to illustrate the concept of multi-level DSPs as discussed in Section 2. There are some differences in terminology between Example 1 and those of this paper. The reason for this is that the terminology in this paper has been kept general in order that problems from other disciplines can be handled. However, since the first example

specifically handles ship structure design, the terminology has been adapted to that use in ship structures. For example, the terms "catastrophic" and "non-catastrophic" have been used to define two categories of failure modes. The equivalent terms in this case study are "collapse" and "unserviceability." Also, the term "strake" is used instead of "subsystem." However, the formulation of the compromise DSPs follows the same format presented in Section 4.

The second case illustrates the coupled problem presented in Section 4.6. This problem is formulated to select one of three materials and to optimize the weight and strength of a three-bar truss. The specific math formulation is derived from a word problem to demonstrate the solution of what might be seen as an open-ended problem.

5.1 Example 1: Limit States Levels and Types

In a structure there are many types of limit states and many ways of categorizing them. First, there are substructure limit states that involve only one substructure and overall limit states that involve more than one substructure and which therefore cannot be dealt with at the substructure level. In a semi-monocoque structure there are two main types of overall collapse: longitudinal collapse which occurs when the overall longitudinal bending moment M exceeds the limit value M_{ult} , and transverse collapse which occurs when the transverse framing has suffered sufficient individual failures (e.g., plastic hinge, flexural-torsional buckling) to form an overall failure mechanism. Fatigue failure normally corresponds to the substructure level, but for structures in which the overall loading is cyclic (ship hulls, aircraft, etc.) it can also constitute an overall limit state. In this case, the limit can be expressed in terms of a minimum required section modulus Z_R such that the cyclic stresses are kept within acceptable limits, as determined by Miner's Rule or another method of fatigue analysis.

In addition to the collapse limit states, there are various other ways in which a structure or substructure can become unsuitable or "unserviceable." For example, there are often limits on structural flexibility arising from aeroelastic or hydroelastic considerations (such as flutter) or from vibration or other dynamic response. In a semi-monocoque structure, these limits can be expressed in terms of a minimum required value of cross sectional moment of inertia I_R .

5.2 Example 1: Optimization of Ship Structures

In even a medium-size structure there are typically 100 to 200 design variables, and a nonlinear optimization problem of this size involves far too much computation to be solved as a single problem. Therefore one of the prerequisites for rationally based structural design is a method or strategy for subdividing the overall problem while still retaining true overall optimization and the capability of dealing with overall constraints. In this section, a brief outline of a dual-level strategy which meets these requirements is presented.

5.2.1 Subdivision of the overall optimization problem

The subdivision of the overall optimization problem is based on the concept of a substructure, which is a region of structure in which a sufficient number of

the scantlings (dimensions) are linked, either by fixed structural geometry or by explicit constraints linking two or more scantlings, such that the region forms a logical entry from an optimization point of view. The characteristics which most clearly make a region suitable as a substructure are geometric uniformity and identical, repetitive structural members. Such characteristics are frequently imposed on portions of structure in order to simplify the design and to thereby gain increased economy and efficiency in nearly all aspects of the structure's existence. Any such uniformity provides an opportunity for reducing the amount of computation, and the choice of substructures should reflect and take full advantage of uniformity.

Figure 4 shows the most common type of substructure for a semi-monocoque hull. For simplicity, it will be called a "strake." It consists of a longitudinal row of panels, transverse frame segments, and if applicable, longitudinal girder segments. In most ships, these members are uniform and repetitive in the longitudinal direction over quite large distances. Local changes in geometry are disregarded because they are dealt with in detail design. Whatever the length of the uniformity, that is the length of the substructure. This reduces the number of design variables. In Figure 4, the strake substructure has 12 design variables: four for the stiffened panel, four for the frame segments, and four for the girder segment.

Substructures also reduce the number of limit values that have to be calculated because identical members all have the same value. Hence, there is just one constraint for each mode of member failure, and to formulate each constraint it is necessary only to scan for and utilize the largest value of each relevant load effect.

5.2.2 Design variables of the overall optimization problem

A parent system design variable is any mathematical combination or function of subsystem design variables which plays the role of an independent variable in an overall limit state. There are two different groups of parent system design variables, one for hull girder collapse and one for constraints relating to hull girder section properties Z and I .

The first group of parent system design variables consists of those member limit values which are involved in the collapse of the hull girder, either longitudinal or transverse. These will be denoted as $Q_{L,hg}$. For longitudinal collapse, the number of panels varies, depending on the structural geometry of the ship, but it is usually less than 10. The constraint against overall longitudinal collapse may be expressed symbolically in the form

$$M_{ult} (Q_{L,hg}) \geq \gamma_{s,o} M$$

in which $\gamma_{s,o}$ is the partial safety factor for overall collapse.

Transverse overall collapse involves a number of different loads, some of which are independent. Hence, the load is not a simple scalar quantity as is hull girder bending moment; rather it is a set or group of individual loads which we shall denote as \underline{F} . The symbol $\underline{F_d}$ represents the set of design loads; for those loads which are random, a characteristic value or design extreme value is used. The magnitude of each vector is characterized by its norm, which we denote as \bar{F}

$$\bar{F} = F^T F$$

The transverse ultimate strength of the ship F_{ult} is the set values of F which cause collapse of the transverse framing. Since there are several load vectors F_{ult} is always taken as the worst of these, that is, the particular combination and sequence which causes collapse for the smallest value of F .

In terms of $Q_{L,hg}$ the constraint against transverse collapse is

$$\bar{F}_{ult}(Q_{L,hg}) \geq \gamma_{s,o} \bar{F}_d$$

in which the parentheses signify the functional dependence of the overall ultimate strength on $Q_{L,hg}$, the member limit values that are involved in the collapse, and indicate that these latter values are the "design variables" in the overall level of optimization.

In the overall limit states relating to hull girder fatigue and flexibility the hull girder section modulus Z and moment of inertia I take the place of the load effects. These geometric quantities can be expressed in terms of the cross-sectional areas of the substructures which comprise the ship's cross section. Therefore these areas are treated as parent system design variables, represented by A , and the constraints relating to hull girder fatigue and flexibility are then functions of these variables, which are few in number, rather than as a function of the many independent design variables. In symbolic form these constraints are

$$Z_B(A) \geq Z_{B,R}$$

$$Z_D(A) \geq Z_{D,R}$$

$$I(A) \geq I_R$$

in which subscripts B and D stand for bottom and deck respectively, and R signifies the required minimum value of Z and I .

The use of subsystems and overall design variables makes it possible to divide the system design problem into several smaller problems, one for each of the substructures and one for the overall structure. In each substructure problem the design variables are the structural dimensions, denoted as X . In the overall problem the design variables are $Q_{L,hg}$ and A . Using the generic compromise DSP developed in Section 4.5, we now formulate the compromise DSP for the overall structure (parent system) and other compromise DSPs for the substructures. The parent system is coupled by multilevel goal constraints. These constraints are a function of the cross section area variable (deck or bottom) and the pertinent values of the subsystem dimension variables. Similar constraints are given in the subsystem model. A multiplier is used with the parent system values A_B and A_D to model the fractional portion of the parent system that the subsystem represents.

5.2.3 Parent system: compromise DSP

The compromise DSP formulation follows:

GIVEN

M = longitudinal bending moment

M_{ult} = ultimate longitudinal bending moment

$\gamma_{s,o}$ = partial safety factor for overall collapse

\bar{F}_d = set of design loads

\bar{F}_{ult} = loads that would cause transverse collapse

σ_w = working stress

Z = hull girder section modulus

I = moment of inertia

KG = distance of the vertical center of gravity from the keel
(lowermost point of the ship structure)

I_T = transverse moment of inertia of the hull compartment

n = percentage area represented by a particular subsystem

FIND

S_D - section modulus of the deck

S_B - section modulus of the bottom

A_D - section area of the deck

A_B - section area of the bottom

Q_L - member limit values

$\underline{e}, \underline{e}^+$ - parent system deviation variables

SATISFY

Parent System Constraints

Collapse

- Longitudinal Collapse

$$M_{ult} (Q_{L,hg}) / M \geq \gamma_{s,o}$$

- Transverse Collapse

$$\bar{F}_{ult} (Q_{L,hg}) / \bar{F}_d \geq \gamma_{s,o}$$

- Hull Girder Bending Stress

$$f_1 (S_D, A_D) \leq \sigma_w|_{deck}$$

$$f_2 (S_B, A_B) \leq \sigma_w|_{bottom}$$

- Hull Girder Fatigue

$$Z_B (A_B) \geq Z_{B,R}$$

$$Z_D (A_D) \geq Z_{D,R}$$

Unserviceability

- Hull Girder Rigidity

$$I (\underline{A}) \geq I_R$$

Bounds on Parent System Variables

$$\underline{L}_A \leq \underline{A} \leq \underline{U}_A$$

$$\underline{L}_S \leq \underline{S} \leq \underline{U}_S$$

Goal Constraints (Dimensionless)

- Vertical Center of Gravity

$$f_3 (S_D, A_D, S_B, A_B) / KG + e_1^- - e_1^+ = 1$$

- Moment of Inertia

$$f_4 (A_D, A_B) / I_T + e_2^- - e_2^+ = 1$$

- Weight

$$f_5(A_D, A_B)/V^E + e_3^- - e_3^+ = 0$$

- Cost

$$f_6(A_D, A_B)/K^E + e_4^- - e_4^+ = 0$$

- Multilevel constraints

$$f_7(nA_D, \underline{P}, \underline{S}) + e_5^- - e_5^+ = 1$$

$$f_8(nA_B, \underline{P}, \underline{S}) + e_6^- - e_6^+ = 1$$

Bounds on Deviation Variables

$$0 \leq e_i^- \leq 1; 0 \leq e_i^+ \leq 1 \text{ for } i=1,2,3,4,5,6$$

MINIMIZE

$$Z = P_1(e_1^- + e_1^+) + P_2(e_2^- + e_2^+) + P_3e_3^+ + P_4e_4^+ + P_5(e_5^- + e_5^+) + P_6(e_6^- + e_6^+)$$

5.2.4 Strake (subsystem) compromise: with plate and stiffeners only

The strake compromise formulation follows:

GIVEN As in the generic compromise DSP (Section 4.5)

FIND

\underline{P} - plate dimensions (thickness, length, width)

\underline{s} - stiffener dimensions (height, web thickness, width of flange, thickness of flange)

$\underline{d}^-, \underline{d}^+$ - deviation variables

SATISFY

Strake Constraints

Panel Collapse

- Stiffener Failure

$$C_1(\underline{s})/D_1(\underline{s}) \geq R_1^C$$

- Combined Buckling

$$C_2(\underline{P}, \underline{s})/D_2(\underline{P}, \underline{s}) \geq R_2^C$$

- Membrane Yield

$$C_3(\underline{P})/D_3(\underline{P}) \geq R_3^C$$

- Stiffener Buckling

$$C_4(\underline{s})/D_4(\underline{s}) \geq R_4^C$$

Panel Unserviceability

- Yield in Tension in Stiffener Flange

$$C_5(\underline{s})/D_5(\underline{s}) \geq R_1$$

- Yield in Tension in Plating

$$C_6(\underline{P})/D_6(\underline{P}) \geq R_2$$

- Yield in Compression in Stiffener Flange

$$C_7(\underline{s})/D_7(\underline{s}) \geq R_3$$

- Yield in Compression in Plating

$$C_8(\underline{P})/D_8(\underline{P}) \geq R_4$$

- Plate Bending

$$C_9(\underline{P}, \underline{s})/D_9(\underline{P}, \underline{s}) \geq R_5$$

- Local Buckling

$$C_{10}(\underline{P}) / D_{10}(\underline{P}) \geq R_6$$

Bounds on Strake Variables

$$\underline{L}_P \leq P \leq \underline{U}_P$$

$$\underline{L}_S \leq s \leq \underline{U}_S$$

Goal Constraints (Dimensionless)

- Collapse Goals

$$\frac{1}{4} \sum_{i=1}^4 C_i(\underline{P}, \underline{s}) / D_i(\underline{P}, \underline{s}) / S^C + d_1^- - d_1^+ = 1$$

$$B_{\max}^C / B_{\min}^C + d_2^- - d_2^+ = 1$$

- Unserviceability

$$(1/6) \sum_{j=1}^6 C_j(\underline{P}, \underline{s}) / C_j(\underline{P}, \underline{s}) / S + d_3^- - d_3^+ = 1$$

$$B_{\max} / B_{\min} + d_4^- - d_4^+ = 1$$

- Weight

$$V(\underline{P}, \underline{s}) / V^E + d_5^- - d_5^+ = 0$$

- Cost

$$K(\underline{P}, \underline{s}) / K^E + d_6^- - d_6^+ = 0$$

- Multilevel Constraints

$$f_1(nA_D, \underline{P}, \underline{s}) + d_7^- - d_7^+ = 1$$

$$f_2(nA_B, \underline{P}, \underline{s}) + d_8^- - d_8^+ = 1$$

Bounds on Deviation Variables

$$0 \leq d_i^- \leq 1; \quad 0 \leq d_i^+ \leq 1 \quad ; i = 1, 2, \dots, 8$$

MINIMIZE

$$Z = P_1(d_1^- + d_1^+) + P_2(d_2^- + d_2^+) + P_3(d_3^- + d_3^+) + \dots + P_8(d_8^- + d_8^+)$$

This model only includes plates and stiffeners. However, inclusion of girders and/or frames is possible and requires only the addition of the appropriate system variables and associated constraints.

5.2.4 Integration of compromise DSPs in the design cycle

In Section 1, Figure 1 was presented as a flow chart of a systematic approach to structural design. Figure 5 is now presented to show how the math models in this section fit into the overall scheme.

The design cycle remains the same. The additions worthy of attention are in the constraint formulation boxes. As shown, the constraint categories are now known. The same goes for the hull subsystem. Thus, the formulations given in this section fit into the design method and thus are not isolated problems.

5.3 Example 2: A Coupled Decision Support Problem

The usefulness of the generic coupled problem will be illustrated by treating a simple three-member indeterminate structure involving two distinct load conditions and the selection of a structural material from among three alternatives.

5.3.1 Problem situation

Given a three-bar truss with geometry as shown in Figure 6, the system parameters are

$$H = 10 \text{ in}$$

$$\beta_1 = 135^\circ$$

$$\beta_2 = 90^\circ$$

$$\beta_3 = 45^\circ$$

$$\sigma_{11} = 20,000 \left(\frac{1}{A_1} - \frac{A_2}{2A_1 A_2 + \sqrt{2} A_1^2} \right)$$

$$\sigma_{21} = \frac{20,000 \sqrt{2} A_1}{2A_1 A_2 + \sqrt{2} A_1^2}$$

$$\sigma_{31} = \frac{20,000 A_2}{2A_1 A_2 + \sqrt{2} A_1^2}$$

The material alternatives are malleable cast iron, gray cast iron, and steel. Their properties are given in Table 1. The cross-sectional areas of the three members should be sized so as to prevent failure and yet yield a low-weight design.

| Alternative | Attributes | | | |
|---------------------|--------------------------|--------------------------------------|------------------------------------|----------------|
| | Allowable Stresses (psi) | Corrosion Resistance (Relative Rank) | Elastic Moduli $\times 10^6$ (psi) | Cost \$/cu. ft |
| Malleable Cast Iron | 5400 | 4 | 25 | 100.0 |
| Gray Cast Iron | 4500 | 3 | 13 | 110.0 |
| Steel | 240000 | 5 | 30 | 150.0 |

TABLE 1 - MATERIAL ALTERNATIVES

5.3.2 Word problem for the three-bar truss

The word problem for the three-bar truss is as follows:

GIVEN

- The system configuration shown in Figure 6
- The equations relating applied forces to resulting stresses
- That two distinct load conditions are present
- Member 2 is always in tension
- Members 1 and 3 may be in tension or compression depending on the load
- The material alternatives are malleable cast iron, gray cast iron, and steel
- Material properties are given in Table 1

FIND

- The most appropriate material from among three alternatives
- Cross-sectional area of members 1 and 3
- Cross-sectional area of member 2

SATISFY

SELECTION

1. Only one material can be chosen
2. The relative merits should be as close to unity as possible

COMPROMISE

System constraints

3. The tensile stress in member 1 is not to exceed the permissible stress level
4. The tensile stress in member 2 is not to exceed the permissible stress level
5. The compressive stress in member 3 is not to exceed the permissible stress level

Goal constraints

6. The weight of the entire structure is to be kept as close to zero as possible (i.e., minimize weight)
7. The material used in constructing member 1 is to be used as efficiently as possible
8. The material used in constructing member 2 is to be used as efficiently as possible

Bounds: System variables

9. The areas of members are non-negative
10. The areas of members are less than a designer-specified value

Bounds: Deviation variables

11. The values of the normalized deviation variables are non-negative
12. The values of the normalized deviation variables are less than unity

MINIMIZE

- The overachievement of the weight goal first and then the deviation from the most efficient utilization of the material

5.3.3 Math formulation

The math formulation is as follows:

GIVEN

As in the word problem

FIND

X_1 [in²] - cross sectional area of A_1 , A_3

X_2 [in²] - cross sectional area of A_2

\underline{d}^- , \underline{d}^+ - compromise deviation variables

Y_1 , Y_2 , Y_3 - material selection variables (Boolean)

\underline{D}^- , \underline{D}^+ - selection deviation variables

SATISFY

SELECTION

1. System Constraints

$$Y_1 + Y_2 + Y_3 = 1$$

2. Goal Constraints

$$(I_1 R_{11} + I_2 R_{12} + I_3 R_{13} + I_4 R_{14}) Y_1 + \underline{D}_1^- - \underline{D}_1^+ = 1$$

$$(I_1 R_{21} + I_2 R_{22} + I_3 R_{23} + I_4 R_{24}) Y_2 + \underline{D}_2^- - \underline{D}_2^+ = 1$$

$$(I_1 R_{31} + I_2 R_{32} + I_3 R_{33} + I_4 R_{34}) Y_3 + \underline{D}_3^- - \underline{D}_3^+ = 1$$

COMPROMISE

System Constraints

3. Stress in member 1

$$\sigma_{11} - (5400 Y_1 + 4500 Y_2 + 24000 Y_3) \leq 0$$

4. Stress in member 2

$$\sigma_{21} - (5400 Y_1 + 4500 Y_2 + 24000 Y_3) \leq 0$$

5. Stress in member 3

$$-\sigma_{31} - (5400 Y_1 + 4500 Y_2 + 24000 Y_3)(0.75) \leq 0$$

Goal Constraints (Dimensionless)

6. Weight

$$(0.276 Y_1 + 0.276 Y_2 + 0.283 Y_3) H (2\sqrt{2}A_1 + A_2)/4.0 + d_1^- - d_1^+ = 0$$

7. Utilization of member 1

$$\frac{(5400Y_1 + 4500Y_2 + 24000 Y_3)}{\sigma_{11}} + d_2^- - d_2^+ = 1$$

8. Utilization of member 2

$$\frac{(5400Y_1 + 4500Y_2 + 24000Y_3)}{\sigma_{21}} + d_3^- - d_3^+ = 1$$

Bounds on System Variables

$$9. \quad X_1, X_2 \geq 0$$

$$10. \quad X_1, X_2 \leq 4 \text{ in}^2$$

Bounds on Deviation Variables

$$11. \quad 0 \leq \underline{d}^- \leq 1 ; 0 \leq \underline{d}^+ \leq 1$$

$$12. \quad 0 \leq \underline{D}^- \leq 1; 0 \leq \underline{D}^+ \leq 1$$

MINIMIZE

$$Z = P_1 (D_1^- + D_1^+ + D_2^- + D_2^+ + D_3^- + D_3^+) \\ + P_2 (d_1^- + d_1^+) + P_3 (d_2^- + d_2^+ + d_3^- + d_3^+)$$

$$P_1 \gg P_2 \gg P_3$$

5.3.4 Solution

The solution obtained from using SLIP2(6) on an AS/9000N computer is:

$$Y_1 = 0.0$$

$$Y_2 = 0.0$$

$$Y_3 = 1.0$$

$$X_1 = 0.56 \text{ in}^2$$

$$X_2 = 0.51 \text{ in}^2$$

The material selected is steel ($Y_3 = 1.0$). Member 2 has a cross-sectional area of 0.51 in. sq. while members 1 and 3 have cross-sectional areas of 0.56 in. sq. The active constraint is the tension on member 1. The tension constraint on member 2 and the compression constraint on member 3 are well within their limits.

This type of problem would be useful in any design where selection of material and optimized weight and strength are critical, e.g., for space structures.

6. A PROTOTYPE SYSTEM: FUTURE RESEARCH AND DEVELOPMENT

In the first section of this paper a design method based on current technology was described. In this section future developments and research will be outlined that will lend support in creating a viable design system for the design of structural systems. Further research is required in several areas.

- Further investigation of the character of the system design problem is needed. This includes the development of constraints for various classes of problems.
- Establishment of values for the target factors of safety that are reliability based is required. (The AISC has released a reliability based code within the past year.)
- Formulation and solution of multiple-level DSPs should be further explored and expanded.
- Further research is required to determine the effective use of sensitivity analysis and the impact of soft information on the design of structural systems.
- The feasibility of employing expert systems to aid a designer in structural design should be investigated. The application of expert systems to constraint banks (compilations of appropriate constraints based on different structural failure theories) will be shown by Shupe, J. A. and Mistree, F., University of Houston, (work in progress).

- In this paper, the compromise DSP for intact strength has been presented. More work needs to be done to develop the compromise DSP for coupled intact and residual strength. One approach has been presented by Mistree (5).

It may be appropriate at this stage to identify an overall strategy which is suitable for system design. There are two possible approaches to design synthesis that could allow one to take advantage of the different analysis (or failure) theories. One strategy is to develop multiple failure analysis modules using different theories of failure (plasticity, fatigue, reliability, etc.). The system would feature a controller which would use the appropriate module and direct the flow of information between the different modules. This concept is illustrated in Figure 7. As can be seen, the controller interacts with the different failure analyses modules and the of the parent system.

The second approach for design synthesis that could be developed is a single synthesis model that can accommodate the various analysis modules directly, and it is presented in Figure 8. This synthesis model should be able to accommodate different failure modes. This model is similar to the multi-level DSP model presented earlier. The important feature here is that the synthesis model is an adaptive one. Thus the same synthesis model is capable of synthesizing the impact of different modes of failure. The second approach is favored by the authors.

ACKNOWLEDGEMENTS

The financial contributions of NL Technology Systems - MWD towards the establishment of a research program to improve the effectiveness of designers operating in a computer-assisted environment are gratefully acknowledged. The technical contribution of Mr. N. Kuppuraju, a graduate student at the University of Houston, in Section 4 is gratefully acknowledged.

REFERENCES

1. O. F. Hughes, F. Mistree, V. Zanic, "A Practical Method for the Rational Design of Ship Structures", Journal of Ship Research, Vol. 26, No. 2, June 1980, pp. 101-113.
2. O. F. Hughes, Ship Structural Design: A Rationally-Based, Computer-Aided, Optimization Approach, Wiley & Sons, 1983.
3. N. Kuppuraju, "Computer Based Design-Synthesis An Approach to Problem Solving", M. S. Thesis, Department of Mechanical Engineering, University of Houston, May 1984.
4. F. Mistree, D. Muster, "Design Harmonization: A Computer-based Approach for Design in the Systems Age", Optimization in Computer-aided Design, (ed. J. S. Gero), North-Holland, 1984.
5. F. Mistree, "Design of Damage Tolerant Structural Systems", Engineering Optimization, Vol. 6, 1983, pp. 141-144.

6. F. Mistree, O. F. Hughes, H. B. Phuoc, "An Optimization Method for the Design of Large, Highly Constrained Complex Systems", Engineering Optimization, Vol. 5, No. 3, 1981, pp.179-197.
7. N. Kuppuraju, F. Mistree, "Compromise - An Effective Approach to Solve Multi-objective Structural Design Problems", Paper Submitted to Computers and Structures, 1984.
8. J. S. Riggs, Engineering Economy, McGraw-Hill, 1977.
9. O. F. Hughes, "A Method for Nonlinear Optimum Design of Large Structures and Applications to Naval Ship Design," Intl. Symp. on Opt. Struc. Des., University of Arizona, Tucson, Section 10, Oct. 1981, p. 5.
10. J. D. Davis, O. F. Hughes, F. Mistree, "Automated Limit State Design of Steel Structures," Proceedings, 6th Australasian Conference on Mechanics of Structures and Materials, Christchurch, New Zealand, Aug. 1977, pp. 98-106.
11. D. Lin, O. F. Hughes, J. Mahowald, "Applications of a Computer-Aided, Optimal Preliminary Ship Structural Design Method," Transactions SNAME, 1981.
12. F. Mistree, T. D. Lyon, J. A. Shupe, "Design of Damage Tolerant Offshore Structures", Proceedings MTS-IEEE Oceans 82, 20-24 Sept, 1982, pp. 1201-1206.
13. T. D. Lyon, "An Advanced Computer-based Method for the Design of Engineering Systems", M. S. Thesis, Department of Mechanical Engineering, University of Houston, February 1983.
14. P. Ittimakin, "Design of Advanced Engineering Systems Using a Micro Computer", M. S. Thesis, Department of Mechanical Engineering, University of Houston, May 1984.

ORIGINAL PAGE IS
OF POOR QUALITY

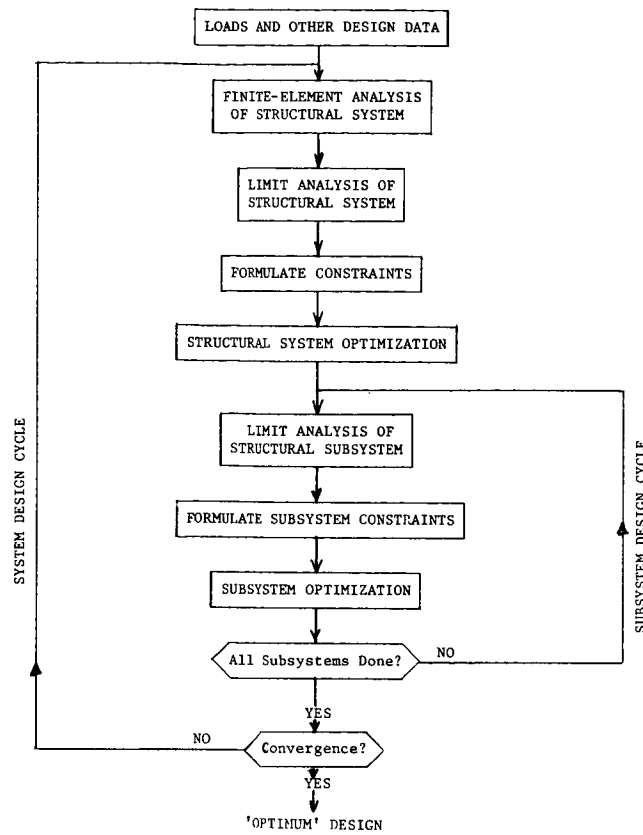


Figure 1.- Structural Design Cycle.

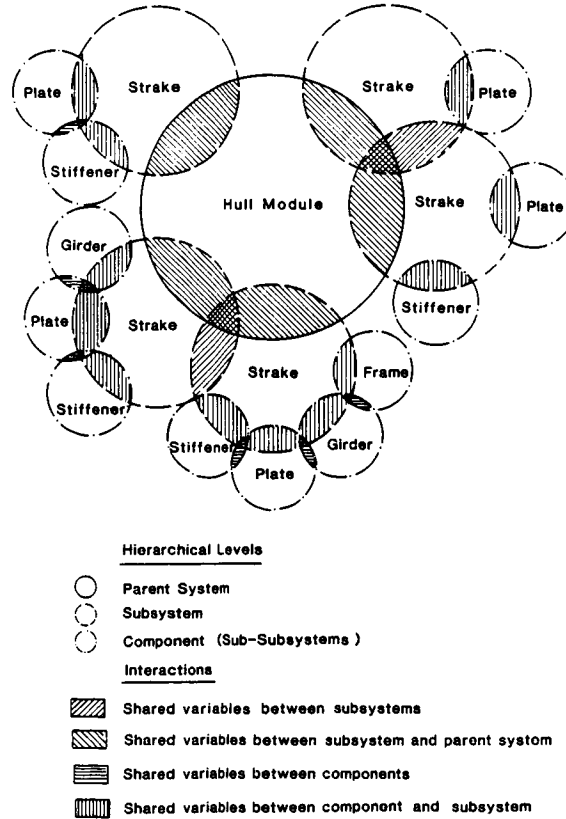


Figure 2.- Hierarchical Nature of a Structural System.

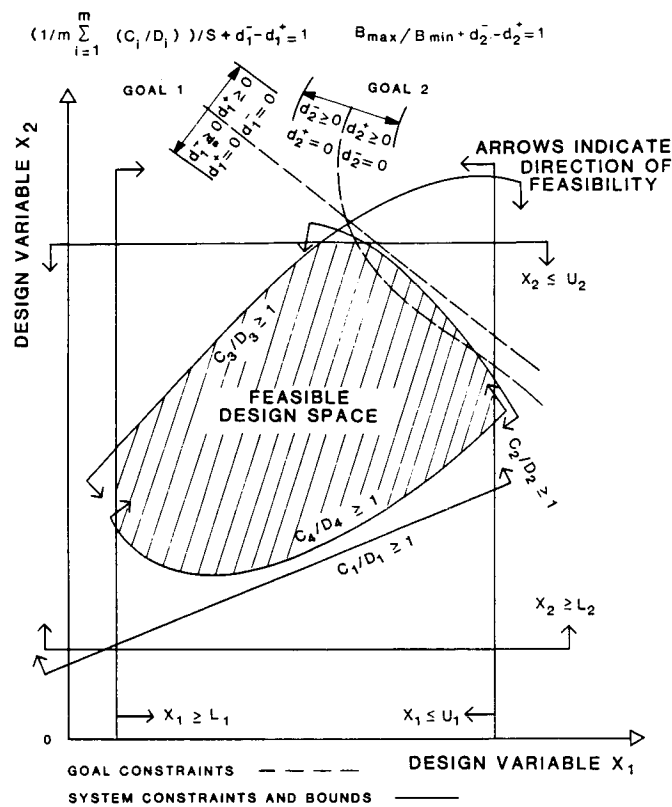


Figure 3.- Typical Design Space: Two-Variable Compromise DSP.

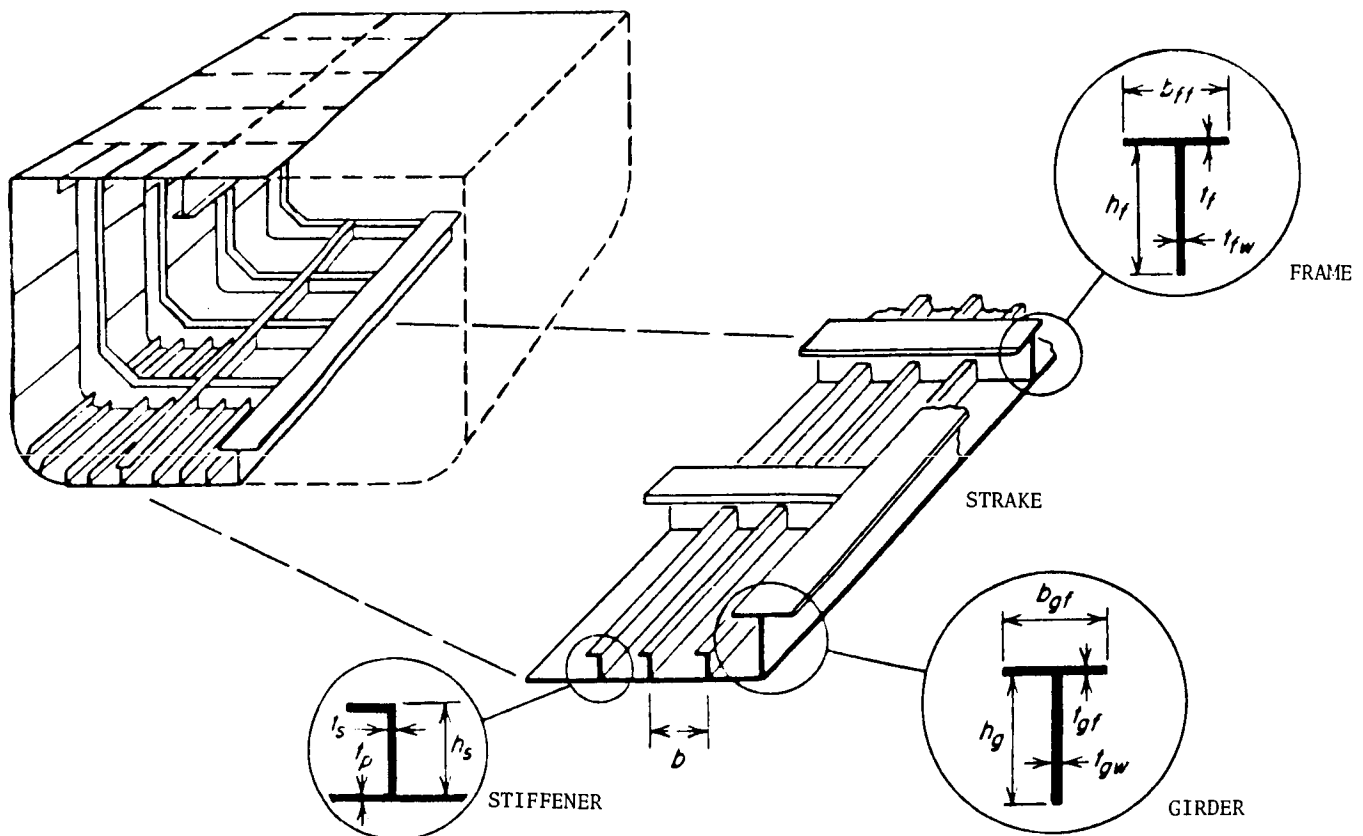


Figure 4.- Strake Subsystem.

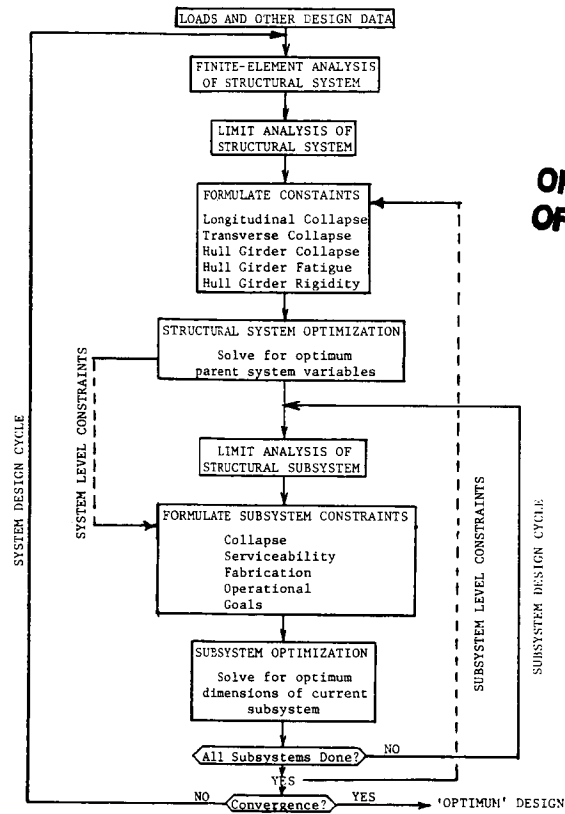


Figure 5.- Multi-Level System Design.

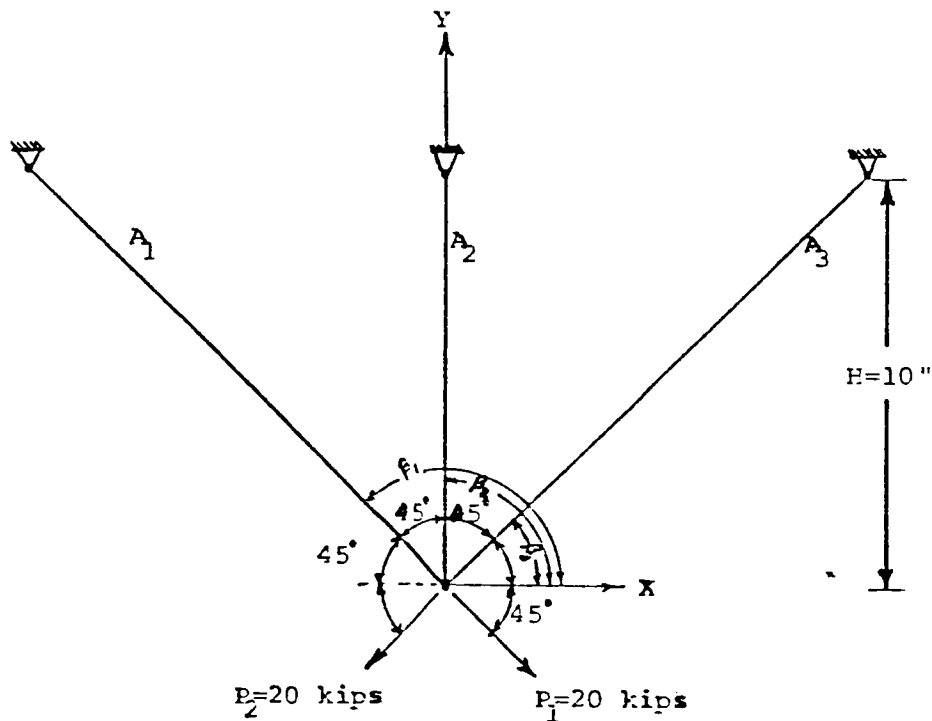


Figure 6.- Three-Bar Truss.

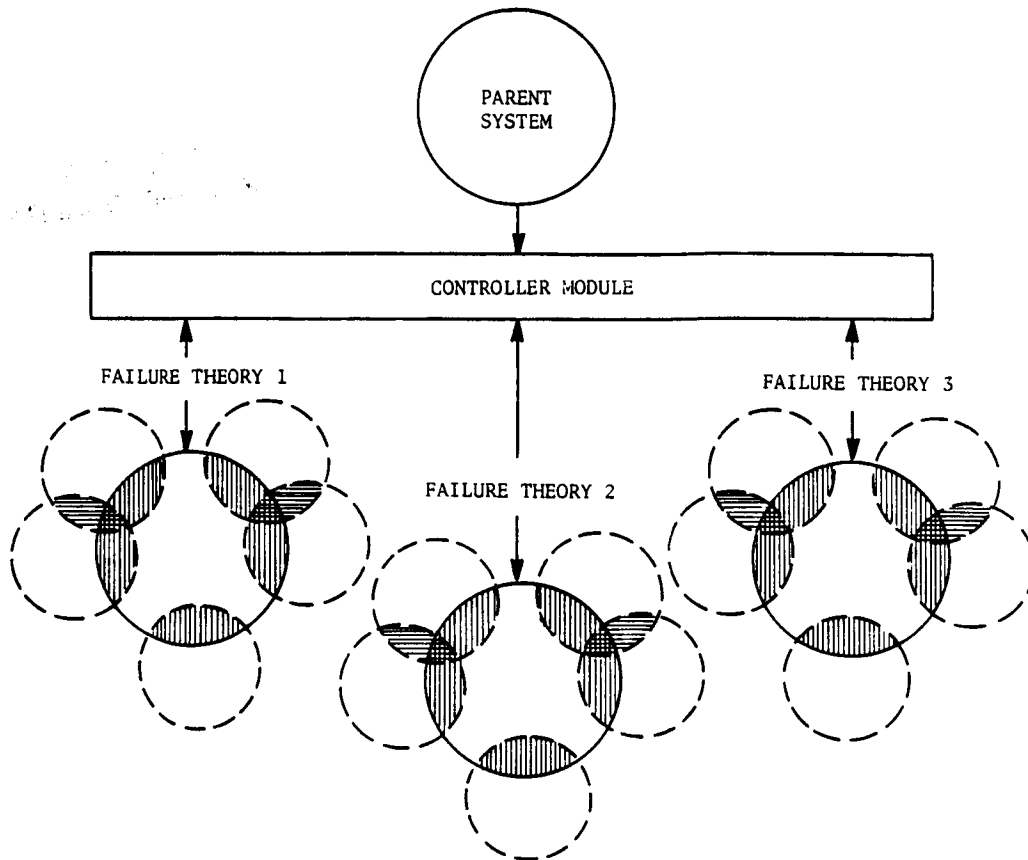
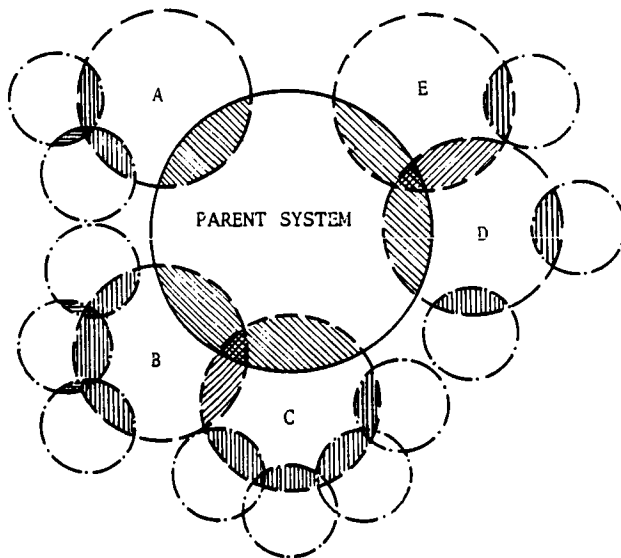


Figure 7.- Parent System/Controller/Analysis Modules.



1. The parent system is defined in terms of subsystems A - E.
2. Two pairs of subsystems have shared variables. (B and C; D and E)
3. Subsystem A has variables that are independent from the other subsystems.

Figure 8.- Parent System and Analysis Modules.

N87-11774

COMMENTS ON GUST RESPONSE CONSTRAINED OPTIMIZATION

Prabhat Hajela
Department of Engineering Sciences
University of Florida
Gainesville, Florida

ABSTRACT

Recent research pertaining to optimum structural design with probabilistic constraints is reviewed. The limitations and complexities introduced in the design as a result of the transition from deterministic to probabilistic constraints are underscored. A concise development of the theoretical aspects of optimum design of aircraft structures subjected to random wind loads is presented and suggestions for future research are offered. An emphasis is placed on the incorporation of recent developments in fracture mechanics in the design constraints.

INTRODUCTION

An overwhelming majority of recent developments in optimum structural design have dealt primarily with the minimum weight design of a statically loaded structure. Structural design with constraints on the dynamic response characteristics introduces an additional degree of complexity and has been the subject of recent research. A random vibration environment necessitates a reformulation of the optimization problem and presents significant new problems that are the subject of this paper.

Optimum design of structural systems with random parameters and probabilistic constraints is a physically realistic problem. Ground excitation during an earthquake or unsteady wind shears are examples of random loads. A similar situation exists for an airplane flying into patches of storm or nonstorm turbulence. There are two levels of difficulty that can be identified in this problem:

- (a) A systematic description of the random loads and the choice of a statistical process that would allow the computation of the dynamic response parameters of interest
- (b) The interpretation of these parameters for the optimum design problem (this would include the formulation of constraints that would minimize the conservativeness in the design but would still be computationally viable)

A considerable body of literature exists in the civil engineering discipline that deals specifically with the description of random loads. A power spectral density description is perhaps the most common approach to the problem wherein the frequency spectrum of ground motion or air pressure distribution is specified. Reference 1 reviews the subject in some detail. There were considerably fewer publications pertaining to probabilistic or reliability based optimum design. References 2-4 are indicative of attempts at optimization in a nondeterministic environment for simplistic structural configurations.

The primary focus of the present paper is to review the state-of-art approaches for probabilistic design in aerospace applications. Research efforts in this area are typified by References 5-8. The deficient areas are defined and new methodology presently under study is outlined. The numerical results obtained under this study will be presented in a separate publication.

AIR TURBULENCE MODELS

Measurements of various air turbulence samples indicate both a time and a spatial variation. A rapid penetration of the gust field justifies assumption of freezing the gust in time (ref. 9). This assumption would be invalid in rotorcraft applications and for air vehicles that have a significant hover mode. In most response calculations, the spatial variation of the gust field along a spanwise direction is neglected and only a variation in the flight direction is taken into consideration. This one-dimensional model (fig. 1) needs to be reassessed for light, high aspect ratio airplanes.

Computation of the system response in the frequency domain is more elegant than the time domain solution and is therefore emphasized in this paper. Following this approach a turbulence field is typically characterized by the gust velocity power spectral density (PSD) distribution shown in figure 2.

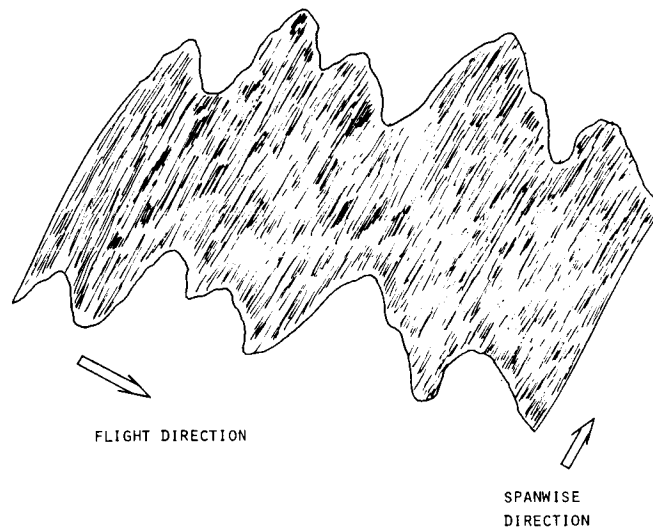


Figure 1.- One-dimensional turbulence model.

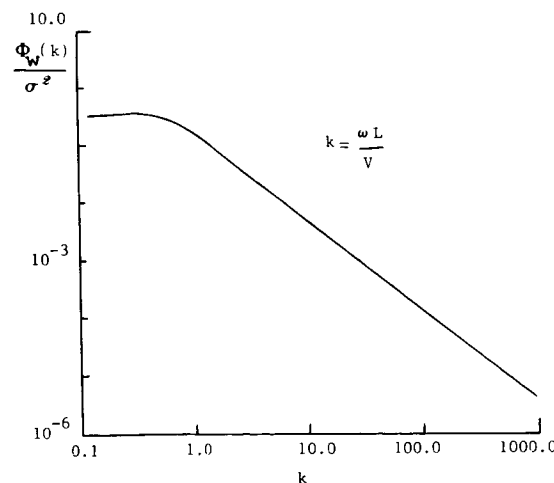


Figure 2.- von Karman power spectra.

The power spectral density function is representative of the variation of the mean square values of the gust velocities with frequency and is established on the basis of a stationary, isotropic, homogeneous, one-dimensional gust field characterized by a Gaussian probability distribution. The power spectral density distribution for the gust intensity is used in conjunction with the response admittance functions to compute the linear response of the system to the gust loading (Figure 3). The von Karman spectra given by

$$\phi(\Omega) = \frac{\sigma^2 L}{\pi} \frac{1 + \frac{8}{3} (1.339 L \Omega)^2}{[1 + (1.339 L \Omega)^2]^{11/6}}$$

provides a good fit to recorded turbulence data. Here, σ is the rms turbulence intensity and 'L' is the "scale of turbulence" which is representative of a spatial distance over which no correlation exists in the gust intensities. Flight measurements indicate some disagreement with the stationarity assumption. This lack of agreement is in the higher turbulence load levels where the computed response underestimates the actual response. This suggests a modification in the Gaussian model for turbulence.

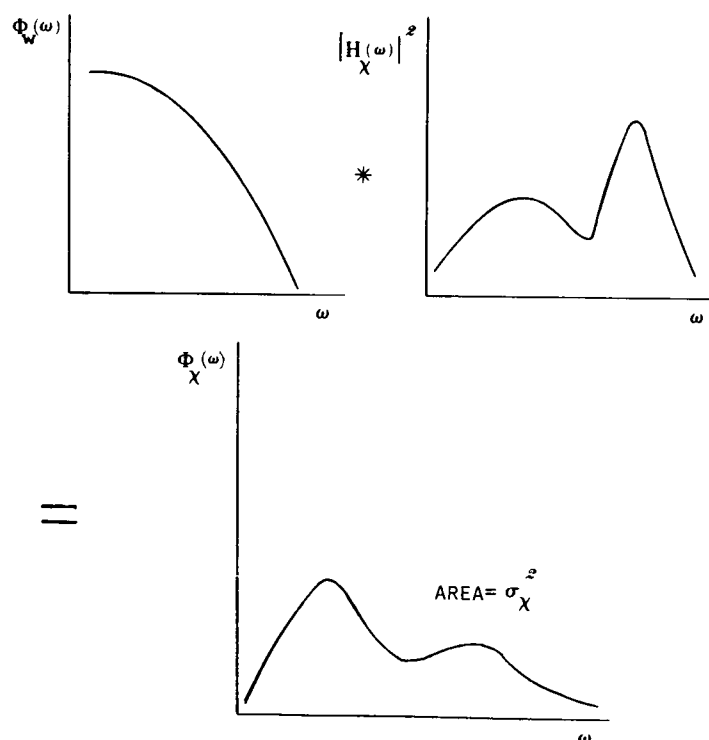


Figure 3.- Linear response analysis in the frequency domain.

GUST RESPONSE ANALYSIS

A modal response approach is customarily preferred for the dynamic analysis of large structural systems. A finite number of elastic modes and dominant rigid body modes are used to model the structural deformations. In terms of the displacement vector w , the system equations of motion are written as

$$(-\omega^2 [M] + [K] - [A])\{w\} = \{G\}$$

where $[M]$ and $[K]$ are the mass and stiffness matrices, $[A]$ is the matrix of loads due to oscillation at frequency ω , and $\{G\}$ is the force coefficient array per unit gust velocity. The displacements $\{w\}$ can be represented approximately by the superposition of the characteristic modes:

$$\{w\} = [\Phi] \{q\}$$

where $[\Phi]$ is the matrix of 'm' normalized eigenmodes and $\{q\}$ is an m-dimensional vector of modal participation factors. The system equation is rewritten as

$$(-\omega^2 [I] + [\omega_m^2] - [\bar{A}]) \{q\} = \{\bar{G}\}$$

Here ω_m^2 is the m-th natural frequency and arrays $[\bar{A}]$ and $\{\bar{G}\}$ are defined as

$$[\bar{A}] = [\Phi]^T [A] [\Phi]$$

$$\{\bar{G}\} = [\Phi]^T \{G\}$$

The above set of simultaneous algebraic equations is solved for a range of reduced frequencies of interest. The forces and the stresses are computed in terms of the displacements.

THE STRUCTURAL OPTIMIZATION PROBLEM

Structural optimization problem in a stochastic environment must account for the random variation in design parameters in addition to the random dynamic loads. The problem formulation is stated as

$$\begin{aligned}
 &\text{Minimize} && F(\bar{d}) \\
 &\text{Subject to} && P\left[\bigcup_{i=1}^k \{R_i(\bar{w}(\bar{d}, t)) > r_i\} \right] < [p_f] \\
 &&& a < t < b \\
 &&& R_j(\bar{d}) < r_j \\
 &&& d_i^L < d_i < d_i^U
 \end{aligned}$$

Here $F(\bar{d})$ is typically the structural weight, \bar{d} is the vector of design variables and \bar{w} is the time varying dynamic response. R_i is the response function with a deterministic or random bound specified by r_i , and $[p_f]$ represents the upper bound on the probability of failure. The design variables have prescribed lower and upper bounds.

In the event that $R_i(\bar{w}(\bar{d}, t))$ is a stationary random process, the constraint can be rewritten in a deterministic, time independent manner (ref. 10).

$$P\left[\bigcup_{i=1}^k \{R_i(\bar{w}(\bar{d}, t)) > r_i\} \right] \approx \sum_{i=1}^k q_i(\bar{d}) < (p_f)$$

$a < t < b$

where, for R and r both conforming to a normal distribution and exhibiting statistical independence,

$$q(\bar{d}) = \frac{1}{\sqrt{2\pi}} \int_{\mu_r - \mu_R / \sqrt{\sigma_r^2 + \sigma_R^2}}^{\infty} e^{-u^2/2} du$$

where the μ 's and σ 's denote the mean and rms values, respectively. The solution to the ensuing deterministic problem can be approached by any standard nonlinear programming strategy. While this approach may perform well for simplistic situations involving single response quantities, gust response design poses significant new problems. The power spectral density approach used in aircraft gust design leads to the rms values of individual loads such as shear, bending moment and torsion at various points within the structure. However, the statistical nature of these loads conceals information regarding their combination characteristic (sign and magnitude), which is very important from the standpoint of design. A constant probability of combination criterion has been suggested to circumvent this

problem. The normal probability distribution density function (fig. 4) for two variables, x and y , is given as

$$p(x,y) = \frac{1}{2\pi\sigma_x\sigma_y\sqrt{1-\rho_{xy}^2}} \exp\left[-\frac{1}{2(1-\rho_{xy}^2)}\left[\left(\frac{x-\mu_x}{\sigma_x}\right)^2 - 2\rho_{xy}\left(\frac{x-\mu_x}{\sigma_x}\right)\left(\frac{y-\mu_y}{\sigma_y}\right) + \left(\frac{y-\mu_y}{\sigma_y}\right)^2\right]\right]$$

This equation represents ellipses in planes parallel to the x - y plane and the infinite load combinations on the boundary of the ellipse have an equal probability of occurrence. The shape and orientation of the ellipse depend upon the mean and mean square values of x and y and on a quantity ρ_{xy} , referred to as the correlation coefficient. In an attempt to define a finite number of dominant load combinations, Stauffer and Hoblitt (ref. 7) propose a technique to circumscribe the ellipse by an octagon (fig. 5) and use the eight vertices of the octagon as critical load combinations in the structural design. This procedure would be intractable if a higher number of equally probable loads were to be combined.

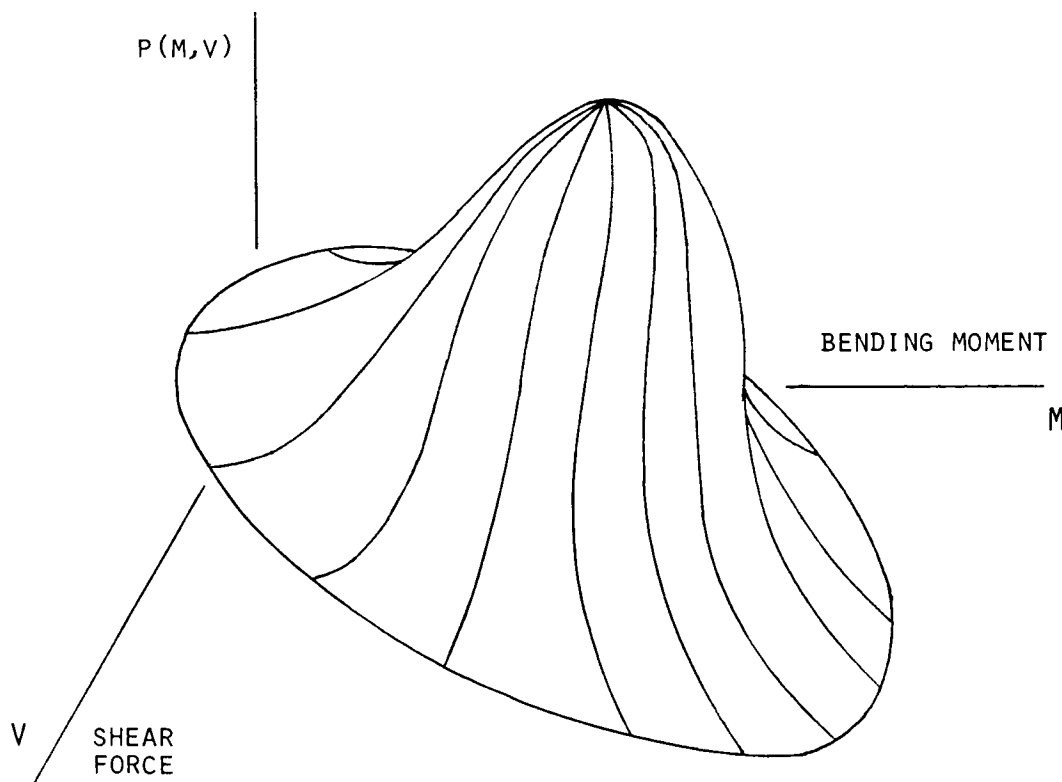


Figure 4.- Probability density.

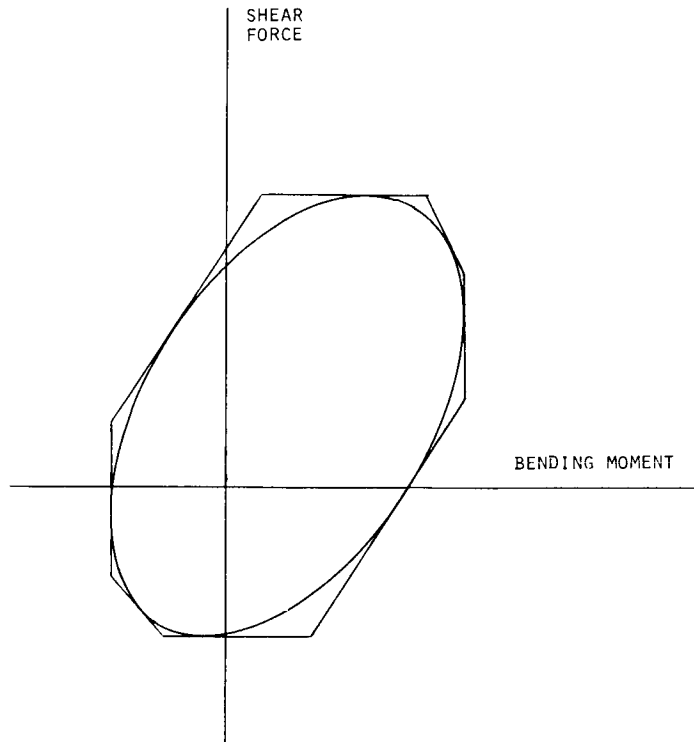


Figure 5.- Equal probability of load combination.

Gross and Sobieski (ref. 6) suggest an alternate procedure which would be applicable to a general multivariate normal density distribution. This approach discretizes the equal probability curve/hypersurface into a finite number of design-load-combination conditions. In an optimization framework this would translate into a very large number of constraints, a situation that is countered by recourse to the "cumulative constraint" idea which permits folding these constraints into a single representative measure.

In both these strategies the correlation coefficient ρ_{xy} plays a key role. This quantity is defined as follows

$$\rho_{xy} = \frac{1}{\bar{A}_x \bar{A}_y} \int_0^{\infty} \phi_w(\omega) [H_{x_{\text{real}}}(\omega) * H_{y_{\text{real}}}(\omega) + H_{x_{\text{imag}}}(\omega) * H_{y_{\text{imag}}}(\omega)] d\omega$$

where $\phi_w(\omega)$ is the gust power spectral density; H_x and H_y are the frequency response functions for the load quantities x and y ; \bar{A}_x and \bar{A}_y are the ratios of the design rms loads σ_x and σ_y to the design rms gust intensity σ_w , respectively. The value of ρ_{xy} varies between +1 and -1 with ± 1 representing complete statistical dependence and a value of 0 representing complete statistical independence. Since this quantity varies with the change in the stiffness and mass distribution, it is imperative to define approximations to this coefficient which would be computationally less cumbersome.

DIRECT APPROACH

The approach presently under study computes the power spectral density for a combined stress function and constrains the rms values of this function by prescribed bounds. Consider a combined stress constraint of the form

$$R(\sigma_x, \sigma_y, \tau_{xy}) \leq R_{all}$$

where R is a stress interaction curve and is constrained by an upper bound R_{all} . By the methods of an earlier section, the generalized force vector can be written as

$$\{F\} = ([A] - \omega^2[M])\{w\} + \{G\}$$

The quantities σ_x , σ_y and τ_{xy} are functions of the shear V , torque T , bending moment M , and the material properties MP .

The constraint can be expressed as

$$R(V, T, M, MP) \leq R_{all}$$

Furthermore, the forces and moments can be expressed in terms of the force vector $\{F\}$ through a transfer matrix based on the structural geometry:

$$\{V\} = [T_1]\{F\}$$

$$\{M\} = [T_2]\{F\}$$

$$\{T\} = [T_3]\{F\}$$

The admittance for the composite response function R , denoted here as H_R , can be computed over a range of frequencies of interest and the rms response value evaluated as

$$\sigma_R^2 = \int_0^\infty |H_R|^2 \phi_w(\omega) d\omega$$

It is obvious that the procedure requires considerable numerical resources and an important emphasis in the ongoing study would be to establish guidelines to minimize this investment.

RELIABILITY CONSTRAINTS IN PROBABILISTIC DESIGN

In a stochastic excitation environment, there are two logical failure criteria of comparable significance:

- (1) Single excursion failure which corresponds to an overstress in any one cycle of loading
- (2) Fatigue failure that results from a gradual degradation in the structural strength due to cyclic loading

Johnson (ref. 11) formulates constraints for a response function $x(t)$ that is stationary and has a Gaussian distribution. An assumption that large values of $x(t)$ arrive independently leads to a Poisson probability function for the number of times n that a large magnitude \bar{x} is exceeded in time t . If T_s denotes the desired life for the structure and \bar{x}_s is the specified value that the response cannot exceed, the constraint to guard against a single excursion failure is written as

$$g_{s.e} = 1 - \frac{T_s}{\pi} \frac{\sigma_x^*}{\sigma_x} \exp(-\bar{x}_s^2 / 2\sigma_x^2) > 0$$

For a fatigue failure analysis, the classical Palmgren-Miner theory provides an estimate of the rate of fatigue damage and the constraint is formulated as

$$g_{f.f} = 1 - \frac{\sigma_x^* L_f}{\pi c} (2)^{\frac{b-2}{2}} \sigma_x^{b-1} \Gamma\left(\frac{b+2}{2}\right) > 0$$

Here, L_f is the desired fatigue life; σ_x and σ_x^* are the rms value of the response and the response rate and b and c are constants obtained from an empirical relation

$$N(x) = \frac{c}{x^b}$$

where $N(x)$ is the number of cycles to failure at stress level x . The above formulation is based on an analysis in the frequency domain and is applicable to response functions taken one at a time or to a combined response function.

RELIABILITY CONSTRAINTS FROM THE FRACTURE MECHANICS STANDPOINT

Reference 12 presents a comprehensive discussion on recent advances in fracture mechanics. Empirical relationships express the degradation in the material in terms of fault or crack propagation rates and provide better estimates of the useful life of the structure than the Palmgren-Miner theory. Incorporation of these ideas in the design constraints is a principal focus of the ongoing study. Consider the cracked specimen shown in figure 6. The differences between various cracked components is expressed in terms of a stress intensity factor, k . This factor describes the stress field around a crack tip and is functionally dependent on the stress σ and the crack geometry denoted by 'a'. There is a critical stress intensity constant k_c for a given material. For the crack shown in Fig. 6, this functional relationship can be expressed in terms of the range of stress intensity factor Δk and the range of stress variation $\Delta\sigma$:

$$\Delta k = \Delta\sigma \sqrt{\pi a}$$

The factor $\pi^{1/2}$ changes as the crack size increases in comparison to the characteristic width of the specimen.

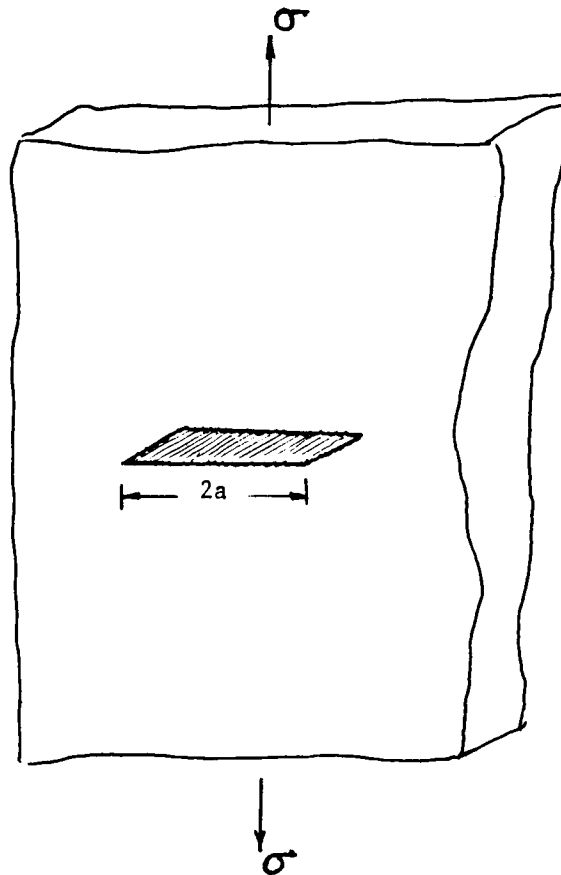


Figure 6.- Cracked material specimen.

The crack propagation rate per cycle of load is given as

$$\frac{da}{dn} = c \Delta k^b$$

where c and b are constants dependent on the material of the specimen. For a value of $b = 2$ (steel) one can write an expression for the crack size after t flight hours as

$$a(t) = a_0 e^{c \pi \Delta \sigma^2 N_0 t}$$

where N_0 is the number of gust loads per flight hour; $(\Delta \sigma)^2$ is the mean square value of a Gaussian response function σ . The Griffith Irwin equation* indicates the residual strength in a material with crack size 'a' in terms of the critical stress intensity constant k_c :

$$k_c = R \sqrt{\frac{\pi a}{2}}$$

The time to reach a critical crack size a_c is obtained as**

$$t_c = \frac{1}{c \pi \Delta \sigma^2 N_0} \ln \frac{a_c}{a_0}$$

At t_f flight hours after t_c , the crack size is

$$a_f = a_c e^{c \pi \Delta \sigma^2 N_0 t_f}$$

and the residual strength at this time is obtained as

$$R_f = R_c e^{c \pi \Delta \sigma^2 N_0 t_f}$$

* Equation is valid for determinate structures only and modifications are necessary for redundant structures.

**Note that a_c generally corresponds to the material ultimate strength, R_c .

Design constraints can thus be formulated to require t_c to be greater than a specified time T_c

$$g_1 \equiv 1 - \frac{T_c}{\ln \frac{a_c}{a_0}} c \pi \Delta \sigma^2 N_0$$

Another constraint could be formulated that required the residual strength to be above a certain bound ($R_f/R_c > K_1$), T_f flight hours after the critical crack size is reached. Such a constraint would be prescribed from a maintenance schedule:

$$g_2 \equiv 1 - \frac{T_f}{\ln K_1} c \pi \Delta \sigma^2 N_0 > 0$$

SUMMARY

The major finding of the present survey can be outlined as follows.

- (a) The frequency domain analysis provides an elegant solution strategy to the gust response problem. However, the lack of agreement in measured data with assumptions such as stationarity, normality and the one-dimensional variation in gust velocity dictate the need for reassessing the turbulence modeling.
- (b) The phase information regarding load combinations is suppressed in a frequency domain solution. This is problematic when combined stress constraints are prescribed in the design. Strategies to circumvent these problems are stated.
- (c) The definition of realistic constraints for the optimum design is addressed from the standpoint of recent developments in fracture mechanics.

ACKNOWLEDGEMENTS

The author would like to thank Mr. Bruce Ainbinder for his assistance in this study.

REFERENCES

1. Gould, P. L.; Abu-Sitta, S. H.: Dynamic Response of Structures to Wind and Earthquake Loading. John Wiley and Sons, 1980.
2. Nigam, N. C.; Narayanan, S.: Structural Optimization in Aseismic Design. 5th World Conference on Earthquake Engineering, Rome, June 1973, Paper No. 374.
3. Rao, S. S.: Reliability-Based Optimization Under Random Vibration Environment. Computers and Structures, Vol. 14, pp 345-355, 1981.

4. Kato, B.; Nakamura, V.; Anraku, H.: Optimum Earthquake Design of Shear Buildings. ASCE Journal of the Engineering Mechanics Division, Vol. 98, No. EM4, Aug 1972, pp 891-910.
5. Gross, D. W.: A Multi-Disciplinary Approach to Structural Design for Stochastic Loads. Presented at the 17th AIAA Aerospace Sciences Meeting, New Orleans, 1979.
6. Gross, D. W.; Sobieski, J. E.: Application to Aircraft Design of Nonlinear Optimization Methods which Include Probabilistic Constraints. Presented at the 18th AIAA Aerospace Sciences Meeting, San Diego, 1980.
7. Stauffer, W. A.; Hoblitt, F. M.: Loads Determination in the Design of the L-1011. Journal of Aircraft, Vol. 10, No. 8, August 1973, pp. 459-467.
8. Pratt, K. G.: Performance and Dynamics of Aerospace Vehicles, NASA SP-258, 1971.
9. Turner, E. W.: An Exposition on Aircraft Response to Atmospheric Turbulence Using Power Spectral Density Analysis Techniques. AFFDL-TR-76-162, 1977.
10. Nigam, N. C.: Structural Optimization in Random Vibration Environment. AIAA Journal, Vol. 10, No. 4, April 1972, pp. 551-553.
11. Johnson, E. H.: Optimization of Structures Undergoing Harmonic or Stochastic Excitation. Stanford University, SUDAAR No. 501, 1976.
12. Hertzberg, R. W.: Deformation and Fracture Mechanics of Engineering Materials. John Wiley and Sons, 1976.

N87-11775

APPLYING OPTIMIZATION
SOFTWARE LIBRARIES TO
ENGINEERING PROBLEMS

M. J. Healy
Boeing Computer Services Company
Seattle, Washington

NONLINEAR PROGRAMMING

The nonlinear programming applications encountered in a large aerospace company are a real challenge to those who provide mathematical software libraries and consultation services. Typical applications include preliminary design studies, data fitting and filtering, jet engine simulations, control system analysis, and trajectory optimization and optimal control. Problem sizes range from single-variable unconstrained minimization to constrained problems with highly nonlinear functions and hundreds of variables. Most of the applications can be posed as nonlinearly constrained minimization problems.

Sample Applications

DATA FITTING/APPROXIMATION

DIGITAL FILTERING

FLIGHT MANAGEMENT COMPUTER SYSTEMS

PRELIMINARY DESIGN

STRUCTURAL OPTIMIZATION

TRAJECTORY OPTIMIZATION

Minimization (Maximization)

minimize $f(x)$ (minimize $-f(x)$)

subject to

$$c_i(x) = 0 \quad (i = 1, \dots, m_e),$$

$$c_i(x) \geq 0 \quad (i = m_e+1, \dots, m),$$

$$\text{and} \quad l_j \leq x_j \leq u_j \quad (j = 1, \dots, n).$$

Figure 1

ORIGINAL PAGE IS
OF POOR QUALITY

PRELIMINARY DESIGN

Preliminary design problems typically have several performance indices with up to 30 independent variables. The independent variables might represent, for example, overall airframe and engine design parameters such as wing aspect ratio and engine cycle pressure ratio. Evaluating the performance indices at different combinations of values for these variables allows a design concept to be explored. The optimization method drives the independent variables to a minimum or maximum of a selected performance index subject to performance level constraints on the others. Varying the constraint levels an increment at a time and solving for a new optimum at each increment allow a "frontier" of non-dominated designs to be explored.

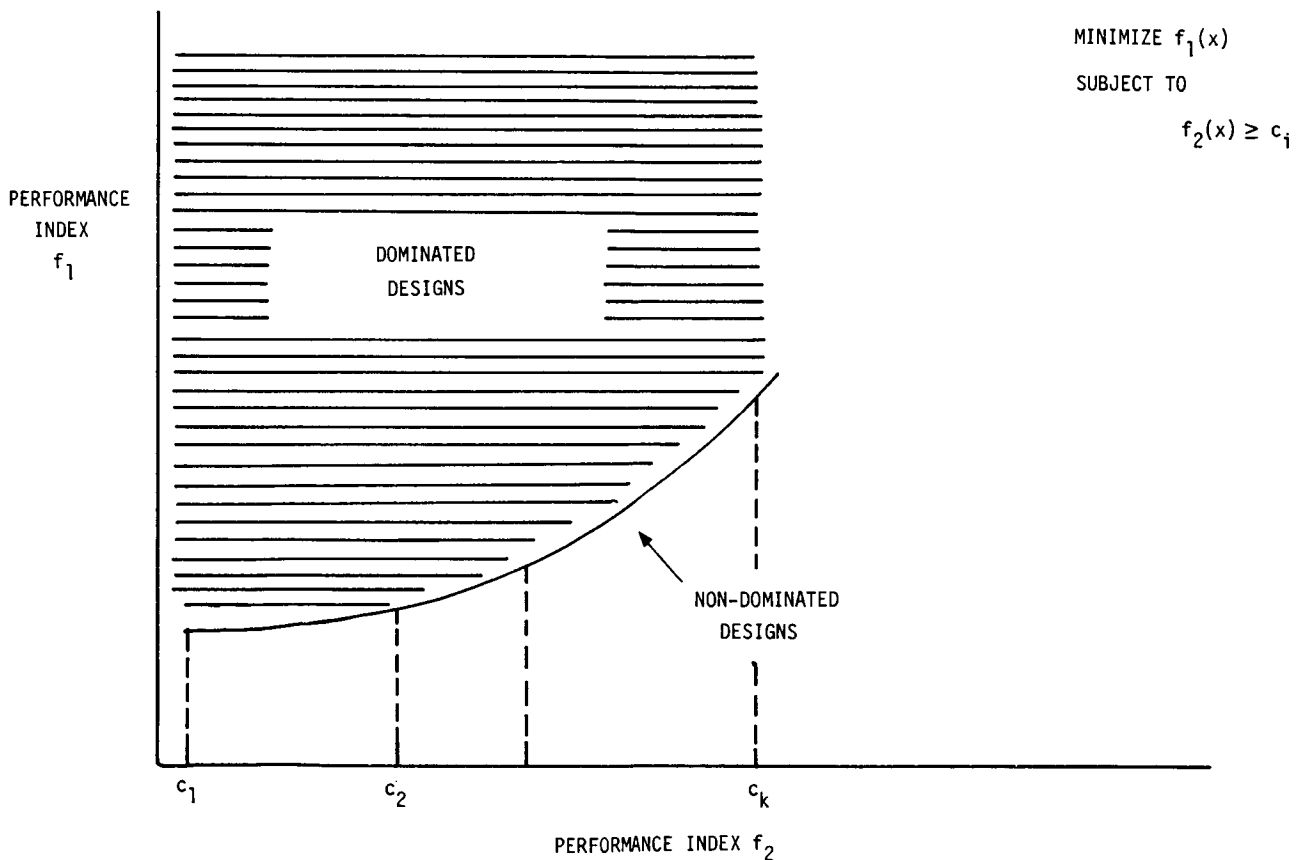


Figure 2

PERFORMANCE SIMULATION PROBLEMS

A major problem with this type of analysis is that the performance index values are usually output from a complex performance simulation which was originally programmed to do analyses at a fixed design point. When evaluated over a range of design points, the performance functions are computationally expensive to evaluate and contain discontinuities. Sometimes, the computational process is unstable when design points are varied and the resulting performance surfaces in multi-dimensional space contain a significant noise component. Many compromises in performance evaluation may have to be made to allow modern, fast-converging optimization methods to be used.

ENGINE DESIGN

BPR, CPR, ETC.

MISSION DESCRIPTION

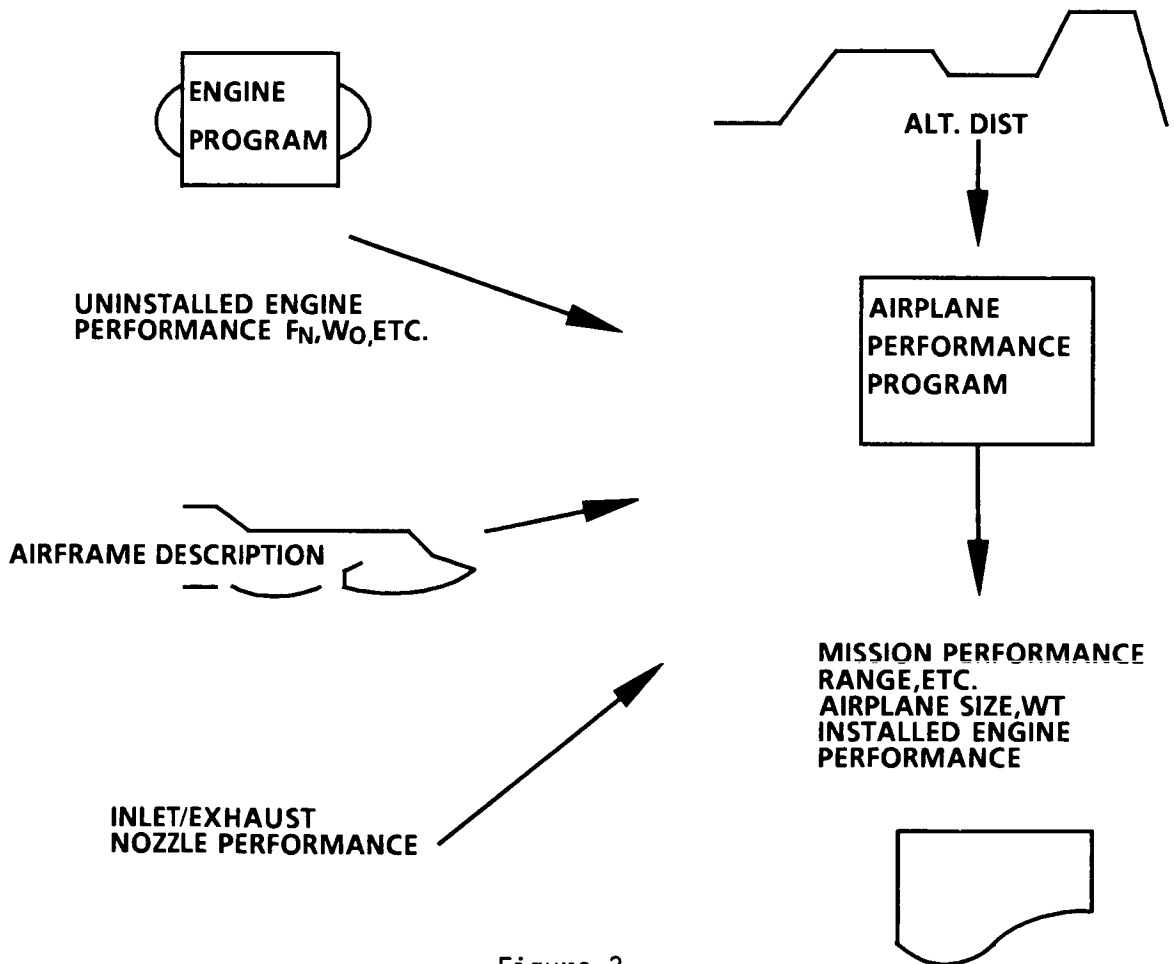


Figure 3

TRAJECTORY OPTIMIZATION

Trajectory optimization problems are being reformulated as nonlinear programming problems in different ways. An infinite-dimensional problem must be reformulated as a finite-dimensional one, so some form of discretization or approximation is involved. A recent method is to express each state and control variable as a linear combination of B-splines and find optimal values for the coefficients. The resulting nonlinear programming problem may have hundreds of variables and constraints.

A major problem with this type of approach is insuring that nonlinear programming solutions correspond to optimal trajectories - some solutions may be extraneous local minima. Another problem is the numerical conditioning of the Jacobian matrix of the constraints in certain parameter subspaces.

$$\text{minimize } f_0(x^p, t_p)$$

subject to

$$f(x^i, \dot{x}^i, \ddot{x}^i, t_i) = 0$$

$$(i = 1, \dots, p)$$

$$x_k^i = \sum_{j=1}^n x_{k,j} B_j(t_i)$$

Figure 4

OPTIMIZATION ON FLIGHT COMPUTERS

Flight management algorithms include in-flight optimal control, an attempt to do optimization in real time. The optimal solutions, usually obtained in a single-variable minimization, may control the flight directly (e. g., via the throttle) or serve as an informational aid to the pilot.

A common difficulty is the small word length and limited arithmetic capabilities of many flight computers (e. g., a 16-bit word length). Even a single-variable problem may be hard to solve, since the large roundoff error level leads to "choppy" curves with many false local minima.

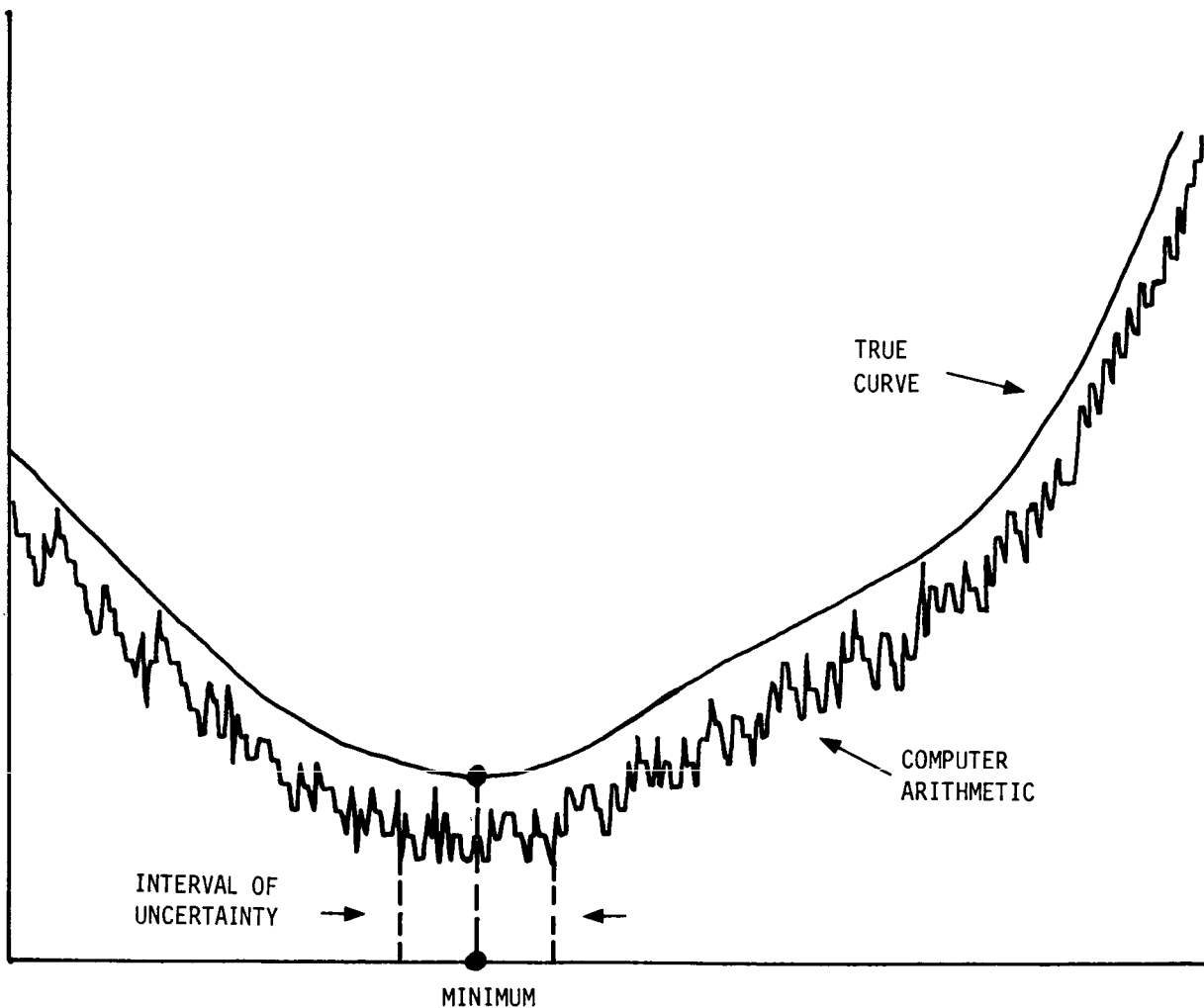


Figure 5

ILL-CONDITIONED PROBLEMS

Ill-conditioned problems are common in nonlinear programming. The objective function curvature around an optimum may be sensitive to variations in certain directions in the space of independent variables but relatively insensitive in other directions. Or, two or more important constraints may be redundant or nearly so. In either case, small errors in satisfying the exact conditions for finding a solution (e. g., in satisfying constraints) can cause a large uncertainty in locating an optimum. This can make a problem appear to have many local optima when in fact a single solution exists. Ill-conditioning has a direct impact on the iterative process of finding a solution, since the iteration matrices involved are essentially singular. A simple method such as steepest descent, which does not use matrices directly, will require a prohibitive number of iterations to converge.

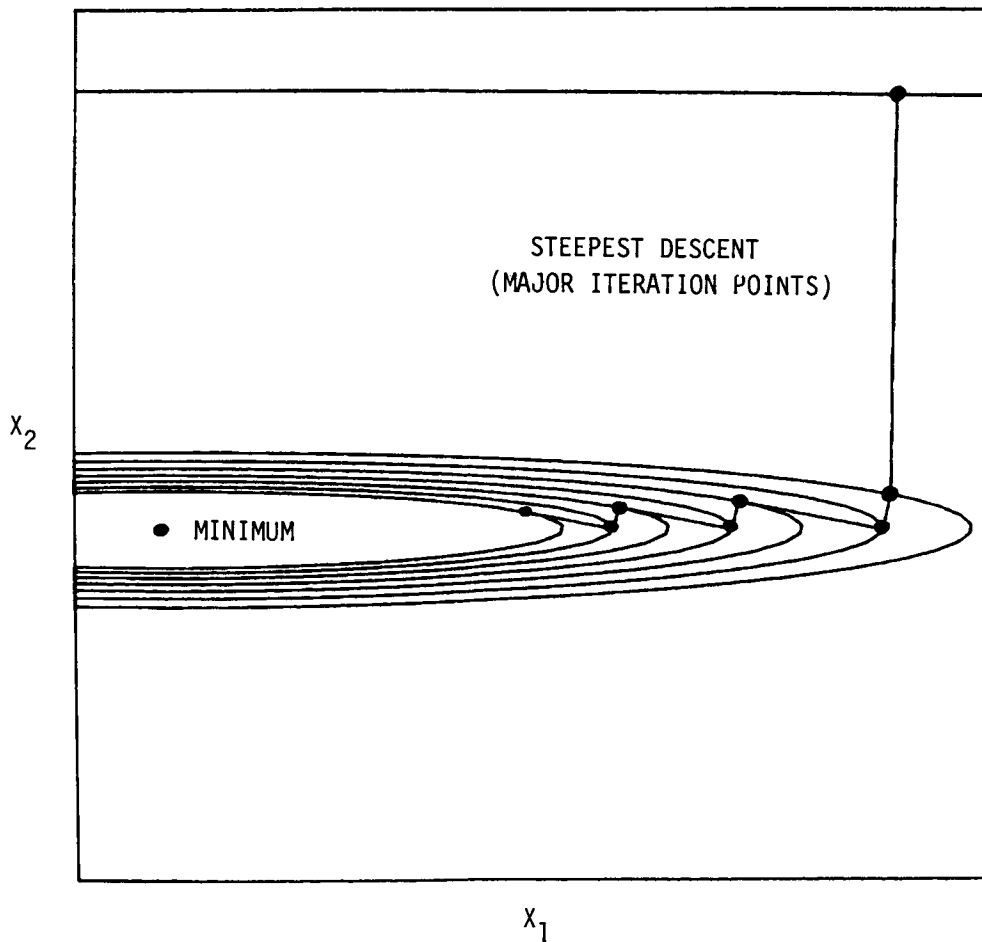


Figure 6

ACCURACY

If extremely accurate solutions are not required, which they are not in some engineering applications, why worry about problem conditioning? The answer is that solutions may contain such a large degree of uncertainty that some solution parameters have no accuracy at all. An example can be given for a simple unconstrained minimization problem, where the objective function is a convex quadratic in two variables. The function has elliptical contours, and locating the minimum numerically corresponds to finding a point that lies within some contour curve representing the tolerance on the minimum function value. If the ratio of lengths of the major and minor axes of the ellipses is large relative to the accuracy of the calculations employed, a solution can lie anywhere within a very large region. In particular, the solution value for an independent variable can have an error whose magnitude is as large as that of the variable itself.

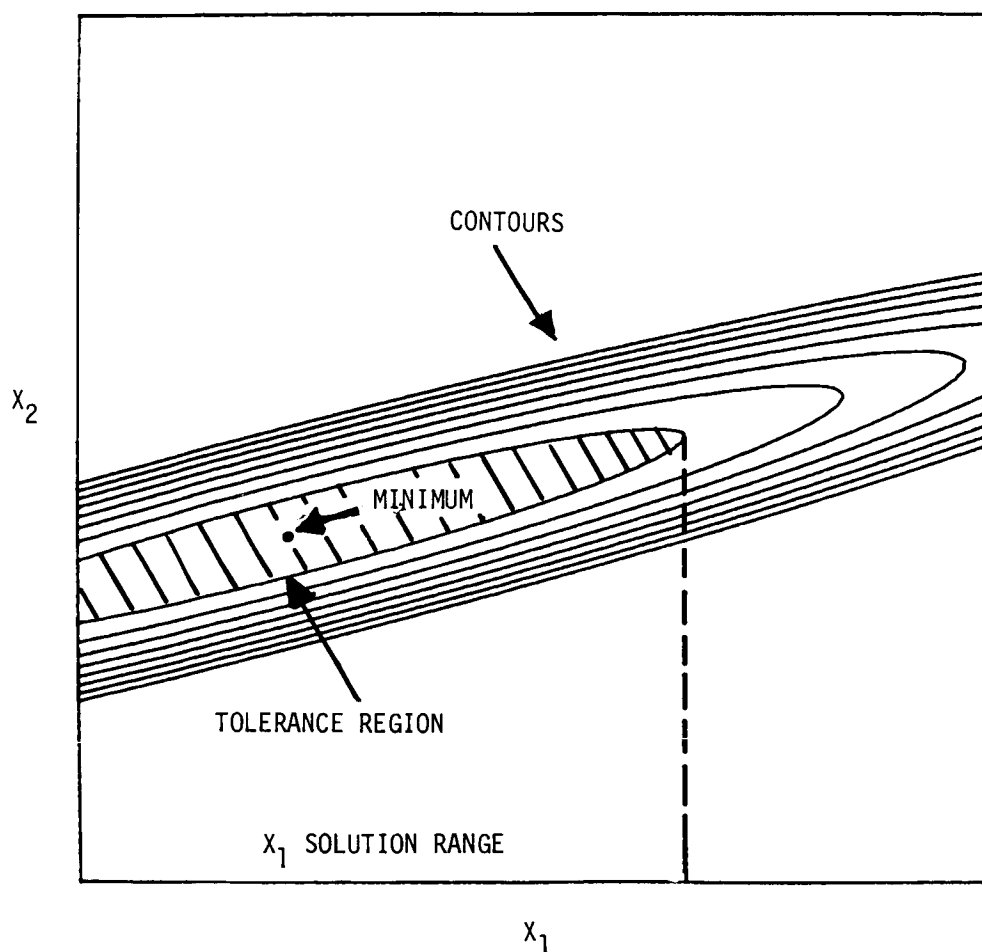


Figure 7

PORTABILITY AND THE MACHINE ENVIRONMENT

Added to the numerical difficulties of the applications is the great variety of host computer systems served by a single software library operating in a large company. At one time, a mathematical subroutine could be entered into a library system which was expected to serve only a single type mainframe. Now, host environments range over several types of mainframe and also minis, micros (e. g., flight computers), and supercomputers.

For efficiency, the codes included in a modern library must be portable and well-equipped for maintenance. Source code comments and usage documentation may receive almost as much attention in code development as the numerical method itself. A typical software library is programmed mostly in portable Fortran, with a core of subroutines which have portable usage but different code on each system. These core subroutines serve to interface the library with a specific machine environment, for example, by specifying the local single precision accuracy.

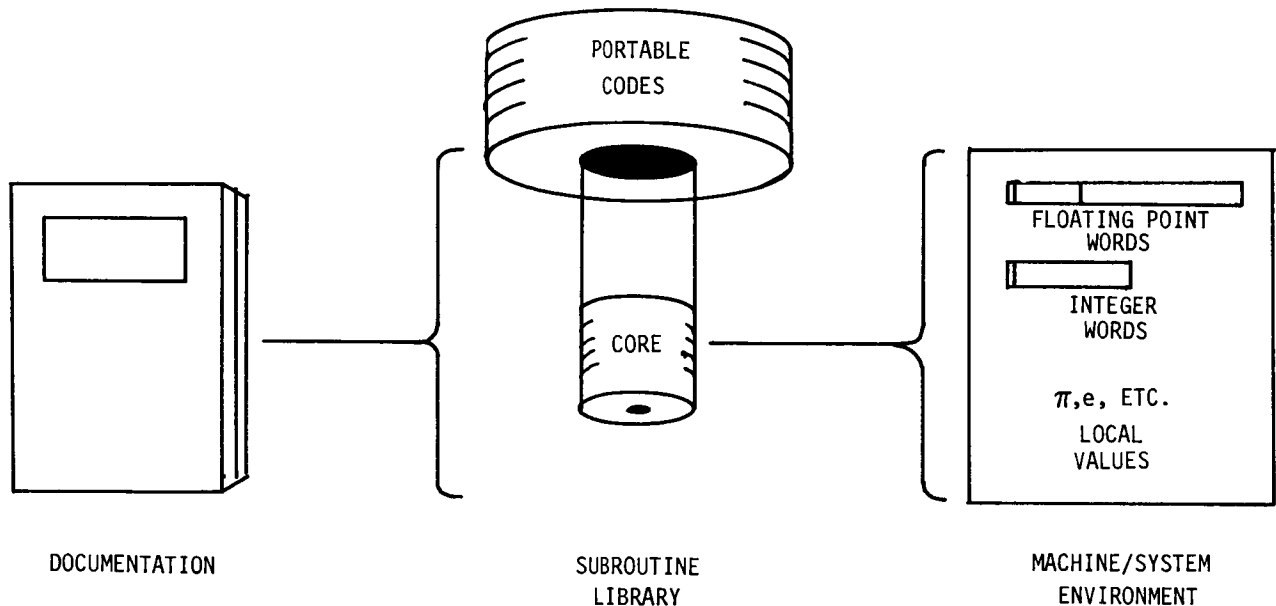


Figure 8

A BRIEF HISTORY

Fast-converging methods embodied in numerically stable codes have proved to be the key to success in overcoming many of the difficulties in nonlinear programming. The earliest fast method was Newton's method. However, steepest descent or some "direct search" method was often used due to the instability of Newton's method and to the fact that it requires second derivatives for solving a minimization problem. Quasi-Newton methods, requiring only first derivatives, were developed in the 1960's. However, early methods of this type were unstable and often slow to converge. Conjugate gradient methods, also developed in the 1960's, were fast on certain types of problems but were often as slow as steepest descent. Techniques for handling constraints, such as penalty functions and gradient projection, had similar problems.

Stabilized Newton and quasi-Newton methods appeared on early optimization software libraries beginning in about 1971. These methods were soon coupled to new gradient projection techniques, yielding efficient codes for linearly constrained problems. More recently, sparse matrix techniques and projected Lagrangian methods have extended the range of efficient codes to large-scale and nonlinearly-constrained optimization.

pre-1959

Minimization

- Newton
- Steepest descent
- Direct search methods

Constraints

- Penalty function
- Simplex method for Linear Programming

1959 - 1969

Minimization

- Nonlinear simplex search method
- Quasi-Newton methods (Davidon, 1959 - Fletcher/Powell, 1963) (refs. 1, 2)
- Conjugate gradient minimization (Fletcher/Reeves, 1964) (ref. 3)
- Sequential polynomial line search
- Early trust region methods (Levenberg, 1944 - Marquardt, 1963) (refs. 4, 5)

Constraints

- Projected/reduced gradient methods (Rosen, 1960 - Wolfe, 1962) (refs. 6, 7)
- Generalized reduced gradient method (Abadie and Carpentier, 1969) (ref. 8)
- Advanced penalty function theory - SUMT (Fiacco/McCormick, 1968) (ref. 9)

1970 - present

Minimization

- Stabilized Newton/quasi-Newton methods
- BFGS update (1970) (ref. 10)
- Modified Cholesky Factorization (Gill/Murray, 1971 - 1974) (ref. 11, 12)
- Trust region methods

Constraints

- Modern projected/reduced gradient methods
- Active set strategies, Lagrange multiplier estimates (1971 - 1974) (ref. 13)
- Null-space/range-space decomposition (1974 - 1976) (ref. 14)
- Projected Lagrangian methods (refs. 15-17)
- Sequential quadratic programming

Figure 9

OPTIMIZATION CATEGORIES AND METHODS

Contemporary optimization methods were developed within an orderly problem classification scheme. Problems are classified in categories based on their structure (e. g., nonlinear least squares) and the computational resources available for solving the problem (e. g., whether or not partial derivatives of the problem functions can be calculated analytically). This scheme reflects current knowledge of the most effective methods for the different categories of smooth or differentiable optimization and also linear programming.

For some categories, no overall method can be recommended. For example, when the problem functions or their derivatives are discontinuous, the problem must be carefully analyzed, and solution methods often rely heavily on problem-specific heuristics. In many cases, it is best to reformulate the problem. The situation for discontinuous optimization is reminiscent of the old days of smooth optimization.

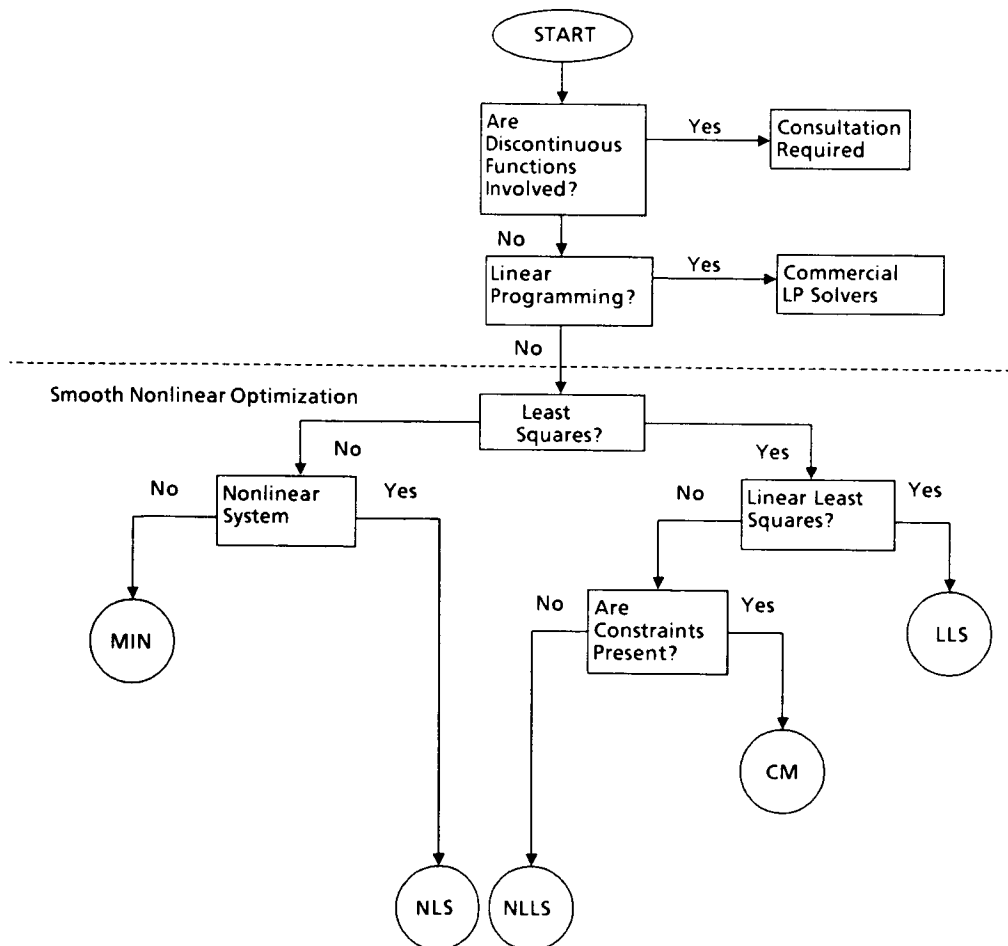


Figure 10

NONLINEAR SYSTEMS AND NONLINEAR LEAST SQUARES

Because of its fast convergence, Newton's method is the basis for most smooth nonlinear optimization algorithms, including nonlinear system solvers and nonlinear least squares. However, the method is not robust and the required derivatives (including second derivatives for minimization problems) are not always available. Powell's hybrid method and the Levenberg-Marquardt method are two forms of trust region or restricted-step methods which modify Newton's method to obtain robust solution algorithms. They also eliminate the need for second derivatives in nonlinear least squares problems. Quasi-Newton and finite-difference approximations make up for the missing first derivatives and usually maintain fast convergence. Some problems, however, do require more specialized methods in order for fast solutions to be obtained.

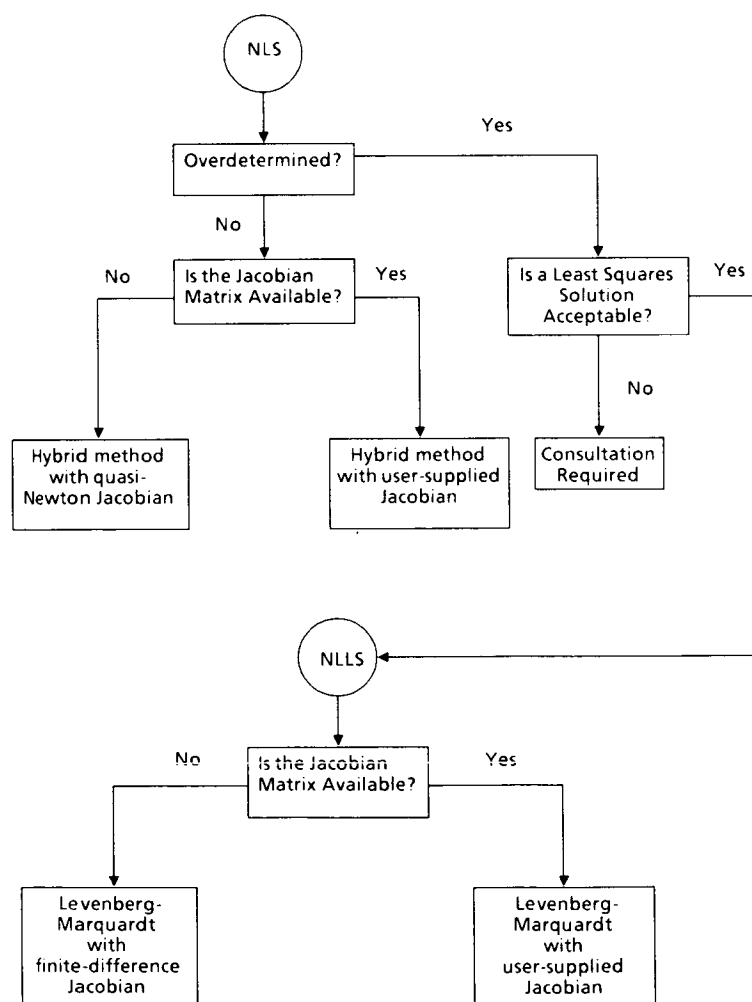


Figure 11

UNCONSTRAINED MINIMIZATION

Although most optimization problems have constraints, it is worthwhile to study the modern methods for unconstrained minimization because they are incorporated in contemporary methods for constrained problems. This is especially true of the Newton, quasi-Newton, and single variable methods. If the problem has fewer than, say, 200 variables (depending on computer resources available), Newton-type methods are preferable. However, they require the storage and use of a search matrix whose size is roughly the square of the problem size. Conjugate gradient methods are much less efficient but use no matrices.

For single-variable problems, safeguarded polynomial search methods minimize a sequence of approximating polynomials within bounds. Recent bounding strategies have been developed to maintain the fast convergence of the polynomial search.

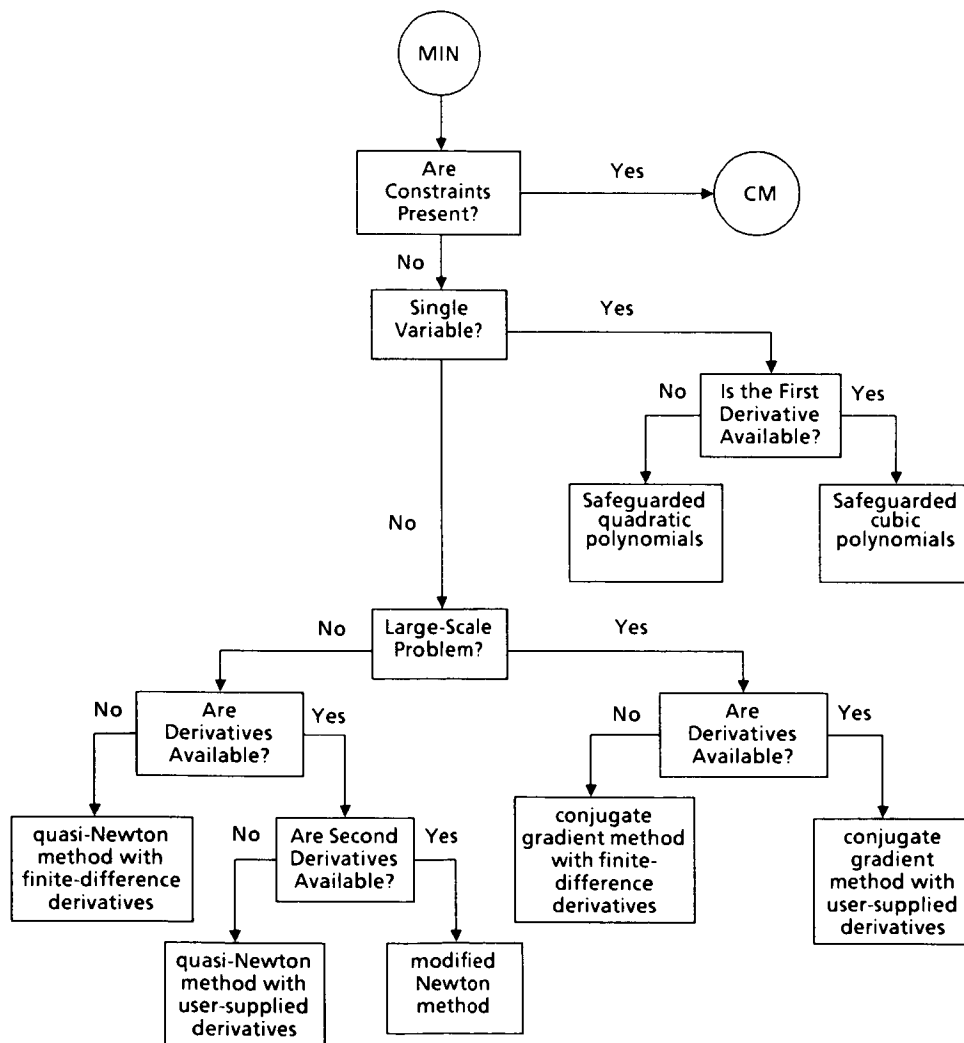


Figure 12

PROJECTED GRADIENTS AND REDUCED GRADIENTS

Modern constrained methods use a projection strategy coupled with a Newton-type minimization method. During the iterative process, the search steps of the unconstrained method are essentially projected into a linear subspace defined by the currently active constraints, i. e., those that would be violated in an unconstrained search. Lagrange multiplier approximations are used in deciding when to drop a constraint from the active set.

For linear constraints, projection methods maintain feasibility after first locating a feasible point. Projection methods for nonlinear constraints use linear approximations but take account of the constraint nonlinearities by adding Lagrangian and penalty function terms to the original objective function. The methods for nonlinear constraints are often referred to as projected Lagrangian methods.

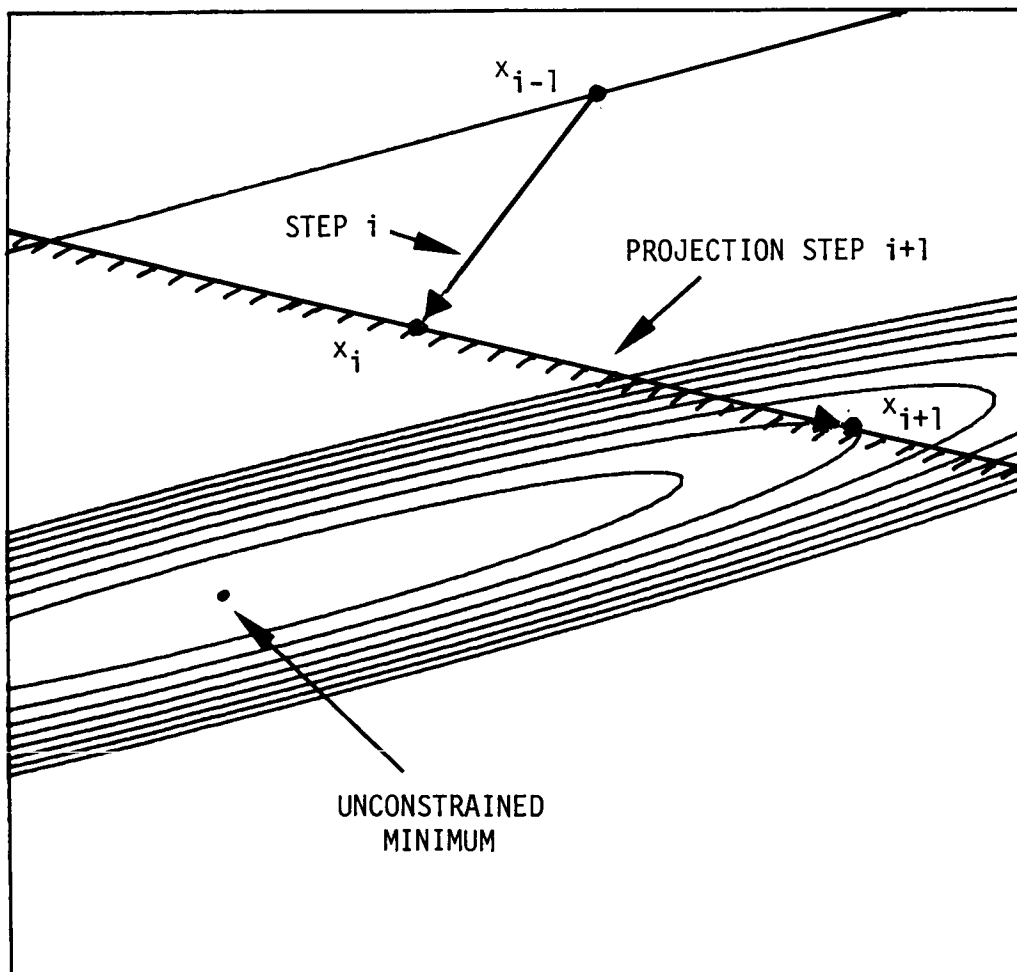


Figure 13

LINEAR LEAST SQUARES

Linear least squares problems can be solved using standard numerical linear algebra techniques if there are no constraints. If there are constraints, an iterative method must be used. The problem then is a special type of quadratic program, or minimization of a quadratic function (in this case, an L2-norm) subject to linear equations and inequalities. Most quadratic programming methods are projected gradient methods. However, specialized methods have been developed for the particular case of the minimum-norm problem.

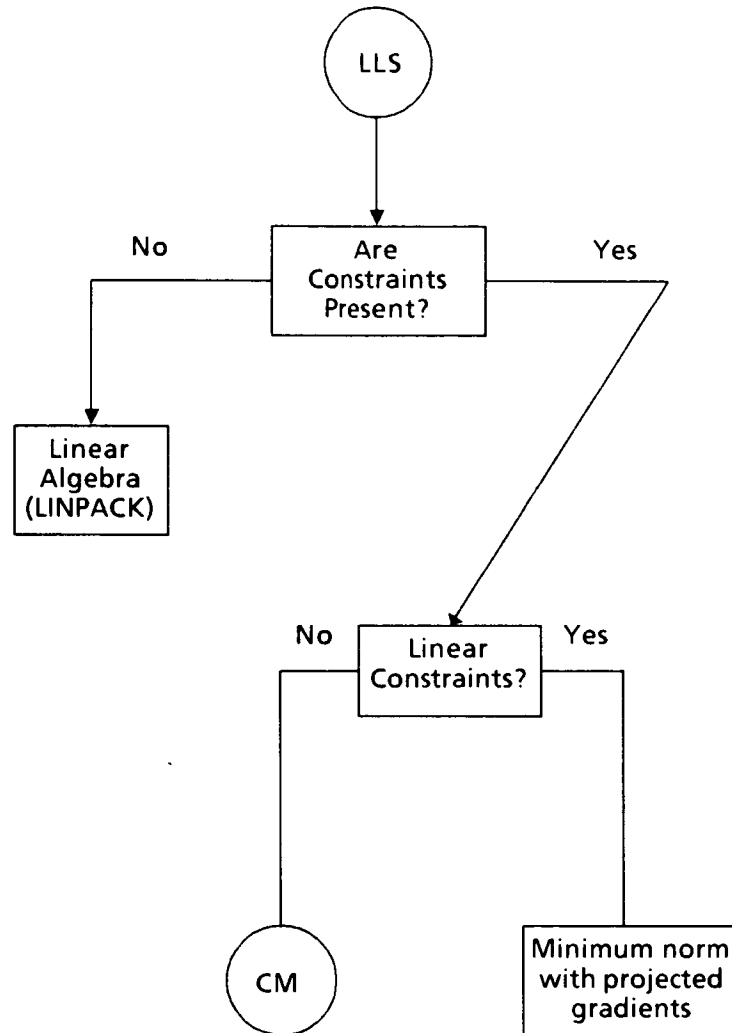


Figure 14

GENERAL CONSTRAINED MINIMIZATION

The distinction between linear and nonlinear constraints has long been fundamental to optimization methods. Only recently have reliable, fast-converging methods evolved for nonlinear constraints, and as mentioned before they use a form of projection, a strategy which has always been used for linear constraints. The null-space method refers to a particularly efficient form of projection, for which good codes have recently become available.

The development of sparse matrix techniques has added a new category of optimization problems which can be solved efficiently. This refers to large-scale nonlinear problems, which often have thousands of variables.

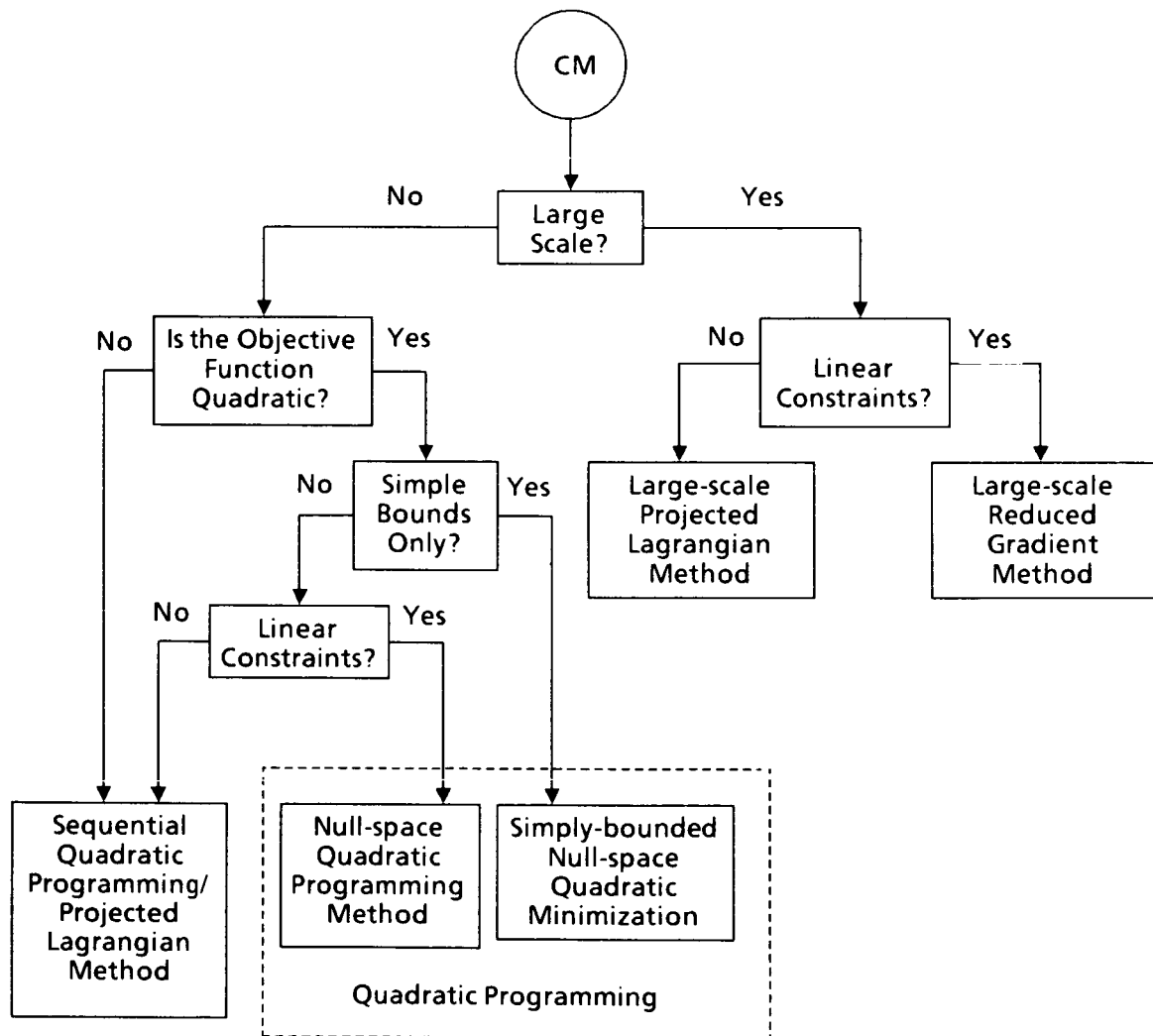


Figure 15

CONCLUSION

Highly complex optimization problems with many variables were formulated in the early days of computing. At the time, many problems had to be reformulated or bypassed entirely, and solution methods often relied on problem-specific strategies. Problems with more than ten variables usually went unsolved.

Modern optimization software libraries represent a complete change in this situation. Advances in optimality and convergence theory and in numerical analysis, especially linear algebra, have made possible codes that are both fast and robust. Advances in mathematical software techniques encourage the packaging of software for implementation in a great variety of computing environments. A major challenge in optimization software at present is in increasing user awareness of these developments and expanding the scope of future applications.

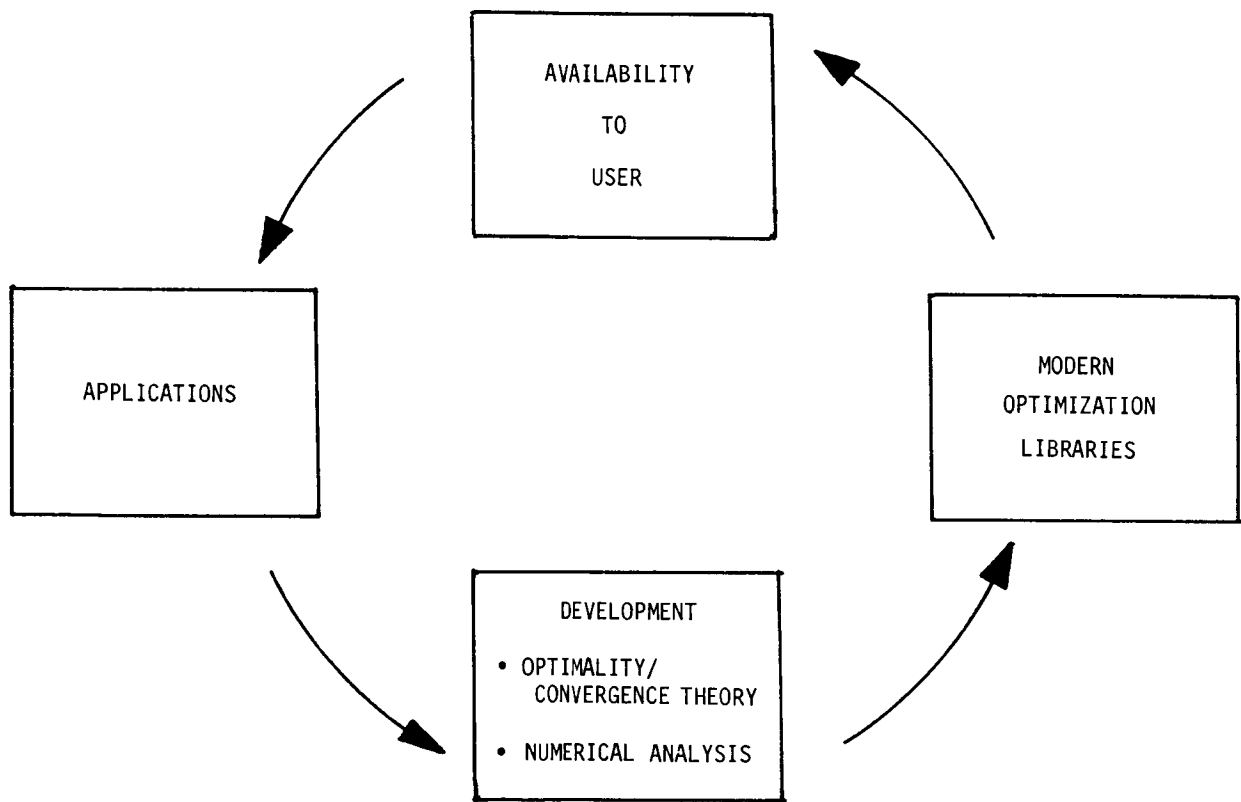


Figure 16

SYMBOLS AND ABBREVIATIONS

| | |
|--------------------------------------|--|
| ALT | Altitude |
| BPR | Bypass ratio |
| $B_j(t_i)$ | B-spline function evaluated at point t_i |
| CPR | Cycle pressure ratio |
| $c_i(x)$ | Constraint function i evaluated at point x |
| DIST | Distance |
| $f(x)$ | Objective function evaluated at point x |
| f_1, f_2 | Performance indices - used as either objective or constraint functions |
| $f_0(x^p, t_p)$ | Objective function for B-spline formulation of trajectory problem |
| $f(x^i, \dot{x}^i, \ddot{x}^i, t_i)$ | Constraint function for B-spline formulation of trajectory problem; expresses system dynamics at point i |
| F_n | Net thrust |
| i, j, k | Indices |
| l_j | Lower bound on independent variable j |
| m | Number of constraints |
| m_e | Number of equality constraints |
| n | Number of variables in Figure 1, number of test points in Figure 4 |
| p | Number of B-spline evaluation points |
| P_S | Specific excess power |
| t_i | The i -th B-spline point |
| t_p | Final time |

| | |
|-------------------------|---|
| u_j | Upper bound on independent variable j |
| WT | Airplane weight |
| x_j | Independent variable j |
| x^p | Final time vector of trajectory variables |
| x_k^i | Trajectory variable k evaluated at B-spline point i |
| $x_{k,j}$ | The j -th B-spline coefficient of trajectory variable k |
| \dot{x}^i, \ddot{x}^i | Trajectory time derivatives evaluated at B-spline point i |
| Σ | Summation |

REFERENCES

1. Davidon, W.: Variable Metric Methods for Minimization. AEC Research and Development Rep. ANL-5590, Argonne Natl. Labs., 1959.
2. Fletcher, R.; and Powell, M.J.D.: A Rapidly Convergent Descent Method for Minimization. Computer J., vol. 6, 1963, pp. 163-168.
3. Fletcher, R.; and Reeves, C.M.: Function Minimization by Conjugate Gradient. Computer J., vol. 7, 1964, pp. 149-154.
4. Levenberg, K.: A Method for the Solution of Certain Problems in Least Squares. Quart. Appl. Math., vol. 2, 1944, pp.164-168.
5. Marquardt, D.: An Algorithm for Least Squares Estimation of Nonlinear Parameters. SIAM J. Appl. Math., vol. 11, 1963, pp. 431-441.
6. Rosen, J.B.: The Gradient Projection Method for Nonlinear Programming. Part I: Linear Constraints. SIAM J. Appl. Math., vol. 8, 1960, pp. 181-217.
7. Wolfe, P.: Recent Developments in Nonlinear Programming. Rand. Corp. Rep. R-401-PR, 1962.
8. Abadie, J.; and Carpentier, J.: Generalization of the Wolfe Reduced Gradient Method to the Case of Nonlinear Constraints. Optimization, edited by R. Fletcher, Academic Press, 1969, pp. 37-49.
9. Fiacco, A.V.; and McCormick, G.P.: Nonlinear Programming: Sequential Unconstrained Minimization Techniques. John Wiley and Sons, NY, 1968.
10. Broyden, C.G.: The Convergence of a Class of Double-Rank Minimization Algorithms. J. Inst. Math. Applic., vol. 6, pp. 76-90, 1970.
11. Gill, P.E.; and Murray, W.: Quasi-Newton Methods for Unconstrained Optimization. J. Inst. Math. Applic., vol. 9, pp. 91-108, 1972.
12. Gill, P.E.; and Murray, W.: Quasi-Newton Methods for Linearly Constrained Optimization. Chapter 3. Numerical Methods for Constrained Optimization, Academic Press, 1974.
13. Gill, P.E.; and Murray, W.: Quasi-Newton Methods for Linearly Constrained Optimization. Natl. Phys. Labs. Rep. NAC 32, Teddington, Middlesex, UK, 1973.
14. Gill, P.E.; and Murray, W.: Newton-Type Methods for Linearly Constrained Optimization. Chapter 2. Numerical Methods for Constrained Optimization, Academic Press, 1974.
15. Murray, W.; and Wright, M.H.: Computation of the Search Direction in Constrained Optimization Algorithms. Algorithms for Constrained Minimization of Smooth Nonlinear Functions, A.G. Buckley and J.-L. Goffin, eds., Math. Proj. Study 16, Mathematical Programming Soc., pp. 62-83, 1982.
16. Murtagh, B.A.; and Saunders, M.A.: A Projected Lagrangian Algorithm and Its

Implementation for Sparse Nonlinear Constraints. Algorithms for Constrained Minimization of Smooth Nonlinear Functions, A.G. Buckley and J.-L. Goffin, eds., Math. Proj. Study 16, Mathematical Programming Soc., 1982.

17. Powell, M.J.D.: A Fast Algorithm for Nonlinearly Constrained Optimization Calculations. Rep. DAMTP 77-NA 2, Univ. Cambridge, UK, 1977.

OPTDES.BYU: AN INTERACTIVE OPTIMIZATION
PACKAGE WITH 2D/3D GRAPHICS

R. J. Balling
A. R. Parkinson
J. C. Free
Brigham Young University
Provo, Utah

PRECEDING PAGE BLANK NOT FILMED

I. INTRODUCTION

The OPTDES.BYU package was developed to assist the engineer in obtaining efficient designs. In particular, the package helps the engineer to perform the following fundamental tasks in the design process:

- (1) Interfacing with existing analysis software
- (2) Defining and redefining the design problem
- (3) Searching for improved designs
- (4) Interpreting results from the design process

II. INTERFACING WITH ANALYSIS

The OPTDES package obtains results from analysis for a particular application by calling the user-supplied subroutine:

```
SUBROUTINE ANFUNC (NAV, NAF, AV, IAF, AF)
AV(NAV) = given "analysis variables"
AF(NAF) = returned "analysis functions"
IAF(NAF) = given flags indicating which analysis
           functions need to be computed
```

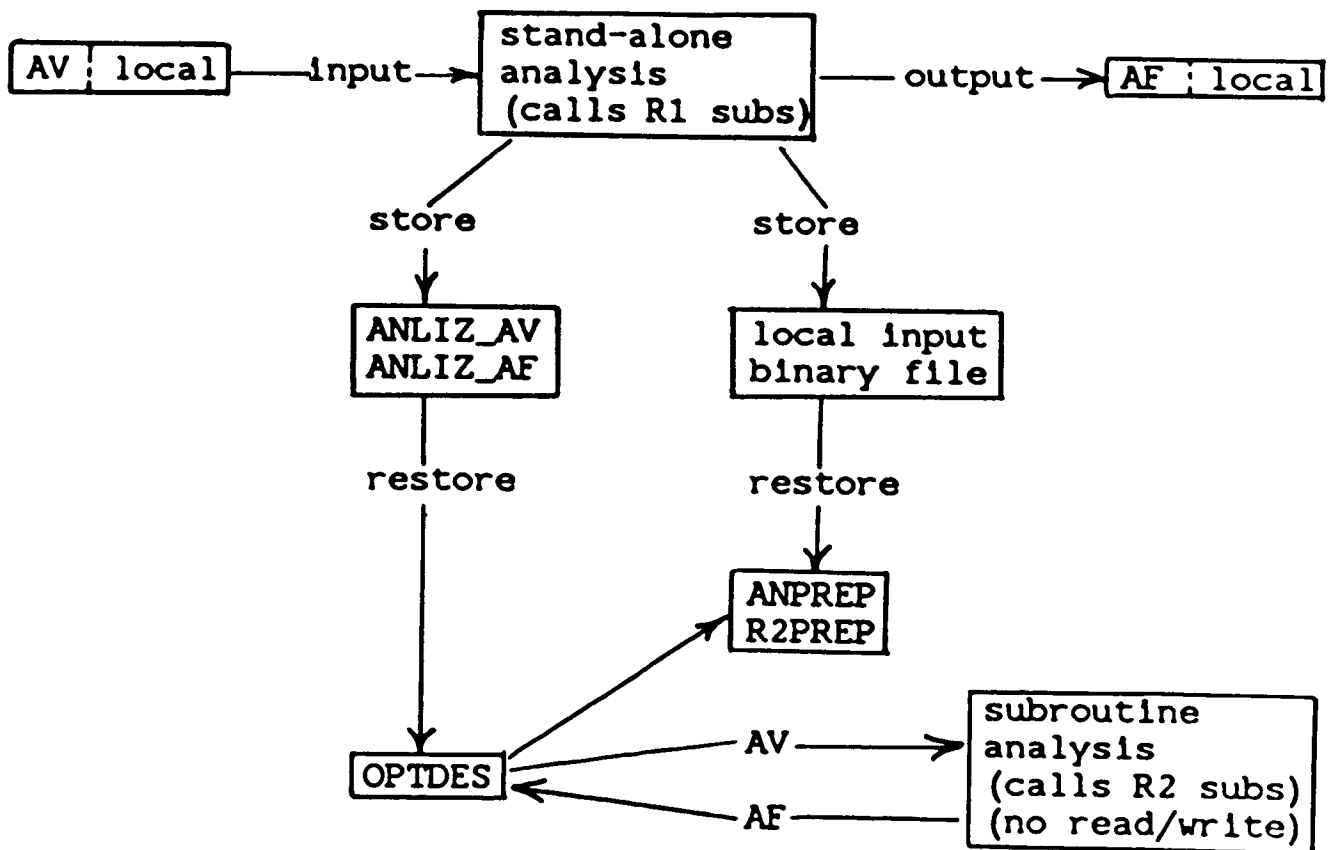
Analysis variables may potentially become design variables, and analysis functions may potentially become design functions (objective, constraints) when the design problem is later defined.

In addition to the ANFUNC subroutine the user must supply the file "ANLIZ_AV" which contains the initial values of the analysis variables as well as optional character descriptions by which the analysis variables will be referred in the OPTDES software. Character descriptions for the analysis functions may also be supplied in an optional "ANLIZ_AF" file:

| ANLIZ_AV FILE | ANLIZ_AF FILE |
|-----------------------|--------------------|
| -30.0, x-coor node 1 | weight |
| 30.0, x-coor node 2 | stress tube 1 |
| 35.0, y-coor node 3 | stress tube 2 |
| 2.0, diameter tube 1 | buck stress tube 1 |
| 2.0, diameter tube 2 | buck stress tube 2 |
| 0.3, thickness tube 1 | x-defl node 3 |
| 0.3, thickness tube 2 | y-defl node 3 |

The user may supply an optional subroutine ANGRAD which returns values for analytical derivatives of specified analysis functions with respect to specified analysis variables. In the absence of a user-supplied ANGRAD subroutine such derivatives are approximated by finite differences in OPTDES. Optional subroutines named ANPREP, ANPOST, and ANITER may be supplied for interfacing to analysis pre, post, and intermediate processing, respectively. Such processing is defined to be computing which is independent from the derivation of analysis functions from analysis variables. These subroutines may call processing software directly or just store/restore data to/from files for stand-alone processing software.

A general method for interfacing any existing stand-alone analysis package to OPTDES will now be sketched. Analysis packages typically contain "READ" and "WRITE" statements throughout. When linked with optimization, this input/output must be performed only once and eliminated thereafter in the several calls to analysis. The OPTDES package contains a set of "R1" and "R2" subroutines. Calls to the "R1" subroutines should be inserted into the analysis source code following all "READ" and "WRITE" statements. When the stand alone analysis package is then executed, the "ANLIZ_AV" and "ANLIZ_AF" files are automatically generated along with a binary file containing local analysis input. The stand alone analysis program is then changed to a subroutine, the calls to "R1" subroutines are replaced by calls to corresponding "R2" subroutines, and all "READ" and "WRITE" statements are deleted. The ANFUNC subroutine to be linked with OPTDES simply calls this new analysis subroutine. An ANPREP subroutine is also linked with OPTDES which calls the subroutine "R2PREP" which restores the local analysis input from the binary file.



After the user-supplied subroutines and files have been created, they may be linked to the OPTDES "DEBUG" module for testing. This module allows one to interactively perform analysis, derivative analysis, and processing:

ENTERING DEBUG

```
>deb> help
"dis av,af 1-2 5"      display listed analysis variables or functions
                        (default = all)
"set av 1-2 5"          set values for listed analysis variables (default =
                        all)
"fun af 1-2 5"          compute listed analysis functions (default = all)
"gra af 1-2 5"          compute gradients of listed analysis functions
                        (default = all)
"ite"                  analysis intermediate process
"pos"                  analysis post-process
"bat"                  switch to batch mode
"qui"                  exit program
```

III. DEFINING THE DESIGN PROBLEM: SETUP

The SETUP module in OPTDES provides a means for interactively defining or redefining an optimization problem. Design variables and design functions (objective, inequality constraints, equality constraints) may be added with the commands shown below:

```
>set> add dv
<mapped analysis variable number (def=1)> 3
<minimum value (def=-1.00)> 10
<maximum value (def=1.00)> 40

>set> add df
<mapped analysis function number (def=1)> 2
<type: objective(=1), inequality(=2), equality(=3) (def=1)> 2
<less than(=1) or greater than(=2) (def=1)>
<reference value (def=0.00)> 100
<range value (def=1.00)> 50
```

It is also possible to add "fancy" design variables which allows one to map several analysis variables to the same design variable, or which allow one to add a group of design variables having the same minimum and maximum bounds with one command. Fancy design functions may be added in like manner.

The analysis variables, analysis functions, design variables, or design functions may be displayed in the SETUP module. The following is an example:

```
>set>      dis dv
d.v.#      scaled      a.v.#      unscaled      minimum      maximum      description
  1          0.667        3          35.0          10.0          40.0          y-coor node 3
  2         -0.500        4           2.00          1.0           5.0          diameter tube 1
                                   5           2.00                                   diameter tube 2
```

```
>set>      dis df
d.f.#      a.f.#      ty      reference      range      description
  1          2          lt      100.000      50.000      stress tube 1
  2          1          mn       80.000      30.000      weight
  3          4          lt       0.250       0.100      y-defl node 3
```

Several commands are available for redefining a design problem. One can delete design variables or functions. One can rescale design variables or functions. It is also possible to relatively rescale all design variables with a single "zoom" command. The values of design variables and unmapped analysis variables may be manually changed. A very useful command is available for changing the status of design functions (i.e. objective to inequality constraint, inequality constraint to equality constraint, etc).

After a design problem has been defined (or redefined), it should be stored to a file. Similarly, a previously defined problem may be restored from a file. The store and restore commands allow the user to specify the file name.

At this point it is useful to comment on the "DIALOGUE" file in OPTDES. All terminal input and output from the interactive modules in OPTDES is automatically echoed to a file named "DIALOGUE" for the user's record.

The Bureau of Reclamation used the OPTDES package in the planning stages for a billion-dollar water project in central Utah. They found the interactive capability for defining and redefining design problems to be valuable as the following comments suggest:

"The most important use of the computer model was the ability to explore a lot of alternatives, to do the 'what ifs'. With OPTDES.BYU it was possible to respond to such questions fairly quickly."

IV. SEARCHING FOR IMPROVED DESIGNS: OPTMIZ

The OPTMIZ module allows one to interactively search for improved designs. Three general techniques are available for doing this. The first technique is brute force trial-and-error. This is accomplished by manually setting values of design variables which automatically initiates a call to analysis:

```
>opt> set dv 2 6-8 14
<scaled values given (def="n")?>
<dv# 2: unscaled value (def=-33.0)> -35
<dv# 6: unscaled value (def=190.0)> 187
<dv# 7: unscaled value (def= 73.0)> 80
<dv# 8: unscaled value (def= 70.0)> 60
<dv# 14: unscaled value (def= 4.00)> 2
```

The second technique is to run a formal optimization algorithm. The software currently contains four fundamentally different nonlinear constrained optimization algorithms, namely: generalized reduced gradient, sequential linear programming, method of multipliers, and feasible directions. Algorithms are easily added to the software, and work is currently under way to add a sequential quadratic programming algorithm. A command is given to select an algorithm followed by a command to run a specified number of iterations where an iteration is defined as the generation of a new design. After the specified number of iterations has been completed (assuming the algorithm's convergence criteria were not satisfied) any OPTMIZ command may be given (such as run more iterations, select a new algorithm, display variables, etc). One may also make variations in the selected algorithm by changing algorithm parameters with a command.

The third technique for searching consists of geometric ideas. A gridding command allows one to create a uniform mesh in design space or any of its subspaces. Analysis is automatically performed at each mesh point and the best design among these points is found. A line command causes analysis to be performed at uniformly spaced points along a line in a specified direction from the current design in design space. The direction may be specified directly, taken as the direction of steepest descent, or taken as a combination of the objective and active constraint gradients. The use of grid and line searching is illustrated as follows:

```
>opt> grid
<number of dimensions (def=2)>
<same spacing all dimensions (def="y")?>
<dim# 1: design variable number (def=1)>
<dim# 1: number of mesh points (def=2)> 10
<dim# 1: backward distance (def=2.0)>
<dim# 1: forward distance (def=2.0)>
<dim# 2: design variable number (def=2)>
FINISHED -- best design was 66 iterations ago

>opt> line
<direction: input (=1), steepest(=2), gradient(=3) (def=1)> 2
<starting distance (def=0.00)>
<ending distance (def=2.35)>
<number of points (def=2)> 10
FINISHED -- best design was 3 iterations ago
```

Print flags may be set to regulate the amount of printout which occurs at each new design (or iteration):

```
> opt> change print
<print out optimization indicators (def="n")?> y
<print out analysis counters (def="n")?> y
<print out design variables (def="n")?>
<print out design functions (def="n")?>
```

| | | | |
|-------------------|-------------------|-------------------|-------------------|
| ITERATION -- : 1 | | | |
| <u>step size</u> | <u>objective</u> | <u>max ineq</u> | <u>max equ</u> |
| 1.59 | -1.22 | -1.39 | 0. |
| <u>anal-calls</u> | <u>anal-evals</u> | <u>grad-calls</u> | <u>grad-evals</u> |
| 2 | 8 | 0 | 0 |

As new designs are generated at each iteration, the values of design variables, design functions, analysis variables, and analysis functions are written to a direct-access binary file with the same name as the problem definition file followed by "_H". This permits the designer to backtrack as well as recover from program crashes. The following commands enable one to access this file:

```
> opt> dis iter
<starting iteration (def=0)>
<ending iteration (def=107)>
```

| | |
|--------------|-------------------------------|
| <u>iter#</u> | <u>algorithm type</u> |
| 0 | first iteration |
| 1 | trial and error |
| 3 | grid searching |
| 103 | backtrack to iteration 36 |
| 104 | generalized reduced gradient |
| 107 | sequential linear programming |

```
> opt > set iter
<iteration (def=107)> 103

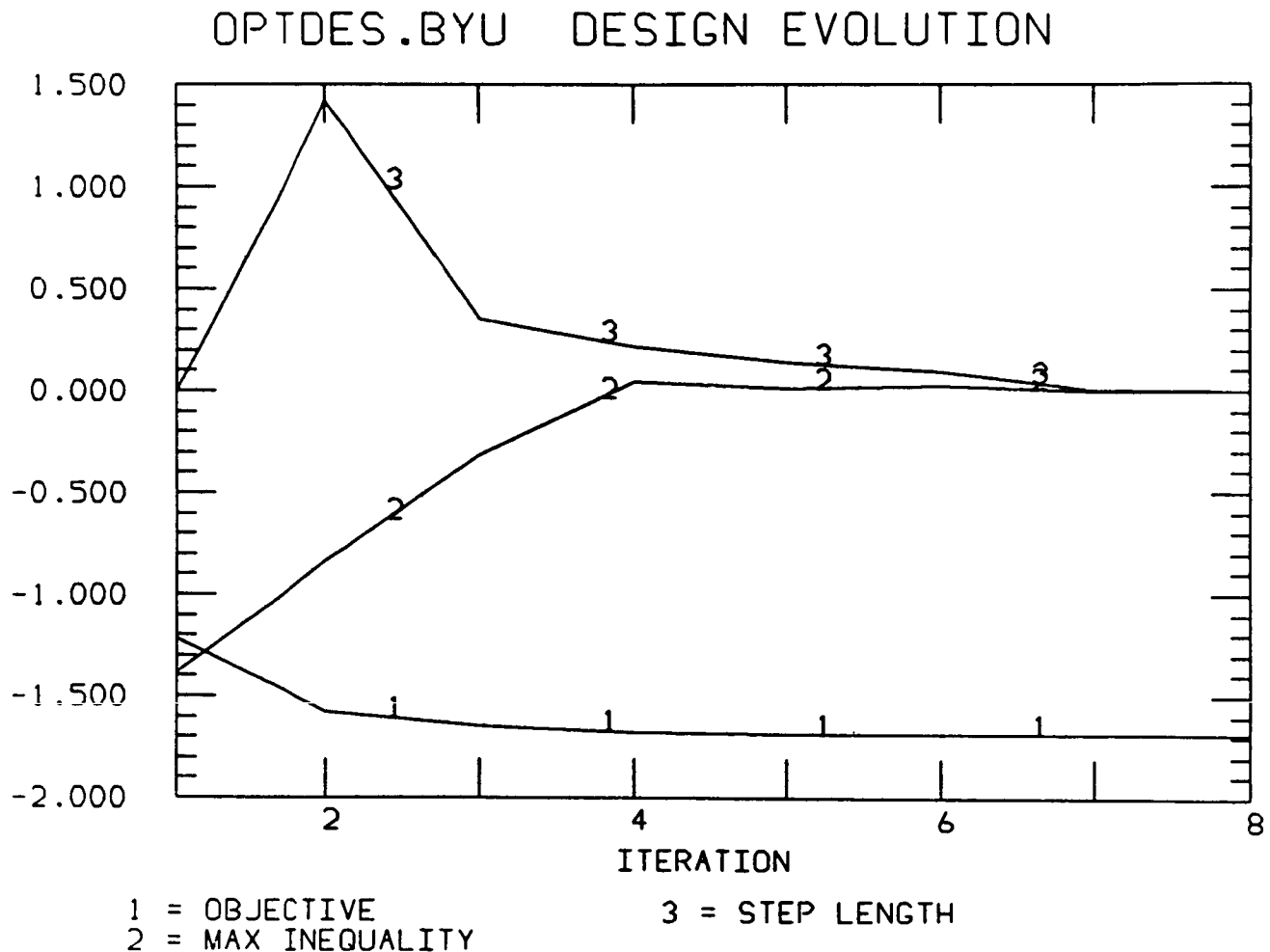
> opt > purge
<first iteration deleted (def=0)>
<first iteration retained (def=108)>
```

For large design problems, a semi-interactive mode is possible. The batch command causes OPTDES input to be taken from a specified file rather than from the terminal. For example, the contents of the file might be the commands: grg, run, 20, quit. This would cause 20 iterations of the grg algorithm to be performed in batch mode. The user could then leave the terminal and return later to restore the results and continue.

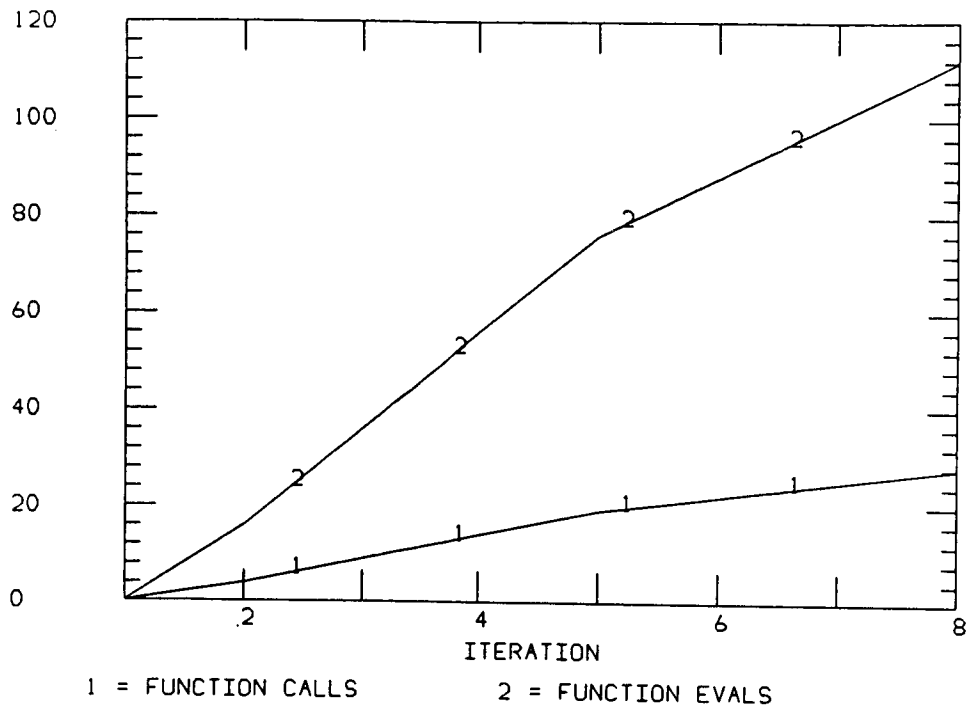
The optional user-supplied analysis subroutines may be activated in the OPTMIZ module. Specifically, commands are available to cause gradients to be computed by the ANGRAD subroutine, to set the regularity at which the ANITER subroutine is called and to execute the ANPOST subroutine. The ANPREP subroutine is always executed at the top of the program.

V. INTERPRETING RESULTS: GRAPH

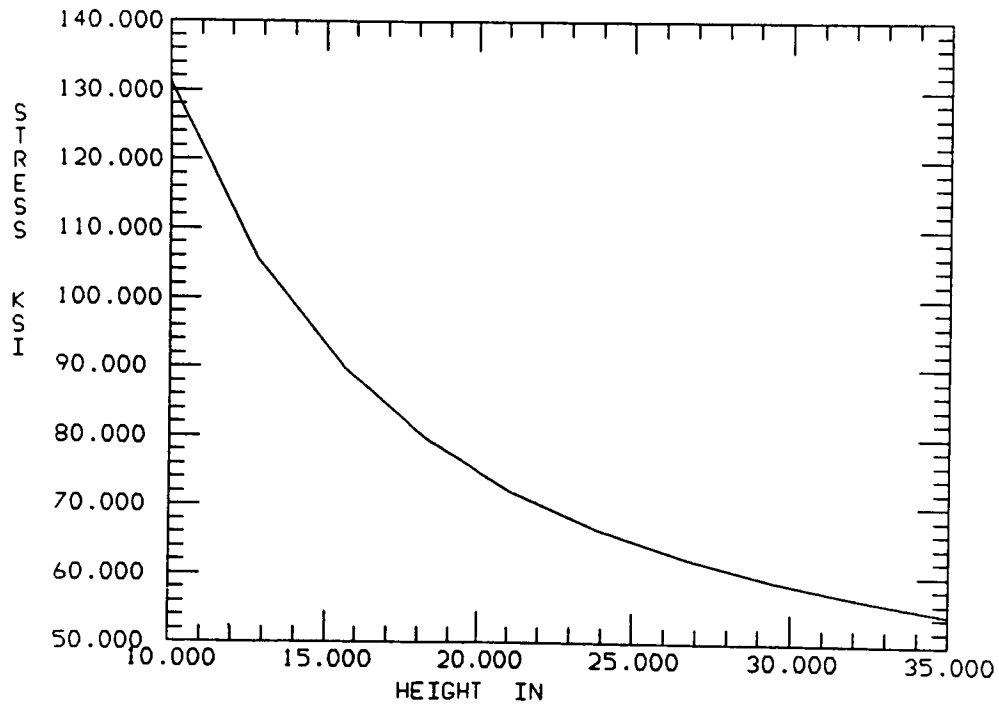
Graphics are used to interpret results. The GRAPH module allows one to interactively generate history and sensitivity plots on the terminal screen or on a plotter or other hard copy device. The user must supply move and draw subroutines for the particular graphics device if the available move and draw subroutines (Tektronix Plot-10) do not work. Example plots are shown below and on the next page.



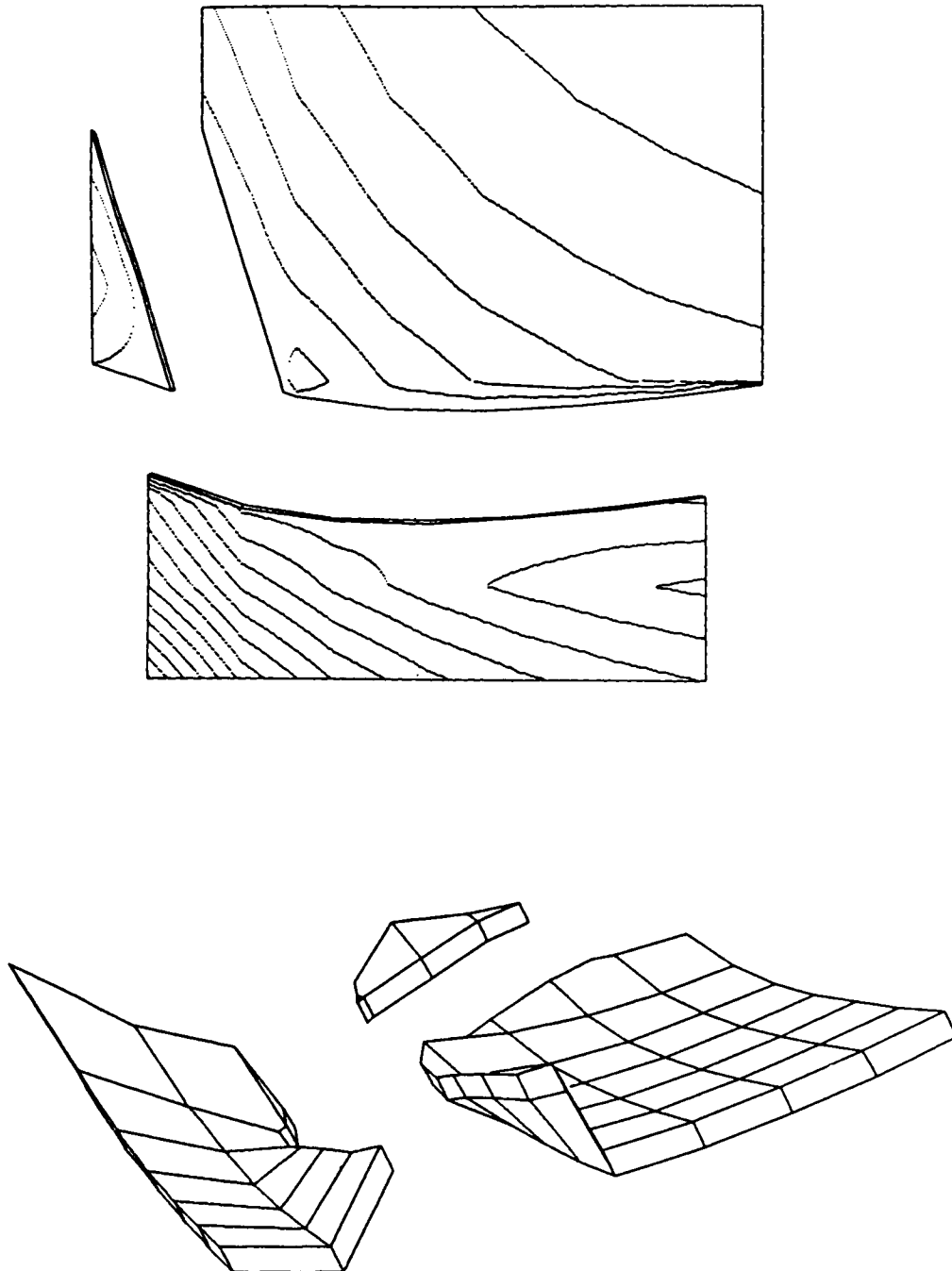
OPTDES.BYU AMOUNT OF ANALYSIS

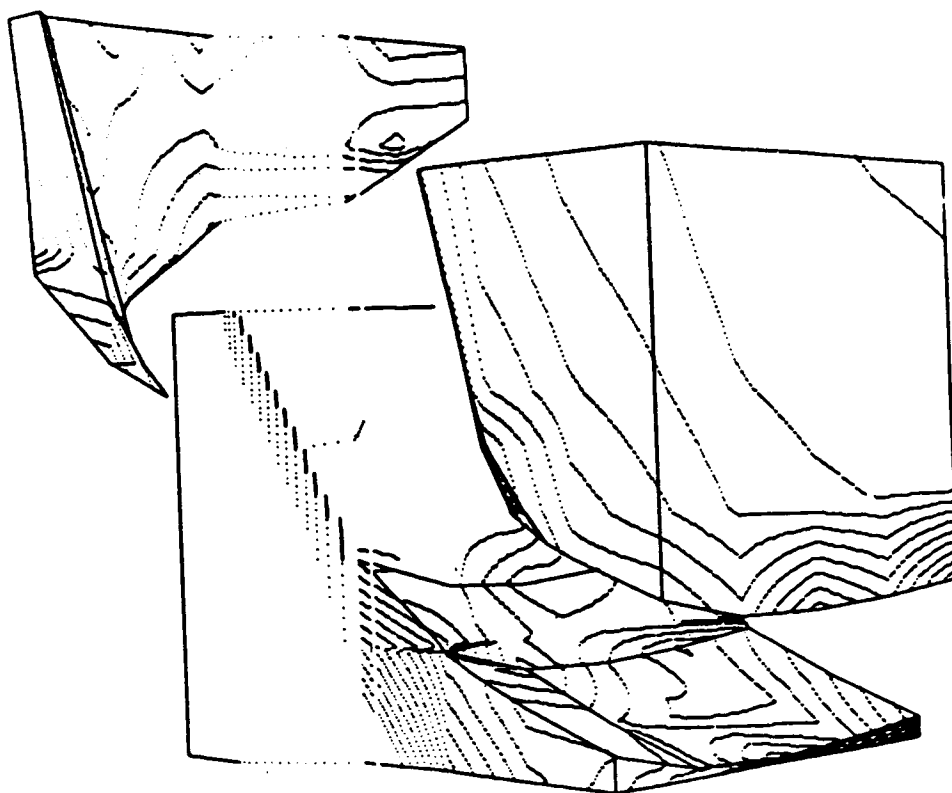
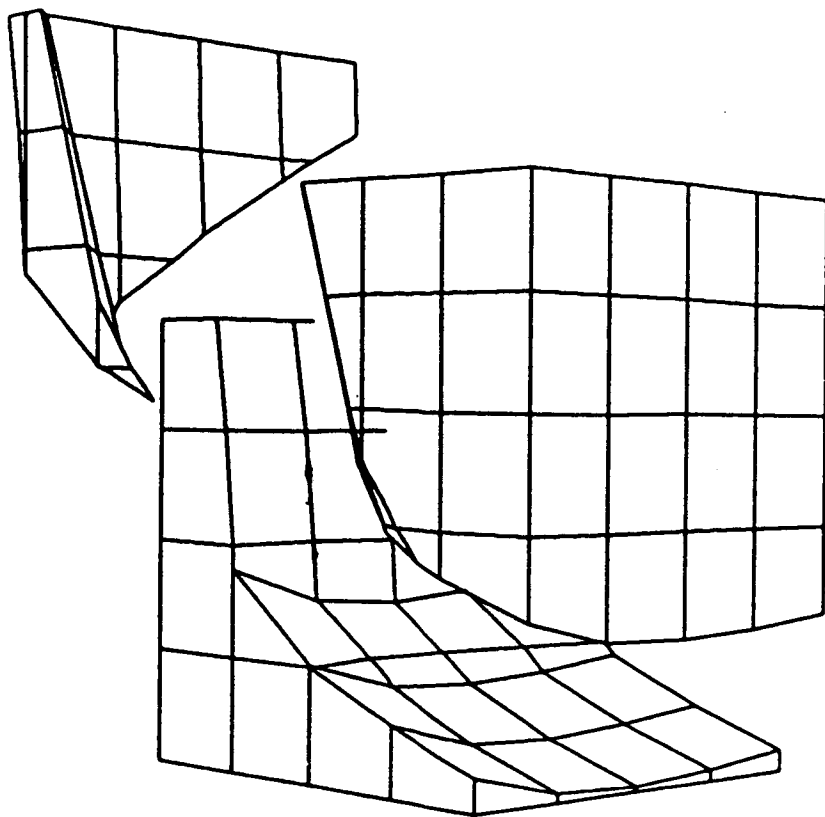


OPTDES.BYU ONE-DIMENSIONAL GRID



Two and three dimensional images of design space (or subspace) may be produced. OPTDES creates input files for the high-performance graphics package MOVIE.BYU. Infeasible regions are clipped away. Objective function values may be depicted by contours and/or color. In a two-dimensional image, the objective value may also be displayed by warping the plane in the third dimension. It is also possible to cut the 3-dimensional feasible region apart with planes and explode the resulting pieces. Data for these images is generated by the gridding command in the OPTMIZ module. Of course if the design space is of dimension higher than 3, the non-displayed dimensions are held constant. Some examples follow.





VI. PROGRAMMING STANDARDS

Strict programming standards were enforced during the development of the OPTDES package. Standard FORTRAN-77 was the language that was used. All arrays are allocated dynamically. Changing storage size simply requires changing the dimension of the integer, real, and/or character vector at the top of the program. Only a handful of common blocks are used. The source code is structured. The only statement labels used are for FORMAT statements. All input is screened to prevent unnecessary program aborts. File handling is performed in one central subroutine.

N87-11777

ON THE UTILIZATION OF ENGINEERING
KNOWLEDGE IN DESIGN OPTIMIZATION

Panos Papalambros
Department of Mechanical Engineering
and Applied Mechanics
The University of Michigan

INTRODUCTION

A long-standing difficulty in the use of formal optimization techniques in design is the often nonmathematical form in which design knowledge is available. In general, engineering knowledge incorporated in a design optimization problem has the form of a mathematical model, such as a nonlinear programming one. The solution to the problem is provided by an optimization technique which operates on the model exclusively. Typically the solution technique is iterative in nature.

Thus, knowledge which has not been included in the analytical model cannot be used. Moreover, knowledge (possibly mathematical in nature) which is not compatible in form with the iterative structure of optimization algorithms cannot be used in an automated way, although the designer/analyst may use that knowledge implicitly in a heuristic way. For any real design problem, it is evident that additional knowledge is available, which however cannot be modelled easily or properly. Typical examples are manufacturing considerations in structural design which are usually expressed as simple upper and lower bounds on the design variables and subtly called "technological constraints."

In this article, some current research work conducted at the University of Michigan is described to illustrate efforts for incorporating knowledge in optimization in a nontraditional way. Much of this research is yet unpublished.

The incorporation of available knowledge in a logic structure is examined in two circumstances. The first examines the possibility of introducing global design information in a local active set strategy implemented during the iterations of projection-type algorithms for nonlinearly constrained problems (ref. 1). The technique used combines global and local monotonicity analysis of the objective and constraint functions (refs. 2 and 3). The second examines a knowledge-based program which aids the user to create configurations that are most desirable from the manufacturing assembly viewpoint. The data bank used is the classification scheme suggested by Boothroyd (ref. 4). The important aspect of this program is that it is an aid for synthesis intended for use in the design concept phase in a way similar to the so-called "idea-triggers" in creativity-enhancement techniques like brainstorming. The idea generation, however, is not random but it is driven by the goal of achieving the best acceptable configuration.

LOCAL MONOTONICITY ANALYSIS

For problems of this form, minimize $f(x)$ subject to $g(x) \leq 0$ and $h(x) = 0$ with x as a vector in a n -dimensional real space; the question of which constraints g_i are active is important mathematically, but more so in the design context, since the active constraints represent critical design requirements. An active set strategy selects active constraints at each iteration based on local information. There are different strategies to do that. One of them is based on local monotonicity, i.e., the signs of the partial derivatives of the functions with respect to the design variables. The program ACCME (Automated Constraint Criticality by Monotonicity Evaluations) outlined in figure 1 implements such a strategy, in conjunction with a reduced-gradient type of search. The partial derivatives are calculated in the tangent space of the subspace of active inequality and equality constraints (constrained derivatives).

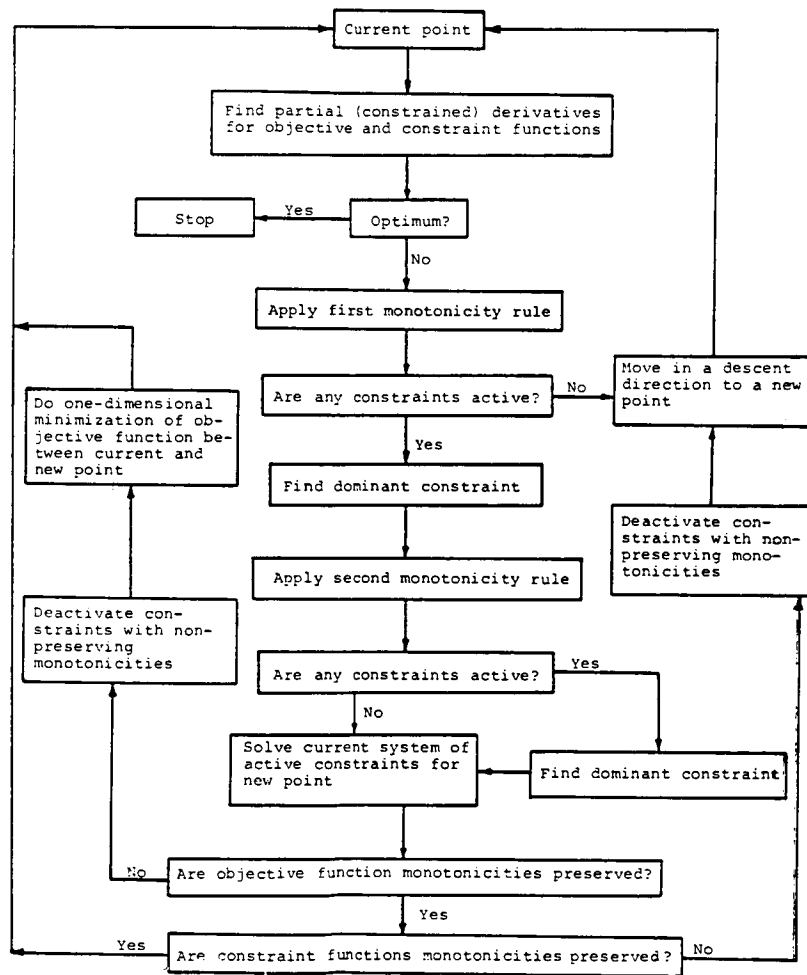


Figure 1

MONOTONICITY AND DOMINANCE RULES

The following two monotonicity rules can be proved (even when nondifferentiable functions are involved).

Rule 1: If the objective function is monotonic with respect to (wrt) a particular variable in the neighborhood of a local minimum, then there exists at least one active constraint with opposite monotonicity wrt that variable in that neighborhood.

Rule 2: If the objective function is stationary wrt a particular variable in the neighborhood of a local minimum, then either all constraints containing that variable are inactive, or there exist at least two active constraints having opposite monotonicities wrt that variable in that neighborhood.

When more than one candidate active constraint exists, then a dominance strategy is employed to select the constraint which is most likely active. In ACCME this is done by selecting the minimum or maximum distance $d_j = x_i - g_j(x_i) / [\partial g_j(x_i) / \partial x_i]$ for all appropriate j , depending on whether the g_j 's are locally increasing or decreasing wrt x_i , as shown schematically in figure 2.

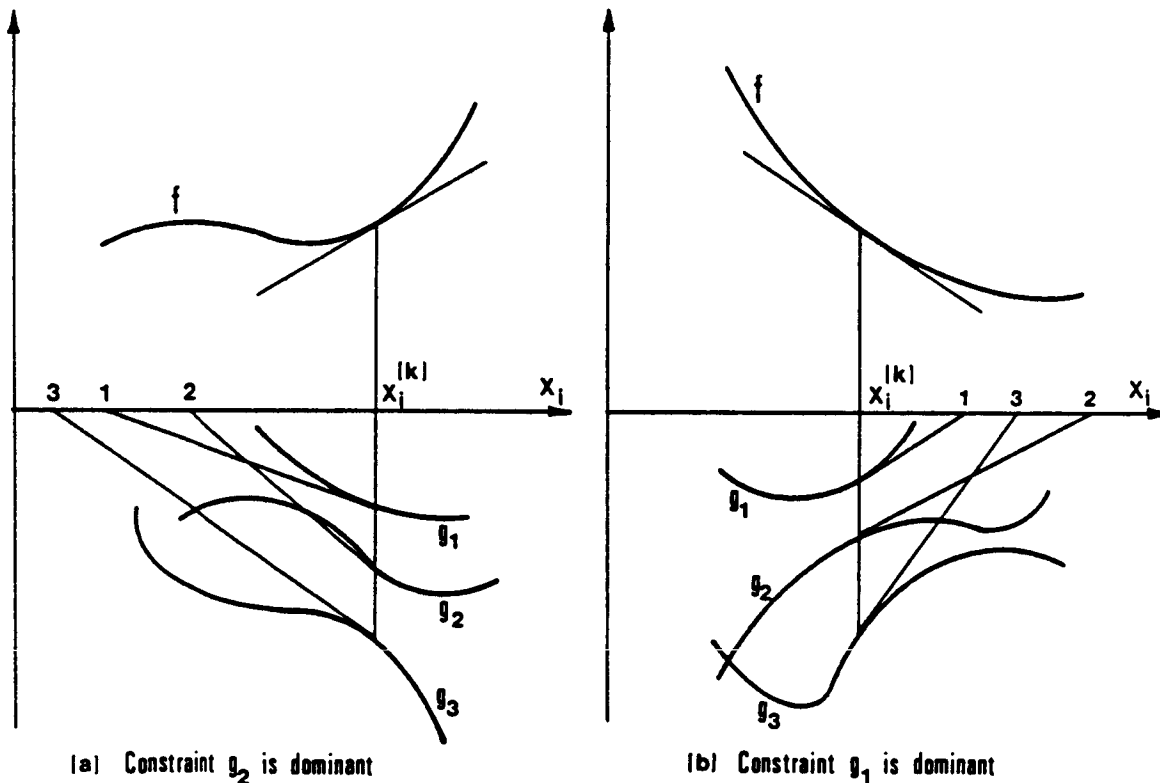


Figure 2

A LOCAL STRATEGY EXAMPLE

A two-dimensional example representing the design of a helical compression spring is shown in figure 3, together with the iteration path followed by ACCME. The corner solution is identified after three iterations. In the first one, g_7 is put in the active set; in the second, g_7 is dropped and g_1 is brought in; in the third, g_1 is retained and g_3 is added. There are now zero degrees of freedom, the Karush-Kuhn-Tucker conditions are satisfied and the algorithm terminates.

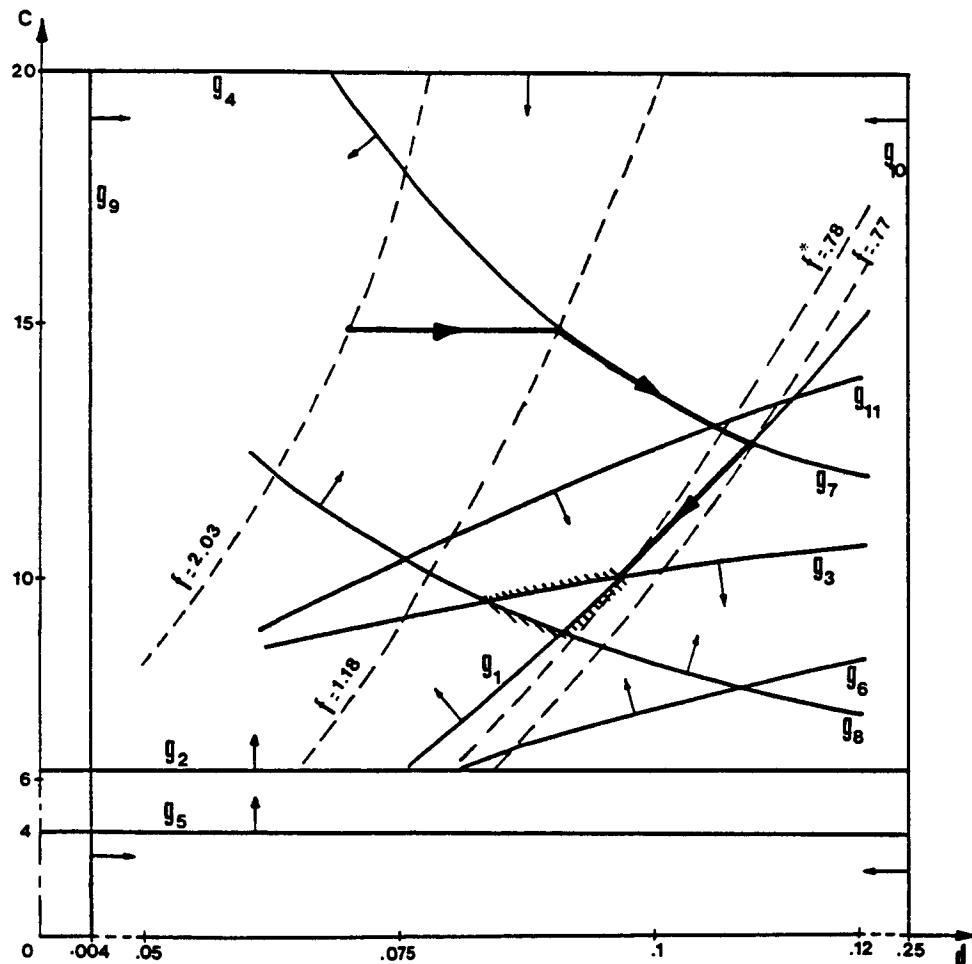
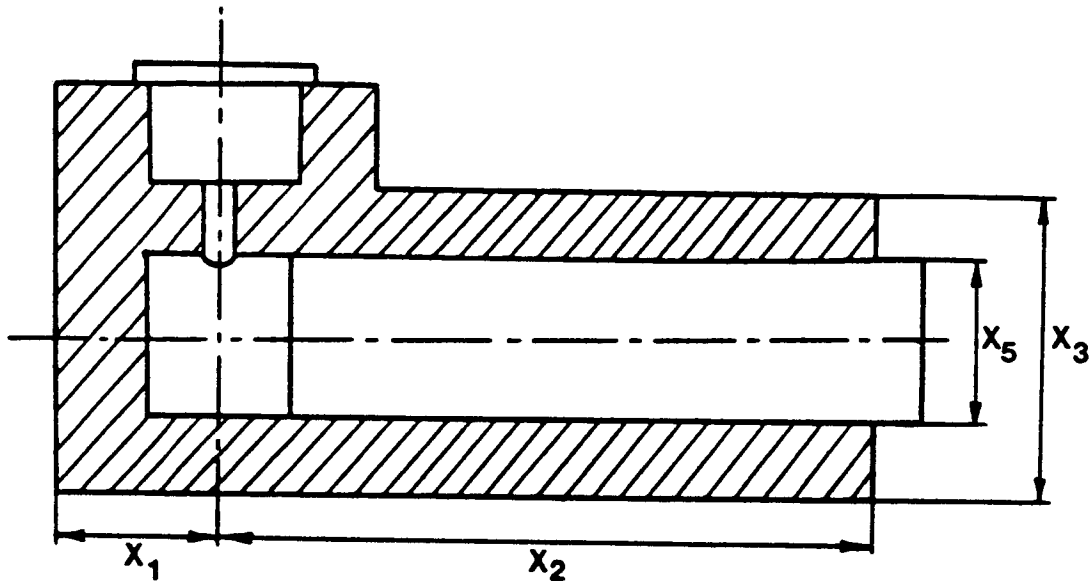


Figure 3

A LOCAL/GLOBAL STRATEGY EXAMPLE

The monotonicity and dominance rules can be applied globally if the monotonicity properties are globally established. This was in fact the way the original theory was developed. These global results can be derived analytically, often without too much effort. The global rules can be used in an overriding mode to influence the decision making at each iteration. A separate subroutine containing the global rules is included in ACCME and called upon in the active set decisions. Note that the form of the logic allows the introduction of any global rules, not just those derived from monotonicity arguments. An example involving an explosively actuated cylinder is shown in figures 4, 5 and 6. The global rules were derived independently in ref. 5. Figures 5 and 6 are the output from ACCME.



- X_1 = UNSWEPT CYLINDER LENGTH, IN
- X_2 = WORKING STORE OF PISTON, IN
- X_3 = OUTSIDE DIAMETER OF CYLINDER, IN
- X_4 = INITIAL PRESSURE OF COMBUSTION, KPSI
- X_5 = PISTON DIAMETER, IN

Figure 4

ORIGINAL PAGE IS
OF POOR QUALITY

>>>>Automated Constraint Criticality by Monotonicity Evaluations<<<<

*****ITERATION NO.(1)*****

Current point:

Values of design variables:

x(1)= 0.20000

x(2)= 1.50000

x(3)= 0.80000

x(4)= 10.000

x(5)= 0.32000

Value of objective function:

f= 1.7000

Values of constraints:

g(1)=-0.20000

g(2)= -1.50000

g(3)=-0.80000

g(4)= -10.000

g(5)=-0.32000

g(6)=-0.20000

g(7)= -26.426

g(8)= 104.25

g(9)= -17.857

g(10)=-0.48000

g(11)=-0.30000

THIS POINT IS INFEASIBLE!!!

Monotonicity and dominance analysis:

For this point, based on first monotonicity rule,
one of the following constraints wrt x(1) may be active:

g(1)

g(7)

NOTE: At any point, based on first monotonicity rule,
wrt x(1) constraint g(7) is GLOBALLY active.

For this point, based on second monotonicity rule,
one of the following constraints wrt x(4) may be active:

g(8)

g(9)

For this point, wrt x(4) constraint g(8) may be dominant.

Decisions taken for this iteration:

>>>>AT THIS ITERATION, BASED ON FIRST MONOTONICITY RULE,

>>>>WRT x(1) CONSTRAINT g(7) IS ACTIVE.

>>>>AT THIS ITERATION, BASED ON SECOND MONOTONICITY RULE,

>>>>WRT x(4) CONSTRAINT g(8) IS ACTIVE.

*****ITERATION NO.(2)*****

Current point:

Values of design variables:

x(1)= 0.16409E-01

x(2)= 1.50000

x(3)= 0.80000

x(4)= 8.7038

x(5)= 0.32000

Value of objective function:

f= 1.5164

Values of constraints:

g(1)=-0.16409E-01

g(2)= -1.50000

g(3)=-0.80000

g(4)= -8.7038

g(5)=-0.32000

g(6)=-0.20000

g(7)= 0.27780E-01

g(8)= 0.56843E-13

g(9)= -20.943

g(10)=-0.48000

g(11)=-0.48359

Monotonicity and dominance analysis:

For this point, based on first monotonicity rule,
one of the following constraints wrt x(5) may be active:

g(1)

g(5)

g(9)

For this point, wrt x(5) constraint g(1) may be dominant.
Monotonicity of active constraints are preserved.

Decisions taken for this iteration:

>>>>AT THIS ITERATION, BASED ON FIRST MONOTONICITY RULE,

>>>>WRT x(5) CONSTRAINT g(1) IS ACTIVE.

>>>>FROM ITERATION(1): WRT x(1) CONSTRAINT g(7) IS ACTIVE.

>>>>FROM ITERATION(1): WRT x(4) CONSTRAINT g(8) IS ACTIVE.

Figure 5

*****ITERATION NO.(3)*****

Current point:

Values of design variables:
x(1)=-0.47003E-23
x(2)= 1.5000
x(3)= 0.80000
x(4)= 8.8405
x(5)= 0.31752
Value of objective function:
f= 1.5000
Values of constraints:
g(1)= 0.47003E-23
g(2)= -1.5000
g(3)=-0.80000
g(4)= -8.8405
g(5)=-0.31752
g(6)=-0.20000
g(7)= 0.81819E-11
g(8)= 0.19423E-09
g(9)= -20.680
g(10)=-0.4E248
g(11)=-0.50000

Monotonicity and dominance analysis:

For this point, based on first monotonicity rule,
one of the following constraints wrt x(2) may be active:
g(2)
g(5)
g(9)
For this point, wrt x(2) constraint g(9) may be dominant.

For this point, based on second monotonicity rule,
one of the following constraints wrt x(3) may be active:
g(6)
NOTE: At any point, based on second monotonicity rule,
constraints g(6) and g(9) MUST be simultaneously active.

Decisions taken for this iteration:

>>>>AT THIS ITERATION,BASED ON FIRST MONOTONICITY RULE,
>>>>WRT x(2)CONSTRAINT g(9)IS ACTIVE.
>>>>AT THIS ITERATION,BASED ON SECOND MONOTONICITY RULE,
>>>>WRT x(3)CONSTRAINT g(6)IS ACTIVE.
>>>>FROM ITERATION(1):WRT x(1)CONSTRAINT g(7)IS ACTIVE.
>>>>FROM ITERATION(1):WRT x(4)CONSTRAINT g(8)IS ACTIVE.
>>>>FROM ITERATION(2):WRT x(5)CONSTRAINT g(1)IS ACTIVE.

*****ITERATION NO.(4)*****

Current point:

Values of design variables:
x(1)= 0.23799E-23
x(2)= 1.0777
x(3)= 1.0000
x(4)= 19.900
x(5)= 0.21163
Value of objective function:
f= 1.0777
Values of constraints:
g(1)=-0.23799E-23
g(2)= -1.0777
g(3)= -1.0000
g(4)= -19.900
g(5)=-0.21163
g(6)= 0.0
g(7)=-0.39790E-12
g(8)=-0.11369E-12
g(9)=-0.35527E-14
g(10)=-0.78637
g(11)=-0.9222E

Decisions taken for this iteration:

>>>>FROM ITERATION(1):WRT x(1)CONSTRAINT g(7)IS ACTIVE.
>>>>FROM ITERATION(1):WRT x(4)CONSTRAINT g(8)IS ACTIVE.
>>>>FROM ITERATION(2):WRT x(5)CONSTRAINT g(1)IS ACTIVE.
>>>>FROM ITERATION(3):WRT x(2)CONSTRAINT g(9)IS ACTIVE.
>>>>FROM ITERATION(3):WRT x(3)CONSTRAINT g(6)IS ACTIVE.

TERMINATION CRITERION MET, KARUSH-KUHN-TUCKER CONDITIONS SATISFIED

Figure 6

A PRODUCTION SYSTEM WITH GLOBAL RULES

Looking at the utilization of global rules only, without local monotonicity analysis, one can create an optimization procedure that includes problem-dependent knowledge supplied by the user. The general form of such a procedure is shown in figure 7.

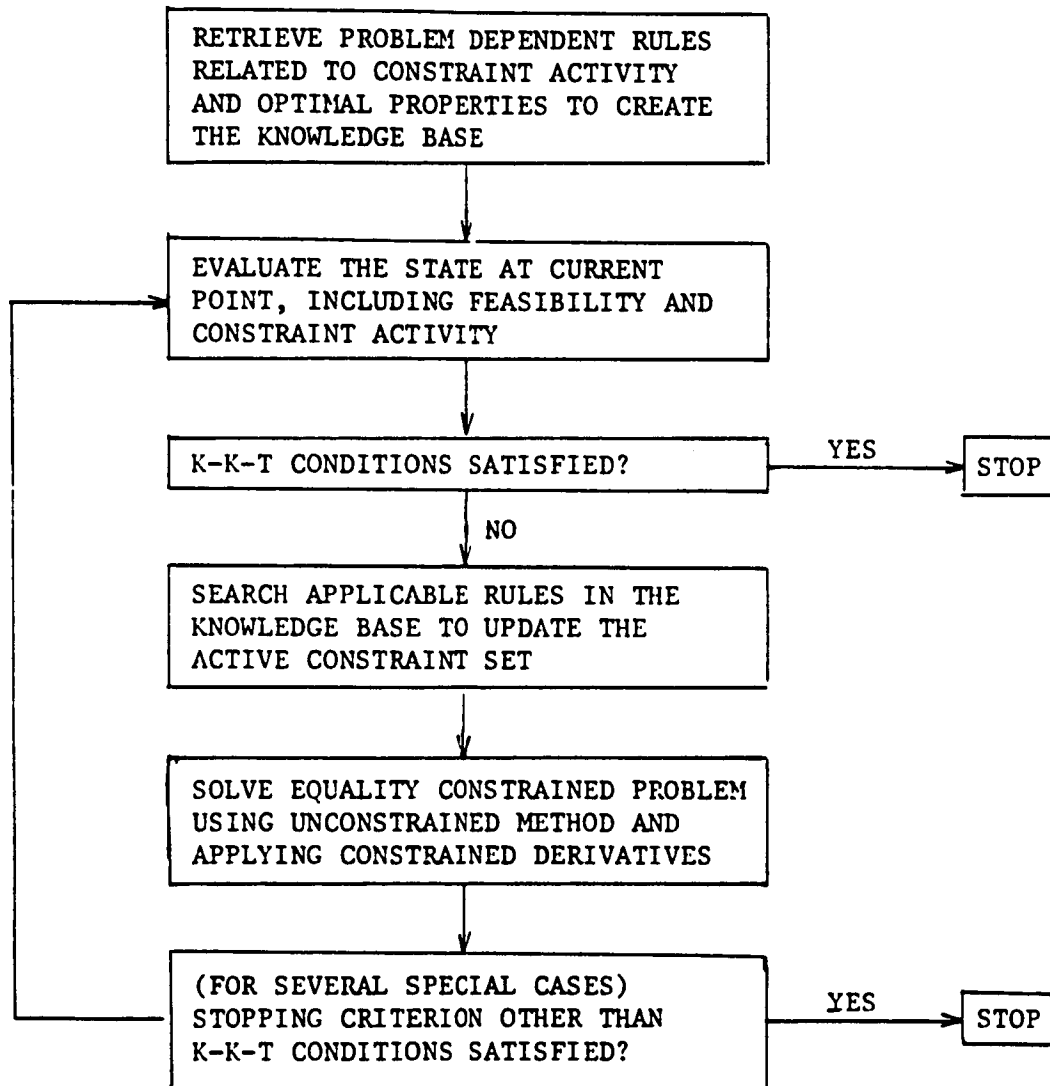


Figure 7

PRODUCTION RULES TYPES

Following the original way that global monotonicity analysis was implemented, a set of rule types can be identified as the first few elements of the production system. In figure 8, seven different rules are listed pertaining to constraint activity and possible properties of the optimum. It should be noted that any number of rule types can be included as more knowledge types are identified as important in the entire process. This of course presumes types requiring knowledge attainable prior to complete solution.

Provide model information type by type to aid the solution process

Type 1. The following inequality constraints are always active:
1.

Type 2. one or more constraints within each of the following groups must be active:
<start with number of constraints in each group>

Type 3. if $A < X(I) < B$, then $G(K)$ is active <or inactive with K as a minus integer>:

Type 4. if $G(I)$ active, then one or more constraints within the following group must be active:
<following I is the number of constraints in each group>

Type 5. if $A < X(I) < B$, then $G(K)$ is dominant to a group of $G(J)$ s:
<following I, K is the number of constraints in each group>

Type 6. if $G(I)$ active, then $G(J)$ redundant and vice versa:

Type 7. if $X(I)$ in (A, B) , then $X(I)$ in $RANDOM(C, D)$:

Figure 8

RULE-BASED DECISIONS

The user provides the available knowledge for a specific problem, according to the different rule types. In figure 9, the input knowledge for a simple example is shown in the top half. The rules are connected so that several decisions can be reached. These are shown in the bottom half of figure 9. Note that most of these decisions are in fact global conclusions.

```

**** Summary of the problem-dependent knowledge provided by the user ****

Type 1:  3 rules
Constraint G( 1) is always active
Constraint G( 3) is always active
Constraint G( 6) is always active

Type 2:  1 rules
One or more of the following constraints must be active: G( 5), G( 8)

Type 3:  1 rules
If X( 2) is in (0.300000E+01,0.100000E+02), then G( 5) is active

Type 4:  1 rules
If G( 1) is active, then one or more of the following constraints must be active: G( 4)

Type 6:  1 rules
If G( 4) is active, then G( 5) is redundant

Type 7:  1 rules
If X( 3) is in (0.0          ,0.280000E+01), then it is moved to (0.280500E+01,0.300000E+03)

Using Type 1 rules,
constraint G( 1) is added to the active set
constraint G( 3) is added to the active set
constraint G( 6) is added to the active set

Using Type 2 rules,
constraint G( 8) is added to the active set

Using Type 3 rules,
constraint G( 5) is added to the active set

Using Type 4 rules,
constraint G( 4) is added to the active set
Constraint G( 5) is deleted from the active set
(This deletion is caused by applying Type 6 rules)

Using Type 7 rules,
X( 3) is changed to 0.196552E+03

The rule search of the current iteration is finished. The current active set contains  5 constraints
 0 equality constraints:
 5 inequality constraints:
G( 1), G( 3), G( 6), G( 8), G( 4)

```

Figure 9

DESIGN DATA FOR AUTOMATED ASSEMBLY

The data collected and organized by Boothroyd is the only quantified measure of how good a design may be from the assembly viewpoint. A typical data structure from ref. 4 is shown in figure 10. Two main performance criteria, orienting efficiency (OE) and relative feeder cost (FC), must be established based on geometric characteristics codified in the form of indices. The goal is to maximize OE and minimize FC. The charts, or interactive program versions of them, are used to analyze existing design and/or assist in redesign.

AUTOMATIC HANDLING — DATA FOR ROTATIONAL PARTS (first digit 0, 1 or 2)

KEY: OE FC

| | | |
|---|------|-----|
| 0 | 0.3 | 1 |
| 1 | 0.15 | 1.5 |
| 2 | 0.45 | 1.5 |

first digit

Diagram labels: SIDE SURFACE, END SURFACES, Principal axis, D, L, I

| | | part is symmetrical about its principal axis (BETA symmetric) (see note 2) | part is not BETA symmetric (code the main feature or features requiring orientation about the principal axis) | | | | | | | | slightly asymmetric or small features less than D/10 and L/10 OR holes or recesses which cannot be seen in outer shape of silhouette | |
|---|---|--|---|---------------------------|---------------------------------|--|---|-------------------------|-------------------------|---|--|--|
| | | | BETA asymmetric projections, steps, or chamfers (can be seen in silhouette) | | | BETA asymmetric grooves or flats (can be seen in silhouette) | | | | | | |
| | | | on side surface only | on end surface(s) only | on both side and end surface(s) | through groove or flat can be seen in end view | through groove can be seen in side view | | | | | |
| | | | | | | | on end surface | on side surface | | | | |
| | | | 0 | 2 | 3 | 4 | 5 | 6 | 7 | 8 | | |
| part is not ALPHA symmetric (code the main feature or features requiring end-to-end orientation) (see note 1) | part is ALPHA symmetric (see note 1) | 0 | 0.7 1 0.7 1 0.9 1 | 0.3 1 0.15 1 0.45 1 | 0.5 1 0.2 1 0.9 2 | 0.3 1 0.15 1 0.45 1 | 0.35 1 0.2 1 0.9 1 | 0.2 1 0.2 1 0.9 2 | 0.5 1 0.2 1 0.9 2 | | | |
| | part can be fed in a slot supported by large end or protruding flange with center of mass below supporting surfaces | 1 | 0.4 1 0.3 1 0.9 1 | | | | | | | | | |
| | BETA symmetric steps or external surfaces (see note 3) | 2 | 0.4 1 0.3 1 0.75 1 | | | | | | | | | |
| | BETA symmetric grooves, holes or recesses (see note 3) | on both side and end surface(s) | 3 | 0.5 1 0.2 1 0.85 1 | | | | | | | - MANUAL HANDLING REQUIRED - | |
| | | on side surface only | 4 | 0.5 1 0.1 1 0.85 1 | | | | | | | | |
| | | on end surface(s) only | 5 | 0.5 1 0.2 1 0.6 1 | | | | | | | | |
| | BETA symmetric hidden features with no corresponding exposed features (see note 4) | 6 | 0.6 1 | | | | | | | | | |
| | BETA asymmetric features on side or end surface(s) | 7 | | | | | | | | | | |
| | slightly asymmetric or small features; amount of asymmetry or feature size less than D/10 and L/10 | 8 | | | | | | | | | | |

-MANUAL HANDLING REQUIRED-

(ref. 4)

Figure 10

BINARY TREE DECISION AID

From a practical viewpoint, it is best to guide the designer in the initial development phase towards meeting the goals, rather than redesign. This can be achieved by interacting with a program that makes optimal suggestions - a situation different from the expert system configuration. A natural logic for this program, based on the original format of the data, is a binary tree structure (fig. 11). This attempts to suggest first general configuration decisions and then more specific ones.

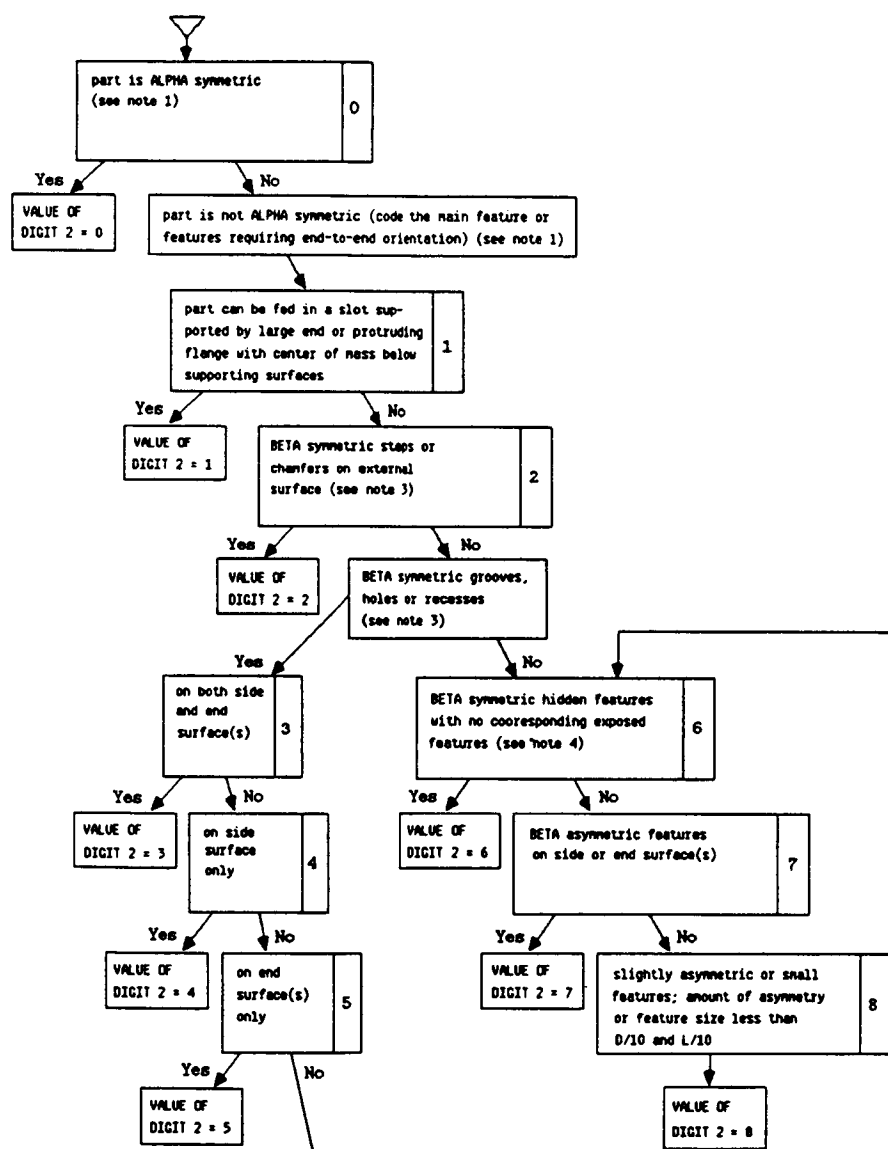


Figure 11

SERIAL DECISION REPRESENTATION

The binary-tree structure has certain flaws, in spite of its intuitive appeal. By attempting to assign digit values one by one, it may arrive at configurations worse than actually possible, because the actual chart data are not perfectly structured along the diagonal (fig. 10). If the binary tree structure is used, additional searches will be required to guarantee optimal configuration. Instead, a serial representation can be used where decisions are based on examining all best possibilities by attempting to assign several digits at once, e.g. a single triplet value for the first three digits to give OE and FC values. This structure is shown in figure 12. It represents a heuristic search appropriate for small data bases, but is it compatible with the way the designer should be aided naturally.

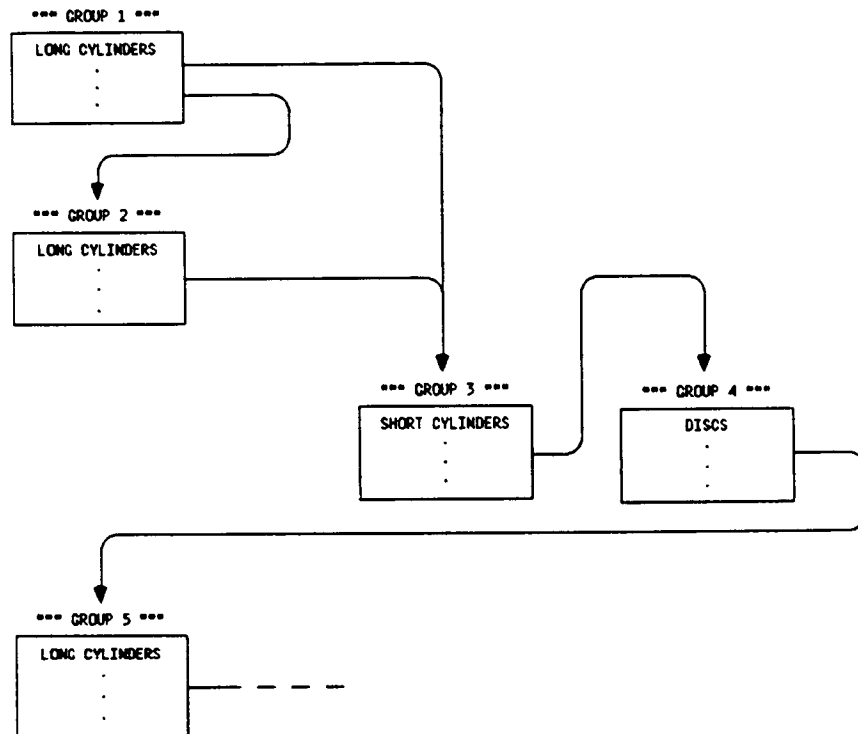


Figure 12

AN EXAMPLE DESIGN

An example of a typical interaction for the first three digit assignment and final design results is shown in figure 13. Note that the program makes just optimal recommendations. The designer is forced to conceptualize the design and examine different possibilities as suggested.

```

*** ASSIGN DIGITS 1,2,3 FOR ROTATIONAL PART ***

[ATTEMPTING TO ASSIGN
OE = 0.90 FC = 1.00]

IT IS RECOMMENDED THAT ...
(1,2) LONG CYLINDERS L/D > 1.5
IS THIS POSSIBLE ? ...
Y

IT IS RECOMMENDED THAT ...
(2,0) ALPHA SYM.

OR

(2,1) NOT ALPHA SYM., SLOT FED WITH C.M. BELOW SUPPORTING S'FACES
IS THIS POSSIBLE ? ...
Y

IT IS RECOMMENDED THAT ...
(3,0) BETA SYM.

OR

(3,5) BETA ASYM. THRU GROOVE OR FLAT SEEN IN END VIEW
IS THIS POSSIBLE ? ...
Y
*** OPTIMAL PARAMETERS ASSIGNED ***

*****
RESULTS OF SEARCH

OE = 0.90 FC = 1.00
*****

PLEASE INPUT THE SPECIFIC 1,2,3 BOOTHROYD DIGITS
YOU PICKED, IN THAT ORDER AS INTEGERS ...
2,0,0

*****
RESULTS OF DESIGN STUDY
*****

--- ROTATIONAL PART ---

MAXIMUM PART DIMENSION = 25.00 MM.
REQUIRED RATE OF ASSEMBLY = 60.00 PARTS/MIN
NUMBER OF SIMULTANEOUS OPERATIONS = 2

FIVE DIGIT AUTOMATIC HANDLING CODE =
20000

ORIENTING EFFICIENCY 'OE' = 0.90
RELATIVE FEEDER COST CR = FC + DC = 1.00
MAXIMUM BASIC FEED RATE FM = 54.00 PARTS/MIN
DIFFICULTY RATING FOR AUTOMATIC HANDLING DF = 1.11
COST OF AUTOMATIC HANDLING PER PART CF = 0.03 * DF = 0.03 CENTS

TWO DIGIT AUTOMATIC INSERTION CODE =
38

RELATIVE WORKHEAD COST WC = 0.80
DIFFICULTY RATING FOR AUTOMATIC INSERTION DI = 0.80
COST OF AUTOMATIC INSERTION PER PART CI = 0.06 * DI = 0.05 CENTS

OPERATION COST = 0.16 CENTS

```

Figure 13

ACKNOWLEDGMENTS

The work described in this article has been supported by NSF Grants CME 80-06687 and MEA 83-00158 and also by the IBM Corporation Contract "Optimal Design for Robotic Assembly" at the University of Michigan. This support is gratefully acknowledged. The program ACCME was developed by S. Azarm, the production rules program by H.L. Li and the assembly consultant program by M. Jakiela with the aid of A.G. Ulsoy.

REFERENCES

1. Azarm, S.; Papalambros, P.: A Case for a Knowledge-Based Active Set Strategy. ASME Paper No. 83-DET-38, September 1983.
2. Azarm, S.; Papalambros, P.: An Automated Procedure for Local Monotonicity Analysis. ASME Paper No. 83-DET-48, September 1983.
3. Azarm, S.: Local Monotonicity in Optimal Design. Ph.D. Dissertation, Dept of Mechanical Engineering and Applied Mechanics, The University of Michigan, Ann Arbor, 1984.
4. Boothroyd, G.; and Dewhurst, P.: Design for Assembly-A Designer's Handbook. The University of Massachusetts at Amherst, 1981.
5. Papalambros, P; Wilde, D.J.: Regional Monotonicity in Optimum Design. Trans. ASME, J. of Mechanical Design, Vol. 102, No. 3, 1980, pp. 497-500.

COMPUTER AIDED ANALYSIS AND OPTIMIZATION
OF
MECHANICAL SYSTEM DYNAMICS

E. J. Haug
Center for Computer Aided Design
The University of Iowa
Iowa City, Iowa

The field of mechanical system dynamics has traditionally been focused on rigid body linkages and machines that consist of a few interconnected bodies. Significant developments have occurred that allow expansion of the capability in computer aided analysis of mechanisms and machines. A two week Advanced Study Institute, sponsored by NATO, NSF, and the Army Research Office in August 1983, focused on this area. Presentations by leaders in the field from North America and Europe highlighted gains that are bringing the technology of machine dynamics closer to the status of better developed fields such as finite element structural analysis.

The purpose of this paper is to outline a computational approach to spatial dynamics of mechanical systems that substantially enlarges the scope of consideration to include flexible bodies, feedback control, hydraulics, and related interdisciplinary effects. Design sensitivity analysis and optimization is the ultimate goal. The approach to computer generation and solution of the system dynamic equations and graphical methods for creating animations as output is outlined in this paper, with references given for more detail.

DYNAMICS OF LARGE SCALE, CONSTRAINED, MECHANICAL SYSTEMS

- * SPATIAL DYNAMICS OF RIGID AND FLEXIBLE BODY SYSTEMS
- * INTERDISCIPLINARY EFFECTS (CONTROLS, HYDRAULICS, IMPACT,...)
- * COMPUTER GENERATION AND SOLUTION OF EQUATIONS OF MOTION
- * ANIMATED GRAPHICS OUTPUT
- * DESIGN SENSITIVITY ANALYSIS

A building block approach is employed to allow for a general formulation and creation of a modular code to which new capabilities and special purpose models can be attached as they are developed and needed. The basic building blocks available to the user are bodies (either rigid or flexible) that represent individual components within the system, a library of kinematic joints that connect components in the system, force elements that can be used to represent the effect of nonlinear springs, dampers, and actuators, and complete interdisciplinary modules that may represent subsystems, control systems, or hydraulic subsystems.

Once the user has specified the structure of the system and its innerconnection using standard components, the equations of motion are automatically formulated and integrated to predict dynamic performance of the system. Graphic computation of hidden line removal is then carried out to create display instructions that are presented at a higher frame rate, creating an animated graphic output.

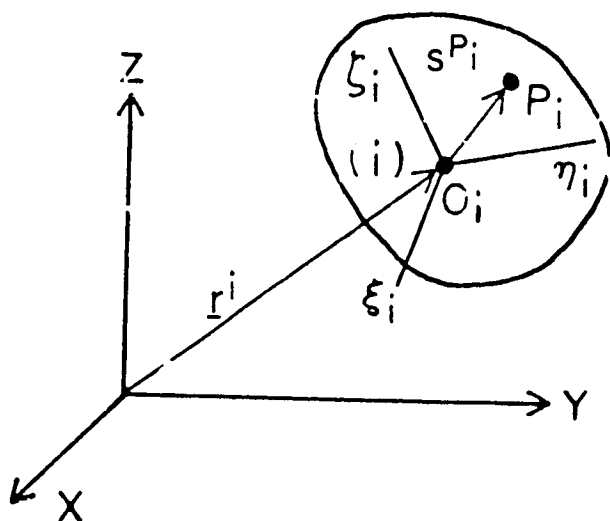
BUILDING BLOCKS

- * BODIES
- * KINEMATIC JOINTS
- * SPRING-DAMPER-ACTUATORS

Individual bodies used in modelling a mechanical system are located in a global XYZ coordinate system, using Cartesian coordinates of the origin of a body fixed ξ - η - ζ coordinate system and Euler parameters [1] to orient the body. The ξ - η - ζ coordinate system may be viewed as the front, side, and top views of the component on a drafting board. Special points that are needed to locate joints between bodies and points of force application are defined in the natural drafting board coordinates system.

Modal deformation coordinates, including both vibration modes and static correction modes that are calculated with standard finite element computer programs, are employed to represent elastic deformation of the body [2].

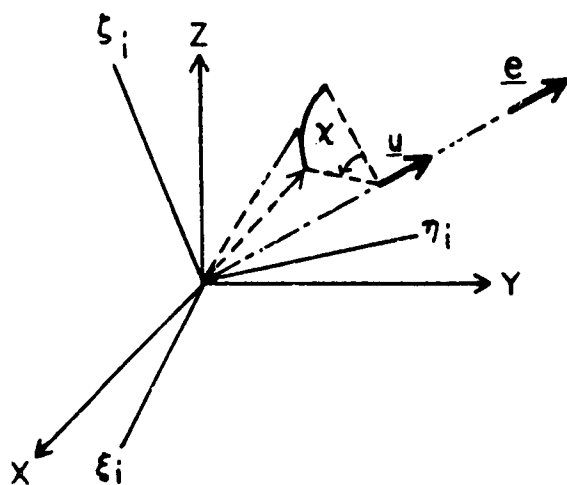
INDIVIDUAL BODY



- * EULER PARAMETER
ORIENTATION COORDINATES
- * MODAL DEFORMATION
COORDINATES
 - vibration modes
 - static correction modes

The method used in the DADS formulation for orienting bodies in space employs Euler parameter generalized coordinates that have been used extensively in astronomy to overcome essential singularity characteristics that are associated with more conventional orientation variables such as Euler angles [1]. Euler's theorem states that if a pair of coordinate systems have their origin in common, then there exists a unit vector \underline{u} about which one coordinate system can be rotated by an angle χ to bring it into coincidence with the other coordinate system. Defining the vector \underline{e} to be the unit vector \underline{u} times the sine of half the angle of rotation and a scalar variable e_0 to be the cosine of half that angle, one can define a four-vector \underline{p} of Euler parameters the sum of the squares of whose components is one, to uniquely orient a coordinate system in space. The mathematical properties of Euler parameters are discussed in Ref. 1.

EULER PARAMETERS



$$\underline{e} \equiv \underline{u} \sin \frac{\chi}{2}$$

$$e_0 \equiv \cos \frac{\chi}{2}$$

$$\underline{p} = [e_0, e_1, e_2, e_3]^T$$

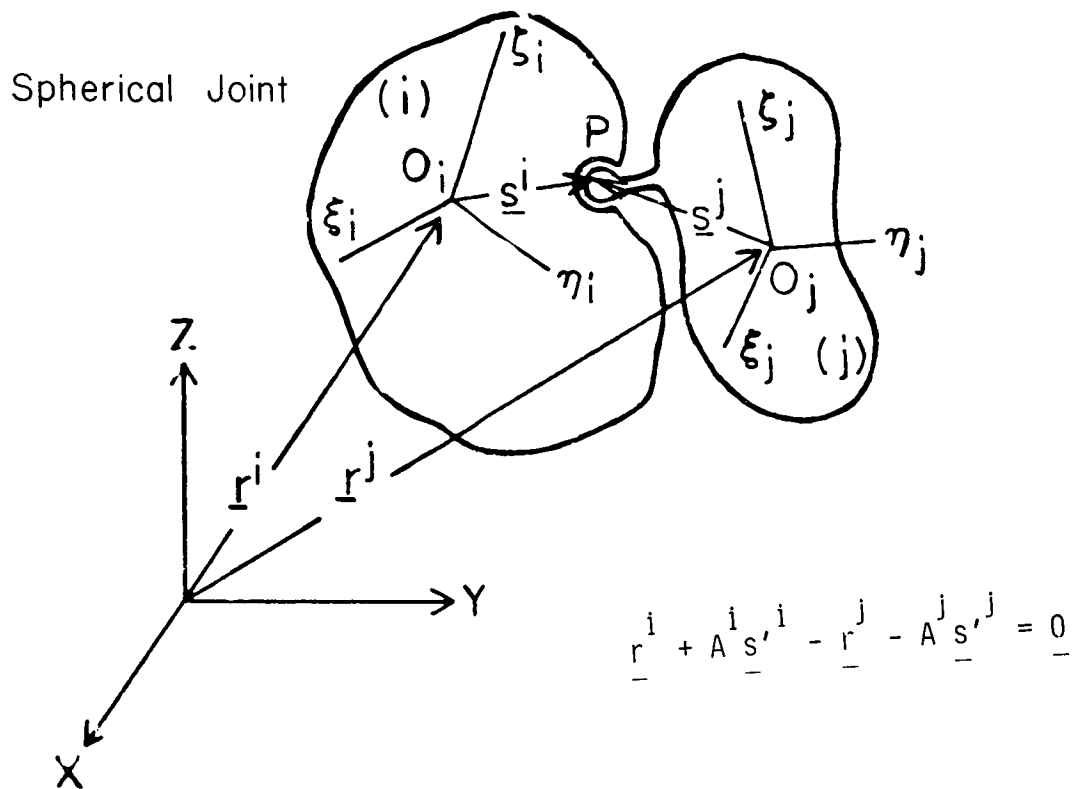
$$e_0^2 + e_1^2 + e_2^2 + e_3^2 = 1$$

A library of kinematic joints is provided to allow the engineer to connect mechanical components of the system. The library of standard joints listed on the left contains the most common kinematic connections between mechanical components that are used in mechanical design. In addition to the standard joint types, composite joints are used to represent bodies with small mass and higher pair joints are admitted.

KINEMATIC JOINTS

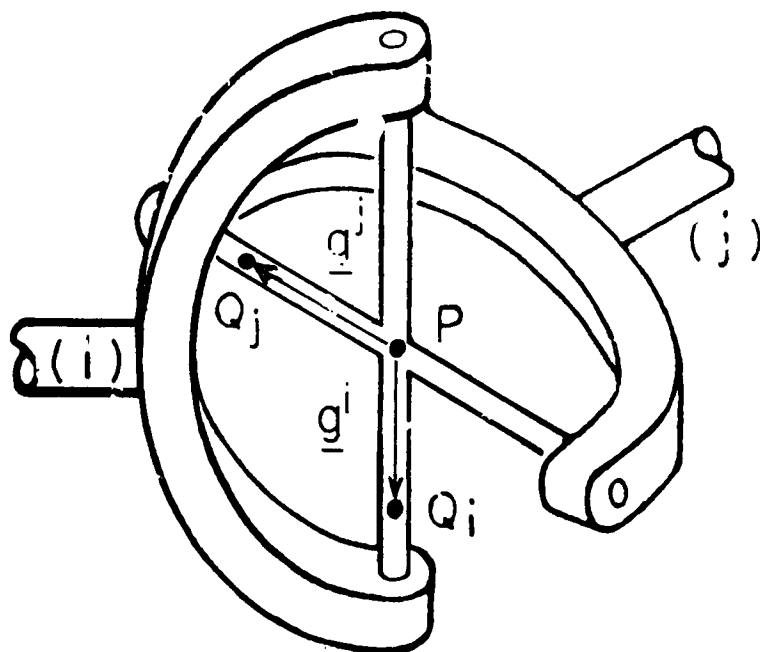
| | |
|---------------|------------------------|
| SPHERICAL | COMPOSITE |
| UNIVERSAL | SPHERICAL-SPHERICAL |
| REVOLUTE | REVOLUTE-REVOLUTE |
| TRANSLATIONAL | REVOLUTE-TRANSLATIONAL |
| CYLINDRICAL | CAM |
| SCREW | SLOT |
| | GEAR |

To illustrate the approach for user definition of kinematic joints, consider first the spherical (ball and socket) joint. The mathematical definition of a spherical joint is simply that the center of the ball on body j and the center of socket on body i must be in common. The vector equation that defines this condition is shown. Notice that this equation involves the generalized coordinates of each of the two bodies and the coordinates of vectors \underline{s}^i and \underline{s}^j that define the location of the joint on each of the two bodies in their undeformed drafting board coordinate system. Thus, the user must supply only the designation of the pair of bodies connected and the three coordinates of the attachment point on each of the bodies. The DADS code automatically constructs the equations of constraint [3].



As a second example, the universal joint shown is specified by constructing the spherical equations for point P, which is common to both of the bodies, and writing the condition that the vectors \underline{g}^i and \underline{g}^j are orthogonal; i.e., their scalar product is zero. To specify a universal joint, the user is required only to locate the center of the cross (point P) on each of the two bodies that are connected and a second point on the cross on each of the two bodies.

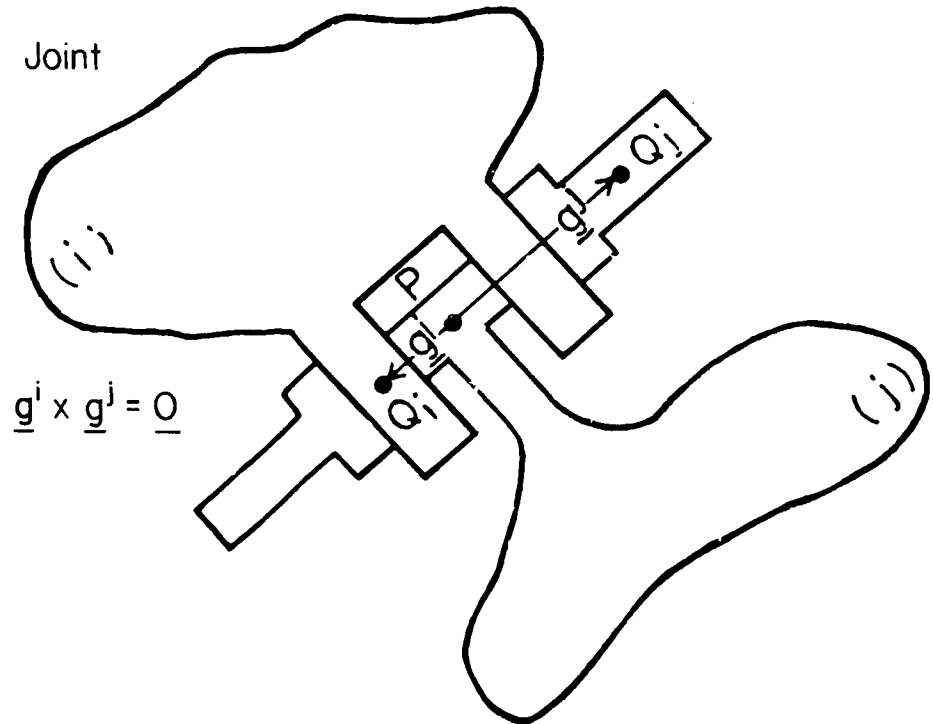
UNIVERSAL JOINT



$$\underline{g}^i \cdot \underline{g}^j = 0$$

A third kinematic joint that is commonly used in machines is the rotational or revolute joint, which allows rotation about a specified axis on each of two bodies, but no relative translation along that common line. To specify this joint, a point P at the center of the bearing must be common to the two bodies, hence it must satisfy the spherical joint equations. In addition, vectors \underline{g}^i and \underline{g}^j on each of the two bodies, which are to coincide with the axis of relative rotation, must remain parallel; i.e., their vector product must be zero.

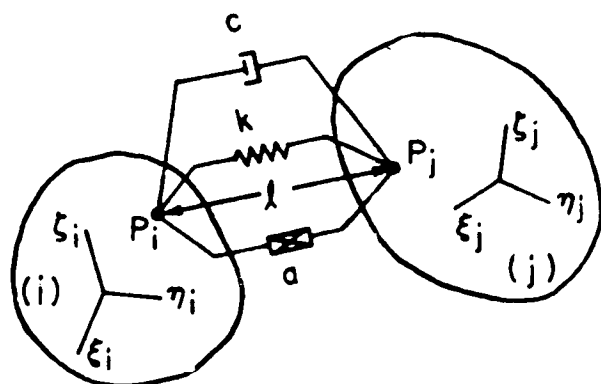
Revolute Joint



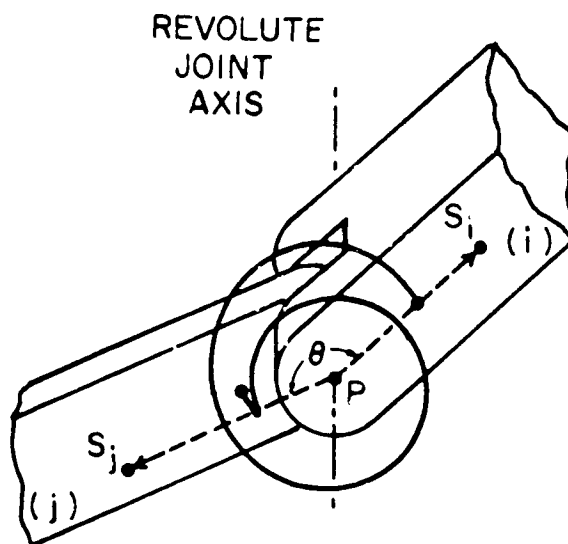
Having defined the kinematics of a mechanical system, it remains to prescribe forces acting on the system. Externally applied forces are defined by their point of application and direction and are automatically included in the system generalized force. Two force elements that are commonly applied between bodies are shown here. The translational spring-damper-actuator is a general nonlinear force element that applies equal and opposite forces on attachment points P_i and P_j , along the line between these two points. The damping coefficient c , spring rate k , and actuator force a may be specified as nonlinear functions of \dot{l} or \dot{l} , specified by input data.

Similarly, a torsional spring-damper-actuator is allowed around each revolute joint, providing torque action and reaction on the connected bodies.

TRANSLATIONAL SPRING-DAMPER-ACTUATOR



ROTATIONAL SPRING-DAMPER-ACTUATOR



Having specified all the kinematic joints, a nonlinear system of algebraic constraint equations is automatically assembled [3]. Similarly, once the mass m^i and matrix of moments and products of inertia I^i are specified for the i th body, the equations of motion are automatically assembled and constraints are accounted for using the Lagrange multiplier λ . The result is a mixed system of differential and algebraic equations of motion.

A generalized coordinate partitioning algorithm [4,5] is used to automatically identify an independent set of generalized coordinates and a standard numerical integration algorithm is employed to systematically solve the system of equations.

DIFFERENTIAL-ALGEBRAIC EQUATIONS OF MOTION

Composite algebraic constraint equations

$$\Phi(\underline{r}^1, \underline{p}^1, \underline{r}^2, \underline{p}^2, \dots, \underline{r}^n, \underline{p}^n) = 0$$

Differential equations of motion

$$m^i \ddot{\underline{r}}^i + \Phi_{\underline{r}}^T \lambda = \underline{f}^i$$

$$4B^i \dot{\underline{I}}^i \dot{\underline{B}}^i \dot{\underline{p}}^i + \Phi_{\underline{p}}^T \lambda = \underline{b}^i + 8B^i \dot{\underline{I}}^i \dot{\underline{B}}^i \dot{\underline{p}}^i$$

Interdisciplinary effects are treated in the formulation using the same approach as outlined for defining characteristics of mechanical components. Flexible bodies are represented by vibration and static correction mode deformation coordinates [2]. Preprocessing with a finite element code is employed to create the reduced mass and stiffness characteristics of each flexible body, which are subsequently read into the DADS code to characterize deformation and its full nonlinear coupling with the gross motion variables.

Feedback control and hydraulic subsystems [6,7] are modelled using a library of components that are defined in a state input-force output module whose governing equations are fully coupled with the dynamic system equations.

Intermittent motion is defined through an impact event in which generalized momentum balance is used to prescribe velocity discontinuity due to impact and continues the integration [8].

INTERDISCIPLINARY EFFECTS

* FEEDBACK CONTROL AND HYDRAULICS

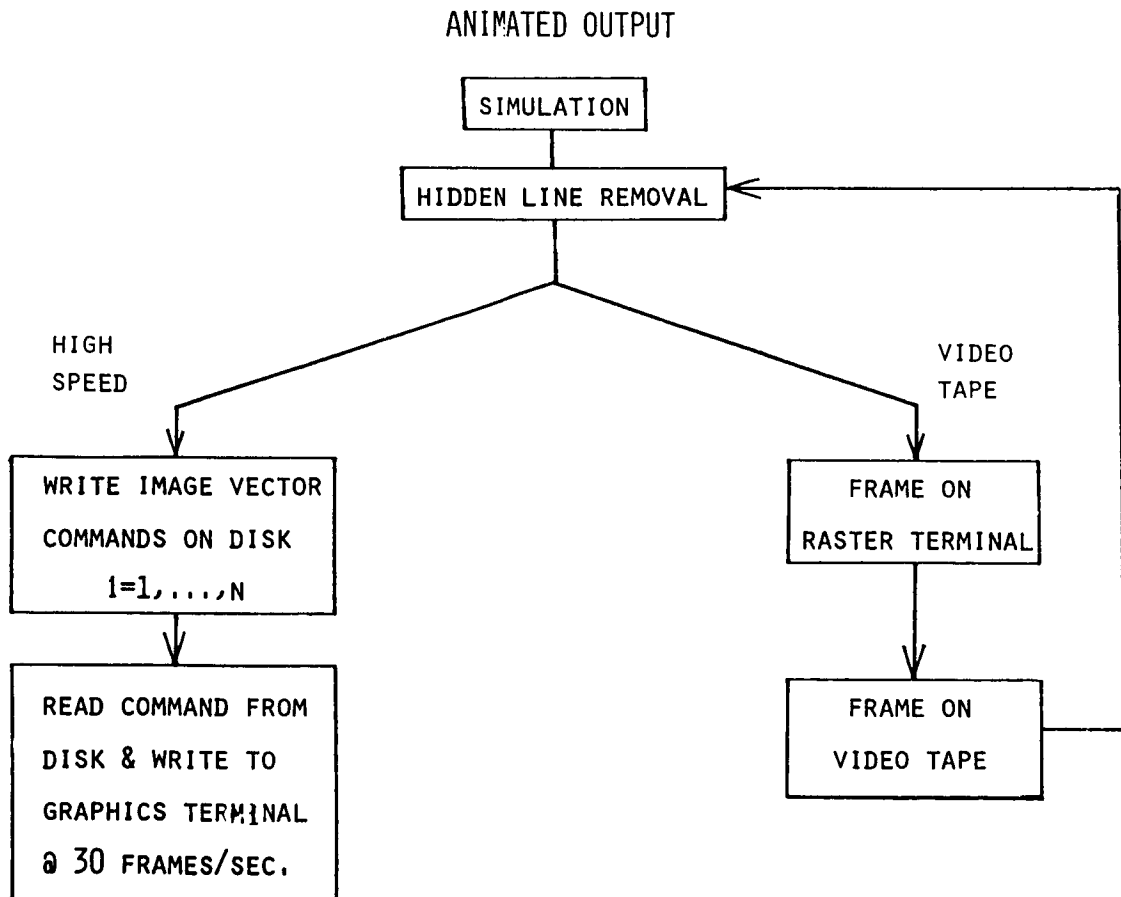
- ' library of components
- ' state variable input
- ' force output
- ' fully coupled

* INTERMITTENT MOTION

- ' impact event times
- ' generalized momentum balance
- ' velocity discontinuity

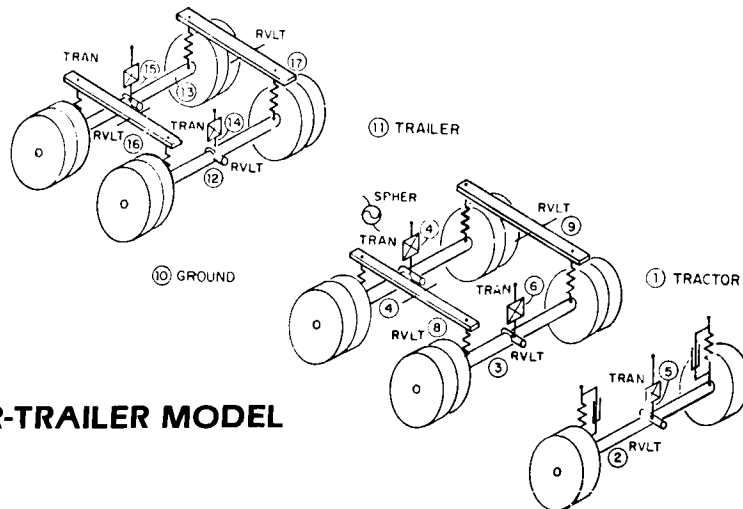
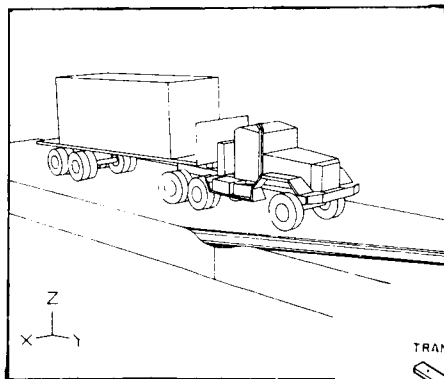
The output of large scale dynamic simulation is the position and orientation of each body in the system and the forces acting in the system. In order to visualize the results of such a prediction, standard graphics software is used to construct the graphic image of the system, with all hidden lines removed [9]. In one mode of display, these images are stored on a disk and, when complete, read from the disk and transmitted to a high speed graphics terminal to yield 30 frames per second of animated output.

An alternative and less expensive mode of operation is to use a video tape deck controller to transmit each frame to video tape as it is generated, allowing the engineer to play the tape back and view the output of his simulation at his leisure.



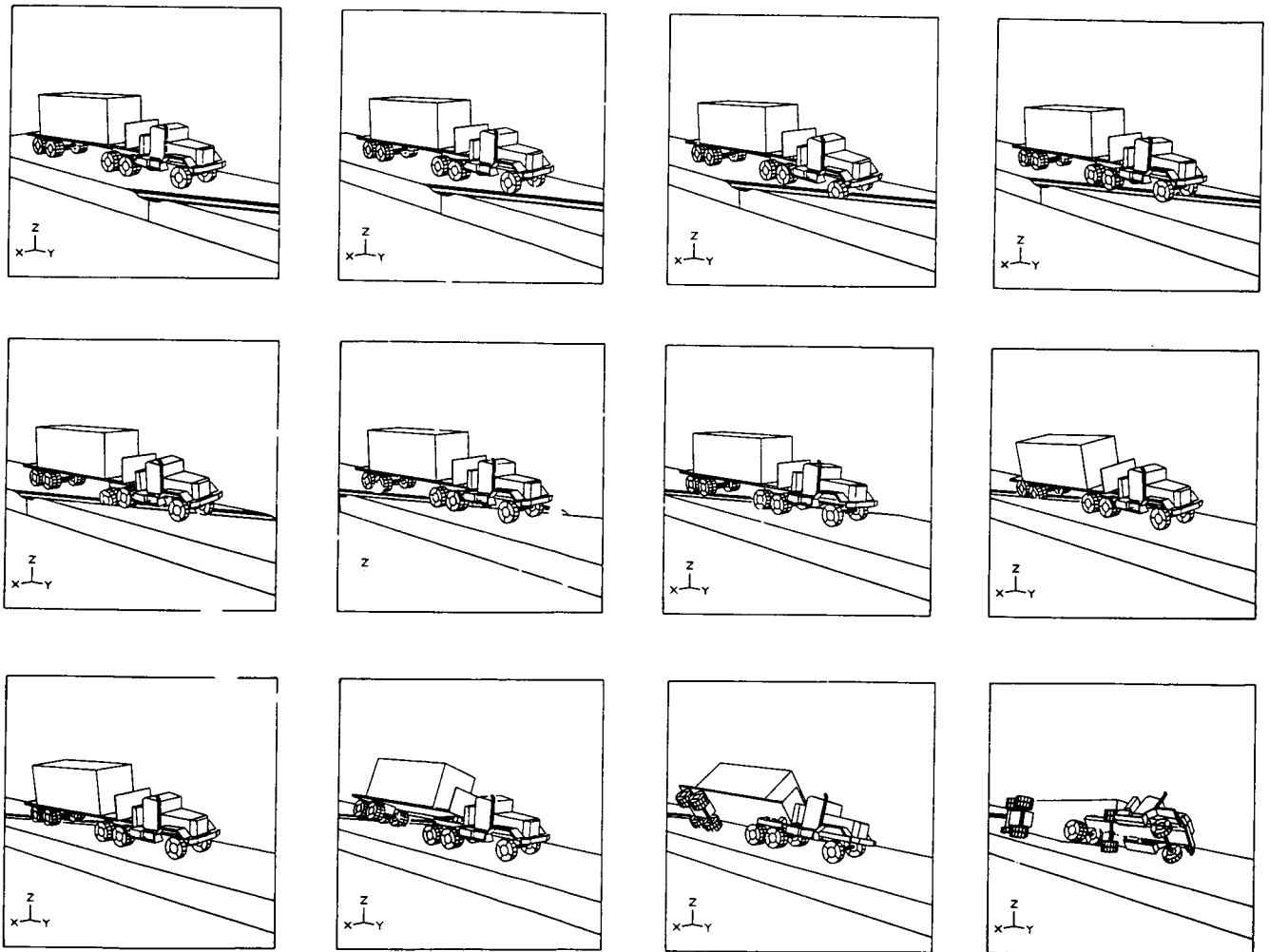
As a large-scale example of use of the software, a tractor-trailer vehicle with load-leveling tandem axles was modelled and propelled along a road with an angled ditch that served to induce roll dynamics. As indicated schematically, the kinematics of vehicle and axle movement was modelled using spherical, revolute, and translational joints. Translational spring-dampers were used to represent flexibility and damping characteristics of suspension springs and shock absorbers. Hysteresis loops were included in the springs to account for substantial friction losses that occur in heavy leaf springs of vehicles.

MODELING WITH DADS

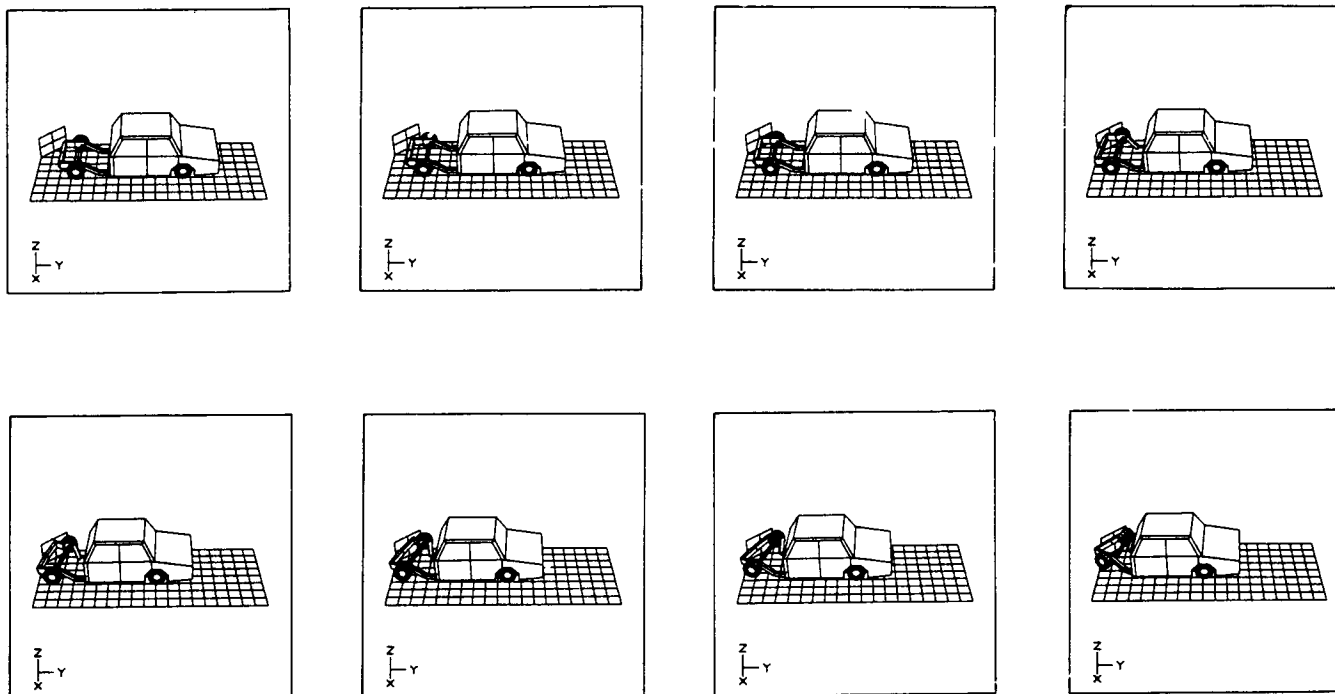


TRACTOR-TRAILER MODEL

The sequence of snapshots shown illustrates the prediction of position of the vehicle during various phases of crossing the ditch. In this case, a severe roll motion of the trailer is predicted, which cannot be compensated for by the suspension of the tractor. The alternative to graphics is digital printout, which locates all the bodies in space. This is clearly not as attractive as the graphics display of predictions. With graphics, and in fact animation at 30 frames per second, the analyst can obtain a clear physical understanding of how the vehicle performs and perhaps why difficulties arise.



A second example, illustrated in the figure, involves the prediction of structural collapse [10] during automobile impact with an obstacle. Collapse of the structure is modelled, employing the DADS code to represent kinematics of the collapse mechanism and plastic hinge data to represent structural collapse characteristics. As indicated by the sequence of snapshots, the nature of collapse of the structure during an oblique impact is predicted in a form that assists in visualization of the collapse mechanism. The code also predicts acceleration of the passenger compartment, which provides information on severity of the crash event on passengers.



Design sensitivity analysis has been implemented in the DADS software [11] to predict the change in state due to a change in design parameters, denoted here as a vector b . The governing equations for design sensitivity are derived by direct differentiation of the system constraint equations and equations of motion to obtain the matrix equations for derivatives of dynamic response with respect to design. These equations are integrated to calculate the derivative of state with respect to design, which is then made available for predicting the effect of a design perturbation on dynamic performance. Note that both the equations of motion and the direct sensitivity equations are integrated forward in time, comprising a rather large system of equations that are automatically integrated by the code.

DIRECT DESIGN SENSITIVITY

Equations of Motion

$$\Phi(q) = 0$$

$$M\ddot{q} + \Phi_q^T \lambda = Q + R$$

$$q_b = \left[\frac{\partial q_i}{\partial b_j} \right]$$

Direct Sensitivity Equations;

$$\Phi_q q_b + \Phi_b = 0$$

$$M\ddot{q}_b + (\Phi_q^T \lambda)_b q_b - Q_q q_b - R_q q_b \dots = Q_b + \dots$$

An alternate method of design sensitivity analysis [11] with attractive efficiency characteristics has been implemented using an adjoint variable technique that was borrowed from the control and structural fields. Using this technique, a set of adjoint equations, shown at the bottom of the chart, are integrated backward in time after the dynamic simulation is completed. Upon completion of this integration, the derivative of a general response measure is calculated, as shown by the last equation on the chart. This method has the attractive feature that only two integrations are required to obtain sensitivity results. It does, however, require that dynamic information predicted during the forward sweep be stored and recalled for use in forming and integrating the adjoint equations backward in time.

ADJOINT DESIGN SENSITIVITY

Response Measure

$$\psi = g(q(\tau), \dot{q}(\tau), b) + \int_0^\tau f(q, \dot{q}, \lambda, b) dt$$

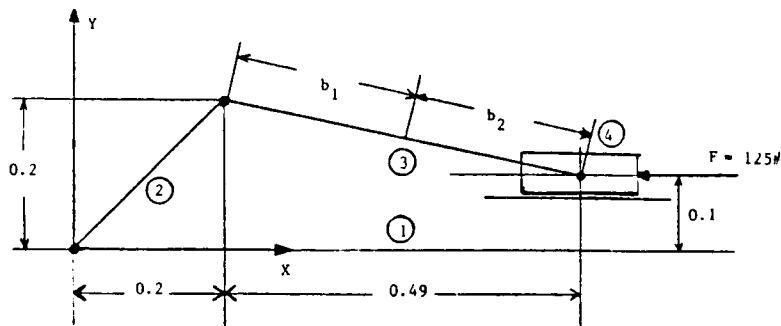
Adjoint Equations $(0 \xleftarrow{\text{integ.}} \tau)$

$$\phi_q^\mu = f_\lambda^T$$

$$M_\mu'' + \phi_q^T v + \dots = f_q^T + \dots$$

$$\frac{d\psi}{db} = g_b + \int_0^\tau [f_b + \mu^T Q_b + \dots]$$

As a simple illustration of design sensitivity analysis, the slider-crank mechanism shown was analyzed with dimensions b_1 and b_2 of the coupler link as design variables. The graph shown at the bottom of the chart plots the predicted variation in acceleration of the slider and the change in acceleration that was obtained by perturbing the design and reanalyzing. As indicated, the sensitivity prediction and reanalysis result coincide, indicating that accurate design sensitivity can be achieved. A functional ψ_0 shown on the chart was used to calculate performance design sensitivity associated with these design parameters. As indicated, the change due to perturbation and change predicted by design sensitivity agree to the third place of numerical accuracy. Design sensitivity results of this kind have been used in design optimization [11] to indicate feasibility of use of this formulation of the equations of dynamics and design sensitivity in performance optimization.

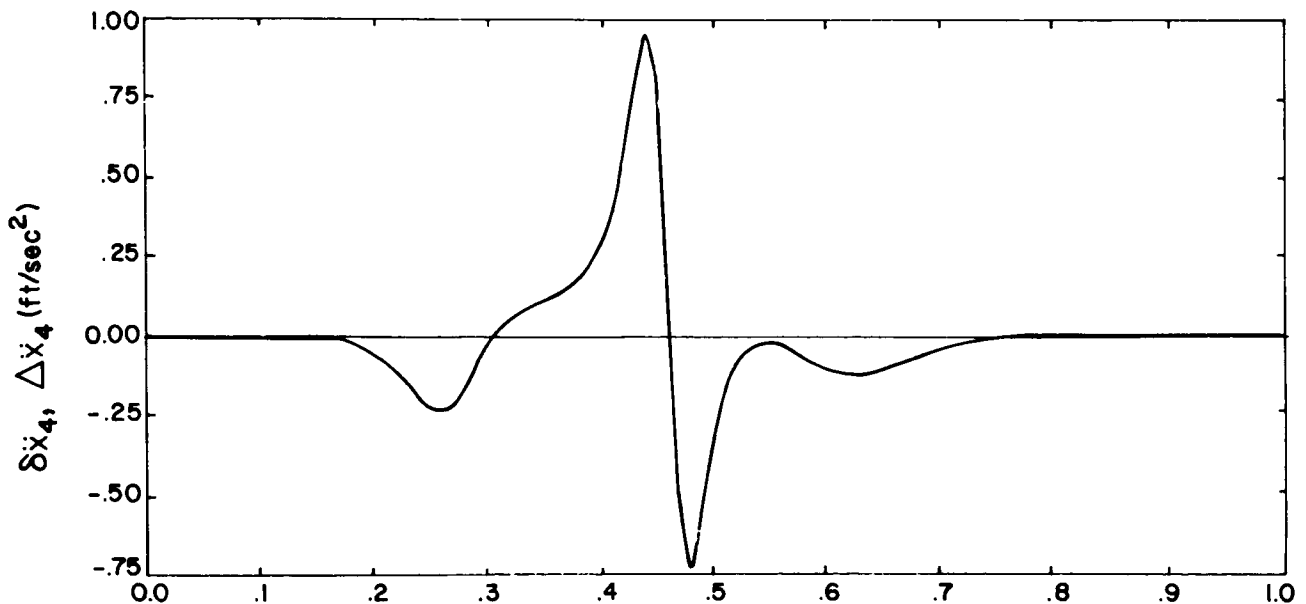


$$b = [-0.25, 0.25]^T$$

$$\delta b = [-1, 1]^T \times 10^{-3}$$

$$\psi_0 = \int_0^1 (x_4 - 20)^2 dt$$

$$\Delta \psi_0 = -0.0184, \delta \psi_0 = -0.0812$$



REFERENCES

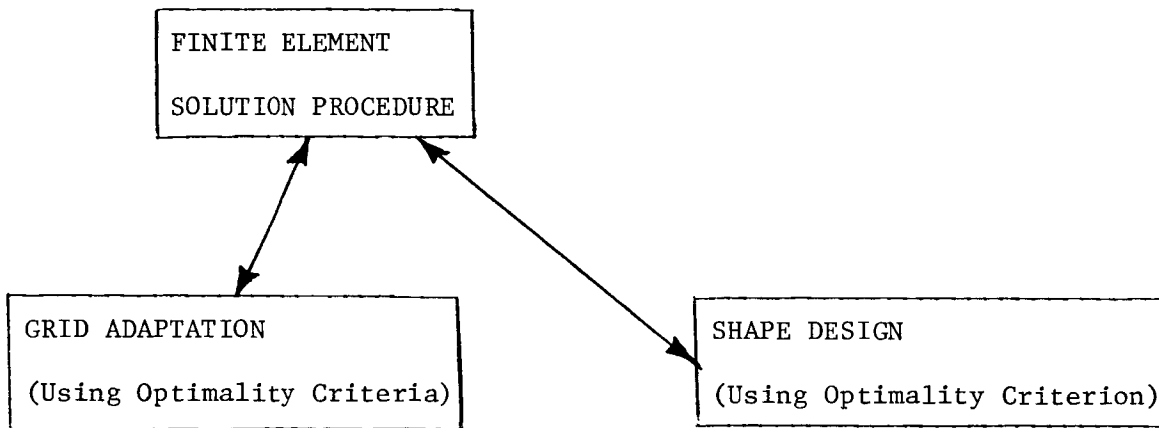
1. Wittenburg, J., Dynamics of Systems of Rigid Bodies, Teubner, Stuttgart, 1977.
2. Yoo, W. S. and Haug, E. J., "Large Displacement Dynamics of Machines with Flexible Components," Journal of Structural Mechanics, to appear, 1984.
3. Haug, E. J., Nikravesh, P. E., Sohoni, V. N., and Wehage, R. A., "Computer Aided Analysis of Large-scale, Constrained, Mechanical Systems," Proceedings, Fourth International Symposium on Large Engineering Systems, Calgary, Alberta, Canada, June 1982.
4. Wehage, R. A. and Haug, E. J., "Generalized Coordinate Partitioning for Dimension Reduction in Analysis of Constrained Dynamic Systems," Journal of Mechanical Design, Vol. 104, No. 1, 1982.
5. Mani, N. K. and Haug, E. J., Singular Value Decomposition for Analysis and Optimization of Mechanical System Dynamics, Technical Report, Center for Computer Aided Design, The University of Iowa, July 1984.
6. Vanderploeg, M. and Lance, G. M., "Controlled Dynamic System Modelling," Computer Aided Analysis and Optimization of Mechanical System Dynamics, (ed. E. J. Haug), Springer Verlag, Heidelberg, 1984.
7. Lance, G. M., Liang, C. G., McCleary, M. A., and Mousseau, C. W., Simulation of Integrated Vehicular Systems, Part I, Technical Report, Center for Computer Aided Design, The University of Iowa, January 1984.
8. Wehage, R. A. and Haug, E. J., "Dynamic Analysis of Mechanical Systems with Intermittent Motion," Journal of Mechanical Design, Vol. 104, No. 3, 1982.
9. Nikravesh, P. E., "Application of Animated Graphics in Large Scale Mechanical System Dynamics," Computer Aided Analysis and Optimization of Mechanical System Dynamics (ed. E. J. Haug), Springer Verlag, Heidelberg, 1984.
10. Nikravesh, P. E. and Chung, I. S., "Structural Collapse and Vehicular Crash Simulation Using a Plastic Hinge Technique," Journal of Structural Mechanics, Vol. 12, No. 3, 1984.
11. Haug, E. J., Mani, N. K., and Krishnaswami, P., "Design Sensitivity Analysis and Optimization of Dynamically Driven Systems," Computer Aided Analysis and Optimization of Mechanical System Dynamics (ed. E. J. Haug), Springer Verlag, Heidelberg, 1984.

SHAPE OPTIMIZATION
INCLUDING FINITE ELEMENT GRID ADAPTATION

Noboru Kikuchi
and
J. E. Taylor
The University of Michigan
Ann Arbor, MI

OBJECTIVES

The prediction of optimal shape design for structures depends on having a sufficient level of precision in the computation of structural response. These requirements become critical in situations where the region to be designed includes stress concentrations or unilateral contact surfaces, for example. In the approach to shape optimization discussed in this paper, a means to obtain grid adaptation is incorporated into the finite element procedures. This facility makes it possible to maintain a level of quality in the computational estimate of response that is surely adequate for the shape design problem.



A SHAPE OPTIMIZATION PROBLEM

We consider the design of a plane, elastic disc for minimum volumes, as indicated in the figure. Traction and displacements are prescribed over respective portions of the boundary. The shape design is expressed by function $R(\theta)$ over the specified interval $A < \theta < B$. The von Mises equivalent stress $\bar{\sigma}$ must satisfy the performance constraint $\bar{\sigma} \leq \bar{\sigma}_{\max}$ on the design boundary; $\bar{\sigma}_{\max}$ is a given bound value. The domain of the disc is taken to be simply connected, and a ray from the origin intersects the boundary only once (i.e., the domain is star-shaped). We note that $\bar{\sigma}$ may exceed $\bar{\sigma}_{\max}$ on the boundary outside the design interval or in the domain of the disc.

MIN VOLUME

SUBJECT TO

- * EQUIL. EQUATIONS
- * BOUNDARY CONDITIONS
- * LOCAL CRITERION

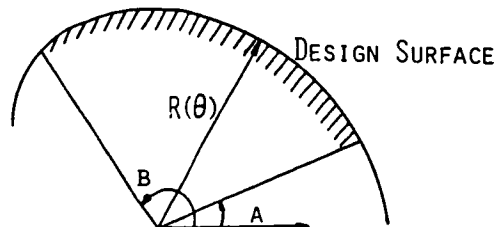
$$\bar{\sigma} \leq \bar{\sigma}_{\max} \quad \text{IN } A \leq \theta \leq B$$

$$\text{VOLUME} = (\text{CONSTANT THICKNESS}) * (\text{AREA})$$

$$\text{AREA} = \int_A^B \int_0^{R(\theta)} r \, dr \, d\theta + A_0$$

$$\text{DOMAIN} = \text{SINGLY CONNECTED AND STAR SHAPED}$$

$$R(\theta) = \text{THE DESIGN VARIABLE ON AN INTERVAL } (A, B)$$



OPTIMALITY CRITERION FOR SHAPE DESIGN

A variational interpretation of the nonlinear programming problem (*) leads to the necessary conditions:

$$\lambda \geq 0; \quad \bar{\sigma}(R(\theta), \theta) - \bar{\sigma}_{\max} \leq 0; \quad \lambda [\bar{\sigma}(R(\theta), \theta) - \bar{\sigma}_{\max}] = 0$$

$$\int_a^b R \delta R d\theta - \int_a^b \lambda \hat{\delta \bar{\sigma}}|_{r=R(\theta)} d\theta = 0$$

Here $\hat{\delta \bar{\sigma}}$ symbolizes the variation of $\bar{\sigma}$ with respect to R within the requirements of the equilibrium boundary value problem statement. An interpretation of these equations provides that $\lambda \neq 0$ and $\bar{\sigma} = \bar{\sigma}_{\max}$ along the design boundary for the optimal shape. This suggests an iterative approach for the determination of optimal design $R(\theta)$ according to the relationship:

$$R^{(K+1)} = R^{(K)} - \mu \frac{\Delta R_{\max}}{\bar{\sigma}_{\max}} (\bar{\sigma}^{(K)} - \bar{\sigma}_{\max})$$

Superscript K represents iterate number, ΔR_{\max} equals the 'maximum design change' per iterate step, and μ is a normalization scale factor with magnitude on the order of unity.

FINITE ELEMENT GRID ADAPTATION

The grid adaptation is formulated as an optimal design problem in the form: minimize the maximum value of local error by relocating nodal points of an initially specified finite element grid. With node position identified by x_α the problem is stated:

$$\min_{x_\alpha} \left\{ \max_{e=1,2,\dots,E} (E_e^h) \right\}$$

where E_e^h represents the (nonnegative) measure of error for the e^{th} element, and E equals the number of elements in the grid. The choice of error measure may be tailored according to the ultimate purpose of performing finite element computations.

Within the broad context of techniques for achieving higher precision in finite element computation, one might consider a systematic increase in the number of degrees of freedom, either by increasing the number of elements (h-method), or by increasing the degree of polynomial shape functions (p-method). In contrast, for the grid adaptation problem defined here the number of degrees of freedom is held fixed. In a broader treatment of the grid adaptation problem, one might consider methods for simultaneous adjustment of element shape function, number of elements, and grid configuration.

OPTIMALITY CONDITION

$$E_e^h = \text{CONSTANT}, \quad e=1,2,\dots,E$$

MEASURE OF LOCAL ERROR

To help explain the definition of error indicator E^h for the grid adaptation problem, we consider as an example problem the simple interpolation using a piecewise linear polynomial for function $f(x)$ in the interval (a,b) . Let the interval be decomposed into segments

$$\Omega_e = (x_e, x_{E+1}), \quad e=1,2,\dots,E, \quad x_1=a$$

and $x_E=b$. Then the following relationship between interpolant $f_I(x)$ and the function $f(x)$ holds:

$$\max_{x \in \Omega_e} |f(x) - f_I(x)| \leq h_e \max_{x \in \Omega_e} |df/dx|$$

In other words, the interpolation error in element Ω_e is bounded by the product of element size h_e and the maximum absolute value in Ω_e of the derivative df/dx . Following this idea, the error indicator E^h for the finite element mesh is defined as the maximum of the difference between the value $\bar{\sigma}^h$ of computed equivalent stress in Ω_e and the values $\bar{\sigma}^h_{em}$ for elements adjacent to Ω_e (see Figure below).

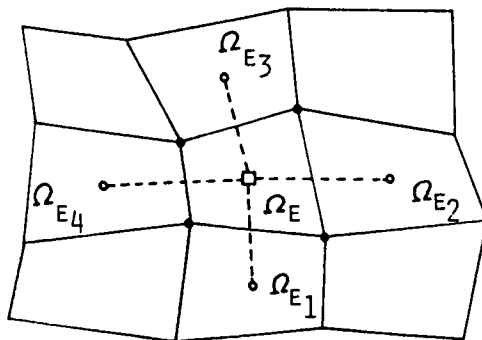
ERROR INDICATORS

$$E^h_E = \max_{M=1,\dots,M_E} \left| \bar{\sigma}^h_{E_M} - \bar{\sigma}^h_E \right|$$

$\bar{\sigma}^h_E$ = THE EQUIVALENT STRESS OF Ω_E

$\bar{\sigma}^h_{E_M}$ = THE EQUIVALENT STRESS OF Ω_{E_M}

M_E = THE TOTAL NUMBER OF ADJACENT ELEMENTS



RELOCATION METHODS

There are infinitely many ways to relocate nodes. Here we shall use the scheme described below. The idea of the relocation scheme is that if the value of error indicator is large, the size of the element must be reduced. Although the relocation scheme tends not to provide nonconvex four-node elements, it is possible to generate non-convex elements. Thus, at each step of node relocation process, we have to check whether or not non-convex elements are generated. It is also noted that the nodes on the outside boundary do not have complete freedom to be relocated, since these nodes must lie on the specified boundary.

In order to determine whether or not the new location of nodes improves quality of approximations, the quantity QI is introduced, which is the ratio of the maximum value vs. the average value of error indicators. If QI is close to the value of unity, the grid is close to the optimum. Similarly, if the quantities QI_e , $e=1, \dots, E$, are defined as the ratio of the maximum value of error indicators vs. error indicator E_e in each finite element, the portion where the approximation is "poor" can be easily identified. Indeed, if QI_e is large, then the quality of the computational result for the e^{th} element is poor. On the other hand, if QI_e is close to the value of unity, the quality of the e^{th} element is, relatively speaking, good.

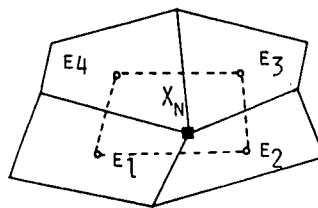
NODE RELOCATION METHODS

$$\bar{X}_N = \frac{\sum_{i=1}^{E_N} \bar{X}_{N_i} (E_{E_i}^H / A_{E_i})}{\sum_{i=1}^{E_N} E_{E_i}^H / A_{E_i}}$$

$E_{E_i}^H$ = ERROR INDICATOR

A_{E_i} = AREA OF ELEMENT

\bar{X}_{N_i} = COORDINATES OF THE CENTROID



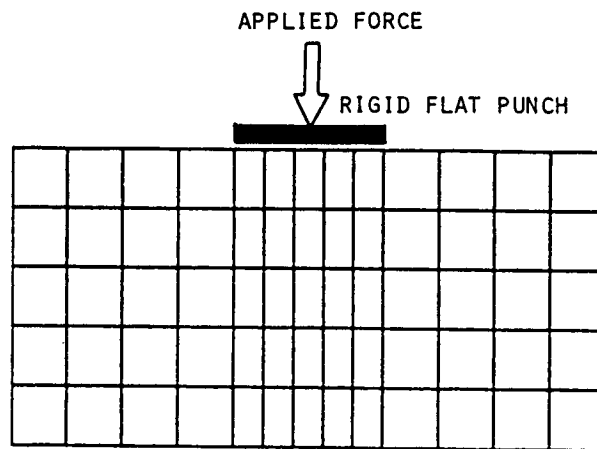
QUALITY INDEX

$$Q.I. = \text{MAX } E_E^H / E_{AV}^H$$

E_{AV}^H = THE AVERAGE ERROR INDICATOR

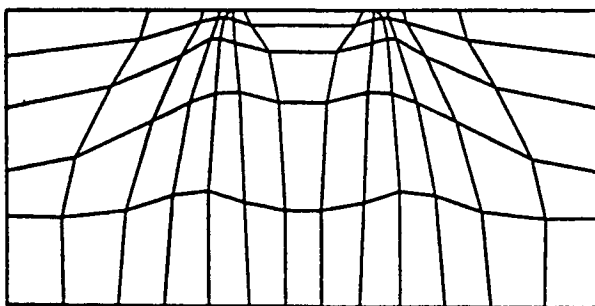
EXAMPLE-GRID OPTIMIZATION

The figure shows an example of application of the grid optimization. A thin linearly elastic plate is subject to both horizontal and downward vertical forces through a flat rigid punch. Because of the horizontal force, the stress distribution is not symmetric while the stress becomes infinity at both edges of a rigid punch. If a uniform grid is used to analyze this problem, singular behavior or of the stress cannot be simulated well. However, the grid optimization algorithm provides at least improved grids which are capable of simulating singular behavior rather realistically.



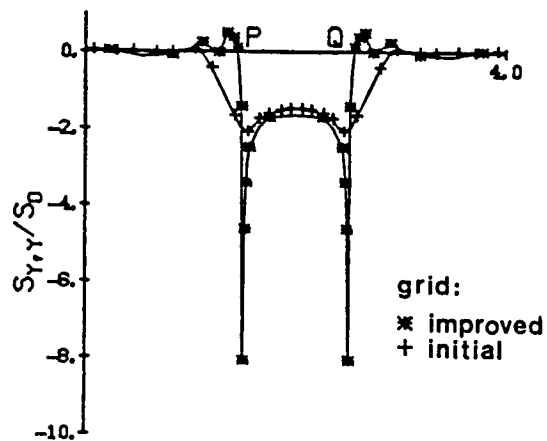
"UNIFORM" INITIAL GRID

* AFTER FOUR ITERATIONS



OPTIMAL GRID

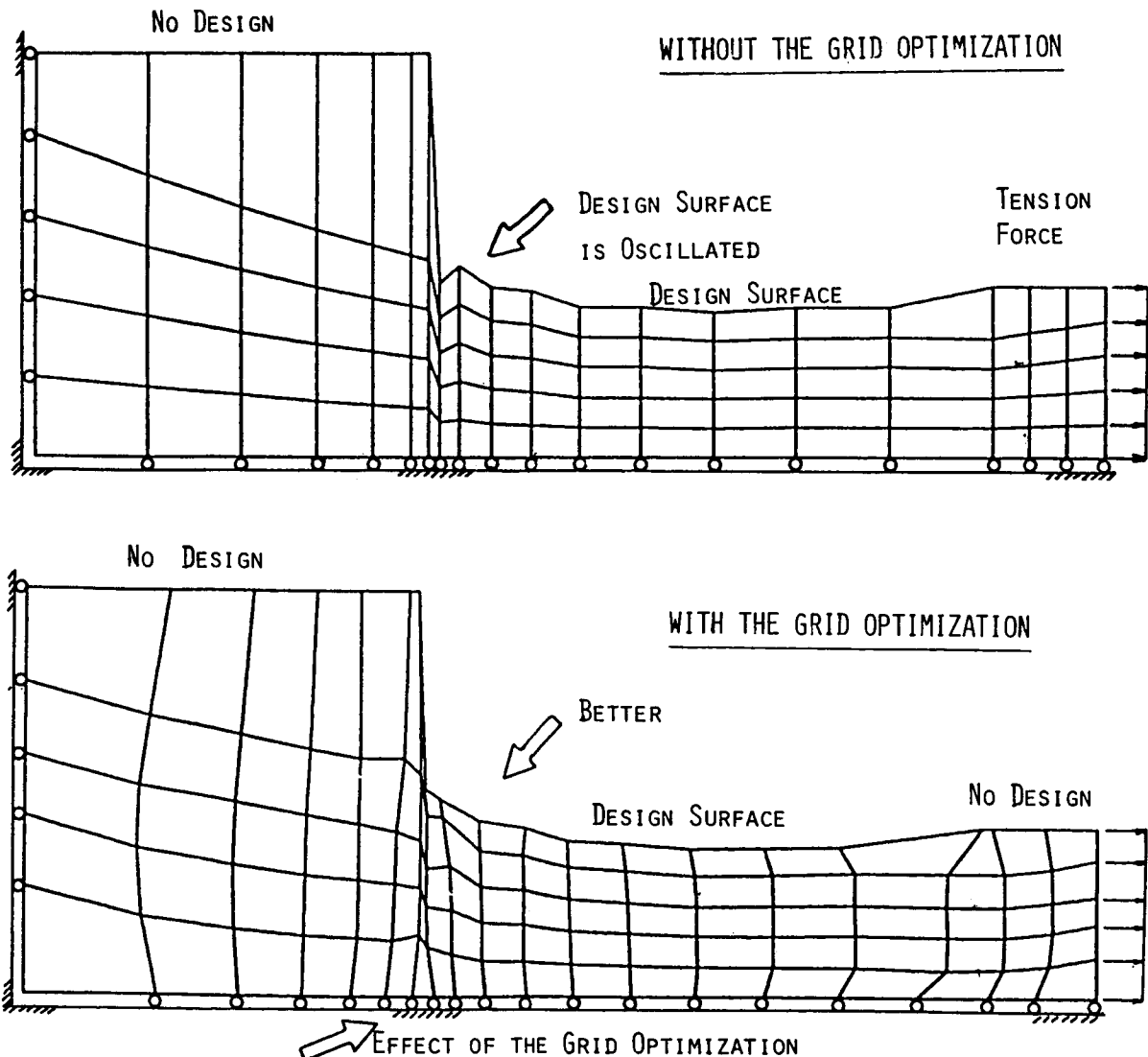
SINGULARITIES AT PUNCH EDGES ARE RECREATED BY THE OPTIMAL GRID



STRESS DISTRIBUTION IN
Y-DIRECTION

EXAMPLE-SHAPE OPTIMIZATION

The figure shows an application of both shape and grid optimization algorithms. It is an interesting observation that both shape and grid optimization problems possess a similar optimality criterion. Indeed, the "fully" stressed condition $\bar{\sigma}_e = \sigma_{\max}^e$ must be reached if any design restrictions are not imposed for shape optimization. On the other hand, the equal distribution of errors $E^h = \text{constant}$ must be realized at the optimal finite element grid. Both optimization problems thus have very similar nature, especially so far as numerical algorithms are concerned. Implementation is as follows. At the first several iterations of shape optimization we would not apply any grid optimization algorithm, since the design change is substantial at the beginning stage of the shape design iteration process, using the optimality criterion method. After the design change becomes moderate, the grid design by relocation of nodes becomes active. Since the design change is small, grid modification should not have too large an effect on the shape design. Examples show that this method is effective.



CONCLUSION

A provision for grid adaptation is incorporated into computational procedures for the prediction of optimal structural shape. The inclusion of such means to improve the quality of computational results from finite element analysis facilitates solution for shape optimization, particularly in situations where local variations would have a strong effect on shape.

Acknowledgements

The authors express their gratitude to Dr. A. R. Diaz for his efforts on the developments of codes for shape and grid optimization. The developments reports in this paper were supported by the National Science Foundation under Grant CEE 8118158.

N87-11780

**MULTIDISCIPLINARY APPROACH TO THE
DESIGN OF HIGH PRESSURE OXYGEN SYSTEMS**

**R. L. Johnston
Lyndon B. Johnson Space Center
Houston, Texas**

PROBLEM

Much of the design, manufacture, inspection, test, and operation of current high pressure oxygen components and systems has been driven by weight, cost, functional, and schedule requirements. As a result, little coordination has been expended on design for safe operation. While the number of oxygen related fires has not been large, their cost, including program losses and delays, has been very large. Most of these failures need not have occurred.

BACKGROUND

The incidents listed are examples of preventable fires. The Apollo 13 fire was caused by improper operating procedures during the prelaunch period. The failure was facilitated by a design that permitted the tank heaters to be electrically overloaded. The cost of this failure exceeded \$100,000,000 when the loss of mission is considered. Good fortune prevented the loss of three astronauts.

The oxygen flow control valve test failure occurred because possible internal particle impact ignition mechanisms were not understood or considered in the design. Material selection could also have been better in that materials less susceptible to ignition (Inconel, Monel, etc.) could have been selected.

The extravehicular mobility unit fire was caused by failure to carefully consider possible internal ignition mechanisms in the design. Ignitable materials (aluminum, stainless steel) were used to reduce weight. Testing was largely performed with inert gases; hence little opportunity to detect incompatibility of the design with high pressure existed. The cost of this incident exceeded \$30,000,000.

- APOLLO 13** — IN-FLIGHT FIRE IN A CRYOGENIC OXYGEN PRESSURE VESSEL RESULTED IN VESSEL RUPTURE AND CAUSED ABORT OF A LUNAR LANDING MISSION. FIRE CAUSED BY IMPROPER GROUND OPERATION AND PERMISSIVE DESIGN
- SHUTTLE OXYGEN FLOW CONTROL VALVE** — TESTS RESULTED IN IGNITION OF THE VALVE AND COMPLETE DESTRUCTION OF THE COMPONENT. MATERIAL SELECTION WAS POOR. SEVERAL IGNITION MECHANISMS WERE NOT CONSIDERED
- EXTRAVEHICULAR MOBILITY UNIT** — FIRE DESTROYED A TEST UNIT AND SPACE SUIT AND SERIOUSLY INJURED A TECHNICIAN. ACCEPTANCE AND QUALIFICATION TESTS WERE CONDUCTED USING NITROGEN. DESIGN ENCOURAGED INTERNAL GENERATION OF CONTAMINATION

DISCIPLINE BIASES

The solution to the problem of fires in high pressure oxygen systems clearly requires a multidisciplinary approach extending through the life of the system. Major improvements over current designs (circa 1970's) can be made in material selection and in design. However, these two disciplines cannot solve the total problem. Continuing concern and determination to respect the operating limits and conditions, as well as the exercise of care in the manufacturing and inspection phases, are required in component production if safe operation is to be achieved.

- DESIGN** — PRIMARILY CONCERNED WITH FUNCTIONAL REQUIREMENTS
- MATERIALS** — PRIMARILY CONCERNED WITH MECHANICAL PROPERTIES, WEIGHT, AND EASE OF MANUFACTURING
- MANUFACTURING** — PRIMARILY CONCERNED WITH MINIMIZING MANUFACTURING PROBLEMS
- QUALITY** — PRIMARILY CONCERNED WITH CONFORMANCE TO DRAWING AND PROCESS SPECIFICATIONS
- CLEANING** — PRIMARILY CONCERNED WITH INITIAL CONTAMINATION
- TEST** — PRIMARILY CONCERNED WITH FUNCTIONAL BEHAVIOR. TESTS CONDUCTED WITH BENIGN FLUIDS TO MINIMIZE FACILITY AND TEST COSTS
- OPERATION** — PRIMARILY CONCERNED WITH WORKING CONDITION OF THE SYSTEM AND WITH PREVENTION OF LAUNCH DELAY

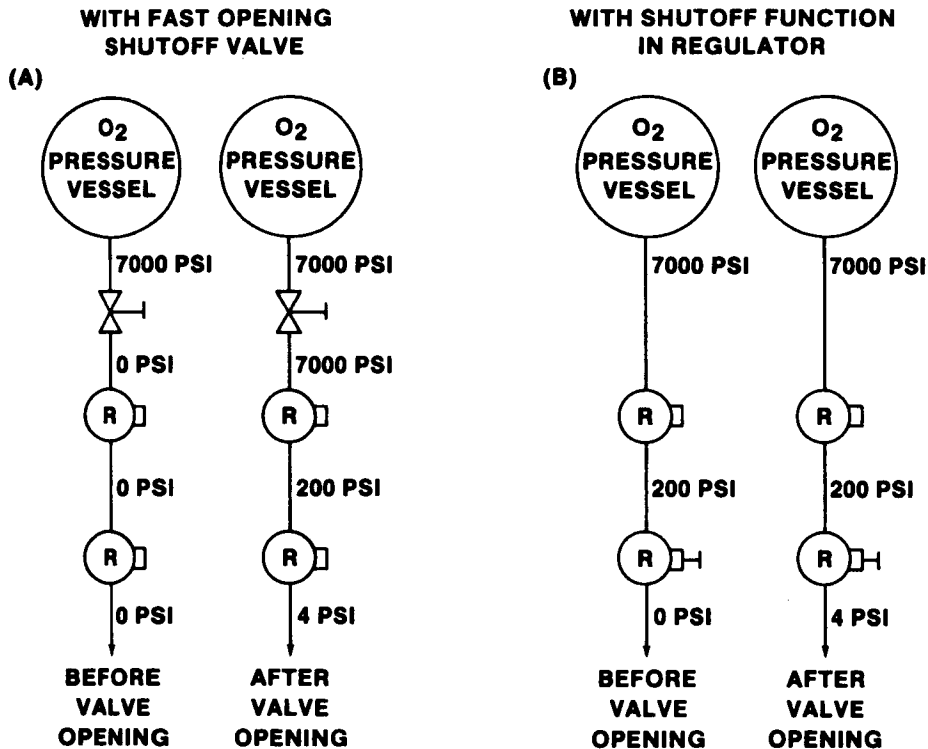
POTENTIAL IGNITION SOURCES

The list of potential ignition sources, while not exhaustive, illustrates both the complexity and the subtle nature of prevention of fires by concentration on elimination of ignition sources only. The designer must be aware of the possible ignition mechanisms that could be included in his design and prevent the inclusion of as many as possible. However, elimination of the total list is probably not possible.

- ELECTRICAL FAILURE** — INSULATION LOSS OR FAILURE
- PARTICLE IMPACT** — ENERGETIC IMPACT CAUSED BY PARTICLES ACCELERATED TO SONIC VELOCITIES
- CONTAMINATION** — IMPROPER CLEANING OR INTERNAL GENERATION AND COLLECTION
- PNEUMATIC SHOCK** — RAPID VALVE OPENING ACROSS LARGE PRESSURE DIFFERENCES
- ADIABATIC COMPRESSION** — INADEQUATE DISSIPATION OF HEAT GENERATED BY PRESSURE INCREASES
- FRETTING OR GALLING** — GENERATION OF LOCALIZED HIGH TEMPERATURES BY RUBBING OR PRESSURE WELDING
- HELMHOLTZ RESONANCE** — GENERATION OF HIGH TEMPERATURES BY RESONATING GAS COLUMNS IN BLIND PASSAGES
- FRICTIONAL HEATING** — GENERATION OF HIGH TEMPERATURES BY RAPID GAS FLOW PAST THIN SECTIONS
- STATIC DISCHARGE** — GENERATION OF STATIC ARCS BY RAPID GAS FLOW OVER INSULATING MATERIALS

EXAMPLE OF A DESIGN RELATED HAZARD

By transferring the shut-off function to the lowest level pressure regulator, rapid pneumatic surges can be prevented. This type of design does require that the low pressure regulator be capable of withstanding full system pressure in the event that a failed-open condition occurs in the intermediate regulator. Some weight may be added to the component by this design approach, but the advantage of this type of design in reducing surge ignition of internal contaminations appears to be well worth while.



EXAMPLE OF MATERIAL SELECTION RELATED HAZARD

The use of materials with large heats of combustion can result in rapid fire propagation rather than self-extinguishment. The probability of impact ignition is also increased. The use of such materials for weight savings or ease of manufacturing reasons can be easily offset by the cost of recovering from a single incident.

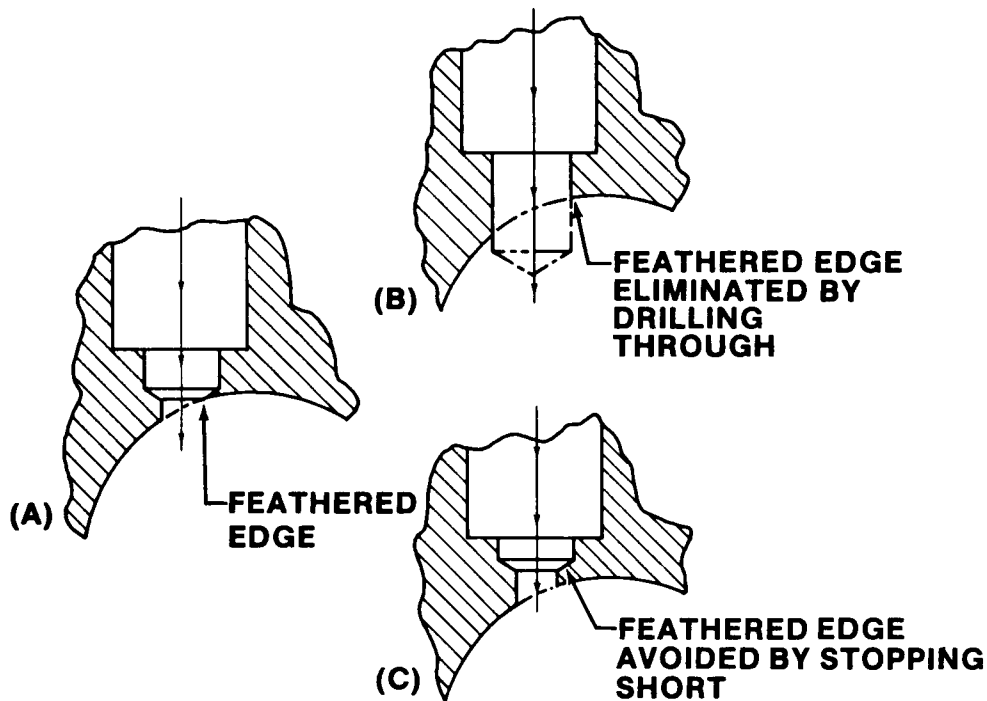
PHYSICAL PROPERTIES OF TYPICAL OXYGEN SYSTEM METALLIC MATERIALS

| Material | Density, lb/in ³ (kg/m ³) | Ultimate Tensile Strength 1000 lb/in ² (MN/m ²) | Max. Use Temp., °F (K) | Heat of Combustion, Btu/lb (MJ/kg) | Impact Ignition Sensitivity Pressure Threshold lb/in ² (N/m ²) |
|--------------------|---|--|------------------------------|--|--|
| Aluminum alloys | 0.10 (2800) | 40 (276) | 350 (450) | 130 000 (302) | 1050 (7.24) |
| Stainless Steel | 0.28 (7800) | 140 (965) | 950 (783) | 33 500 (77.8) | 1050 (7.24) |
| Inconel 718 | 0.30 (8300) | 180 (1240) | 1200 (922) | 15 100 (35.1) | 8000 (55.2) |
| Monel 400 | 0.31 (8600) | 145 (1000) | 1000 (811) | 14 200 (33.1) | 8000 (55.2) |

EXAMPLE OF MANUFACTURING TECHNIQUE RELATED HAZARD

The elimination of "feather edges" by careful manufacturing and inspection can remove one source of internally generated contamination. Even if the thin edge does not separate and become contamination, it could be ignited by friction in high flow regions if the heat dissipation paths are small.

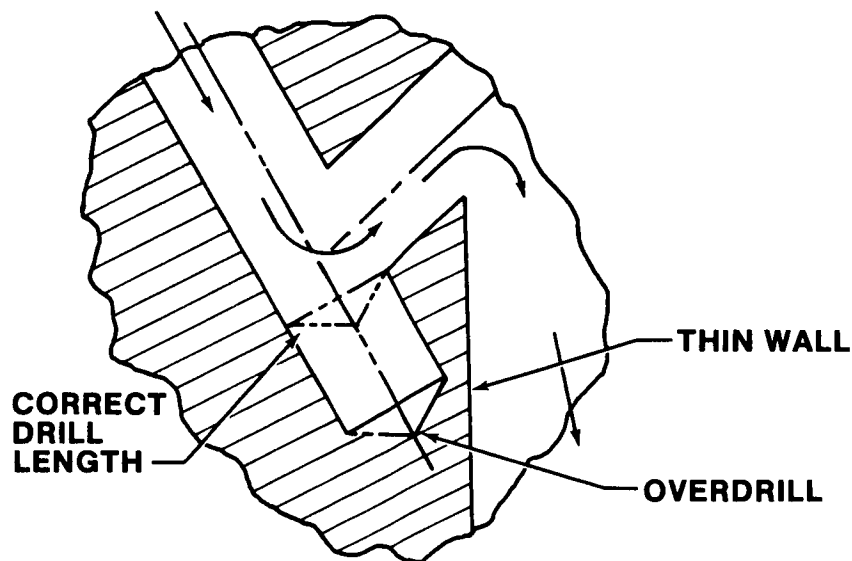
Numerous other manufacturing related ignition sensitive conditions and techniques for their elimination are discussed in reference 1.



EXAMPLE OF A QUALITY RELATED HAZARD

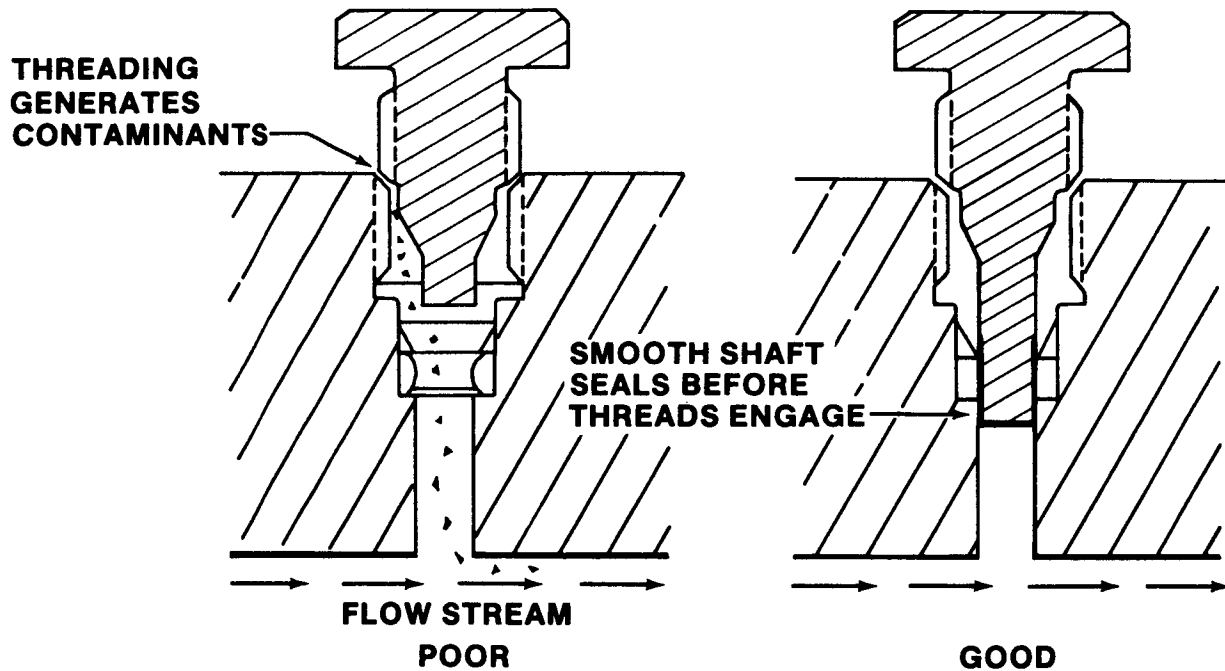
The overdrill condition (which actually occurred in manned maneuvering unit hardware) can result in ignition caused by several different mechanisms. It can act as a debris or contamination trap, it can resonate producing high temperature, high temperatures can be produced by system actuation due to adiabatic compression, or the thin section may be torn free to become a high velocity particle upon exposure to repeated pneumatic impact. One of these mechanisms probably initiated the EMU fire.

X-ray inspection conducted by an inspector trained to recognize such conditions would serve to reduce ignition probabilities. The use of a clear plastic tooling "proof block" to permit visualization of such conditions is also highly desirable (if not mandatory) for parts with complex internal flow paths.



EXAMPLE OF CONTAMINATION RELATED HAZARD

The assembly of previously cleaned and particle free parts can generate internal contamination which may not be removed by subsequent cleaning. The condition may be reduced or eliminated by clever design. Careful selection of the level of assembly prior to intermediate or final cleaning may also help.



EXAMPLE OF A TEST RELATED HAZARD

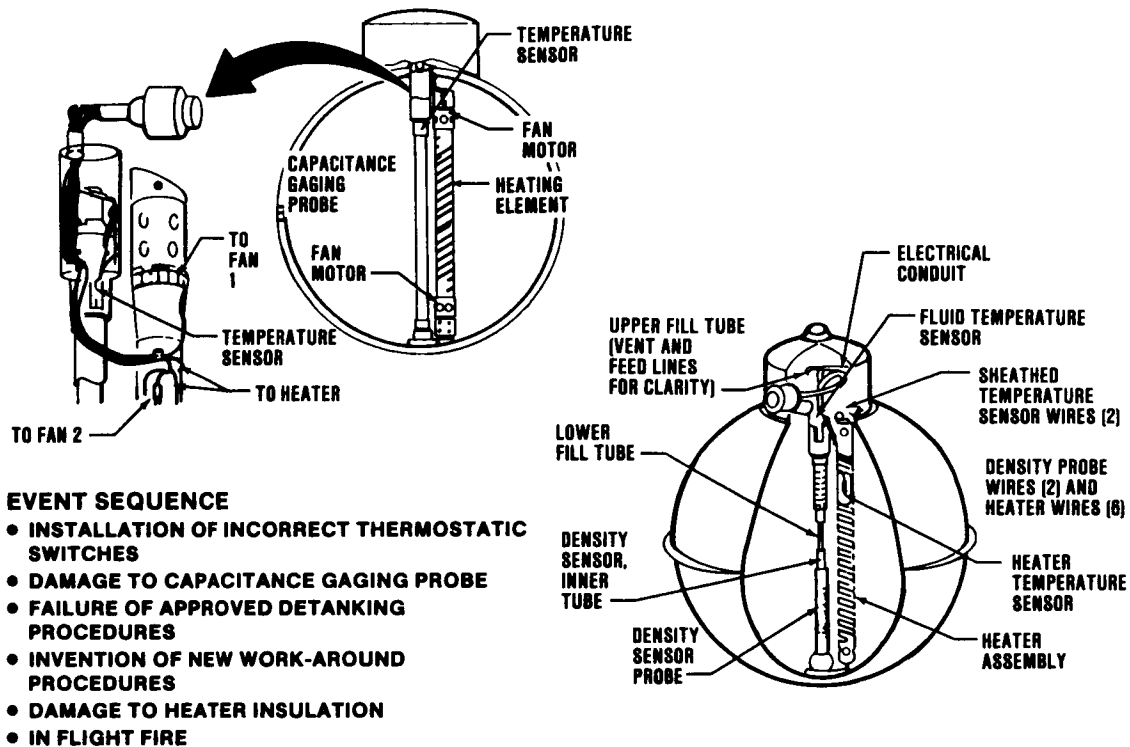
Most extravehicular mobility unit qualification testing and all individual unit acceptance testing was conducted using nitrogen. As a result, the first exposure to oxygen for the unit involved in the fires was with technicians in close proximity. The fire occurred on the 19th actuation of the oxygen control valve during a bench test of the system. Had oxygen been used more extensively in acceptance testing, the fire would have occurred in a remotely operated hazardous test area.

Post-manufacturing acceptance testing and most qualification testing should be conducted with oxygen. While some fires may be delayed until a substantial period of operation has passed, some "infant mortality" cases may be prevented from reaching the user. All acceptance testing and qualification testing should be considered hazardous and should be conducted remotely in facilities designed for this purpose.

- **QUALIFICATION AND ACCEPTANCE TESTS
CONDUCTED WITH NITROGEN**
- **OXYGEN NOT USED TO REDUCE TEST COMPLEXITY
AND TO AVOID REQUIREMENTS FOR HAZARDOUS
TEST AREA**
- **FIRST EXPOSURES TO OXYGEN OCCURRED WITH
TECHNICIANS PRESENT**
- **FIRE OCCURRED ON 19TH ACTUATION OF SYSTEM
USING OXYGEN**

EXAMPLE OF AN OPERATIONALLY RELATED HAZARD

The invention of ad hoc procedures to work around an equipment problem can lead to more problems than it solves. If fully coordinated review cannot be obtained, then such procedures should not be attempted.



OBSERVATIONS AND CONCLUSIONS

- o Every facet of design, manufacturing, inspection, test and operation must cooperate to prevent high pressure oxygen fires
- o The information and skills exist which, if applied, can reduce both the number and magnitude of high pressure oxygen fires

REFERENCE

1. Bond, A.C., et al.: Design Guide for High Pressure Oxygen Systems, NASA RP-1113, 1983.

| | | | | | |
|---|--|-----------------------------|--|---|--|
| 1. Report No. NASA CP-2327, Part 2 | | 2. Government Accession No. | | 3. Recipient's Catalog No. | |
| 4. Title and Subtitle RECENT EXPERIENCES IN MULTIDISCIPLINARY ANALYSIS AND OPTIMIZATION | | | | 5. Report Date September 1984 | |
| | | | | 6. Performing Organization Code 505-33-53-12 | |
| 7. Author(s) Jaroslaw Sobieski, Compiler | | | | 8. Performing Organization Report No. L-15830 | |
| 9. Performing Organization Name and Address NASA Langley Research Center Hampton, Virginia 23665 | | | | 10. Work Unit No. | |
| | | | | 11. Contract or Grant No. | |
| 12. Sponsoring Agency Name and Address National Aeronautics and Space Administration Washington, DC 20546 | | | | 13. Type of Report and Period Covered Conference Publication | |
| | | | | 14. Sponsoring Agency Code | |
| 15. Supplementary Notes | | | | | |
| 16. Abstract <p>This conference publication contains the papers presented at the NASA Symposium on Recent Experiences in Multidisciplinary Analysis and Optimization, held at NASA Langley Research Center, Hampton, Virginia, April 24-26, 1984. The purposes of the symposium were to exchange information about the status of the application of optimization and the associated analyses in industry or research laboratories to real life problems, and to examine the directions of future developments. Within the broad statement of the symposium's purpose, information exchange has encompassed examples of successful application; identification of potential applications and benefits, even though no attempt to apply optimization may have been made as yet; synergistic effects of optimized interaction and trade-offs occurring among two or more engineering disciplines (e.g., structural engineering and aerodynamics) and/or subsystems in a system (e.g., propulsion and airframe in aircraft); and computer technology in the context of the foregoing. This information exchange has covered aerospace and other industries as well as universities and government agencies.</p> <p>The goal of the meeting was to reach a better understanding of the extent to which optimization and the associated analyses are being used, development directions, the future potential, and actions that ought to be taken to realize the potential sooner. That goal was attained and there was a consensus that multidisciplinary analysis and optimization have an important potential as aids to human intellect in the design process, and that the cooperation of industry, academia, and government, under NASA leadership, is needed to realize that potential.</p> | | | | | |
| 17. Key Words (Suggested by Author(s)) Optimization Synthesis Systems Sensitivity Computers | | | 18. Distribution Statement [REDACTED] | | |
| 19. Security Classif. (of this report) Unclassified | 20. Security Classif. (of this page) Unclassified | 21. No. of Pages 519 | 22. Price | | |